

6

Transport of Sodium, Chloride, and Potassium

James A. McCormick | David B. Mount | David H. Ellison

CHAPTER OUTLINE

INTRODUCTION TO NA, CL, AND K TRANSPORT, 156

POTASSIUM TRANSPORT, 188

INTRODUCTION TO NA, CL, AND K TRANSPORT

SODIUM AND CHLORIDE TRANSPORT

Daily sodium (Na^+) intake for adults in the United States is approximately 180 mmol (4.2 g) for men and 150 mmol (3.5 g) for women (<https://www.cdc.gov/nchs/nhanes/wwc.htm>). As Na^+ is the principal osmole in extracellular fluid, the total body content of Na^+ and chloride (Cl^-), its primary anion, determine the extracellular fluid volume. Renal excretion or retention of salt ($\text{Na}^+\text{-Cl}^-$) is thus the major determinant of the extracellular fluid volume, such that genetic loss- or gain-of-function in renal $\text{Na}^+\text{-Cl}^-$ transport can be associated with relative hypotension or hypertension, respectively. On a quantitative level, at a glomerular filtration rate (GFR) of 180 L/day and serum Na^+ of about 140 mmol/L, the kidney filters some 25,000 mmol/day of Na^+ ; this is equivalent to about 1.5 kg of salt, which would occupy roughly 10 times the extracellular space.¹ Minute changes in renal $\text{Na}^+\text{-Cl}^-$ excretion can thus have massive effects on the extracellular fluid volume. In addition, 99.6% of filtered $\text{Na}^+\text{-Cl}^-$ must be reabsorbed to excrete 140 mmol/L per day. Energetically, this renal absorption of Na^+ consumes 1 molecule of adenosine triphosphate (ATP) per five molecules of Na^+ .¹ This is gratifyingly economical, given that the absorption of $\text{Na}^+\text{-Cl}^-$ is primarily, but not exclusively, driven by basolateral $\text{Na}^+\text{-K}^+\text{-ATPase}$, which has a stoichiometry of three molecules of transported Na^+ per molecule of ATP.² This estimate reflects a net expenditure, however, because the cost of transepithelial $\text{Na}^+\text{-Cl}^-$ transport varies considerably along the nephron, from a predominance of passive transport by thin ascending limbs to the purely active transport mediated by the “aldosterone-sensitive distal nephron” (distal convoluted tubule [DCT], connecting tubule [CNT], and collecting duct).

As much as 60% to 70% of filtered $\text{Na}^+\text{-Cl}^-$ is reabsorbed along the proximal tubule (PT), and approximately 25% along the thick ascending limb (TAL; Fig. 6.1). Whereas the PT

can theoretically absorb as much as nine Na^+ molecules for each hydrolyzed ATP, paracellular Na^+ transport by the TAL doubles the efficiency of transepithelial $\text{Na}^+\text{-Cl}^-$ transport (six Na^+ molecules per ATP).^{1,3} By the time filtered fluid reaches the macula densa, more than 90% of filtered Na^+ has been reabsorbed,⁴ a percentage that varies only slightly, when dietary NaCl intake ranges from very low to very high.⁵ Thus the terminal segments of the nephron, while reabsorbing only 5% to 10% of filtered Na^+ , are a primary site of transport regulation. Here, renal $\text{Na}^+\text{-Cl}^-$ absorption occurs at full cost (3 Na^+ per ATP) in the aldosterone-sensitive distal nephron while affording the generation of considerable transepithelial gradients.¹

The nephron thus constitutes a serial arrangement of tubule segments with considerable heterogeneity in the physiologic consequences, mechanisms, and regulation of transepithelial $\text{Na}^+\text{-Cl}^-$ transport. These issues will be reviewed in this section in anatomic order.

PROXIMAL TUBULE

A primary function of the renal PT is the near-isosmotic reabsorption of two-thirds to three-quarters of the glomerular ultrafiltrate. This encompasses the reabsorption of at least 60% of filtered Na^+ with accompanying anions (Fig. 6.1), such that this nephron segment plays a critical role in the maintenance of extracellular fluid volume. Although all segments of the PT share the ability to transport a variety of inorganic and organic solutes, there are considerable differences in the transport characteristics and capacity of early, mid, and late segments of the PT. There is thus a gradual reduction in the volume of transported fluid and solutes as one proceeds along the proximal nephron. This corresponds to distinct ultrastructural characteristics in the tubular epithelium, moving from the S1 segment (early proximal convoluted tubule [PCT]) to the S2 segment (late PCT and beginning of the proximal straight tubule) and the S3 segment (remainder of the proximal straight tubule). Cells of the S1 segment are thus characterized by a tall brush

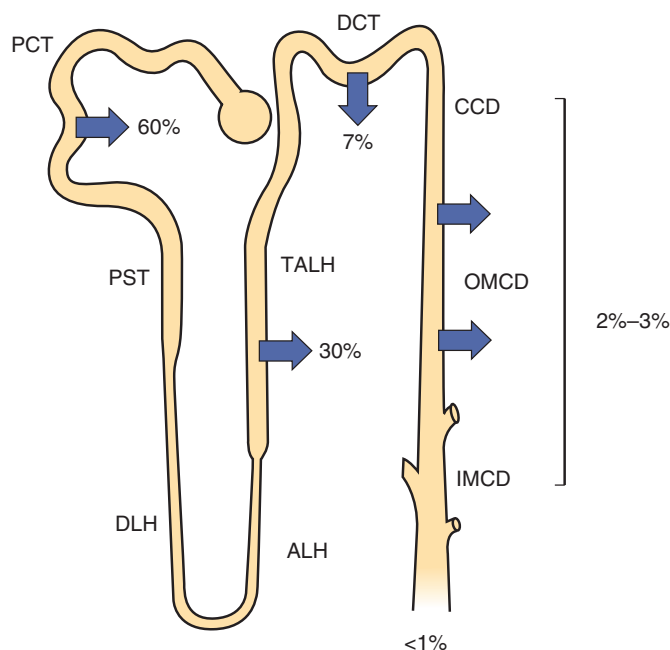


Fig. 6.1 Percentage reabsorption of filtered $\text{Na}^+\text{-Cl}^-$ along the euvolemic nephron. *ALH*, Thin ascending limb of the loop of Henle; *CCD*, cortical collecting duct; *DCT*, distal convoluted tubule; *DLH*, descending thin limb of the loop of Henle; *IMCD*, inner medullary collecting duct; *OMCD*, outer medullary collecting duct; *PCT*, proximal convoluted tubule; *PST*, proximal straight tubule; *TALH*, thick ascending limb of the loop of Henle. (From Moe OW, Baum M, Berry CA, Rector Jr FC. Renal transport of glucose, amino acids, sodium, chloride, and water. In: Brenner BM, ed. *Brenner and Rector's the Kidney*. Philadelphia: WB Saunders; 2004:413–452.)

border, with extensive lateral invaginations of the basolateral membrane.⁶ Numerous elongated mitochondria are located in lateral cell processes, with a proximity to the plasma membrane that is characteristic of epithelial cells involved in active transport. Ultrastructure of the S2 segment is similar, albeit with a shorter brush border, fewer lateral invaginations, and less prominent mitochondria. In epithelial cells of the S3 segment, lateral cell processes and invaginations are essentially absent, with small mitochondria that are randomly distributed within the cell.⁶ The extensive brush border of proximal tubular cells serves to amplify the apical cell surface that is available for reabsorption; again, this amplification is axially distributed, increasing the apical area 36-fold in S1 and 15-fold in S3.⁷ At the functional level, bicarbonate reabsorption rates decline by at least 80% between the first and last portions of the PT, whereas Cl^- reabsorption declines by approximately 50%.⁸

There is also considerable axial heterogeneity in the quantitative capacity of the proximal nephron for organic solutes such as glucose and amino acids, with predominant reabsorption of these substrates in S1 segments.⁹ The Na^+ -dependent reabsorption of glucose, amino acids, and other solutes in S1 segments results in a transepithelial potential difference (PD) that is initially lumen negative due to electrogenic removal of Na^+ from the lumen (Fig. 6.2).¹⁰ This is classically considered the first phase of volume reabsorption by the PT.¹¹ The lumen-negative PD serves to drive both

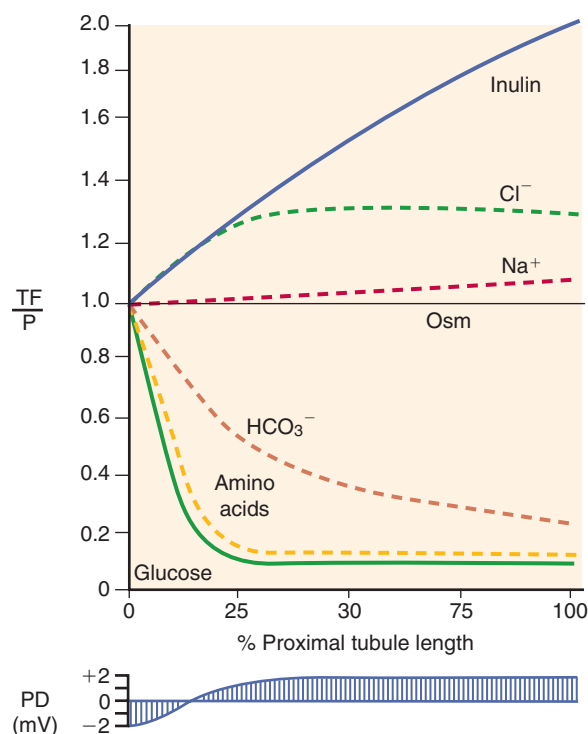


Fig. 6.2 Reabsorption of solutes along the proximal tubule in relation to the transepithelial potential difference (PD). *Osm*, Osmolality; *TF/P*, ratio of tubule fluid to plasma concentration. (From Rector Jr FC. Sodium, bicarbonate, and chloride absorption by the proximal tubule. *Am J Physiol*. 1983;244:F461–F471.)

paracellular Cl^- absorption and a backleak of Na^+ from the peritubular space to the lumen. Paracellular Cl^- absorption in this setting accomplishes the net transepithelial absorption of a solute such as glucose, along with equal amounts of Na^+ and Cl^- ; by contrast, backleak of Na^+ leads only to reabsorption of the organic solute, with no net transepithelial transport of Na^+ or Cl^- . The amount of Cl^- reabsorption that is driven by this lumen-negative PD thus depends on the relative permeability of the paracellular pathway to Na^+ and Cl^- . There appears to be considerable heterogeneity in the relative paracellular permeability to Na^+ and Cl^- ; for example, whereas superficial PCTs and proximal straight tubules in the rabbit are Cl^- selective, juxtamedullary PTs in this species are reportedly Na^+ selective.^{12,13} Regardless, the component of paracellular Cl^- transport that is driven by this lumen-negative PD is restricted to the very early PT.

The second phase of volume reabsorption by the PT is dominated by $\text{Na}^+\text{-Cl}^-$ reabsorption via paracellular and transcellular pathways.¹¹ In addition to the Na^+ -dependent reabsorption of organic solutes, the early PT has a much higher capacity for HCO_3^- absorption via the coupling of apical $\text{Na}^+\text{-H}^+$ exchange, carbonic anhydrase, and basolateral $\text{Na}^+\text{-HCO}_3^-$ cotransport.⁹ As the luminal concentrations of HCO_3^- and other solutes begin to drop, the concentration of $\text{Na}^+\text{-Cl}^-$ rises to a value greater than that of the peritubular space.¹⁴ This is accompanied by a reversal of the lumen-negative PD to a lumen-positive value generated by passive Cl^- diffusion (Fig. 6.2).¹⁵ This lumen-positive PD serves

to drive paracellular Na^+ transport, whereas the chemical gradient between the lumen and peritubular space provides the driving force for paracellular reabsorption of Cl^- . This passive paracellular pathway is thought to mediate about 40% of transepithelial $\text{Na}^+\text{-Cl}^-$ reabsorption by the mid to late PT.¹² Of note, however, there may be heterogeneity in the relative importance of this paracellular pathway, with evidence that active (i.e., transcellular) reabsorption predominates in PCTs from juxtamedullary versus superficial nephrons.¹⁶ Regardless, the combination of passive and active transport of $\text{Na}^+\text{-Cl}^-$ explains how the PT is able to reabsorb about 60% of filtered $\text{Na}^+\text{-Cl}^-$, despite $\text{Na}^+\text{-K}^+\text{-ATPase}$ activity that is considerably lower than that of distal segments of the nephron (Fig. 6.3).¹⁷

The transcellular component of $\text{Na}^+\text{-Cl}^-$ reabsorption initially emerged from studies of the effect of cyanide, ouabain, luminal anion transport inhibitors, cooling, and luminal-peritubular K^+ removal.¹¹ For example, the luminal addition of SITS (4-acetamido-4'-isothiocyano-stilbene-2,2'-disulfonic acid), an inhibitor of anion transporters, reduces volume reabsorption of PCTs perfused with a high Cl^- , low HCO_3^- solution that mimics the luminal composition of the late PT; this occurs in the absence of an effect on carbonic anhydrase.¹⁴ This transcellular component of $\text{Na}^+\text{-Cl}^-$ reabsorption is clearly electroneutral. For example, in the absence of anion gradients across the perfused PT, there is no change in transepithelial PD after the inhibition of active transport by ouabain, despite a marked reduction in volume reabsorption.¹⁸

Transcellular $\text{Na}^+\text{-Cl}^-$ reabsorption is accomplished by the coupling of luminal $\text{Na}^+\text{-H}^+$ exchange or $\text{Na}^+\text{-SO}_4^{2-}$ cotransport with a heterogeneous population of anion exchangers, as reviewed later.

PARACELLULAR $\text{Na}^+\text{-Cl}^-$ TRANSPORT

A number of factors serve to optimize the conditions for paracellular $\text{Na}^+\text{-Cl}^-$ transport by the mid to late PT. First, the PT is a low-resistance, so-called leaky epithelium, with tight junctions that are highly permeable to both Na^+ and Cl^- .^{12,13} Second, these tight junctions are preferentially permeable to Cl^- over HCO_3^- , a feature that helps generate the lumen-positive PD in the mid to late PT.¹⁴ Third, the increase in luminal $\text{Na}^+\text{-Cl}^-$ concentrations in the mid to late PT generates a chemical driving force for paracellular reabsorption of Cl^- .¹⁵ This increase in luminal $\text{Na}^+\text{-Cl}^-$ is the direct result of the robust reabsorption of HCO_3^- and other solutes by the early S1 segment, combined with the isosmotic reabsorption of filtered water.^{9,19}

A highly permeable paracellular pathway is a consistent feature of epithelia that function in the near-isosmolar reabsorption of $\text{Na}^+\text{-Cl}^-$, including the small intestine, PT, and gallbladder. Morphologically, the apical tight junction of proximal tubular cells and other leaky epithelia is considerably less complex than that of tight epithelia. Freeze-fracture microscopy thus reveals that the tight junction of proximal tubular cells is comparatively shallow, with as few as one junctional strand (Fig. 6.4); by contrast, high-resistance

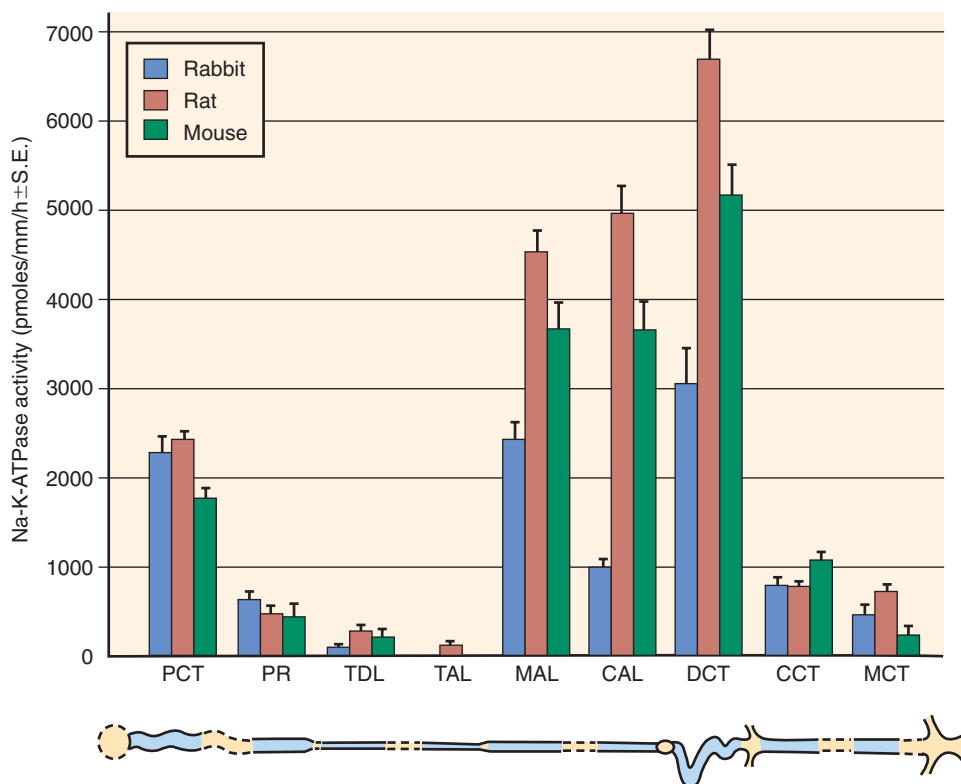


Fig. 6.3 Distribution of $\text{Na}^+\text{-K}^+\text{-ATPase}$ activity along the nephron. *CCD*, Cortical collecting duct; *cTAL*, cortical thick ascending limb; *DCT*, distal convoluted tubule; *MCD*, medullary collecting duct; *mTAL*, medullary thick ascending limb; *PCT*, proximal convoluted tubule; *PST*, proximal straight tubule; *tAL*, thin ascending limb of the loop of Henle; *tDL*, descending thin limb of the loop of Henle. (From Katz AI, Doucet A, Morel F. $\text{Na}^+\text{-K}^+\text{-ATPase}$ activity along the rabbit, rat, and mouse nephron. *Am J Physiol.* 1979;237:F114–F120.)

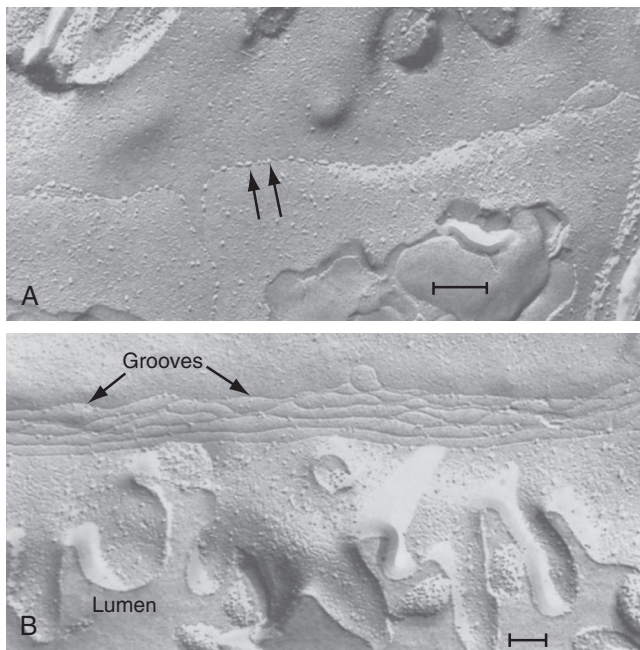


Fig. 6.4 Freeze-fracture electron microscopy images of tight junctions in mouse proximal and distal nephron. (A) Proximal convoluted tubule, a “leaky” epithelium; the tight junction contains only one junctional strand, seen as a groove in the fracture face (arrows). (B) Distal convoluted tubule, a “tight” epithelium. The tight junction is deeper and contains several anastomosing strands, seen as grooves in the fracture face. (From Claude P, Goodenough DA. Fracture faces of zonulae occludentes from “tight” and “leaky” epithelia. *J Cell Biol.* 1973;58: 390–400.)

epithelia have deeper tight junctions, with a complex and extensive network of junctional strands.²⁰ At the functional level, tight junctions of epithelia function as charge- and size-selective paracellular tight junction channels, physiologic characteristics that are thought to be conferred by integral membrane proteins that cluster together at the tight junction. Changes in the expression of these proteins can have marked effects on permeability without affecting the number of junctional strands.^{14,21,22} In particular, the charge and size selectivity of tight junctions appears to be conferred in large part by the claudins, a large (>20) gene family of tetraspan transmembrane proteins,^{23–25} one of which was recently crystallized.²⁶ The repertoire of claudins expressed by proximal tubular epithelial cells may thus determine the high paracellular permeability of this nephron segment. At a minimum, proximal tubular cells coexpress claudin-2, claudin-10, and claudin-17.^{14,27,28}

The robust expression of claudin-2 in the PT is of particular interest because this claudin can dramatically decrease the resistance of transfected epithelial cells.²² Overexpression of claudin-2, but not claudin-10, also increases Na^+ -dependent water flux in epithelial cell lines, suggesting that claudin-2 directly modulates paracellular water permeability.²⁹ Consistent with this cellular phenotype, targeted deletion of claudin-2 in mice generates a tight epithelium in the PT, with a reduction in Na^+ , Cl^- , and fluid absorption.³⁰ Loss of claudin-2 expression does not affect the ultrastructure of tight junctions, but leads to a reduction in paracellular cation permeability and secondary reduction in transepithelial Cl^- transport.³⁰

This action enhances the energy efficiency of proximal solute reabsorption. Although reabsorption is lower in claudin-2 knockout mice, overall sodium handling is normal because solute transport is increased along more distal segments. This requirement for more transcellular solute transport along the loop of Henle contributes to lower medullary oxygen tension, and increased susceptibility to renal ischemia.³¹ Terminal differentiation of proximal tubular claudin-2 expression requires the integrin β_1 -subunit, such that deletion of this protein in mice converts the PT to a tight epithelium expressing low levels of claudin-2.³²

The molecular identification of anion-selective claudins in the PT has lagged, but claudin-17 has been shown to generate a predominantly anion-selective paracellular conductance in Madin-Darby canine kidney (MDCK) C7 cells, whereas knockdown of the protein was able to reverse a predominantly cation-selective LLC-PK(1) epithelial cell line to an anion-selective cell line.²⁸ Claudin-17 is expressed along the PT, suggesting a significant role in paracellular chloride absorption by this nephron segment. Recently, it has been suggested that a form of claudin-10, claudin-10a, is another anion-selective paracellular pathway along the PT.³³

The reabsorption of HCO_3^- and other solutes from the glomerular ultrafiltrate would be expected to generate an osmotic gradient across the epithelium, resulting in a hypotonic lumen. This appears to be the case, although the absolute difference in osmolality between the lumen and peritubular space has been a source of considerable controversy.¹⁹ Another controversial issue has been the relative importance of paracellular versus transcellular water transport from this hypotonic lumen. These issues have been elegantly addressed through characterization of knockout mice with a targeted deletion of aquaporin-1, a water channel protein expressed at the apical and basolateral membranes of the PT. Mice deficient in aquaporin-1 have an 80% reduction in water permeability in perfused S2 segments, with a 50% reduction in transepithelial fluid transport.³⁴ Aquaporin-1 deficiency also results in a marked increase in luminal hypotonicity, providing definitive proof that near-isosmotic reabsorption by the PT requires transepithelial water transport via aquaporin-1.¹⁹ The residual water transport in the PTs of aquaporin-1 knockout mice is mediated in part by aquaporin-7 and/or by claudin-2-dependent paracellular water transport.^{30,35} Combined knockout of aquaporin-1 and claudin-2 in mice demonstrates sustained PT water reabsorption (25% of wild type), suggestive of compensation from other pathways.³⁶ Alternative pathways for water reabsorption may include cotransport of H_2O via the multiple Na^+ -dependent solute transporters in the early PT; this novel hypothesis is, however, a source of considerable controversy.^{37,38} A related issue is the relative importance of diffusional versus convective (solvent drag) transport of $\text{Na}^+\text{-Cl}^-$ across the paracellular tight junction; convective transport of $\text{Na}^+\text{-Cl}^-$ with water would seem to play a lesser role than diffusion, given the evidence that the transcellular pathway is the dominant transepithelial pathway for water in the PT.^{12,19,34,35}

TRANSCELLULAR $\text{Na}^+\text{-Cl}^-$ TRANSPORT

Apical Mechanisms

Apical $\text{Na}^+\text{-H}^+$ exchange plays a critical role in the transcellular and paracellular reabsorption of $\text{Na}^+\text{-Cl}^-$ by the PT. In addition

to providing an entry site in the transcellular transport of Na^+ , $\text{Na}^+\text{-H}^+$ exchange plays a dominant role in the functional “absorption” of HCO_3^- by the early PT (HCO_3^- does not actually move across the apical membrane, but rather is generated within cells together with H^+); as the movement of Na^+ and HCO_3^- drives osmotic water movement, it also acts to increase the luminal concentration of Cl^- , which in turn increases the driving forces for the passive paracellular transport of Cl^- .³⁹ Increases in luminal Cl^- also help drive the apical uptake of Cl^- during transcellular transport. Not surprisingly, there is a considerable reduction in fluid transport of perfused PTs exposed to concentrations of amiloride that are sufficient to inhibit proximal tubular $\text{Na}^+\text{-H}^+$ exchange.¹⁴

$\text{Na}^+\text{-H}^+$ exchange is predominantly mediated by the NHE proteins, encoded by the nine members of the *SLC9* gene family; NHE3 in particular plays an important role in proximal tubular physiology.⁴⁰ The NHE3 protein is expressed at the apical membrane of S1, S2, and S3 segments.⁴¹ The apical membrane of the PT also expresses alternative Na^+ -dependent H^+ transporters, including NHE8.^{40,42} NHE8 predominates over NHE3 in the neonatal PT, with subsequent induction of NHE3 and downregulation of NHE8 in mature, adult nephrons.⁴⁰ The primacy of NHE3 in mature PTs is illustrated

by the renal phenotype of NHE3 knockout mice, which have a 62% reduction in proximal fluid absorption and a 54% reduction in baseline chloride absorption.^{43,44} A recent study in which *Nhe3* was disrupted specifically in the kidney showed that it plays a role in maintaining blood pressure at baseline, and plasma Na^+ in response to increased or reduced dietary $\text{Na}^+\text{-Cl}^-$, with compensatory upregulation of $\text{Na}^+\text{-Cl}^-$ cotransporter (NCC) and epithelial Na^+ channel (ENaC) occurring.⁴⁵ The severe salt-wasting phenotype seen in global *Nhe3* knockout mice occurs due to its deletion in intestine.

Much as amiloride and other inhibitors of $\text{Na}^+\text{-H}^+$ exchange have revealed an important role for this transporter in transepithelial salt transport by the PT, evidence for the involvement of an apical anion exchanger first came from the use of anion transport inhibitors; DIDS (4,4'-diisothiocyanostilbene-2,2'-disulfonic acid), furosemide, and SITS all reduce fluid absorption from the lumen of PT segments perfused with solutions containing $\text{Na}^+\text{-Cl}^-$.¹⁴ In the simplest arrangement for the coupling of $\text{Na}^+\text{-H}^+$ exchange to Cl^- exchange, Cl^- would be exchanged with the OH^- ion during $\text{Na}^+\text{-Cl}^-$ transport (Fig. 6.5). Evidence for such a $\text{Cl}^-\text{-OH}^-$ exchanger was reported by a number of groups in the early 1980s that used membrane vesicles isolated from

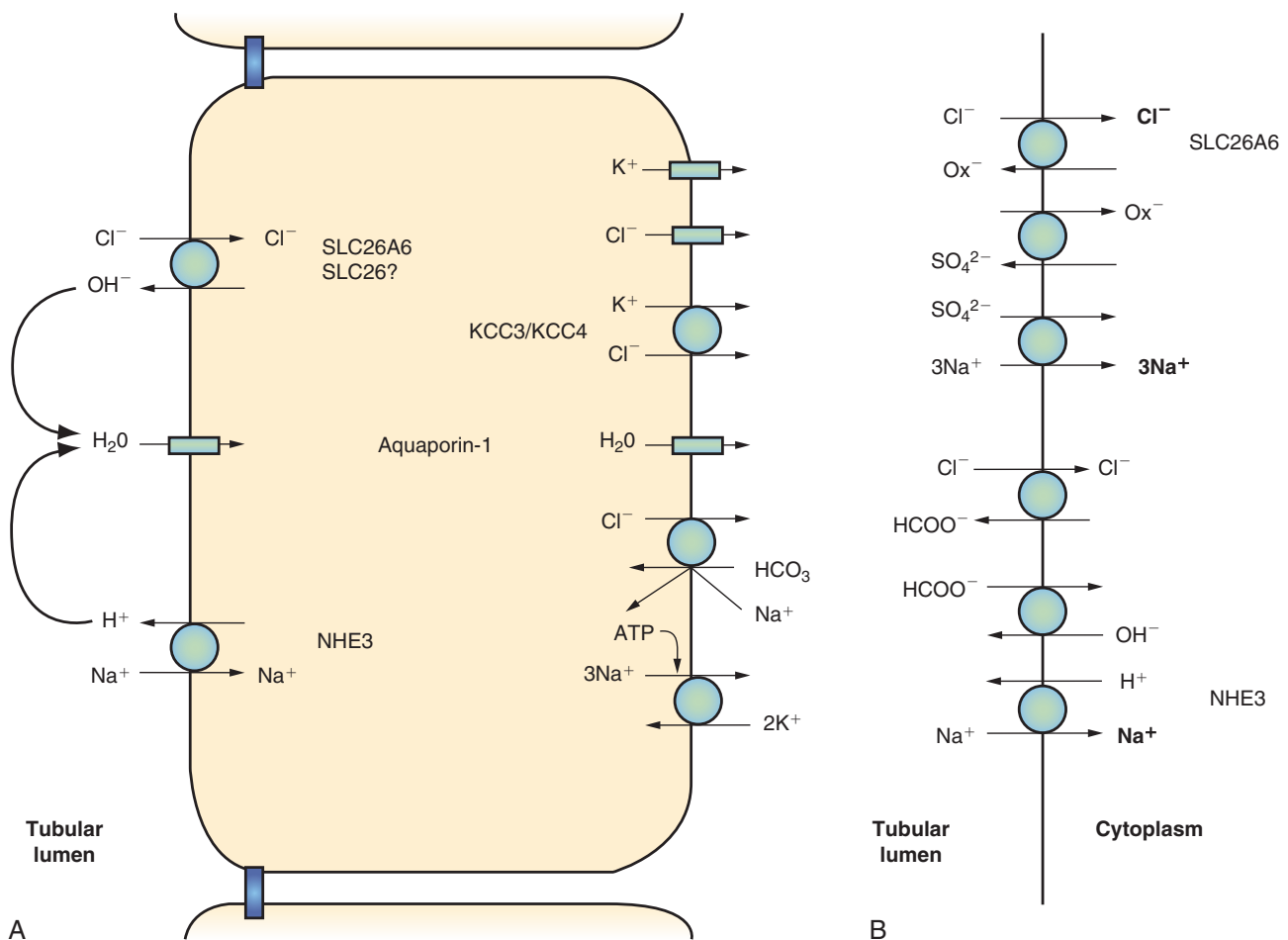


Fig. 6.5 Transepithelial $\text{Na}^+\text{-Cl}^-$ transport in the proximal tubule. (A) In the simplest scheme, Cl^- enters the apical membrane via a Cl^- - OH^- exchanger, coupled to Na^+ entry via NHE3. (B) Alternative apical anion exchange activities that couple to $\text{Na}^+\text{-H}^+$ exchange and $\text{Na}^+\text{-SO}_4^{2-}$ cotransport. See text for details.

the PT.⁴⁶ These findings could not, however, be replicated in similar studies from other groups.^{46,47} Moreover, experimental evidence was provided for the existence of a dominant Cl⁻-formate exchange activity in brush border vesicles in the absence of significant Cl⁻-OH⁻ exchange.⁴⁷ It was postulated that recycling of formate by the back diffusion of formic acid would sustain the net transport of Na⁺-Cl⁻ across the apical membrane. Vesicle formate transport stimulated by a pH gradient (H⁺-formate cotransport or formate-OH⁻ exchange) is saturable, consistent with a carrier-mediated process rather than diffusion of formic acid across the apical membrane of the PT.⁴⁸ Transport studies using brush border vesicles have also detected the presence of Cl⁻-oxalate exchange mechanisms in the apical membrane of the PT, in addition to SO₄²⁻-oxalate exchange.^{39,49} Based on differences in the affinities and inhibitor sensitivity of the Cl⁻-oxalate and Cl⁻-formate exchange activities, it was suggested that there are two separate apical exchangers in the proximal nephron, a Cl⁻-formate exchanger and a Cl⁻-formate-oxalate exchanger capable of transporting both formate and oxalate (Fig. 6.5).

The physiological relevance of apical Cl⁻-formate and Cl⁻-oxalate exchange has been addressed by perfusing individual PT segments with solutions containing Na⁺-Cl⁻ and formate or oxalate. Both formate and oxalate significantly increased fluid transport under these conditions in rabbit, rat, and mouse PTs.⁴⁴ This increase in fluid transport was inhibited by DIDS, suggesting involvement of the DIDS-sensitive anion exchanger(s) detected in brush border vesicle studies. A similar mechanism for Na⁺-Cl⁻ transport in the DCT has also been detected, independent of thiazide-sensitive Na⁺-Cl⁻ cotransport.⁵⁰ Further experiments have indicated that the oxalate- and formate-dependent anion transporters in the PT are coupled to distinct Na⁺ entry pathways, to Na⁺-SO₄²⁻ cotransport and Na⁺-H⁺ exchange, respectively.⁵¹ The coupling of Cl⁻-oxalate transport to Na⁺-SO₄²⁻ cotransport requires the additional presence of SO₄²⁻-oxalate exchange, which has been demonstrated in brush border membrane vesicle studies.⁵² The obligatory role for NHE3 in formate-stimulated Cl⁻ transport was illustrated using *Nhe3* null mice, in which the formate effect is abolished; as expected, oxalate stimulation of Cl⁻ transport is preserved in the *Nhe3* null mice.⁴⁴ Finally, tubular perfusion data from superficial and juxtamedullary PCTs have suggested that there is heterogeneity in the dominant mode of anion exchange along the PT, such that Cl⁻-formate exchange is absent in juxtamedullary PCT, in which Cl⁻-OH⁻ exchange may instead be dominant.¹⁴

The molecular identity of the apical anion exchanger(s) involved in transepithelial Na⁺-Cl⁻ reabsorption by the PT has been the object of almost 3 decades of investigation. A key breakthrough was the observation that the SLC26A4 anion exchanger, also known as pendrin, is capable of Cl⁻-formate exchange when expressed in *Xenopus laevis* oocytes.⁵³ However, expression of SLC26A4 in the PT is minimal or absent in several species, and formate-stimulated Na⁺-Cl⁻ transport in this nephron segment is unimpaired in *Slc26a4* null mice.¹⁴ There is, however, robust expression of SLC26A4 in distal type B intercalated cells; the role of this exchanger in Cl⁻ transport by the distal nephron is reviewed elsewhere in this chapter (see the “[Connecting Tubules and the Cortical Collecting Duct: Cl⁻ Transport](#)” section).⁵⁴ Regardless, these data for SLC26A4 led to the identification and characterization of SLC26A6, a widely expressed member of the SLC26 family

that is expressed at the apical membrane of proximal tubular cells. Murine SLC26A6, when expressed in *Xenopus* oocytes, mediates the multiple modes of anion exchange that have been implicated in transepithelial Na⁺-Cl⁻ by the PT, including Cl⁻-formate, Cl⁻-OH⁻, Cl⁻-SO₄²⁻, and SO₄²⁻-oxalate exchange.⁵⁵ However, tubule perfusion experiments in mice deficient in SLC26A6 did not reveal a reduction in baseline Cl⁻ or fluid transport, indicative of considerable heterogeneity in apical Cl⁻ transport by the PT.⁵⁶ Candidates for the residual Cl⁻ transport in SLC26A6-deficient mice include SLC26A7 and SLC26A9, which are expressed at the apical membrane of PTs; however, these members of the SLC26 family appear to function as Cl⁻ channels rather than as exchangers.^{57–59} SLC26A2 may also contribute to apical anion exchange in the PT.⁶⁰ It does, however, appear that SLC26A6 is the dominant Cl⁻-oxalate exchanger of the proximal brush border; the usual increase in tubular fluid transport induced by oxalate is abolished in *Slc26a6* knockout mice, with an attendant loss of Cl⁻-oxalate exchange in brush border membrane vesicles.^{56,61}

Somewhat surprisingly, SLC26A6 mediates electrogenic Cl⁻-OH⁻ and Cl⁻-HCO₃⁻ exchange, and most if not all the members of this family are electrogenic in at least one mode of anion transport.^{14,55,58,62,63} This begs the question of how the electroneutrality of transcellular Na⁺-Cl⁻ transport is preserved. Notably, however, the stoichiometry and electrophysiology of Cl⁻-base exchange differ for individual members of the family; for example, SLC26A6 exchanges one Cl⁻ for two HCO₃⁻ anions, whereas SLC26A3 exchanges two Cl⁻ anions for one HCO₃⁻ anion.^{14,63} Coexpression of two or more electrogenic SLC26 exchangers in the same membrane may thus yield a net electroneutrality of apical Cl⁻ exchange. Alternatively, apical K⁺ channels in the PT may function to stabilize membrane potential during Na⁺-Cl⁻ absorption.⁶⁴

Another puzzle is why Cl⁻-formate exchange preferentially couples to Na⁺-H⁺ exchange mediated by NHE3 (Fig. 6.5), without evident coupling of Cl⁻-oxalate exchange to Na⁺-H⁺ exchange or Cl⁻-formate exchange to Na⁺-SO₄²⁻ cotransport; it is evident that SLC26A6 is capable of mediating SO₄²⁻-formate exchange, which would be necessary to support coupling between Na⁺-SO₄²⁻ cotransport and formate.^{44,55} Scaffolding proteins may serve to cluster these different transporters together in separate microdomains, leading to preferential coupling. Notably, whereas both SLC26A6 and NHE have been reported to bind to the scaffolding protein PDZK1, distribution of SLC26A6 is selectively impaired in *Pdzk1* knockout mice.⁶⁵ Petrovic and colleagues have also reported a novel activation of proximal Na⁺-H⁺ exchange by luminal formate, suggesting a direct effect of formate per se on NHE3; this may in part explain the preferential coupling of Cl⁻-formate exchange to NHE3.⁶⁶ Despite these intriguing observations, the relative importance of transcellular versus passive paracellular Cl⁻ reabsorption in the PT remains to be established with certainty.

Basolateral Mechanisms

As in other absorptive epithelia, basolateral Na⁺-K⁺-ATPase activity establishes the Na⁺ gradient for transcellular Na⁺-Cl⁻ transport by the PT and provides a major exit pathway for Na⁺. To preserve the electroneutrality of transcellular Na⁺-Cl⁻ transport, this exit of Na⁺ across the basolateral membrane must be balanced by an equal exit of Cl⁻.¹⁸ Several

exit pathways for Cl^- have been identified in proximal tubular cells, including $\text{K}^+\text{-Cl}^-$ cotransport, Cl^- channels, and various modalities of Cl^- - HCO_3^- exchange (Fig. 6.5).

Several lines of evidence support the existence of a swelling-activated basolateral $\text{K}^+\text{-Cl}^-$ cotransporter (KCC) in the PT.⁶⁷ The KCC proteins are encoded by four members of the cation-chloride cotransporter gene family; *Kcc1*, *Kcc3*, and *Kcc4* are all expressed in the kidney. In particular, there is very heavy coexpression of KCC3 and KCC4 at the basolateral membrane of the PT, from S1 to S3.⁶⁸ At the functional level, basolateral membrane vesicles from the renal cortex reportedly contain $\text{K}^+\text{-Cl}^-$ cotransport activity.⁶⁷ The use of ion-sensitive microelectrodes, combined with luminal charge injection and manipulation of bath K^+ and Cl^- , suggest the presence of an electroneutral KCC at the basolateral membrane of proximal straight tubules. Increases or decreases in basolateral K^+ increase or decrease intracellular Cl^- activity, respectively, with reciprocal effects of basolateral Cl^- on K^+ activity; these data are consistent with coupled $\text{K}^+\text{-Cl}^-$ transport.^{69,70} Notably, a 1-mmol/L concentration of furosemide, sufficient to inhibit all four of the KCCs, does not inhibit this $\text{K}^+\text{-Cl}^-$ cotransport under baseline conditions.⁶⁹ However, only 10% of baseline K^+ efflux in the PT is mediated by furosemide-sensitive $\text{K}^+\text{-Cl}^-$ cotransport, which is likely quiescent in the absence of cell swelling. Thus the activation of apical Na^+ -glucose transport in proximal tubular cells strongly activates a barium-resistant (Ba^{2+}) K^+ efflux pathway that is 75% inhibited by 1-mmol/L furosemide.⁷¹ In addition, a volume regulatory decrease (VRD) in Ba^{2+} -blocked PTs swollen by hypotonic conditions is blocked by 1-mmol/L furosemide.⁶⁷ Cell swelling in response to apical Na^+ absorption is postulated to activate a volume-sensitive basolateral KCC, which participates in transepithelial absorption of $\text{Na}^+\text{-Cl}^-$.¹⁴ Notably, targeted deletion of *Kcc3* and *Kcc4* in the respective knockout mice reduces VRD in the PT.⁷² Furthermore, perfused PTs from KCC3-deficient mice have a considerable reduction in transepithelial fluid transport, suggesting an important role for basolateral $\text{K}^+\text{-Cl}^-$ cotransport in transcellular $\text{Na}^+\text{-Cl}^-$ reabsorption.⁷³

The basolateral chloride conductance of mammalian proximal tubular cells is relatively low, suggesting a lesser role for Cl^- channels in transepithelial $\text{Na}^+\text{-Cl}^-$ transport. Basolateral anion substitutions have minimal effect on the membrane potential, despite considerable effects on intracellular Cl^- activity, nor for that matter do changes in basolateral membrane potential affect intracellular Cl^- .^{69,70,74} However, as with basolateral $\text{K}^+\text{-Cl}^-$ cotransport, basolateral Cl^- channels in the PT may be relatively inactive in the absence of cell swelling. Cell swelling thus activates both K^+ and Cl^- channels at the basolateral membranes of proximal tubular cells.^{14,75,76} Seki and associates have reported the presence of a basolateral Cl^- channel in S3 segments of the rabbit nephron, wherein they did not see an effect of the KCC inhibitor H74 on intracellular Cl^- activity.⁷⁷ The molecular identity of these and other basolateral Cl^- channels in the proximal nephron is not known with certainty, although S3 segments have been shown to express messenger RNA (mRNA) exclusively for the swelling-activated Cl^- channel; the role of this channel in transcellular $\text{Na}^+\text{-Cl}^-$ reabsorption is not as yet clear.⁷⁸

Finally, there is functional evidence for Na^+ -dependent and Na^+ -independent Cl^- - HCO_3^- exchange at the basolateral

membrane of proximal tubular cells.^{13,74,79} The impact of Na^+ -independent Cl^- - HCO_3^- exchange on basolateral exit is thought to be minimal.⁷⁴ First, this exchanger is expected to mediate Cl^- entry under physiologic conditions.⁷⁹ Second, there is only a modest difference between the rate of decrease in intracellular Cl^- activity and the combined removal of Na^+ and Cl^- versus Cl^- and HCO_3^- , suggesting that pure Cl^- - HCO_3^- exchange does not contribute significantly to Cl^- exit. By contrast, there is a 75% reduction in the rate of decrease in intracellular Cl^- activity after the removal of basolateral Na^+ .⁷⁴ The Na^+ -dependent Cl^- - HCO_3^- exchanger may thus play a considerable role in basolateral Cl^- exit, with recycled exit of Na^+ and HCO_3^- via the basolateral $\text{Na}^+\text{-HCO}_3^-$ cotransporter NBC1 (Fig. 6.5). The molecular identity of this proximal tubular Na^+ -dependent Cl^- - HCO_3^- exchanger is not as yet known.

REGULATION OF PROXIMAL TUBULAR $\text{Na}^+\text{-Cl}^-$ TRANSPORT

Glomerulotubular Balance

A fundamental property of the kidney is the phenomenon of glomerulotubular balance, wherein changes in the GFR are offset by changes in tubular reabsorption, thus maintaining a constant fractional reabsorption of fluid and $\text{Na}^+\text{-Cl}^-$ (Fig. 6.6). Although the distal nephron is capable of adjusting reabsorption in response to changes in tubular flow, the impact of GFR on $\text{Na}^+\text{-Cl}^-$ reabsorption by the PT is particularly pronounced (Fig. 6.7).⁸⁰ Glomerulotubular balance is independent of direct neuronal and systemic hormonal control, and is thought to be mediated by the additive effects of luminal and peritubular factors.⁸¹

Until recently, there was some controversy regarding the role of luminal factors in glomerulotubular balance because experiments performed using isolated rabbit PTs failed to demonstrate a significant effect of tubular flow on fluid absorption.⁸² This issue has largely been resolved, however,

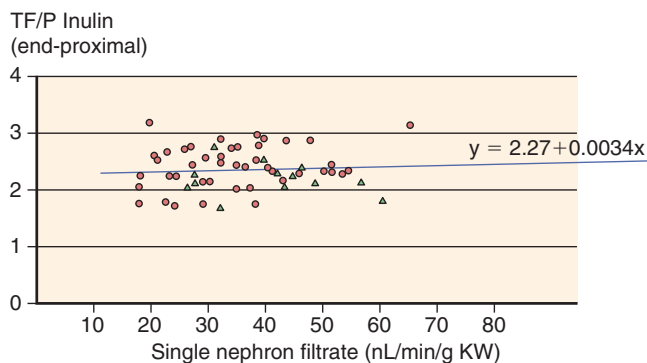


Fig. 6.6 Glomerulotubular balance. The tubular fluid-to-plasma ratio of the nonreabsorbable marker, inulin (TF/P inulin), at the end of the proximal tubule, which is used as a measure of fractional water absorption by the proximal tubule, does not change as a function of single-nephron glomerular filtration rate. Measurements were done during antidiuresis (triangles) and water diuresis (circles). (From Schnermann J, Wahl M, Liebau G, Fischbach H. Balance between tubular flow rate and net fluid reabsorption in the proximal convolution of the rat kidney. I. Dependency of reabsorptive net fluid flux upon proximal tubular surface area at spontaneous variations of filtration rate. *Pflügers Arch.* 1968;304:90–103.)

with clear evidence that fluid shear stress (FSS) increases solute and water absorption.⁸³ Du and coworkers reported linear flow dependence of fluid and HCO_3^- transport in isolated perfused murine PTs (Fig. 6.8),^{81,84} mediated by NHE3 and the H^+ -ATPase, as discussed later. These data were analyzed using a mathematical model that estimated microvillus torque as a function of tubular flow; accounting for increases in tubular diameter, which reduce torque, there is a linear relationship between calculated torque and fluid and HCO_3^- absorption.^{81,84} Consistent with an effect of torque rather than flow per se, increasing viscosity of the perfusate by the addition of dextran increases the effect on fluid transport; the extra viscosity increases the hydrodynamic effect of flow and thus increases torque. The mathematical analysis of Du and associates provides an excellent explanation of the discrepancy between their results and those of Burg and Orloff.⁸² Whereas Burg and Orloff performed their

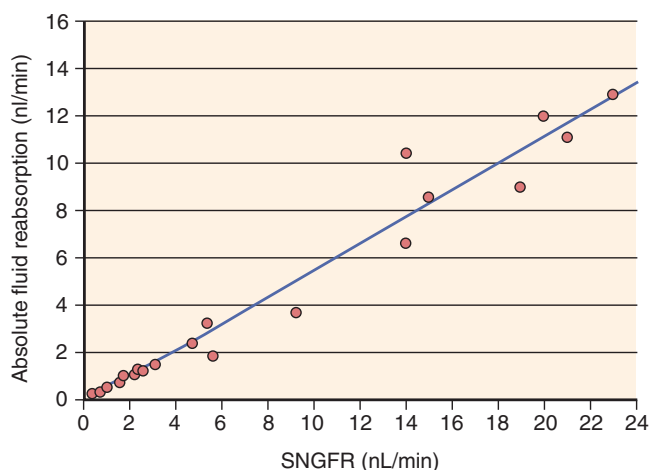


Fig. 6.7 Glomerulotubular balance. Shown is the linear increase in absolute fluid reabsorption by the late proximal tubule as a function of single-nephron glomerular filtration rate (SNGFR). (From Spitzer A, Brandis M. Functional and morphologic maturation of the superficial nephrons. Relationship to total kidney function. *J Clin Invest.* 1974;53: 279–287.)

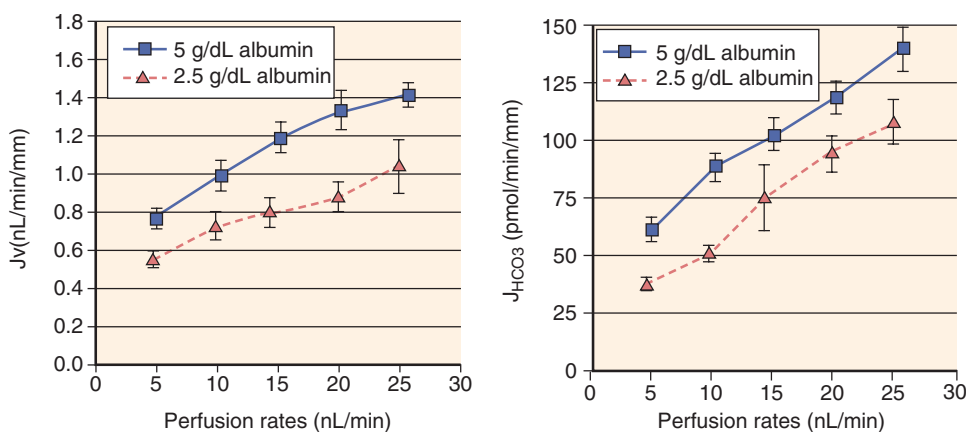


Fig. 6.8 Glomerulotubular balance; flow-dependent increases in fluid (J_v) and HCO_3^- (J_{HCO_3}) absorption by perfused mouse proximal tubules. Absorption also increases when bath albumin concentration increases from 2.5 to 5 g/dL. (From Du Z, Yan Q, Duan Y, et al. Axial flow modulates proximal tubule NHE3 and H-ATPase activities by changing microvillus bending moments. *Am J Physiol Renal Physiol.* 2006;290:F289–F296.)

experiments in rabbits, the more recent report used mice; other studies that had found an effect of flow used perfusion of rat PTs, presumably more similar to mouse than rabbit.^{80–82,84} Increased flow has a considerably greater effect on tubular diameter in the rabbit PT, thus reducing the increase in torque. Mathematical analysis of the rabbit data thus predicts a 43% increase in torque due to a 41% increase in tubule diameter at a threefold increase in flow; this corresponds to the statistically insignificant 36% increase in volume reabsorption reported by Burg and Orloff.⁸²

Pharmacologic inhibition reveals that tubular flow activates proximal HCO_3^- reabsorption mediated by NHE3 and apical H^+ -ATPase.⁸¹ The flow-dependent increase in proximal fluid and HCO_3^- reabsorption is also attenuated in NHE3-deficient knockout mice.^{81,84} Inhibition of the actin cytoskeleton with cytochalasin D reduces the effect of flow on fluid and HCO_3^- transport. This maneuver blocked the effects of flow on NHE3 and Na^+/K^+ -ATPase, but not on H^+ -ATPase. It also blocks the effects of FSS on movement of these transporters to the plasma membranes, suggesting that flow-dependent movement of microvilli activates these transport proteins via their linkage to the cytoskeleton (see Fig. 6.12 for NHE3).⁸⁵ FSS induces densely distributed peripheral actin bands and increases the formation of tight junctions and adherens junctions in cultured tubule cells; this junctional buttressing is hypothesized to maximize flow-activated transcellular salt and water absorption.⁸⁶

The roles of dopamine, angiotensin II (Ang II), and calcium on FSS-induced sodium and bicarbonate transport have been examined. Luminal dopamine completely inhibited the flow-induced increase in Na^+ transport,⁸³ with the major effects being mediated through the D_{1A} receptor. Deletion of AT_{1A} receptors in mice also abrogated flow-induced increments in Na^+ transport,⁸⁷ but these effects may be related to the profound basal reductions in NHE3 activity. When AT_1 receptor blockers are employed, flow-induced Na^+ transport remained.^{87,88} Intracellular activation of IP₃ through a local calcium signal may mediate the effects of flow on NHE3 activity, although increased calcium influx does not appear to play a role.⁸⁹ Flow and torque were not found to have any effects on chloride absorption, suggesting no convective flow of chloride through the paracellular pathway.

Another mechanism for glomerulotubular balance operating from the luminal side involves limiting solute concentration. Solutes, such as bicarbonate, amino acids, and glucose, that are reabsorbed coupled to sodium will be depleted earlier along the PT when flow is low, thereby limiting reabsorption rates along the segment as a whole.⁹⁰

Peritubular factors also play an important additive role in glomerulotubular balance, perhaps accounting for the difficulties in documenting flow-induced alterations using isolated rabbit PTs. Specifically, increases in GFR result in an increase in filtration fraction and an attendant increase in postglomerular protein and peritubular oncotic pressure. It has long been appreciated that changes in peritubular protein concentration have important effects on proximal tubular $\text{Na}^+\text{-Cl}^-$ reabsorption; these effects are also seen in combined capillary and tubular perfusion experiments.^{81,91} Peritubular protein also has an effect in isolated perfused PT segments, where the effect of hydrostatic pressure is abolished.⁸¹ Increases in peritubular protein concentration have an additive effect on the flow-dependent activation of proximal fluid and HCO_3^- absorption (Fig. 6.8). The effect of peritubular protein on HCO_3^- absorption, which is a predominantly transcellular phenomenon, suggests that changes in peritubular oncotic pressure do not affect transport

via the paracellular pathway.¹⁴ However, the mechanism of the stimulatory effect of peritubular protein on transcellular transport is still not completely clear.⁸¹ There are also changes in absorption that correlate with changes in peritubular hydrostatic pressure, as occurs during expansion or contraction of the extracellular fluid volume.⁹¹

Neurohumoral Influences

Fluid and $\text{Na}^+\text{-Cl}^-$ reabsorption by the PT are affected by a number of hormones and neurotransmitters. The major hormonal influences on renal $\text{Na}^+\text{-Cl}^-$ transport are shown in Fig. 6.9. Renal sympathetic tone exerts a particularly important stimulatory influence, as does Ang II; dopamine is a major inhibitor of proximal tubular $\text{Na}^+\text{-Cl}^-$ reabsorption.

Unilateral denervation of the rat kidney causes a marked natriuresis and a 40% reduction in proximal $\text{Na}^+\text{-Cl}^-$ reabsorption, without effects on single-nephron GFR or on the contralateral innervated kidney.⁹² By contrast, low-frequency electrical stimulation of renal sympathetic nerves increases proximal tubular fluid absorption, with a 32% drop in natriuresis and no change in GFR.⁹³ Basolateral epinephrine and/or norepinephrine stimulate proximal $\text{Na}^+\text{-Cl}^-$ reabsorption via both α - and β -adrenergic receptors. Several lines of evidence suggest that α_1 -adrenergic receptors exert a

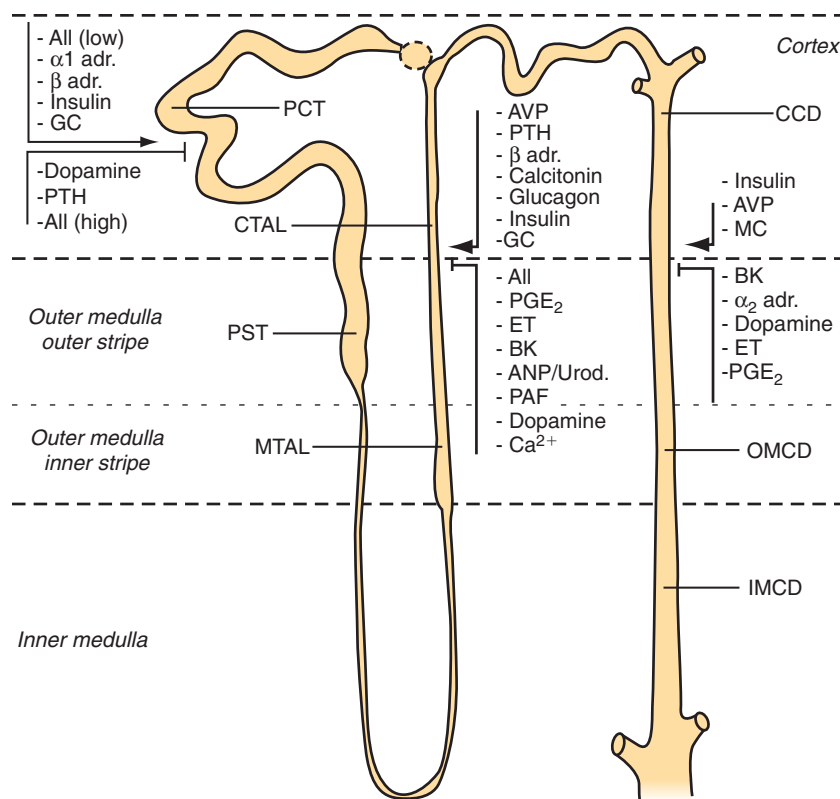


Fig. 6.9 Neurohumoral influences on $\text{Na}^+\text{-Cl}^-$ absorption by the proximal tubule, thick ascending limb, and collecting duct. Factors that stimulate (\rightarrow) and inhibit (\leftarrow) sodium reabsorption are as follows: *ANG II*, Angiotensin II (low and high referring to picomolar and micromolar concentrations, respectively); *ANP/Urod*, atrial natriuretic peptide and urodilatin; *AVP*, arginine vasopressin; *BK*, bradykinin; *CCD*, cortical collecting duct; *cTAL*, cortical thick ascending limb; *ET*, endothelin; *GC*, glucocorticoids; *IMCD*, inner medullary collecting duct; *MC*, mineralocorticoids; *mTAL*, medullary thick ascending limb of the loop of Henle; *OMCD*, outer medullary collecting duct; *PAF*, platelet-activating factor; *PCT*, proximal convoluted tubule; *PGE₂*, prostaglandin E₂; *PST*, proximal straight tubule; *PTH*, parathyroid hormone; α_1 *adr*, α_1 -adrenergic agonist; β *adr*, β -adrenergic agonist. (From Feraille E, Doucet A. Sodium-potassium-adenosine triphosphatase-dependent sodium transport in the kidney: hormonal control. *Physiol Rev.* 2001;81:345–418.)

stimulatory effect on proximal $\text{Na}^+\text{-Cl}^-$ transport via activation of basolateral $\text{Na}^+\text{-K}^+\text{-ATPase}$ and apical $\text{Na}^+\text{-H}^+$ exchange; the role of α_2 -adrenergic receptors is more controversial.⁹⁴ Ligand-dependent recruitment of the scaffolding protein NHE regulatory factor-1 (NHERF-1) by β_2 -adrenergic receptors results in direct activation of apical NHE3, bypassing the otherwise negative effect of downstream cyclic adenosine monophosphate (cAMP; see later).^{95,96} Ang II has potent effects on proximal $\text{Na}^+\text{-Cl}^-$ reabsorption and therefore on blood pressure. Genetic deletion of $\text{AT}_{1\text{A}}$ receptors from PT cells reduced proximal fluid reabsorption, lowered basal blood pressure, shifted the pressure natriuresis, and attenuated the hypertensive response to Ang II infused chronically.⁹⁶ Although basal abundances of NHE3 and $\text{NaPi}2$ were similar in PTs from control and knockout mice, the abundance of NHE3 and $\text{NaPi}2$ was lower following Ang II infusion in mice lacking $\text{AT}_{1\text{A}}$, suggesting that these effects are mediated, at least in part, through these two prominent Na^+ transport pathways.

Despite this clear stimulatory effect, it has also been appreciated for 3 decades that Ang II has a bimodal (sometimes called “biphasic”) effect on the PT Na^+ transport in rats, rabbits, and mice; stimulation of $\text{Na}^+\text{-Cl}^-$ reabsorption occurs at 10^{-12} to 10^{-10} M, whereas inhibition of $\text{Na}^+\text{-Cl}^-$ reabsorption occurs at concentrations greater than 10^{-7} M (Fig. 6.10).⁹⁷ Note, however, that plasma Ang II concentrations typically do not exceed 10^{-9} M, even during pathological states, such as 2 kidney/1 clip Goldblatt hypertension.⁹⁸ Furthermore, this biphasic role of Ang II may not hold true for all species, and in human PT samples, obtained during nephrectomy, concentrations up to 10^{-6} M Ang II stimulate $\text{Na}^+\text{-Cl}^-$ reabsorption, primarily owing to a stimulatory effect of the nitric oxide (NO)–cyclic guanosine monophosphate

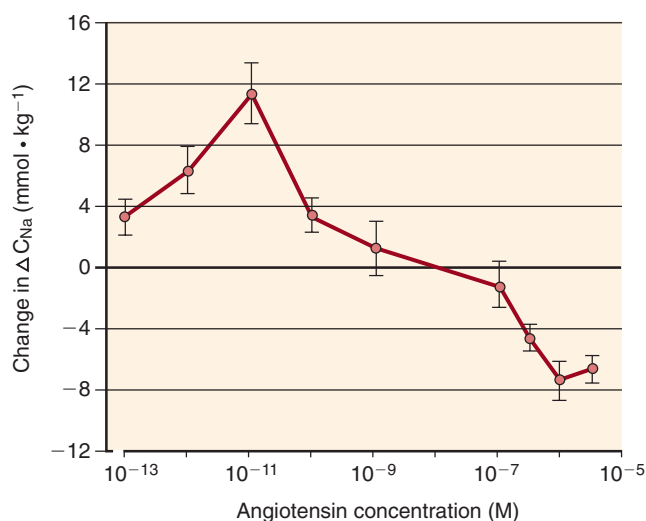


Fig. 6.10 Biphasic effect of angiotensin II (Ang II) on Na^+ reabsorption in microperfused proximal tubules. The steady-state transepithelial Na^+ concentration gradient (peritubular-luminal), ΔC_{Na} , that developed in a stationary split droplet is used as an indication of the rate of active Na^+ reabsorption. This is plotted as a function of peritubular Ang II concentration; low concentrations activate Na^+ absorption by the proximal tubule, whereas higher concentrations inhibit it. (From Harris PJ, Navar LG. Tubular transport responses to angiotensin. *Am J Physiol.* 1985;248:F621–F630)

(cGMP) pathway on extracellular signal-regulated kinase (ERK) phosphorylation.⁹⁹ Although the plasma Ang II concentration is typically below the inhibitory concentration, it should be noted, as discussed further later, that the concentration of Ang II in the lumen of the PT frequently exceeds that in plasma, and thus plasma concentrations may not be the sole determining factor. Given the substantial effects of proximal $\text{AT}_{1\text{A}}$ receptor deletion to reduce blood pressure and shift the pressure natriuresis,⁹⁶ it seems likely that the predominant effect of Ang II is stimulatory along the PT under most physiological conditions.

Further complexity of Ang II signaling arises from the presence of AT_1 receptors at both the luminal and basolateral membranes in the PT.¹⁰⁰ Ang II application to the luminal or peritubular side of perfused tubules has a similar bimodal effect on fluid transport, albeit with more potent effects at the luminal side.¹⁰¹ Traditionally, experiments using receptor antagonists and knockout mice have indicated that the stimulatory and inhibitory effects of Ang II are both mediated via AT_1 receptors due to signaling at the luminal and basolateral membranes.¹⁰² However, other work has identified that AT_2 receptors working through NO-cGMP pathway are able to downregulate NHE3 and $\text{Na}^+\text{-K}^+\text{-ATPase}$, leading to natriuresis and reduced blood pressure.¹⁰³ Finally, Ang II is also synthesized and secreted by the PT, exerting a potent autocrine effect on proximal tubular $\text{Na}^+\text{-Cl}^-$ reabsorption.¹⁰⁴ Proximal tubular cells thus express mRNA for angiotensinogen, renin, and angiotensin-converting enzyme (ACE),⁹⁴ allowing for the autocrine generation of Ang II. Indeed, luminal concentrations of Ang II can be 100- to 1000-fold higher than circulating levels of the hormone.⁹⁴ Proximal tubular and systemic synthesis of Ang II may be subject to different control. In fact, intrarenal Ang II appears to stimulate proximal $\text{Na}^+\text{-Cl}^-$ and fluid reabsorption even when dietary salt intake is high, thereby helping to prevent rises in glomerular filtration from increasing late proximal flow.¹⁰⁵ It should be recalled, however, that in this, as in many salt loading studies in rodents, animals received 1% saline as drinking solution. Thus the high salt load was accompanied by free water deprivation, a circumstance shown recently to lead to stress and inflammation.¹⁰⁶

The PT is also a target for natriuretic hormones; in particular, dopamine synthesized in the PT has negative autocrine effects on proximal $\text{Na}^+\text{-Cl}^-$ reabsorption.⁹⁴ Proximal tubular cells have the requisite enzymatic machinery for the synthesis of dopamine, using L-dopa reabsorbed from the glomerular ultrafiltrate. Dopamine synthesis by proximal tubular cells and release into the tubular lumen are increased after volume expansion or a high-salt diet, resulting in a considerable natriuresis.^{107,108} Luminal dopamine antagonizes the stimulatory effect of epinephrine on volume absorption in perfused PCTs, consistent with an autocrine effect of dopamine released into the tubular lumen.^{107,109} Dopamine primarily exerts its natriuretic effect via D_1 -like dopamine receptors (D_1 and D_5 in humans); as is the case for the AT_1 receptors for Ang II, D_1 receptors are expressed at the apical and luminal membranes of PTs.^{100,110} Targeted deletion of the $\text{D}_{1\text{A}}$ and D_5 receptors in mice leads to hypertension by mechanisms that include reduced proximal tubular natriuresis.^{111,112} The proximal tubular-specific deletion of aromatic amino acid decarboxylase, which produces dopamine, generates mice that are a vivid demonstration of the role of intrarenal

dopamine. This intrarenal dopamine deficiency leads to upregulation of sodium transporters along the nephron, upregulation of the intrarenal renin–angiotensin axis, decreased natriuresis in response to L-dopa, and reduced medullary cyclooxygenase-2 (COX-2) expression, with reduced urinary prostaglandin levels. These mice also exhibit salt-sensitive hypertension and ultimately a significantly shorter life span compared with wild type mice.¹¹³

The natriuretic effect of dopamine in the PT is modulated by atrial natriuretic peptide (ANP), which inhibits apical $\text{Na}^+\text{-H}^+$ exchange via a dopamine-dependent mechanism.¹⁴ ANP appears to induce recruitment of the D_1 dopamine receptor to the plasma membrane of proximal tubular cells, thus sensitizing the tubule to the effect of dopamine.¹¹⁴ The inhibitory effect of ANP on basolateral $\text{Na}^+\text{-K}^+\text{-ATPase}$ occurs via a D_1 -dependent mechanism, with a synergistic inhibition of $\text{Na}^+\text{-K}^+\text{-ATPase}$ by the two hormones.¹¹⁴ Furthermore, dopamine and D_1 receptors appear to play critical permissive roles in the *in vivo* natriuretic effect of ANP.¹⁴

Finally, there is considerable crosstalk between the major antinatriuretic and natriuretic influences on the PT. For example, ANP inhibits Ang II–dependent stimulation of proximal tubular fluid absorption, presumably via the dopamine-dependent mechanisms discussed earlier.^{14,115} Dopamine also decreases the expression of AT_1 receptors for Ang II in cultured proximal tubular cells.¹¹⁶ Furthermore, the provision of L-dopa in the drinking water of rats decreases AT_1 receptor expression in the PT, suggesting that dopamine synthesis in the PT resets the sensitivity to Ang II.¹¹⁶ Ang II signaling through AT_1 receptors decreases expression of the D_5 dopamine receptor, whereas renal cortical expression of AT_1 receptors is in turn increased in knockout mice deficient in the D_5 receptor.¹¹⁷ Similar interactions have been found between proximal tubular AT_1 receptors and the D_2 -like D_3 receptor.¹¹⁸

Regulation of Proximal Tubular Transporters

The apical $\text{Na}^+\text{-H}^+$ exchanger NHE3 and the basolateral $\text{Na}^+\text{-K}^+\text{-ATPase}$ are primary targets for signaling pathways elicited by the various antinatriuretic and natriuretic stimuli discussed earlier; NHE3 mediates the rate-limiting step in transepithelial $\text{Na}^+\text{-Cl}^-$ absorption and, as such, is the dominant target for regulatory pathways.⁸⁴ NHE3 is regulated by the combined effects of direct phosphorylation and dynamic, carboxyl-terminal interaction with scaffolding proteins and signal transduction proteins, which primarily regulate transport via changes in trafficking of the exchanger protein to and from the brush border membrane (Fig. 6.11).^{40,119} Basal activity of the exchanger is also dependent on carboxyl-terminal binding of casein kinase 2 (CK2); phosphorylation of serine 719 by CK2 contributes significantly to the transport activity of NHE3 by modulating membrane trafficking of the transport protein.¹²⁰

Increases in cAMP have a profound inhibitory effect on apical $\text{Na}^+\text{-H}^+$ exchange in the PT. Intracellular cAMP is increased in response to dopamine signaling via D_1 -like receptors and/or parathyroid hormone (PTH)–dependent signaling via the PTH receptor, whereas Ang II–dependent activation of NHE3 is associated with a reduction in cAMP.¹²¹ PTH is a potent inhibitor of NHE3, presumably so as to promote the distal delivery of $\text{Na}^+\text{-HCO}_3^-$ and an attendant stimulation of distal calcium reabsorption.¹²² The activation of protein kinase A (PKA) by increased cAMP results in direct phosphorylation of NHE3; although several sites in NHE3 are phosphorylated by PKA, the phosphorylation of serine 552 (S552) and 605 (S605) has been specifically implicated in the inhibitory effect of cAMP on $\text{Na}^+\text{-H}^+$ exchange.¹²³ So-called phospho-specific antibodies, which specifically recognize the phosphorylated forms of S552 and S605, have demonstrated dopamine-dependent increases in the phosphorylation of both these serines.¹²⁴ Moreover,

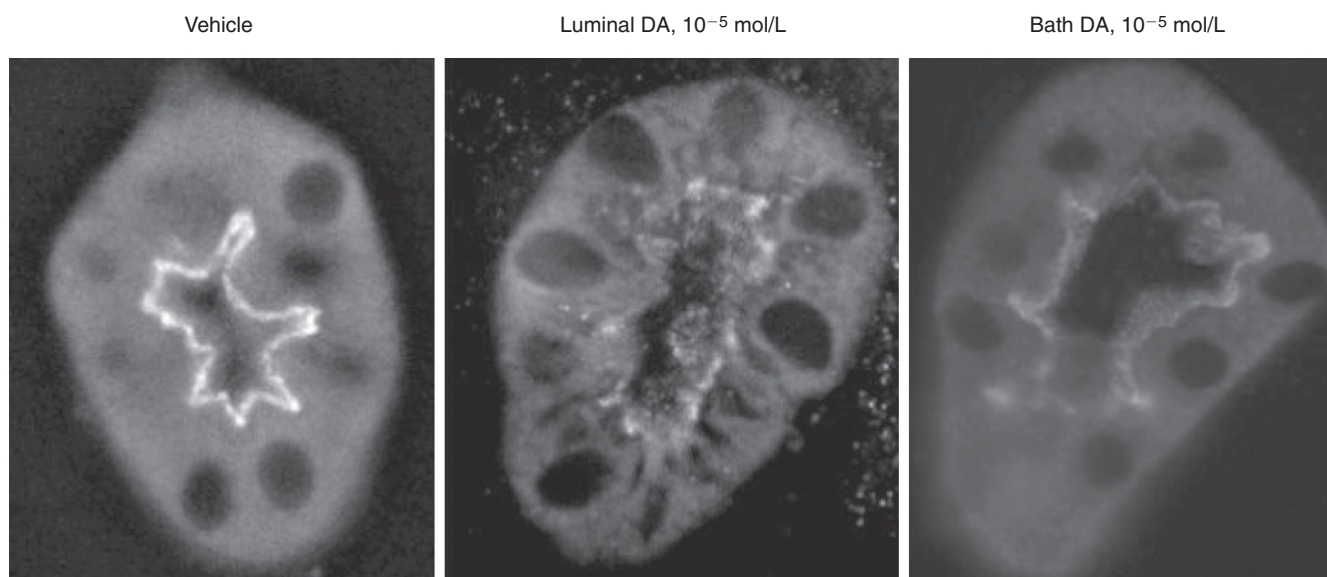


Fig. 6.11 Effect of dopamine on trafficking of the $\text{Na}^+\text{-H}^+$ exchanger NHE3 in the proximal tubule. Microdissected proximal convoluted tubules were perfused for 30 minutes with 10^{-5} mol/L dopamine (DA), in the lumen or the bath, inducing a retraction of immunoreactive NHE3 protein from the apical membrane. (From Bacic D, Kaissling B, McLeroy P, et al. Dopamine acutely decreases apical membrane Na/H exchanger NHE3 protein in mouse renal proximal tubule. *Kidney Int.* 2003;64:2133–2141.)

immunostaining of rat kidney has revealed that S552-phosphorylated NHE3 localizes at the coated pit region of the brush border membrane, where the oligomerized inactive form of NHE3 predominates.^{124,125} The cAMP-stimulated phosphorylation of NHE3 by PKA thus results in a redistribution of the transporter from the microvillar membrane to an inactive submicrovillar population (Fig. 6.11). Notably, however, phosphorylation of these residues appears to be necessary but not sufficient for regulation of NHE3.⁴⁰ A number of regulators of NHE3, including gastrin and uroguanylin, have been found to exert a functional effect through phosphorylation of S552 and/or S605.^{126,127}

The regulation of NHE3 by cAMP also requires the participation of a family of homologous scaffolding proteins that contain protein–protein interaction motifs known as PDZ domains (named for the PSD95, *Drosophila* disc large, and ZO-1 proteins in which these domains were first discovered; Fig. 6.12). The first of these proteins, NHERF-1, was purified as a cellular factor required for the inhibition of NHE3 by PKA.¹²⁸ NHERF-2 was in turn cloned by yeast two-hybrid screens as a protein that interacts with the carboxyl-terminus of NHE3; NHERF-1 and NHERF-2 have very similar effects on the regulation of NHE3 in cultured cells. The related protein PDZK1 interacts with NHE3 and a number of other epithelial transporters and is required for expression of the anion exchanger SLC26A6 at brush border membranes of the PT.⁶⁵

NHERF-1 and NHERF-2 are both expressed in human and mouse PT cells; NHERF-1 colocalizes with NHE3 in microvilli of the brush border, whereas NHERF-2 is predominantly expressed at the base of microvilli in the vesicle-rich

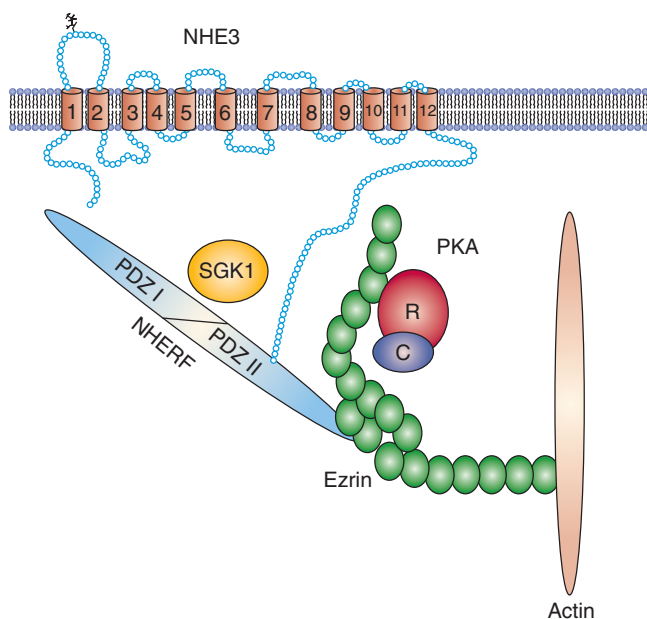


Fig. 6.12 Scaffolding protein NHERF ($\text{Na}^+\text{-H}^+$ exchanger regulatory factor) links the $\text{Na}^+\text{-H}^+$ exchanger NHE3 to the cytoskeleton and signaling proteins. NHERF binds to ezrin, which in turn links to protein kinase A (PKA) and the actin cytoskeleton. NHERF also binds to SGK1 (serum- and glucocorticoid-regulated kinase 1), which activates NHE3. C, Catalytic; PDZ, domain named for the PSD95, *Drosophila* disc large (*Drosophila*), and ZO-1 proteins; R, regulatory.

domain.¹²⁸ The NHERFs assemble a multiprotein, dynamically regulated signaling complex that includes NHE3 and several other transport proteins. In addition to NHE3, they bind to the actin-associated protein, ezrin, thus linking NHE3 to the cytoskeleton; this linkage to the cytoskeleton may be particularly important for the mechanical activation of NHE3 by microvillar bending, as has been implicated in glomerulotubular balance (see earlier discussion).^{81,84,128} Ezrin also interacts directly with NHE3, binding to a separate binding site within the carboxyl-terminus of the transport protein.¹¹⁹ Ezrin functions as an anchoring protein for PKA, bringing PKA into close proximity with NHE3 and facilitating its phosphorylation (Fig. 6.12).¹²⁸ Analysis of knockout mice for *Nherf-1* has revealed that it is not required for baseline activity of NHE3; as expected, however, it is required for cAMP-dependent regulation of the exchanger by PTH.¹²⁸ One long-standing paradox has been that β -adrenergic receptors, which increase cAMP in the PT, cause an activation of apical $\text{Na}^+\text{-H}^+$ exchange.⁹⁴ This was resolved by the observation that the first PDZ domain of NHERF-1 interacts with the β_2 -adrenergic receptor in an agonist-dependent fashion; this interaction serves to disrupt the interaction between the second PDZ domain and NHE3, resulting in a stimulation of the exchanger, despite the catecholamine-dependent increase in cAMP.¹²⁸

As discussed earlier, at concentrations higher than 10^{-7} M (Fig. 6.10), Ang II has an inhibitory effect on proximal tubular $\text{Na}^+\text{-Cl}^-$ absorption.⁹⁷ This inhibition is dependent on the activation of brush border phospholipase A_2 (PLA₂), which results in the liberation of arachidonic acid.¹⁰¹ Metabolism of arachidonic acid by cytochrome P450 monooxygenases, in turn, generates 20-hydroxyeicosatetraenoic acid (20-HETE) and epoxyeicosatrienoic acids (EETs), compounds that inhibit NHE3 and the basolateral $\text{Na}^+\text{-K}^+\text{-ATPase}$.^{94,129} EETs and 20-HETE have also been implicated in the reduction in proximal $\text{Na}^+\text{-Cl}^-$ absorption that occurs during pressure natriuresis, inhibiting $\text{Na}^+\text{-K}^+\text{-ATPase}$ and retracting NHE3 from the brush border membrane.¹³⁰

Antinatriuretic stimuli such as Ang II acutely increase the expression of NHE3 at the apical membrane, at least in part by inhibiting the generation of cAMP.¹²¹ Low-dose Ang II 0.1 nmol/L (10^{-10} M) also increases exocytic insertion of NHE3 into the plasma membrane via a mechanism that is dependent on phosphatidylinositol-3-kinase (PI3K).¹³¹ Treatment of rats with captopril thus results in a retraction of NHE3 and associated proteins from the brush border of PT cells.¹³² Glucocorticoids also increase NHE3 activity due to transcriptional induction of the *Nhe3* gene and an acute stimulation of exocytosis of the exchanger to the plasma membrane.⁴⁰ Glucocorticoid-dependent exocytosis of NHE3 appears to require NHERF-2, which acts in this context as a scaffolding protein for the glucocorticoid-induced serine-threonine kinase SGK1 (see the “Regulation of $\text{Na}^+\text{-Cl}^-$ Transport in the Connecting Tubule and Cortical Collecting Duct: Aldosterone” section).¹³³ The acute effect of dexamethasone has thus been shown to require direct phosphorylation of serine 663 in the NHE3 protein by SGK1.¹³⁴

Finally, many of the natriuretic and antinatriuretic pathways that influence NHE3 have parallel effects on the basolateral $\text{Na}^+\text{-K}^+\text{-ATPase}$ (see Feraille and Doucet⁹⁴ for a detailed review). The molecular mechanisms underlying inhibition of $\text{Na}^+\text{-K}^+\text{-ATPase}$ by dopamine have been particularly well characterized.

Inhibition by dopamine is associated with removal of active $\text{Na}^+\text{-K}^+\text{-ATPase}$ units from the basolateral membrane, somewhat analogous to the effect on NHE3 expression at the apical membrane.¹³⁵ This inhibitory effect is primarily mediated by protein kinase C (PKC), which directly phosphorylates the α_1 -subunit of $\text{Na}^+\text{-K}^+\text{-ATPase}$, the predominant α -subunit in the kidney.⁹⁴ The effect of dopamine requires phosphorylation of serine 18 of the α_1 -subunit by PKC; this phosphorylation does not affect enzymatic activity of the $\text{Na}^+\text{-K}^+\text{-ATPase}$, but rather induces a conformational change that enhances the binding of PI3K to an adjacent, proline-rich domain. The PI3K recruited by this phosphorylated α_1 -subunit then stimulates the dynamin-dependent endocytosis of the $\text{Na}^+\text{-K}^+\text{-ATPase}$ complex via clathrin-coated pits.¹³⁵

LOOP OF HENLE

The loop of Henle encompasses the thin descending limb, thin ascending limb, and TAL. The descending and ascending thin limbs function in passive absorption of water and $\text{Na}^+\text{-Cl}^-$, respectively, whereas the TAL reabsorbs about 30% of filtered $\text{Na}^+\text{-Cl}^-$ via active transport.^{136,137} There is considerable cellular and functional heterogeneity along the entire length of the loop of Henle, with consequences for the transport of water, $\text{Na}^+\text{-Cl}^-$, and other solutes. The thin descending limb begins in the outer medulla after an abrupt transition from S3 segments of the PT, marking the boundary between the outer and inner stripes of the outer medulla. Thin descending limbs end at a hairpin turn at the end of the loop of Henle. Short-looped nephrons that originate from superficial and midcortical nephrons have a short descending limb within the inner stripe of the outer medulla; these tubules merge abruptly into the TAL close to the hairpin turn of the loop (see also discussion later). Long-looped nephrons originating from juxtamedullary glomeruli have a long ascending thin limb that then merges with the TAL. The TALs of long-looped nephrons begin at the boundary between the inner and outer medulla, whereas the TALs of short-looped nephrons may be entirely cortical. The ratio of medullary to cortical TAL for a given nephron is a function of the depth of its origin, such that superficial nephrons are primarily composed of cortical TALs, whereas juxtamedullary nephrons primarily possess medullary TALs.

The TAL begins abruptly after the thin ascending limb of long-looped nephrons and after the aquaporin-negative segment of short-limbed nephrons.¹³⁸ The TAL extends into the renal cortex, where it meets its parent glomerulus at the vascular pole; the plaque of cells at this junction form the macula densa, which function as the tubular sensor for tubuloglomerular feedback (TGF) and tubular regulation of renin release by the juxtaglomerular apparatus. Cells in the medullary TAL are 7 to 8 μm in height, with extensive invaginations of the basolateral plasma membrane and interdigitations between adjacent cells.⁶ As in the PT, these lateral cell processes contain numerous elongated mitochondria, perpendicular to the basement membrane. Cells in the cortical TAL are considerably shorter, 2 μm in height at the end of the cortical TAL in rabbits, with fewer mitochondria and a simpler basolateral membrane.⁶ Macula densa cells also lack the lateral cell processes and interdigitations characteristic of medullary TAL cells.⁶ However, scanning electron microscopy has revealed that the TAL of rat and

hamster contains two morphologic subtypes, a rough-surfaced cell type (R cells) with prominent apical microvilli and a smooth-surfaced cell type (S cells) with an abundance of subapical vesicles.^{6,139–141} In the hamster TAL, cells can also be separated into those with high apical and low basolateral K^+ conductance and weak basolateral Cl^- conductance (LBC cells) versus a second population with low apical and high basolateral K^+ conductance combined with high basolateral Cl^- conductance (HBC).^{140,142} The relative frequency of the morphologic and functional subtypes in the cortical and medullary TAL suggests that HBC cells correspond to S cells and LBC cells to R cells.¹⁴⁰

TRANSPORT CHARACTERISTICS OF THE DESCENDING THIN LIMB

It has long been appreciated that the osmolality of tubular fluid increases progressively between the corticomedullary junction and papillary tip due to active secretion of solutes or passive absorption of water along the descending thin limb.¹⁴³ Subsequent reports have revealed a very high water permeability of perfused outer medullary thin descending limbs in the absence of significant permeability to $\text{Na}^+\text{-Cl}^-$.¹⁴⁴ Notably, however, the permeability properties of descending thin limbs vary as a function of depth in the inner medulla and inclusion in short- versus long-looped nephrons.^{145,146} Descending thin limbs from short-looped nephrons contain type I cells, very flat, endothelial-like cells, with intermediate-depth tight junctions suggesting a relative tight epithelium.^{145,146} The epithelium of descending limbs from long-looped nephrons is initially more complex, with taller type II cells possessing more elaborate apical microvilli and more prominent mitochondria. In the lower medullary portion of long-looped nephrons, these cells change into a type III morphology, endothelial-like cells similar to the type I cells from short-looped nephrons.¹⁴⁵ The permeability properties appear to change as a function of cell type, with a progressive axial drop in water permeability of long-looped descending limbs; the water permeability of descending thin limbs in the middle part of the inner medulla is thus about 42% that of outer medullary thin descending limbs.¹⁴⁷ Furthermore, the distal 20% of descending thin limbs have a very low water permeability.¹⁴⁷ These changes in water permeability along the descending thin limb are accompanied by a progressive increase in $\text{Na}^+\text{-Cl}^-$ permeability, although the ionic permeability remains considerably less than that of the ascending thin limb.¹⁴⁶

Consistent with a primary role in passive water and solute absorption, $\text{Na}^+\text{-K}^+\text{-ATPase}$ activity in the descending thin limb is almost undetectable,¹⁷ suggesting that these cells do not actively transport $\text{Na}^+\text{-Cl}^-$; those ion transport pathways that have been identified in descending thin limb cells are thought to contribute primarily to cellular volume regulation.¹⁴⁸ In contrast to the relative lack of $\text{Na}^+\text{-Cl}^-$ transport, transcellular water reabsorption by the thin descending limb is a critical component of the renal countercurrent concentrating mechanism (see Chapter 10).^{136,144}

$\text{Na}^+\text{-Cl}^-$ TRANSPORT BY THE THIN ASCENDING LIMB

Fluid entering the thin ascending limb has a very high concentration of $\text{Na}^+\text{-Cl}^-$ due to osmotic equilibration by the water-permeable descending limbs. The passive reabsorption of this delivered $\text{Na}^+\text{-Cl}^-$ by the thin ascending limb is a

critical component of the passive equilibration model of the renal countercurrent multiplication system (see Chapter 10). Consistent with this role, the permeability properties of the thin ascending limb are dramatically different from those of the descending thin limb, with a much higher permeability to $\text{Na}^+\text{-Cl}^-$ and vanishingly low water permeability.^{146,149} Passive $\text{Na}^+\text{-Cl}^-$ reabsorption by thin ascending limbs occurs via a combination of paracellular Na^+ transport and transcellular Cl^- transport.^{137,142,150–153} The inhibition of paracellular conductance by protamine thus selectively inhibits Na^+ transport across perfused thin ascending limbs, consistent with paracellular transport of Na^+ .¹⁵⁰ As in the descending limb, thin ascending limbs have a modest $\text{Na}^+\text{-K}^+\text{-ATPase}$ activity (Fig. 6.3); however, the active transport of Na^+ across thin ascending limbs accounts for only an estimated 2% of Na^+ reabsorption by this nephron segment.¹⁵⁴ Chloride channel blockers reduce Cl^- permeability of the thin ascending limb, consistent with passive transcellular Cl^- transport.¹⁵³ Direct measurement of the membrane potential of impaled hamster thin ascending limbs has also yielded evidence for apical and basolateral Cl^- channel activity.¹⁴² This transepithelial transport of Cl^- , but not Na^+ , is activated by vasopressin, with a pharmacologic profile that is consistent with direct activation of thin ascending limb Cl^- channels.¹⁵⁵

Both apical and basolateral Cl^- transport in the thin ascending limb appear to be mediated by the CLC-K1 Cl^- channel in cooperation with the Barttin subunit (see also the “ $\text{Na}^+\text{-Cl}^-$ Transport by the Thick Ascending Limb: Basolateral Mechanisms” section). Immunofluorescence and in situ hybridization indicate a selective expression of CLC-K1 (homologous to the human chloride channel Kb , CLC-NKB) in thin ascending limbs, although single-tubule, reverse transcriptase-polymerase chain reaction (RT-PCR) studies

have suggested additional expression in the TAL, DCT, and cortical collecting duct (CCD).^{156–158} Notably, immunofluorescence and immunogold labeling indicate that CLC-K1 is expressed exclusively at both the apical and basolateral membranes of thin ascending limbs, such that both the luminal and basolateral Cl^- channels of this nephron segment are encoded by the same gene.^{142,156} Homozygous knockout mice with a targeted deletion of *Clc-k1* have a vasopressin-resistant nephrogenic diabetes insipidus, reminiscent of the phenotype of aquaporin-1 knockout mice.^{136,159} Given that CLC-K1 is potentially expressed in the TAL, dysfunction of this nephron segment might also contribute to the renal phenotype of *Clc-k1* knockout mice; however, the closely homologous channel CLC-K2 (CLC-NKB) is clearly expressed in the TAL, where it can likely substitute for CLC-K1 .¹⁵⁸ Furthermore, loss-of-function mutations in *CLC-NKB* cause Bartter syndrome, which is phenocopied in *Clc-k2* knockout mice, indicating that CLC-K2 , rather than CLC-K1 , is critical for transport function of the TAL.^{160–162}

Detailed characterization of *Clc-k1* knockout mice has revealed a selective impairment in Cl^- transport by the thin ascending limb.¹³⁷ Whereas Cl^- absorption is profoundly reduced, Na^+ absorption by thin ascending limbs is not significantly impaired (Fig. 6.13). The diffusion voltage induced by a transepithelial $\text{Na}^+\text{-Cl}^-$ gradient is reversed by the absence of CLC-K1 , from +15.5 mV in homozygous wild type controls (+/+) to -7.6 mV in homozygous knockout mice (-/-). This change in diffusion voltage is due to the dominance of paracellular Na^+ transport in the CLC-K1 -deficient -/- mice, leading to a lumen-negative potential; this corresponds to a marked reduction in the relative permeability of Cl^- to that of Na^+ ($P_{\text{Cl}}/P_{\text{Na}}$), from 4.02 to 0.63 (Fig. 6.13). Protamine, an inhibitor of paracellular Na^+ transport, has a comparable effect on

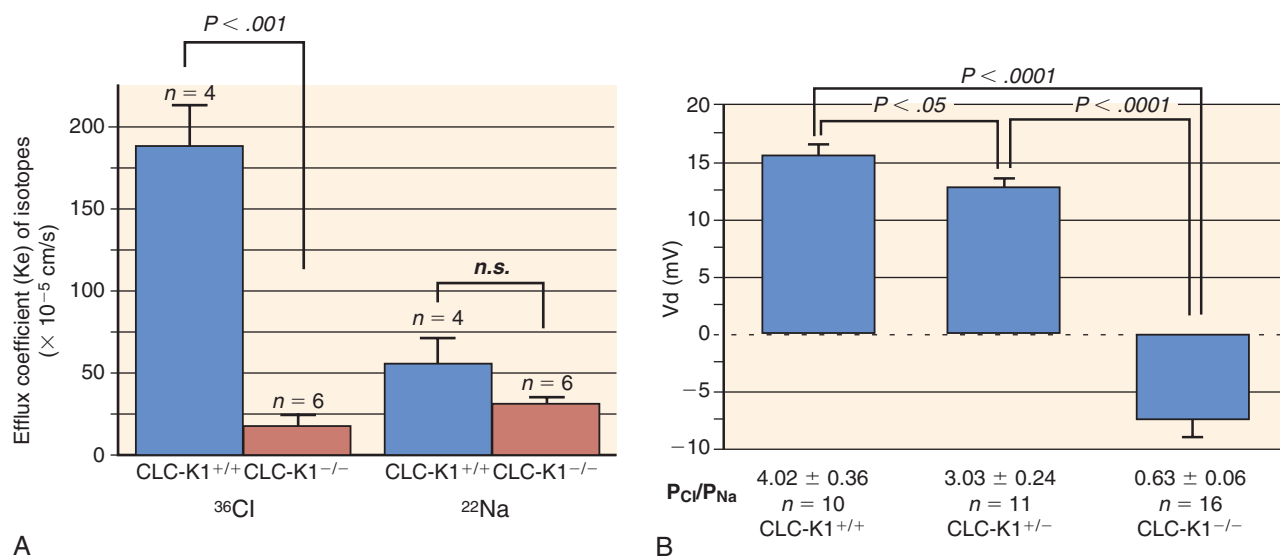


Fig. 6.13 Role of the CLC-K1 chloride channel in Na^+ and Cl^- transport by the thin ascending limbs. Homozygous knockout mice ($\text{CLC-K1}^{-/-}$) are compared with their littermate controls ($\text{CLC-K1}^{+/+}$). (A) Efflux coefficients for $^{36}\text{Cl}^-$ and $^{22}\text{Na}^+$ in the thin ascending limbs. Cl^- absorption is essentially abolished in the knockout mice, whereas there is no significant effect of CLC-K1 deficiency on Na^+ transport. (B) The diffusion voltage (VD), induced by a transepithelial $\text{Na}^+\text{-Cl}^-$ gradient, is reversed by the absence of CLC-K1 , from +15.5 mV in controls to -7.6 mV in homozygous knockout mice. This change in diffusion voltage is due to the dominance of paracellular Na^+ transport in the CLC-K1 -deficient -/- mice, leading to a lumen-negative potential; this corresponds to a marked reduction in the relative permeability of Cl^- to that of Na^+ ($P_{\text{Cl}}/P_{\text{Na}}$), from 4.02 to 0.63. (From Liu W, Morimoto T, Kondo Y, et al. Analysis of NaCl transport in thin ascending limb of the loop of Henle in CLC-K1 null mice. *Am J Physiol Renal Physiol*. 2002;282:F451–F457.)

the diffusion voltage in $-/-$ mice versus $+/-$ and $+/+$ mice that have been treated with 5-nitro-2-(3-phenylpropylamino)-benzoate (NPPB) to inhibit CLC-K1; the respective diffusion voltages are 7.9 mV ($-/-$ plus protamine), 8.6 mV ($+/-$ plus protamine and NPPB), and 9.8 mV ($+/+$ plus protamine and NPPB). Therefore the paracellular Na^+ conductance is unimpaired and essentially the same in *Clc-k1* knockout mice when compared with littermate controls. This study thus provided elegant proof for the relative independence of paracellular and transcellular conductances for Na^+ and Cl^- , respectively, in thin ascending limbs.¹³⁷

CLC-K1 associates with Barttin, an accessory subunit identified via positional cloning of the gene for Bartter syndrome with sensorineural deafness (see the “[Na⁺-Cl⁻ Transport by the Thick Ascending Limb: Basolateral Mechanisms](#)” section).¹⁶³ Barttin is expressed with CLC-K1 in thin ascending limbs, in addition to the TAL, DCT, and α -intercalated cells.^{158,163} Rat CLC-K1 is unique among the CLC-K orthologs and paralogs (CLC-K1/2 in rodents, CLC-NKB/NKA in humans) in that it can generate Cl^- channel activity in the absence of coexpression with Barttin; however, its human ortholog CLC-NKA is nonfunctional in the absence of Barttin.^{156,158,164} Regardless, Barttin coimmunoprecipitates with CLC-K1 and increases expression of the channel protein at the cell membrane.^{158,164} This so-called chaperone function seems to involve the transmembrane core of Barttin, whereas domains within the cytoplasmic carboxy terminus modulate channel properties (open probability and unitary conductance).¹⁶⁴

With respect to regulation in this nephron segment, vasopressin has stimulatory effects on Cl^- transport by the thin ascending limb, acting as in principal cells and TAL through V2 receptors and cAMP.¹⁵⁵ Water deprivation induces a fourfold increase in CLC-K1 mRNA, indicating transcriptional effects of vasopressin or medullary tonicity.¹⁶⁵ Basolateral calcium in turn inhibits Cl^- and Na^+ transport in the thin ascending limb via activation of the calcium-sensing receptor (CaSR).¹⁶⁶

NA⁺-CL⁻ TRANSPORT BY THE THICK ASCENDING LIMB

Apical Na⁺-Cl⁻ Transport

The TAL reabsorbs about 30% of filtered $\text{Na}^+\text{-Cl}^-$ (Fig. 6.1). In addition to an important role in the defense of the extracellular fluid volume, $\text{Na}^+\text{-Cl}^-$ reabsorption by the water-impermeable TAL is a critical component of the renal countercurrent multiplication system. The separation of $\text{Na}^+\text{-Cl}^-$ and water by the TAL is thus responsible for the capability of the kidney to dilute or concentrate the urine. In concert with the countercurrent mechanism, $\text{Na}^+\text{-Cl}^-$ reabsorption by the thin ascending limb and TAL increases medullary tonicity, facilitating water absorption by the collecting duct.

Notwithstanding the morphological heterogeneity described earlier, the cells of the medullary TAL, cortical TAL, and macula densa share the same basic transport mechanisms (Fig. 6.14). $\text{Na}^+\text{-Cl}^-$ reabsorption by the TAL is thus a secondarily active process, driven by the favorable electrochemical gradient for Na^+ established by the basolateral $\text{Na}^+\text{-K}^+\text{-ATPase}$.^{14,167} Na^+ , K^+ , and Cl^- are cotransported across the apical membrane by an electroneutral $\text{Na}^+\text{-K}^+\text{-2Cl}^-$ cotransporter, which generally requires the simultaneous presence of all three ions.¹⁴ Of note, under certain circumstances,

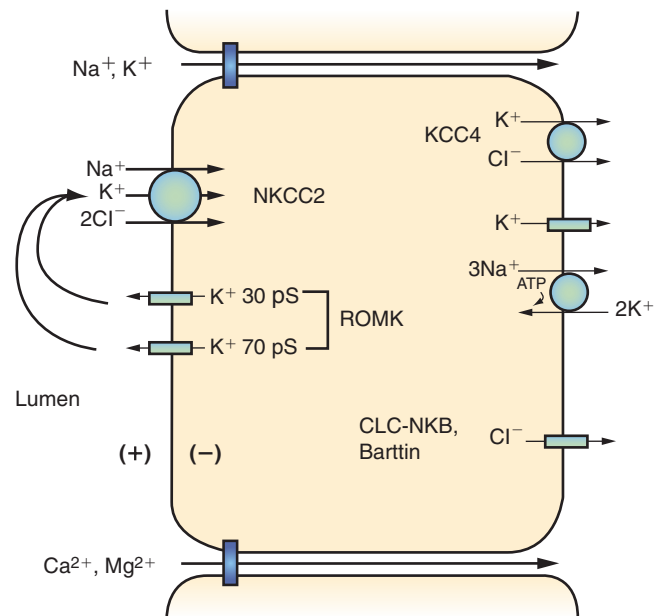


Fig. 6.14 Transepithelial $\text{Na}^+\text{-Cl}^-$ transport pathways in the thick ascending limb. *CLC-K2*, Cl^- channel, Barttin; *KCC4*, $\text{K}^+\text{-Cl}^-$ cotransporter-4; *NKCC2*, $\text{Na}^+\text{-K}^+\text{-2Cl}^-$ cotransporter-2; *ROMK*, renal outer medullary K^+ channel.

apical $\text{Na}^+\text{-Cl}^-$ transport in the TAL appears to be K^+ independent; this issue is reviewed later (see the “[Regulation of Na⁺-Cl⁻ Transport by the Thick Ascending Limb](#)” section). Apical $\text{Na}^+\text{-K}^+\text{-2Cl}^-$ cotransport is mediated by the cation-chloride cotransporter NKCC2, encoded by *SLC12A1*.¹⁶⁸ This is a member of the cation chloride cotransporter family of proteins that includes the thiazide-sensitive transporter NCC, and the potassium chloride cotransporters. Functional expression of NKCC2 in *Xenopus* oocytes yields Cl^- - and Na^+ -dependent uptake of Rb^+ (a radioactive substitute for K^+) and Cl^- - and K^+ -dependent uptake of $^{22}\text{Na}^+$.^{97,168-170} As expected, NKCC2 is sensitive to micromolar concentrations of furosemide, bumetanide, and other loop diuretics.¹⁶⁸

Immunofluorescence indicates expression of NKCC2 protein along the entire length of the TAL.¹⁶⁸ In particular, immunoelectron microscopy reveals expression in both rough (R) and smooth (S) cells of the TAL (see earlier discussion).¹⁴¹ NKCC2 expression in subapical vesicles is particularly prominent in smooth cells, suggesting a role for vesicular trafficking in the regulation of NKCC2 (see the “[Regulation of Na⁺-Cl⁻ Transport by the Thick Ascending Limb](#)” section).¹⁴¹ NKCC2 is also expressed in macula densa cells, which have been shown to possess apical $\text{Na}^+\text{-K}^+\text{-2Cl}^-$ cotransport activity.^{141,171} This latter observation is of considerable significance, given the role of the macula densa in TGF and renal renin secretion; luminal loop diuretics block TGF and the suppression of renin release by luminal Cl^- .¹⁴

Alternative splicing of exon 4 of the *SLC12A1* gene yields NKCC2 proteins that differ within transmembrane domain 2 and the adjacent intracellular loop; the functional significance of these variants appears primarily related to differences in binding to chloride.¹⁷² There are thus three different variants of exon 4, denoted “A,” “B,” and “F”; the variable inclusion of these cassette exons yields NKCC2-A, NKCC2-B,

and NKCC2-F proteins.^{168,170} Kinetic characterization reveals that these isoforms differ dramatically in ion affinities.^{168,170} In particular, NKCC2-F has a very low affinity for Cl^- ($K_m = 113$ mmol/L) and NKCC2-B has a very high affinity ($K_m = 8.9$ mmol/L); NKCC2-A has an intermediate affinity for Cl^- ($K_m = 44.7$ mmol/L).¹⁷⁰ These isoforms differ in axial distribution along the tubule, with the F cassette expressed in the inner stripe of the outer medulla, the A cassette in the outer stripe, and the B cassette in cortical TAL.¹⁴ There is thus an axial distribution of the anion affinity of NKCC2 along the TAL, from a low-affinity, high-capacity transporter (NKCC2-F) to a high-affinity, low-capacity transporter (NKCC2-B). Although technically compromised by the considerable homology between the 3' end of these 96-base pair exons, *in situ* hybridization has suggested that rabbit macula densa exclusively expresses the NKCC2-B isoform.¹⁴ Notably, however, selective knockout of the B cassette exon 4 does not eliminate NKCC2 expression in the murine macula densa, which also seems to express NKCC2-A by *in situ* hybridization.¹⁷³ The comparative phenotypes of NKCC2-A and NKCC2-B knockout mice are consistent with the relative Cl^- affinity of each isoform, with NKCC2-B functioning as a high-affinity, low-capacity isoform and NKCC2-A functioning as a low-affinity, high-capacity isoform. Thus targeted deletion of NKCC2-A selectively reduces TGF responses at the higher range of tubular flow rates (a low-affinity, high-capacity situation), whereas NKCC2-B deletion reduces responses at low flow rates.¹⁷⁴ Loss of NKCC2-A almost abolishes the suppression of plasma renin activity by isotonic saline infusion, which is, if anything, more robust in NKCC2-B knockout mice than wild type littermates.¹⁷⁴

It should be mentioned in this context that the $\text{Na}^+\text{-H}^+$ exchanger NHE3 functions as an alternative mechanism for apical Na^+ absorption by the TAL. There is also evidence in mouse cortical TAL for $\text{Na}^+\text{-Cl}^-$ transport via parallel $\text{Na}^+\text{-H}^+$ and $\text{Cl}^-\text{-HCO}_3^-$ exchange, although the role of this mechanism in transepithelial $\text{Na}^+\text{-Cl}^-$ transport seems less prominent than in the PT.¹⁴ Indeed, apical $\text{Na}^+\text{-H}^+$ exchange mediated by NHE3 appears to function primarily in HCO_3^- absorption by the TAL.¹⁷⁵ There is thus a considerable upregulation of both apical $\text{Na}^+\text{-H}^+$ exchange and NHE3 protein in the TAL of acidotic animals, paired with an induction of AE2, a basolateral $\text{Cl}^-\text{-HCO}_3^-$ exchanger.^{176,177} NHE3 in the TAL is also upregulated by increased flow. However, this is not via shear stress, as demonstrated in the PT, but by the production of endogenous O_2^- and activation of PKC, a potential pathway for flow-stimulated bicarbonate reabsorption.¹⁷⁸

Apical K^+ Channels

Microperfused TALs develop a lumen-positive PD during perfusion with $\text{Na}^+\text{-Cl}^-$.^{179,180} This lumen-positive PD plays a critical role in the physiology of the TAL, driving the paracellular transport of Na^+ , Ca^{2+} , and Mg^{2+} (Fig. 6.14). Originally attributed to electrogenic Cl^- transport, the lumen-positive transepithelial PD in the TAL is generated by the combination of apical K^+ channels and basolateral Cl^- channels.^{14,167,180} The conductivity of the apical membrane of TAL cells is predominantly, if not exclusively, K^+ selective. Luminal recycling of K^+ via $\text{Na}^+\text{-K}^+\text{-2Cl}^-$ cotransport and apical K^+ channels, along with basolateral depolarization due to Cl^- exit through Cl^- channels, results in the lumen-positive transepithelial PD.^{14,167}

Several lines of evidence have indicated that apical K^+ channels are required for transepithelial $\text{Na}^+\text{-Cl}^-$ transport by the TAL.^{14,167} First, the removal of K^+ from luminal perfusate results in a marked decrease in $\text{Na}^+\text{-Cl}^-$ reabsorption by the TAL, as measured electrophysiologically; the residual $\text{Na}^+\text{-Cl}^-$ transport in the absence of luminal K^+ is sustained by K^+ movement into the luminal fluid apical K^+ channels, because the combination of K^+ removal and a luminal K^+ channel inhibitor (barium) almost abolishes the equivalent short circuit current.¹⁴ Apical K^+ channels are thus required for continued functioning of NKCC2, the apical $\text{Na}^+\text{-K}^+\text{-2Cl}^-$ cotransporter; the low luminal concentration of K^+ in this nephron segment would otherwise become limiting for transepithelial $\text{Na}^+\text{-Cl}^-$ transport.

Second, the net transport of K^+ across perfused TAL is less than 10% that of Na^+ and Cl^- ; about 90% of the K^+ transported by NKCC2 is recycled across the apical membrane via K^+ channels, resulting in minimal net K^+ absorption by the TAL.^{14,181}

Third, the intracellular K^+ activity of perfused TAL cells is about 15 to 20 mV above equilibrium due to furosemide-sensitive entry of K^+ via NKCC2.¹⁸² Given an estimated apical K^+ conductivity of about 12 mS/cm², this intracellular K^+ activity yields a calculated K^+ current of about 200 $\mu\text{A}/\text{cm}^2$, which corresponds quantitatively to the uptake of K^+ by the apical $\text{Na}^+\text{-K}^+\text{-2Cl}^-$ cotransporter.¹⁶⁷

Fourth, the observation that Bartter syndrome can be caused by mutations in renal outer medullary potassium (ROMK, encoded by *KCNJ1*) provides genetic proof for the importance of K^+ channels in $\text{Na}^+\text{-Cl}^-$ absorption by the TAL (see later).¹⁸³ Finally, a novel ROMK inhibitor functions as a potent diuretic *in vivo*, primarily due to inhibition of TAL $\text{Na}^+\text{-Cl}^-$ transport.¹⁸⁴

Three types of apical K^+ channels have been identified in the TAL, a channel with a conductance of 30 picosiemen (30 pS), a channel with a conductance of 70 pS, and a high-conductance, calcium-activated maxi- K^+ channel (Fig. 6.14).¹⁸⁵⁻¹⁸⁷ The higher P_o and greater density of the 30-pS and 70-pS channels versus the maxi- K^+ channel suggest that these are the primary routes for K^+ recycling across the apical membrane; the 70-pS channel in turn appears to mediate about 80% of the apical K^+ conductance of TAL cells.¹⁸⁸ The low-conductance, 30-pS channel shares several electrophysiologic and regulatory characteristics with ROMK, the cardinal inward-rectifying K^+ channel that was initially cloned from renal outer medulla.¹⁴ In humans, three isoforms of ROMK (ROMK1, 2, and 3) are generated by alternative splicing of the *KCNJ1* gene; ROMK3 has not been detected in rat or mouse.¹⁸⁹ ROMK2 has the shortest amino terminus, ROMK1 has an additional 16 residues, and ROMK3 an additional 22 residues (compared with ROMK2). ROMK1 mRNA is expressed in the mid and late distal tubule and the CCD, and in the outer medullary collecting duct (OMCD), but not along the TAL (see later). ROMK2 mRNA is expressed from the medullary TAL through the CCD, but is absent from the OMCD.¹⁸⁹ ROMK3 is expressed from the medullary TAL through the DCT. ROMK protein has been identified at the apical membrane of medullary TAL, cortical TAL, and macula densa.¹⁹⁰ Furthermore, the 30-pS channel is also absent from the apical membrane of mice with homozygous deletion of the gene encoding ROMK.¹⁹¹ Notably, not all cells in the TAL are labeled with ROMK antibody, suggesting that ROMK

might be absent in the so-called HBC cells with HBC and low apical K^+ conductance (also see earlier discussion).^{140,142} HBC cells are thought to correspond to the smooth-surfaced morphologic subtype of TAL cells (S cells)¹⁴⁰; however, distribution of ROMK protein by immunoelectron microscopy has not as yet been reported.

ROMK clearly plays a critical role in Na^+ - Cl^- absorption by the TAL, given that loss-of-function mutations in this gene are associated with Bartter syndrome.¹⁸³ The role of ROMK in Bartter syndrome was initially discordant with the data, suggesting that the 70-pS K^+ channel is the dominant conductance at the apical membrane of TAL cells; heterologous expression of the ROMK protein in *Xenopus* oocytes had yielded a channel with a conductance of about 30 pS, suggesting that the 70-pS channel was distinct from ROMK.^{14,188} This paradox has been resolved by the observation that the 70-pS channel is absent from the TAL of ROMK knockout mice, indicating that ROMK proteins form a subunit of the 70-pS channel.¹⁹² A recent study specifically examined the effects of ROMK1 disruption in mice, and consistent with its absence along the TAL, discussed earlier, these mice did not display a Bartter syndrome phenotype.¹⁹³

ROMK activity in the TAL is clearly modulated by association with other proteins, such that coassociation with other subunits to generate the 70-pS channel is perfectly compatible with the known physiology of this protein. ROMK thus associates with scaffolding proteins NHERF-1 and NHERF-2 (see the “[Regulation of Proximal Tubular \$Na^+\$ - \$Cl^-\$ Transport: Neurohumoral Influences](#)” section) via the carboxyl-terminal PDZ-binding motif of ROMK; NHERF-2 is coexpressed with ROMK in the TAL.¹⁹⁴ The association of ROMK with NHERFs serves to bring ROMK into closer proximity to the cystic fibrosis transmembrane regulator protein (CFTR).¹⁹⁴ This ROMK-CFTR interaction is, in turn, required for the native ATP and glibenclamide sensitivity of apical K^+ channels in the TAL.¹⁹⁵

Paracellular Transport

TALs perfused with Na^+ - Cl^- develop a lumen-positive, transepithelial PD generated by the combination of apical K^+ secretion and basolateral Cl^- efflux.^{14,167,179,180,182} This lumen-positive PD plays a critical role in the paracellular reabsorption of Na^+ , Ca^{2+} , and Mg^{2+} by the TAL (Fig. 6.14). In the transepithelial transport of Na^+ , the stoichiometry of NKCC2 ($1Na^+:1K^+:2Cl^-$) is such that other mechanisms are necessary to balance the exit of Cl^- at the basolateral membrane; consistent with this requirement, data from mouse TAL have indicated that about 50% of transepithelial Na^+ transport occurs via the paracellular pathway.^{3,196} For example, the ratio of net Cl^- transepithelial absorption to net Na^+ absorption through the paracellular pathway is 2.4 ± 0.3 in microperfused mouse medullary TAL segments, and the expected ratio of 50% of Na^+ transport occurs via the paracellular pathway. In the absence of vasopressin, apical Na^+ - Cl^- cotransport is not K^+ dependent (see the “[Regulation of \$Na^+\$ - \$Cl^-\$ Transport by the Thick Ascending Limb](#)” section), reducing the lumen-positive PD; switching to K^+ -dependent Na^+ - K^+ - $2Cl^-$ cotransport in the presence of vasopressin results in a doubling of Na^+ - Cl^- reabsorption, without an effect on oxygen consumption.^{3,196} Therefore, the combination of a cation-permeable paracellular pathway and an “active transport,” lumen-positive PD,¹⁶⁷ generated indirectly by the basolateral Na^+ - K^+ -ATPase,

results in a doubling of active Na^+ - Cl^- transport for a given level of oxygen consumption.^{3,197}

Unlike in the PT, the voltage-positive PD in the TAL is generated almost entirely by transcellular transport, rather than by diffusion across the lateral tight junction.¹⁵ Mouse TAL segments primarily express claudin-14, -16, -19, and -10.^{14,198–200} In vasopressin-stimulated mouse TAL segments, with a lumen-positive PD of 10 mV, the maximal increase in Na^+ - Cl^- in the lateral interspace is about 10 mmol/L.¹⁹⁶ Tight junctions in the TAL are cation selective, with P_{Na^+}/P_{Cl^-} ratios of 2 to 5.^{167,196} Notably, however, P_{Na^+}/P_{Cl^-} ratios can be highly variable in individual tubules, ranging from 2 to 5 in a single study of perfused mouse TAL.¹⁹⁶ Recently, it has been suggested that the claudin profile of cells along the TAL represents a mosaic, with some cell interfaces expressing the Na^+ -selective claudin-10, whereas others express claudin-3, -16, or -19. It was suggested that this mosaic pattern reveals the existence of spatially separated paracellular routes for Na^+ and Ca^{2+}/Mg^{2+} .²⁰¹ Regardless, assuming a net P_{Na^+}/P_{Cl^-} ratio of about 3, the maximal dilution potential in the mouse TAL is between 0.7 and 1.1 mV, consistent with a dominant effect of transcellular processes on the lumen-positive PD.¹⁹⁶

The reported transepithelial resistance in the TAL is between 10 and 50 $\Omega \cdot cm^2$; although this resistance is higher than that of the PT, the TAL is not considered a tight epithelium.^{14,167} Notably, however, water permeability of the TAL is extremely low, less than 1% that of the PT.¹⁶⁷ These hybrid characteristics—relatively low resistance and very low water permeability—allow the TAL to generate and sustain Na^+ - Cl^- gradients of up to 120 mmol/L.^{14,167} Not unexpectedly, given its lack of water permeability, the TAL does not express aquaporin water channels; as in the PT, the particular repertoire of claudins expressed in the TAL determines the resistance and ion selectivity of this nephron segment.

Mutations in human claudin-16 (previously called paracellin-1) and claudin-19 are associated with hereditary hypomagnesemia, suggesting that these claudins are particularly critical for the cation selectivity of TAL tight junctions.^{14,199} Heterologous expression of claudin-16 (paracellin-1) in the anion-selective LLC-PK1 cell line markedly increases Na^+ permeability without affecting Cl^- permeability; this generates a significant increase in the P_{Na^+}/P_{Cl^-} ratio (Fig. 6.15).²⁰² LLC-PK1 cells expressing claudin-16 also have increased permeability to other monovalent cations. There is, however, only a modest increase in Mg^{2+} permeability, suggesting that claudin-16 does not form an Mg^{2+} -specific pathway in the tight junction; rather, it may serve to increase the overall cation selectivity of the tight junction. Claudin-19 appears in turn to reduce P_{Cl^-} in LLC-PK1 cells, without having much effect on Mg^{2+} or Na^+ permeability.²⁰³ The claudin-16 and claudin-19 proteins interact in multiple systems, and coexpression of claudin-16 and claudin-19 synergistically increases the P_{Na^+}/P_{Cl^-} ratio in LLC-PK1 cells.^{203,204} Knockdown of claudin-16 in transgenic mice increases Na^+ absorption in the downstream collecting duct, with the development of hypovolemic hyponatremia after treatment with amiloride; claudin-19 knockdown mice exhibit an increase in fractional excretion of Na^+ and a doubling in serum aldosterone levels.^{204,205} In summary, therefore, claudin-16 and claudin-19 interact to confer the cation selectivity of tight junctions in the TAL, contributing significantly to the transepithelial absorption of Na^+ in this nephron segment.

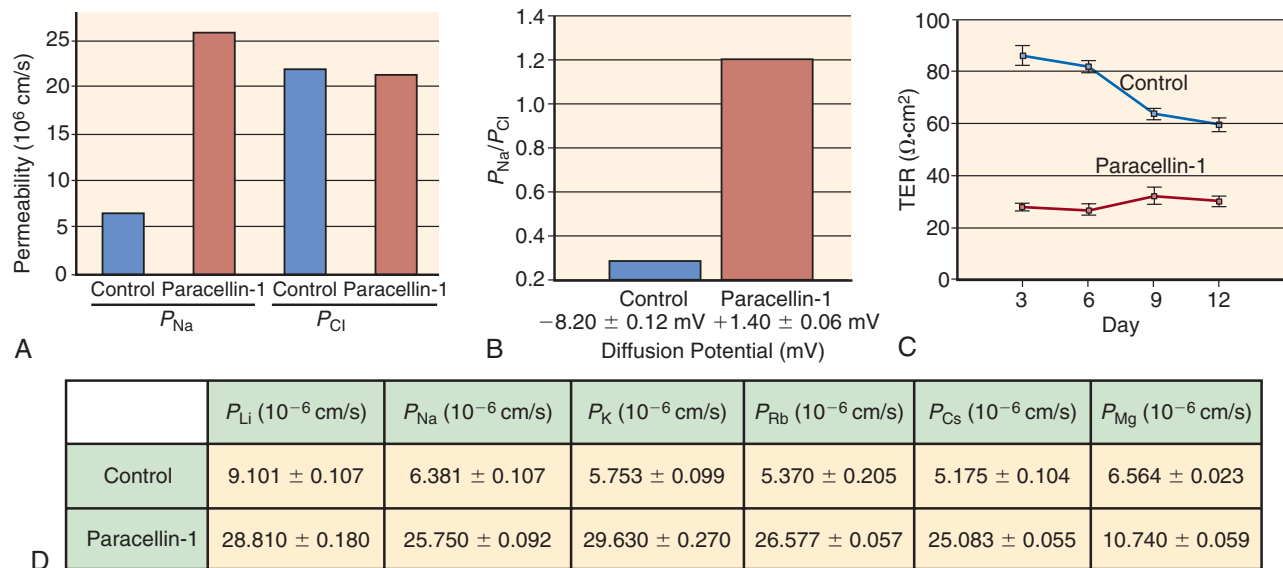


Fig. 6.15 Effect of claudin-16 (formerly called paracellin-1) overexpression in LLC-PK1 cells. (A) Effects of claudin-16 on the permeability of Na^+ and Cl^- in LLC-PK1 cells. (B) Ratio of P_{Na} to P_{Cl} and diffusion potential (*bottom*) across an LLC-PK1 cell monolayer. (C) Transepithelial resistance across an LLC-PK1 cell monolayer over a period of 12 days in cells expressing claudin-16 and control cells. (D) Summary of the effects of claudin-16 on permeability of various cations in LLC-PK1 cells. (From Hou J, Paul DL, Goodenough DA. Paracellin-1 and the modulation of ion selectivity of tight junctions. *J Cell Sci.* 2005;118:5109–5118.)

Other claudins expressed in the TAL modulate the function of claudin-16–claudin-19 heterodimers or have independent effects. Claudin-14 interacts with claudin-16, disrupting cation selectivity of the paracellular barrier in cells that also coexpress claudin-19.²⁰⁶ Claudin-14 expression in the TAL is calcium dependent via the CaSR, providing a novel axis for calcium-dependent regulation of paracellular calcium transport (see later).^{206–208} Claudin-10 appears to modulate paracellular Na^+ permeability specifically, with impaired paracellular Na^+ transport in claudin-10 knockout mice and a salt-wasting nephropathy in humans bearing compound heterozygous claudin-10 mutations.^{33,209}

Basolateral Mechanisms

The basolateral $\text{Na}^+\text{-K}^+\text{-ATPase}$ is the primary exit pathway for Na^+ at the basolateral membrane of TAL cells. The Na^+ gradient generated by $\text{Na}^+\text{-K}^+\text{-ATPase}$ activity is also thought to drive the apical entry of Na^+ , K^+ , and Cl^- via NKCC2, the furosemide-sensitive $\text{Na}^+\text{-K}^+\text{-2Cl}^-$ cotransporter.¹⁴ Inhibition of $\text{Na}^+\text{-K}^+\text{-ATPase}$ with ouabain thus collapses the lumen-positive PD and abolishes transepithelial $\text{Na}^+\text{-Cl}^-$ transport in the TAL.^{179,180,197} Basolateral exit of Cl^- from TAL cells is primarily but not exclusively electrogenic, mediated by an approximately 10-pS Cl^- channel.^{14,167,210} Reductions in basolateral Cl^- depolarize the basolateral membrane, whereas decreases in intracellular Cl^- induced by luminal furosemide have a hyperpolarizing effect.¹⁴ Intracellular Cl^- activity during transepithelial $\text{Na}^+\text{-Cl}^-$ transport is above its electrochemical equilibrium,¹⁴ with an intracellular negative voltage of -40 to -70 mV that drives basolateral Cl^- exit.^{14,167}

At least two CLC chloride channels, CLC-K1 and CLC-K2 (CLC-NKA and CLC-NKB in humans), are coexpressed in this nephron segment.^{158,163} However, an increasing body of evidence has indicated that the dominant Cl^- channel in the TAL is encoded by CLC-K2. First, CLC-K1 is heavily expressed

at the apical and basolateral membranes of the thin ascending limb, and the phenotype of the corresponding knockout mouse is consistent with primary dysfunction of thin ascending limbs, rather than the TAL (see $\text{Na}^+\text{-Cl}^-$ transport by the thin ascending limb).^{3,137,156,159} Second, loss-of-function mutations in CLC-NKB are associated with Bartter syndrome, providing genetic evidence for a dominant role of this channel in $\text{Na}^+\text{-Cl}^-$ transport in the TAL.¹⁶⁰ More recently, a very common T481S polymorphism in human CLC-NKB was shown to increase channel activity by a factor of 20; preliminary data have indicated an association with hypertension, suggesting that this gain-of-function in CLC-NKB increases $\text{Na}^+\text{-Cl}^-$ transport by the TAL and/or other segments of the distal nephron.^{211–213} Finally, CLC-K2 protein is heavily expressed at the basolateral membrane of the mouse TAL, with additional expression in the DCT, CNT, and α -intercalated cells.²¹⁴ Recently, *Clc-k2* was deleted from mice, leading to salt wasting, resembling Bartter syndrome, and to a loss of the around 10-pS chloride channel in TAL cells.¹⁶² Deletion of this gene also abrogated the response to furosemide, indicating the central role that this channel plays in transepithelial NaCl transport. This approach also permitted conclusions to be drawn regarding the location of CLC-K1 and CLC-K2 in the kidney, even though antibodies cross-react against the two related chloride channels. In the *Clc-k2* knockout mice, the reaction product could be seen to extend beyond the thin ascending limb into the medullary TAL, suggesting that CLC-K1 plays a role there.

A key advance was the characterization of the Barttin subunit of CLC-K channels, which is coexpressed with CLC-K1 and CLC-K2 in several nephron segments, including TAL.^{158,163} Unlike rat CLC-K1, the rat CLC-K2, human CLC-NKA, and human CLC-NKB paralogs are not functional in the absence of Barttin coexpression.^{163,164} CLC-NKB coexpressed with Barttin is highly selective for Cl^- , with a permeability series

of $\text{Cl}^- \gg \text{Br}^- = \text{NO}_3^- > \text{I}^-$.^{14,158,163} CLC-NKB/Barttin channels are activated by increases in extracellular Ca^{2+} and are pH sensitive, with activation at an alkaline extracellular pH and marked inhibition at an acidic pH.¹⁶³ CLC-NKA/Barttin channels have similar pH and calcium sensitivities, but exhibit higher permeability to Br^- .¹⁶³ Strikingly, despite the considerable homology between the CLC-NKA/NKB proteins, these channels also differ considerably in pharmacologic sensitivity to various Cl^- channel blockers, potential lead compounds for the development of paralogue-specific inhibitors.²¹⁵

Correlation between functional characteristics of CLC-K proteins with native Cl^- channels in TAL has been problematic, but the recent knockout work discussed earlier has begun to provide clarity. Wide variation in single-channel conductance has been reported for basolateral Cl^- channels in the TAL.²¹⁶ This is perhaps due to the use of collagenase and other conditions for the preparation of tubule fragments and/or basolateral vesicles, manipulations that potentially affect channel characteristics.²¹⁶ Notably, single-channel conductance has not been reported for CLC-NKB/Barttin channels because of the difficulty in expressing the channel in heterologous systems; this complicates the comparison of CLC-NKB/Barttin with native Cl^- channels. Single-channel conductance has, however, been reported for the V166E mutant of rat CLC-K1, which alters gating of the channel without expected effects on single-channel amplitude – coexpression with Barttin increases the single-channel conductance of V166E CLC-K1 from about 7 to 20 pS.¹⁶⁴ Therefore, part of the reported variability in native single-channel conductance may reflect heterogeneity in the interaction between CLC-NKB and/or CLC-NKA with Barttin. Regardless, a study using whole-cell recording techniques has suggested that CLC-K2 (CLC-NKB in humans) is the dominant Cl^- channel in TAL and other segments of the distal nephron.²¹⁶ Like CLC-NKB/Barttin, this native channel is highly Cl^- selective, with considerably weaker conductance for Br^- and I^- ; CLC-NKA/Barttin channels exhibit higher permeability to Br^- .^{14,158,163,216} TAL cells from wild type mice exhibited a dominant basolateral chloride conductance of 8 pS, which was entirely absent in *Clc-k2* knockout mice. Coupled with the strong Bartter syndrome phenotype, these results support the key role of this chloride channel in driving transepithelial NaCl transport along the TAL.

Electroneutral $\text{K}^+\text{-Cl}^-$ cotransport has also been implicated in transepithelial $\text{Na}^+\text{-Cl}^-$ transport in the TAL (Fig. 6.14), functioning in K^+ -dependent Cl^- exit at the basolateral membrane.¹⁴ The KCC KCC4 is thus expressed at the basolateral membrane of medullary and cortical TAL, in addition to the macula densa.^{217,218} There is also functional evidence for $\text{K}^+\text{-Cl}^-$ cotransport at the basolateral membrane of this section of the nephron. First, TAL cells contain a Cl^- -dependent NH_4^+ transport mechanism that is sensitive to 1.5-mmol/L furosemide and 10-mmol/L barium (Ba^{2+}).²¹⁹ NH_4^+ ions have the same ionic radius as K^+ and are transported by KCC4 and other KCCs; KCC4 is also sensitive to Ba^{2+} and millimolar furosemide, consistent with the pharmacology of $\text{NH}_4^+\text{-Cl}^-$ cotransport in the TAL.^{219–221} Second, to account for the effects on the transmembrane PD of basolateral Ba^{2+} and/or increased K^+ , it has been suggested that the basolateral membrane of TAL contains a Ba^{2+} -sensitive $\text{K}^+\text{-Cl}^-$ transporter; this is also consistent with the known expression of Ba^{2+} -sensitive KCC4 at the basolateral membrane.^{14,217,218,221} Third,

increases in basolateral K^+ cause Cl^- -dependent cell swelling in *Amphiuma* early distal tubule, an analog of the mammalian TAL; in *Amphiuma* LBC cells with low basolateral conductance, analogous to mammalian LBC cells (see the “ $\text{Na}^+\text{-Cl}^-$ Transport by the Thick Ascending Limb: Apical $\text{Na}^+\text{-Cl}^-$ Transport” section), this cell swelling was not accompanied by changes in basolateral membrane voltage or resistance, consistent with $\text{K}^+\text{-Cl}^-$ transport.^{140,142,222}

There is thus considerable evidence for basolateral $\text{K}^+\text{-Cl}^-$ cotransport in the TAL, mediated by KCC4.^{217,218} However, direct confirmation of a role for basolateral $\text{K}^+\text{-Cl}^-$ cotransport in transepithelial $\text{Na}^+\text{-Cl}^-$ transport is lacking. Indeed, KCC4-deficient mice do not have a prominent defect in function of the TAL, but exhibit instead a renal tubular acidosis.²¹⁷ The renal tubular acidosis in these mice has been attributed to defects in acid extrusion by $\text{H}^+\text{-ATPase}$ in α -intercalated cells; however, this phenotype is conceivably the result of a reduction in medullary NH_4^+ reabsorption by the TAL due to the loss of basolateral NH_4^+ exit mediated by KCC4.^{217,220,223}

Finally, there is also evidence for the existence of Ba^{2+} -sensitive K^+ channel activity at the basolateral membrane of the TAL, providing an alternative exit pathway for K^+ to that mediated by KCC4.^{224–226} Such channel activity may help stabilize the basolateral membrane potential above the equilibrium potential for Cl^- , thus maintaining a continuous driving force for Cl^- exit via CLC-NKB/Barttin Cl^- channels.²²⁶ Patch-clamp experiments have identified two types of K^+ channels in the basolateral membrane of the TAL: a 40-pS inwardly rectifying K^+ channel and an Na^+ - and Cl^- -activated, 80- to 150-pS K channel (Kca4.1 or slo2.2).^{225,227} The 40-pS K^+ channel was absent in the TAL of *Kcnj10* knockout mice, suggesting that the 40-pS K^+ channel is a KIR4.1 and KIR4.5 heterotetramer.²²⁷ Although KIR4.1 is also detected in human TAL, loss-of-function *KCNJ10* mutations do not show the phenotype of Bartter syndrome, suggesting that the disruption of KIR4.1 has no significant effect on transport function in the TAL.²²⁸ This may reflect secondary activation of alternative K^+ channels along TAL, as *Kcnj10* knockout mice demonstrate vasopressin-induced stimulation of the 80- to 150-pS K channel. Basolateral K^+ channels may also attenuate the increases in intracellular K^+ that are generated by the basolateral $\text{Na}^+\text{-K}^+\text{-ATPase}$, thus maintaining transepithelial $\text{Na}^+\text{-Cl}^-$ transport.^{224–226}

REGULATION OF $\text{Na}^+\text{-Cl}^-$ TRANSPORT BY THE THICK ASCENDING LIMB

Activating Influences

Transepithelial $\text{Na}^+\text{-Cl}^-$ transport by the TAL is regulated by a complex blend of competing neurohumoral influences, which are required to maintain the urinary concentrating capacity, and modulate salt balance. In particular, increases in intracellular cAMP tonically stimulate ion transport in the TAL; the stimulatory hormones and mediators that increase cAMP in this nephron segment include vasopressin, PTH, glucagon, calcitonin, and β -adrenergic activation (Fig. 6.9). These overlapping cAMP-dependent stimuli are thought to result in maximal baseline stimulation of transepithelial $\text{Na}^+\text{-Cl}^-$ transport.⁹⁴ For example, characterization of the in vivo effect of these hormones requires the prior simultaneous suppression or absence of circulating vasopressin, PTH, calcitonin, and glucagon.⁹⁴ This baseline activation is, in turn,

modulated by a number of negative influences, most prominently prostaglandin E₂ (PGE₂) and extracellular Ca²⁺ (Fig. 6.9). Other hormones and autoids working through cGMP-dependent signaling, including NO, have potent negative effects on Na⁺-Cl⁻ transport within the TAL.²³⁰ By contrast, Ang II has a stimulatory effect on Na⁺-Cl⁻ transport within the TAL.²³¹

Vasopressin is perhaps the most extensively studied positive modulator of transepithelial Na⁺-Cl⁻ transport in the TAL. The TAL, with the exception of macula densa cells,²³² expresses type 2 vasopressin receptors (V₂Rs) at both the mRNA and protein levels, and microdissected TALs respond to the hormone with an increase in intracellular cAMP.²³³ Vasopressin activates apical Na⁺-K⁺-2Cl⁻ cotransport within minutes in perfused mouse TAL segments and also exerts a longer-term influence on NKCC2 expression and function. The acute activation of apical Na⁺-K⁺-2Cl⁻ cotransport is achieved at least in part by the stimulated exocytosis of NKCC2 proteins, from subapical vesicles to the plasma membrane.²³⁴ This trafficking-dependent activation is abrogated by treatment of perfused tubules with tetanus toxin, which cleaves the vesicle-associated membrane proteins VAMP-2 and VAMP-3.²³⁴ As V₂Rs are prominently expressed along the collecting duct, as well as along the TAL and DCT, it has been difficult to separate the roles of vasopressin signaling in the two sites. This limitation was recently overcome by introducing a dominant-negative V₂R mutant into TAL cells of rat. The rats demonstrated polyuria and defective urinary concentration, as well as hypercalciuria, reminiscent of mild Bartter syndrome.²³² The absence of V₂R expression by macula densa cells was suggested to maintain TGF independent of vasopressin signaling.

Activation of NKCC2 by vasopressin is also associated with the phosphorylation of a cluster of amino-terminal threonines in the transporter protein; treatment of rats with the V₂ agonist desmopressin (DDAVP) induces phosphorylation of these residues *in vivo*, as measured with a phosphospecific antibody.²³⁴ These threonine residues are substrates for SPAK (STE20/SPS1-related proline/alanine-rich kinase) and OSR1 (oxidative stress-responsive kinase 1), first identified by Gagnon and colleagues as key regulatory kinases for NKCC1 and other cation-chloride cotransporters.²³⁵ SPAK and OSR1 are in turn activated by upstream WNK (*with no lysine* [K] kinases), such that SPAK or OSR1 requires coexpression with WNK4 to activate NKCC1 fully, at least in *in vitro* systems.²³⁵ By contrast, two reports of *Wnk4* knockout mice suggested that WNK4 does not regulate NKCC2 *in vivo*.^{236,237} Regardless, expression of WNK3 in *Xenopus* oocytes results in activatory phosphorylation of the amino-terminal threonines in NKCC2 that are phosphorylated in TAL cells after treatment with DDAVP.^{234,238}

The amino-terminal phosphorylation of NKCC2 by SPAK and/or OSR1 kinases appears to be important for activity of the transporter in the native TAL. The amino-terminus of NKCC2 contains a predicted binding site for SPAK,²³⁹ proximal to the sites of regulatory phosphorylation; the analogous binding site is required for activation of the NKCC1 cotransporter.²⁴⁰ SPAK also requires the sorting receptor SORLA (sorting protein-related receptor with A-type repeats) for proper trafficking within TAL cells, such that targeted deletion of *Sorla* results in a marked reduction in amino-terminal NKCC2 phosphorylation.²⁴¹ The role of the upstream WNK kinases is illustrated by the phenotype of a “knock-in” mouse

strain, in which the knocked-in mutant SPAK cannot be activated by upstream WNK kinases; these mice have a marked reduction in amino-terminal phosphorylation of both NKCC2 and the thiazide-sensitive NCC, with associated salt-sensitive hypotension.²⁴² The upstream WNK kinases appear to regulate SPAK and NKCC2 in a chloride-dependent fashion, phosphorylating and activating SPAK and the transporter in response to a reduction in intracellular chloride concentration (see the “Integrated Na⁺-Cl⁻ and K⁺ Transport in the Distal Nephron” section).²⁴³

Of the two kinases, SPAK and OSR1, OSR1 is perhaps more critical for NKCC2 function in the TAL, because pan-renal epithelial-specific deletion of *Osr1* leads to decreased amino-terminal phosphorylation of NKCC2, and a Bartter syndrome-like phenotype.²⁴⁴ Several groups reported an increase in NKCC2 amino-terminal phosphorylation and an increased response to furosemide in *Spak* knockout mice, suggesting overcompensation by OSR1.^{245–247} By contrast, it was reported that baseline Na⁺ absorption by isolated perfused TAL segments is profoundly impaired in SPAK-deficient mice, though this may reflect an absence of activating factors present *in vivo*.²⁴⁸ Truncated species of SPAK protein have also been detected in kidney due to generation of alternative mRNA species that lack the amino-terminal kinase domain and to proteolytic degradation; both forms of SPAK function as dominant-negative inhibitors of the full-length kinase, abrogating the usual stimulatory effect on coexpressed NKCC2 or NKCC1.^{247,249} A lack of these species in SPAK knockout mice may also contribute to the increased amino-terminal NKCC2 phosphorylation observed, due to the removal of a dominant-negative effect on OSR1. Further complexity arises from the influence of the adaptor protein calcium-binding protein 39 (CAB39, also called mouse protein-25, MO25²⁵⁰), which can both increase SPAK/OSR1-driven phosphorylation of NKCC2 and also activate SPAK/OSR1 directly, without the need for upstream phosphorylation by WNK kinases, by promoting dimerization of the kinases.^{250,251} WNK4 is also capable of direct interaction with CAB39, promoting activation of NKCC2 in the absence of SPAK or OSR1 expression.²⁵² In support of SPAK/OSR1-independent activation of NKCC2, in mice in which both SPAK and OSR1 were disrupted in the kidney, significant amino-terminal phosphorylation of NKCC2 was still detected. However, although this could reflect a direct effect of WNK4 on NKCC2, it could also result from phosphorylation by an as-yet unidentified kinase. Therefore, there appear to be at least three potential pathways for NKCC2 activation—a WNK4-dependent SPAK/OSR1 pathway, a WNK4-independent SPAK/OSR1 pathway, and a SPAK/OSR1-independent WNK4 pathway.²⁵² It should be noted, however, that amino-terminal phosphorylation has a smaller effect on NKCC2 activity than it does on NKCC1 and NCC.²³⁸ Thus changes in NKCC2 phosphorylation may not always reflect changes in NKCC2 activity.²⁵³

Vasopressin has also been shown to alter the stoichiometry of furosemide-sensitive apical Cl⁻ transport in the TAL, from a K⁺-independent Na⁺-Cl⁻ mode to the classic Na⁺-K⁺-2Cl⁻ cotransport stoichiometry.³ In the absence of vasopressin, ²²Na⁺ uptake by mouse medullary TAL cells is not dependent on the presence of extracellular K⁺, whereas the addition of the hormone induces a switch to K⁺-dependent ²²Na⁺ uptake. Underscoring the metabolic advantages of paracellular Na⁺ transport, which is critically dependent on the apical entry

of K^+ via $Na^+K^+2Cl^-$ cotransport (see previously), vasopressin accomplishes a doubling of transepithelial Na^+Cl^- transport without affecting $^{22}Na^+$ uptake (an indicator of transcellular Na^+Cl^- transport); this doubling in transepithelial absorption occurs without an increase in O_2 consumption, highlighting the energy efficiency of ion transport by the TAL.³ The mechanism of this shift in the apparent stoichiometry of NKCC2 is not completely clear. However, splice variants of mouse NKCC2 with a novel, shorter carboxyl-terminus have been found to confer sensitivity to cAMP when coexpressed with full-length NKCC2.²⁵⁴ Notably, these shorter splice variants appear to encode furosemide-sensitive, K^+ -independent NCCs when expressed alone in *Xenopus* oocytes.²⁵⁵ The in vivo relevance of these phenomena is not clear, however, nor is it known whether similar splice variants exist in species other than mouse.

In addition to its acute effects on NKCC2, the apical $Na^+K^+2Cl^-$ cotransporter, vasopressin increases transepithelial Na^+Cl^- transport by activating apical K^+ channels and basolateral Cl^- channels in the TAL.^{94,233} Details have yet to emerge of the regulation of the basolateral $ClC-K2/Barttin$ Cl^- channel complex by vasopressin, cAMP, and related pathways. However, the apical K^+ channel ROMK is directly phosphorylated by PKA on three serine residues (S25, S200, and S294 in the ROMK2 isoform). Phosphorylation of at least two of these three serines is required for detectable K^+ channel activity in *Xenopus* oocytes; mutation of all three serines to alanine abolishes phosphorylation and transport activity, and all three serines are required for full channel activity.²⁵⁶ These three phospho acceptor sites have distinct effects on ROMK activity and expression.²⁵⁷ Phosphorylation of the amino-terminal S25 residue appears to regulate trafficking of the channel to the cell membrane, without effects on channel gating; this serine is also a substrate for the SGK1 kinase, which activates the channel via an increase in expression at the membrane.²⁵⁷ By contrast, phosphorylation of the two carboxyl-terminal serines modulates open channel probability via effects on pH-dependent gating and on activation by the binding of phosphatidylinositol 4,5-bisphosphate (PIP2) to the carboxyl-terminal domain of the channel.^{258,259}

Vasopressin also has considerable long-term effects on transepithelial Na^+Cl^- transport by the TAL. Sustained increases in circulating vasopressin result in marked hypertrophy of medullary TAL cells, accompanied by a doubling in baseline active Na^+Cl^- transport.²³³ Water restriction or treatment with DDAVP also results in an increase in abundance of the NKCC2 protein in rat TAL cells. Consistent with a direct effect of vasopressin-dependent signaling, expression of NKCC2 is reduced in mice with a heterozygous deletion of the G_s stimulatory G protein, through which the V_2R activates cAMP generation.²³³ Increases in cAMP are thought to induce transcription of the *Slc12a1* gene that encodes NKCC2 directly, given the presence of a cAMP-response element in the 5' promoter.^{233,234} Abrogation of the tonic negative effect of PGE_2 on cAMP generation with indomethacin also results in a considerable increase in abundance of the NKCC2 protein.²³³ Finally, in addition to these effects on NKCC2 expression, water restriction or DDAVP treatment increases abundance of the ROMK protein at the apical membrane of TAL cells.²⁶⁰

Recently, a role for β_3 -adrenergic receptors in activation of NKCC2 was proposed, with administration of the selective

agonist BRL37344 increasing NKCC2 phosphorylation *in vivo* in wild type but not β_3 -adrenergic receptor knockout mice, which also displayed a mild Na^+ - and K^+ -wasting phenotype.²⁶¹

Inhibitory Influences

The stimulation of transepithelial Na^+Cl^- transport by cAMP-generating hormones (e.g., vasopressin, PTH) is modulated by a number of negative neurohumoral influences (Fig. 6.9).⁹⁴ In particular, extracellular Ca^{2+} and PGE_2 exert dramatic inhibitory effects on ion transport by this and other segments of the distal nephron through a plethora of synergistic mechanisms. Extracellular Ca^{2+} and PGE_2 both activate the G_i inhibitory G protein in TAL cells, opposing the stimulatory, G_s -dependent effects of vasopressin on intracellular levels of cAMP.^{262,263} Extracellular Ca^{2+} exerts its effect through the CaSR, which is heavily expressed at the basolateral membrane of TAL cells; PGE_2 primarily signals through EP_3 prostaglandin receptors.^{94,263,264} The increases in intracellular Ca^{2+} due to the activation of the CaSR and other receptors directly inhibit cAMP generation by a Ca^{2+} -inhibitable adenylate cyclase that is expressed in the TAL, accompanied by an increase in phosphodiesterase-dependent degradation of cAMP (Fig. 6.16).^{263,265} These negative stimuli likely inhibit baseline transport in the TAL; abrogation of the negative effect of PGE_2 with indomethacin results in a considerable increase in abundance of the NKCC2 protein, whereas targeted deletion of the CaSR in mouse TAL activates NKCC2 via increased amino-terminal phosphorylation.^{189,209}

Activation of the CaSR and other receptors in the TAL also results in the downstream generation of arachidonic acid metabolites, with potent negative effects on Na^+Cl^- transport (Fig. 6.16). Extracellular Ca^{2+} thus activates PLA_2 in TAL cells, leading to the liberation of arachidonic acid. This arachidonic acid is in turn metabolized by cytochrome P450 ω -hydroxylase to 20-HETE or by COX-2 to PGE_2 ; cytochrome P450 ω -hydroxylation generally predominates in response to activation of the CaSR in TAL.²⁶³ 20-HETE has very potent negative effects on apical $Na^+K^+2Cl^-$ cotransport, apical K^+ channels, and the basolateral $Na^+K^+ATPase$.^{94,263} PLA_2 -dependent generation of 20-HETE also underlies in part the negative effect of bradykinin and Ang II on Na^+Cl^- transport.^{94,263} Activation of the CaSR also induces tumor necrosis factor- α expression in the TAL, which activates COX-2 and thus generation of PGE_2 (Fig. 6.16); this PGE_2 in turn results in additional inhibition of Na^+Cl^- transport.²⁶³

The relative importance of the CaSR in the regulation of Na^+Cl^- transport by the TAL is dramatically illustrated by the phenotype of a handful of patients with gain-of-function mutations in this receptor. In addition to suppressed PTH and hypocalcemia, the usual phenotype caused by gain-of-function mutations in the CaSR (autosomal dominant hypoparathyroidism), these patients manifest a hypokalemic alkalosis, polyuria, and increases in circulating renin and aldosterone.^{266,267} Therefore, the persistent inhibition of Na^+Cl^- transport in the TAL by these overactive mutants of the CaSR causes a rare subtype of Bartter syndrome, type V, in the genetic classification of this disease.²⁶³

Activation of the CaSR also affects claudin expression in TAL cells via downregulation of microRNAs, leading to PTH-independent hypercalciuria (see Chapter 7).^{206–208,268}

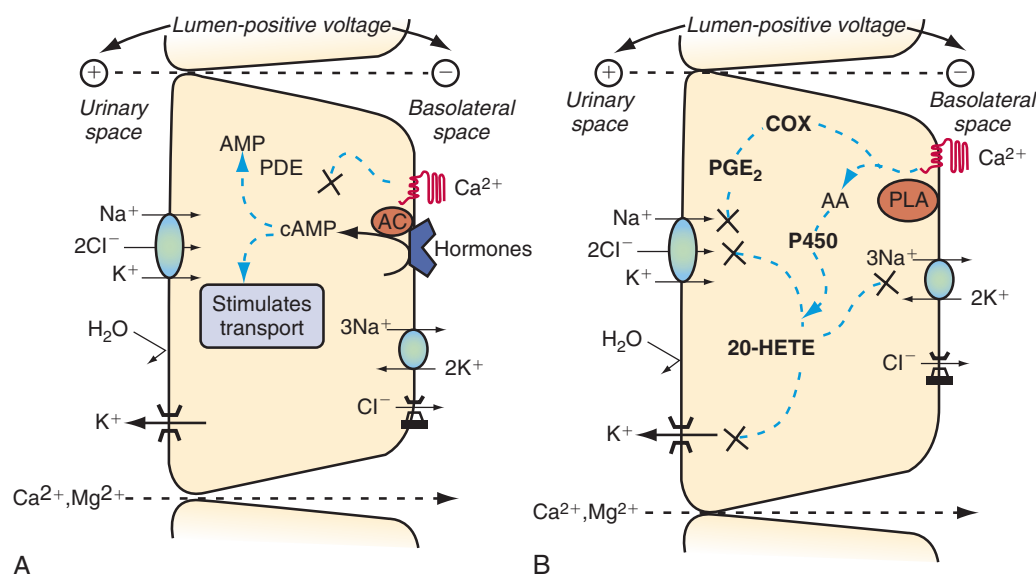


Fig. 6.16 Inhibitory effects of the calcium-sensing receptor (CaSR) on transepithelial $\text{Na}^+\text{-Cl}^-$ transport in the thick ascending limb. (A) Activation of the basolateral CaSR inhibits the generation of cAMP in response to vasopressin and other hormones (see text for details). (B) Stimulation of phospholipase A_2 by the CaSR leads to liberation of arachidonic acid, which is in turn metabolized by cytochrome P450 ω -hydroxylase to 20-HETE (20-hydroxyeicosatetraenoic acid), or by cyclooxygenase-2 (COX-2) to prostaglandin E_2 (PGE_2). 20-HETE is a potent natriuretic factor, inhibiting apical $\text{Na}^+\text{-K}^+\text{-2Cl}^-$ cotransport, apical K^+ channels, and the basolateral $\text{Na}^+\text{-K}^+\text{-ATPase}$. Activation of the CaSR also induces tumor necrosis factor- α (TNF- α) expression in the TAL, which activates COX-2 and thus generation of PGE_2 , leading to additional inhibition of $\text{Na}^+\text{-Cl}^-$ transport. (From Hebert SC. Calcium and salinity sensing by the thick ascending limb: a journey from mammals to fish and back again. *Kidney Int Suppl.* 2004;91:S28–S33.)

Uromodulin

TAL cells are unique in expressing the membrane-bound, glycosylphosphatidylinositol (GPI)-anchored protein, uromodulin (Tamm-Horsfall glycoprotein), which is not expressed by macula densa cells or the downstream DCT. Uromodulin is released by proteolytic cleavage at the apical membrane and is secreted as the most abundant protein in normal human urine (20 to 100 mg/day).²⁶⁹ Uromodulin has a host of emerging roles in the physiology and biology of the TAL. A high-salt diet increases uromodulin expression, suggesting a role in ion transport.²⁶⁹ In this regard, uromodulin facilitates membrane trafficking and function of the NKCC2 protein, with similar effects on apical ROMK protein.^{270,271}

Autosomal dominant mutations in the *UMOD* gene encoding uromodulin are associated with medullary cystic disease type 2 and familial juvenile hyperuricemic nephropathy. Now referred to as uromodulin-associated kidney disease, this syndrome includes progressive tubulointerstitial damage and chronic kidney disease (CKD), variably penetrant hyperuricemia and gout, and variably penetrant renal cysts that are typically confined to the corticomedullary junction.²⁶⁹ The causative mutations tend to affect conserved cysteine residues within the amino-terminal half of the protein, leading to protein misfolding and retention within the endoplasmic reticulum.^{269,272} More common genetic variants in the *UMOD* promoter have recently been linked in genomewide association studies with a risk of CKD and hypertension.²⁶⁹ These susceptibility variants have a high frequency (≈ 0.8) and confer an approximately 20% higher risk for CKD and a 15% risk for hypertension.²⁷³ These polymorphisms are associated with more abundant renal uromodulin transcript and higher urinary uromodulin excretion due to activating effects on the *UMOD* promoter.^{273,274} Overexpression of uromodulin in

transgenic mice leads to distal tubular injury, with segmental dilation and an increased tubular cast area relative to wild type mice; similar lesions are increased in frequency in older adults homozygous for susceptibility variants in *UMOD* when compared with those homozygous for protective variants.²⁷³

Uromodulin-transgenic mice also manifest salt-sensitive hypertension due to activation of the SPAK kinase and activating amino-terminal phosphorylation of NKCC2. Human hypertensive individuals homozygous for susceptibility variants in *UMOD* appear to have an analogous phenotype, with exaggerated natriuresis in response to furosemide compared with those who are homozygous for protective variants.²⁷³ These findings are compatible with the stimulatory effects of uromodulin on NKCC2 and ROMK—that is, a net gain of function in TAL transport.^{270,271} Uromodulin excretion also appears to parallel transport activity of the TAL, with common polymorphisms in the *KCNJ1* gene encoding ROMK and two genes involved in regulating SPAK and OSR1 kinase activity (*SORL1* and *CAB39*).²⁷⁴

ANATOMY OF THE DISTAL NEPHRON

The distal nephron that extends beyond the TAL is the final arbiter of urinary $\text{Na}^+\text{-Cl}^-$ excretion and a critical target for natriuretic and antinatriuretic stimuli. The understanding of the cellular organization and molecular phenotype of the distal nephron continues to evolve and merits a brief review in this context. The DCT begins at a variable distance after the macula densa, with an abrupt transition between NKCC2-positive cortical TAL cells and DCT cells that express the thiazide-sensitive NCC. Considerable progress has been made in the phenotypic classification of cell types in the DCT and adjacent nephron segments, based on the expression of an

expanding list of transport proteins and other markers.²⁷⁵ This analysis has revealed considerable differences in the organization of the DCT, CNT, and CCD in rodent, rabbit, and human kidneys. In general, rabbit kidneys are unique in the axial demarcation of DCT, CNT, and CCD segments, at both a molecular and morphologic level; the organization of the DCT to CCD is considerably more complex in other species, with boundaries that are much less absolute.²⁷⁵ Notably, however, the overall repertoire of transport proteins expressed does not vary among these species; what differs is the specific cellular and molecular organization of this segment of the nephron.

The early DCT (DCT1) of mouse kidney expresses NCC and a specific marker, parvalbumin, which also distinguishes the DCT1 from the adjacent cortical TAL (Fig. 6.17).²⁷⁶ Targeted deletion of parvalbumin in mice reveals that this intracellular Ca^{2+} -binding protein is required for full activity of NCC in the DCT.²⁷⁷ Cells of the late DCT (DCT2) in mice coexpress NCC with proteins involved in transcellular Ca^{2+} transport, including the apical calcium channel, TRPV5 (previously ECaC1), the cytosolic calcium-binding protein calbindin $\text{D}_{28\text{K}}$, and the basolateral Na^+ - Ca^{2+} exchanger NCX1.²⁷⁶ NCC is coexpressed with ENaC in the late DCT2 of mouse, where the two proteins physically and may functionally interact,²⁷⁸ with robust expression of ENaC continuing in the downstream CNT and CCD.²⁷⁶ By contrast, rabbit kidney does not have a DCT1 or DCT2 and exhibits abrupt transitions between NCC- and ENaC-positive DCT and CNT segments, respectively.²⁷⁵ Human kidneys that have been studied thus far exhibit expression of calbindin $\text{D}_{28\text{K}}$ all along the DCT and CNT, extending into the CCD; however, the intensity of expression varies at these sites. Approximately 30% of cells in the distal convolution of human kidney express NCC, with 70% expressing ENaC (CNT cells); ENaC and NCC overlap in expression at the end of the human DCT segment. Finally, cells of the early CNT of human kidneys express ENaC in the absence of aquaporin-2, the apical vasopressin-sensitive water channel.²⁷⁵

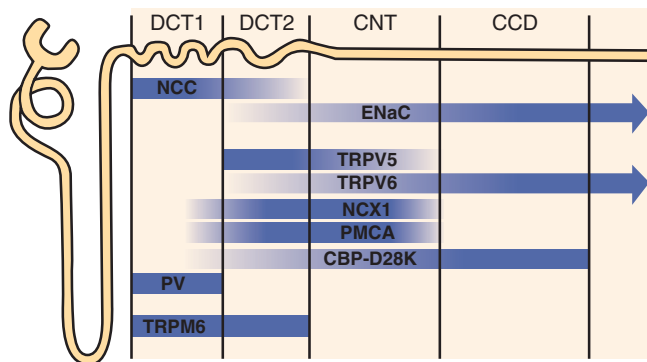


Fig. 6.17 Schematic representation of the segmentation of the mouse distal nephron and distribution and abundance of Na^+ , Ca^{2+} , and Mg^{2+} -transporting proteins. *CBP-D28K*, calbindin-D28K; *CCD*, cortical collecting duct; *CNT*, connecting tubule; *DCT1* and *DCT 2*, distal convoluted tubules 1 and 2, respectively; *ENaC*, epithelial Na^+ channel; *NCC*, thiazide-sensitive Na^+ - Cl^- cotransporter; *NCX1*, Na^+ - Ca^{2+} exchanger; *PMCA*, plasma membrane Ca^{2+} -ATPase; *PV*, parvalbumin; *TRPM6*, apical Mg^{2+} entry channel; *TRPV5* and *TRPV6*, apical Ca^{2+} entry channels.^{276,614,615}

Although primarily contiguous with the DCT, CNT cells share several traits with principal cells of the CCD, including apical expression of ENaC and ROMK, the K^+ secretory channel; the capacity for Na^+ - Cl^- reabsorption and K^+ secretion in this nephron segment is as much as 10 times higher than that of the CCD.²⁷⁹ Intercalated cells are the minority cell type in the distal nephron, emerging within the DCT and CNT and extending into the early inner medullary collecting duct (IMCD).²⁸⁰ Three subtypes of intercalated cells have been defined, based on differences in the subcellular distribution of the H^+ -ATPase and the presence or absence of the basolateral AE1 Cl^- - HCO_3^- exchanger. Type A intercalated cells extrude protons via an apical H^+ -ATPase in series with basolateral AE1 ; type B intercalated cells secrete HCO_3^- and OH^- via an apical anion exchanger (SLC26A4 or pendrin) in series with basolateral H^+ -ATPase.²⁸⁰ In rodents, the most prevalent subtype of intercalated cells in the CNT is the non-A, non-B intercalated cell, which possesses an apical Cl^- - HCO_3^- exchanger (SLC26A4 or pendrin) along with apical H^+ -ATPase.²⁸⁰ Although intercalated cells play a dominant role in acid-base homeostasis, Cl^- transport by type B intercalated cells performs an increasingly appreciated role in distal nephron Na^+ - Cl^- transport (see the “Connecting Tubules and the Cortical Collecting Duct: Cl^- Transport” section).

The OMCD encompasses two separate subsegments corresponding to the outer and inner stripes of the outer medulla, OMCD_o and OMCD_i, respectively. OMCD_o and OMCD_i contain principal cells with apical amiloride-sensitive Na^+ channels (ENaCs); however, the primary role of this nephron segment is renal acidification, with a particular dominance of type A intercalated cells in OMCD_i.^{6,281} The OMCD may also play a role in K^+ reabsorption via the activity of apical H^+ - K^+ -ATPase pumps,²⁸²⁻²⁸⁴ although deletion of this transport protein does not alter the ability to conserve K^+ substantially.²⁸⁵

Finally, the IMCD begins at the boundary between the outer and inner medulla and extends to the tip of the papilla. The IMCD is arbitrarily separated into three equal zones, denoted IMCD1, IMCD2, and IMCD3; at the functional level, an early IMCD (IMCD_i) and a terminal portion (IMCD_t) can be appreciated.⁶ The IMCD plays a particularly prominent role in vasopressin-sensitive water and urea transport.⁶ The early IMCD contains principal cells and intercalated cells; all three subsegments (IMCD1–3) express apical ENaC protein, albeit considerably weaker expression than in the CNT and CCD.²⁸⁶ The roles of the IMCD and OMCD in Na^+ - Cl^- homeostasis have been more elusive than those of the CNT and CCD; however, to the extent that ENaC is expressed in the IMCD and OMCD, homologous mechanisms are expected to function in Na^+ - Cl^- reabsorption by the CNT, CCD, OMCD, and IMCD segments.

DISTAL CONVOLUTED TUBULE

Mechanisms of Na^+ - Cl^- Transport in the Distal Convoluted Tubule

Earlier micropuncture studies that did not distinguish between early and late DCT indicated that this nephron segment reabsorbs about 10% of filtered Na^+ - Cl^- .^{5,287} The apical absorption of Na^+ and Cl^- by the DCT is mutually dependent; ion substitution does not affect transepithelial voltage, suggesting electroneutral transport.²⁸⁸ The absorption of Na^+ by perfused

DCT segments is also inhibited by chlorothiazide, localized proof that this nephron segment is the target for thiazide diuretics.²⁸⁹ Similar thiazide-sensitive $\text{Na}^+\text{-Cl}^-$ cotransport exists in the urinary bladder of winter flounder, the species in which the thiazide-sensitive NCC was first identified by expression cloning.²⁹⁰ Functional characterization of rat NCC indicates very high affinities for both Na^+ and Cl^- (Michaelis–Menten constants of 7.6 ± 1.6 and 6.3 ± 1.1 mmol/L, respectively); equally high affinities had previously been obtained by Velázquez and associates in perfused rat DCT.^{288,291} The measured Hill coefficients of rat NCC are about 1 for each ion, consistent with electroneutral cotransport.²⁹¹

NCC expression is the defining characteristic of the DCT (Fig. 6.18).²⁷⁵ There is also evidence for expression of this transporter in osteoblasts, peripheral blood mononuclear cells, and intestinal epithelium; however, the functional significance of expression reported for these sites remains unclear.^{168,292} The human *SLC12A3* gene encodes three isoforms (NCC1, NCC2, and NCC3), but only NCC3 has been studied extensively, because NCC1 and NCC2 are not expressed in rats or mice.²⁹³ These isoforms may undergo differential regulation. For example, NCC1 and NCC2 contain a region in their carboxyl-termini that is absent from NCC3 and contain a serine (S811), which undergoes phosphorylation and contributes to cotransporter activity.²⁹⁴ Loss-of-function mutations in the *SLC12A3* gene encoding human NCC cause Gitelman syndrome, familial hypokalemic alkalosis with hypomagnesemia, and hypocalciuria (see Chapter 44). Mice with homozygous deletion of the *Slc12a3* gene encoding NCC exhibit marked morphologic defects in the early DCT, with a reduction in the absolute number of DCT cells and changes

in ultrastructural appearance.^{295,296} Similarly, thiazide treatment promotes marked apoptosis of the proximal part of DCT, suggesting that thiazide-sensitive $\text{Na}^+\text{-Cl}^-$ cotransport plays an important role in modulating growth and regression of this nephron segment.²⁹⁷

Coexpression of NCC and ENaC occurs in the “late DCT” (DCT2) and CNT segments of many species, either in the same cells or in adjacent cells in the same tubule.²⁷⁵ Notably, ENaC is the primary Na^+ transport pathway of CNT and CCD cells, rather than DCT. There is, however, evidence for other Na^+ and Cl^- entry pathways in DCT cells. In particular, the $\text{Na}^+\text{-H}^+$ exchanger NHE2 (SLC9A2) is coexpressed with NCC at the apical membrane of rat DCT cells.²⁹⁸ As in the PT, perfusion of the DCT with formate and oxalate stimulates DIDS-sensitive $\text{Na}^+\text{-Cl}^-$ transport that is distinct from the thiazide-sensitive transport mediated by NCC.⁵⁰ Therefore a parallel arrangement of $\text{Na}^+\text{-H}^+$ exchange and Cl^- anion exchangers may play an important role in electroneutral $\text{Na}^+\text{-Cl}^-$ absorption by the DCT (Fig. 6.18). The $\text{Na}^+\text{-H}^+$ antiporter NHA2 (SLC9B2) has been localized to the DCT, and the anion exchanger SLC26A6 may be expressed in DCT cells; NHE2, NHA2, and SLC26A6 are thus candidate mechanisms for this alternative pathway of DCT $\text{Na}^+\text{-Cl}^-$ absorption.^{298–300}

At the basolateral membrane, as in other nephron segments, Na^+ exits via $\text{Na}^+\text{-K}^+\text{-ATPase}$; bearing in mind the considerable caveats in morphologic identification of the DCT, this nephron segment appears to have the highest $\text{Na}^+\text{-K}^+\text{-ATPase}$ activity of the entire nephron (Fig. 6.3).^{17,275} Basolateral membranes of DCT cells in both rabbit and mouse express the KCC KCC4, a potential exit pathway for

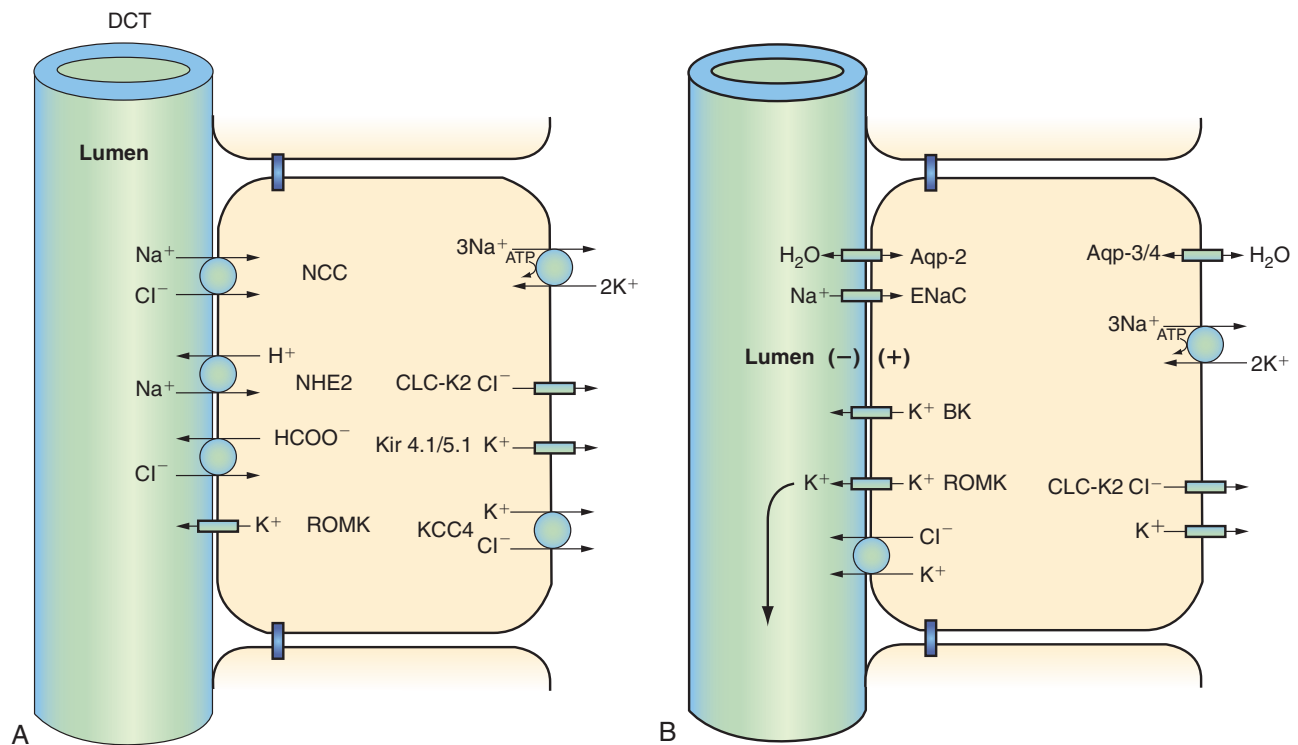


Fig. 6.18 Transport pathways for $\text{Na}^+\text{-Cl}^-$ and K^+ in distal convoluted tubule (DCT) cells (A) and principal cells of the connecting tubule (CNT) and cortical collecting duct (CCD) (B). *Aqp-2*, 3/4, Aquaporin-2, aquaporin-3/4; *ENaC*, epithelial Na^+ channel; *KCC4*, $\text{K}^+\text{-Cl}^-$ cotransporter-4; *NCC*, thiazide-sensitive $\text{Na}^+\text{-Cl}^-$ cotransporter; *NHE-2*, $\text{Na}^+\text{-H}^+$ exchanger-2; *ROMK*, renal outer medullary K^+ channel.

Cl^- .^{218,301} However, several lines of evidence have indicated that Cl^- primarily exits DCT cells via basolateral Cl^- channels. First, the basolateral membrane of rabbit DCT contains Cl^- channel activity, with functional characteristics similar to those of CLC-K2 .^{216,302} Second, CLC-K2 protein is expressed at the basolateral membrane of DCT and CNT cells. Although mRNA for CLC-K1 can also be detected by RT-PCR of microdissected DCT segments,^{158,214} recent data show that deletion of CLC-K2 from mice leads to a loss of response to furosemide, and a markedly blunted one to thiazide, implicating this channel in chloride reabsorption along both the TAL and the DCT.¹⁶² Finally, loss-of-function mutations in CLC-NKB , the human ortholog of CLC-K2 , cause classic Bartter syndrome; this Bartter subtype has a phenotype that is typically intermediate between Bartter syndrome type I, and Gitelman syndrome, consistent with loss of function of DCT segments.^{160,162,303}

K^+ channels at the basolateral membrane of DCT cells play a critical role in the function of this nephron segment. Cell-attached patches in basolateral membranes of microdissected DCTs detect an inward rectifying K^+ channel, with characteristics similar to those of heteromeric KIR4.1/KIR5.1 and KIR4.2/KIR5.1 channels.^{228,304–306} Basolateral membranes of the DCT express immunoreactive KIR4.1 and KIR5.1 protein, and DCT cells express KIR4.2 mRNA.^{228,304–306} Patients with loss-of-function mutations in the *KCNJ10* gene that encodes KIR4.1 develop a syndrome encompassing epilepsy, ataxia, sensorineural deafness, and tubulopathy (EAST or SeSAME syndrome).^{228,307} The associated tubulopathy includes hypokalemia, metabolic alkalosis, hypocalciuria, and hypomagnesemia.^{228,307} Mice in which *Kcnj10* has been deleted following development demonstrate hypokalemic alkalosis with hypocalciuria, and suppression of NCC abundance,³⁰⁸ indicating a key role of this channel in supporting trans-epithelial NaCl transport.^{228,308,309} While KIR4.1 activity is detected in the TAL, KIR4.1 disruption in mice has no significant effect on TAL membrane potential or NKCC2 expression, so the physiological relevance of this is unclear.³¹⁰ By contrast, *Kcnj10* disruption markedly depolarizes the basolateral cell membrane of DCT cells, indicating that these K^+ channels play a key role in setting the membrane potential in the DCT.^{308,311} In addition to sensing the membrane potential, the KIR4.1/KIR5.1 channels at the basolateral membrane of DCT cells are hypothesized to function in basolateral K^+ recycling, maintaining adequate $\text{Na}^+\text{-K}^+\text{-ATPase}$ activity for $\text{Na}^+\text{-Cl}^-$ absorption and other aspects of DCT function. Notably, the CaSR coassociates with KIR4.1 and KIR4.2 proteins and inhibits their activity, providing a mechanism for the dynamic modulation of $\text{Na}^+\text{-Cl}^-$, calcium, and magnesium transport by the DCT.³⁰⁵

Regulation of $\text{Na}^+\text{-Cl}^-$ Transport in the Distal Convoluted Tubule

Our understanding of factors that regulate solute transport by the DCT has advanced rapidly, during the past 5 years. Studies performed in the 1990s showed that dietary NaCl deprivation activates thiazide-sensitive NaCl transport along the DCT.⁵ When distal salt delivery was increased further, by administering loop diuretics continuously and administering saline, as drinking solution, additional increases in transport capacity were observed, together with considerable hypertrophy of DCT cells. One contributor to this phenotype is

Ang II. DCT cells express AT_1 receptors, and Ang II activates NCC, through a mechanism that requires the kinase WNK4 (see discussion later).^{237,312–316}

Aldosterone has also been suggested as a factor that modulates NCC, which would make the DCT part of the aldosterone-sensitive distal nephron. Aldosterone, given to adrenalectomized rats, activated NCC.³¹⁷ Dietary salt restriction and exogenous mineralocorticoids were also shown to increase the abundance of NCC, and phosphorylated NCC.³¹⁸ DCT cells, at least in rats, were shown to express 11 beta hydroxysteroid dehydrogenase type 2 ($11\beta\text{-HSD2}$),³¹⁹ at least at low levels, and its deletion from mice resulted in a phenotype that includes hypertrophy of DCT cells, and increases in the abundance of phosphorylated NCC.³²⁰ Aldosterone has been reported to enhance NCC activity acutely in cultured DCT cells.³²¹ Roy and colleagues identified two alternatively spliced exons in WNK1 that contain PY motifs, which bind the E3 ubiquitin ligase NEDD4-2 . These motifs were suggested to mediate NCC activation by aldosterone.³²²

It was only the recognition that dietary potassium intake is a powerful NCC and DCT regulatory factor that has modified the view of aldosterone's role. Vallon and colleagues documented that dietary potassium deprivation increased the abundance of phosphorylated NCC in mice.³²³ Two groups subsequently showed that low potassium intake can increase NCC abundance and activity even in the setting of high salt intake, and another showed that high potassium intake can suppress NCC, even when dietary salt intake is low.³²⁴ Thus it appears that the effects of potassium predominate over those of sodium. These effects of high potassium intake raised the possibility that aldosterone may not be playing a dominant role in NCC regulation, as high potassium diets are associated with high aldosterone secretion and low NCC activity.³²⁴ Increasingly, it has become apparent that DCT cells, and NCC, are exquisitely sensitive to plasma $[\text{K}^+]$. These effects occur very rapidly, as a short-term gavage with high potassium solution leads to rapid dephosphorylation of the NCC.³²⁵ Similarly, raising the plasma potassium concentration, either by potassium infusion,³²⁶ by administering the sodium channel blocking drug amiloride,³²⁷ or by deleting Na^+ channels,³²⁸ strikingly reduces the abundance of phosphorylated NCC. These effects on the abundance of phosphorylated NCC are functionally relevant, as several groups have documented that directional changes in pNCC abundance, in the setting of potassium challenge, are associated with concordant changes in thiazide-sensitive NaCl excretion.³²⁹ The mechanisms involved in the potassium effect will be discussed later, with the discussion of WNK kinases.

The recognition that potassium plays a dominant role in regulating NCC and the DCT suggested that some effects observed during aldosterone infusion might be secondary to induced potassium imbalance. Mice with nephron-specific disruption of the mineralocorticoid receptor (MR) did exhibit low NCC activity, as would be expected if aldosterone stimulates NCC directly, but NCC could be stimulated to normal levels by dietary K^+ restriction, proving that it was effects of MR deletion on potassium balance that were responsible for changes in NCC.^{329,330} A second group showed that in mice with deletion of MR in approximately 20% of renal tubule cells, which allowed side-by-side comparison of cells in the same segment, no differences in NCC abundance and phosphorylation were observed between DCT cells that did

and did not express mineralocorticoid receptors; dietary Na^+ restriction upregulated NCC to similar extent in both types of cell.³³¹ By contrast, along the collecting duct ENaC expression and apical membrane localization were not detected on control diet nor in response to dietary Na^+ restriction in knockout cells. Finally, studies in adult mice with inducible disruption of the MR target α -ENaC showed that a high Na^+ /low K^+ diet, which normalized plasma $[\text{K}^+]$, also normalized the reduced abundances of total and phosphorylated NCC seen on a normal diet.³²⁸ In summary, the preponderance of evidence suggests that the effects of plasma $[\text{K}^+]$ are dominant, and that aldosterone plays only a modifying role in regulating NCC; the effects of potassium on NCC and aldosterone on ENaC appear to comprise a potassium switch in the kidney (see later).

A central role in the regulation of DCT Na^+ and Cl^- transport is played by WNK1 and WNK4, key regulatory kinases in the distal nephron that were initially identified as two of the causative genes for familial hyperkalemic hypertension (FHHt; also known as pseudohypoaldosteronism type II or Gordon syndrome). FHHt is in every respect the mirror image of Gitelman syndrome, encompassing hypertension, hyperkalemia, hyperchloremic metabolic acidosis, suppressed plasma renin activity and aldosterone, and hypercalciuria.³³²

Furthermore, FHHt behaves like a gain-of-function in NCC and/or the DCT in that treatment with thiazides typically results in resolution of the entire syndrome³³²; however, simple transgenic overexpression of NCC in DCT cells does not replicate the phenotype in mice, indicating specific effects of the mutant WNK1 and WNK4 alleles.^{332,333}

WNK kinases have pleiotropic effects, and initial experiments involving WNK expression in heterologous systems have often produced results that now seem contradictory. Yet, a consensus view of the predominant effects of WNK kinases in regulating NCC has begun to emerge. According to a highly simplified scheme (Fig. 6.19), WNK kinases activate the downstream kinases SPAK and/or OSR1 by binding to them along their conserved carboxyl-terminal domains, and directly phosphorylating them. When so activated, and enhanced by interactions with MO25 (Cab39),²⁵⁰ these secondary kinases bind to and activate NCC by enhancing phosphorylation of key residues in the NCC amino terminal cytoplasmic domain.³³⁴

Mutations in both WNK1 and WNK4 can cause FHHt. Intronic mutations in WNK1 enhance the expression of a full-length kinase-active form of WNK1 along the DCT, where it is normally expressed only at low levels³³⁵; WNK4-point mutations cluster around an acid-rich conserved region of

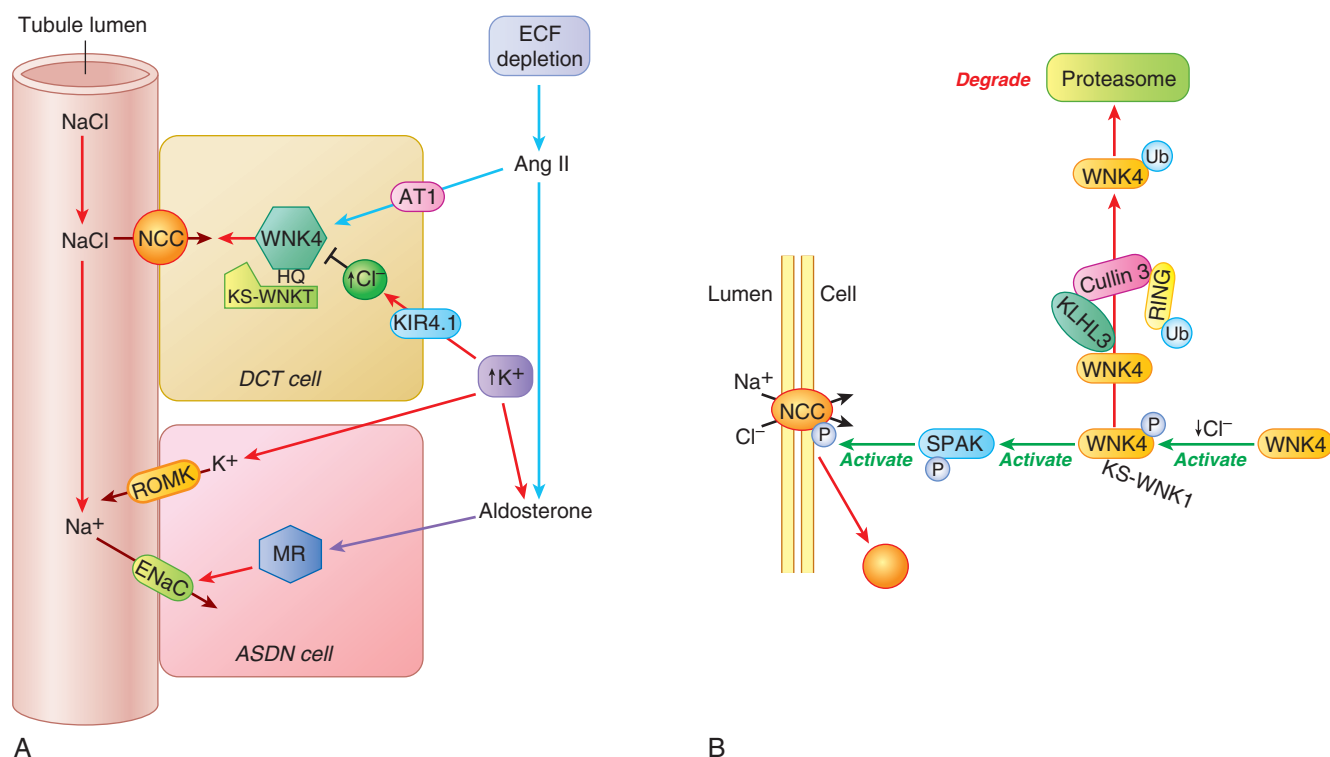


Fig. 6.19 Regulation of distal transport by WNK kinases. (A) Comparison of effects of extracellular fluid (ECF) volume depletion and hyperkalemia ($\uparrow[\text{K}^+]$) on transport along the distal nephron. In the lumen, Na^+ delivery to the aldosterone-sensitive distal nephron (ASDN) is determined by entry into the distal convoluted tubule (DCT) and reabsorption by the thiazide-sensitive NaCl cotransporter (NCC). WNK4, likely together with WNK1-S [also known as kidney-specific (KS)-WNK1], activates NCC.⁶¹⁶ This process is stimulated by angiotensin II (*Ang II*), which also enhances aldosterone secretion by the adrenal gland to stimulate the epithelial Na^+ channel (ENaC), via the mineralocorticoid receptor (MR). Sodium reabsorption along both the DCT and ASDN corrects ECF volume depletion. During hyperkalemia, NCC is turned off via increased intracellular chloride (modulated by K^+ flux through KIR4.1 channels), and Na^+ is reabsorbed primarily by ENaC, favoring K^+ secretion. (B) Detailed scheme of WNK kinase regulation. NCC is phosphorylated and activated by STE20/SPS1-related proline/alanine-rich kinase (SPAK), which is phosphorylated and activated by WNK4, which is activated by low intracellular chloride concentration. WNKs can interact with a cullin-ring ligase, via the adaptor Kelch-Like 3 (KLHL3), leading to WNK ubiquitination and subsequent degradation by the proteasome. When dephosphorylated, NCC can be removed from the apical plasma membrane.

the protein, or near the carboxyl-terminal domain.³³⁶ These mutations disrupt WNK binding to adaptor proteins that are essential for WNK degradation (see later).^{337–339} Thus both WNK mutant forms of FHHt result in increased abundance of WNKs along the DCT.

The WNK1 and WNK4 proteins are coexpressed within the distal nephron in DCT and CCD cells, where they both localize to the cytoplasm (diffusely, and also in punctate structures) and apical membrane.^{340,341} Although both WNK4 and WNK1 can stimulate NCC activity in expression systems, only deletion of WNK4 has been shown to reduce NCC activity in mice.^{236,237} In mice in which an FHHt-like phenotype has been generated by mutation of the protein KLHL3 (see later), increased WNK1 abundance does not compensate for deletion of WNK4, suggesting a key role for WNK4.³³ Generation of mice with WNK1 deletion specifically in the kidney may shed more light on its contribution to NCC regulation in vivo.

WNKs, especially WNK4, appear to be sensitive to inhibition by chloride,^{342,343} so that when intracellular chloride concentration is low, the stimulatory effect is maximal; when intracellular chloride concentration is higher, there is less stimulation.³⁴⁴ For WNK1, chloride binds to the catalytic site of the kinase and inhibits autophosphorylation and activation of the kinase.³⁴² This chloride binding has a major role in the potassium-sensing function of DCT cells. Reduction in potassium intake and/or hypokalemia lead to reduced basolateral K⁺ concentration in the DCT; the subsequent hyperpolarization is dependent on basolateral KIR4.1-containing K⁺ channels.^{308,311,327} Hyperpolarization has been proposed to lead to chloride exit via basolateral CLC-K2 chloride channels and a reduction in intracellular chloride; the reduction in intracellular chloride activates the SPAK and OSR1-WNK cascade, resulting in phosphorylation of NCC and activation of the transporter.³²⁷ This model helps explain the activating effect of potassium depletion on NCC and the inhibitory effect of potassium loading on NCC, and they go a long way to explain the critical role of the DCT and NCC in potassium homeostasis.³²⁷

To develop in vivo models relevant to FHHt, two groups developed mice expressing WNK4 carrying a mutation that causes the disease. Lalioti and coworkers generated BAC-transgenic mice that is an FHHt mutant of WNK4 (TgWnk4^{PHAI}), bearing a Q562E mutation associated with the disease,³⁴⁵ and Yang and colleagues developed a knock-in mouse expressing D568. Both models were hypertensive,^{345a} with biochemical phenotypes similar to that of FHHt (i.e., hyperkalemia, acidosis, and hypercalciuria). TgWnk4^{PHAI} mice also exhibit marked hyperplasia of the DCT. Of particular significance, the DCT hyperplasia of TgWnk4^{PHAI} mice was completely suppressed on an NCC-deficient background, generated by mating TgWnk4^{PHAI} mice with NCC knockout mice.^{295,296} Therefore the DCT is the primary target for FHHt-associated mutations in WNK4. In addition, as suggested by prior studies, changes in Na⁺-Cl⁻ entry via NCC can evidently modulate hyperplasia or regression of the DCT.^{275,295,296,345} Vidal-Petiot and colleagues have also generated mice that lack the orthologous intron of WNK1 involved in patients with FHHt, recapitulating the phenotype.³³⁵ Treatment with the calcineurin inhibitor tacrolimus has a similar effect as in FHHt.³⁴⁸

WNK proteins are regulated by Cullin 3 (CUL3) and Kelch-like 3 (KLHL3), components of an E3 ubiquitin ligase

complex that targets the WNKs for degradation.^{339,349,350} Mutations in the *CUL3* and *KLHL3* genes also cause FHHt and account for the majority of cases. Disease-associated mutations in KLHL3 abrogate binding to WNK4 and vice versa.³³⁹ In turn, disease-associated mutations in CUL3 may deplete levels of KLHL3, preventing WNK degradation.³⁵¹ Physiologically, phosphorylation of KLHL3 by PKC, downstream of Ang II, also abrogates the interaction between KLHL3 and WNK4, leading to NCC activation.³⁵² More information about the mechanisms of FHHt, and the roles of regulatory proteins can be found in Chapters 17 and 44.

The various mechanistic models for the regulation of NCC by upstream WNK1, WNK4, and the SPAK-OSR1 kinases have recently been reviewed; interactions between WNK4 and both WNK3 and SGK1 also contribute to the complexity, as do CUL3 and KLHL3.^{339,349–356} Competing divergent mechanisms can be reconciled by the likelihood that the physiologic context determines whether WNK4 will have an activating or inhibitory effect on NCC. For example, the activation of NCC by the Ang II receptor type 1 appears to require the downstream activation of SPAK by WNK4.^{315,357} Changes in circulating and local levels of Ang II, aldosterone, vasopressin, and K⁺ are thus expected to have different and often opposing effects on the activity of NCC in the DCT (see also Fig. 6.19 and the “Integrated Na⁺-Cl⁻ and K⁺ Transport in the Distal Nephron” section).^{315,353,357–361}

WNK kinases exhibit effects in expression systems that may seem anomalous, but which likely reflect their pleiotropic properties. In *Xenopus* oocytes, for example, WNK4 can inhibit NCC, through its carboxyl-terminal domain, which binds to protein phosphatase 1.³⁶² It now appears that this effect results from WNK4 inhibiting endogenously expressed WNK kinases in the setting of high intracellular chloride concentrations.³⁶³ WNK4 coexpression with NCC reduces transporter expression at the membrane of both *Xenopus* oocytes and mammalian cells, suggesting a prominent effect on membrane trafficking.^{353,357} The WNK4 kinase activates lysosomal degradation of the transporter protein, rather than inducing dynamin- and clathrin-dependent endocytosis.^{364,365} This occurs through effects of WNK4 on the interaction of NCC with the lysosomal targeting receptor sortilin and AP-3 adaptor complex.^{364,365} Dynamin-dependent endocytosis of NCC is induced by ERK1/2 phosphorylation via activation of H-Ras, Raf, and MEK1/2, resulting in ubiquitination of NCC and endocytosis of the transporter, suggesting a significant role in the down-regulation of NCC by PTH.^{366–368} Ubiquitination of NCC is catalyzed by the ubiquitin-ligase NEDD4-2, causing down-regulation of NCC.³²¹ NCC is highly ubiquitinated at multiple specific sites, but it is unclear whether ubiquitination at all of these sites involves NEDD4-2.³⁶⁹ Ubiquitination at these different sites has different effects on NCC, either modulating its endocytosis or degradation. The full implications of these effects observed in cell culture systems regarding in vivo behavior awaits additional study.

CONNECTING TUBULES AND THE CORTICAL COLLECTING DUCT

Apical Na⁺ Transport

The apical membrane of CNT cells and principal cells contain prominent Na⁺ and K⁺ conductances, without a measurable apical conductance for Cl⁻.^{216,279,370,371} The entry

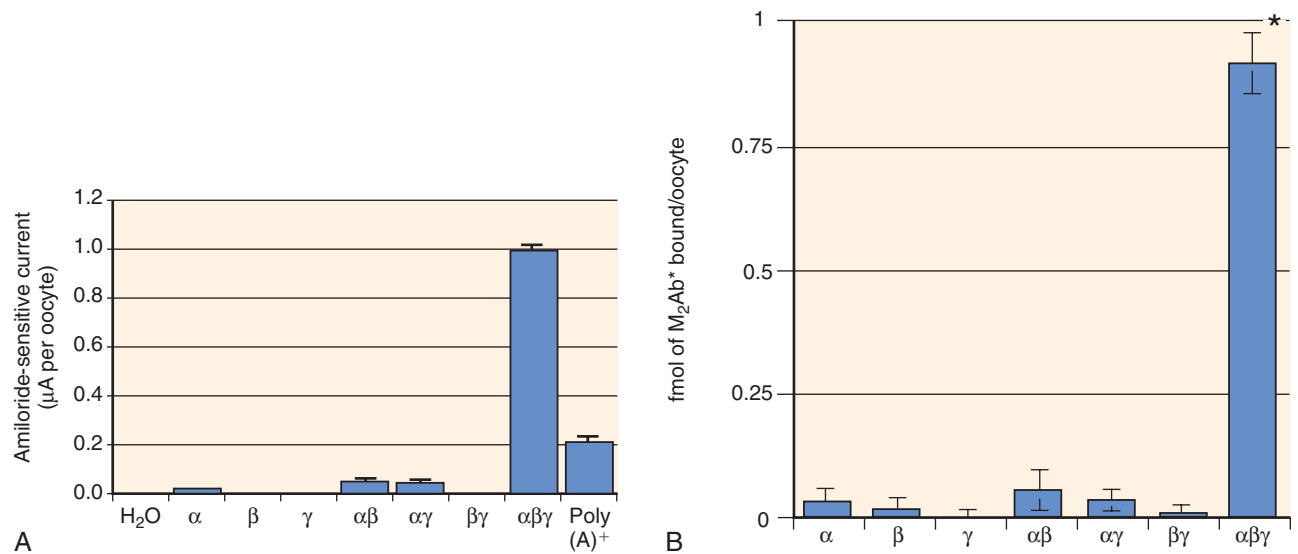


Fig. 6.20 Maximal expression of the amiloride-sensitive epithelial Na⁺ channel (ENaC) at the plasma membrane requires the coexpression of all three subunits (α -, β -, and γ -ENaC). (A) Amiloride-sensitive current in *Xenopus* oocytes expressing the individual subunits and various combinations thereof. (B) Surface expression is markedly enhanced in *Xenopus* oocytes that coexpress all three subunits. The individual complementary DNAs (cDNAs) were engineered with an external epitope tag; expression of the channel proteins at the cell surface is measured by binding of a monoclonal antibody (M₂Ab*) to the tag. Poly A⁺, Polyadenylated messenger RNA (mRNA). (A from Canessa CM, Schild L, Buell G, et al. Amiloride-sensitive epithelial Na⁺ channel is made of three homologous subunits. *Nature*. 1994;367:463–467; B from Firsov, D, Schild L, Gautschi I, et al. Cell surface expression of the epithelial Na channel and a mutant causing Liddle syndrome: a quantitative approach. *Proc Natl Acad Sci U S A*. 1996;93:15370–15375.)

of Na⁺ occurs via the highly selective epithelial Na⁺ channel (ENaC), which is sensitive to micromolar concentrations of amiloride (Fig. 6.20).³⁷² This selective absorption of positive charge generates a lumen-negative PD, the magnitude of which varies considerably as a function of mineralocorticoid status and other factors. This lumen-negative PD serves to drive the following critical processes: (1) K⁺ secretion via apical K⁺ channels; (2) paracellular Cl⁻ transport through the adjacent tight junctions; and/or (3) electrogenic H⁺ secretion via adjacent type A intercalated cells.³⁷³

ENaC is a heteromeric channel complex formed by the assembly of separate, homologous subunits, denoted α -, β -, and γ -ENaC.¹⁴ These channel subunits share a common structure, with intracellular amino- and carboxyl-terminal domains, two transmembrane segments, and a large glycosylated extracellular loop.¹⁴ *Xenopus* oocytes expressing α -ENaC alone have detectable Na⁺ channel activity (Fig. 6.20), which facilitated the initial identification of this subunit by expression cloning; functional complementation of this modest activity was then used to clone the other two subunits by expression cloning.¹⁴ Full channel activity requires the coexpression of all three subunits, which causes a dramatic increase in expression of the channel complex at the plasma membrane (Fig. 6.20).³⁷⁴ The subunit stoichiometry has been a source of considerable controversy, with some reports favoring a tetramer with ratios of two α -ENaC proteins to one each of β - and γ -ENaC (2 α :1 β :1 γ) and others favoring a higher-order assembly with a stoichiometry of 3 α :3 β :3 γ .³⁷⁵ Regardless, the single-channel characteristics of heterologously expressed ENaC are essentially identical to those of the amiloride-sensitive channel detectable at the apical membrane of CCD cells.^{14,372}

ENaC plays a critical role in renal Na⁺-Cl⁻ reabsorption and maintenance of the extracellular fluid volume. In particular, recessive loss-of-function mutations in the three subunits of ENaC are a cause of pseudohypoaldosteronism type I.^{14,376} Patients with this syndrome typically present with severe neonatal salt wasting, hypotension, acidosis, and hyperkalemia; this dramatic phenotype underscores the critical roles of ENaC activity in renal Na⁺-Cl⁻ reabsorption, K⁺ secretion, and H⁺ secretion. Gain-of-function mutations in all three ENaC subunits have been reported to cause Liddle syndrome, an autosomal dominant hypertensive syndrome accompanied by suppressed aldosterone and variable hypokalemia.³⁷⁷ The majority of ENaC mutations associated with Liddle syndrome disrupt interactions between a PPxY motif in the carboxyl-terminus of channel subunits with the NEDD4-2 ubiquitin-ligase leading to increased surface expression of the channel. Mutations in the extracellular loops of α -ENaC and γ -ENaC have also been identified,^{378,379} with the α -ENaC mutation increasing intrinsic activity of the channel.³⁷⁹

The ENaC protein is detectable at the apical membrane of CNT cells and principal cells in the CCD, OMCD, and IMCD.^{281,286} Notably, however, several lines of evidence have supported the hypothesis that the CNT makes the dominant contribution to amiloride-sensitive Na⁺ reabsorption by the distal nephron:

1. Amiloride-sensitive Na⁺ currents in the CNT are twofold to fourfold higher than in the CCD; the maximal capacity of the CNT for Na⁺ reabsorption is estimated to be about 10 times higher than that of the CCD.²⁷⁹
2. Targeted deletion of α -ENaC in the collecting duct abolishes amiloride-sensitive currents in CCD principal

- cells, but does not affect Na^+ or K^+ homeostasis; the residual ENaC expression in the late DCT and CNT of these knockout mice easily compensates for the loss of the channel in CCD cells.³⁸⁰
- $\text{Na}^+\text{-K}^+\text{-ATPase}$ activity in the CCD is considerably less than that of the DCT (see also Fig. 6.4); this speaks to a greater capability for transepithelial $\text{Na}^+\text{-Cl}^-$ absorption by the DCT and CNT.¹⁷
 - The apical recruitment of ENaC subunits in response to dietary Na^+ restriction begins in the CNT, with progressive recruitment of subunits in the downstream CCD at lower levels of dietary Na^+ ; although the CNT plays a dominant role in ENaC-mediated sodium transport, it does so primarily in an aldosterone-independent mechanism, with aldosterone-mediated sodium transport in the CCD involved in the finely tuned regulation of sodium transport.^{381,382}
 - Patch-clamp analysis of knock-in mice homozygous for a Liddle syndrome ENaC mutant showed that the primary site of increased Na^+ reabsorption is the DCT2/CNT rather than the CNT/CCD.³⁸³

Cl^- Transport

There are two major pathways for Cl^- absorption in the CNT and CCD – paracellular transport across the tight junction and transcellular transport across type B intercalated cells (Fig. 6.21).^{280,384} The CNT and CCD are “tight” epithelia, with comparatively low paracellular permeability that is not selective for Cl^- over Na^+ ; however, voltage-driven, paracellular Cl^- transport in the CCD may play a considerable role in transepithelial $\text{Na}^+\text{-Cl}^-$ absorption.³⁸⁵ The CNT, DCT, and collecting duct coexpress claudin-3, -4, and -8; claudin-8 in particular may function as a paracellular cation barrier that prevents backleak of Na^+ , K^+ , and H^+ in this segment of the nephron.^{14,386} Several lines of evidence have indicated that claudin-4 and claudin-8 interact to form a paracellular pathway for Cl^- in the collecting duct, thus mediating transcellular Cl^- absorption via the paracellular pathway.³⁸⁷ CCD-specific knockout of claudin-4 in mice leads to NaCl wasting and hypotension,³⁸⁸ while CCD-specific disruption of claudin-8 causes hypotension, hypokalemia, and metabolic alkalosis, which resembles Gitelman syndrome.³⁸⁹ Regulated changes in paracellular permeability may also contribute to Cl^- absorption by the CNT and CCD. In particular, wild type WNK4 appears to increase paracellular Cl^- permeability in transfected MDCK II cell lines; a WNK4 FHHt mutant has a much larger effect, with no effect seen in cells expressing kinase-dead WNK4 constructs.³⁹⁰ Yamauchi and colleagues have also reported that FHHt-associated WNK4 increases paracellular permeability, due perhaps to an associated hyperphosphorylation of claudin proteins.³⁹¹ The claudin-4-mediated chloride conductance is also negatively regulated by cleavage in its second extracellular loop by channel-activating protease 1 (cap1).³⁸⁸ Similar to WNK4-mediated degradation by CUL3/KLHL3 (see the “Regulation of $\text{Na}^+\text{-Cl}^-$ Transport in the Distal Convoluted Tubule” section), claudin-8 was shown to be a target of KLHL3-mediated degradation, with FHHt-associated KLHL3 displaying impaired interaction.³⁸⁹

Transcellular Cl^- absorption across intercalated cells is thought to play a quantitatively greater role in the CNT and CCD than that of paracellular transport.³⁸⁴ In the simplest

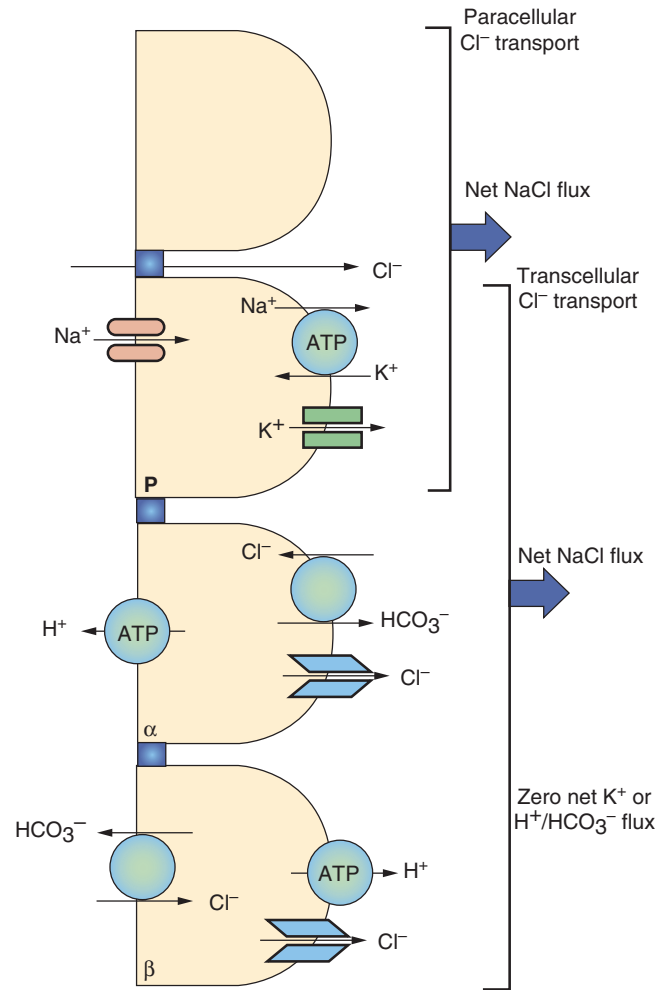


Fig. 6.21 Transepithelial Cl^- transport by principal and intercalated cells. The lumen-negative potential difference (PD) generated by principal cells drives paracellular Cl^- absorption. Alternatively, transepithelial transport occurs in type B intercalated cells via apical $\text{Cl}^-/\text{HCO}_3^-$ exchange (SLC26A4/pendrin) and basolateral Cl^- exit via ClC-K2 . (Modified from Moe OW, Baum M, Berry CA, Rector Jr FC. Renal transport of glucose, amino acids, sodium, chloride, and water. In: Brenner BM, ed. *Brenner and Rector's the Kidney*. Philadelphia: WB Saunders; 2004:413–452.)

scheme, this process requires the concerted function of type A and type B intercalated cells, achieving net electrogenic Cl^- absorption without affecting HCO_3^- or H^+ excretion (see also Fig. 6.21).³⁸⁴ Chloride thus enters type B intercalated cells via apical $\text{Cl}^-/\text{HCO}_3^-$ exchange, followed by exit from the cell via basolateral Cl^- channels. Recycling of Cl^- at the basolateral membrane of adjacent type A intercalated cells also results in HCO_3^- absorption and extrusion of H^+ at the apical membrane. The net effect of apical $\text{Cl}^-/\text{HCO}_3^-$ exchange in type B intercalated cells, leading to apical secretion of HCO_3^- , and recycling of Cl^- at the basolateral membrane type A intercalated cells, leading to apical secretion of H^+ , is electrogenic Cl^- absorption across type B intercalated cells (Fig. 6.21).

At the basolateral membrane, intercalated cells have a very robust Cl^- conductance, with transport characteristics similar to those of $\text{ClC-K2}/\text{Barttin}$.^{216,392} ClC-K2 protein is

also detected at the basolateral membrane of type A intercalated cells, and CLC-K2 activity has been observed in type B cells.^{214,393} The basolateral $\text{Na}^+\text{-K}^+\text{-2Cl}^-$ cotransporter NKCC1 in adjacent type A intercalated cells also plays an evident role in transepithelial Cl^- absorption by the CCD.³⁹⁴ At the apical membrane, the SLC26A4 exchanger (also known as pendrin) has been conclusively identified as the elusive Cl^- - HCO_3^- exchanger of type B and non-A, non-B intercalated cells; this exchanger functions as the apical entry site during transepithelial Cl^- transport by the distal nephron.²⁸⁰ Human *SLC26A4* is mutated in Pendred syndrome, which encompasses sensorineural hearing loss and goiter; these patients do not have an appreciable renal phenotype.²⁸⁰ However, *Slc26a4* knockout mice are sensitive to restriction of dietary $\text{Na}^+\text{-Cl}^-$, developing hypotension during severe restriction.³⁹⁵ *Slc26a4* knockout mice are also resistant to mineralocorticoid-induced hypertension.³⁹⁶ Pendrin has indirect effects on ENaC abundance and activity, apparently by modulating luminal ATP and HCO_3^- concentrations; pendrin and ENaC are also both coactivated by Ang II^{397–400} and pendrin expression is also induced by aldosterone.⁴⁰¹ The overexpression of pendrin in intercalated cells thus causes hypertension in transgenic mice, with an increase in ENaC activity and activity of electroneutral $\text{Na}^+\text{-Cl}^-$ absorption (see later).⁴⁰² Conversely, disruption of pendrin in mice decreased ENaC-mediated Na^+ absorption by reducing channel open probability and channel density at the apical membrane.⁴⁰³ Finally, dietary Cl^- restriction with provision of $\text{Na}^+\text{-HCO}_3^-$ results in Cl^- wasting in *Slc26a4* knockout mice and increased apical expression of SLC26A4 protein in the type B intercalated cells of normal littermate controls.⁴⁰⁴ Several groups have reported that SLC26A4 expression is exquisitely responsive to changes in distal chloride delivery.⁴⁰⁵ Therefore SLC26A4 plays a critical role in distal nephron Cl^- absorption, underlining the particular importance of transcellular Cl^- transport in this process. Of broader relevance, these studies have served to underline the important role for Cl^- homeostasis in the maintenance of extracellular volume and pathogenesis of hypertension.⁴⁰⁵

Electroneutral $\text{Na}^+\text{-Cl}^-$ Cotransport

Thiazide-sensitive $\text{Na}^+\text{-Cl}^-$ cotransport is considered the exclusive provenance of the DCT, which expresses the canonical thiazide-sensitive transporter NCC (see the “Mechanisms of $\text{Na}^+\text{-Cl}^-$ Transport in the Distal Convoluted Tubule” section). However, Tomita and coworkers demonstrated many years ago that approximately 50% of $\text{Na}^+\text{-Cl}^-$ transport in rat CCD is electroneutral, amiloride resistant, and thiazide sensitive.^{406,407} Thiazide-sensitive electroneutral $\text{Na}^+\text{-Cl}^-$ transport has also been demonstrated in mouse CCD.⁴⁰⁸ This transport activity is preserved in CCDs from mice with genetic disruption of NCC and ENaC, indicating independence from the dominant apical Na^+ transport pathways in the distal nephron. This thiazide-sensitive, electroneutral $\text{Na}^+\text{-Cl}^-$ transport appears to be mediated by the parallel activity of the Na^+ -driven SLC4A8 Cl^- - HCO_3^- exchanger and SLC26A4 Cl^- - HCO_3^- exchanger (pendrin; see earlier discussion).⁴⁰⁸ *Slc4a8* knockout mice display only a mild perturbation of $\text{Na}^+\text{-Cl}^-$ and water balance due to compensation by NCC; combined SLC4A8 and NCC disruption caused intravascular volume contraction and hypokalemia.⁴⁰⁹ Notably, however, heterologously expressed recombinant SLC4A8 and SLC26A4 are resistant

and partially sensitive to thiazide, respectively, such that the in vivo pharmacology of this electroneutral $\text{Na}^+\text{-Cl}^-$ absorption is not completely explained. Immunolocalization of Slc4a8 within the CCD has been problematic; hence, it is unknown whether SLC4A8 and SLC26A4 are coexpressed in type B intercalated cells. Regardless, the combined activity of SLC4A8 and SLC26A4 appears to play a major role in $\text{Na}^+\text{-Cl}^-$ transport within the CCD, with significant implications for $\text{Na}^+\text{-Cl}^-$ and K^+ homeostasis (see also the “Integrated $\text{Na}^+\text{-Cl}^-$ and K^+ Transport in the Distal Nephron” section).

The apical entry of Na^+ via SLC4A8 requires a basolateral exit of Na^+ in type B intercalated cells, evidently mediated by the basolateral $\text{Na}^+\text{-HCO}_3^-$ transporter SLC4A9.² Another puzzle was the energetics of transcellular $\text{Na}^+\text{-Cl}^-$ transport in intercalated cells, which possess minimal, if any, detectable $\text{Na}^+\text{-K}^+\text{-ATPase}$ activity. A series of elegant experiments have revealed that electroneutral $\text{Na}^+\text{-Cl}^-$ transport in type B intercalated cells is energized by and thus dependent on the activity of the basolateral $\text{H}^+\text{-ATPase}$.² Type B intercalated cells are therefore unique among mammalian renal epithelial cells in that transcellular ion transport is driven by $\text{H}^+\text{-ATPase}$ rather than $\text{Na}^+\text{-K}^+\text{-ATPase}$ activity.

REGULATION OF $\text{Na}^+\text{-Cl}^-$ TRANSPORT IN THE CONNECTING TUBULE AND CORTICAL COLLECTING DUCT

Aldosterone

The DCT, CNT, and collecting ducts collectively constitute the aldosterone-sensitive distal nephron, expressing the mineralocorticoid receptor and $11\beta\text{-HSD2}$ enzyme that protects against illicit activation by glucocorticoids.²⁷⁵ Aldosterone plays a dominant positive role in the regulation of distal nephron $\text{Na}^+\text{-Cl}^-$ transport, with a plethora of mechanisms and transcriptional targets.⁴¹⁰ For example, aldosterone increases the expression of the $\text{Na}^+\text{-K}^+\text{-ATPase}$ α_1 - and β_1 -subunits in the CCD, in addition to inducing SLC26A4, the apical Cl^- - HCO_3^- exchanger of intercalated cells.^{396,411} Aldosterone may also affect paracellular permeability of the distal nephron via posttranscriptional modification of claudins and other components of the tight junction.⁴¹² However, particularly impressive progress has been made in the understanding of the downstream effects of aldosterone on synthesis, trafficking, and membrane-associated activity of ENaC subunits. A detailed discussion of aldosterone’s actions may be found in Chapter 12; here we summarize the major findings of relevance to $\text{Na}^+\text{-Cl}^-$ transport.

Aldosterone increases abundance of α -ENaC via a glucocorticoid response element in the promoter of the *SCNN1A* gene that encodes this subunit.⁴¹³ Aldosterone also relieves a tonic inhibition of the *SCNN1A* gene by a complex that includes the Dot1a (disruptor of telomere silencing splicing variant *a*) and AF9 and AF17 transcription factors.⁴¹⁴ An aldosterone-dependent reduction in promoter methylation is also involved.⁴¹⁵ This transcriptional activation results in an increased abundance of α -ENaC protein in response to exogenous aldosterone or dietary $\text{Na}^+\text{-Cl}^-$ restriction (Fig. 6.22); the response to $\text{Na}^+\text{-Cl}^-$ restriction is blunted by spironolactone, indicating involvement of the mineralocorticoid receptor.^{416–418} At baseline, α -ENaC transcripts in the kidney are less abundant than those encoding β - and γ -ENaC⁴¹⁹ (Fig. 6.22). All three subunits are required for efficient processing

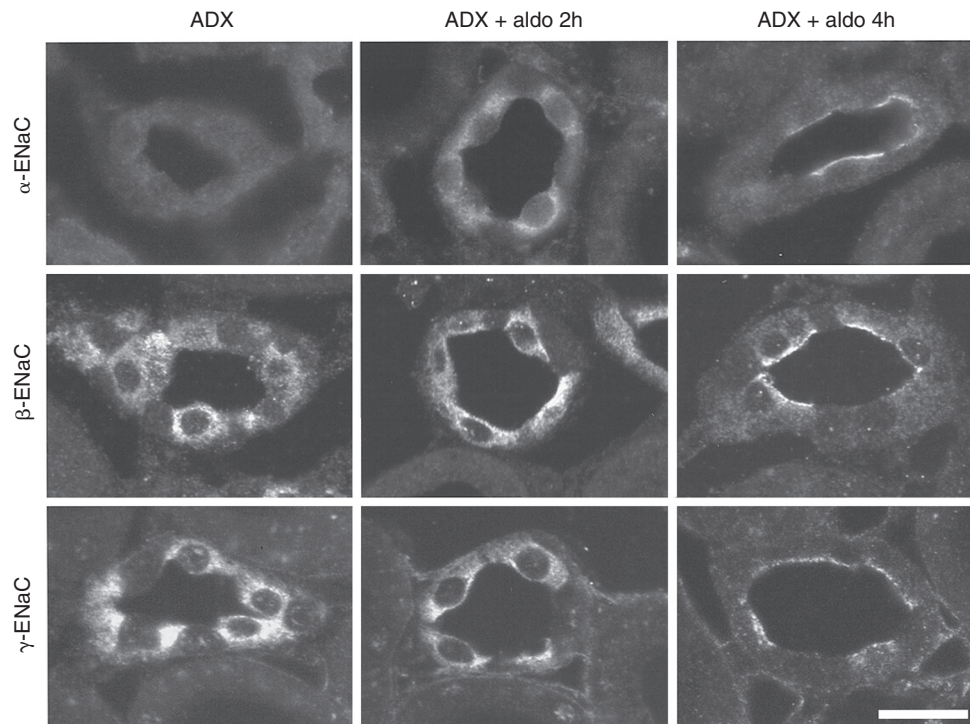


Fig. 6.22 Immunofluorescence images of connecting tubule profiles in kidneys from adrenalectomized rats (ADX) and from ADX rats 2 and 4 hours after aldosterone (aldo) injection. Antibodies against the α , β , and γ subunits of epithelial Na^+ channel (ENaC) reveal absent expression of the former in ADX rats, with progressive induction by aldosterone. All three subunits traffic to the apical membrane in response to aldosterone. This coincides with rapid aldosterone induction of the SGK kinase in the same cells; SGK is known to increase the expression of ENaC at the plasma membrane (see text for details). Bar \equiv 15 μm . (From Loffing J, Zecevic M, Féraille E, et al. Aldosterone induces rapid apical translocation of ENaC in early portion of renal collecting system: possible role of SGK. *Am J Physiol Renal Physiol*. 2001;280:F675–F682.)

of heteromeric channels in the endoplasmic reticulum and trafficking to the plasma membrane (Fig. 6.20), such that the induction of α -ENaC is thought to relieve a major bottleneck in the processing and trafficking of active ENaC complexes.⁴¹⁹

Aldosterone also plays an indirect role in the regulated trafficking of ENaC subunits to the plasma membrane via the regulation of accessory proteins that interact with preexisting ENaC subunits. Aldosterone rapidly induces expression of a serine-threonine kinase denoted SGK1 (serum and glucocorticoid-induced kinase-1); coexpression of SGK1 with ENaC subunits in *Xenopus* oocytes results in a dramatic activation of the channel due to increased expression at the plasma membrane.^{418,420,421} Notably, an analogous redistribution of ENaC subunits occurs in the CNT and early CCD, from a largely cytoplasmic location during dietary $\text{Na}^+\text{-Cl}^-$ excess to a purely apical distribution after aldosterone or $\text{Na}^+\text{-Cl}^-$ restriction (Fig. 6.22).^{381,416,418} Furthermore, there is a temporal correlation between the appearance of induced SGK1 protein in the CNT and the redistribution of ENaC protein to the plasma membrane.⁴¹⁸

SGK1 modulates membrane expression of ENaC by interfering with regulated endocytosis of its channel subunits. Specifically, the kinase interferes with interactions between ENaC subunits and the ubiquitin ligase NEDD4-2.⁴¹⁹ PPxY domains in the C termini of all three ENaC subunits bind to WW domains of NEDD4-2⁴²²; these PPxY domains are deleted, truncated, or mutated in patients with Liddle syndrome, leading to a gain of function in channel activity.^{374,377} Coexpres-

sion of NEDD4-2 with the wild type ENaC channel results in a marked inhibition of channel activity due to retrieval from the cell membrane, whereas channels bearing Liddle syndrome mutations are resistant; NEDD4-2 is thought to ubiquitinate ENaC subunits, resulting in the removal of channel subunits from the cell membrane and degradation in lysosomes and the proteasome.⁴¹⁹ A PPxY domain in SGK1 also binds to NEDD4-2, which is a phosphorylation substrate for the kinase; phosphorylation of NEDD4-2 by SGK1 abrogates its inhibitory effect on ENaC subunits.^{423,424} Aldosterone also stimulates NEDD4-2 phosphorylation in vivo.⁴²⁵ NEDD4-2 phosphorylation in turn results in ubiquitin-mediated degradation of SGK1, suggesting that there is considerable feedback regulation in this system.⁴²⁶ Aldosterone also reduces NEDD4-2 protein expression in cultured CCD cells, and acetylation of ENaC antagonizes ENaC ubiquitination, suggesting additional levels of in vivo regulation.^{427,428}

The induction of SGK1 by aldosterone thus appears to stimulate the redistribution of ENaC subunits from the cytoplasm to the apical membrane of CNT and CCD cells. This phenomenon involves SGK1-dependent phosphorylation of the NEDD4-2 ubiquitin ligase, which is coexpressed with ENaC and SGK1 in the distal nephron.⁴²⁷ Of note, there is considerable axial heterogeneity in the recruitment and redistribution of ENaC to the plasma membrane, which begins in the CNT and only extends into the CCD and OMCD in $\text{Na}^+\text{-Cl}^-$ -restricted or aldosterone-treated animals.^{275,418} The underlying causes of this progressive axial recruitment are not as yet clear.²⁷⁵ However, NEDD4-2 expression is inversely

related to the apical distribution of ENaC, with low expression in the CNT and increased expression levels in the CCD. In all likelihood, the relative balance among SGK1, ENaC, and NEDD4-2 figures prominently in the recruitment of the channel subunits to the apical membrane.⁴²⁷

NEDD4-2 and ENaC are part of a larger regulatory complex that includes the signaling protein Raf-1, stimulatory aldosterone-induced chaperone GILZ1 (glucocorticoid-induced leucine zipper-1), and scaffolding protein CNK3.^{429,430} The mTORC2 (mammalian target of rapamycin complex 2) kinase complex is another component, catalyzing upstream activation of SGK1 and thus inducing activation of ENaC.^{431,432}

Although many studies have supported a central role for SGK1 in mediating the effects of aldosterone on ENaC, a recent study found that despite altered apical trafficking of ENaC in SGK1 knockout mice, ENaC activity is normal even after aldosterone administration. This suggests that other aldosterone-induced proteins play a role in ENaC activation via mineralocorticoid receptors.^{433,434} For example, another aldosterone-induced protein, Ankyrin G, a cytoskeletal protein involved in vesicular trafficking, increases ENaC activity in cultured CCD cells by promoting its plasma membrane insertion from recycling endosomes.⁴³⁵

Finally, aldosterone indirectly activates ENaC channels through the induction of channel-activating proteases, which increase open channel probability by cleavage of the extracellular domains of α - and γ -ENaC. Western blotting of renal tissue from rats subjected to Na⁺-Cl⁻ restriction or treatment with aldosterone has revealed α - and γ -ENaC subunits of lower molecular mass than those detected in control animals, indicating that aldosterone induces proteolytic cleavage.^{417,436} Proteases that have been implicated in the processing of ENaC include furin, elastase, and three membrane-associated proteases denoted CAP1–3 (channel activating proteases-1, -2, and -3).^{437–439} Filtered proteases such as plasmin may also contribute to ENaC activation in nephrotic syndrome.⁴³⁹ CAP1 was initially identified from *Xenopus* A6 cells as an ENaC-activating protease; the mammalian ortholog is an aldosterone-induced protein in principal cells.^{440,441} Urinary excretion of CAP1, also known as prostaticin, is increased in hyperaldosteronism, with a reduction after adrenalectomy.⁴⁴¹ CAP1 is tethered to the plasma membrane by a GPI linkage, whereas CAP2 and CAP3 are transmembrane proteases.^{438,440} All three of these proteases activate ENaC by increasing the P_o of the channel, without increasing expression at the cell surface.⁴³⁸ However, analysis of CAP2 knockout mice indicates that it does not play a role in ENaC regulation and sodium balance in vivo.⁴⁴² Proteolytic cleavage of ENaC appears to activate the channel by removing the self-inhibitory effect of external Na⁺; in the case of furin-mediated proteolysis of α -ENaC, this appears to involve the removal of an inhibitory domain from within the extracellular loop.^{438,443} Extracellular Na⁺ appears to interact with a specific acidic cleft in the extracellular loop of α -ENaC, causing inhibition of the channel.⁴⁴⁴ The structures of the extracellular domains of ENaC and related channels resemble an outstretched hand holding a ball, with defined subdomains termed the “wrist,” “finger,” “thumb,” “palm,” “ β -ball,” and “knuckle”; functionally relevant proteolytic events target the finger domains of ENaC subunits.⁴³⁹ Unprocessed channels at the plasma membrane are thought to function as a reserve pool, capable of rapid activation by membrane-associated luminal proteases.⁴³⁷

Vasopressin and Other Factors

Although not typically considered an antinatriuretic hormone, vasopressin has well-characterized stimulatory effects on Na⁺-Cl⁻ transport by the CCD.^{94,445} Vasopressin directly activates ENaC in murine CCD, increasing the open probability (P_o) of the channel.⁴⁴⁶ In perfused rat CCD segments, vasopressin and aldosterone can have synergistic effects on Na⁺ transport, with a combined effect that exceeds that of the individual hormones.⁴⁴⁵ In addition, water and Na⁺ restriction synergistically increase the P_o of ENaC in murine CCDs.⁴⁴⁶ Prostaglandins inhibit this effect of vasopressin, particularly in the rabbit CCD; this inhibition occurs at least in part through reductions in vasopressin-generated cAMP.^{94,445} There are, however, considerable species-dependent differences in the interactions between vasopressin and negative modulators of Na⁺-Cl⁻ transport in the CCD, which include prostaglandins, bradykinin, endothelin, and α_2 -adrenergic tone.^{94,445} Regardless, cAMP causes a rapid increase in the Na⁺ conductance of apical membranes in the CCD; this effect appears to be due to increases in the surface expression of ENaC subunits at the plasma membrane⁴⁴⁷ in addition to effects on open channel probability.^{446,448} Notably, cAMP inhibits retrieval of ENaC subunits from the plasma membrane via PKA-dependent phosphorylation of the phosphoacceptor sites in NEDD4-2 that are targeted by SGK1; therefore both aldosterone and vasopressin converge on NEDD4-2 in the regulation of ENaC activity in the distal nephron.⁴⁴⁹ Analogous to the effect on trafficking of aquaporin-2 in principal cells, cAMP also seems to stimulate exocytosis of ENaC subunits to the plasma membrane.⁴⁴⁸ Finally, similar to the long-term effects of vasopressin on aquaporin-2 expression and NKCC2 expression, chronic treatment with DDAVP results in an increase in abundance of the β - and γ -ENaC subunits.^{233,450}

The activation of ENaC by vasopressin appears to have additional direct effects on water homeostasis. Hypernatremic mice treated with the ENaC inhibitor benzamil thus exhibit further increases in tonicity due to a reduction in urinary osmolality.⁴⁵¹ In adrenalectomized mice, which lack circulating aldosterone, vasopressin maintains ENaC activity in the distal nephron.⁴⁵² This vasopressin-dependent activation of ENaC may, by extension, play a role in generating hyponatremia in the setting of primary adrenal failure. Systemic generation of circulating Ang II induces aldosterone release by the adrenal gland, with downstream activation of ENaC. However, Ang II also directly activates amiloride-sensitive Na⁺ transport in perfused CCDs; blockade by losartan or candesartan suggests that this activation is mediated by Ang II receptors type 1.⁴⁵³ Of particular significance, the effect of luminal Ang II (10⁻⁹ M) was greater than that of bath Ang II, suggesting that intratubular Ang II may regulate ENaC in the distal nephron. Ang II also activates chloride absorption across intercalated cells via a pendrin (SLC26A4) and an H⁺-ATPase-dependent mechanism.⁴⁵⁴ Stimulation of ENaC is seen when tubules are perfused with Ang I; this effect is blocked by ACE inhibition with captopril, suggesting that intraluminal conversion of Ang I to Ang II can occur in the CCD.⁴⁵⁵ Notably, CNT cells express considerable amounts of immunoreactive renin versus the vanishingly low expression of renin mRNA in the PT.⁴⁵⁶ Angiotensinogen secreted into the tubule by PT cells may thus be converted to Ang II in the CNT via locally generated renin and ACE and/or related proteases.⁴⁵⁶

Luminal perfusion with ATP or uridine triphosphate (UTP) inhibits amiloride-sensitive Na^+ transport and reduces ENaC P_o in the CCD via activation of luminal P2Y_2 purinergic receptors.^{457,458} Targeted deletion of the murine P2Y_2 receptor results in salt-resistant hypertension due in part to an upregulation of NKCC2 activity in the TAL; resting ENaC activity is also increased, but suppressed aldosterone and downregulation of the α -subunit of ENaC blunts the role of amiloride-sensitive transport.^{458,459} Clamping mineralocorticoid activity at higher levels, via the administration of exogenous mineralocorticoid, reveals that P2Y_2 receptor activation may be a major mechanism for the modulation of ENaC P_o in response to changes in dietary $\text{Na}^+\text{-Cl}^-$.³²³ Increased dietary $\text{Na}^+\text{-Cl}^-$ thus leads to increased urinary ATP and UTP excretion in mice⁴⁵⁸; endogenous ATP from principal cells inhibits ENaC, and ENaC activity is not responsive to increased dietary $\text{Na}^+\text{-Cl}^-$ in P2Y_2 receptor knockout mice.^{323,458} In addition, the activation of apical ionotropic purinergic receptors, likely P2X_4 and/or $\text{P2X}_4/\text{P2X}_6$, can inhibit or activate ENaC, depending on luminal Na^+ concentration; these receptors may also participate in fine-tuning ENaC activity in response to dietary $\text{Na}^+\text{-Cl}^-$.⁴⁶⁰

As in other segments of the nephron, $\text{Na}^+\text{-Cl}^-$ transport by the CNT and CCD is modulated by metabolites of arachidonic acid generated by cytochrome P450 monooxygenases. In particular, arachidonic acid inhibits ENaC channel activity in the rat CCD via generation of the epoxygenase product 11,12-EET by the CYP2C23 enzyme expressed in principal cells.⁴⁶¹ Targeted deletion of the murine *Cyp4a10* gene, encoding, another P450 monooxygenase, results in salt-sensitive hypertension; urinary excretion of 11,12-EET is reduced in these knockout mice, with a blunted effect of arachidonic acid on ENaC channel activity in the CCD.⁴⁶² These mice also became normotensive after treatment with amiloride, indicative of *in vivo* activation of ENaC. It appears that deletion of *Cyp4a10* reduces activity of the murine ortholog of rat CYP2C23 (*Cyp2c44* in mouse) and/or related epoxygenases via reduced generation of a ligand for PPAR α (peroxisome proliferator-activated receptor α) that induces epoxygenase activity.⁴⁶² The mechanism(s) whereby 11,12-EET inhibits ENaC are unknown as yet. However, renal 11,12-EET production is known to be salt-sensitive, suggesting that generation of this mediator may serve to reduce ENaC activity during high dietary $\text{Na}^+\text{-Cl}^-$ intake.⁴⁶¹

Finally, activation of PPAR γ by thiazolidinediones (TZDs) results in amiloride-sensitive hypertension, suggesting *in vivo* activation of ENaC.^{463,464} TZDs (e.g., rosiglitazone, pioglitazone, troglitazone) are insulin-sensitizing drugs used for the treatment of type II diabetes. Treatment with these agents is frequently associated with fluid retention, suggesting an effect on renal $\text{Na}^+\text{-Cl}^-$ transport. Given robust expression of PPAR γ in the collecting duct, activation of ENaC was an attractive hypothesis for this TZD-associated edema syndrome.^{463,464} This appears to be the case, in that selective deletion of the murine PPAR γ gene in principal cells abrogates the increase in amiloride-sensitive transport seen in response to TZDs.^{463,464} Conversely, mice with disruption of α -ENaC specifically along CNT/CCD display blunted increases in total body water and extracellular fluid volume in response to rosiglitazone administration, providing direct evidence that the effects of PPAR γ are mediated through ENaC.⁴⁶⁵ TZDs appear to induce transcription of the *Scn1g* gene encoding γ -ENaC in addition

to inducing SGK1; targeted deletion of SGK1 in knockout mice attenuates but does not abolish TZD-associated edema.^{463,466,467} Notably, however, other studies have failed to detect an effect of TZDs on ENaC activity, which may instead activate a nonspecific cation channel within the IMCD.^{468,469} Regardless, the beneficial effect of spironolactone in type II diabetics with TZD-associated volume expansion is consistent with *in vivo* activation of $\text{Na}^+\text{-Cl}^-$ absorption in the aldosterone-responsive distal nephron.⁴⁷⁰ In addition, the risk of peripheral edema is increased considerably in patients treated with both TZDs and insulin therapy. Notably, insulin appears to activate ENaC via SGK1-dependent mechanisms; PPAR γ is required for the full activating effect of insulin on ENaC, such that this clinical observation may reflect synergistic activation of ENaC by insulin and TZDs.^{468,471,472}

POTASSIUM TRANSPORT

Maintenance of K^+ balance is important for a multitude of physiologic processes. Changes in intracellular K^+ affect cell volume regulation, regulation of intracellular pH, enzymatic function, protein synthesis, DNA synthesis, and apoptosis.¹⁴ Changes in the ratio of intracellular to extracellular K^+ affect the resting membrane potential, leading to depolarization in hyperkalemia and hyperpolarization in hypokalemia. Thus, disorders of extracellular K^+ have a dominant effect on excitable tissues, chiefly heart and muscle. In addition, a growing body of evidence has implicated hypokalemia and/or reduced dietary K^+ in the pathobiology of hypertension, heart failure, and stroke; these and other clinical consequences of K^+ disorders are reviewed in Chapter 17.

Potassium is predominantly an intracellular cation, with only 2% of total body K^+ residing in the extracellular fluid. Extracellular K^+ is maintained within a very narrow range by three primary mechanisms. First, the distribution of K^+ between the intracellular and extracellular space is determined by the activity of a number of transport pathways—namely, $\text{Na}^+\text{-K}^+\text{-ATPase}$, the $\text{Na}^+\text{-K}^+\text{-2Cl}^-$ cotransporter NKCC1, the four KCCs, and a plethora of K^+ channels. In particular, skeletal muscle contains as much as 75% of total body potassium and exerts considerable influence on extracellular K^+ . Short-term and long-term regulation of muscle $\text{Na}^+\text{-K}^+\text{-ATPase}$ play a dominant role in determining the distribution of K^+ between the intracellular and extracellular spaces; the various hormones and physiologic conditions that affect the uptake of K^+ by skeletal muscle are reviewed in Chapter 17. Second, the colon has the ability to absorb and secrete K^+ , with considerable mechanistic and regulatory similarities to renal K^+ secretion. K^+ secretion in the distal colon is increased after dietary loading and in end-stage renal disease.^{14,473,474} However, the colon has a relatively limited capacity for K^+ excretion, such that changes in renal K^+ excretion play the dominant role in responding to changes in K^+ intake. In particular, regulated K^+ secretion by the CNT and CCD plays a critical role in the response to hyperkalemia and K^+ loading; increases in the reabsorption of K^+ by intercalated cells of the CCD and OMCD function in the response to hypokalemia or K^+ deprivation.

This section reviews the mechanisms and regulation of transepithelial K^+ transport along the nephron. As in other sections of this chapter, the emphasis is on particularly recent

developments in the molecular physiology of renal K^+ transport. Of note, transport pathways for K^+ play important roles in renal Na^+-Cl^- transport, particularly within the TAL. Furthermore, Na^+ absorption via ENaC in the aldosterone-sensitive distal nephron generates a lumen-negative PD that drives distal K^+ excretion. These pathways are primarily discussed in the section on renal Na^+-Cl^- transport; related issues relevant to K^+ homeostasis per se will be specifically addressed in this section.

PROXIMAL TUBULE

The PT reabsorbs some 50% to 70% of filtered K^+ (Fig. 6.23). PTs generate minimal transepithelial K^+ gradients, and fractional reabsorption of K^+ is similar to that of Na^+ .²⁸² K^+ absorption follows that of fluid, Na^+ , and other solutes, such that this nephron segment does not play a direct role in regulated renal excretion.^{475,476} Notably, however, changes in Na^+-Cl^- reabsorption by the PT have considerable effects on distal tubular flow and distal tubular Na^+ delivery, with attendant effects on the excretory capacity for K^+ (see the section “Distal Nephron, K^+ secretion” below).

The mechanisms involved in transepithelial K^+ transport by the PT are not completely clear, although active transport does not appear to play a major role.^{476,477} Luminal barium has modest effects on transepithelial K^+ transport by the PT, suggesting a component of transcellular transport via barium-sensitive K^+ channels.⁴⁷⁸ However, the bulk of K^+ transport is thought to occur via the paracellular pathway, driven by the lumen-positive PD in the mid to late PT (Fig. 6.2).^{478,479} The total K^+ permeability of the PT is thus rather high, apparently due to features of the paracellular pathway.^{478,479}

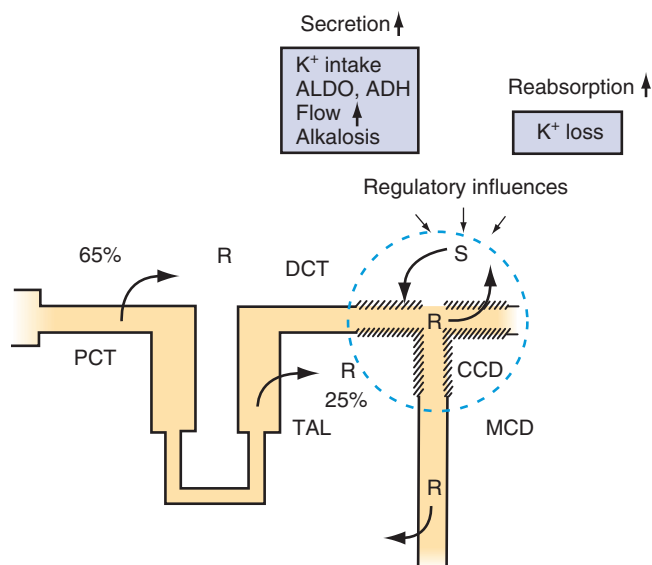


Fig. 6.23 K^+ transport along the nephron. Approximately 90% of filtered K^+ is reabsorbed by the proximal tubule and the loop of Henle. K^+ is secreted along the initial and cortical collecting duct. Net reabsorption occurs in response to K^+ depletion, primarily within the medullary collecting duct. *ADH*, Antidiuretic hormone; *ALDO*, aldosterone; *CCD*, cortical collecting duct; *DCT*, distal convoluted tubule; *MCD*, medullary collecting duct; *PCT*, proximal convoluted tubule; *R*, reabsorption; *S*, secretion; *TAL*, thick ascending limb.

The combination of luminal K^+ concentrations that are about 10% higher than that of plasma, a lumen-positive PD of about 2 mV (Fig. 6.2), and high paracellular permeability leads to considerable paracellular absorption in the PT. This absorption is thought to primarily proceed via convective transport—solvent drag due to frictional interactions between water and K^+ —rather than diffusional transport.⁴⁸⁰ Notably, however, the primary pathway for water movement in the PT is conclusively transcellular via aquaporin-1 and aquaporin-7 water channels in the apical and basolateral membrane.^{19,34,35} Therefore the apparent convective transport of K^+ would have to constitute so-called pseudosolvent drag, with hypothetical uncharacterized interactions between water traversing the transcellular route and diffusion of K^+ along the paracellular pathway.⁴⁸⁰

LOOP OF HENLE

Transport by the loop of Henle plays a critical role in medullary K^+ recycling (Fig. 6.24). Several lines of evidence have indicated that a considerable fraction of K^+ secreted by the CCD is reabsorbed by the medullary collecting ducts and then secreted into the late PT and/or descending thin

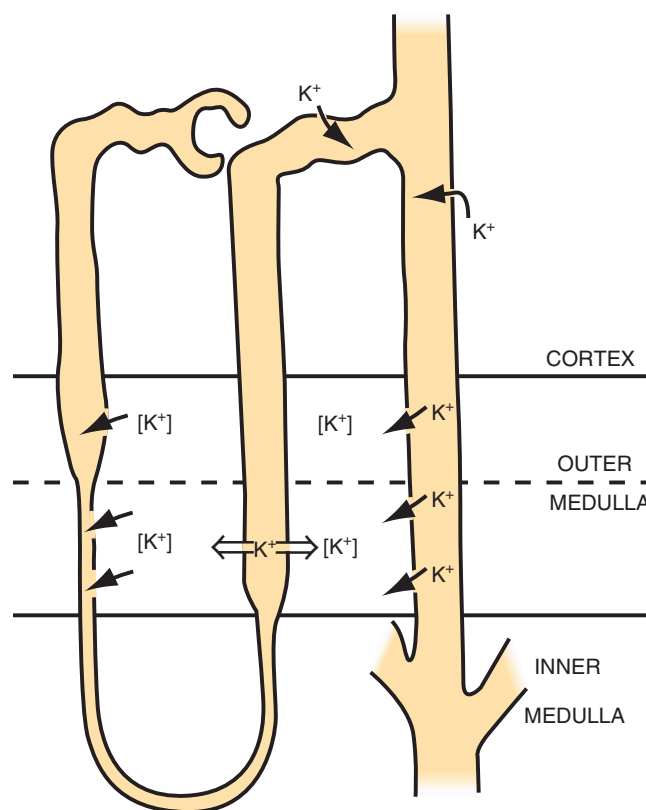


Fig. 6.24 Schematic representation of medullary K^+ recycling. Medullary interstitial K^+ increases considerably after dietary K^+ loading due to the combined effects of secretion in the cortical collecting duct, absorption in the outer medullary collecting duct, thick ascending limb, and inner medullary collecting duct, and secretion in the descending thin limb. See text for details. (From Stokes JB. Consequences of potassium recycling in the renal medulla. Effects of ion transport by the medullary thick ascending limb of the loop of Henle. *J Clin Invest.* 1982;70:219–229.)

limbs of long-looped nephrons.⁴⁸¹ In potassium-loaded rats, there is thus a doubling of luminal K^+ in the terminal thin descending limbs, with a sharp drop after inhibition of CCD K^+ secretion by amiloride.⁴⁸² Enhancement of CCD K^+ secretion by treatment with DDAVP also results in an increase in luminal K^+ in the descending thin limbs.⁴⁸³ This recycling pathway (secretion in CCD, absorption in OMCD and IMCD, secretion in descending thin limb) is associated with a marked increase in medullary interstitial K^+ . Passive transepithelial K^+ absorption by the thin ascending limb and active absorption by the TAL also contribute to this increase in interstitial K^+ (Fig. 6.24).¹⁸¹ Specifically, the absorption of K^+ by the ascending thin limb, TAL, and OMCD exceeds the secretion by the descending thin limbs, thus trapping K^+ in the interstitium.

The physiologic significance of medullary K^+ recycling is not completely clear. However, an increase in interstitial K^+ concentration from 5 to 25 mmol/L dramatically inhibits Cl^- (and to a lesser extent, Na^+) transport by perfused TALs.¹⁸¹ By inhibiting Na^+Cl^- absorption by the TAL, increases in interstitial K^+ contribute to the well-documented diuretic effects of a high- K^+ diet,⁴⁸⁴ and would increase Na^+ delivery to the CNT and CCD, thus enhancing the lumen-negative PD in these tubules and increasing K^+ secretion.¹⁸¹ Alternatively, the marked increase in medullary interstitial K^+ after dietary K^+ loading serves to limit the difference between luminal and peritubular K^+ in the CCD, thus minimizing passive K^+ loss from the collecting duct.

K^+ is secreted into the descending thin limbs by passive diffusion, driven by the high medullary interstitial K^+ concentration. Descending thin limbs thus have a very high- K^+ permeability, without evidence for active transepithelial K^+ transport.⁴⁸⁵ Transepithelial K^+ transport by ascending thin limbs has not to our knowledge been measured; however, as is the case for Na^+Cl^- transport (see the “[Na⁺Cl⁻ Transport by the Thin Ascending Limb](#)” section), the absorption of K^+ by the thin ascending limbs is presumably passive. Active transepithelial K^+ transport across the TAL includes a transcellular component, via apical $Na^+K^+2Cl^-$ cotransport mediated by NKCC2, and a paracellular pathway (Fig. 6.14). Luminal K^+ channels play a critical role in generating the lumen-positive PD in the TAL, as summarized earlier (see the “[Na⁺Cl⁻ Transport by the Thick Ascending Limb: Apical K⁺ Channels](#)” section). Secretion of K^+ through these may also play a role in the response to high dietary K^+ . Patch-clamp analysis of split-open TALs revealed that 70-pS ROMK exhibited a higher open probability (P_o) in mice placed on a low- Na^+ /high- K^+ diet.⁴⁸⁶ This may be dependent on NKCC2 activity, because micropuncture showed that furosemide increased K^+ secretion in the early distal tubule in mice on a normal diet, but decreased it in mice on the low- Na^+ /high- K^+ diet.

DISTAL NEPHRON

K^+ SECRETION

Approximately 90% of filtered K^+ is reabsorbed by the PT and loop of Henle (Fig. 6.23); the fine-tuning of renal K^+ excretion occurs in the remaining distal nephron. The bulk of regulated secretion occurs in principal cells within the CNT and CCD, whereas K^+ reabsorption primarily occurs in the OMCD (see later). A low rate of K^+ secretion is initially detectable in the early DCT, in which NCC-positive cells

express ROMK, the apical K^+ secretory channel.^{190,487} Generally, the CCD is considered the primary site for distal K^+ secretion, partially due to the greater ease with which this segment is perfused and studied. However, as is the case for Na^+Cl^- absorption (see the “[Connecting Tubules and the Cortical Collecting Duct: Apical Na⁺ Transport](#)” section), the bulk of distal K^+ secretion appears to occur prior to the CCD, within the CNT.^{282,371}

In principal cells, apical Na^+ entry via ENaC generates a lumen-negative PD, which drives passive K^+ exit through apical K^+ channels. Distal K^+ secretion is therefore dependent on delivery of adequate luminal Na^+ to the CNT and CCD, essentially ceasing when luminal Na^+ drops below 8 mmol/L.^{488–490} Dietary Na^+ intake also influences K^+ excretion, such that excretion is enhanced by excess Na^+ intake and reduced by Na^+ restriction.^{488,489} Secreted K^+ enters principal cells via the basolateral $Na^+K^+ATPase$, which also generates the gradient that drives apical Na^+ entry via ENaC (Fig. 6.23).

Two major subtypes of apical K^+ channels function in secretion by the CNT and CCD, with or without the DCT; a small-conductance (SK), 30-pS channel and a large-conductance, Ca^{2+} -activated, 150-pS (maxi-K or BK) channel.^{191,371,491} The density and high P_o of the SK channel indicates that this pathway alone is sufficient to mediate the bulk of K^+ secretion in the CCD under baseline conditions—hence, its designation as the secretory K^+ channel.⁴⁹² Notably, SK channel density is considerably higher in the CNT than in the CCD, consistent with the greater capacity for Na^+ absorption and K^+ secretion in the CNT.³⁶ The characteristics of the SK channel are similar to those of the ROMK K^+ channel, and ROMK protein has been localized at the apical membrane of principal cells.^{188,493} SK channel activity is absent from apical membranes of the CCD in homozygous knockout mice with a targeted deletion of the *Kcnj1* gene that encodes ROMK, definitive proof that ROMK is the SK channel.¹⁹¹ The observation that these knockout mice are normokalemic, with an increased excretion of K^+ , illustrates the considerable redundancy in distal K^+ secretory pathways; distal K^+ secretion in these mice is mediated by apical BK channels (see later).^{191,494} However, dietary K^+ loading induced hyperkalemia in ROMK1 knockout mice, consistent with a role in K^+ secretion along the CCD.¹⁹³ Of interest, loss-of-function mutations in human *KCNJ1* genes are associated with Bartter syndrome; ROMK expression is critical for the 30- and 70-pS channels that generate the lumen-positive PD in the TAL (Fig. 6.14).^{191,192} These patients typically have slightly higher serum K^+ levels than those with other genetic forms of Bartter syndrome, and affected patients with severe neonatal hyperkalemia have also been described; this neonatal hyperkalemia is presumably the result of a transient developmental deficit in apical BK channel activity.^{14,183} Note that Bartter syndrome due to *KCNJ1* disruption may specifically reflect a defect in ROMK2 and/or ROMK3 function since mice with disruption of ROMK1, consistent with its absence along the TAL, do not display a Bartter syndrome phenotype.¹⁹³

The apical Ca^{2+} -activated BK channel plays a critical role in flow-dependent K^+ secretion by the CNT and CCD.⁴⁹¹ BK channels have a heteromeric structure, with α -subunits that form the ion channel pore and modulatory β -subunits that affect the biophysical, regulatory, and pharmacologic characteristics of the channel complex.⁴⁹¹ BK α -subunit transcripts

are expressed in multiple nephron segments, and channel protein is detectable at the apical membrane of principal and intercalated cells in the CCD and CNT.⁴⁹¹ The β -subunits are differentially expressed within the distal nephron. Thus β_1 -subunits are restricted to the CNT, with no expression in intercalated cells, whereas β_4 -subunits are detectable at the apical membranes of the TAL, DCT, and intercalated cells.^{491,495} Increased distal flow has a well-established stimulatory effect on K^+ secretion, due in part to enhanced delivery and absorption of Na^+ and to increased removal of secreted K^+ .^{488,489} The pharmacology of flow-dependent K^+ secretion in the CCD is consistent with dominant involvement of BK channels, and flow-dependent K^+ secretion is reduced in mice with targeted deletion of the α_1 - and β_1 -subunits.^{491,496–498} Both mice strains develop hyperaldosteronism that is exacerbated by a high- K^+ diet, leading to hypertension in the α_1 -subunit knockout.⁴⁹⁸ Disruption of the β_2 subunit also leads to hyperaldosteronism, but flow-induced K^+ secretion is normal, suggesting compensation by other isoforms.⁴⁹⁹ Ca^{2+} -dependence of BK activation involves TRPV4.^{500–502} A high- K^+ diet increases TRPV4 expression, and leads to its redistribution to the apical membrane in CCD. The importance of this process in BK activation was demonstrated in TRPV4 knockout mice, which display decreased BK activity in CCD, and hyperkalemia after dietary K^+ loading.

One enigma has been the greater density of BK channels in intercalated cells in both the CCD and CNT.^{503,504} This has suggested a major role for intercalated cells in K^+ secretion; however, the much lower density of Na^+K^+ -ATPase activity in intercalated cells has been considered inadequate to support K^+ secretion across the apical membrane.⁵⁰⁵ More recent evidence has revealed a major role for the basolateral $Na^+K^+2Cl^-$ cotransporter NKCC1 in K^+ secretion mediated by apical BK channels. NKCC1 is expressed almost exclusively at the basolateral membrane of intercalated cells, providing an alternative entry pathway for basolateral K^+ secreted at the apical membrane.^{506,507} This still begs the question of how basolateral Na^+ recycles across the basolateral membrane in the absence of significant Na^+K^+ -ATPase activity; one possibility is an alternative basolateral Na^+ pump, the ouabain-insensitive furosemide-sensitive Na^+ -ATPase, a transport activity that has been detected in cell culture models of intercalated cells.⁵⁰⁶ At the apical membrane, BK-mediated K^+ secretion is only partially dependent on luminal Na^+ ; K^+ secretion would eventually hyperpolarize the membrane in the absence of apical Na^+ entry, which is mediated by ENaC in principal cells.⁵⁰⁸ An intriguing possibility is that apical Cl^- channels allow for the parallel secretion of K^+ and Cl^- in intercalated cells.⁵⁰⁹

BK channels also play a critical role in cell volume regulation by intercalated cells, with indirect, flow-mediated influences on distal K^+ secretion. MDCK-C11 cells have an intercalated cell phenotype and express BK α - and β_4 -subunits, as do intercalated cells; shear stress activates BK channels in these cells, leading to loss of K^+ and cell shrinkage.^{495,510} Mice with a targeted deletion of the β_4 -subunit exhibit normal K^+ excretion on a normal diet.⁵⁰⁵ However, when fed a high- K^+ diet, which increases urinary and tubular flow rates and tubular shear stress, the β_4 -knockout mice develop hyperkalemia with a blunted increase in K^+ excretion and urinary flow rates. Intercalated cells from β_4 -knockouts fail to significantly decrease cell volume in response to high- K^+ diet.

Intercalated cells thus function as so-called speed bumps that protrude into the lumen of distal tubules; flow-activated BK channels reduce the cell volume of intercalated cells after K^+ loading, reducing tubular resistance, increasing tubular flow rates, and increasing distal K^+ secretion.⁵⁰⁵

The physiologic rationale for the presence of two apical secretory K^+ channels, ROMK/SK and BK channels, is not completely clear. However, the high density and higher P_o of ROMK/SK channels are perhaps better suited for a role in basal K^+ secretion, with additional recruitment of the higher capacity, flow-activated BK channels when additional K^+ secretion is required.⁴⁹¹ Evolving evidence has also indicated that BK channels function in partially Na^+ -independent K^+ secretion by intercalated cells, with ROMK functioning in ENaC- and Na^+ -dependent K^+ excretion by DCT, CNT, and CCD cells. Regardless, at the whole-organ level, the two K^+ channels can substitute for one another, with BK-dependent K^+ secretion in ROMK knockout mice and an upregulation of ROMK in the distal nephron of α_1 -subunit BK knockouts.^{494,497}

Other K^+ channels reportedly expressed at the luminal membranes of the CNT and CCD include voltage-sensitive channels such as Kv1.3, the calcium-activated, small-conductance SK3 channel, and double-pore K^+ channels, such as TWIK-1 and KCNQ1.^{511–514} KCNQ1 mediates K^+ secretion in the inner ear and is expressed at the apical membrane of principal cells in the CCD, whereas TWIK-1 is expressed at the apical membrane of intercalated cells.^{514,515} The roles of these channels in renal K^+ secretion or absorption are not fully characterized. However, Kv1.3 may play a role in distal K^+ secretion in that luminal margatoxin, a specific blocker of this channel, reduces K^+ secretion in CCDs of rat kidneys from animals on a high- K^+ diet.⁵¹⁶ Other apical K^+ channels in the distal nephron may subservise other physiologic functions. For example, the apical Kv1.1 channel is critically involved in Mg^{2+} transport by the DCT, likely by hyperpolarizing the apical membrane and increasing the driving force for Mg^{2+} influx via TRPM6 (transient receptor potential cation channel 6); missense mutations in *KVL1* are a cause of genetic hypomagnesemia.⁵¹⁷

K^+ channels present at the basolateral membrane of principal cells appear to set the resting potential of the basolateral membrane and function in K^+ secretion and Na^+ absorption at the apical membrane, the latter via K^+ recycling at the basolateral membrane to maintain activity of the Na^+K^+ -ATPase. A variety of different K^+ channels have been described in the electrophysiologic characterization of the basolateral membrane of principal cells, which has a number of technical barriers to overcome.⁵¹⁸ However, a single predominant activity has been identified in principal cells from the rat CCD using whole-cell recording techniques under conditions in which ROMK is inhibited (low intracellular pH or presence of the ROMK inhibitor tertiapin-Q).⁵¹⁸ This basolateral current is tetraethylammonium-insensitive, barium-sensitive, and acid-sensitive ($pK_a \cong 6.5$), with a conductance of about 17 pS and weak inward rectification. These properties do not correspond exactly to specific characterized K^+ channels or combinations thereof. However, candidate inward-rectifying K^+ channel subunits that have been localized at the basolateral membrane of the CCD include KIR4.1, KIR5.1, KIR7.1, and KIR2.3.⁵¹⁸ KIR4.1 and KIR5.1 channels generate a predominant 40-pS basolateral K^+ channel in murine

principal cells,⁵¹⁹ with both KIR4.1 and KIR5.1 participating in generating the membrane potential that permits Na⁺ entry through ENaC.^{227,520} Notably, basolateral K⁺ channel activity increases on a high-K⁺ diet, suggesting a role in transepithelial K⁺ secretion.⁵¹⁸ Disruption of KIR5.1 in rats reveals it plays a critical role in mediating collecting duct function, particularly with respect to maintenance of K⁺ homeostasis.⁵²⁰ Activation of KIR4.1/5.1 by insulin and insulin-like growth factor-1 (IGF-1) may also facilitate Na⁺ reabsorption along the CCD by hyperpolarizing the basolateral membrane.⁵²¹

In addition to apical K⁺ channels, considerable evidence has implicated apical K⁺-Cl⁻ cotransport (or functionally equivalent pathways) in distal K⁺ secretion.^{67,488,522,523} Thus, in rat distal tubules, a reduction in luminal Cl⁻ markedly increases K⁺ secretion; the replacement of luminal Cl⁻ with SO₄⁻ or gluconate has an equivalent stimulatory effect on K⁺ secretion.⁵²⁴ This anion-dependent component of K⁺ secretion is not influenced by luminal Ba²⁺, suggesting that it does not involve apical K⁺ channel activity.⁵²⁴ Perfused surface distal tubules are a mixture of the DCT, connecting segment, and initial collecting duct; however, Cl⁻-coupled K⁺ secretion is detectable in the DCT and in early CNT.⁵²⁵ In addition, similar pathways are detectable in rabbit CCD, where a decrease in luminal Cl⁻ concentration from 112 to 5 mmol/L increases K⁺ secretion by 48%.⁵²⁶ A reduction in basolateral Cl⁻ also decreases K⁺ secretion without an effect on transepithelial voltage or Na⁺ transport, and the direction of K⁺ flux can be reversed by a lumen to bath Cl⁻ gradient, resulting in K⁺ absorption.⁵²⁶ In perfused CCDs from rats treated with mineralocorticoid, vasopressin increases K⁺ secretion; because this increase in K⁺ secretion is resistant to luminal Ba²⁺ (2 mmol/L), vasopressin may stimulate Cl⁻-dependent K⁺ secretion.^{14,527} Pharmacologic study results of perfused tubules are consistent with K⁺-Cl⁻ cotransport mediated by the KCCs; however, of the three renal KCCs, only KCC1 is apically expressed along the nephron.^{67,523} Other functional possibilities for Cl⁻-dependent K⁺ secretion include parallel operation of apical H⁺-K⁺-exchange and Cl⁻-HCO₃⁻ exchange in type B intercalated cells.⁵²²

A provocative study by Frindt and Palmer serves to underline the importance of ENaC-independent K⁺ excretion, whether it is mediated by apical K⁺-Cl⁻ cotransport and/or by other mechanisms (see also the “[Integrated Na⁺-Cl⁻ and K⁺ Transport in the Distal Nephron](#)” section).⁵²⁸ Rats were infused with amiloride via osmotic minipumps, generating urinary concentrations considered sufficient to inhibit more than 98% of ENaC activity. Whereas amiloride almost abolished K⁺ excretion in rats on a normal K⁺ intake, acute and long-term high-K⁺ diets led to an increasing fraction of K⁺ excretion that was independent of ENaC activity (≈50% after 7–9 days on a high-K⁺ diet).

K⁺ REABSORPTION BY THE COLLECTING DUCT

In addition to K⁺ secretion, the distal nephron is capable of considerable reabsorption, primarily during restriction of dietary K⁺.^{282–284} This reabsorption is accomplished largely by intercalated cells in the OMCD via the activity of apical H⁺/K⁺-ATPase pumps. Under K⁺-replete conditions, apical H⁺/K⁺-ATPase activity recycles K⁺ with an apical K⁺ channel, without an effect on transepithelial K⁺ absorption. Under K⁺-restricted basolateral conditions, K⁺ absorbed via apical

H⁺/K⁺-ATPase appears to exit intercalated cells via a K⁺ channel, thus achieving the transepithelial transport of K⁺.⁵²⁹

H⁺-K⁺-ATPase holoenzymes are members of the P-type family of ion transport ATPases, which also includes subunits of the basolateral Na⁺-K⁺-ATPase.⁵³⁰ HKα₁ and HKα₂ are also referred to as the gastric and colonic subunits, respectively; humans also have an HKα₄-subunit.^{530,531} A specific HKβ subunit interacts with the HKα subunits to ensure delivery to the cell surface and complete expression of H⁺-K⁺-ATPase activity; HKα₂ and HKα₄ subunits are also capable of interaction with Na⁺-K⁺-ATPase β-subunits.^{14,532} The pharmacology of H⁺-K⁺-ATPase holoenzymes differs considerably, such that the gastric HKα₁ subunit is typically sensitive to the H⁺-K⁺-ATPase inhibitors SCH-28080 and omeprazole and resistant to ouabain; the colonic HKα₂ subunit is usually sensitive to ouabain and resistant to SCH-28080.⁵³² Within the kidney, the HKα₁ subunit is expressed at the apical membrane of at least a subset of type A intercalated cells in the distal nephron.⁵³¹ HKα₂-subunit distribution in the distal nephron is more diffuse, with robust expression at the apical membrane of types A and B intercalated cells and connecting segment cells and lesser expression in principal cells.^{533–535} The human HKα₄ subunit is reportedly expressed in intercalated cells.⁵³¹

HKα₁ and HKα₂ subunits are both constitutively expressed in the distal nephron. However, tubule perfusion of K⁺-replete animals suggests a functional dominance of omeprazole/SCH-28080-sensitive, ouabain-resistant H⁺-K⁺-ATPase activity, consistent with holoenzymes containing the HKα₁ subunit.⁵³⁶ K⁺ deprivation increases the overall activity of H⁺-K⁺-ATPase in the collecting duct, with the emergence of ouabain-sensitive H⁺-K⁺-ATPase activity; this is consistent with a relative dominance of the HKα₂ subunit during K⁺-restricted conditions.¹⁴ K⁺ restriction also induces a dramatic upregulation of the HKα₂-subunit transcript and protein in the outer and inner medulla during K⁺ depletion; HKα₁-subunit expression is unaffected.¹⁴ Mice with targeted deletion of the HKα₂ subunit exhibit lower plasma and muscle K⁺ than wild type littermates when maintained on a K⁺-deficient diet. However, this appears to be due to marked loss of K⁺ in the colon rather than in the kidney, because renal K⁺ excretion is appropriately reduced in the K⁺-depleted knockout mice.²⁸⁵ Presumably the lack of an obvious renal phenotype in HKα₁- or HKα₂-subunit knockout mice reflects the marked redundancy in the expression of HKα subunits in the distal nephron.^{285,537} Indeed, collecting ducts from the HKα₁-subunit knockout mice have significant residual ouabain-resistant and SCH-28080-sensitive H⁺-K⁺-ATPase activities, consistent with the expression of other HKα-subunits that confer characteristics similar to the “gastric” H⁺-K⁺-ATPase.⁵³⁸ However, data from HKα₁- and HKα₂-subunit knockout mice have suggested that compensatory mechanisms in these mice are not accounted for by ATPase-type mechanisms.⁵³⁹

The importance of K⁺ reabsorption mediated by the collecting duct is dramatically illustrated by the phenotype of transgenic mice with generalized overexpression of a gain-of-function mutation in H⁺-K⁺-ATPase, effectively bypassing the redundancy and complexity of this reabsorptive pathway. This transgene expresses a mutant form of the HKβ subunit, in which a tyrosine-to-alanine mutation within the carboxyl-terminal tail abrogates regulated endocytosis from the plasma membrane; these mice have higher plasma K⁺ than their

wild type littermates, with approximately half the fractional excretion of K^+ .⁵⁴⁰

The H^+ , K^+ -ATPase may also serve to recycle K^+ , facilitating downregulation of ENaC by the purinergic signaling system during high dietary Na^+ intake. ENaC activity in $HK\alpha_1$ knockout mice is uncoupled from dietary Na^+ intake, and urinary [ATP] is not increased by a high- Na^+ diet, as in wild type mice.⁵⁴¹

REGULATION OF DISTAL K^+ TRANSPORT

MODULATION OF RENAL OUTER MEDULLARY POTASSIUM CHANNEL ACTIVITY

ROMK and other Kir channels are inward-rectifying—that is, K^+ flows inward more readily than outward (Kir, inward rectifying renal K^+ channel). Even though outward conductance is usually less than inward conductance, K^+ efflux through the ROMK predominates in the CNT and CCD because the membrane potential is more positive than the equilibrium potential for K^+ . Intracellular magnesium (Mg^{2+}) and polyamines play key roles in inward rectification, binding, and blocking the pore of the channel from the cytoplasmic side.^{542–544} A single transmembrane residue, asparagine-171 in ROMK1, controls the affinity and blocking effect of Mg^{2+} and polyamines.^{542,543} Intracellular Mg^{2+} in the TAL, DCT, CNT, and principal cells is thought to have a significant effect on ROMK activity because it inhibits outward ROMK-dependent currents in principal cells.⁵⁴⁵ The blocking affinity of Mg^{2+} is enhanced at lower extracellular K^+ concentrations, which should aid in reducing K^+ secretion during hypokalemia and K^+ deficiency.⁵⁴⁵ A reduction of this intracellular Mg^{2+} block may also explain the hypokalemia associated with hypomagnesemia, wherein distal K^+ secretion is enhanced.^{544,545}

In addition to inward rectification, the endogenous ROMK channels in the TAL and principal cells exhibit a very high channel P_o . The high P_o of ROMK is maintained by the combined effects of binding of PIP2 to the channel protein, direct channel phosphorylation by PKA, ATP binding to the ROMK-CFTR complex, and cytoplasmic pH. PIP2 binding to ROMK is thus required to maintain the channel in an open state, whereas cytoplasmic acidification inhibits the channel.⁵⁴⁶ PKA phosphorylates ROMK protein at one amino-terminal serines and two carboxyl-terminal serines—S25, S200, and S294 in the ROMK2 isoform.²⁵⁶ Phosphorylation of all three sites is required for full channel function. Phosphorylation of the amino-terminal site overrides the effect of a carboxy-terminal endoplasmic reticulum retention signal, thus increasing expression of the channel protein at the cell membrane.⁵⁴⁷ Phosphorylation of S200 and S294 maintains the channel in a high P_o state, in part by modulating the effects of PIP2, ATP, and pH.^{195,258,259}

Because ROMK channels exhibit such a high P_o , physiologic regulation of the channel is primarily achieved by regulated changes in the number of active channels on the plasma membrane. The associated mechanisms are discussed in the context of the adaptation to K^+ loading and hyperkalemia and K^+ deprivation and hypokalemia.

ALDOSTERONE AND K^+ LOADING

Aldosterone has a potent kaliuretic effect, with important interrelationships between circulating K^+ and aldosterone.⁵⁴⁸ Aldosterone release by the adrenal is thus induced by

hyperkalemia and/or a high- K^+ diet, suggesting an important feedback effect of aldosterone on K^+ homeostasis.⁵⁴⁹ Aldosterone also has clinically relevant effects on K^+ homeostasis, with a clear relationship at all levels of serum K^+ between circulating levels of the hormone and the ability to excrete K^+ .

Aldosterone has no effect on the density of apical ROMK channels in the CCD; it does, however, induce a marked increase in the density of apical Na^+ channels in the CNT and CCD.⁵⁵⁰ This hormone activates ENaC via interrelated effects on the synthesis, trafficking, and membrane-associated activity of the subunits encoding the channel (see the “[Regulation of \$Na^+\$ - \$Cl^-\$ Transport in the Connecting Tubule and Cortical Collecting Duct](#)” section). Aldosterone is thus induced by a high- K^+ diet and strongly stimulates apical ENaC activity, which provides the lumen-negative PD that stimulates K^+ secretion by principal cells.

The important relationships between K^+ and aldosterone notwithstanding, it is increasingly clear that much of the adaptation to a high- K^+ intake is aldosterone independent. For example, a high- K^+ diet in adrenalectomized animals increases apical Na^+ reabsorption and K^+ secretion in the CCD.⁵⁵¹ At the tubular level, when basolateral K^+ is increased, there is significant activation of Na^+ - K^+ -ATPase, accompanied by a secondary activation of apical Na^+ and K^+ channels.⁵⁵² Increased dietary K^+ also markedly increases the density of ROMK channels in the CCD, along with a modest increase in Na^+ channel (ENaC) density; this is associated with changes in the subcellular distribution of the ROMK protein, with an increase in apical expression.^{550,553} Notably, this increase in ENaC and ROMK density in the CCD occurs within hours of consuming a high- K^+ diet, with a minimal associated increase in circulating aldosterone (Table 6.1).⁵⁵⁴ By contrast, a week of low Na^+ - Cl^- intake, with almost a 1000-fold increase in aldosterone, has no effect on ROMK channel density, nor for that matter does 2 days of aldosterone infusion, despite the development of hypokalemia (Table 6.1).⁵⁵⁴ Unlike the marked increase seen in the CCD, the density of ROMK channels in the CNT is not increased by high dietary K^+ ,^{371,550,554} but this may reflect difficulties in estimating channel densities in small membrane patches. Measurement of whole cell currents using the ROMK inhibitor tertiapin-Q indicates an upregulation of ROMK activity in the CNT by a high- K^+ diet.⁵⁵⁵

BK channels in the CNT and CCD play an important role in the flow-activated component of distal K^+ excretion; these channels are also activated by dietary K^+ loading.⁴⁹¹ Flow-stimulated K^+ secretion by the CCD of mice and rats is thus enhanced on a high- K^+ diet, with an absence of flow-dependent K^+ secretion in rats on a low- K^+ diet.^{494,556} This is accompanied by the appropriate changes in transcript levels for α and β_{2-4} subunits of the BK channel proteins in microdissected CCDs (β_1 subunits are restricted to the CNT).⁴⁹¹ Trafficking of BK subunits is also affected by dietary K^+ , with a largely intracellular distribution of α subunits in K^+ -restricted rodents and prominent apical expression in K^+ -loaded rodents.^{500,556} Aldosterone does not contribute to the regulation of BK channel activity or expression in response to a high- K^+ diet.⁵⁵⁷

The changes in trafficking and/or activity of the ROMK channel that are induced by dietary K^+ appear in large part to involve tyrosine phosphorylation and dephosphorylation of the ROMK protein (see later). However, a series of reports have linked changes in expression of WNK1 kinase subunits

Table 6.1 Effect of High-K⁺ Diet, Aldosterone, and/or Na⁺-Cl⁻ Restriction on SK Channel Density in the Rat Cortical Collecting Duct

Parameter	K ⁺ Channel Density (μm ²)	Plasma Aldosterone (ng/dL)	Plasma K (mmol/L)
Control	0.41	15	3.68
High-K ⁺ diet, 6 hours	1.51	36	NM
High-K ⁺ diet, 48 hours	2.13	98	4.37
Low-Na ⁺ diet, 7 days	0.48	1260	NM
Aldosterone infusion, 48 hours	0.44	550	2.44
Aldosterone + high-K ⁺ diet	0.32	521	3.80

NM, Not measured.

Modified from Palmer LG, Frindt G. Regulation of apical K channels in rat cortical collecting tubule during changes in dietary K intake. *Am J Physiol.* 1999;277:F805-F812.

in the response to a high-K⁺ diet. WNK1 and WNK4 were initially identified as causative genes for FHHt (see also the “Regulation of Na⁺-Cl⁻ Transport in the Distal Convulated Tubule” section). ROMK expression at the membrane of *Xenopus* oocytes is dramatically reduced by coexpression of WNK4; FHHt-associated mutations dramatically increase this effect, suggesting a direct inhibition of SK channels in FHHt.⁵⁵⁸ This is further supported by a recent patch-clamp study that showed DCT2/CNT isolated from transgenic mice expressing FHHt-causing mutant WNK4 has lower ENaC and ROMK activity, suggesting direct, NCC-independent effects of the mutant.⁵⁵⁹ The aldosterone-induced SGK1 is activated by the upstream kinase mTORC2. Disruption of mTORC2 in renal epithelia in mice causes profound hyperkalemia when they are placed on a high-K⁺ diet. Patch-clamp analysis showed that in CNT/CCD, while ENaC activity was unaltered, Ba²⁺-sensitive K⁺ currents were almost absent. SGK1 phosphorylation was ablated, suggesting that hyperkalemia may result from unchecked WNK4-mediated ROMK endocytosis.⁵⁶⁰

The study of WNK1 is further complicated by the transcriptional complexity of its gene, which has at least three separate promoters and a number of alternative splice forms. In particular, the predominant intrarenal WNK1 isoform is generated by a distal nephron transcriptional site that bypasses the amino-terminal exons that encode the kinase domain, yielding a kinase-deficient short form of the protein (WNK1-S, also known as kidney-specific [KS]-WNK1).⁵⁶¹ Full-length WNK1 (WNK1-L) inhibits ROMK activity by inducing endocytosis of the channel protein; kinase activity and/or the amino-terminal kinase domain of WNK1 appear to be required for this effect, although Cope and colleagues have reported that a kinase-dead mutant of WNK1 is unimpaired.⁵⁶²⁻⁵⁶⁴ WNK1 and WNK4 induce endocytosis of ROMK via interaction with intersectin, a multimodular endocytic scaffold protein.⁵⁶⁵ Additional binding of ROMK to the clathrin adaptor protein termed “autosomal recessive hypercholesterolemia” (ARH) is required for basal and WNK1-stimulated endocytosis of the channel protein.⁵⁶⁶ Ubiquitination of ROMK protein is also involved in clathrin-dependent endocytosis, requiring interaction between the channel and the U3 ubiquitin ligase POSH (plenty of SH domains).⁵⁶⁷

The shorter WNK1-S isoform, which lacks the kinase domain, appears to inhibit the effect of WNK1-L.^{563,564} The ratio of WNK1-S to WNK1-L transcripts is reduced by K⁺

restriction (greater endocytosis of ROMK) and increased by K⁺ loading (reduced endocytosis of ROMK), suggesting that this ratio between WNK1-S and WNK1-L functions as a type of switch to regulate distal K⁺ secretion.^{563,564,568} The inhibitory effect of WNK1-S tracks to the first 253 amino acids of the protein, encompassing the initial 30 amino acids unique to this isoform and an adjacent autoinhibitory domain.⁵⁶⁹ Transgenic mice that overexpress this inhibitory domain of WNK1-S have lower serum K⁺ concentrations, higher fractional excretion of K⁺, and increased expression of ROMK protein at the apical membrane of CNT and CCD cells—all consistent with an important inhibitory effect of WNK1-S.⁵⁶⁹

The BK channel is also regulated by the WNK kinases. WNK4 thus inhibits BK channel activity and protein expression, whereas FHHt-associated mutations in WNK4 also enhance the inhibitory effect via ubiquitination.⁵⁷⁰⁻⁵⁷² A high-K⁺ diet increases WNK1-L expression selectively in intercalated cells,⁵⁷³ and activates BK by reducing ERK1/2 signaling-mediated lysosomal degradation of the channel protein.⁵²⁹

K⁺ DEPRIVATION

A reduction in dietary K⁺ leads within 24 hours to a dramatic drop in urinary K⁺ excretion.^{568,574} This drop in excretion is due to both an induction of reabsorption by intercalated cells in the OMCD and to a reduction in SK channel activity in principal cells.^{14,283,284} The mechanisms involved in K⁺ reabsorption by intercalated cells are discussed earlier; notably, H⁺/K⁺-ATPase activity in the collecting duct does not appear to be regulated by aldosterone.⁵⁷⁵

Considerable progress has been made in defining the signaling pathways that regulate the activity of the SK channel (ROMK) in response to changes in dietary K⁺. Dietary K⁺ intake modulates trafficking of the ROMK channel protein to the plasma membrane of principal cells, with a marked increase in the relative proportion of intracellular channel protein in K⁺-depleted animals and clearly defined expression at the plasma membrane of CCD cells from animals on a high-K⁺ diet.^{553,576} The membrane insertion and activity of ROMK are modulated by tyrosine phosphorylation of the channel protein, such that phosphorylation of tyrosine residue 337 stimulates endocytosis and dephosphorylation induces exocytosis; this tyrosine phosphorylation appears to play a key role in the regulation of ROMK by dietary K⁺.⁵⁷⁷⁻⁵⁷⁹ Whereas the levels of protein tyrosine phosphatase-1D do not vary with K⁺ intake, intrarenal activity of the cytoplasmic

tyrosine kinases c-src and c-yes are inversely related to dietary K^+ intake, with a decrease under high- K^+ conditions and a marked increase after several days of K^+ restriction.^{14,580} Localization studies have indicated coexpression of c-src with ROMK in the TAL and principal cells of the CCD.⁵⁵³ Moreover, inhibition of protein tyrosine phosphatase activity, leading to a dominance of tyrosine phosphorylation, dramatically increases the proportion of intracellular ROMK in the CCD of animals on a high- K^+ diet.⁵⁵³

The neurohumoral factors that induce the K^+ -dependent trafficking and expression of apical ROMK and BK channels have only come into focus rather recently.^{553,556,576} Several studies have implicated the intrarenal generation of superoxide anions in the activation of cytoplasmic tyrosine kinases.^{581–583} Potential candidates for the upstream kaliuretic factor include Ang II and growth factors such as IGF-1.⁵⁸¹ Ang II inhibits ROMK activity in K^+ -restricted rats, but not rats on a normal K^+ diet.⁵⁸⁴ This inhibition involves downstream activation of superoxide production and c-src activity, such that the well-known induction of Ang II by a low- K^+ diet appears to play a major role in reducing distal tubular K^+ secretion.⁵⁸⁵

Reports of transient postprandial kaliuresis in sheep, independent of changes in plasma K^+ or aldosterone, have suggested that an enteric or hepatoportal K^+ sensor controls kaliuresis via a sympathetic reflex; tissue kallikrein (TK) has recently emerged as a candidate mediator for this postprandial kaliuresis (see later).⁵⁸⁶ Regardless of the signaling involved, changes in dietary K^+ absorption have a direct anticipatory effect on K^+ homeostasis in the absence of changes in plasma K^+ . Such a feed-forward control has the theoretical advantage of greater stability because it operates prior to changes in plasma K^+ .⁵⁸⁷ Notably, changes in ROMK phosphorylation status and insulin-sensitive muscle uptake can be seen in K^+ -deficient animals in the absence of a change in plasma K^+ , suggesting that upstream activation of the major mechanisms that serve to reduce K^+ excretion (reduced K^+ secretion in the CNT and CCD, decreased peripheral uptake, and increased K^+ reabsorption in the OMCD) does not require changes in plasma K^+ .⁵⁸⁸ Consistent with this hypothesis, moderate K^+ restriction, without an associated drop in plasma K^+ , is sufficient to induce Ang II-dependent superoxide generation and c-src activation, leading to inhibition of ROMK channel activity.⁵⁸⁵

VASOPRESSIN

Vasopressin has a well-characterized stimulatory effect on K^+ secretion by the distal nephron.^{483,589} From an evolutionary viewpoint, this vasopressin-dependent activation serves to preserve K^+ secretion during dehydration and extracellular volume depletion, when circulating levels of vasopressin are high and tubular delivery of Na^+ and fluid is reduced. The stimulation of basolateral V_2 R_s results in an activation of ENaC, which increases the driving force for K^+ secretion by principal cells; the relevant mechanisms have been discussed earlier in this chapter (see the “Regulation of Na^+ - Cl^- Transport in the Connecting Tubule and Cortical Collecting Duct: Vasopressin and Other Factors” section). In addition, vasopressin activates SK channels directly in the CCD, as does cAMP.^{492,590} The ROMK is directly phosphorylated by PKA on three serine residues (S25, S200, and S294 in the ROMK2 isoform), with phosphorylation of all three sites required

for full activity in *Xenopus* oocytes (see the “Regulation of Na^+ - Cl^- Transport by the Thick Ascending Limb: Activating Influences” section). Finally, the stimulation of luminal V_1 receptors also stimulates K^+ secretion in the CCD, apparently via activation of BK channels.⁵⁹¹

TISSUE KALLIKREIN

The serine protease TK is involved in the generation of kinins, ultimately stimulating the formation of bradykinin.⁵⁹² Within the kidney, TK is synthesized in CNT cells and released into the tubular lumen and peritubular interstitium. Although TK-induced bradykinin has a number of effects on distal tubular physiology, more recent data have revealed a provocative role in postprandial kaliuresis.⁵⁹² Thus oral K^+ - Cl^- loading leads to a spike in urinary K^+ and TK excretion in rats, mice, and humans.⁵⁹² The increase in urinary TK after K^+ loading is not accompanied by changes in urinary aldosterone and can be detected in aldosterone synthase knockout mice.⁵⁹³ Mice deficient in TK demonstrate postprandial hyperkalemia, indicating a role for the protease in postprandial kaliuresis. This transient hyperkalemia is accompanied by a marked increase in K^+ reabsorption by perfused CCDs due to an upregulation of H^+ / K^+ -ATPase activity and an increase in $HK\alpha_2$ -subunit transcript. The addition of luminal but not basolateral TK inhibits the activated CCD H^+ / K^+ -ATPase activity in the TK knockout mice, consistent with direct proteolytic activation. There is also a marked increase in Na^+ reabsorption by perfused CCDs from TK knockout mice, without development of a lumen-negative PD; this is consistent with an increased activity of the electroneutral Na^+ - Cl^- cotransport mediated by the Na^+ -driven SLC4A8 Cl^- - HCO_3^- exchanger and the SLC26A4 Cl^- - HCO_3^- exchanger (see later discussion as well).⁴⁰⁸ This electroneutral transport pathway had previously been shown to be inhibited by bradykinin; hence the activation by TK deletion presumably reflected loss of tonic inhibition by TK-generated bradykinin.⁴⁰⁶ Previous data had indicated that TK mediates proteolytic cleavage of the γ subunit of ENaC, with reduced ENaC activity in TK-deficient mice; net Na^+ balance is thus neutral in these mice.⁵⁹⁴

In summary, TK secretion from CNT cells is induced by oral K^+ - Cl^- loading, causing proteolytic activation of ENaC and thus an increase in ENaC-driven K^+ secretion, bradykinin-dependent inhibition of electroneutral Na^+ - Cl^- cotransport in the CCD.^{406,408,594} There is consequently a further augmentation of electrogenic Na^+ transport (favoring K^+ secretion), and direct luminal inhibition of H^+ / K^+ -ATPase activity and thus a decrease or tonic inhibition of K^+ reabsorption. TK may very well be the postprandial factor that functions in feed-forward control of plasma K^+ .^{586,587}

INTEGRATED Na^+ - Cl^- AND K^+ TRANSPORT IN THE DISTAL NEPHRON

Segmentation of the renal epithelia into distinct sections does not mean that different segments function independently. Increasing evidence from *in vivo* studies in mice with multiple genes disrupted, or from studies in which knockout mice are subjected to drug treatment or dietary manipulation, shows that effects in one segment exert compensatory effects to maintain homeostasis. For example, *Slc26a4* knockout mice with combined genetic ablation of NCC⁵⁹⁵ or administration of hydrochlorothiazide⁵⁹⁶ display salt wasting and volume

contraction. Similarly, ENaC blockade with amiloride leads to enhanced natriuresis in NCC knockout mice.⁵⁹⁷ In mice with disruption of MR specifically in renal epithelia, while activities of both ENaC and NCC are diminished, the effect on NCC is secondary to the hyperkalemia induced by lower ENaC activity.^{329,330} These mice are hypotensive, but normalization of plasma $[K^+]$ by dietary K^+ restriction stimulates NCC activity resulting in normalization of blood pressure. Grimm and colleagues performed microarray studies on SPAK knockout mice, which display lower NCC activity, and proposed that α -ketoglutarate may serve as a downstream signaling molecule that mediates compensatory responses.⁵⁹⁸ These interactions between segments are likely to be similar to those seen with diuretic treatment and may contribute to diuretic resistance (see Chapter 50). In the following sections, other examples of this intersegment crosstalk are described in more depth.

In the classic model of renal K^+ secretion, the lumen-negative PD generated by Na^+ entry via ENaC induces the exit of K^+ via apical K^+ -selective channels. This general scheme explains much of the known physiology and pathophysiology of renal K^+ secretion, yet has several key consequences that bear emphasis. First, enhanced Na^+Cl^- reabsorption upstream of the CNT and CCD will reduce the delivery of luminal Na^+ to the CNT and CCD, decrease the lumen-negative PD, and thus decrease K^+ secretion; K^+ secretion by the CCD essentially stops when luminal Na^+ drops below 8 mmol/L.^{488–490} In this respect, the increasingly refined phenotypic understanding of FHHT, caused by kinase-induced gain of function of the DCT, has served to underscore that variation in NCC-dependent Na^+Cl^- absorption, just upstream of the CNT, has truly profound effects on the ability to excrete dietary K^+ (Fig. 6.19).³⁴⁵ Second, aldosterone is a kaliuretic hormone, induced by hyperkalemia. However, under certain circumstances associated with marked induction of aldosterone, such as dietary sodium restriction, sodium balance is maintained without effects on K^+ homeostasis. This so-called aldosterone paradox—how the kidney independently regulates Na^+Cl^- and K^+ handling by the aldosterone-sensitive distal nephron—is only recently beginning to yield to investigative efforts. The major factors in the integrated control of Na^+Cl^- and K^+ transport appear to include electroneutral thiazide-sensitive Na^+Cl^- transport within the CCD, ENaC-independent K^+ excretion within the distal nephron, and the differential regulation of various signaling pathways by aldosterone, Ang II, and dietary K^+ .^{406–408,528,599,600}

Thiazide-sensitive electroneutral Na^+Cl^- transport within the CCD is evidently mediated by the parallel activity of the Na^+ -driven SLC4A8 $Cl^-HCO_3^-$ exchanger and the SLC26A4 $Cl^-HCO_3^-$ exchanger.⁴⁰⁸ The molecular identity of this transport mechanism has only emerged rather recently, so regulatory influences are not fully characterized.⁴⁰⁸ However, electroneutral Na^+Cl^- transport within the CCD is evidently induced by volume depletion and mineralocorticoid treatment.^{406–408} This mechanism appears to mediate about 50% of Na^+ reabsorption in the CCD under these conditions, all without affecting the luminal PD and thus without direct effect on K^+ excretion. Therefore electroneutral, thiazide-sensitive Na^+Cl^- transport affords the ability to increase the reabsorption of Na^+ within the CCD without affecting K^+ excretion. The converse occurs after several days of accommodation to a high- K^+ diet, which increases the fraction of

ENaC-independent, amiloride-resistant K^+ excretion to about 50%. Again, this presumptively electroneutral, aldosterone-independent pathway for K^+ excretion serves to uncouple distal tubular Na^+ and K^+ excretion.⁵²⁸

WNK-dependent signaling constitutes a major pathway for integrating Na^+Cl^- and K^+ transport within the distal nephron, and is regulated by the differential influence of K^+ intake on circulating Ang II, ROMK activity (i.e., K^+ secretory capacity), ratio of WNK1 isoforms, and activity of NCC in the DCT. Thus Ang II activates NCC via the WNK4-SPAK pathway, reducing delivery of Na^+ to the CNT and limiting K^+ secretion.^{312,315,601} By contrast, Ang II inhibits ROMK activity via several mechanisms, including downstream activation of c-src tyrosine kinases.^{583–585} Whereas K^+ restriction induces renin and circulating Ang II, increases in dietary K^+ are suppressive.^{585,602} A decrease in circulating and local Ang II partially explains why NCC phosphorylation and activity are down-regulated by a high- K^+ diet; teleologically, this serves to increase delivery of Na^+ to the CNT, thus increasing K^+ secretion.³⁶¹

The DCT also clearly functions as a potassium sensor, directly responding to changes in circulating potassium (Fig. 6.19). Evidence that a key role of the DCT is to act as a plasma $[K^+]$ sensor, rather than to maintain plasma $[Na^+]$, is demonstrated by the observation that acute K^+ loading dephosphorylates NCC even in Na^+ -restricted mice.⁶⁰³ Reduction in potassium intake and/or hypokalemia thus lead to reduced basolateral $[K^+]$ in the DCT; the subsequent hyperpolarization of DCT cells is dependent on basolateral KIR4.1-containing K^+ channels.^{308,327} Hyperpolarization leads to chloride exit via basolateral CLC-K2 chloride channels; the resulting decrease in intracellular chloride disinhibits WNK kinases, resulting in phosphorylation of NCC and activation of the transporter by SPAK/OSR1.³²⁷ Ex vivo studies (micro-perfusion and kidney slices) have provided evidence that increased phosphorylation of NCC resulting in response to lower extracellular $[K^+]$ is dependent on increased intracellular chloride.⁶⁰⁴ Along the DCT, WNK4 appears to be the major WNK activating NCC,²³⁶ and WNK4 is also more sensitive to changes in intracellular chloride than WNK1 or WNK3.³⁴³ The essential role of this pathway in mediating responses to dietary K^+ restriction is clearly demonstrated by the development of severe hypokalemia in mice lacking KIR4.1,³¹¹ WNK4,⁶⁰⁵ SPAK/OSR1,⁶⁰⁶ and NCC (D.H. Ellison, unpublished observations; see Fig. 6.19 for summary of model). An alternative mechanism has been proposed in which KLHL3, part of the ubiquitin ligase complex that degrades WNK4, is phosphorylated in response to K^+ depletion. This prevents WNK4 binding to the complex, decreasing WNK4 degradation, which promotes NCC activation.⁶⁰⁷

NCC undergoes rapid dephosphorylation in response to K^+ loading,^{604,608} a process that appears to be largely independent of increased intracellular chloride, which would inhibit WNKs.⁶⁰⁴ This suggests a role for protein phosphatases; one study suggested that PP3 (calcineurin) is responsible for NCC dephosphorylation,⁶⁰⁸ while another found no role for PP1, PP2A, or PP3.⁶⁰⁴ Glucocorticoid-induced leucine zipper protein (GILZ) may also play a role in the response to high dietary K^+ by inhibiting SPAK activity and hence NCC. Compared with wild type mice, *Gilz* knockout mice are more sensitive to NCC inhibition by thiazides and have greater abundance of phosphorylated NCC. *Gilz* knockout

mice display elevated plasma $[K^+]$ at baseline, with dietary Na^+ restriction increasing it further. When plasma $[K^+]$ increases, GILZ-mediated inhibition of NCC may serve to maintain distal Na^+ delivery to ENaC to drive kaliuresis.⁶⁰⁹ Most studies have used diets completely almost deficient in K^+ , or with very high levels, for example, 5% KCl, to examine NCC activation status. Relatively small changes in plasma $[K^+]$ also alter the degree of NCC phosphorylation in vivo, suggesting that the role of NCC to maintain plasma $[K^+]$ is homeostatically important under dietary K^+ levels that do not show extreme deviation from normal.³⁴³

A mouse model in which NCC activity was increased specifically along DCT1, by expressing a constitutively active SPAK mutant only in this segment, suggests that altering NCC activity may affect distal K^+ secretion by inducing remodeling of the CNT, and not just by altering Na^+ delivery to ENaC.⁶¹⁰ These mice displayed hyperkalemia, which was associated with lower volume of the CNT and lower ROMK abundance, which may limit K^+ secretion. Chronic blockade of NCC led to increased CNT volume and ROMK abundance, and normalized plasma K^+ , suggesting that altered Na^+ delivery to the CNT may induce remodeling.

Finally, within principal cells, increases in aldosterone induce the SGK1 kinase, which phosphorylates WNK4 and attenuates the effect of WNK4 on ROMK, while activating ENaC via NEDD4-2-dependent effects.⁶¹¹ However, when dietary K^+ intake is reduced, c-src tyrosine kinase activity increases under the influence of increased Ang II, causing direction inhibition of ROMK activity via tyrosine phosphorylation of the channel.^{577,579,612} The increase in c-src tyrosine kinase activity also abrogates the effect of SGK1 on WNK4.^{600,613} While NEDD4-2 can regulate NCC during K^+ restriction,³²¹ ENaC regulation may be more important. In NEDD4-2 knockout mice, chronic K^+ restriction led to hypokalemia and urinary K^+ wasting that was reversed with the ENaC blocker benzamil.³⁴⁰ Higher phosphorylation of NCC and lower ROMK abundance were observed, but not sufficient to compensate for the effect on ENaC activation. While both insulin and IGF-1 activate ENaC, insulin promotes kaliuresis whereas IGF-1 exerts an antikaliuretic response. Patch-clamp analysis of isolated mouse CCD cells showed that this differential effect on K^+ secretion may be due to differential effects on CLC-K2 (which is expressed in intercalated cells).³⁹² IGF-1 stimulates CLC-K2, which may promote net Na^+ -Cl⁻ reabsorption, thus reducing the driving force for K^+ secretion by the CCD. By contrast, insulin inhibits CLC-K2, which would enhance the generation of the electrogenic drive for K^+ secretion.

 Complete reference list available at ExpertConsult.com.

KEY REFERENCES

- Chambrey R, Kurth I, Peti-Peterdi J, et al. Renal intercalated cells are rather energized by a proton than a sodium pump. *Proc Natl Acad Sci USA*. 2013;110:7928–7933.
- Sun A, Grossman EB, Lombardi M, et al. Vasopressin alters the mechanism of apical Cl⁻ entry from Na⁺:Cl⁻ to Na⁺:K⁺:2Cl⁻ cotransport in mouse medullary thick ascending limb. *J Membr Biol*. 1991;120:83–94.
- Kokko JP. Proximal tubule potential difference. Dependence on glucose, HCO₃⁻, and amino acids. *J Clin Invest*. 1973;52:1362–1367.
- Alpern RJ, Howlin KJ, Preisig PA. Active and passive components of chloride transport in the rat proximal convoluted tubule. *J Clin Invest*. 1985;76:1360–1366.
- Barratt LJ, Rector FC Jr, Kokko JP, et al. Factors governing the transepithelial potential difference across the proximal tubule of the rat kidney. *J Clin Invest*. 1974;53:454–464.
- Katz AI, Doucet A, Morel F. Na-K-ATPase activity along the rabbit, rat, and mouse nephron. *Am J Physiol*. 1979;237:F114–F120.
- Muto S, Hata M, Taniguchi J, et al. Claudin-2-deficient mice are defective in the leaky and cation-selective paracellular permeability properties of renal proximal tubules. *Proc Natl Acad Sci USA*. 2010;107:8011–8016.
- Schnermann J, Chou CL, Ma T, et al. Defective proximal tubular fluid reabsorption in transgenic aquaporin-1 null mice. *Proc Natl Acad Sci USA*. 1998;95:9660–9664.
- Schnermann J, Huang Y, Mizel D. Fluid reabsorption in proximal convoluted tubules of mice with gene deletions of claudin-2 and/or aquaporin1. *Am J Physiol Renal Physiol*. 2013;305:F1352–F1364.
- Bacic D, Kaissling B, McLeroy P, et al. Dopamine acutely decreases apical membrane Na⁺/H exchanger NHE3 protein in mouse renal proximal tubule. *Kidney Int*. 2003;64:2133–2141.
- Schultheis PJ, Clarke LL, Meneton P, et al. Renal and intestinal absorptive defects in mice lacking the NHE3 Na⁺/H⁺ exchanger. *Nat Genet*. 1998;19:282–285.
- Wang T, Agulian SK, Giebisch G, et al. Effects of formate and oxalate on chloride absorption in rat distal tubule. *Am J Physiol*. 1993;264:F730–F736.
- Wang T. Flow-activated transport events along the nephron. *Curr Opin Nephrol Hypertens*. 2006;15:530–536.
- Thomson SC, Deng A, Wead L, et al. An unexpected role for angiotensin II in the link between dietary salt and proximal reabsorption. *J Clin Invest*. 2006;116:1110–1116.
- Zhang MZ, Yao B, Wang S, et al. Intrarenal dopamine deficiency leads to hypertension and decreased longevity in mice. *J Clin Invest*. 2011;121:2845–2854.
- Waldegger S, Jeck N, Barth P, et al. Barttin increases surface expression and changes current properties of ClC-K channels. *Pflugers Arch*. 2002;444:411–418.
- Simon DB, Bindra RS, Mansfield TA, et al. Mutations in the chloride channel gene, CLCNKB, cause Bartter syndrome type III. *Nat Genet*. 1997;17:171–178.
- Estevez R, Boettger T, Stein V, et al. Barttin is a Cl⁻ channel beta-subunit crucial for renal Cl⁻ reabsorption and inner ear K⁺ secretion. *Nature*. 2001;414:558–561.
- Rocha AS, Kokko JP. Sodium chloride and water transport in the medullary thick ascending limb of Henle. Evidence for active chloride transport. *J Clin Invest*. 1973;52:612–623.
- Stokes JB. Consequences of potassium recycling in the renal medulla. Effects of ion transport by the medullary thick ascending limb of Henle's loop. *J Clin Invest*. 1982;70:219–229.
- Xu JZ, Hall AE, Peterson LN, et al. Localization of the ROMK protein on apical membranes of rat kidney nephron segments. *Am J Physiol*. 1997;F739–F748.
- Lu M, Wang T, Yan Q, et al. ROMK is required for expression of the 70-pS K channel in the thick ascending limb. *Am J Physiol Renal Physiol*. 2004;286:F490–F495.
- Gagnon KB, England R, Delpire E. Volume sensitivity of cation-Cl⁻ cotransporters is modulated by the interaction of two kinases: Ste20-related proline-alanine-rich kinase and WNK4. *Am J Physiol Cell Physiol*. 2006;290:C134–C142.
- Riccardi D, Hall AE, Chattopadhyay N, et al. Localization of the extracellular Ca²⁺/polyvalent cation-sensing protein in rat kidney. *Am J Physiol*. 1998;274:F611–F622.
- Trudu M, Janas S, Lanzani C, et al; Swiss Kidney Project on Genes in Hypertension (SKIPOGH) team. Common noncoding UMOD gene variants induce salt-sensitive hypertension and kidney damage by increasing uromodulin expression. *Nat Med*. 2013;19:1655–1660.
- Loffing J, Kaissling B. Sodium and calcium transport pathways along the mammalian distal nephron: from rabbit to human. *Am J Physiol Renal Physiol*. 2003;284:F628–F643.
- Zhang C, Wang L, Zhang J, et al. KCNJ10 determines the expression of the apical Na-Cl cotransporter (NCC) in the early distal convoluted tubule (DCT1). *Proc Natl Acad Sci USA*. 2014;111:11864–11869.
- Terker AS, Zhang C, McCormick JA, et al. Potassium modulates electrolyte balance and blood pressure through effects on distal cell voltage and chloride. *Cell Metab*. 2015;21:39–50.
- Vidal-Petiot E, Elvira-Matlot E, Mutig K, et al. WNK1-related familial hyperkalemic hypertension results from an increased expression

- of L-WNK1 specifically in the distal nephron. *Proc Natl Acad Sci USA*. 2013;110:14366–14371.
345. Lalioti MD, Zhang J, Volkman HM, et al. Wnk4 controls blood pressure and potassium homeostasis via regulation of mass and activity of the distal convoluted tubule. *Nat Genet*. 2006;38:1124–1132.
349. Boyden LM, Choi M, Choate KA, et al. Mutations in Kelch-like 3 and cullin 3 cause hypertension and electrolyte abnormalities. *Nature*. 2012;482:98–102.
404. Verlander JW, Kim YH, Shin W, et al. Dietary Cl⁻ restriction upregulates pendrin expression within the apical plasma membrane of type B intercalated cells. *Am J Physiol Renal Physiol*. 2006;291:F833–F839.
423. Snyder PM, Olson DR, Thomas BC. Serum and glucocorticoid-regulated kinase modulates Nedd4-2-mediated inhibition of the epithelial Na⁺ channel. *J Biol Chem*. 2002;277:5–8.
430. Soundararajan R, Ziera T, Koo E, et al. Scaffold protein connector enhancer of kinase suppressor of Ras isoform 3 (CNK3) coordinates assembly of a multiprotein epithelial sodium channel (ENaC)-regulatory complex. *J Biol Chem*. 2012;287:33014–33025.
439. Kleyman TR, Carattino MD, Hughey RP. ENaC at the cutting edge: regulation of epithelial sodium channels by proteases. *J Biol Chem*. 2009;284:20447–20451.
444. Kashlan OB, Blobner BM, Zuzek Z, et al. Na⁺ inhibits the epithelial Na⁺ channel by binding to a site in an extracellular acidic cleft. *J Biol Chem*. 2015;290:568–576.
446. Bugaj V, Pochynyuk O, Stockand JD. Activation of the epithelial Na⁺ channel in the collecting duct by vasopressin contributes to water reabsorption. *Am J Physiol Renal Physiol*. 2009;297:F1411–F1418.
451. Mironova E, Chen Y, Pao AC, et al. Activation of ENaC by AVP contributes to the urinary concentrating mechanism and dilution of plasma. *Am J Physiol Renal Physiol*. 2015;308:F237–F243.
462. Nakagawa K, Holla VR, Wei Y, et al. Salt-sensitive hypertension is associated with dysfunctional Cyp4a10 gene and kidney epithelial sodium channel. *J Clin Invest*. 2006;116:1696–1702.
463. Guan Y, Hao C, Cha DR, et al. Thiazolidinediones expand body fluid volume through PPAR γ stimulation of ENaC-mediated renal salt absorption. *Nat Med*. 2005;11:861–866.
504. Palmer LG, Frindt G. High-conductance K channels in intercalated cells of the rat distal nephron. *Am J Physiol Renal Physiol*. 2007;292:F966–F973.
505. Holtzclaw JD, Grimm PR, Sansom SC. Intercalated cell BK α /beta4 channels modulate sodium and potassium handling during potassium adaptation. *J Am Soc Nephrol*. 2010;21:634–645.
523. Amorim JB, Bailey MA, Musa-Aziz R, et al. Role of luminal anion and pH in distal tubule potassium secretion. *Am J Physiol Renal Physiol*. 2003;284:F381–F388.
545. Yang L, Frindt G, Palmer LG. Magnesium modulates ROMK channel-mediated potassium secretion. *J Am Soc Nephrol*. 2010;21:2109–2116.
549. Palmer LG, Frindt G. Aldosterone and potassium secretion by the cortical collecting duct. *Kidney Int*. 2000;57:1324–1328.
550. Palmer LG, Antonian L, Frindt G. Regulation of apical K and Na channels and Na/K pumps in rat cortical collecting tubule by dietary K. *J Gen Physiol*. 1994;104:693–710.
554. Palmer LG, Frindt G. Regulation of apical K channels in rat cortical collecting tubule during changes in dietary K intake. *Am J Physiol*. 1999;277:F805–F812.
600. Yue P, Lin DH, Pan CY, et al. Src family protein tyrosine kinase (PTK) modulates the effect of SGK1 and WNK4 on ROMK channels. *Proc Natl Acad Sci USA*. 2009;106:15061–15066.
604. Penton D, Czogalla J, Wengi A, et al. Extracellular K⁺ rapidly controls NaCl cotransporter phosphorylation in the native distal convoluted tubule by Cl⁻-dependent and independent mechanisms. *J Physiol*. 2016;594(21):6319–6331.

REFERENCES

- Greger R. Physiology of renal sodium transport. *Am J Med Sci*. 2000;319:51–62.
- Chambrey R, Kurth I, Peti-Peterdi J, et al. Renal intercalated cells are rather energized by a proton than a sodium pump. *Proc Natl Acad Sci USA*. 2013;110:7928–7933.
- Sun A, Grossman EB, Lombardi M, et al. Vasopressin alters the mechanism of apical Cl⁻ entry from Na⁺:Cl⁻ to Na⁺:K⁺:2Cl⁻ cotransport in mouse medullary thick ascending limb. *J Membr Biol*. 1991;120:83–94.
- Palmer LG, Schnermann J. Integrated control of Na transport along the nephron. *Clin J Am Soc Nephrol*. 2015;10:676–687.
- Ellison DH, Velazquez H, Wright FS. Adaptation of the distal convoluted tubule of the rat. Structural and functional effects of dietary salt intake and chronic diuretic infusion. *J Clin Invest*. 1989;83:113–126.
- Madsen KM, Tishler CC. Anatomy of the kidney. In: Brenner BM, ed. *Brenner and Rector's The Kidney*. Philadelphia: WB Saunders; 2004:3–72.
- Welling LW, Welling DJ. Surface areas of brush border and lateral cell walls in the rabbit proximal nephron. *Kidney Int*. 1975;8:343–348.
- Liu FY, Cogan MG. Axial heterogeneity of bicarbonate, chloride, and water transport in the rat proximal convoluted tubule. Effects of change in luminal flow rate and of alkalemia. *J Clin Invest*. 1986;78:1547–1557.
- Maddox DA, Gennari FJ. The early proximal tubule: a high-capacity delivery-responsive reabsorptive site. *Am J Physiol*. 1987;252:F573–F584.
- Kokko JP. Proximal tubule potential difference. Dependence on glucose, HCO₃⁻, and amino acids. *J Clin Invest*. 1973;52:1362–1367.
- Alpern RJ, Howlin KJ, Preisig PA. Active and passive components of chloride transport in the rat proximal convoluted tubule. *J Clin Invest*. 1985;76:1360–1366.
- Schild L, Giebisch G, Green R. Chloride transport in the proximal renal tubule. *Annu Rev Physiol*. 1988;50:97–110.
- Moe OW, Baum M, Berry CA, et al. Renal transport of glucose, amino acids, sodium, chloride, and water. In: Brenner BM, ed. *Brenner and Rector's The Kidney*. Philadelphia: WB Saunders; 2004.
- Mount DB, Yu AS. Transport of inorganic solutes: sodium, potassium, calcium, magnesium, and phosphate. In: Brenner BM, ed. *Brenner and Rector's The Kidney*. Philadelphia: WB Saunders; 2004:156–213.
- Barratt LJ, Rector FC Jr, Kokko JP, et al. Factors governing the transepithelial potential difference across the proximal tubule of the rat kidney. *J Clin Invest*. 1974;53:454–464.
- Jacobson HR. Characteristics of volume reabsorption in rabbit superficial and juxtamedullary proximal convoluted tubules. *J Clin Invest*. 1979;63:410–418.
- Katz AI, Doucet A, Morel F. Na-K-ATPase activity along the rabbit, rat, and mouse nephron. *Am J Physiol*. 1979;237:F114–F120.
- Baum M, Berry CA. Evidence for neutral transcellular NaCl transport and neutral basolateral chloride exit in the rabbit proximal convoluted tubule. *J Clin Invest*. 1984;74:205–211.
- Vallon V, Verkman AS, Schnermann J. Luminal hypotonicity in proximal tubules of aquaporin-1-knockout mice. *Am J Physiol Renal Physiol*. 2000;278:F1030–F1033.
- Claude P, Goodenough DA. Fracture faces of zonulae occludentes from “tight” and “leaky” epithelia. *J Cell Biol*. 1973;58:390–400.
- Yu AS. Paracellular solute transport: more than just a leak? *Curr Opin Nephrol Hypertens*. 2000;9:513–515.
- Furuse M, Furuse K, Sasaki H, et al. Conversion of zonulae occludentes from tight to leaky strand type by introducing claudin-2 into Madin-Darby canine kidney I cells. *J Cell Biol*. 2001;153:263–272.
- Yu AS, Enck AH, Lencer WI, et al. Claudin-8 expression in Madin-Darby canine kidney cells augments the paracellular barrier to cation permeation. *J Biol Chem*. 2003;278:17350–17359.
- Nitta T, Hata M, Gotoh S, et al. Size-selective loosening of the blood-brain barrier in claudin-5-deficient mice. *J Cell Biol*. 2003;161:653–660.
- Hou J, Rajagopal M, Yu AS. Claudins and the kidney. *Annu Rev Physiol*. 2013;75:479–501.
- Suzuki H, Nishizawa T, Tani K, et al. Crystal structure of a claudin provides insight into the architecture of tight junctions. *Science*. 2014;344:304–307.
- Enck AH, Berger UV, Yu AS. Claudin-2 is selectively expressed in proximal nephron in mouse kidney. *Am J Physiol Renal Physiol*. 2001;281:F966–F974.
- Krug SM, Gunzel D, Conrad MP, et al. Claudin-17 forms tight junction channels with distinct anion selectivity. *Cell Mol Life Sci*. 2012;69:2765–2778.
- Rosenthal R, Milatz S, Krug SM, et al. Claudin-2, a component of the tight junction, forms a paracellular water channel. *J Cell Sci*. 2010;123:1913–1921.
- Muto S, Hata M, Taniguchi J, et al. Claudin-2-deficient mice are defective in the leaky and cation-selective paracellular permeability properties of renal proximal tubules. *Proc Natl Acad Sci USA*. 2010;107:8011–8016.
- Pei L, Solis G, Nguyen MT, et al. Paracellular epithelial sodium transport maximizes energy efficiency in the kidney. *J Clin Invest*. 2016;126:2509–2518.
- Elias BC, Mathew S, Srichai MB, et al. The integrin beta1 subunit regulates paracellular permeability of kidney proximal tubule cells. *J Biol Chem*. 2014;289:8532–8544.
- Bongers E, Shelton LM, Milatz S, et al. A novel hypokalemic-alkalotic salt-losing tubulopathy in patients with CLDN10 mutations. *J Am Soc Nephrol*. 2017;28:3118–3128.
- Schnermann J, Chou CL, Ma T, et al. Defective proximal tubular fluid reabsorption in transgenic aquaporin-1 null mice. *Proc Natl Acad Sci USA*. 1998;95:9660–9664.
- Sohara E, Rai T, Miyazaki J, et al. Defective water and glycerol transport in the proximal tubules of AQP7 knockout mice. *Am J Physiol Renal Physiol*. 2005;289:F1195–F1200.
- Schnermann J, Huang Y, Mizel D. Fluid reabsorption in proximal convoluted tubules of mice with gene deletions of claudin-2 and/or aquaporin1. *Am J Physiol Renal Physiol*. 2013;305:F1352–F1364.
- Zeuthen T, Meinild AK, Loo DD, et al. Isotonic transport by the Na⁺-glucose cotransporter SGLT1 from humans and rabbit. *J Physiol*. 2001;531:631–644.
- Charron FM, Blanchard MG, Lapointe JY. Intracellular hypertonicity is responsible for water flux associated with Na⁺/glucose cotransport. *Biophys J*. 2006;90:3546–3554.
- Maddox DA, Gennari FJ. Load dependence of HCO₃⁻ and H₂O reabsorption in the early proximal tubule of the Munich-Wistar rat. *Am J Physiol*. 1985;248:F113–F121.
- Bobulescu IA, Moe OW. Luminal Na⁽⁺⁾/H⁽⁺⁾ exchange in the proximal tubule. *Pflugers Arch*. 2009;458:5–21.
- Bacic D, Kaissling B, McLeroy P, et al. Dopamine acutely decreases apical membrane Na⁺/H⁺ exchanger NHE3 protein in mouse renal proximal tubule. *Kidney Int*. 2003;64:2133–2141.
- Choi JY, Shah M, Lee MG, et al. Novel amiloride-sensitive sodium-dependent proton secretion in the mouse proximal convoluted tubule. *J Clin Invest*. 2000;105:1141–1146.
- Schultheis PJ, Clarke LL, Meneton P, et al. Renal and intestinal absorptive defects in mice lacking the NHE3 Na⁺/H⁺ exchanger. *Nat Genet*. 1998;19:282–285.
- Wang T, Yang CL, Abbiati T, et al. Essential role of NHE3 in facilitating formate-dependent NaCl absorption in the proximal tubule. *Am J Physiol Renal Physiol*. 2001;281:F288–F292.
- Fenton RA, Poulsen SB, de la Mora Chavez S, et al. Renal tubular NHE3 is required in the maintenance of water and sodium chloride homeostasis. *Kidney Int*. 2017;92:397–414.
- Kurtz I, Nagami G, Yanagawa N, et al. Mechanism of apical and basolateral Na⁽⁺⁾-independent Cl⁻/base exchange in the rabbit superficial proximal straight tubule. *J Clin Invest*. 1994;94:173–183.
- Karniski LP, Aronson PS. Chloride/formate exchange with formic acid recycling: a mechanism of active chloride transport across epithelial membranes. *Proc Natl Acad Sci USA*. 1985;82:6362–6365.
- Saleh AM, Rudnick H, Aronson PS. Mechanism of H⁽⁺⁾-coupled formate transport in rabbit renal microvillus membranes. *Am J Physiol*. 1996;271:F401–F407.
- Karniski LP, Aronson PS. Anion exchange pathways for Cl⁻ transport in rabbit renal microvillus membranes. *Am J Physiol*. 1987;253:F513–F521.
- Wang T, Agulian SK, Giebisch G, et al. Effects of formate and oxalate on chloride absorption in rat distal tubule. *Am J Physiol*. 1993;264:F730–F736.
- Wang T, Egbert AL Jr, Abbiati T, et al. Mechanisms of stimulation of proximal tubule chloride transport by formate and oxalate. *Am J Physiol*. 1996;271:F446–F450.

52. Kuo SM, Aronson PS. Pathways for oxalate transport in rabbit renal microvillus membrane vesicles. *J Biol Chem.* 1996;271:15491–15497.
53. Scott DA, Karniski LP. Human pendrin expressed in *Xenopus laevis* oocytes mediates chloride/formate exchange. *Am J Physiol Cell Physiol.* 2000;278:C207–C211.
54. Royaux IE, Wall SM, Karniski LP, et al. Pendrin, encoded by the Pendred syndrome gene, resides in the apical region of renal intercalated cells and mediates bicarbonate secretion. *Proc Natl Acad Sci USA.* 2001;98:4221–4226.
55. Xie Q, Welch R, Mercado A, et al. Molecular characterization of the murine Slc26a6 anion exchanger: functional comparison with Slc26a1. *Am J Physiol Renal Physiol.* 2002;283:F826–F838.
56. Wang Z, Wang T, Petrovic S, et al. Renal and intestinal transport defects in Slc26a6-null mice. *Am J Physiol Cell Physiol.* 2005;288:C957–C965.
57. Dudas PL, Mentone S, Greineder CF, et al. Immunolocalization of anion transporter Slc26a7 in mouse kidney. *Am J Physiol Renal Physiol.* 2006;290:F937–F945.
58. Kim KH, Shcheynikov N, Wang Y, et al. SLC26A7 is a Cl⁻ channel regulated by intracellular pH. *J Biol Chem.* 2005;280:6463–6470.
59. Simao S, Gomes P, Pinho MJ, et al. Identification of SLC26A transporters involved in the Cl⁽⁻⁾/HCO⁽³⁻⁾ exchange in proximal tubular cells from WKY and SHR. *Life Sci.* 2013;93:435–440.
60. Chapman JM, Karniski LP. Protein localization of SLC26A2 (DTDST) in rat kidney. *Histochem Cell Biol.* 2010;133:541–547.
61. Jiang Z, Asplin JR, Evan AP, et al. Calcium oxalate urolithiasis in mice lacking anion transporter Slc26a6. *Nat Genet.* 2006;38:474–478.
62. Chang MH, Plata C, Zandi-Nejad K, et al. Slc26a9—anion exchanger, channel and Na⁺ transporter. *J Membr Biol.* 2009;228:125–140.
63. Ohana E, Yang D, Shcheynikov N, et al. Diverse transport modes by the solute carrier 26 family of anion transporters. *J Physiol.* 2009;587:2179–2185.
64. Vallon V, Grahmmer F, Volk H, et al. KCNQ1-dependent transport in renal and gastrointestinal epithelia. *Proc Natl Acad Sci USA.* 2005;102:17864–17869.
65. Thomson RB, Wang T, Thomson BR, et al. Role of PDZK1 in membrane expression of renal brush border ion exchangers. *Proc Natl Acad Sci USA.* 2005;102:13331–13336.
66. Petrovic S, Barone S, Weinstein AM, et al. Activation of the apical Na⁺/H⁺ exchanger NHE3 by formate: a basis of enhanced fluid and electrolyte reabsorption by formate in the kidney. *Am J Physiol Renal Physiol.* 2004;287:F336–F346.
67. Mount DB, Gamba G. Renal potassium-chloride cotransporters. *Curr Opin Nephrol Hypertens.* 2001;10:685–691.
68. Mercado A, Vazquez N, Song L, et al. NH2-terminal heterogeneity in the KCC3 K⁺-Cl⁻ cotransporter. *Am J Physiol Renal Physiol.* 2005;289:F1246–F1261.
69. Ishibashi K, Rector FC Jr, Berry CA. Chloride transport across the basolateral membrane of rabbit proximal convoluted tubules. *Am J Physiol.* 1990;258:F1569–F1578.
70. Sasaki S, Ishibashi K, Yoshiyama N, et al. KCl co-transport across the basolateral membrane of rabbit renal proximal straight tubules. *J Clin Invest.* 1988;81:194–199.
71. Avison MJ, Gullans SR, Ogino T, et al. Na⁺ and K⁺ fluxes stimulated by Na⁺-coupled glucose transport: evidence for a Ba²⁺-insensitive K⁺ efflux pathway in rabbit proximal tubules. *J Membr Biol.* 1988;105:197–205.
72. Boettger T, Rust MB, Maier H, et al. Loss of K-Cl co-transporter KCC3 causes deafness, neurodegeneration and reduced seizure threshold. *EMBO J.* 2003;22:5422–5434.
73. Wang T, Delpire E, Giebisch G, et al. Impaired fluid and bicarbonate absorption in proximal tubules (PT) of KCC3 knockout mice. *FASEB J.* 2003;17:A464.
74. Ishibashi K, Rector FC Jr, Berry CA. Role of Na-dependent Cl⁻/HCO³⁻ exchange in basolateral Cl transport of rabbit proximal tubules. *Am J Physiol.* 1993;264:F251–F258.
75. Macri P, Breton S, Beck JS, et al. Basolateral K⁺, Cl⁻, and HCO³⁻ conductances and cell volume regulation in rabbit PCT. *Am J Physiol.* 1993;264:F365–F376.
76. Welling PA, O'Neil RG. Cell swelling activates basolateral membrane Cl and K conductances in rabbit proximal tubule. *Am J Physiol.* 1990;258:F951–F962.
77. Seki G, Taniguchi S, Uwatoko S, et al. Evidence for conductive Cl⁻ pathway in the basolateral membrane of rabbit renal proximal tubule S3 segment. *J Clin Invest.* 1993;92:1229–1235.
78. Obermuller N, Gretz N, Kriz W, et al. The swelling-activated chloride channel ClC-2, the chloride channel ClC-3, and ClC-5, a chloride channel mutated in kidney stone disease, are expressed in distinct subpopulations of renal epithelial cells. *J Clin Invest.* 1998;101:635–642.
79. Alpern RJ, Chambers M. Basolateral membrane Cl⁻/HCO³⁻ exchange in the rat proximal convoluted tubule. Na-dependent and -independent modes. *J Gen Physiol.* 1987;89:581–598.
80. Wang T. Flow-activated transport events along the nephron. *Curr Opin Nephrol Hypertens.* 2006;15:530–536.
81. Du Z, Yan Q, Duan Y, et al. Axial flow modulates proximal tubule NHE3 and H-ATPase activities by changing microvillus bending moments. *Am J Physiol Renal Physiol.* 2006;290:F289–F296.
82. Burg MB, Orloff J. Control of fluid absorption in the renal proximal tubule. *J Clin Invest.* 1968;47:2016–2024.
83. Wang T, Weinbaum S, Weinstein AM. Regulation of glomerulotubular balance: flow-activated proximal tubule function. *Pflugers Arch.* 2017;469:643–654.
84. Du Z, Duan Y, Yan Q, et al. Mechanosensory function of microvilli of the kidney proximal tubule. *Proc Natl Acad Sci USA.* 2004;101:13068–13073.
85. Duan Y, Weinstein AM, Weinbaum S, et al. Shear stress-induced changes of membrane transporter localization and expression in mouse proximal tubule cells. *Proc Natl Acad Sci USA.* 2010;107:21860–21865.
86. Duan Y, Gotoh N, Yan Q, et al. Shear-induced reorganization of renal proximal tubule cell actin cytoskeleton and apical junctional complexes. *Proc Natl Acad Sci USA.* 2008;105:11418–11423.
87. Du Z, Wan L, Yan Q, et al. Regulation of glomerulotubular balance: II: impact of angiotensin II on flow-dependent transport. *Am J Physiol Renal Physiol.* 2012;303:F1507–F1516.
88. Du Z, Yan Q, Wan L, et al. Regulation of glomerulotubular balance. I. Impact of dopamine on flow-dependent transport. *Am J Physiol Renal Physiol.* 2012;303:F386–F395.
89. Du Z, Weinbaum S, Weinstein AM, et al. Regulation of glomerulotubular balance. III. Implication of cytosolic calcium in flow-dependent proximal tubule transport. *Am J Physiol Renal Physiol.* 2015;308:F839–F847.
90. Barfuss DW, Schafer JA. Flow dependence of nonelectrolyte absorption in the nephron. *Am J Physiol.* 1979;236:F163–F174.
91. Brenner BM, Troy JL. Postglomerular vascular protein concentration: evidence for a causal role in governing fluid reabsorption and glomerulotubular balance by the renal proximal tubule. *J Clin Invest.* 1971;50:336–349.
92. Bello-Reuss E, Colindres RE, Pastoriza-Munoz E, et al. Effects of acute unilateral renal denervation in the rat. *J Clin Invest.* 1975;56:208–217.
93. Bell-Reuss E, Trevino DL, Gottschalk CW. Effect of renal sympathetic nerve stimulation on proximal water and sodium reabsorption. *J Clin Invest.* 1976;57:1104–1107.
94. Feraille E, Doucet A. Sodium-potassium-adenosinetriphosphatase-dependent sodium transport in the kidney: hormonal control. *Physiol Rev.* 2001;81:345–418.
95. Hall RA, Premont RT, Chow CW, et al. The beta2-adrenergic receptor interacts with the Na⁺/H⁺-exchanger regulatory factor to control Na⁺/H⁺ exchange. *Nature.* 1998;392:626–630.
96. Gurley SB, Riquier-Brisson AD, Schnermann J, et al. AT1A angiotensin receptors in the renal proximal tubule regulate blood pressure. *Cell Metab.* 2011;13:469–475.
97. Harris PJ, Young JA. Dose-dependent stimulation and inhibition of proximal tubular sodium reabsorption by angiotensin II in the rat kidney. *Pflugers Arch.* 1977;367:295–297.
98. Caravaggi AM, Bianchi G, Brown JJ, et al. Blood pressure and plasma angiotensin II concentration after renal artery constriction and angiotensin infusion in the dog. (5-Isoleucine)angiotensin II and its breakdown fragments in dog blood. *Circ Res.* 1976;38:315–321.
99. Shirai A, Yamazaki O, Horita S, et al. Angiotensin II dose-dependently stimulates human renal proximal tubule transport by the nitric oxide/guanosine 3',5'-cyclic monophosphate pathway. *J Am Soc Nephrol.* 2014;25:1523–1532.
100. Harrison-Bernard LM, Navar LG, Ho MM, et al. Immunohistochemical localization of ANG II AT1 receptor in adult rat kidney using a monoclonal antibody. *Am J Physiol.* 1997;273:F170–F177.
101. Li L, Wang YP, Capparelli AW, et al. Effect of luminal angiotensin II on proximal tubule fluid transport: role of apical phospholipase A2. *Am J Physiol.* 1994;266:F202–F209.

102. Zheng Y, Horita S, Hara C, et al. Biphasic regulation of renal proximal bicarbonate absorption by luminal AT(1A) receptor. *J Am Soc Nephrol*. 2003;14:1116–1122.
103. Kemp BA, Howell NL, Gildea JJ, et al. AT(2) receptor activation induces natriuresis and lowers blood pressure. *Circ Res*. 2014;115:388–399.
104. Quan A, Baum M. Endogenous production of angiotensin II modulates rat proximal tubule transport. *J Clin Invest*. 1996;97:2878–2882.
105. Thomson SC, Deng A, Wead L, et al. An unexpected role for angiotensin II in the link between dietary salt and proximal reabsorption. *J Clin Invest*. 2006;116:1110–1116.
106. Kitada K, Daub S, Zhang Y, et al. High salt intake reprioritizes osmolyte and energy metabolism for body fluid conservation. *J Clin Invest*. 2017.
107. Wang ZQ, Siragy HM, Felder RA, et al. Intrarenal dopamine production and distribution in the rat. Physiological control of sodium excretion. *Hypertension*. 1997;29:228–234.
108. Hegde SS, Jadhav AL, Lokhandwala MF. Role of kidney dopamine in the natriuretic response to volume expansion in rats. *Hypertension*. 1989;13:828–834.
109. Baum M, Quigley R. Inhibition of proximal convoluted tubule transport by dopamine. *Kidney Int*. 1998;54:1593–1600.
110. Yu P, Asico LD, Luo Y, et al. D1 dopamine receptor hyperphosphorylation in renal proximal tubules in hypertension. *Kidney Int*. 2006;70:1072–1079.
111. Albrecht FE, Drago J, Felder RA, et al. Role of the D1A dopamine receptor in the pathogenesis of genetic hypertension. *J Clin Invest*. 1996;97:2283–2288.
112. Hollon TR, Bek MJ, Lachowicz JE, et al. Mice lacking D5 dopamine receptors have increased sympathetic tone and are hypertensive. *J Neurosci*. 2002;22:10801–10810.
113. Zhang MZ, Yao B, Wang S, et al. Intrarenal dopamine deficiency leads to hypertension and decreased longevity in mice. *J Clin Invest*. 2011;121:2845–2854.
114. Holtback U, Brismar H, DiBona GF, et al. Receptor recruitment: a mechanism for interactions between G protein-coupled receptors. *Proc Natl Acad Sci USA*. 1999;96:7271–7275.
115. Harris PJ, Thomas D, Morgan TO. Atrial natriuretic peptide inhibits angiotensin-stimulated proximal tubular sodium and water reabsorption. *Nature*. 1987;326:697–698.
116. Cheng HF, Becker BN, Harris RC. Dopamine decreases expression of type-1 angiotensin II receptors in renal proximal tubule. *J Clin Invest*. 1996;97:2745–2752.
117. Zeng C, Yang Z, Wang Z, et al. Interaction of angiotensin II type 1 and D5 dopamine receptors in renal proximal tubule cells. *Hypertension*. 2005;45:804–810.
118. Zeng C, Liu Y, Wang Z, et al. Activation of D3 dopamine receptor decreases angiotensin II type 1 receptor expression in rat renal proximal tubule cells. *Circ Res*. 2006;99:494–500.
119. Donowitz M, Mohan S, Zhu CX, et al. NHE3 regulatory complexes. *J Exp Biol*. 2009;212:1638–1646.
120. Sarker R, Gronborg M, Cha B, et al. Casein kinase 2 binds to the C terminus of Na⁺/H⁺ exchanger 3 (NHE3) and stimulates NHE3 basal activity by phosphorylating a separate site in NHE3. *Mol Biol Cell*. 2008;19:3859–3870.
121. Liu FY, Cogan MG. Angiotensin II stimulates early proximal bicarbonate absorption in the rat by decreasing cyclic adenosine monophosphate. *J Clin Invest*. 1989;84:83–91.
122. Collazo R, Fan L, Hu MC, et al. Acute regulation of Na⁺/H⁺ exchanger NHE3 by parathyroid hormone via NHE3 phosphorylation and dynamin-dependent endocytosis. *J Biol Chem*. 2000;275:31601–31608.
123. Zhao H, Wiederkkehr MR, Fan L, et al. Acute inhibition of Na/H exchanger NHE-3 by cAMP. Role of protein kinase a and NHE-3 phosphoserines 552 and 605. *J Biol Chem*. 1999;274:3978–3987.
124. Kocinsky HS, Girardi AC, Biemesderfer D, et al. Use of phospho-specific antibodies to determine the phosphorylation of endogenous Na⁺/H⁺ exchanger NHE3 at PKA consensus sites. *Am J Physiol Renal Physiol*. 2005;289:F249–F258.
125. Biemesderfer D, DeGray B, Aronson PS. Active (9.6 s) and inactive (21 s) oligomers of NHE3 in microdomains of the renal brush border. *J Biol Chem*. 2001;276:10161–10167.
126. Lessa LM, Carraro-Lacroix LR, Crajoins RO, et al. Mechanisms underlying the inhibitory effects of uroguanylin on NHE3 transport activity in renal proximal tubule. *Am J Physiol Renal Physiol*. 2012;303:F1399–F1408.
127. Liu T, Jose PA. Gastrin induces sodium-hydrogen exchanger 3 phosphorylation and mTOR activation via a phosphoinositide 3-kinase-/protein kinase C-dependent but AKT-independent pathway in renal proximal tubule cells derived from a normotensive male human. *Endocrinology*. 2013;154:865–875.
128. Weinman EJ, Cunningham R, Shenolikar S. NHERF and regulation of the renal sodium-hydrogen exchanger NHE3. *Pflugers Arch*. 2005;450:137–144.
129. Sanchez-Mendoza A, Lopez-Sanchez P, Vazquez-Cruz B, et al. Angiotensin II modulates ion transport in rat proximal tubules through CYP metabolites. *Biochem Biophys Res Commun*. 2000;272:423–430.
130. Dos Santos EA, Dahly-Vernon AJ, Hoagland KM, et al. Inhibition of the formation of EETs and 20-HETE with 1-aminobenzotriazole attenuates pressure natriuresis. *Am J Physiol Regul Integr Comp Physiol*. 2004;287:R58–R68.
131. du Cheyron D, Chalumeau C, Defontaine N, et al. Angiotensin II stimulates NHE3 activity by exocytic insertion of the transporter: role of PI 3-kinase. *Kidney Int*. 2003;64:939–949.
132. Leong PK, Devillez A, Sandberg MB, et al. Effects of ACE inhibition on proximal tubule sodium transport. *Am J Physiol Renal Physiol*. 2006;290:F854–F863.
133. Yun CC, Chen Y, Lang F. Glucocorticoid activation of Na⁽⁺⁾/H⁽⁺⁾ exchanger isoform 3 revisited. The roles of SGK1 and NHERF2. *J Biol Chem*. 2002;277:7676–7683.
134. Wang D, Sun H, Lang F, et al. Activation of NHE3 by dexamethasone requires phosphorylation of NHE3 at Ser663 by SGK1. *Am J Physiol Cell Physiol*. 2005;289:C802–C810.
135. Pedemonte CH, Efendiev R, Bertorello AM. Inhibition of Na_oK-ATPase by dopamine in proximal tubule epithelial cells. *Semin Nephrol*. 2005;25:322–327.
136. Chou CL, Knepper MA, Hoek AN, et al. Reduced water permeability and altered ultrastructure in thin descending limb of Henle in aquaporin-1 null mice. *J Clin Invest*. 1999;103:491–496.
137. Liu W, Morimoto T, Kondo Y, et al. Analysis of NaCl transport in thin ascending limb of Henle's loop in CLC-K1 null mice. *Am J Physiol Renal Physiol*. 2002;282:F451–F457.
138. Nielsen S, Pallone T, Smith BL, et al. Aquaporin-1 water channels in short and long loop descending thin limbs and in descending vasa recta in rat kidney. *Am J Physiol*. 1995;268:F1023–F1037.
139. Allen F, Tisher CC. Morphology of the ascending thick limb of Henle. *Kidney Int*. 1976;9:8–22.
140. Tsuruoka S, Koseki C, Muto S, et al. Axial heterogeneity of potassium transport across hamster thick ascending limb of Henle's loop. *Am J Physiol*. 1994;267:F121–F129.
141. Nielsen S, Maunsbach AB, Ecelbarger CA, et al. Ultrastructural localization of Na-K-2Cl cotransporter in thick ascending limb and macula densa of rat kidney. *Am J Physiol*. 1998;275:F885–F893.
142. Yoshitomi K, Kondo Y, Imai M. Evidence for conductive Cl⁻ pathways across the cell membranes of the thin ascending limb of Henle's loop. *J Clin Invest*. 1988;82:866–871.
143. Gottschalk CW, Lassiter WE, Mylle M, et al. Micropuncture study of composition of loop of Henle fluid in desert rodents. *Am J Physiol*. 1963;204:532–535.
144. Kokko JP. Sodium chloride and water transport in the descending limb of Henle. *J Clin Invest*. 1970;49:1838–1846.
145. Imai M, Taniguchi J, Yoshitomi K. Transition of permeability properties along the descending limb of long-loop nephron. *Am J Physiol*. 1988;254:F323–F328.
146. Chou CL, Knepper MA. In vitro perfusion of chinchilla thin limb segments: urea and NaCl permeabilities. *Am J Physiol*. 1993;264:F337–F343.
147. Chou CL, Knepper MA. In vitro perfusion of chinchilla thin limb segments: segmentation and osmotic water permeability. *Am J Physiol*. 1992;263:F417–F426.
148. Lopes AG, Amzel LM, Markakis D, et al. Cell volume regulation by the thin descending limb of Henle's loop. *Proc Natl Acad Sci USA*. 1988;85:2873–2877.
149. Imai M. Function of the thin ascending limb of Henle of rats and hamsters perfused in vitro. *Am J Physiol*. 1977;232:F201–F209.
150. Koyama S, Yoshitomi K, Imai M. Effect of protamine on ion conductance of ascending thin limb of Henle's loop from hamsters. *Am J Physiol*. 1991;261:F593–F599.
151. Takahashi N, Kondo Y, Fujiwara I, et al. Characterization of Na⁺ transport across the cell membranes of the ascending thin limb of Henle's loop. *Kidney Int*. 1995;47:789–794.

152. Kondo Y, Yoshitomi K, Imai M. Effects of anion transport inhibitors and ion substitution on Cl⁻ transport in TAL of Henle's loop. *Am J Physiol*. 1987;253:F1206-F1215.
153. Iozaki T, Yoshitomi K, Imai M. Effects of Cl⁻ transport inhibitors on Cl⁻ permeability across hamster ascending thin limb. *Am J Physiol*. 1989;257:F92-F98.
154. Kondo Y, Abe K, Igarashi Y, et al. Direct evidence for the absence of active Na⁺ reabsorption in hamster ascending thin limb of Henle's loop. *J Clin Invest*. 1993;91:5-11.
155. Takahashi N, Kondo Y, Ito O, et al. Vasopressin stimulates Cl⁻ transport in ascending thin limb of Henle's loop in hamster. *J Clin Invest*. 1995;95:1623-1627.
156. Uchida S, Sasaki S, Nitta K, et al. Localization and functional characterization of rat kidney-specific chloride channel, ClC-K1. *J Clin Invest*. 1995;95:104-113.
157. Wolf K, Meier-Meitingner M, Bergler T, et al. Parallel down-regulation of chloride channel ClC-K1 and barttin mRNA in the thin ascending limb of the rat nephron by furosemide. *Pflugers Arch*. 2003;446:665-671.
158. Waldegger S, Jeck N, Barth P, et al. Barttin increases surface expression and changes current properties of ClC-K channels. *Pflugers Arch*. 2002;444:411-418.
159. Matsumura Y, Uchida S, Kondo Y, et al. Overt nephrogenic diabetes insipidus in mice lacking the ClC-K1 chloride channel. *Nat Genet*. 1999;21:95-98.
160. Simon DB, Bindra RS, Mansfield TA, et al. Mutations in the chloride channel gene, CLCNKB, cause Bartter's syndrome type III. *Nat Genet*. 1997;17:171-178.
161. Grill A, Schiessl IM, Gess B, et al. Salt-losing nephropathy in mice with a null mutation of the Clcnk2 gene. *Acta Physiol (Oxf)*. 2016;218:198-211.
162. Hennings JC, Andriani O, Picard N, et al. The ClC-K2 chloride channel is critical for salt handling in the distal nephron. *J Am Soc Nephrol*. 2017;28:209-217.
163. Estevez R, Boettger T, Stein V, et al. Barttin is a Cl⁻ channel beta-subunit crucial for renal Cl⁻ reabsorption and inner ear K⁺ secretion. *Nature*. 2001;414:558-561.
164. Scholl U, Hebeisen S, Janssen AG, et al. Barttin modulates trafficking and function of ClC-K channels. *Proc Natl Acad Sci USA*. 2006;103:11411-11416.
165. Uchida S, Sasaki S, Furukawa T, et al. Molecular cloning of a chloride channel that is regulated by dehydration and expressed predominantly in kidney medulla. *J Biol Chem*. 1993;268:3821-3824.
166. Sugawara N, Morimoto T, Farajov EI, et al. Calcium and calcimimetics regulate paracellular Na⁺ transport in the thin ascending limb of Henle's loop in mouse kidney. *Pflugers Arch*. 2010;460:197-205.
167. Greger R. Ion transport mechanisms in thick ascending limb of Henle's loop of mammalian nephron. *Physiol Rev*. 1985;65:760-797.
168. Hebert SC, Mount DB, Gamba G. Molecular physiology of cation-coupled Cl⁻ cotransport: the SLC12 family. *Pflugers Arch*. 2004;447:580-593.
169. Plata C, Mount DB, Rubio V, et al. Isoforms of the Na-K-2Cl cotransporter in murine TAL II. Functional characterization and activation by cAMP. *Am J Physiol*. 1999;276:F359-F366.
170. Gimenez I, Isenring P, Forbush B. Spatially distributed alternative splice variants of the renal Na-K-Cl cotransporter exhibit dramatically different affinities for the transported ions. *J Biol Chem*. 2002;277:8767-8770.
171. Lapointe JY, Laamarti A, Bell PD. Ionic transport in macula densa cells. *Kidney Int Suppl*. 1998;67:S58-S64.
172. Castrop H, Schiessl IM. Physiology and pathophysiology of the renal Na-K-2Cl cotransporter (NKCC2). *Am J Physiol Renal Physiol*. 2014;307:F991-F1002.
173. Oppermann M, Mizel D, Huang G, et al. Macula densa control of renin secretion and preglomerular resistance in mice with selective deletion of the B isoform of the Na,K,2Cl co-transporter. *J Am Soc Nephrol*. 2006;17:2143-2152.
174. Castrop H, Schnermann J. Isoforms of renal Na-K-2Cl cotransporter NKCC2: expression and functional significance. *Am J Physiol Renal Physiol*. 2008;295:F859-F866.
175. Good DW, Watts BA 3rd. Functional roles of apical membrane Na⁺/H⁺ exchange in rat medullary thick ascending limb. *Am J Physiol*. 1996;270:F691-F699.
176. Laghmani K, Borensztein P, Ambuhl P, et al. Chronic metabolic acidosis enhances NHE-3 protein abundance and transport activity in the rat thick ascending limb by increasing NHE-3 mRNA. *J Clin Invest*. 1997;99:24-30.
177. Quentin F, Eladari D, Frische S, et al. Regulation of the Cl⁻/HCO₃⁻-exchanger AE2 in rat thick ascending limb of Henle's loop in response to changes in acid-base and sodium balance. *J Am Soc Nephrol*. 2004;15:2988-2997.
178. Hong NJ, Garvin JL. Endogenous flow-induced superoxide stimulates Na/H exchange activity via PKC in thick ascending limbs. *Am J Physiol Renal Physiol*. 2014;307:F800-F805.
179. Burg MB, Green N. Function of the thick ascending limb of Henle's loop. *Am J Physiol*. 1973;224:659-668.
180. Rocha AS, Kokko JP. Sodium chloride and water transport in the medullary thick ascending limb of Henle. Evidence for active chloride transport. *J Clin Invest*. 1973;52:612-623.
181. Stokes JB. Consequences of potassium recycling in the renal medulla. Effects of ion transport by the medullary thick ascending limb of Henle's loop. *J Clin Invest*. 1982;70:219-229.
182. Greger R, Weidtko C, Schlatter E, et al. Potassium activity in cells of isolated perfused cortical thick ascending limbs of rabbit kidney. *Pflugers Arch*. 1984;401:52-57.
183. Simon DB, Karet FE, Rodriguez-Soriano J, et al. Genetic heterogeneity of Bartter's syndrome revealed by mutations in the K⁺ channel, ROMK. *Nat Genet*. 1996;14:152-156.
184. Garcia ML, Priest BT, Alonso-Galicia M, et al. Pharmacologic inhibition of the renal outer medullary potassium channel causes diuresis and natriuresis in the absence of kaliuresis. *J Pharmacol Exp Ther*. 2014;348:153-164.
185. Taniguchi J, Guggino WB. Membrane stretch: a physiological stimulator of Ca²⁺-activated K⁺ channels in thick ascending limb. *Am J Physiol*. 1989;257:F347-F352.
186. Bleich M, Schlatter E, Greger R. The luminal K⁺ channel of the thick ascending limb of Henle's loop. *Pflugers Arch*. 1990;415:449-460.
187. Wang WH. Two types of K⁺ channel in thick ascending limb of rat kidney. *Am J Physiol*. 1994;267:F599-F605.
188. Wang W, Lu M. Effect of arachidonic acid on activity of the apical K⁺ channel in the thick ascending limb of the rat kidney. *J Gen Physiol*. 1995;106:727-743.
189. Boim MA, Ho K, Shuck ME, et al. ROMK inwardly rectifying ATP-sensitive K⁺ channel. II. Cloning and distribution of alternative forms. *Am J Physiol*. 1995;268:F1132-F1140.
190. Xu JZ, Hall AE, Peterson LN, et al. Localization of the ROMK protein on apical membranes of rat kidney nephron segments. *Am J Physiol*. 1997;273:F739-F748.
191. Lu M, Wang T, Yan Q, et al. Absence of small conductance K⁺ channel (SK) activity in apical membranes of thick ascending limb and cortical collecting duct in ROMK (Bartter's) knockout mice. *J Biol Chem*. 2002;277:37881-37887.
192. Lu M, Wang T, Yan Q, et al. ROMK is required for expression of the 70-pS K channel in the thick ascending limb. *Am J Physiol Renal Physiol*. 2004;286:F490-F495.
193. Dong K, Yan Q, Lu M, et al. Romk1 knockout mice do not produce bartter phenotype but exhibit impaired K excretion. *J Biol Chem*. 2016;291:5259-5269.
194. Yoo D, Flagg TP, Olsen O, et al. Assembly and trafficking of a multiprotein ROMK (Kir 1.1) channel complex by PDZ interactions. *J Biol Chem*. 2004;279:6863-6873.
195. Lu M, Leng Q, Egan ME, et al. CFTR is required for PKA-regulated ATP sensitivity of Kir1.1 potassium channels in mouse kidney. *J Clin Invest*. 2006;116:797-807.
196. Hebert SC, Andreoli TE. Ionic conductance pathways in the mouse medullary thick ascending limb of Henle. The paracellular pathway and electrogenic Cl⁻ absorption. *J Gen Physiol*. 1986;87:567-590.
197. Hebert SC, Culpepper RM, Andreoli TE. NaCl transport in mouse medullary thick ascending limbs. II. ADH enhancement of transcellular NaCl cotransport; origin of transepithelial voltage. *Am J Physiol*. 1981;241:F432-F442.
198. Gong Y, Hou J. Claudins in barrier and transport function-the kidney. *Pflugers Arch*. 2017;469:105-113.
199. Konrad M, Schaller A, Seelow D, et al. Mutations in the tight-junction gene claudin 19 (CLDN19) are associated with renal magnesium wasting, renal failure, and severe ocular involvement. *Am J Hum Genet*. 2006;79:949-957.
200. Angelow S, El-Husseini R, Kanzawa SA, et al. Renal localization and function of the tight junction protein, claudin-19. *Am J Physiol Renal Physiol*. 2007;293:F166-F177.

201. Milatz S, Himmerkus N, Wulfmeyer VC, et al. Mosaic expression of claudins in thick ascending limbs of Henle results in spatial separation of paracellular Na⁺ and Mg²⁺ transport. *Proc Natl Acad Sci USA*. 2017;114:E219–E227.
202. Hou J, Paul DL, Goodenough DA. Paracellin-1 and the modulation of ion selectivity of tight junctions. *J Cell Sci*. 2005;118:5109–5118.
203. Hou J, Renigunta A, Konrad M, et al. Claudin-16 and claudin-19 interact and form a cation-selective tight junction complex. *J Clin Invest*. 2008;118:619–628.
204. Hou J, Renigunta A, Gomes AS, et al. Claudin-16 and claudin-19 interaction is required for their assembly into tight junctions and for renal reabsorption of magnesium. *Proc Natl Acad Sci USA*. 2009;106:15350–15355.
205. Himmerkus N, Shan Q, Goerke B, et al. Salt and acid-base metabolism in claudin-16 knockdown mice: impact for the pathophysiology of FHHNC patients. *Am J Physiol Renal Physiol*. 2008;295:F1641–F1647.
206. Gong Y, Renigunta V, Himmerkus N, et al. Claudin-14 regulates renal Ca⁺(+) transport in response to CaSR signalling via a novel microRNA pathway. *EMBO J*. 2012;31:1999–2012.
207. Toka HR, Al-Romaih K, Koshy JM, et al. Deficiency of the calcium-sensing receptor in the kidney causes parathyroid hormone-independent hypocalciuria. *J Am Soc Nephrol*. 2012;23:1879–1890.
208. Dimke H, Desai P, Borovac J, et al. Activation of the Ca²⁺-sensing receptor increases renal claudin-14 expression and urinary Ca²⁺ excretion. *Am J Physiol Renal Physiol*. 2013;304:F761–F769.
209. Breiderhoff T, Himmerkus N, Stuver M, et al. Deletion of claudin-10 (Cldn10) in the thick ascending limb impairs paracellular sodium permeability and leads to hypermagnesemia and nephrocalcinosis. *Proc Natl Acad Sci USA*. 2012;109:14241–14246.
210. Greger R, Schlatter E. Properties of the basolateral membrane of the cortical thick ascending limb of Henle's loop of rabbit kidney. A model for secondary active chloride transport. *Pflugers Arch*. 1983;396:325–334.
211. Jeck N, Waldegger P, Doroszewicz J, et al. A common sequence variation of the CLCNKB gene strongly activates ClC-Kb chloride channel activity. *Kidney Int*. 2004;65:190–197.
212. Sile S, Velez DR, Gillani NB, et al. CLCNKB-T481S and essential hypertension in a Ghanaian population. *J Hypertens*. 2009;27:298–304.
213. Jeck N, Waldegger S, Lampert A, et al. Activating mutation of the renal epithelial chloride channel ClC-Kb predisposing to hypertension. *Hypertension*. 2004;43:1175–1181.
214. Kobayashi K, Uchida S, Mizutani S, et al. Intrarenal and cellular localization of CLC-K2 protein in the mouse kidney. *J Am Soc Nephrol*. 2001;12:1327–1334.
215. Picollo A, Liantonio A, Didonna MP, et al. Molecular determinants of differential pore blocking of kidney ClC-K chloride channels. *EMBO Rep*. 2004;5:584–589.
216. Palmer LG, Frindt G. Cl⁻ channels of the distal nephron. *Am J Physiol Renal Physiol*. 2006;291:F1157–F1168.
217. Boettger T, Hubner CA, Maier H, et al. Deafness and renal tubular acidosis in mice lacking the K-Cl co-transporter Kcc4. *Nature*. 2002;416:874–878.
218. Song L, Delpire E, Gamba G, et al. Localization of the K-Cl cotransporters KCC3 and KCC4 in mouse kidney. *FASEB J*. 2000;A341.
219. Amlal H, Paillard M, Bichara M. Cl⁻-dependent NH₄⁺ transport mechanisms in medullary thick ascending limb cells. *Am J Physiol*. 1994;267:C1607–C1615.
220. Bergeron MJ, Gagnon E, Wallendorff B, et al. Ammonium transport and pH regulation by K⁺-Cl⁻ cotransporters. *Am J Physiol Renal Physiol*. 2003;285:F68–F78.
221. Mercado A, Song L, Vazquez N, et al. Functional comparison of the K-Cl cotransporters KCC1 and KCC4. *J Biol Chem*. 2000;275:30326–30334.
222. Guggino WB. Functional heterogeneity in the early distal tubule of the Amphiuma kidney: evidence for two modes of Cl⁻ and K⁺ transport across the basolateral cell membrane. *Am J Physiol*. 1986;250:F430–F440.
223. Good DW. Ammonium transport by the thick ascending limb of Henle's loop. *Annu Rev Physiol*. 1994;56:623–647.
224. Hurst AM, Duplain M, Lapointe JY. Basolateral membrane potassium channels in rabbit cortical thick ascending limb. *Am J Physiol*. 1992;263:F262–F267.
225. Paulais M, Lachheb S, Teulon J. A Na⁺- and Cl⁻-activated K⁺ channel in the thick ascending limb of mouse kidney. *J Gen Physiol*. 2006;127:205–215.
226. Paulais M, Lourdel S, Teulon J. Properties of an inwardly rectifying K⁺ channel in the basolateral membrane of mouse TAL. *Am J Physiol Renal Physiol*. 2002;282:F866–F876.
227. Su XT, Zhang C, Wang L, et al. Disruption of KCNJ10 (Kir4.1) stimulates the expression of ENaC in the collecting duct. *Am J Physiol Renal Physiol*. 2016;310:F985–F993.
228. Bockenhauer D, Feather S, Stanescu HC, et al. Epilepsy, ataxia, sensorineural deafness, tubulopathy, and KCNJ10 mutations. *N Engl J Med*. 2009;360:1960–1970.
229. Liu Y, Song X, Shi Y, et al. WNK1 activates large-conductance Ca²⁺-activated K⁺ channels through modulation of ERK1/2 signaling. *J Am Soc Nephrol*. 2015;26:844–854.
230. Ares GR, Caceres PS, Ortiz PA. Molecular regulation of NKCC2 in the thick ascending limb. *Am J Physiol Renal Physiol*. 2011;301:F1143–F1159.
231. Wu P, Wang M, Luan H, et al. Angiotensin II stimulates basolateral 10-pS Cl channels in the thick ascending limb. *Hypertension*. 2013;61:1211–1217.
232. Mutig K, Borowski T, Boldt C, et al. Demonstration of the functional impact of vasopressin signaling in the thick ascending limb by a targeted transgenic rat approach. *Am J Physiol Renal Physiol*. 2016;311:F411–F423.
233. Knepper MA, Kim GH, Fernandez-Llana P, et al. Regulation of thick ascending limb transport by vasopressin. *J Am Soc Nephrol*. 1999;10:628–634.
234. Ortiz PA. cAMP increases surface expression of NKCC2 in rat thick ascending limbs: role of VAMP. *Am J Physiol Renal Physiol*. 2006;290:F608–F616.
235. Gagnon KB, England R, Delpire E. Volume sensitivity of cation-Cl⁻ cotransporters is modulated by the interaction of two kinases: Ste20-related proline-alanine-rich kinase and WNK4. *Am J Physiol Cell Physiol*. 2006;290:C134–C142.
236. Takahashi D, Mori T, Nomura N, et al. WNK4 is the major WNK kinase positively regulating NCC in the mouse kidney. *Biosci Rep*. 2014;9:e00107.
237. Castaneda-Bueno M, Cervantes-Perez LG, Vazquez N, et al. Activation of the renal Na⁺-Cl⁻ cotransporter by angiotensin II is a WNK4-dependent process. *Proc Natl Acad Sci USA*. 2012;109:7929–7934.
238. Rinehart J, Kahle KT, de Los Heros P, et al. WNK3 kinase is a positive regulator of NKCC2 and NCC, renal cation-Cl⁻ cotransporters required for normal blood pressure homeostasis. *Proc Natl Acad Sci USA*. 2005;102:16777–16782.
239. Delpire E, Gagnon KB. Genome-wide analysis of SPAK/OSR1 binding motifs. *Physiol Genomics*. 2007;28:223–231.
240. Gagnon KB, England R, Delpire E. A single binding motif is required for SPAK activation of the Na-K-2Cl cotransporter. *Cell Physiol Biochem*. 2007;20:131–142.
241. Reiche J, Theilig F, Rafiqi FH, et al. SORLA/SORL1 functionally interacts with SPAK to control renal activation of Na⁺-K⁺-Cl⁻ cotransporter 2. *Mol Cell Biol*. 2010;30:3027–3037.
242. Rafiqi FH, Zuber AM, Glover M, et al. Role of the WNK-activated SPAK kinase in regulating blood pressure. *EMBO Mol Med*. 2010;2:63–75.
243. Ponce-Coria J, San-Cristobal P, Kahle KT, et al. Regulation of NKCC2 by a chloride-sensing mechanism involving the WNK3 and SPAK kinases. *Proc Natl Acad Sci USA*. 2008;105:8458–8463.
244. Lin SH, Yu IS, Jiang ST, et al. Impaired phosphorylation of Na⁺-K⁺-2Cl⁻ cotransporter by oxidative stress-responsive kinase-1 deficiency manifests hypotension and Bartter-like syndrome. *Proc Natl Acad Sci USA*. 2011;108:17538–17543.
245. Grimm PR, Taneja TK, Liu J, et al. SPAK isoforms and OSR1 regulate sodium-chloride co-transporters in a nephron-specific manner. *J Biol Chem*. 2012;287:37673–37690.
246. Yang SS, Lo YF, Wu CC, et al. SPAK-knockout mice manifest Gitelman syndrome and impaired vasoconstriction. *J Am Soc Nephrol*. 2010;21:1868–1877.
247. McCormick JA, Mutig K, Nelson JH, et al. A SPAK isoform switch modulates renal salt transport and blood pressure. *Cell Metab*. 2011;14:352–364.
248. Cheng CJ, Yoon J, Baum M, et al. STE20/SPS1-related proline/alanine-rich kinase (SPAK) is critical for sodium reabsorption in isolated, perfused thick ascending limb. *Am J Physiol Renal Physiol*. 2015;308:F437–F443.
249. Markadieu N, Rios K, Spiller BW, et al. Short forms of Ste20-related proline/alanine-rich kinase (SPAK) in the kidney are created by

- aspartyl aminopeptidase (Dnpep)-mediated proteolytic cleavage. *J Biol Chem.* 2014;289:29273–29284.
250. Filippi BM, de los Heros P, Mehellou Y, et al. MO25 is a master regulator of SPAK/OSR1 and MST3/MST4/YSK1 protein kinases. *EMBO J.* 2011;30:1730–1741.
 251. Ponce-Coria J, Gagnon KB, Delpire E. Calcium-binding protein 39 facilitates molecular interaction between Ste20p proline alanine-rich kinase and oxidative stress response 1 monomers. *Am J Physiol Cell Physiol.* 2012;303:C1198–C1205.
 252. Ponce-Coria J, Markadieu N, Austin TM, et al. A novel Ste20-related proline/alanine-rich kinase (SPAK)-independent pathway involving calcium-binding protein 39 (Cab39) and serine threonine kinase with no lysine member 4 (WNK4) in the activation of Na-K-Cl cotransporters. *J Biol Chem.* 2014;289:17680–17688.
 253. Hannemann A, Flatman PW. Phosphorylation and transport in the Na-K-2Cl cotransporters, NKCC1 and NKCC2A, compared in HEK-293 cells. *PLoS ONE.* 2011;6:e17992.
 254. Mount DB, Baekgaard A, Hall AE, et al. Isoforms of the Na-K-2Cl cotransporter in murine TAL I. Molecular characterization and intrarenal localization. *Am J Physiol.* 1999;276:F347–F358.
 255. Plata C, Meade P, Hall A, et al. Alternatively spliced isoform of apical Na(+)-K(+)-Cl(-) cotransporter gene encodes a furosemide-sensitive Na(+)-Cl(-) cotransporter. *Am J Physiol Renal Physiol.* 2001;280:F574–F582.
 256. Xu ZC, Yang Y, Hebert SC. Phosphorylation of the ATP-sensitive, inwardly rectifying K⁺ channel, ROMK, by cyclic AMP-dependent protein kinase. *J Biol Chem.* 1996;271:9313–9319.
 257. Yoo D, Kim BY, Campo C, et al. Cell surface expression of the ROMK (Kir 1.1) channel is regulated by the aldosterone-induced kinase, SGK-1, and protein kinase A. *J Biol Chem.* 2003;278:23066–23075.
 258. Leipziger J, MacGregor GG, Cooper GJ, et al. PKA site mutations of ROMK2 channels shift the pH dependence to more alkaline values. *Am J Physiol Renal Physiol.* 2000;279:F919–F926.
 259. Liou HH, Zhou SS, Huang CL. Regulation of ROMK1 channel by protein kinase A via a phosphatidylinositol 4,5-bisphosphate-dependent mechanism. *Proc Natl Acad Sci USA.* 1999;96:5820–5825.
 260. Ecelbarger CA, Kim GH, Knepper MA, et al. Regulation of potassium channel Kir 1.1 (ROMK) abundance in the thick ascending limb of Henle's loop. *J Am Soc Nephrol.* 2001;12:10–18.
 261. Procino G, Carosino M, Milano S, et al. beta3 adrenergic receptor in the kidney may be a new player in sympathetic regulation of renal function. *Kidney Int.* 2016;90:555–567.
 262. Takaichi K, Kurokawa K. Inhibitory guanosine triphosphate-binding protein-mediated regulation of vasopressin action in isolated single medullary tubules of mouse kidney. *J Clin Invest.* 1988;82:1437–1444.
 263. Hebert SC. Calcium and salinity sensing by the thick ascending limb: a journey from mammals to fish and back again. *Kidney Int Suppl.* 2004;S28–S33.
 264. Riccardi D, Hall AE, Chattopadhyay N, et al. Localization of the extracellular Ca²⁺/polyvalent cation-sensing protein in rat kidney. *Am J Physiol.* 1998;274:F611–F622.
 265. de Jesus Ferreira MC, Helies-Toussaint C, Imbert-Teboul M, et al. Co-expression of a Ca²⁺-inhibitable adenylyl cyclase and of a Ca²⁺-sensing receptor in the cortical thick ascending limb cell of the rat kidney. Inhibition of hormone-dependent cAMP accumulation by extracellular Ca²⁺. *J Biol Chem.* 1998;273:15192–15202.
 266. Watanabe S, Fukumoto S, Chang H, et al. Association between activating mutations of calcium-sensing receptor and Bartter's syndrome. *Lancet.* 2002;360:692–694.
 267. Vargas-Poussou R, Huang C, Hulin P, et al. Functional characterization of a calcium-sensing receptor mutation in severe autosomal dominant hypocalcemia with a Bartter-like syndrome. *J Am Soc Nephrol.* 2002;13:2259–2266.
 268. Loupy A, Ramakrishnan SK, Wootla B, et al. PTH-independent regulation of blood calcium concentration by the calcium-sensing receptor. *J Clin Invest.* 2012;122:3355–3367.
 269. Rampoldi L, Scolari F, Amoroso A, et al. The rediscovery of uromodulin (Tamm-Horsfall protein): from tubulointerstitial nephropathy to chronic kidney disease. *Kidney Int.* 2011;80:338–347.
 270. Mutig K, Kahl T, Saritas T, et al. Activation of the bumetanide-sensitive Na⁺,K⁺,2Cl⁻ cotransporter (NKCC2) is facilitated by Tamm-Horsfall protein in a chloride-sensitive manner. *J Biol Chem.* 2011;286:30200–30210.
 271. Renigunta A, Renigunta V, Saritas T, et al. Tamm-Horsfall glycoprotein interacts with renal outer medullary potassium channel ROMK2 and regulates its function. *J Biol Chem.* 2011;286:2224–2235.
 272. Dahan K, Devuyst O, Smaers M, et al. A cluster of mutations in the UMOD gene causes familial juvenile hyperuricemic nephropathy with abnormal expression of uromodulin. *J Am Soc Nephrol.* 2003;14:2883–2893.
 273. Trudu M, Janas S, Lanzani C, et al. Common noncoding UMOD gene variants induce salt-sensitive hypertension and kidney damage by increasing uromodulin expression. *Nat Med.* 2013;19:1655–1660.
 274. Olden M, Corre T, Hayward C, et al. Common variants in UMOD associate with urinary uromodulin levels: a meta-analysis. *J Am Soc Nephrol.* 2014;25:1869–1882.
 275. Loffing J, Kaissling B. Sodium and calcium transport pathways along the mammalian distal nephron: from rabbit to human. *Am J Physiol Renal Physiol.* 2003;284:F628–F643.
 276. Loffing J, Loffing-Cueni D, Valderrabano V, et al. Distribution of transcellular calcium and sodium transport pathways along mouse distal nephron. *Am J Physiol Renal Physiol.* 2001;281:F1021–F1027.
 277. Belge H, Gailly P, Schwaller B, et al. Renal expression of parvalbumin is critical for NaCl handling and response to diuretics. *Proc Natl Acad Sci USA.* 2007;104:14849–14854.
 278. Mistry AC, Wynne BM, Yu L, et al. The sodium chloride cotransporter (NCC) and epithelial sodium channel (ENaC) associate. *Biochem J.* 2016;473:3237–3252.
 279. Frindt G, Palmer LG. Na channels in the rat connecting tubule. *Am J Physiol Renal Physiol.* 2004;286:F669–F674.
 280. Wall SM. Recent advances in our understanding of intercalated cells. *Curr Opin Nephrol Hypertens.* 2005;14:480–484.
 281. Duc C, Farman N, Canessa CM, et al. Cell-specific expression of epithelial sodium channel alpha, beta, and gamma subunits in aldosterone-responsive epithelia from the rat: localization by in situ hybridization and immunocytochemistry. *J Cell Biol.* 1994;127:1907–1921.
 282. Malnic G, Klose RM, Giebisch G. Micropuncture Study of Renal Potassium Excretion in the Rat. *Am J Physiol.* 1964;206:674–686.
 283. Wingo CS, Armitage FE. Rubidium absorption and proton secretion by rabbit outer medullary collecting duct via H-K-ATPase. *Am J Physiol.* 1992;263:F849–F857.
 284. Okusa MD, Unwin RJ, Velazquez H, et al. Active potassium absorption by the renal distal tubule. *Am J Physiol.* 1992;262:F488–F493.
 285. Meneton P, Schultheis PJ, Greeb J, et al. Increased sensitivity to K⁺ deprivation in colonic H,K-ATPase-deficient mice. *J Clin Invest.* 1998;101:536–542.
 286. Hager H, Kwon TH, Vinnikova AK, et al. Immunocytochemical and immunoelectron microscopic localization of alpha-, beta-, and gamma-ENaC in rat kidney. *Am J Physiol Renal Physiol.* 2001;280:F1093–F1106.
 287. Khuri RN, Strieder N, Wiederholt M, et al. Effects of graded solute diuresis on renal tubular sodium transport in the rat. *Am J Physiol.* 1975;228:1262–1268.
 288. Velázquez H, Good DW, Wright FS. Mutual dependence of sodium and chloride absorption by renal distal tubule. *Am J Physiol.* 1984;247:F904–F911.
 289. Costanzo LS. Localization of diuretic action in microperfused rat distal tubules: Ca and Na transport. *Am J Physiol.* 1985;248:F527–F535.
 290. Gamba G, Saltzberg SN, Lombardi M, et al. Primary structure and functional expression of a cDNA encoding the thiazide-sensitive, electroneutral sodium-chloride cotransporter. *Proc Natl Acad Sci USA.* 1993;90:2749–2753.
 291. Monroy A, Plata C, Hebert SC, et al. Characterization of the thiazide-sensitive Na(+)-Cl(-) cotransporter: a new model for ions and diuretics interaction. *Am J Physiol Renal Physiol.* 2000;279:F161–F169.
 292. Bazzini C, Vezzoli V, Sironi C, et al. Thiazide-sensitive NaCl-cotransporter in the intestine: possible role of hydrochlorothiazide in the intestinal Ca²⁺ uptake. *J Biol Chem.* 2005;280:19902–19910.
 293. Simon DB, Nelson-Williams C, Bia MJ, et al. Gitelman's variant of Bartter's syndrome, inherited hypokalaemic alkalosis, is caused by mutations in the thiazide-sensitive Na-Cl cotransporter. *Nat Genet.* 1996;12:24–30.
 294. Tutakhel OA, Jelen S, Valdez-Flores M, et al. Alternative splice variant of the thiazide-sensitive NaCl cotransporter: a novel player in renal salt handling. *Am J Physiol Renal Physiol.* 2016;310:F204–F216.
 295. Schultheis PJ, Lorenz JN, Meneton P, et al. Phenotype resembling Gitelman's syndrome in mice lacking the apical Na⁺-Cl⁻ cotransporter of the distal convoluted tubule. *J Biol Chem.* 1998;273:29150–29155.
 296. Loffing J, Vallon V, Loffing-Cueni D, et al. Altered renal distal tubule structure and renal Na(+) and Ca(2+) handling in a mouse model for Gitelman's syndrome. *J Am Soc Nephrol.* 2004;15:2276–2288.

297. Loffing J, Loffing-Cueni D, Hegyi I, et al. Thiazide treatment of rats provokes apoptosis in distal tubule cells. *Kidney Int.* 1996; 50:1180–1190.
298. Chambrey R, Warmock DG, Podevin RA, et al. Immunolocalization of the Na⁺/H⁺ exchanger isoform NHE2 in rat kidney. *Am J Physiol.* 1998;275:F379–F386.
299. Kujala M, Tienari J, Lohi H, et al. SLC26A6 and SLC26A7 anion exchangers have a distinct distribution in human kidney. *Nephron Exp Nephrol.* 2005;101:e50–e58.
300. Kondapalli KC, Todd Alexander R, Pluznick JL, et al. NHA2 is expressed in distal nephron and regulated by dietary sodium. *J Physiol Biochem.* 2017;73:199–205.
301. Velazquez H, Silva T. Cloning and localization of KCC4 in rabbit kidney: expression in distal convoluted tubule. *Am J Physiol Renal Physiol.* 2003;285:F49–F58.
302. Lourdel S, Paulais M, Marvao P, et al. A chloride channel at the basolateral membrane of the distal-convoluted tubule: a candidate Cl⁻-K⁺ channel. *J Gen Physiol.* 2003;121:287–300.
303. Jeck N, Konrad M, Peters M, et al. Mutations in the chloride channel gene, CLCNKB, leading to a mixed Bartter-Gitelman phenotype. *Pediatr Res.* 2000;48:754–758.
304. Lourdel S, Paulais M, Cluzeaud F, et al. An inward rectifier K⁽⁺⁾ channel at the basolateral membrane of the mouse distal convoluted tubule: similarities with Kir4-Kir5.1 heteromeric channels. *J Physiol.* 2002;538:391–404.
305. Huang C, Sindic A, Hill CE, et al. Interaction of the Ca²⁺-sensing receptor with the inwardly rectifying potassium channels Kir4.1 and Kir4.2 results in inhibition of channel function. *Am J Physiol Renal Physiol.* 2007;292:F1073–F1081.
306. Tanemoto M, Abe T, Onogawa T, et al. PDZ binding motif-dependent localization of K⁺ channel on the basolateral side in distal tubules. *Am J Physiol Renal Physiol.* 2004;287:F1148–F1153.
307. Scholl UI, Choi M, Liu T, et al. Seizures, sensorineural deafness, ataxia, mental retardation, and electrolyte imbalance (SeSAME syndrome) caused by mutations in KCNJ10. *Proc Natl Acad Sci USA.* 2009;106:5842–5847.
308. Cuevas CA, Su XT, Wang MX, et al. Potassium sensing by renal distal tubules requires Kir4.1. *J Am Soc Nephrol.* 2017;28:1814–1825.
309. Zhang C, Wang L, Zhang J, et al. KCNJ10 determines the expression of the apical Na-Cl cotransporter (NCC) in the early distal convoluted tubule (DCT1). *Proc Natl Acad Sci USA.* 2014;111:11864–11869.
310. Zhang C, Wang L, Su XT, et al. KCNJ10 (Kir4.1) is expressed in the basolateral membrane of the cortical thick ascending limb. *Am J Physiol Renal Physiol.* 2015;308:F1288–F1296.
311. Wang MX, Cuevas CA, Su XT, et al. Potassium intake modulates the thiazide-sensitive sodium-chloride cotransporter (NCC) activity via the Kir4.1 potassium channel. *Kidney Int.* 2018.
312. Sandberg MB, Riquier AD, Pihakaski-Maunsbach K, et al. ANG II provokes acute trafficking of distal tubule Na⁺-Cl⁻ cotransporter to apical membrane. *Am J Physiol Renal Physiol.* 2007;293:F662–F669.
313. Abuladze N, Lee I, Newman D, et al. Axial heterogeneity of sodium-bicarbonate cotransporter expression in the rabbit proximal tubule. *Am J Physiol.* 1998;274:F628–F633.
314. Castaneda-Bueno M, Gamba G. Mechanisms of sodium-chloride cotransporter modulation by angiotensin II. *Curr Opin Nephrol Hypertens.* 2012;21:516–522.
315. San-Cristobal P, Pacheco-Alvarez D, Richardson C, et al. Angiotensin II signaling increases activity of the renal Na-Cl cotransporter through a WNK4-SPAK-dependent pathway. *Proc Natl Acad Sci USA.* 2009;106:4384–4389.
316. van der Lubbe N, Lim CH, Fenton RA, et al. Angiotensin II induces phosphorylation of the thiazide-sensitive sodium chloride cotransporter independent of aldosterone. *Kidney Int.* 2011;79:66–76.
317. Bernstein PL, Velázquez H, Bartiss A, et al. Adrenal steroids stimulate thiazide-sensitive Na-Cl cotransport by rat distal tubules. *J Am Soc Nephrol.* 1994;5:282.
318. Kim GH, Masilamani S, Turner R, et al. The thiazide-sensitive Na-Cl cotransporter is an aldosterone-induced protein. *Proc Natl Acad Sci USA.* 1998;95:14552–14557.
319. Bostanjoglo M, Reeves WB, Reilly RF, et al. 11β-Hydroxysteroid dehydrogenase, mineralocorticoid receptor, and thiazide-sensitive Na-Cl cotransporter expression by distal tubules. *J Am Soc Nephrol.* 1998;9:1347–1358.
320. Hunter RW, Ivy JR, Flatman PW, et al. Hypertrophy in the Distal Convoluted Tubule of an 11β-Hydroxysteroid Dehydrogenase Type 2 Knockout Model. *J Am Soc Nephrol.* 2015;26:1537–1548.
321. Arroyo JP, Lagnaz D, Ronzaud C, et al. Nedd4-2 modulates renal Na⁺-Cl⁻ cotransporter via the aldosterone-SGK1-Nedd4-2 pathway. *J Am Soc Nephrol.* 2011;22:1707–1719.
322. Roy A, Al-Qusairi L, Donnelly BF, et al. Alternatively spliced proline-rich cassettes link WNK1 to aldosterone action. *J Clin Invest.* 2015;125:3433–3448.
323. Pochynyuk O, Rieg T, Bugaj V, et al. Dietary Na⁺ inhibits the open probability of the epithelial sodium channel in the kidney by enhancing apical P2Y2-receptor tone. *FASEB J.* 2010;24:2056–2065.
324. van der Lubbe N, Moes AD, Rosenbaek LL, et al. K⁺-induced natriuresis is preserved during Na⁺ depletion and accompanied by inhibition of the Na⁺-Cl⁻ cotransporter. *Am J Physiol Renal Physiol.* 2013;305:F1177–F1188.
325. Sorensen MV, Grossmann S, Roesinger M, et al. Rapid dephosphorylation of the renal sodium chloride cotransporter in response to oral potassium intake in mice. *Kidney Int.* 2013;83:811–824.
326. Rengarajan S, Lee DH, Oh YT, et al. Increasing plasma [K⁺] by intravenous potassium infusion reduces NCC phosphorylation and drives kaliuresis and natriuresis. *Am J Physiol Renal Physiol.* 2014;306:F1059–F1068.
327. Terker AS, Zhang C, McCormick JA, et al. Potassium modulates electrolyte balance and blood pressure through effects on distal cell voltage and chloride. *Cell Metab.* 2015;21:39–50.
328. Perrier R, Boscardin E, Malsure S, et al. Severe salt-losing syndrome and hyperkalemia induced by adult nephron-specific knockout of the epithelial sodium channel alpha-Subunit. *J Am Soc Nephrol.* 2016;27:2309–2318.
329. Terker AS, Yarbrough B, Ferdaus MZ, et al. Direct and indirect mineralocorticoid effects determine distal salt transport. *J Am Soc Nephrol.* 2016;27:2436–2445.
330. Canonica J, Sergi C, Maillard M, et al. Adult nephron-specific MR-deficient mice develop a severe renal PHA-1 phenotype. *Pflugers Arch.* 2016;468:895–908.
331. Czogalla J, Vohra T, Penton D, et al. The mineralocorticoid receptor (MR) regulates ENaC but not NCC in mice with random MR deletion. *Pflugers Arch.* 2016;468:849–858.
332. Mayan H, Vered I, Mouallem M, et al. Pseudohypoaldosteronism type II: marked sensitivity to thiazides, hypercalciuria, normomagnesiumemia, and low bone mineral density. *J Clin Endocrinol Metab.* 2002;87:3248–3254.
333. McCormick JA, Nelson JH, Yang CL, et al. Overexpression of the sodium chloride cotransporter is not sufficient to cause familial hyperkalemic hypertension. *Hypertension.* 2011;58:888–894.
334. Richardson C, Rafiqi FH, Karlsson HK, et al. Activation of the thiazide-sensitive Na⁺-Cl⁻ cotransporter by the WNK-regulated kinases SPAK and OSR1. *J Cell Sci.* 2008;121:675–684.
335. Vidal-Petiot E, Elvira-Matelet E, Mutig K, et al. WNK1-related Familial Hyperkalemic Hypertension results from an increased expression of L-WNK1 specifically in the distal nephron. *Proc Natl Acad Sci USA.* 2013;110:14366–14371.
336. Wilson FH, Disse-Nicodeme S, Choate KA, et al. Human hypertension caused by mutations in WNK kinases. *Science.* 2001;293:1107–1112.
337. Mori Y, Wakabayashi M, Mori T, et al. Decrease of WNK4 ubiquitination by disease-causing mutations of KLHL3 through different molecular mechanisms. *Biochem Biophys Res Commun.* 2013;439:30–34.
338. Wakabayashi M, Mori T, Isobe K, et al. Impaired KLHL3-mediated ubiquitination of WNK4 causes human hypertension. *Cell Rep.* 2013;3:858–868.
339. Ohta A, Schumacher FR, Mehellou Y, et al. The CUL3-KLHL3 E3 ligase complex mutated in Gordon's hypertension syndrome interacts with and ubiquitylates WNK isoforms: disease-causing mutations in KLHL3 and WNK4 disrupt interaction. *Biochem J.* 2013;451:111–122.
340. Al-Qusairi L, Basquin D, Roy A, et al. Renal tubular ubiquitin-protein ligase NEDD4-2 is required for renal adaptation during long-term potassium depletion. *J Am Soc Nephrol.* 2017;28:2431–2442.
341. Ohno M, Uchida K, Ohashi T, et al. Immunolocalization of WNK4 in mouse kidney. *Histochem Cell Biol.* 2011;136:25–35.
342. Piala AT, Moon TM, Akella R, et al. Chloride sensing by WNK1 involves inhibition of autophosphorylation. *Sci Signal.* 2014;7:ra41.
343. Terker AS, Zhang C, Erspamer KJ, et al. Unique chloride-sensing properties of WNK4 permit the distal nephron to modulate potassium homeostasis. *Kidney Int.* 2016;89:127–134.
344. Kahle KT, Rinehart J, Ring A, et al. WNK protein kinases modulate cellular Cl⁻ flux by altering the phosphorylation state of the Na-K-Cl and K-Cl cotransporters. *Physiology (Bethesda).* 2006;21:326–335.

345. Lalioti MD, Zhang J, Volkman HM, et al. Wnk4 controls blood pressure and potassium homeostasis via regulation of mass and activity of the distal convoluted tubule. *Nat Genet.* 2006;38:1124–1132.
- 345a. Yang SS, Morimoto T, Rai T, et al. Molecular pathogenesis of pseudohypoaldosteronism type II: generation and analysis of a Wnk4(D561A/+) knockin mouse model. *Cell Metab.* 2007;5:331–344.
346. Wilson FH, Kahle KT, Sabath E, et al. Molecular pathogenesis of inherited hypertension with hyperkalemia: the Na-Cl cotransporter is inhibited by wild-type but not mutant WNK4. *Proc Natl Acad Sci USA.* 2003;100:680–684.
347. Golbang AP, Cope G, Hamad A, et al. Regulation of the expression of the Na/Cl cotransporter by WNK4 and WNK1: evidence that accelerated dynamin-dependent endocytosis is not involved. *Am J Physiol Renal Physiol.* 2006;291:F1369–F1376.
348. Hoorn EJ, Walsh SB, McCormick JA, et al. The calcineurin inhibitor tacrolimus activates the renal sodium chloride cotransporter to cause hypertension. *Nat Med.* 2011;17:1304–1309.
349. Boyden LM, Choi M, Choate KA, et al. Mutations in kelch-like 3 and cullin 3 cause hypertension and electrolyte abnormalities. *Nature.* 2012;482:98–102.
350. Shibata S, Zhang J, Puthumana J, et al. Kelch-like 3 and Cullin 3 regulate electrolyte homeostasis via ubiquitination and degradation of WNK4. *Proc Natl Acad Sci USA.* 2013;110:7838–7843.
351. McCormick JA, Yang CL, Zhang C, et al. Hyperkalemic hypertension-associated cullin 3 promotes WNK signaling by degrading KLHL3. *J Clin Invest.* 2014;124:4723–4736.
352. Shibata S, Arroyo JP, Castaneda-Bueno M, et al. Angiotensin II signaling via protein kinase C phosphorylates Kelch-like 3, preventing WNK4 degradation. *Proc Natl Acad Sci USA.* 2014;111:15556–15561.
353. Ko B, Hoover RS. Molecular physiology of the thiazide-sensitive sodium-chloride cotransporter. *Curr Opin Nephrol Hypertens.* 2009;18:421–427.
354. Subramanya AR, Ellison DH. Distal convoluted tubule. *Clin J Am Soc Nephrol.* 2014;9:2147–2163.
355. Yang CL, Zhu X, Ellison DH. The thiazide-sensitive Na-Cl cotransporter is regulated by a WNK kinase signaling complex. *J Clin Invest.* 2007;117:3403–3411.
356. Rozansky DJ, Cornwall T, Subramanya AR, et al. Aldosterone mediates activation of the thiazide-sensitive Na-Cl cotransporter through an SGK1 and WNK4 signaling pathway. *J Clin Invest.* 2009;119:2601–2612.
357. Gamba G. The thiazide-sensitive Na⁺-Cl⁻ cotransporter: molecular biology, functional properties, and regulation by WNKs. *Am J Physiol Renal Physiol.* 2009;297:F838–F848.
358. Chiga M, Rai T, Yang SS, et al. Dietary salt regulates the phosphorylation of OSR1/SPAK kinases and the sodium chloride cotransporter through aldosterone. *Kidney Int.* 2008;74:1403–1409.
359. Pedersen NB, Hofmeister MV, Rosenbaek LL, et al. Vasopressin induces phosphorylation of the thiazide-sensitive sodium chloride cotransporter in the distal convoluted tubule. *Kidney Int.* 2010;78:160–169.
360. Mutig K, Saritas T, Uchida S, et al. Short-term stimulation of the thiazide-sensitive Na⁺-Cl⁻ cotransporter by vasopressin involves phosphorylation and membrane translocation. *Am J Physiol Renal Physiol.* 2010;298:F502–F509.
361. Vallon V, Schroth J, Lang F, et al. Expression and phosphorylation of the Na⁺-Cl⁻ cotransporter NCC in vivo is regulated by dietary salt, potassium, and SGK1. *Am J Physiol Renal Physiol.* 2009;297:F704–F712.
362. Lin DH, Yue P, Rinehart J, et al. Protein phosphatase 1 modulates the inhibitory effect of With-no-Lysine kinase 4 on ROMK channels. *Am J Physiol Renal Physiol.* 2012;303:F110–F119.
363. Chavez-Canales M, Zhang C, Soukaseum C, et al. WNK-SPAK-NCC cascade revisited: WNK1 stimulates the activity of the Na-Cl cotransporter via SPAK, an effect antagonized by WNK4. *Hypertension.* 2014;64:1047–1053.
364. Subramanya AR, Liu J, Ellison DH, et al. WNK4 diverts the thiazide-sensitive NaCl cotransporter to the lysosome and stimulates AP-3 interaction. *J Biol Chem.* 2009;284:18471–18480.
365. Zhou B, Zhuang J, Gu D, et al. WNK4 enhances the degradation of NCC through a sortilin-mediated lysosomal pathway. *J Am Soc Nephrol.* 2010;21:82–92.
366. Ko B, Kamsteeg EJ, Cooke LL, et al. RasGRP1 stimulation enhances ubiquitination and endocytosis of the sodium-chloride cotransporter. *Am J Physiol Renal Physiol.* 2010;299:F300–F309.
367. Ko B, Joshi LM, Cooke LL, et al. Phorbol ester stimulation of RasGRP1 regulates the sodium-chloride cotransporter by a PKC-independent pathway. *Proc Natl Acad Sci USA.* 2007;104:20120–20125.
368. Ko B, Cooke LL, Hoover RS. Parathyroid hormone (PTH) regulates the sodium chloride cotransporter via Ras guanyl releasing protein 1 (Ras-GRP1) and extracellular signal-regulated kinase (ERK)1/2 mitogen-activated protein kinase (MAPK) pathway. *Transl Res.* 2011;158:282–289.
369. Rosenbaek LL, Rizzo F, Wu Q, et al. The thiazide sensitive sodium chloride co-transporter NCC is modulated by site-specific ubiquitylation. *Sci Rep.* 2017;7:12981.
370. Frindt G, Palmer LG. Low-conductance K channels in apical membrane of rat cortical collecting tubule. *Am J Physiol.* 1989;256:F143–F151.
371. Frindt G, Palmer LG. Apical potassium channels in the rat connecting tubule. *Am J Physiol Renal Physiol.* 2004;287:F1030–F1037.
372. Palmer LG, Frindt G. Amiloride-sensitive Na channels from the apical membrane of the rat cortical collecting tubule. *Proc Natl Acad Sci USA.* 1986;83:2767–2770.
373. Wagner CA, Devuyst O, Bourgeois S, et al. Regulated acid-base transport in the collecting duct. *Pflugers Arch.* 2009;458:137–156.
374. Firsov D, Schild L, Gautschi I, et al. Cell surface expression of the epithelial Na channel and a mutant causing Liddle syndrome: a quantitative approach. *Proc Natl Acad Sci USA.* 1996;93:15370–15375.
375. Staruschenko A, Adams E, Booth RE, et al. Epithelial Na⁺ channel subunit stoichiometry. *Biophys J.* 2005;88:3966–3975.
376. Grunder S, Firsov D, Chang SS, et al. A mutation causing pseudohypoaldosteronism type I identifies a conserved glycine that is involved in the gating of the epithelial sodium channel. *EMBO J.* 1997;16:899–907.
377. Findling JW, Raff H, Hansson JH, et al. Liddle's syndrome: prospective genetic screening and suppressed aldosterone secretion in an extended kindred. *J Clin Endocrinol Metab.* 1997;82:1071–1074.
378. Hiltunen TP, Hannila-Handelberg T, Petajaniemi N, et al. Liddle's syndrome associated with a point mutation in the extracellular domain of the epithelial sodium channel gamma subunit. *J Hypertens.* 2002;20:2383–2390.
379. Salih M, Gautschi I, van Bemmelen MX, et al. A missense mutation in the extracellular domain of alphaENaC causes liddle syndrome. *J Am Soc Nephrol.* 2017.
380. Rubera I, Loffing J, Palmer LG, et al. Collecting duct-specific gene inactivation of alphaENaC in the mouse kidney does not impair sodium and potassium balance. *J Clin Invest.* 2003;112:554–565.
381. Loffing J, Pietri L, Aregger F, et al. Differential subcellular localization of ENaC subunits in mouse kidney in response to high- and low-Na diets. *Am J Physiol Renal Physiol.* 2000;279:F252–F258.
382. Nesterov V, Dahmann A, Krueger B, et al. Aldosterone-dependent and -independent regulation of the epithelial sodium channel (ENaC) in mouse distal nephron. *Am J Physiol Renal Physiol.* 2012;303:F1289–F1299.
383. Nesterov V, Krueger B, Bertog M, et al. In liddle syndrome, epithelial sodium channel is hyperactive mainly in the early part of the aldosterone-sensitive distal nephron. *Hypertension.* 2016;67:1256–1262.
384. Schuster VL, Stokes JB. Chloride transport by the cortical and outer medullary collecting duct. *Am J Physiol.* 1987;253:F203–F212.
385. Warden DH, Schuster VL, Stokes JB. Characteristics of the paracellular pathway of rabbit cortical collecting duct. *Am J Physiol.* 1988;255:F720–F727.
386. Li WY, Huey CL, Yu AS. Expression of claudin-7 and -8 along the mouse nephron. *Am J Physiol Renal Physiol.* 2004;286:F1063–F1071.
387. Hou J, Renigunta A, Yang J, et al. Claudin-4 forms paracellular chloride channel in the kidney and requires claudin-8 for tight junction localization. *Proc Natl Acad Sci USA.* 2010;107:18010–18015.
388. Gong Y, Yu M, Yang J, et al. The Cap1-claudin-4 regulatory pathway is important for renal chloride reabsorption and blood pressure regulation. *Proc Natl Acad Sci USA.* 2014;111:E3766–E3774.
389. Gong Y, Wang J, Yang J, et al. KLHL3 regulates paracellular chloride transport in the kidney by ubiquitination of claudin-8. *Proc Natl Acad Sci USA.* 2015;112:4340–4345.
390. Kahle KT, Macgregor GG, Wilson FH, et al. Paracellular Cl⁻ permeability is regulated by WNK4 kinase: insight into normal physiology and hypertension. *Proc Natl Acad Sci USA.* 2004;101:14877–14882.

391. Yamauchi K, Rai T, Kobayashi K, et al. Disease-causing mutant WNK4 increases paracellular chloride permeability and phosphorylates claudins. *Proc Natl Acad Sci USA*. 2004;101:4690–4694.
392. Zaika O, Mamenko M, Boukelmoune N, et al. IGF-1 and insulin exert opposite actions on ClC-K2 activity in the cortical collecting ducts. *Am J Physiol Renal Physiol*. 2015;308:F39–F48.
393. Pinelli L, Nissant A, Edwards A, et al. Dual regulation of the native ClC-K2 chloride channel in the distal nephron by voltage and pH. *J Gen Physiol*. 2016;148:213–226.
394. Pech V, Thumova M, Kim YH, et al. ENaC inhibition stimulates Cl⁻ secretion in the mouse cortical collecting duct through an NKCC1-dependent mechanism. *Am J Physiol Renal Physiol*. 2012;303:F45–F55.
395. Wall SM, Kim YH, Stanley L, et al. NaCl restriction upregulates renal Slc26a4 through subcellular redistribution: role in Cl⁻ conservation. *Hypertension*. 2004;44:982–987.
396. Verlander JW, Hassell KA, Royaux IE, et al. Deoxycorticosterone upregulates PDS (Slc26a4) in mouse kidney: role of pendrin in mineralocorticoid-induced hypertension. *Hypertension*. 2003;42:356–362.
397. Kim YH, Pech V, Spencer KB, et al. Reduced ENaC protein abundance contributes to the lower blood pressure observed in pendrin-null mice. *Am J Physiol Renal Physiol*. 2007;293:F1314–F1324.
398. Gueutin V, Vallet M, Jayat M, et al. Renal beta-intercalated cells maintain body fluid and electrolyte balance. *J Clin Invest*. 2013;123:4219–4231.
399. Pech V, Pham TD, Hong S, et al. Pendrin modulates ENaC function by changing luminal HCO₃⁻. *J Am Soc Nephrol*. 2010;21:1928–1941.
400. Verlander JW, Hong S, Pech V, et al. Angiotensin II acts through the angiotensin 1a receptor to upregulate pendrin. *Am J Physiol Renal Physiol*. 2011;301:F1314–F1325.
401. Xu N, Hirohama D, Ishizawa K, et al. Hypokalemia and Pendrin Induction by Aldosterone. *Hypertension*. 2017;69:855–862.
402. Jacques T, Picard N, Miller RL, et al. Overexpression of pendrin in intercalated cells produces chloride-sensitive hypertension. *J Am Soc Nephrol*. 2013;24:1104–1113.
403. Pech V, Wall SM, Nanami M, et al. Pendrin gene ablation alters ENaC subcellular distribution and open probability. *Am J Physiol Renal Physiol*. 2015;309:F154–F163.
404. Verlander JW, Kim YH, Shin W, et al. Dietary Cl⁻ restriction upregulates pendrin expression within the apical plasma membrane of type B intercalated cells. *Am J Physiol Renal Physiol*. 2006;291:F833–F839.
405. Eladari D, Chambrey R, Frische S, et al. Pendrin as a regulator of ECF and blood pressure. *Curr Opin Nephrol Hypertens*. 2009;18:356–362.
406. Tomita K, Pisano JJ, Burg MB, et al. Effects of vasopressin and bradykinin on anion transport by the rat cortical collecting duct. Evidence for an electroneutral sodium chloride transport pathway. *J Clin Invest*. 1986;77:136–141.
407. Terada Y, Knepper MA. Thiazide-sensitive NaCl absorption in rat cortical collecting duct. *Am J Physiol*. 1990;259:F519–F528.
408. Leviel F, Hubner CA, Houllier P, et al. The Na⁺-dependent chloride-bicarbonate exchanger SLC4A8 mediates an electroneutral Na⁺ reabsorption process in the renal cortical collecting ducts of mice. *J Clin Invest*. 2010;120:1627–1635.
409. Sinning A, Radionov N, Trepiccione F, et al. Double knockout of the Na⁺-Driven Cl⁻/HCO₃⁻ exchanger and Na⁺/Cl⁻ cotransporter induces hypokalemia and volume depletion. *J Am Soc Nephrol*. 2017;28:130–139.
410. Fuller PJ, Young MJ. Mechanisms of mineralocorticoid action. *Hypertension*. 2005;46:1227–1235.
411. Welling PA, Caplan M, Sutters M, et al. Aldosterone-mediated Na⁺/K⁺-ATPase expression is alpha 1 isoform specific in the renal cortical collecting duct. *J Biol Chem*. 1993;268:23469–23476.
412. Le Moellic C, Boulkroum S, Gonzalez-Nunez D, et al. Aldosterone and tight junctions: modulation of claudin-4 phosphorylation in renal collecting duct cells. *Am J Physiol Cell Physiol*. 2005;289:C1513–C1521.
413. Mick VE, Itani OA, Loftus RW, et al. The alpha-subunit of the epithelial sodium channel is an aldosterone-induced transcript in mammalian collecting ducts, and this transcriptional response is mediated via distinct cis-elements in the 5'-flanking region of the gene. *Mol Endocrinol*. 2001;15:575–588.
414. Reisenauer MR, Anderson M, Huang L, et al. AF17 competes with AF9 for binding to Dot1a to up-regulate transcription of epithelial Na⁺ channel alpha. *J Biol Chem*. 2009;284:35659–35669.
415. Yu Z, Kong Q, Kone BC. Aldosterone reprograms promoter methylation to regulate alphaENaC transcription in the collecting duct. *Am J Physiol Renal Physiol*. 2013;305:F1006–F1013.
416. Nielsen J, Kwon TH, Masilamani S, et al. Sodium transporter abundance profiling in kidney: effect of spironolactone. *Am J Physiol Renal Physiol*. 2002;283:F923–F933.
417. Masilamani S, Kim GH, Mitchell C, et al. Aldosterone-mediated regulation of ENaC alpha, beta, and gamma subunit proteins in rat kidney. *J Clin Invest*. 1999;104:R19–R23.
418. Loffing J, Zecevic M, Feraïlle E, et al. Aldosterone induces rapid apical translocation of ENaC in early portion of renal collecting system: possible role of SGK. *Am J Physiol Renal Physiol*. 2001;280:F675–F682.
419. Snyder PM. Minireview: regulation of epithelial Na⁺ channel trafficking. *Endocrinology*. 2005;146:5079–5085.
420. Chen SY, Bhargava A, Mastroberardino L, et al. Epithelial sodium channel regulated by aldosterone-induced protein sgk. *Proc Natl Acad Sci USA*. 1999;96:2514–2519.
421. Naray-Fejes-Toth A, Canessa C, Cleaveland ES, et al. sgk is an aldosterone-induced kinase in the renal collecting duct. Effects on epithelial na⁺ channels. *J Biol Chem*. 1999;274:16973–16978.
422. Kamynina E, Tauxe C, Staub O. Distinct characteristics of two human Nedd4 proteins with respect to epithelial Na⁽⁺⁾ channel regulation. *Am J Physiol Renal Physiol*. 2001;281:F469–F477.
423. Snyder PM, Olson DR, Thomas BC. Serum and glucocorticoid-regulated kinase modulates Nedd4-2-mediated inhibition of the epithelial Na⁺ channel. *J Biol Chem*. 2002;277:5–8.
424. Debonneville C, Flores SY, Kamynina E, et al. Phosphorylation of Nedd4-2 by Sgk1 regulates epithelial Na⁽⁺⁾ channel cell surface expression. *EMBO J*. 2001;20:7052–7059.
425. Flores SY, Loffing-Cueni D, Kamynina E, et al. Aldosterone-induced serum and glucocorticoid-induced kinase 1 expression is accompanied by Nedd4-2 phosphorylation and increased Na⁺ transport in cortical collecting duct cells. *J Am Soc Nephrol*. 2005;16:2279–2287.
426. Zhou R, Snyder PM. Nedd4-2 phosphorylation induces serum and glucocorticoid-regulated kinase (SGK) ubiquitination and degradation. *J Biol Chem*. 2005;280:4518–4523.
427. Loffing-Cueni D, Flores SY, Sauter D, et al. Dietary sodium intake regulates the ubiquitin-protein ligase nedd4-2 in the renal collecting system. *J Am Soc Nephrol*. 2006;17:1264–1274.
428. Butler PL, Staruschenko A, Snyder PM. Acetylation stimulates the epithelial sodium channel by reducing its ubiquitination and degradation. *J Biol Chem*. 2015;290:12497–12503.
429. Soundararajan R, Melters D, Shih IC, et al. Epithelial sodium channel regulated by differential composition of a signaling complex. *Proc Natl Acad Sci USA*. 2009;106:7804–7809.
430. Soundararajan R, Ziera T, Koo E, et al. Scaffold protein connector enhancer of kinase suppressor of Ras isoform 3 (CNK3) coordinates assembly of a multiprotein epithelial sodium channel (ENaC)-regulatory complex. *J Biol Chem*. 2012;287:33014–33025.
431. Gleason CE, Frindt G, Cheng CJ, et al. mTORC2 regulates renal tubule sodium uptake by promoting ENaC activity. *J Clin Invest*. 2015;125:117–128.
432. Lu M, Wang J, Jones KT, et al. mTOR complex-2 activates ENaC by phosphorylating SGK1. *J Am Soc Nephrol*. 2010;21:811–818.
433. Yang L, Frindt G, Lang F, et al. SGK1-dependent ENaC processing and trafficking in mice with high dietary K intake and elevated aldosterone. *Am J Physiol Renal Physiol*. 2017;312:F65–F76.
434. Fejes-Toth G, Frindt G, Naray-Fejes-Toth A, et al. Epithelial Na⁺ channel activation and processing in mice lacking SGK1. *Am J Physiol Renal Physiol*. 2008;294:F1298–F1305.
435. Klemens CA, Edinger RS, Kightlinger L, et al. Ankyrin G expression regulates apical delivery of the epithelial sodium channel (ENaC). *J Biol Chem*. 2017;292:375–385.
436. Ergonul Z, Frindt G, Palmer LG. Regulation of maturation and processing of ENaC subunits in the rat kidney. *Am J Physiol Renal Physiol*. 2006;291:F683–F693.
437. Kleyman TR, Myerburg MM, Hughey RP. Regulation of ENaCs by proteases: an increasingly complex story. *Kidney Int*. 2006;70:1391–1392.
438. Vuagniaux G, Vallet V, Jaeger NE, et al. Synergistic activation of ENaC by three membrane-bound channel-activating serine proteases (mCAP1, mCAP2, and mCAP3) and serum- and glucocorticoid-regulated kinase (Sgk1) in *Xenopus* Oocytes. *J Gen Physiol*. 2002;120:191–201.
439. Kleyman TR, Carattino MD, Hughey RP. ENaC at the cutting edge: regulation of epithelial sodium channels by proteases. *J Biol Chem*. 2009;284:20447–20451.
440. Vallet V, Chraïbi A, Gaeggeler HP, et al. An epithelial serine protease activates the amiloride-sensitive sodium channel. *Nature*. 1997;389:607–610.

441. Narikiyo T, Kitamura K, Adachi M, et al. Regulation of prostasin by aldosterone in the kidney. *J Clin Invest*. 2002;109:401–408.
442. Keppner A, Andreasen D, Merillat AM, et al. Epithelial sodium channel-mediated sodium transport is not dependent on the membrane-bound serine protease CAP2/Tmprss4. *PLoS ONE*. 2015;10:e0135224.
443. Carattino MD, Sheng S, Bruns JB, et al. The epithelial Na⁺ channel is inhibited by a peptide derived from proteolytic processing of its alpha subunit. *J Biol Chem*. 2006;281:18901–18907.
444. Kashlan OB, Blobner BM, Zuzek Z, et al. Na⁺ inhibits the epithelial Na⁺ channel by binding to a site in an extracellular acidic cleft. *J Biol Chem*. 2015;290:568–576.
445. Schafer JA. Abnormal regulation of ENaC: syndromes of salt retention and salt wasting by the collecting duct. *Am J Physiol Renal Physiol*. 2002;283:F221–F235.
446. Bugaj V, Pochynyuk O, Stockand JD. Activation of the epithelial Na⁺ channel in the collecting duct by vasopressin contributes to water reabsorption. *Am J Physiol Renal Physiol*. 2009;297:F1411–F1418.
447. Morris RG, Schafer JA. cAMP increases density of ENaC subunits in the apical membrane of MDCK cells in direct proportion to amiloride-sensitive Na⁽⁺⁾ transport. *J Gen Physiol*. 2002;120:71–85.
448. Butterworth MB, Edinger RS, Johnson JP, et al. Acute ENaC stimulation by cAMP in a kidney cell line is mediated by exocytic insertion from a recycling channel pool. *J Gen Physiol*. 2005;125:81–101.
449. Snyder PM, Olson DR, Kabra R, et al. cAMP and serum and glucocorticoid-inducible kinase (SGK) regulate the epithelial Na⁽⁺⁾ channel through convergent phosphorylation of Nedd4-2. *J Biol Chem*. 2004;279:45753–45758.
450. Ecelbarger CA, Kim GH, Terris J, et al. Vasopressin-mediated regulation of epithelial sodium channel abundance in rat kidney. *Am J Physiol Renal Physiol*. 2000;279:F46–F53.
451. Mironova E, Chen Y, Pao AC, et al. Activation of ENaC by AVP contributes to the urinary concentrating mechanism and dilution of plasma. *Am J Physiol Renal Physiol*. 2015;308:F237–F243.
452. Mironova E, Bugaj V, Roos KP, et al. Aldosterone-independent regulation of the epithelial Na⁺ channel (ENaC) by vasopressin in adrenalectomized mice. *Proc Natl Acad Sci USA*. 2012;109:10095–10100.
453. Peti-Peterdi J, Warnock DG, Bell PD. Angiotensin II directly stimulates ENaC activity in the cortical collecting duct via AT(1) receptors. *J Am Soc Nephrol*. 2002;13:1131–1135.
454. Pech V, Kim YH, Weinstein AM, et al. Angiotensin II increases chloride absorption in the cortical collecting duct in mice through a pendrin-dependent mechanism. *Am J Physiol Renal Physiol*. 2007;292:F914–F920.
455. Komlosi P, Fuson AL, Fintha A, et al. Angiotensin I conversion to angiotensin II stimulates cortical collecting duct sodium transport. *Hypertension*. 2003;42:195–199.
456. Rohrwasser A, Morgan T, Dillon HF, et al. Elements of a paracrine tubular renin-angiotensin system along the entire nephron. *Hypertension*. 1999;34:1265–1274.
457. Lehrmann H, Thomas J, Kim SJ, et al. Luminal P2Y₂ receptor-mediated inhibition of Na⁺ absorption in isolated perfused mouse CCD. *J Am Soc Nephrol*. 2002;13:10–18.
458. Pochynyuk O, Bugaj V, Rieg T, et al. Paracrine regulation of the epithelial Na⁺ channel in the mammalian collecting duct by purinergic P2Y₂ receptor tone. *J Biol Chem*. 2008;283:36599–36607.
459. Rieg T, Bunday RA, Chen Y, et al. Mice lacking P2Y₂ receptors have salt-resistant hypertension and facilitated renal Na⁺ and water reabsorption. *FASEB J*. 2007;21:3717–3726.
460. Wildman SS, Marks J, Turner CM, et al. Sodium-dependent regulation of renal amiloride-sensitive currents by apical P₂ receptors. *J Am Soc Nephrol*. 2008;19:731–742.
461. Wei Y, Lin DH, Kemp R, et al. Arachidonic acid inhibits epithelial Na channel via cytochrome P450 (CYP) epoxygenase-dependent metabolic pathways. *J Gen Physiol*. 2004;124:719–727.
462. Nakagawa K, Holla VR, Wei Y, et al. Salt-sensitive hypertension is associated with dysfunctional Cyp4a10 gene and kidney epithelial sodium channel. *J Clin Invest*. 2006;116:1696–1702.
463. Guan Y, Hao C, Cha DR, et al. Thiazolidinediones expand body fluid volume through PPARgamma stimulation of ENaC-mediated renal salt absorption. *Nat Med*. 2005;11:861–866.
464. Zhang H, Zhang A, Kohan DE, et al. Collecting duct-specific deletion of peroxisome proliferator-activated receptor gamma blocks thiazolidinedione-induced fluid retention. *Proc Natl Acad Sci USA*. 2005;102:9406–9411.
465. Fu Y, Gerasimova M, Batz F, et al. PPARgamma agonist-induced fluid retention depends on alphaENaC expression in connecting tubules. *Nephron*. 2015;129:68–74.
466. Hong G, Lockhart A, Davis B, et al. PPARgamma activation enhances cell surface ENaCalpha via up-regulation of SGK1 in human collecting duct cells. *FASEB J*. 2003;17:1966–1968.
467. Artunc F, Sandulache D, Nasir O, et al. Lack of the serum and glucocorticoid-inducible kinase SGK1 attenuates the volume retention after treatment with the PPARgamma agonist pioglitazone. *Pflugers Arch*. 2008;456:425–436.
468. Pavlov TS, Levchenko V, Karpushev AV, et al. Peroxisome proliferator-activated receptor gamma antagonists decrease Na⁺ transport via the epithelial Na⁺ channel. *Mol Pharmacol*. 2009;76:1333–1340.
469. Vallon V, Hummler E, Rieg T, et al. Thiazolidinedione-induced fluid retention is independent of collecting duct alphaENaC activity. *J Am Soc Nephrol*. 2009;20:721–729.
470. Karaliedde J, Buckingham R, Starkie M, et al. Effect of various diuretic treatments on rosiglitazone-induced fluid retention. *J Am Soc Nephrol*. 2006;17:3482–3490.
471. Alvarez de la Rosa D, Canessa CM. Role of SGK in hormonal regulation of epithelial sodium channel in A6 cells. *Am J Physiol Cell Physiol*. 2003;284:C404–C414.
472. Wang J, Barbry P, Maiyar AC, et al. SGK integrates insulin and mineralocorticoid regulation of epithelial sodium transport. *Am J Physiol Renal Physiol*. 2001;280:F303–F313.
473. Sausbier M, Matos JE, Sausbier U, et al. Distal colonic K⁽⁺⁾ secretion occurs via BK channels. *J Am Soc Nephrol*. 2006;17:1275–1282.
474. Bastl C, Hayslett JP, Binder HJ. Increased large intestinal secretion of potassium in renal insufficiency. *Kidney Int*. 1977;12:9–16.
475. Bomsztyk K, Wright FS. Dependence of ion fluxes on fluid transport by rat proximal tubule. *Am J Physiol*. 1986;250:F680–F689.
476. Kaufman JS, Hamburger RJ. Passive potassium transport in the proximal convoluted tubule. *Am J Physiol*. 1985;248:F228–F232.
477. Wilson RW, Wareing M, Green R. The role of active transport in potassium reabsorption in the proximal convoluted tubule of the anaesthetized rat. *J Physiol*. 1997;500(Pt 1):155–164.
478. Kibble JD, Wareing M, Wilson RW, et al. Effect of barium on potassium diffusion across the proximal convoluted tubule of the anesthetized rat. *Am J Physiol*. 1995;268:F778–F783.
479. Wilson RW, Wareing M, Kibble J, et al. Potassium permeability in the absence of fluid reabsorption in proximal tubule of the anesthetized rat. *Am J Physiol*. 1998;274:F1109–F1112.
480. Wareing M, Wilson RW, Kibble JD, et al. Estimated potassium reflection coefficient in perfused proximal convoluted tubules of the anaesthetized rat in vivo. *J Physiol*. 1995;488(Pt 1):153–161.
481. Johnston PA, Battilana CA, Lacy FB, et al. Evidence for a concentration gradient favoring outward movement of sodium from the thin loop of Henle. *J Clin Invest*. 1977;59:234–240.
482. Battilana CA, Doby DC, Lacy FB, et al. Effect of chronic potassium loading on potassium secretion by the pars recta or descending limb of the juxtamedullary nephron in the rat. *J Clin Invest*. 1978;62:1093–1103.
483. Elalouf JM, Roinel N, de Rouffignac C. Effects of dDAVP on rat juxtamedullary nephrons: stimulation of medullary K recycling. *Am J Physiol*. 1985;249:F291–F298.
484. Keith NM, Binger MW. Diuretic action of potassium salts. *JAMA*. 1935;105:1584–1591.
485. Tabei K, Imai M. K transport in upper portion of descending limbs of long-loop nephron from hamster. *Am J Physiol*. 1987;252:F387–F392.
486. Wang B, Wen D, Li H, et al. Net K⁺ secretion in the thick ascending limb of mice on a low-Na, high-K diet. *Kidney Int*. 2017;92:864–875.
487. Schnermann J, Weihprecht H, Briggs JP. Inhibition of tubuloglomerular feedback during adenosine I receptor blockade. *Am J Physiol*. 1990;258:F553–F561.
488. Giebisch G. Renal potassium transport: mechanisms and regulation. *Am J Physiol*. 1998;274:F817–F833.
489. Muto S. Potassium transport in the mammalian collecting duct. *Physiol Rev*. 2001;81:85–116.
490. Stokes JB. Potassium secretion by cortical collecting tubule: relation to sodium absorption, luminal sodium concentration, and transepithelial voltage. *Am J Physiol*. 1981;241:F395–F402.
491. Pluznick JL, Sansom SC. BK channels in the kidney: role in K⁽⁺⁾ secretion and localization of molecular components. *Am J Physiol Renal Physiol*. 2006;291:F517–F529.

492. Gray DA, Frindt G, Palmer LG. Quantification of K⁺ secretion through apical low-conductance K channels in the CCD. *Am J Physiol Renal Physiol.* 2005;289:F117–F126.
493. Palmer LG, Choe H, Frindt G. Is the secretory K channel in the rat CCT ROMK? *Am J Physiol.* 1997;273:F404–F410.
494. Bailey MA, Cantone A, Yan Q, et al. Maxi-K channels contribute to urinary potassium excretion in the ROMK-deficient mouse model of Type II Bartter's syndrome and in adaptation to a high-K diet. *Kidney Int.* 2006;70:51–59.
495. Grimm PR, Foutz RM, Brenner R, et al. Identification and localization of BK-beta subunits in the distal nephron of the mouse kidney. *Am J Physiol Renal Physiol.* 2007;293:F350–F359.
496. Woda CB, Bragin A, Kleyman TR, et al. Flow-dependent K⁺ secretion in the cortical collecting duct is mediated by a maxi-K channel. *Am J Physiol Renal Physiol.* 2001;280:F786–F793.
497. Rieg T, Vallon V, Sausbier M, et al. The role of the BK channel in potassium homeostasis and flow-induced renal potassium excretion. *Kidney Int.* 2007;72:566–573.
498. Grimm PR, Irsik DL, Settles DC, et al. Hypertension of Kcnnb1^{-/-} is linked to deficient K secretion and aldosteronism. *Proc Natl Acad Sci USA.* 2009;106:11800–11805.
499. Larsen CK, Jensen IS, Sorensen MV, et al. Hyperaldosteronism after decreased renal K⁺ excretion in KCNMB2 knockout mice. *Am J Physiol Renal Physiol.* 2016;310:F1035–F1046.
500. Mamenko MV, Boukelmoune N, Tomilin VN, et al. The renal TRPV4 channel is essential for adaptation to increased dietary potassium. *Kidney Int.* 2017;91:1398–1409.
501. Liu Y, Rafferty TM, Rhee SW, et al. CD8⁺ T cells stimulate Na-Cl co-transporter NCC in distal convoluted tubules leading to salt-sensitive hypertension. *Nat Commun.* 2017;8:14037.
502. Li Y, Hu H, Butterworth MB, et al. Expression of a diverse array of Ca²⁺-activated K⁺ channels (SK1/3, IK1, BK) that functionally couple to the mechanosensitive TRPV4 channel in the collecting duct system of kidney. *PLoS ONE.* 2016;11:e0155006.
503. Pacha J, Frindt G, Sackin H, et al. Apical maxi K channels in intercalated cells of CCT. *Am J Physiol.* 1991;261:F696–F705.
504. Palmer LG, Frindt G. High-conductance K channels in intercalated cells of the rat distal nephron. *Am J Physiol Renal Physiol.* 2007;292:F966–F973.
505. Holtzclaw JD, Grimm PR, Sansom SC. Intercalated cell BK-alpha/beta4 channels modulate sodium and potassium handling during potassium adaptation. *J Am Soc Nephrol.* 2010;21:634–645.
506. Liu W, Schreck C, Coleman RA, et al. Role of NKCC in BK channel-mediated net K(+) secretion in the CCD. *Am J Physiol Renal Physiol.* 2011;301:F1088–F1097.
507. Ginns SM, Knepper MA, Ecelbarger CA, et al. Immunolocalization of the secretory isoform of Na-K-Cl cotransporter in rat renal intercalated cells. *J Am Soc Nephrol.* 1996;7:2533–2542.
508. Muto S, Tsuruoka S, Miyata Y, et al. Basolateral Na⁺/H⁺ exchange maintains potassium secretion during diminished sodium transport in the rabbit cortical collecting duct. *Kidney Int.* 2009;75:25–30.
509. Fernandez R, Bosqueiro JR, Cassola AC, et al. Role of Cl⁻ in electrogenic H⁺ secretion by cortical distal tubule. *J Membr Biol.* 1997;157:193–201.
510. Holtzclaw JD, Liu L, Grimm PR, et al. Shear stress-induced volume decrease in C11-MDCK cells by BK-alpha/beta4. *Am J Physiol Renal Physiol.* 2010;299:F507–F516.
511. Giebisch GH. A trail of research on potassium. *Kidney Int.* 2002;62:1498–1512.
512. Giebisch G. Renal potassium channels: function, regulation, and structure. *Kidney Int.* 2001;60:436–445.
513. Berrout J, Mamenko M, Zaika OL, et al. Emerging role of the calcium-activated, small conductance, SK3 K⁺ channel in distal tubule function: regulation by TRPV4. *PLoS ONE.* 2014;9:e95149.
514. Zheng W, Verlander JW, Lynch JJ, et al. Cellular distribution of the potassium channel KCNQ1 in normal mouse kidney. *Am J Physiol Renal Physiol.* 2007;292:F456–F466.
515. Lesage F, Lazdunski M. Molecular and functional properties of two-pore-domain potassium channels. *Am J Physiol Renal Physiol.* 2000;279:F793–F801.
516. Carrisoza-Gaytan R, Salvador C, Satlin LM, et al. Potassium secretion by voltage-gated potassium channel Kv1.3 in the rat kidney. *Am J Physiol Renal Physiol.* 2010;299:F255–F264.
517. Glaudemans B, van der Wijst J, Scola RH, et al. A missense mutation in the Kv1.1 voltage-gated potassium channel-encoding gene KCNA1 is linked to human autosomal dominant hypomagnesemia. *J Clin Invest.* 2009;119:936–942.
518. Gray DA, Frindt G, Zhang YY, et al. Basolateral K⁺ conductance in principal cells of rat CCD. *Am J Physiol Renal Physiol.* 2005;288:F493–F504.
519. Lachheb S, Cluzeaud F, Bens M, et al. Kir4.1/Kir5.1 channel forms the major K⁺ channel in the basolateral membrane of mouse renal collecting duct principal cells. *Am J Physiol Renal Physiol.* 2008;294:F1398–F1407.
520. Palygin O, Levchenko V, Ilatovskaya DV, et al. Essential role of Kir5.1 channels in renal salt handling and blood pressure control. *JCI Insight.* 2017;2.
521. Zaika O, Palygin O, Tomilin V, et al. Insulin and IGF-1 activate Kir4.1/5.1 channels in cortical collecting duct principal cells to control basolateral membrane voltage. *Am J Physiol Renal Physiol.* 2016;310:F311–F321.
522. Zhou X, Xia SL, Wingo CS. Chloride transport by the rabbit cortical collecting duct: dependence on H,K-ATPase. *J Am Soc Nephrol.* 1998;9:2194–2202.
523. Amorim JB, Bailey MA, Musa-Aziz R, et al. Role of luminal anion and pH in distal tubule potassium secretion. *Am J Physiol Renal Physiol.* 2003;284:F381–F388.
524. Ellison DH, Velazquez H, Wright FS. Unidirectional potassium fluxes in renal distal tubule: effects of chloride and barium. *Am J Physiol.* 1986;250:F885–F894.
525. Velazquez H, Ellison DH, Wright FS. Chloride-dependent potassium secretion in early and late renal distal tubules. *Am J Physiol.* 1987;253:F555–F562.
526. Wingo CS. Potassium secretion by the cortical collecting tubule: effect of Cl gradients and ouabain. *Am J Physiol.* 1989;256:F306–F313.
527. Schafer JA, Troutman SL. Potassium transport in cortical collecting tubules from mineralocorticoid-treated rat. *Am J Physiol.* 1987;253:F76–F88.
528. Frindt G, Palmer LG. K⁺ secretion in the rat kidney: Na⁺ channel-dependent and -independent mechanisms. *Am J Physiol Renal Physiol.* 2009;297:F389–F396.
529. Zhou X, Lynch JJ, Xia SL, et al. Activation of H(+)-K(+)-ATPase by CO(2) requires a basolateral Ba(2+)-sensitive pathway during K restriction. *Am J Physiol Renal Physiol.* 2000;279:F153–F160.
530. Jaisser F, Beggah AT. The nongastric H⁺-K⁺-ATPases: molecular and functional properties. *Am J Physiol.* 1999;276:F812–F824.
531. Kraut JA, Helander KG, Helander HF, et al. Detection and localization of H⁺-K⁺-ATPase isoforms in human kidney. *Am J Physiol Renal Physiol.* 2001;281:F763–F768.
532. Sangan P, Thevananther S, Sangan S, et al. Colonic H-K-ATPase alpha- and beta-subunits express ouabain-insensitive H-K-ATPase. *Am J Physiol Cell Physiol.* 2000;278:C182–C189.
533. Fejes-Toth G, Naray-Fejes-Toth A, Velazquez H. Intrarenal distribution of the colonic H,K-ATPase mRNA in rabbit. *Kidney Int.* 1999;56:1029–1036.
534. Verlander JW, Moudy RM, Campbell WG, et al. Immunohistochemical localization of H-K-ATPase alpha(2c)-subunit in rabbit kidney. *Am J Physiol Renal Physiol.* 2001;281:F357–F365.
535. Fejes-Toth G, Naray-Fejes-Toth A. Immunohistochemical localization of colonic H-K-ATPase to the apical membrane of connecting tubule cells. *Am J Physiol Renal Physiol.* 2001;281:F318–F325.
536. Silver RB, Soleimani M. H⁺-K⁺-ATPases: regulation and role in pathophysiological states. *Am J Physiol.* 1999;276:F799–F811.
537. Spicer Z, Miller ML, Andringa A, et al. Stomachs of mice lacking the gastric H,K-ATPase alpha-subunit have achlorhydria, abnormal parietal cells, and ciliated metaplasia. *J Biol Chem.* 2000;275:21555–21565.
538. Petrovic S, Spicer Z, Greeley T, et al. Novel Schering and ouabain-insensitive potassium-dependent proton secretion in the mouse cortical collecting duct. *Am J Physiol Renal Physiol.* 2002;282:F133–F143.
539. Dherbecourt O, Cheval L, Bloch-Faure M, et al. Molecular identification of Sch28080-sensitive K-ATPase activities in the mouse kidney. *Pflugers Arch.* 2006;451:769–775.
540. Wang T, Courtois-Coutry N, Giebisch G, et al. A tyrosine-based signal regulates H-K-ATPase-mediated potassium reabsorption in the kidney. *Am J Physiol.* 1998;275:F818–F826.
541. Mironova E, Lynch JJ, Berman JM, et al. ENaC activity in the cortical collecting duct of HKalpha1 H⁺-K⁺-ATPase knockout mice is uncoupled from Na⁺ intake. *Am J Physiol Renal Physiol.* 2017;312:F1073–F1080.
542. Lu Z, MacKinnon R. Electrostatic tuning of Mg²⁺ affinity in an inward-rectifier K⁺ channel. *Nature.* 1994;371:243–246.

543. Lopatin AN, Makhina EN, Nichols CG. Potassium channel block by cytoplasmic polyamines as the mechanism of intrinsic rectification. *Nature*. 1994;372:366–369.
544. Huang CL, Kuo E. Mechanism of hypokalemia in magnesium deficiency. *J Am Soc Nephrol*. 2007;18:2649–2652.
545. Yang L, Frindt G, Palmer LG. Magnesium modulates ROMK channel-mediated potassium secretion. *J Am Soc Nephrol*. 2010;21:2109–2116.
546. Huang CL, Feng S, Hilgemann DW. Direct activation of inward rectifier potassium channels by PIP2 and its stabilization by Gbeta-gamma. *Nature*. 1998;391:803–806.
547. O'Connell AD, Leng Q, Dong K, et al. Phosphorylation-regulated endoplasmic reticulum retention signal in the renal outer-membrane K⁺ channel (ROMK). *Proc Natl Acad Sci USA*. 2005;102:9954–9959.
548. August JT, Nelson DH, Thorn GW. Response of normal subjects to large amounts of aldosterone. *J Clin Invest*. 1958;37:1549–1555.
549. Palmer LG, Frindt G. Aldosterone and potassium secretion by the cortical collecting duct. *Kidney Int*. 2000;57:1324–1328.
550. Palmer LG, Antonian L, Frindt G. Regulation of apical K and Na channels and Na/K pumps in rat cortical collecting tubule by dietary K. *J Gen Physiol*. 1994;104:693–710.
551. Muto S, Sansom S, Giebisch G. Effects of a high potassium diet on electrical properties of cortical collecting ducts from adrenalectomized rabbits. *J Clin Invest*. 1988;81:376–380.
552. Muto S, Asano Y, Seldin D, et al. Basolateral Na⁺ pump modulates apical Na⁺ and K⁺ conductances in rabbit cortical collecting ducts. *Am J Physiol*. 1999;276:F143–F158.
553. Lin DH, Sterling H, Yang B, et al. Protein tyrosine kinase is expressed and regulates ROMK1 location in the cortical collecting duct. *Am J Physiol Renal Physiol*. 2004;286:F881–F892.
554. Palmer LG, Frindt G. Regulation of apical K channels in rat cortical collecting tubule during changes in dietary K intake. *Am J Physiol*. 1999;277:F805–F812.
555. Frindt G, Shah A, Edvinsson J, et al. Dietary K regulates ROMK channels in connecting tubule and cortical collecting duct of rat kidney. *Am J Physiol Renal Physiol*. 2009;296:F347–F354.
556. Najjar F, Zhou H, Morimoto T, et al. Dietary K⁺ regulates apical membrane expression of maxi-K channels in rabbit cortical collecting duct. *Am J Physiol Renal Physiol*. 2005;289:F922–F932.
557. Estilo G, Liu W, Pastor-Soler N, et al. Effect of aldosterone on BK channel expression in mammalian cortical collecting duct. *Am J Physiol Renal Physiol*. 2008;295:F780–F788.
558. Kahle KT, Wilson FH, Leng Q, et al. WNK4 regulates the balance between renal NaCl reabsorption and K⁺ secretion. *Nat Genet*. 2003;35:372–376.
559. Zhang C, Wang L, Su XT, et al. ENaC and ROMK activity are inhibited in the DCT2/CNT of TgWnk4PHAI mice. *Am J Physiol Renal Physiol*. 2017;312:F682–F688.
560. Grahmmer F, Nesterov V, Ahmed A, et al. mTORC2 critically regulates renal potassium handling. *J Clin Invest*. 2016;126:1773–1782.
561. Delalay C, Lu J, Houot AM, et al. Multiple promoters in the WNK1 gene: one controls expression of a kidney-specific kinase-defective isoform. *Mol Cell Biol*. 2003;23:9208–9221.
562. Cope G, Murthy M, Golbarg AP, et al. WNK1 affects surface expression of the ROMK potassium channel independent of WNK4. *J Am Soc Nephrol*. 2006;17:1867–1874.
563. Wade JB, Fang L, Liu J, et al. WNK1 kinase isoform switch regulates renal potassium excretion. *Proc Natl Acad Sci USA*. 2006;103:8558–8563.
564. Lazrak A, Liu Z, Huang CL. Antagonistic regulation of ROMK by long and kidney-specific WNK1 isoforms. *Proc Natl Acad Sci USA*. 2006;103:1615–1620.
565. He G, Wang HR, Huang SK, et al. Intersectin links WNK kinases to endocytosis of ROMK1. *J Clin Invest*. 2007;117:1078–1087.
566. Fang L, Garuti R, Kim BY, et al. The ARH adaptor protein regulates endocytosis of the ROMK potassium secretory channel in mouse kidney. *J Clin Invest*. 2009;119:3278–3289.
567. Lin DH, Yue P, Pan CY, et al. POSH stimulates the ubiquitination and the clathrin-independent endocytosis of ROMK1 channels. *J Biol Chem*. 2009;284:29614–29624.
568. O'Reilly M, Marshall E, Macgillivray T, et al. Dietary electrolyte-driven responses in the renal WNK kinase pathway in vivo. *J Am Soc Nephrol*. 2006;17:2402–2413.
569. Liu Z, Wang HR, Huang CL. Regulation of ROMK channel and K⁺ homeostasis by kidney-specific WNK1 kinase. *J Biol Chem*. 2009;284:12198–12206.
570. Zhuang J, Zhang X, Wang D, et al. WNK4 kinase inhibits Maxi K channel activity by a kinase-dependent mechanism. *Am J Physiol Renal Physiol*. 2011;301:F410–F419.
571. Yue P, Zhang C, Lin DH, et al. WNK4 inhibits Ca(2+)-activated big-conductance potassium channels (BK) via mitogen-activated protein kinase-dependent pathway. *Biochim Biophys Acta*. 2013;1833:2101–2110.
572. Wang Z, Subramanya AR, Satlin LM, et al. Regulation of large-conductance Ca²⁺-activated K⁺ channels by WNK4 kinase. *Am J Physiol Cell Physiol*. 2013;305:C846–C853.
573. Webb TN, Carrisoza-Gaytan R, Montalbetti N, et al. Cell-specific regulation of L-WNK1 by dietary K. *Am J Physiol Renal Physiol*. 2016;310:F15–F26.
574. Ornt DB, Tannen RL. Demonstration of an intrinsic renal adaptation for K⁺ conservation in short-term K⁺ depletion. *Am J Physiol*. 1983;245:F329–F338.
575. Eiam-Ong S, Kurtzman NA, Sabatini S. Regulation of collecting tubule adenosine triphosphatases by aldosterone and potassium. *J Clin Invest*. 1993;91:2385–2392.
576. Mennitt PA, Frindt G, Silver RB, et al. Potassium restriction downregulates ROMK expression in rat kidney. *Am J Physiol Renal Physiol*. 2000;278:F916–F924.
577. Lin DH, Sterling H, Lerea KM, et al. K depletion increases protein tyrosine kinase-mediated phosphorylation of ROMK. *Am J Physiol Renal Physiol*. 2002;283:F671–F677.
578. Sterling H, Lin DH, Gu RM, et al. Inhibition of protein-tyrosine phosphatase stimulates the dynamin-dependent endocytosis of ROMK1. *J Biol Chem*. 2002;277:4317–4323.
579. Lin DH, Sterling H, Wang WH. The protein tyrosine kinase-dependent pathway mediates the effect of K intake on renal K secretion. *Physiology (Bethesda)*. 2005;20:140–146.
580. Wei Y, Bloom P, Lin D, et al. Effect of dietary K intake on apical small-conductance K channel in CCD: role of protein tyrosine kinase. *Am J Physiol Renal Physiol*. 2001;281:F206–F212.
581. Babilonia E, Wei Y, Sterling H, et al. Superoxide anions are involved in mediating the effect of low K intake on c-Src expression and renal K secretion in the cortical collecting duct. *J Biol Chem*. 2005;280:10790–10796.
582. Babilonia E, Lin D, Zhang Y, et al. Role of gp91phox-containing NADPH oxidase in mediating the effect of K restriction on ROMK channels and renal K excretion. *J Am Soc Nephrol*. 2007;18:2037–2045.
583. Wang ZJ, Sun P, Xing W, et al. Decrease in dietary K intake stimulates the generation of superoxide anions in the kidney and inhibits K secretory channels in the CCD. *Am J Physiol Renal Physiol*. 2010;298:F1515–F1522.
584. Wei Y, Zavilowitz B, Satlin LM, et al. Angiotensin II inhibits the ROMK-like small conductance K channel in renal cortical collecting duct during dietary potassium restriction. *J Biol Chem*. 2007;282:6455–6462.
585. Jin Y, Wang Y, Wang ZJ, et al. Inhibition of angiotensin type 1 receptor impairs renal ability of K conservation in response to K restriction. *Am J Physiol Renal Physiol*. 2009;296:F1179–F1184.
586. Rabinowitz L. Aldosterone and potassium homeostasis. *Kidney Int*. 1996;49:1738–1742.
587. McDonough AA, Youn JH. Role of muscle in regulating extracellular [K⁺]. *Semin Nephrol*. 2005;25:335–342.
588. Chen P, Guzman JP, Leong PK, et al. Modest dietary K⁺ restriction provokes insulin resistance of cellular K⁺ uptake and phosphorylation of renal outer medulla K⁺ channel without fall in plasma K⁺ concentration. *Am J Physiol Cell Physiol*. 2006;290:C1355–C1363.
589. Field MJ, Stanton BA, Giebisch GH. Influence of ADH on renal potassium handling: a micropuncture and micropfusion study. *Kidney Int*. 1984;25:502–511.
590. Cassola AC, Giebisch G, Wang W. Vasopressin increases density of apical low-conductance K⁺ channels in rat CCD. *Am J Physiol*. 1993;264:F502–F509.
591. Amorim JB, Musa-Aziz R, Mello-Aires M, et al. Signaling path of the action of AVP on distal K⁺ secretion. *Kidney Int*. 2004;66:696–704.
592. Chambrey R, Picard N. Role of tissue kallikrein in regulation of tubule function. *Curr Opin Nephrol Hypertens*. 2011;20:523–528.
593. El Moghrabi S, Houillier P, Picard N, et al. Tissue kallikrein permits early renal adaptation to potassium load. *Proc Natl Acad Sci USA*. 2010;107:13526–13531.
594. Picard N, Eladari D, El Moghrabi S, et al. Defective ENaC processing and function in tissue kallikrein-deficient mice. *J Biol Chem*. 2008;283:4602–4611.

595. Soleimani M, Barone S, Xu J, et al. Double knockout of pendrin and Na-Cl cotransporter (NCC) causes severe salt wasting, volume depletion, and renal failure. *Proc Natl Acad Sci USA*. 2012;109:13368–13373.
596. Alshahrani S, Soleimani M. Ablation of the Cl-/HCO₃- exchanger pendrin enhances hydrochlorothiazide-induced diuresis. *Kidney Blood Press Res*. 2017;42:444–455.
597. Patel-Chamberlin M, Varasteh Kia M, Xu J, et al. The role of epithelial sodium channel ENaC and the apical Cl-/HCO₃- exchanger pendrin in compensatory salt reabsorption in the setting of Na-Cl cotransporter (NCC) inactivation. *PLoS ONE*. 2016;11:e0150918.
598. Grimm PR, Lazo-Fernandez Y, Delpire E, et al. Integrated compensatory network is activated in the absence of NCC phosphorylation. *J Clin Invest*. 2015;125:2136–2150.
599. Welling PA, Chang YP, Delpire E, et al. Multigene kinase network, kidney transport, and salt in essential hypertension. *Kidney Int*. 2010;77:1063–1069.
600. Yue P, Lin DH, Pan CY, et al. Src family protein tyrosine kinase (PTK) modulates the effect of SGK1 and WNK4 on ROMK channels. *Proc Natl Acad Sci USA*. 2009;106:15061–15066.
601. Yang LE, Sandberg MB, Can AD, et al. Effects of dietary salt on renal Na⁺ transporter subcellular distribution, abundance, and phosphorylation status. *Am J Physiol Renal Physiol*. 2008;295:F1003–F1016.
602. Sealey JE, Clark I, Bull MB, et al. Potassium balance and the control of renin secretion. *J Clin Invest*. 1970;49:2119–2127.
603. Jensen IS, Larsen CK, Leipziger J, et al. Na(+) dependence of K(+) -induced natriuresis, kaliuresis and Na(+) /Cl(-) cotransporter dephosphorylation. *Acta Physiol (Oxf)*. 2016;218:49–61.
604. Penton D, Czogalla J, Wengi A, et al. Extracellular K⁺ rapidly controls NaCl cotransporter phosphorylation in the native distal convoluted tubule by Cl⁻-dependent and independent mechanisms. *J Physiol*. 2016;594:6319–6331.
605. Castaneda-Bueno M, Cervantes-Perez LG, Rojas-Vega L, et al. Modulation of NCC activity by low and high K⁺ intake: insights into the signaling pathways involved. *Am J Physiol Renal Physiol*. 2014;306:F1507–F1519.
606. Ferdous MZ, Barber KW, Lopez-Cayuqueo KI, et al. SPAK and OSR1 play essential roles in potassium homeostasis through actions on the distal convoluted tubule. *J Physiol*. 2016;594:4945–4966.
607. Ishizawa K, Xu N, Loffing J, et al. Potassium depletion stimulates Na-Cl cotransporter via phosphorylation and inactivation of the ubiquitin ligase Kelch-like 3. *Biochem Biophys Res Commun*. 2016;480:745–751.
608. Shoda W, Nomura N, Ando F, et al. Calcineurin inhibitors block sodium-chloride cotransporter dephosphorylation in response to high potassium intake. *Kidney Int*. 2017;91:402–411.
609. Rashmi P, Colussi G, Ng M, et al. Glucocorticoid-induced leucine zipper protein regulates sodium and potassium balance in the distal nephron. *Kidney Int*. 2017;91:1159–1177.
610. Grimm PR, Coleman R, Delpire E, et al. Constitutively active SPAK causes hyperkalemia by activating NCC and remodeling distal tubules. *J Am Soc Nephrol*. 2017;28:2597–2606.
611. Ring AM, Leng Q, Rinehart J, et al. An SGK1 site in WNK4 regulates Na⁺ channel and K⁺ channel activity and has implications for aldosterone signaling and K⁺ homeostasis. *Proc Natl Acad Sci USA*. 2007;104:4025–4029.
612. Sterling D, Brown NJ, Supuran CT, et al. The functional and physical relationship between the DRA bicarbonate transporter and carbonic anhydrase II. *Am J Physiol Cell Physiol*. 2002;283:C1522–C1529.
613. Lin DH, Yue P, Yarborough O 3rd, et al. Src-family protein tyrosine kinase phosphorylates WNK4 and modulates its inhibitory effect on KCNJ1 (ROMK). *Proc Natl Acad Sci USA*. 2015;112:4495–4500.
614. Nijenhuis T, Hoenderop JG, van der Kemp AW, et al. Localization and regulation of the epithelial Ca²⁺ channel TRPV6 in the kidney. *J Am Soc Nephrol*. 2003;14:2731–2740.
615. Voets T, Nilius B, Hoefs S, et al. TRPM6 forms the Mg²⁺ influx channel involved in intestinal and renal Mg²⁺ absorption. *J Biol Chem*. 2004;279:19–25.
616. Argañiz ER, Chavez-Canales M, Ostrosky-Frid M, et al. Kidney-specific WNK1 isoform (KS-WNK1) is a potent activator of WNK4 and NCC. *Am J Physiol Renal Physiol*. 2018;315:F734–F745.

BOARD REVIEW QUESTIONS

- Despite being electrically “leaky,” the proximal tubule establishes a large transepithelial gradient for which of the following ions,
 - Sodium
 - Calcium
 - Bicarbonate
 - Magnesium

Answer: c

Rationale: The proximal tubule actively reabsorbs bicarbonate through the concerted actions of an apical Na-H exchanger and basolateral Na-bicarbonate cotransporter, and this occurs in excess of osmotic water reabsorption so that, by the mid-PT, there is a transepithelial gradient with a higher bicarbonate concentration basolaterally than apically.

- Glomerulotubular balance is a term that describes the
 - Decrease in glomerular filtration rate when distal NaCl delivery is high
 - Correspondence between glucose filtration and excretion
 - Increased proximal fluid reabsorption when GFR increases
 - Correspondence between glomerular size and tubule length

Answer: c

Rationale: Glomerulotubular balance refers to the phenomenon wherein changes in the glomerular filtration rate (GFR) are offset by changes in tubular reabsorption, thus maintaining a constant fractional reabsorption of fluid and $\text{Na}^+\text{-Cl}^-$. Glomerulotubular balance is independent of direct neuronal and systemic hormonal control and is thought to be mediated by the additive effects of luminal and peritubular factors.

- The thick ascending limb has a transepithelial voltage oriented in the lumen-positive direction primarily because of the combined actions of
 - Primary active transport of chloride out of the lumen
 - Luminal chloride channels and basolateral potassium channels
 - Apical Na-K-Cl cotransport and basolateral Na/K ATPase
 - The charge carried by the apical Na-K-Cl cotransporter
 - Luminal potassium channels and basolateral chloride channels

Answer: e

Rationale: The lumen-positive transepithelial potential difference in the thick ascending limb of Henle is generated

by the combination of apical K^+ channels and basolateral Cl^- channels. Luminal recycling of K^+ via $\text{Na}^+\text{-K}^+\text{-2Cl}^-$ cotransport and apical K^+ channels, along with basolateral depolarization due to Cl^- exit through Cl^- channels, results in the lumen-positive transepithelial voltage.

- Which of the following is now known to play a dominant role in modulating the activity of the thiazide-sensitive NaCl cotransporter in the distal convoluted tubule?
 - Serum potassium concentration
 - Serum sodium concentration
 - Serum chloride concentration
 - Serum bicarbonate concentration

Answer: a

Rationale: Recent evidence shows that DCT cells, and NCC, are exquisitely sensitive to plasma $[\text{K}^+]$. WNKs, especially WNK4, appear to be sensitive to inhibition by intracellular chloride, and this plays a major role in the potassium-sensing function of DCT cells. Hypokalemia leads to reduced basolateral K^+ concentration in the DCT, and subsequent hyperpolarization that is dependent on basolateral KIR4.1-containing K^+ channels. This hyperpolarization has been proposed to lead to chloride exit via basolateral CLC-K2 chloride channels and a reduction in intracellular chloride; the reduction in intracellular chloride activates the SPAK and OSRI-WNK cascade, resulting in phosphorylation of NCC and activation of the transporter.

- Combined genetic deletion of the thiazide-sensitive NaCl cotransporter and pendrin in mice causes which striking phenotype?
 - Profound hyperkalemic acidosis
 - Hypercalciuria with nephrocalcinosis
 - Nephrogenic diabetes insipidus
 - Profound salt wasting

Answer: d

Rationale: There is increasing evidence that effects on salt transport in one tubule segment induce compensatory effects in other segments to maintain homeostasis. Whereas single deletion of pendrin or the thiazide-sensitive NaCl cotransporter in mice does not cause salt wasting or excessive diuresis, double knockout mice with combined genetic ablation of pendrin and the thiazide-sensitive NaCl cotransporter display severe salt wasting, increased urine output, volume depletion and renal failure.

The Regulation of Calcium, Magnesium, and Phosphate Excretion by the Kidney

Theresa J. Berndt | Rajiv Kumar

CHAPTER OUTLINE

CALCIUM TRANSPORT IN THE KIDNEY, 199	PHOSPHORUS TRANSPORT IN THE KIDNEY, 210
MAGNESIUM TRANSPORT IN THE KIDNEY, 207	

KEY POINTS

- $1\alpha,25(\text{OH})_2\text{D}_3$, parathyroid hormone (PTH), and the phosphatonin, FGF-23, regulate renal tubule function to maintain homeostasis of serum calcium and phosphate concentrations, whereas magnesium handling is regulated largely by dietary magnesium load.
- The hypocalciuric effect of PTH is mediated by increased paracellular Ca_2^+ reabsorption in the thick ascending limb of Henle, via inhibition of claudin-14 and by changes in the expression of apical channels in the distal tubule.
- Sclerostin is an osteocyte-derived glycoprotein that has calciuric effects and appears to serve as a counterbalance to PTH and $1\alpha,25(\text{OH})_2$ in calcium homeostasis.
- Claudin-10b is a tight junction protein that mediates paracellular Na^+ reabsorption in the medullary thick ascending limb, thereby limiting Ca_2^+ reabsorption further downstream in the cortical thick ascending limb.
- Mutations in claudin-10b cause hypermagnesemia and hypokalemic alkalosis, together with various extrarenal manifestations.
- PTH and FGF-23 converge on a common signaling pathway in the proximal tubule, involving phosphorylation of NHERF-1 and dissociation and internalization of the NaPi-IIa cotransporter, to cause phosphaturia.
- $1\alpha,25(\text{OH})_2\text{D}$ stimulates the synthesis of FGF-23, which in turn inhibits 25-hydroxyvitamin D 1α -hydroxylase, serving as a negative feedback loop to limit vitamin D effects on phosphate turnover.

CALCIUM TRANSPORT IN THE KIDNEY

THE ROLE OF CALCIUM IN CELLULAR PROCESSES

Calcium is an abundant cation in the body (Table 7.1). Several biochemical and physiologic processes, including nerve conduction and function, coagulation, enzyme activity, exocytosis, and bone mineralization, are critically dependent on normal calcium concentrations in extracellular fluid.¹⁻³ Not unexpectedly, significant decreases or increases in serum calcium concentrations are associated with marked symptoms and signs. Intricate mechanisms exist to maintain extracellular

fluid calcium concentrations within a narrow range and to maintain calcium balance. Decreases in serum calcium concentrations are associated with numbness and tingling of the extremities and peri-oral region, cramping, Chvostek and Trousseau signs, tetany, and when profound, generalized seizures.⁴⁻⁶ A negative calcium balance that is present when calcium absorption in the intestine is reduced is associated with secondary hyperparathyroidism, hypophosphatemia, and rickets or osteomalacia.^{5,6} Hypercalcemia, especially when severe, is associated with lethargy, confusion, irritability, depression, hallucinations, and in extreme cases, stupor and coma, anorexia, nausea, vomiting and constipation, cardiac ectopy,

Table 7.1 Composition of the Whole Body as Determined by Chemical Analysis (Values per Kilogram Fat-Free Tissue Unless Otherwise Indicated)

Body Weight (kg)	Water ^a (g)	Fat ^a (g)	Water (g)	N (g)	Na (mEq)	K (mEq)	Cl (mEq)	Mg (g)	Ca (g)	P (g)	Fe (mg)	Cu (mg)	Zn (mg)	B (mg)	Co (mg)
70	605	160	720	34	80	69	50	0.47	22.4	12.0	74	1.7	28	0.37	0.02

^aPer kilogram whole body weight.

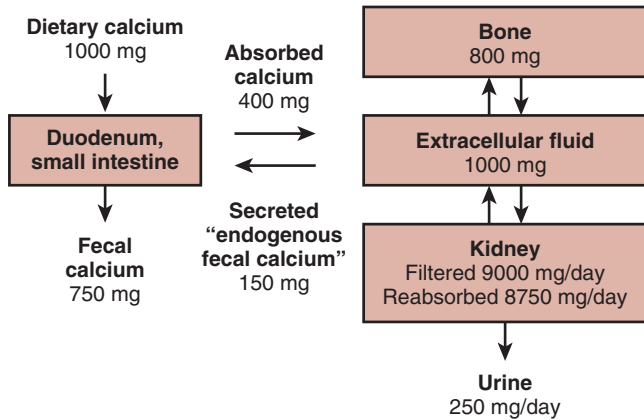


Fig. 7.1 Calcium homeostasis in normal humans showing the amounts of calcium absorbed in the intestine and reabsorbed by the kidney.

and polyuria and renal colic from the passage of renal stones.⁷ The attendant hypercalciuria is associated with a reduced capacity to concentrate urine,^{8–11} volume depletion, and nephrocalcinosis and renal stones.^{12,13} Hypercalcemia occurs as a result of parathyroid hormone (PTH)-dependent or PTH-independent processes, and changes in laboratory values depend on the etiology of hypercalcemia.⁷ Thus, in PTH-dependent hypercalcemia, elevated serum PTH concentrations are present and are the cause of hypercalcemia, whereas in PTH-independent hypercalcemia, PTH concentrations are suppressed, sometimes in association with increases in various vitamin D metabolites.⁷ As shown in Fig. 7.1, the intestine and kidney are important in the absorption and the reabsorption and excretion of calcium. Following the absorption in the intestine, calcium in the extracellular fluid space is deposited in bone (the major repository of calcium in the body) and is filtered in the kidney. The concentration of calcium in serum varies with age and gender, with higher values present in children and adolescent subjects than in adults.

CALCIUM IS PRESENT IN SERUM IN BOUND AND FREE FORMS

Calcium is present in plasma in filterable (60% of total calcium) and bound (40% of total calcium) forms. Filterable calcium is composed of calcium complexed to anions, such as citrate, sulfate, and phosphate (~10% of total calcium) and ionized calcium (~50% of total calcium) (Fig. 7.2).¹⁴ The percentage of calcium bound to proteins (predominantly albumin, and to a lesser extent, globulins), and the amount of filterable calcium, is dependent on plasma pH.¹⁴ Alkalemia is associated with a reduction in free calcium, whereas acidemia is associated with

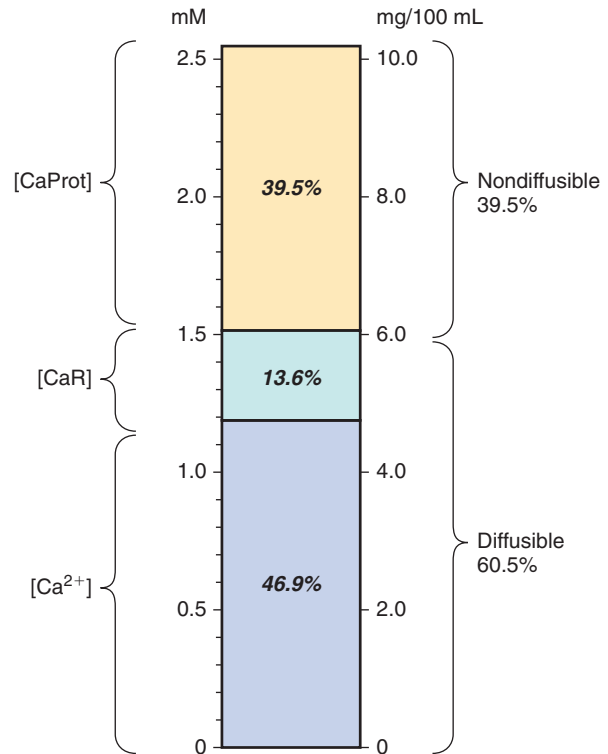


Fig. 7.2 Components of serum total calcium assessed by ultrafiltration data in normal human patients. *CaR*, Diffuse of both calcium complexes; *Ca²⁺*, ionized calcium, *CaProt*, protein-bound calcium. Redrawn from Moore, EW. Ionized calcium in normal serum, ultrafiltrates, and whole blood determined by ion-exchange electrodes. *J Clin Invest.* 1970;49:318–334, with permission of the publisher.

an increase in free calcium. A 1-g/dL change in serum albumin is associated with a 0.8-mg/dL change in total serum calcium, and a 1-g/dL change in globulins is associated with a 0.16-mg/dL change in total serum calcium. An equation defining the amount of calcium (mmol/L) bound to albumin and globulins (g/L) as a function of pH is as follows¹⁴:

$$[CaProt] = 0.019[Alb] - [(0.42) ([Alb]/47.3) (7.42 - pH)] + 0.004[Glob] - [(0.42) ([Glob]/25.0) (7.42 - pH)]$$

If one assumes that all calcium is bound to albumin, the following equation applies:

$$[CaProt] = 0.0211[Alb] - [(0.42) ([Alb]/47.3) (7.42 - pH)],$$

where Alb is albumin, CaProt is protein-bound calcium, and Glob is globulins.

A nomogram describing this relationship is shown in Fig. 7.3.

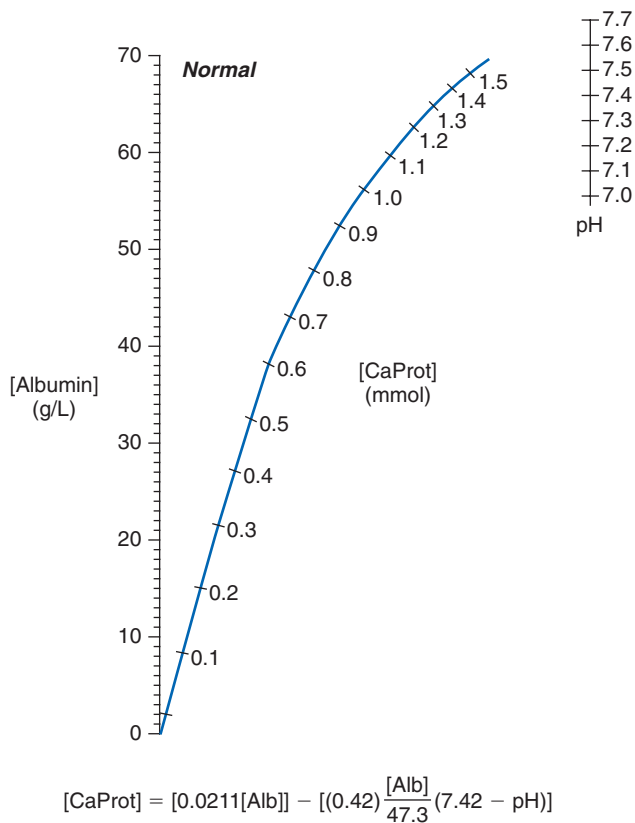


Fig. 7.3 A nomogram for estimating protein-bound calcium levels [CaProt] in normal humans. [CaProt] is obtained by connecting observed albumin and pH values with a straight line and reading the point at which it intersects the curve. The equation describing the relationship between [CaProt] (protein-bound calcium), serum albumin concentrations, and pH is shown at the bottom of the graph. Redrawn from Moore EW. Ionized calcium in normal serum, ultrafiltrates, and whole blood determined by ion-exchange electrodes. *J Clin Invest.* 1970;49:318–334, with permission of the publisher.

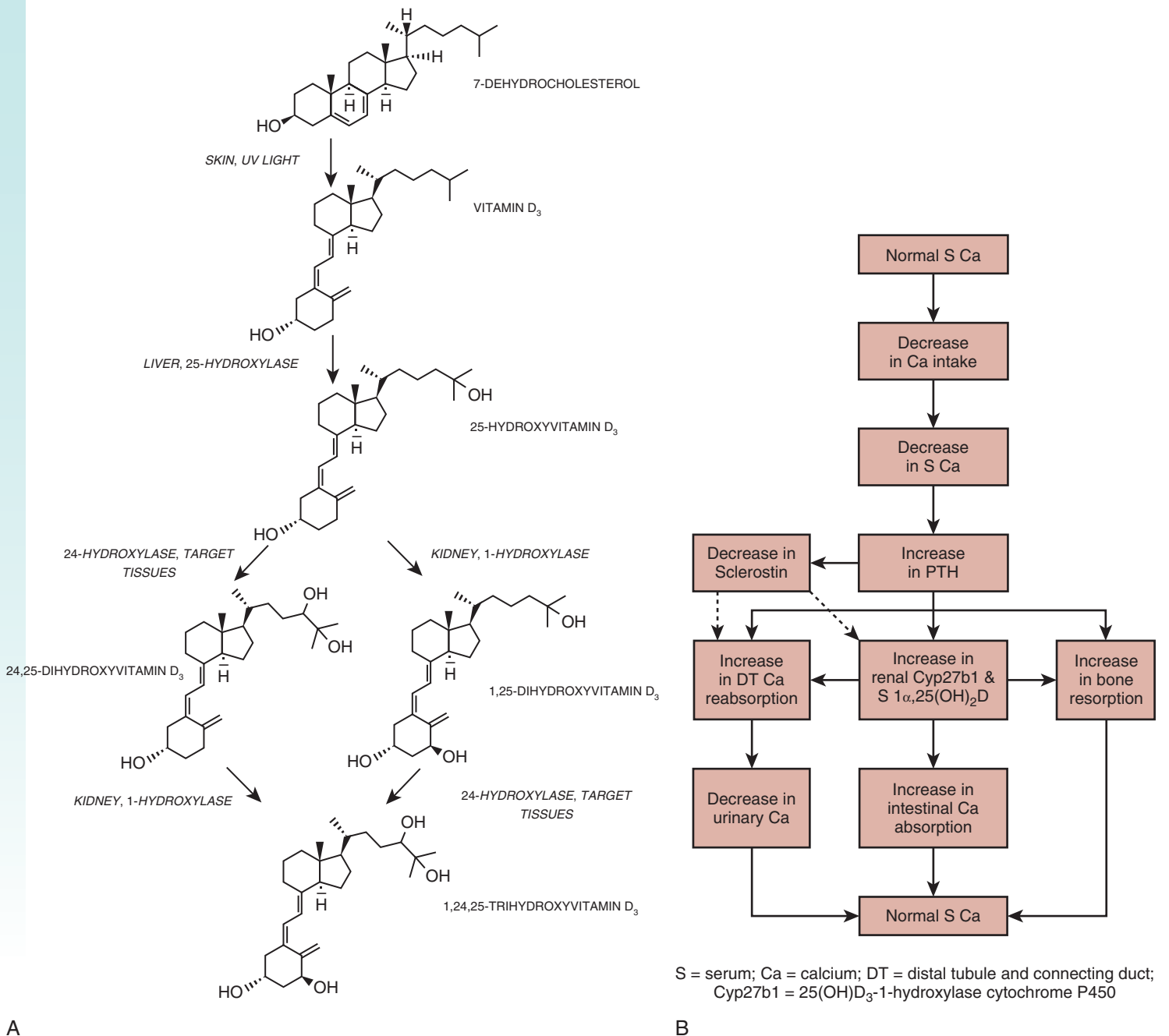
REGULATION OF CALCIUM HOMEOSTASIS BY THE PARATHYROID HORMONE–VITAMIN D ENDOCRINE SYSTEM

In states of neutral calcium balance, the amount of calcium absorbed by the intestine is equivalent to the amount excreted by the kidney. The central role of the vitamin D–PTH endocrine system in the regulation of calcium homeostasis is well recognized.^{15–17} The major physiologic role of vitamin D through the activity of its active metabolite $1\alpha,25\text{-dihydroxyvitamin D}_3$ ($1\alpha,25(\text{OH})_2\text{D}_3$) is the maintenance of normal calcium and phosphorus balance.^{18–21} In Fig. 7.4 the metabolism of vitamin D and the adaptations that occur in response to changes in serum calcium are illustrated. Fig. 7.4A summarizes the salient biochemical transformations that occur endogenously during the formation and metabolism of vitamin D₃. Vitamin D₃ (cholecalciferol) is formed in the skin by the ultraviolet light–mediated photolysis of the B-ring of the sterol precursor, 7-dehydrocholesterol, which gives rise to pre-vitamin D₃ that rapidly undergoes thermal equilibration to vitamin D₃.^{22–30} Vitamin D₂, or ergocalciferol, derived by photolysis of the plant sterol, ergosterol, is ingested orally, after which it is metabolized in a similar manner to

vitamin D₃.³¹ Although vitamin D₂ is less active in birds than mammals, when compared with vitamin D₃, the metabolic transformations of vitamin D₂ and vitamin D₃ are similar.³² Vitamin D₃, bound to vitamin D–binding protein, to which it preferentially binds relative to its precursor, pre-vitamin D₃,²⁹ exits the skin, enters the circulation, and is metabolized in the liver microsomes and mitochondria to 25-hydroxyvitamin D₃ (25(OH)D₃) by the vitamin D₃-25-hydroxylase.^{16,33–43} The CYP2R1 is the cytochrome P450 of the microsomal vitamin D₃-25 hydroxylase.⁴¹ Other vitamin D₃-25-hydroxylases play a role in the transformation of vitamin D₃ to 25(OH)D₃ because deletion of the *Cyp2r1* gene in mice results in reduced (>50% reduction) but detectable serum 25(OH)D₃ concentrations.⁴³

The subsequent metabolism of 25(OH)D₃ is dependent on the calcium and phosphorus requirements of the individual. In states of calcium demand, 25(OH)D₃ is metabolized by the 25-hydroxyvitamin D₃-1 α -hydroxylase to the biologically active vitamin D metabolite, $1\alpha,25\text{-dihydroxyvitamin D}_3$ ($1\alpha,25(\text{OH})_2\text{D}_3$), in mitochondria of kidney proximal and distal tubule cells by PTH-dependent processes (see Fig. 7.4B).^{18,26,44–56} In response to reductions in calcium intake and subsequent decreases in serum calcium, PTH release from the parathyroid glands is increased. The change in serum calcium concentrations is detected by the parathyroid gland calcium-sensing receptor, a G-protein–coupled receptor, which alters PTH release from the parathyroid cell.^{57–60} PTH enhances calcium transport in the distal tubule of the kidney directly,^{61–63} and indirectly through changes in sclerostin expression,^{55,56,64,65} and increases the activity of the renal 25-hydroxyvitamin D 1 α -hydroxylase, and attendant increases in the synthesis of $1\alpha,25(\text{OH})_2\text{D}_3$.⁵² $1\alpha,25(\text{OH})_2\text{D}_3$ increases calcium transport in the intestine^{49,50,66} and kidney.^{67–71} At the same time, both PTH^{72–74} and $1\alpha,25(\text{OH})_2\text{D}_3$ ^{75,76} increase bone calcium mobilization and help to maintain serum calcium concentrations. The converse series of events occurs in hypercalcemic circumstances. In states of calcium sufficiency, the synthesis of $1\alpha,25(\text{OH})_2\text{D}_3$ is reduced, and the synthesis of $24R,25\text{-dihydroxyvitamin D}_3$ ($24R,25(\text{OH})_2\text{D}_3$), a vitamin D metabolite with reduced bioactivity, is increased.^{77–79} The synthesis of $24R,25(\text{OH})_2\text{D}_3$ is mediated by a $1\alpha,25(\text{OH})_2\text{D}_3$ -inducible enzyme, the 25(OH)D₃-24-hydroxylase, that is present in several target tissues of $1\alpha,25(\text{OH})_2\text{D}_3$ including the intestine and the kidney.^{77,80–84}

$1\alpha,25(\text{OH})_2\text{D}_3$, PTH, and the phosphatonin, fibroblast growth factor-23 (FGF-23), regulate and maintain normal phosphorus concentrations.^{85–87} Serum phosphate concentrations also regulate the synthesis of $1\alpha,25(\text{OH})_2\text{D}_3$ by PTH independent mechanisms.⁸⁸ In states of phosphorus demand, 25(OH)D₃ is metabolized to $1\alpha,25(\text{OH})_2\text{D}_3$ and the synthesis of $24R,25(\text{OH})_2\text{D}_3$ is reduced.^{16,46,89–92} The enhanced synthesis of $1\alpha,25(\text{OH})_2\text{D}_3$ in hypophosphatemic states is induced directly by reductions in serum phosphate,^{88,93–95} an increase in the expression of IGF-1,^{96,97} and by inhibition of FGF-23.⁹⁸ The converse occurs in hyperphosphatemic states. A decrease in serum phosphate concentrations is associated with an increase in ionized calcium, a decrease in PTH secretion, and a subsequent decrease in renal phosphate excretion. An increase in renal 25-hydroxyvitamin D-1 α -hydroxylase activity, increased $1\alpha,25(\text{OH})_2\text{D}_3$ synthesis, and increased phosphorus absorption in the intestine and reabsorption in the kidney occur.^{88,92,94,99–105} In the intestine and kidney, $1\alpha,25(\text{OH})_2\text{D}_3$ increases the expression of the sodium–phosphate cotransporters IIB, and IIA and IIC, respectively, thereby regulating



S = serum; Ca = calcium; DT = distal tubule and connecting duct; Cyp27b1 = 25(OH)D₃-1-hydroxylase cytochrome P450

Fig. 7.4 A. The formation and metabolism of vitamin D₃. B. Physiologic changes in response to decreases in serum calcium concentrations. Ca, Calcium; Cyp27b1, 25(OH)D₃-1-hydroxylase cytochrome P450; DT, distal tubule and connection duct; PTH, parathyroid hormone; S, serum; UV, ultraviolet. From Tebben PJ, Singh RJ, Kumar R. Vitamin D-mediated hypercalcemia: mechanisms, diagnosis, and treatment. *Endocr Rev.* 2016;37:521–547.

the efficiency of Pi absorption in enterocytes and proximal tubule (PT) cells.^{87,106–108} In hyperphosphatemic states, renal 25-hydroxyvitamin D-1 α -hydroxylase activity and 1 α ,25(OH)₂D₃ synthesis are diminished, and 25-hydroxyvitamin D-24-hydroxylase activity is increased in association with elevations in FGF-23.^{7,98} Numerous other factors other than calcium and phosphorus alter the activity of the 25(OH)D-1 α -hydroxylase and the reader is referred to reviews on this matter.^{47,109–113}

The bioactivity of vitamin D₃ depends on the formation of 1 α ,25(OH)₂D₃ as pharmacologic amounts of vitamin D₃ or 25(OH)D₃ are required to elicit a biological response in

anephric animals and patients,^{53,75,114} whereas 1 α ,25(OH)₂D₃ readily increases intestinal calcium transport^{49,50} and mobilizes calcium from bone⁷⁵ when given in physiologic amounts. The actions of 1 α ,25(OH)₂D₃ require the presence of the vitamin D receptor (VDR), a steroid hormone receptor, that binds 1 α ,25(OH)₂D₃ with high affinity.^{115–118} Following binding of 1 α ,25(OH)₂D₃ to the ligand binding domain of the VDR, a conformational change in the receptor occurs and is associated with the recruitment of RXR α and coactivator (or corepressor) proteins to DNA binding elements within the transcription start site or other areas of genes regulated by

$1\alpha,25(\text{OH})_2\text{D}_3$.^{20,119–139} The efficiency of calcium absorption increases or decreases inversely with the amount of dietary calcium, and adaptations to changes in calcium intake are dependent on $1\alpha,25(\text{OH})_2\text{D}_3$.^{140,141} Calcium is absorbed by the intestine by passive paracellular and active transcellular mechanisms.^{141–143} Active calcium absorption initially involves the movement of calcium across the apical border of the intestinal cell into the cell down a concentration and electrical gradient and does not require the expenditure of energy.^{17,144} The extrusion of calcium out of the intestinal cell at the basolateral membrane is against an electrical and concentration gradient and requires the energy expenditure.^{17,144} Essential to the process of active calcium transport are several vitamin D-dependent proteins, including the TRPV 5/6 (transient receptor potential vanilloid 5/6) epithelial calcium channels, calbindin $\text{D}_{9\text{K}}$ and $\text{D}_{28\text{K}}$, and the plasma membrane calcium pump.⁸⁷ In the duodenal enterocyte, apically situated TRPV 5/6 cation channels mediate the increase in Ca uptake from the lumen into the cell¹⁴⁵; intracellular Ca binding proteins such as calbindin $\text{D}_{9\text{K}}$ and $\text{D}_{28\text{K}}$ facilitate the movement of Ca across the cell^{17,143}; and the basolateral plasma membrane Ca pump (PMCA)^{2,146,147} and the Na-Ca exchanger (NCX)¹⁴⁸ assist in the extrusion of Ca from within the cell into the extracellular fluid (ECF). The Na gradient for the activity of the NCX is maintained by the Na-K-ATPase. Intestinal transcellular Ca transport is regulated by $1\alpha,25(\text{OH})_2\text{D}_3$, which increases the expression of TRPV 6 channels,¹⁴⁹ the intracellular concentrations of calbindin $\text{D}_{9\text{K}}$ and $\text{D}_{28\text{K}}$,^{17,150–152} and the expression of the plasma membrane pump, isoform 1.^{153,154} The requirement of various intestinal Ca transporter proteins in transcellular Ca transport in vivo has been examined in knockout mice. Deletions of *TrpV6* and *calbindin D_{9K}* genes are not associated with alterations in intestinal Ca transport in vivo in the basal state and following the administration of $1\alpha,25(\text{OH})_2\text{D}_3$,^{155,156} although one report suggests that basal Ca transport on an adequate Ca diet is normal in *TrpV6* knockout mice but adaptations to a low-Ca diet are impaired.¹⁵⁷ We recently showed that deletion of the *Pmca1* in the intestine is associated with reduced growth and bone mineralization and a failure to upregulate calcium absorption in response to $1\alpha,25(\text{OH})_2\text{D}_3$, thereby establishing the essential role of the pump in transcellular intestinal Ca transport.¹⁵⁸

REABSORPTION OF CALCIUM ALONG THE TUBULE

The kidney reabsorbs filtered calcium in amounts that are subject to regulation by calciotropic hormones, PTH and $1\alpha,25(\text{OH})_2\text{D}_3$.^{16,145,159–164} Between 9000 and 10,000 mg of complexed and ionized calcium are filtered by the glomerulus in a 24-hour period. The amount of calcium appearing in the urine is approximately 250 mg/day, and it is therefore evident that a large percentage of filtered calcium is reabsorbed. As a result of reabsorption processes that occur in both the proximal and distal tubule, only 1%–2% of calcium filtered at the glomerulus appears in the urine.^{145,161,164} Fig. 7.5 shows the percentages of calcium reabsorbed along different segments of the nephron.

Ca^{2+} REABSORPTION IN THE PROXIMAL TUBULE

As noted earlier, about 60%–70% of total plasma calcium is free (not protein bound) and is filtered at the glomerulus.^{165,166}

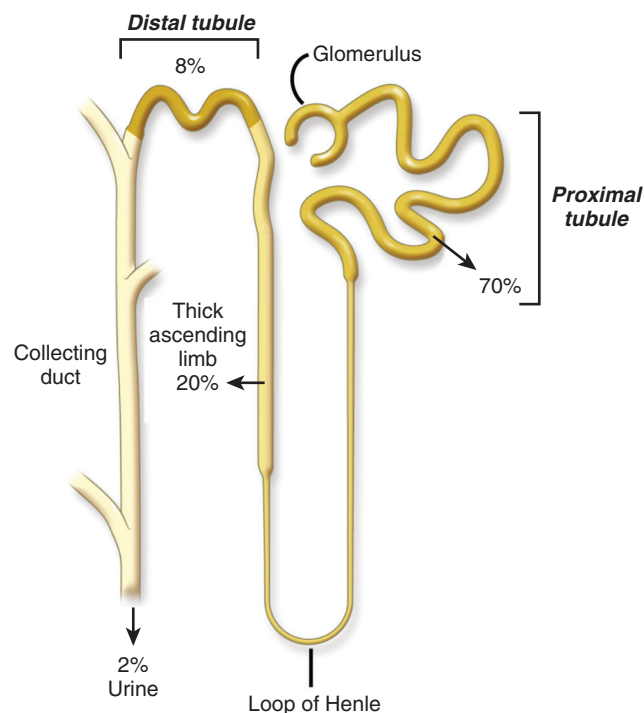


Fig. 7.5 Percentages of filtered calcium reabsorbed along the tubule.

A large percentage (~70%) of filtered calcium (Ca^{2+}) is reabsorbed in the PT mainly by paracellular processes that are linked with sodium (Na^+) reabsorption.^{165,167–170} In this nephron segment, the reabsorption of Na^+ and Ca^{2+} is proportional under a variety of conditions^{169,171} and is not dissociated following the administration of several factors that are known to alter renal Ca^{2+} reabsorption, such as PTH, cyclic AMP, chlorothiazide, furosemide, acetazolamide, or changes in the hydrogen ion content.^{168,169,172,173} The precise cellular and molecular machinery responsible for the movement of Ca^{2+} from the lumen of the PT into the interstitial space is not clearly defined. A majority of Ca^{2+} is believed to move in between cells (paracellular movement) with a smaller, but significant, transcellular component (Fig. 7.6). The components of the paracellular pathway likely include the tight junction protein, claudin-2, which functions as a paracellular cation channel. Ca^{2+} permeates through claudin-2¹⁷⁴ and simultaneously competitively inhibits Na^+ conductance.¹⁷⁵ A transcellular component of Ca^{2+} reabsorption may also be present in the PT. Undefined Ca^{2+} channels and intracellular Ca^{2+} -binding proteins influence the movement of Ca^{2+} into and across the cell. The Na-K-ATPase has been implicated in transcellular Ca^{2+} transport in the PT,¹⁷⁶ and both the Na- Ca^{2+} exchanger¹⁷⁷ and isoforms 1 and 4 of the plasma membrane Ca^{2+} pump^{178,179} are expressed in the PT, and could be important in the movement of Ca^{2+} out of the PT cell. Although the PT reabsorbs large amounts of Ca^{2+} , primarily by paracellular processes, the rate of Ca^{2+} reabsorption is not influenced by factors or hormones that regulate calcium balance.^{168,169,172} Extracellular volume status is the major factor that influences Ca^{2+} reabsorption in the PT, via its effects on Na^+ reabsorption (see later).

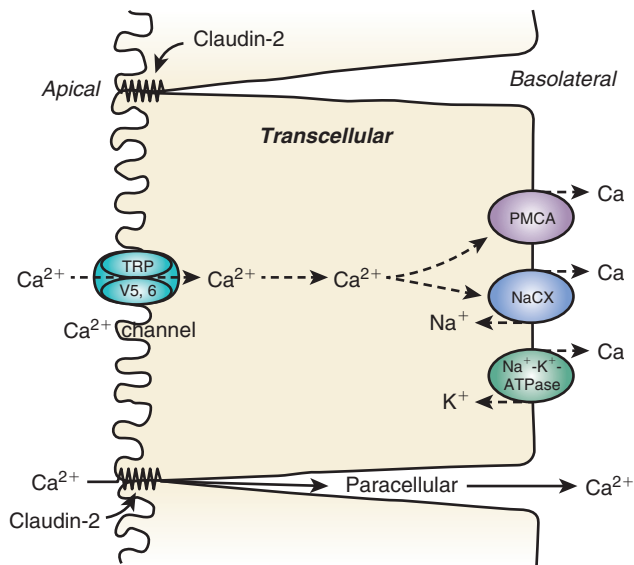


Fig. 7.6 Mechanisms by which calcium is transported in the proximal tubule. The majority of calcium is reabsorbed by paracellular mechanisms. A smaller percentage is reabsorbed by transcellular mechanisms.

CA²⁺ REABSORPTION IN THE LOOP OF HENLE

The thin descending and thin ascending limbs of the loop of Henle do not transport significant amounts of Ca²⁺.^{197,198} Between 20%–25% of filtered Ca²⁺ is reabsorbed in the thick ascending loop of Henle, primarily by the paracellular route involving claudin-16 and -19.^{165,180–191} Thick ascending limb cells express the furosemide-sensitive Na-K-Cl cotransporter, NKCC2,^{192–195} which mediates the reabsorption of Na⁺ and thereby contributes to the driving force for paracellular Ca²⁺ transport. A lumen-positive transepithelial potential is generated in the thick ascending limb of the loop of Henle (TALH) through the activity of the NKCC2 (Na-K-2Cl cotransporter)¹⁹⁶ by two mechanisms: secondary apical recycling of K⁺ via ROMK, and a NaCl diffusion potential generated by reabsorbed NaCl establishing a concentration gradient across the Na-selective paracellular pathway. This transepithelial voltage provides the driving force for passive Ca²⁺ reabsorption through the paracellular pathway.

Claudins, located in the tight junction between cells of the TALH play a role in the paracellular movement of Ca²⁺ (and Mg²⁺ reabsorption, as discussed in the next section)^{197,198} (Fig. 7.7). Claudin-16 (also known as paracellin), together with claudin-19, forms a paracellular pore. A heteromeric claudin-16 and claudin-19 interaction is required to assemble and traffic to the tight junction and to generate cation-selective paracellular channels.^{199,200} It has been postulated that these channels are themselves responsible for permeating divalent cations, Ca²⁺ and Mg²⁺, via the paracellular route.^{197,198} An alternative hypothesis is that claudin-16 and -19 form Na⁺ channels and act primarily to establish the transepithelial NaCl diffusion potential, thus contributing to the driving force for divalent cation reabsorption.^{199–202} Regardless of the mechanism, loss-of-function mutations in the genes encoding claudin-16 and -19 result in familial hypomagnesemia with hypercalciuria and nephrocalcinosis (FHHNC), which is characterized by renal Ca²⁺ and Mg²⁺ wasting due to defective thick ascending

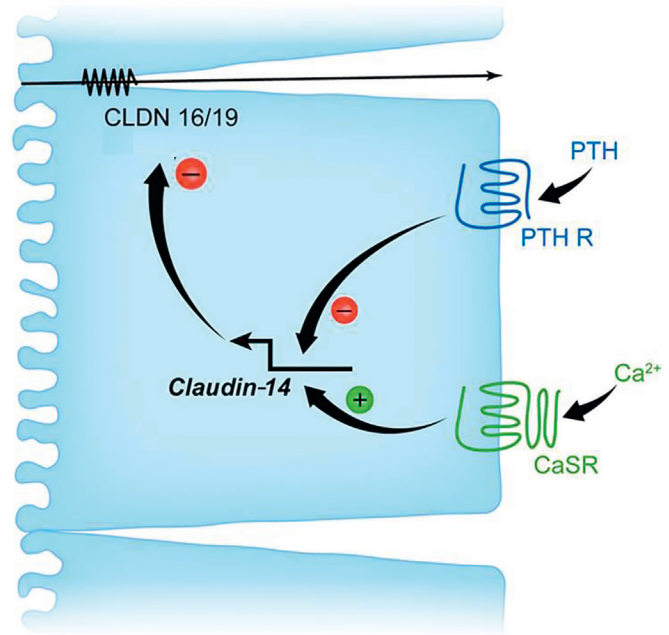


Fig. 7.7 Mechanisms and regulation of calcium transport in the thick ascending limb of Henle (TALH). In the TALH, calcium is reabsorbed via paracellular mechanisms through a pore composed in part by claudin-16 and claudin-19. The activity of the latter proteins is suppressed by claudin-14, whose expression is controlled by parathyroid hormone (PTH) and Ca²⁺. PTH binds to its receptor and inhibits the expression of claudin-14, whereas extracellular fluid Ca²⁺ activates the calcium-sensing receptor (CaSR) and increases claudin-14 expression. The reabsorption of Ca²⁺ in the TALH is the result of opposing activities of PTH and Ca²⁺ through their receptors. CLDN 16/19, Claudin-16 and -19; PTH, parathyroid hormone; PTH R, parathyroid receptor.

limb divalent cation reabsorption. Hou et al. generated claudin-16 and claudin-19 knockdown mouse models using transgenic siRNAs and demonstrated that these mice have significantly reduced plasma Mg²⁺ concentrations and excessive urinary excretion of Mg²⁺ and Ca.^{24, 380} Calcium deposits were observed in the basement membranes of the medullary tubules and the interstitium in the kidney of claudin-16 knockdown mice. Thus, the phenotypes of *Cldn16* and *Cldn19* knockdown mice recapitulate the phenotype of human FHHNC patients. Similarly, mutations of NKCC2 are associated with the common form of Bartter syndrome and can be associated with hypercalciuria²⁰³ (see also Chapters 18 and 44).

Calcium-regulating hormones can regulate reabsorption of Ca²⁺ by the thick ascending limb, but there is considerable species heterogeneity. In the mouse, PTH and calcitonin (CT) stimulate Ca²⁺ transport in the cortical thick ascending limb,^{184,186,204,205} whereas in the rabbit CT stimulates calcium reabsorption in the medullary thick ascending limb but not in the cortical thick ascending limb.¹⁸⁹ Extracellular fluid calcium also regulates calcium reabsorption in this segment through the Ca²⁺-sensing receptor (see later).

CA²⁺ REABSORPTION IN THE DISTAL TUBULE

In the distal convoluted tubule (primarily DCT2) and connecting tubule (together abbreviated as DT), 5%–10% of filtered Ca²⁺ is reabsorbed^{206–208} by active transport processes

against both an electrical and concentration gradient. Ca^{2+} reabsorption in the DT occurs via a transcellular pathway. The apically situated, transient receptor potential cation channels, subfamily V, type 5 and 6 channels (TRPV5, TRPV6) mediate the increase in Ca^{2+} uptake from the lumen into the cell.^{164,209–214} Micropuncture studies in knockout mice indicate that TRPV5 is the gatekeeper of Ca^{2+} reabsorption in the accessible DT in mice (Fig. 7.8A).²¹¹ The intracellular Ca^{2+} -binding proteins, calbindin $\text{D}_{9\text{K}}$ and $\text{D}_{28\text{K}}$, facilitate the movement of Ca^{2+} across the cell.^{160,215} The basolateral plasma membrane calcium ATPase (PMCA) pump,^{159,160,162} Na^+ - Ca^{2+} exchanger (NaCX),^{216–219} and the Na^+ - Ca^{2+} - K^+ exchanger (NaCKX)²²⁰ mediate the active extrusion of Ca^{2+} across the basolateral membrane (see Fig. 7.8B and 7.8C). The Na^+ gradient for the activity of the NaCX and the NaCKX is provided by the Na-K ATPase situated at the basolateral cell membrane (not shown). Ca^{2+} reabsorption in the DT is increased by PTH,^{61–63} CT,^{204,205} and $1\alpha,25(\text{OH})_2\text{D}_3$.^{67–71}

REGULATION OF Ca^{2+} TRANSPORT IN THE KIDNEY

CALCIUM-REGULATING HORMONES

The calcium-regulating hormones, PTH and $1\alpha,25(\text{OH})_2\text{D}_3$, regulate the expression or activity of calcium channels, calcium-binding proteins, calcium pumps, and exchangers in the kidney to increase tubule retention of filtered calcium via the transcellular pathway. PTH increases the activity of TRPV5 channels in the DT by activating cAMP-PKA signaling, and phosphorylating a threonine residue within the channel, resulting in an increase in the open probability of the channel.²²⁰ PTH also activates the PKC pathway, thereby increasing the numbers of TRPV5 channels on the surface

of tubular cells by inhibiting endocytosis of caveolae in which the channels are located.²²¹ $1\alpha,25(\text{OH})_2\text{D}_3$ enhances the expression of TRPV5 and TRPV6 channels present in the distal and connecting tubule and cortical collecting duct by increasing respective mRNA concentrations through increased binding of the VDR to response elements in the gene promoters.^{70,213} $1\alpha,25(\text{OH})_2\text{D}_3$ increases the expression of calbindin $\text{D}_{9\text{K}}$ and $\text{D}_{28\text{K}}$ and the PMCA pump in the kidney and cultured renal cells.^{70,179,222–231} The effect of PTH and $1\alpha,25(\text{OH})_2\text{D}_3$ is to increase the expression of Ca^{2+} channels, binding proteins, pumps and exchangers, thereby increasing the retention of calcium by the kidney.

PTH has also been well described to increase renal tubule Ca^{2+} reabsorption by increasing its passive permeability in the TALH, predominantly in the cortical segment.^{232,233} The mechanism has now been elucidated. PTH, acting through the PTH/PTHrP receptor, has been shown to inhibit the transcription and subcellular trafficking of claudin 14, thereby increasing paracellular Ca^{2+} reabsorption in the TALH²³⁴ (see Fig. 7.7). Claudin-14 binds to claudin-16 and functions to inhibit the paracellular pore comprised of claudins 16 and 19. Tissue-specific knockout of the renal tubule PTH/PTHrP receptor in mice caused hypercalciuria and hypocalcemia, which was completely rescued by claudin-14 deletion, suggesting that the effect of PTH on paracellular Ca^{2+} transport in the TALH may be more important than previously appreciated.

EXTRACELLULAR CALCIUM AND DIET

The level of extracellular calcium regulates renal Ca^{2+} reabsorption by signaling through the Ca-sensing receptor (CaSR). In the kidney, the CaSR is primarily expressed on the basolateral membrane of the TALH. Activation of CaSR reduces renal tubular Ca^{2+} reabsorption and induces calciuresis

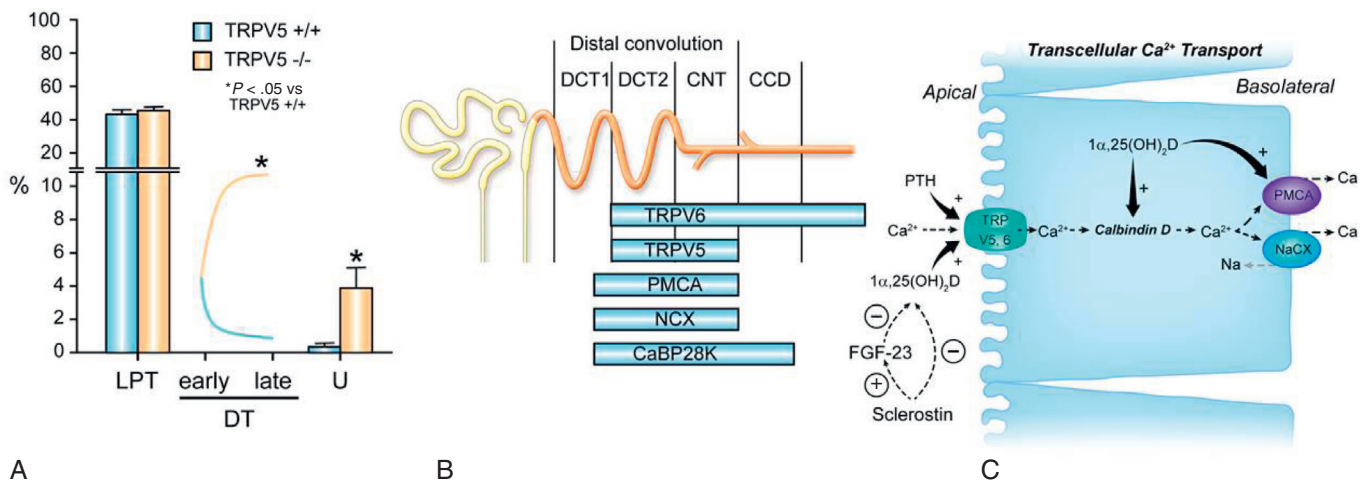


Fig. 7.8 Mechanisms of calcium transport in the distal convoluted tubule. **A.** Role of TRPV5 investigated by micropuncture of kidneys from TRPV5 knockout mice. The figure shows fractional Ca^{2+} delivery to micropuncture sites in the late proximal tubule (LPT) to sites located along the distal convoluted tubule (DC) from early to late DC (as localized using tubule K^+ concentrations) and to the urine. Deletion of TRPV5 in mice prevents Ca^{2+} reabsorption along the DT and there is even evidence for Ca^{2+} leaking back into the lumen, possibly by paracellular routes; TRPV6 may partially compensate in the collecting duct. **B.** Distribution of $1\alpha,25(\text{OH})_2\text{D}_3$ or parathyroid hormone–sensitive channels and transporters along the distal convoluted tubule (DCT1 and DCT2), connecting tubule (CNT), and cortical and medullary collecting ducts (CCD and MCD). **C.** Ca transport in the DT occurs by transcellular mechanisms. Transcellular Ca transport is mediated by several channels, pumps, and exchangers located at the apical and basolateral portions of the cell. Modified from Kumar R, Vallon V. Reduced renal calcium excretion in the absence of sclerostin expression: evidence for a novel calcium-regulating bone kidney axis. *J Am Soc Nephrol.* 2014;25:2159–2168, with permission of the publisher.

in response to a Ca load.^{235,236} One mechanism is by inhibition of NKCC2 expression²³⁶ or activity. More recently, it has been suggested that CaSR acts primarily by regulating paracellular permeability. Loupy et al. showed that a CaSR antagonist increased Ca²⁺ permeability in isolated perfused TALH with no change in transepithelial voltage or Na flux.²³⁷ This appears to be mediated by regulation of the expression of claudin-14. Activation of the CaSR causes robust upregulation of claudin-14,^{238,239} which through physical interaction, inhibits paracellular cation channels formed by claudin-16 and claudin-19²³⁸ (see Fig. 7.7). The signaling mechanism seems to involve CaSR inhibiting calcineurin, a phosphatase that normally activates NFAT to increase transcription of two micro-RNAs miR-9 and miR-374, thereby downregulating claudin-14 expression.^{240,241} The central role of claudin-14 is further supported by the finding that claudin-14 knockout mice are unable to increase their fractional excretion of calcium in response to a high Ca²⁺ diet,²³⁸ and exhibit complete loss of regulation of urinary Ca²⁺ excretion in response to either a CaSR agonist or antagonist.^{240,242} Of note, claudin-14 expression is also decreased in kidney of mice fed a low-calcium diet compared with those fed a high-calcium diet,²³⁴ providing a mechanism by which calcium excretion is matched to dietary intake.

DIURETICS

Loop diuretics such as furosemide increase urinary calcium losses. The mechanism by which furosemide causes hypercalciuria is linked to its ability to bind to and inhibit the furosemide-sensitive Na-K-Cl cotransporter, NKCC2,^{192–195} present in the TALH. NaCl absorption is diminished, as is potassium recycling, resulting in a reduction in lumen positivity that drives Ca²⁺ reabsorption. Subjects with the common form of Bartter syndrome have inactivating mutations of the NKCC2 and associated with calciuria.²⁰³ Compensatory increases occur in the expression of distal tubule transport channels and proteins such as the TRPV5 and TRPV6 channels and calbindin D_{28K} following the administration of furosemide, but fail to compensate for the increase in excretion that occurs in the TALH.²⁴² Thiazide diuretics, on the other hand, cause hypocalciuria^{213,243–245} and the effect appears to be independent of PTH in humans and rodents. Thiazides bind to and inhibit the Na-Cl cotransporter in the distal tubule.^{192,246} Chronic thiazide use is associated with a reduction in extracellular fluid volume, which secondarily enhances Na⁺ and Ca²⁺ reabsorption in the PT of in the kidney.¹⁷³ Distal tubule Ca²⁺ transport is clearly unaffected by “chronic” thiazide use,¹⁷³ in contrast to older reports that thiazide “acutely” increases Ca²⁺ reabsorption in isolated perfused DCT.²⁴⁷ The development of hypocalciuria parallels a compensatory increase in Na⁺ reabsorption secondary to an initial natriuresis following thiazide administration. These observations are supported by the upregulation of the Na⁺/H⁺ exchanger, responsible for the majority of Na⁺ and associated Ca²⁺ reabsorption in the PT, whereas the expression of proteins involved in active Ca²⁺ transport in the distal tubule was unaltered. Indeed, thiazide administration was associated with hypocalciuria in *Trpv5*-knockout mice. Humans with Gitelman syndrome and inactivating mutations of the thiazide-sensitive Na-Cl transporter have hypocalciuria, hypomagnesemia, and volume depletion,^{208,248–250} findings that are recapitulated in the Na-Cl cotransporter knockout mouse.²⁵¹

Clinical Relevance

Hypomagnesemia With Epidermal Growth Factor (EGF) Receptor Inhibitors

Because EGF activates TRPM6 in the distal convoluted tubules, EGF receptor inhibitors, which are widely used as chemotherapeutic agents, cause hypomagnesemia. Monoclonal antibodies targeting the EGF receptor, such as cetuximab and panitumumab, are frequently associated with this complication, whereas the incidence with small-molecule tyrosine kinase inhibitors such as erlotinib seems to be less.

Diuretics in Calcium Disorders

Because of their hypercalciuric effect, loop diuretics are used for the acute treatment of hyperkalemia. Conversely, in patients with idiopathic hypercalciuria, thiazide diuretics are effective at lowering urine calcium concentration and thereby reducing the risk of kidney stone formation.

ESTROGENS

Estrogens influence calcium transport in the kidney as postmenopausal women have higher urinary Ca²⁺ excretion than premenopausal women.²⁵² In the early postmenopausal period the administration of estrogen is associated with a decrease in urine Ca²⁺ excretion and an increase in serum PTH and 1 α ,25(OH)₂D.^{253,254} Estradiol increases the expression of the TRPV5 channel in the kidney in a manner independent of 1 α ,25(OH)₂D.²⁵⁵ These observations are supported by reduced duodenal TRPV5 channel expression in mice lacking the estrogen receptor α .²⁵⁶

EXTRACELLULAR FLUID VOLUME

In conditions such as volume depletion, where PT Na⁺ reabsorption is increased, one also observes enhanced Ca²⁺ reabsorption that can contribute to the hypercalcemia that is sometimes seen in such situations. Conversely, the salutary effects of isotonic saline administration in hypercalcemic patients are attributable to a reduction in Ca²⁺ reabsorption as a result of reduced Na⁺ reabsorption.

METABOLIC ACIDOSIS AND ALKALOSIS

Metabolic acidosis is associated with hypercalciuria, and when prolonged, often results in bone loss and osteoporosis.²⁵⁷ Metabolic acidosis and metabolic alkalosis decrease or increase the reabsorption of Ca²⁺ in the distal tubule,^{172,258–261} the expression TrpV5 in the distal tubule,²⁶² and the activity of TrpV5 channels.^{263–265}

REGULATION OF RENAL CALCIUM TRANSPORT BY NOVEL PROTEINS

KLOTHO

Klotho is a coreceptor for the phosphaturic peptide, FGF 23, with β -glucuronidase activity.^{266–269} It is a kidney- and parathyroid gland-specific protein, which influences epithelial Ca²⁺ transport by deglycosylating TRPV5, thereby trapping the channel in the plasma membrane and sustaining the

activity of the channel.²⁷⁰ Further evaluation of serum Klotho concentrations and their association with changes in renal calcium excretion is required to establish a role of this factor in regulation of renal calcium transport.

SCLEROSTIN

Sclerostin is an osteocyte-derived glycoprotein that influences bone mass.²⁷¹ Patients with sclerosteosis and its milder variant, van Buchem disease,^{272–274} have exceptionally dense bones and skeletal overgrowth that often constricts cranial nerve foramina and the foramen magnum, resulting in premature death. Sclerosteosis is due to inactivating mutations of the sclerostin (*SOST*) gene, and the milder van Buchem disease is due to a 52-kb deletion of a downstream enhancer element of the sclerostin gene.²⁷⁵ Mouse models of sclerosteosis have increases in skeletal mass similar to those found in patients with the disease.^{55,276–278} By using a *Sost* gene knockout model generated in our laboratory⁵⁵ we have demonstrated that sclerostin, either directly or indirectly, through an alteration in the synthesis of $1\alpha,25$ -dihydroxyvitamin D ($1\alpha,25(\text{OH})_2\text{D}$), influences renal calcium reabsorption in the kidney. Urinary calcium excretion and renal fractional excretion of calcium are decreased in *Sost*^{-/-} mice.⁵⁵ Serum $1\alpha,25(\text{OH})_2\text{D}$ concentrations are increased without attendant hypercalcemia; renal $25(\text{OH})\text{D}-1\alpha$ hydroxylase (*Cyp27b1*) mRNA and protein expression are also increased in *Sost*^{-/-} mice, strongly suggesting that the increase in serum $1\alpha,25(\text{OH})_2\text{D}$ concentrations was due to increased $1\alpha,25(\text{OH})_2\text{D}$ synthesis. When recombinant sclerostin is added to cultures of proximal tubular cells the expression of the messenger RNA for *Cyp27b1*, the 1α -hydroxylase cytochrome P450, is diminished. Serum $24,25(\text{OH})_2\text{D}$ concentrations were diminished in *Sost*^{-/-} mice, and PTH concentrations were similar in knockout and wild-type mice. The lack of change in PTH is consistent with previous studies in humans.²⁷⁹ The data suggest that in addition to the hormones traditionally thought to alter calcium reabsorption in the kidney (PTH and $1\alpha,25(\text{OH})_2\text{D}$), sclerostin plays a significant role in altering renal calcium excretion. Whereas PTH and $1\alpha,25(\text{OH})_2\text{D}$ decrease fractional excretion of calcium by increasing the efficiency of calcium reabsorption in the DT, sclerostin increases fractional excretion of calcium (the absence of sclerostin expression being associated with a reduced fractional excretion of calcium).⁵⁵ Thus, the adaptation to a reduction in calcium intake and resultant downstream alterations in hormones may need to be amended to include changes in sclerostin expression (see Fig. 7.4B and Fig. 7.8C).

MAGNESIUM TRANSPORT IN THE KIDNEY

THE ROLE OF MAGNESIUM IN CELLULAR PROCESSES

Magnesium is an abundant cation in the human body (Table 7.1).^{280–285} Magnesium is required for a variety of biochemical functions.²⁸⁶ The activities of magnesium-dependent enzymes are modulated by the metal as a result of binding to the substrate or as a result of direct binding to the enzyme.^{286–289} Enzymes of the glycolytic and citric acid pathways, exonuclease, topoisomerase, RNA and DNA polymerases, and adenylate cyclase are among the many enzymes regulated by

Table 7.2 Distribution and Concentrations of Magnesium in a Healthy Adult

Site	% total-body Mg	Concentration/content
Bone	53	0.5% of bone ash
Muscle	27	9 mmol/kg wet weight
Soft tissue	19	9 mmol/kg wet weight
Adipose tissue	0.012	0.8 mmol/kg wet weight
Erythrocytes	0.5	1.65–2.73 mmol/L
Serum	0.3	0.69–0.94 mmol/L

magnesium.^{286–290} Additionally, magnesium regulates channel activity.²⁸⁶

Given its role in such diverse biological processes, it is not surprising that a deficiency or increase in serum magnesium concentrations is associated with important clinical symptoms.²⁹¹ For example, low magnesium concentrations are associated with muscular weakness, fasciculations, Chvostek and Trousseau signs, and sometimes frank tetany.²⁹¹ The tetany of hypomagnesemia is independent of changes in serum calcium. On occasion, personality changes, anxiety, delirium and psychoses may manifest. Hypocalcemia,^{292–298} reduced PTH secretion,^{299–304} and hypokalemia^{305–308} are sometimes present in hypomagnesemic subjects. Cardiac arrhythmias and prolongation of the corrected QT interval^{309,310} are sometimes observed. Conversely, hypermagnesemia seen in association with the administration of excessive amounts of magnesium in diseases such as eclampsia and in patients with renal failure is manifest as weakness of the voluntary muscles.

MAGNESIUM IS PRESENT IN SERUM IN BOUND AND FREE FORMS

Most magnesium within the body is present in bone or within the cells (Table 7.2).²⁸⁶ Approximately 60% of magnesium is stored in bone. Serum magnesium concentrations vary slightly with age and in adults are 1.6–2.3 mg/dL (0.66–0.94 mmol/L). Within plasma, about 70% of Mg is ultrafiltrable, 55% is free, and about 14% of Mg is in the form of soluble complexes with citrate and phosphate.³¹¹ Because Mg is present largely within cells and bone, there is some interest as to whether serum Mg concentrations reflect tissue stores, especially when Mg is depleted or deficient. When rats^{312–314} and humans^{291,315} are fed Mg-deficient diets, serum Mg decreases within 1 day in rats and in 5–6 days in humans. Bone Mg and blood mononuclear cell Mg concentrations correlate well with total body Mg and serum Mg.^{315–318} The correlations between total body Mg stores and muscle or cardiac Mg, however, are not precise.³¹⁵

REGULATION OF MG HOMEOSTASIS

The intestine and the kidney regulate magnesium balance (Fig. 7.9).²⁸⁶ A diet adequate in magnesium normally contains 200–300 mg of magnesium.³¹⁹ Between 75 and 150 mg of ingested dietary magnesium is absorbed in the jejunum and ileum, primarily by paracellular passive processes.^{320–325} The TRPM6 protein (a mutant form of this protein is present in patients with familial hypomagnesemia) is localized to

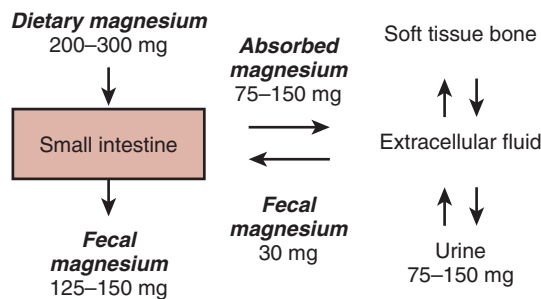


Fig. 7.9 Magnesium homeostasis in normal humans showing the amounts of magnesium absorbed in the intestine and reabsorbed by the kidney.

the apical membrane of intestinal and renal epithelial cells and mediates transcellular magnesium absorption.^{145,326} A homolog of TRPM6, TRPM7 is ubiquitously expressed and plays a role in whole-body magnesium homeostasis and many cellular functions, ranging from control of cell proliferation and cellular magnesium homeostasis to cell adhesion and cell migration.^{327–335} It forms a heteromeric complex with TRPM6 and is necessary for TRPM6 activity and epithelial magnesium absorption.^{336,337} About 30 mg of magnesium is secreted into the intestine via pancreatic and intestinal secretions, giving a net magnesium absorption of approximately 130 mg/24 h. Magnesium that is not absorbed in the intestine and is secreted into the intestinal lumen eventually appears in the feces (125–150 mg). Absorbed magnesium enters the extracellular fluid pool and moves in and out of bone and soft tissues. Approximately 130 mg of magnesium (equivalent to the net and amount absorbed in the intestine) is excreted in the urine.

In experimental animals and humans, feeding a diet low in magnesium results in a rapid decrease in urinary and fecal magnesium and the occurrence of a negative magnesium balance.^{338–347} Conversely, the administration of magnesium is associated with an increase in the renal excretion of magnesium.^{348–350} Unlike the cases of calcium and phosphorus, however, no hormones or molecules have been identified that alter magnesium transport in the intestine or that alter the renal excretion of magnesium in response to changes in magnesium balance.^{286,351,352}

REABSORPTION OF MAGNESIUM ALONG THE TUBULE

Approximately 10% of total body magnesium is filtered daily by the glomeruli (approximately 3000 mg/24 hr). About 75% of total plasma magnesium is filterable. Because urinary magnesium excretion is about 150 mg/24 hr, a substantial fraction of filtered magnesium is reabsorbed along the tubule (approximately 95%).

MG²⁺ REABSORPTION IN THE PROXIMAL TUBULE

Between 15% and 20% of filtered magnesium is reabsorbed in the PT (Fig. 7.10). The cellular and molecular mechanisms by which magnesium is reabsorbed in the proximal nephron are unknown. However, it is speculated that reabsorption of magnesium in the proximal nephron occurs by paracellular mechanisms, likely driven by the concentration gradient

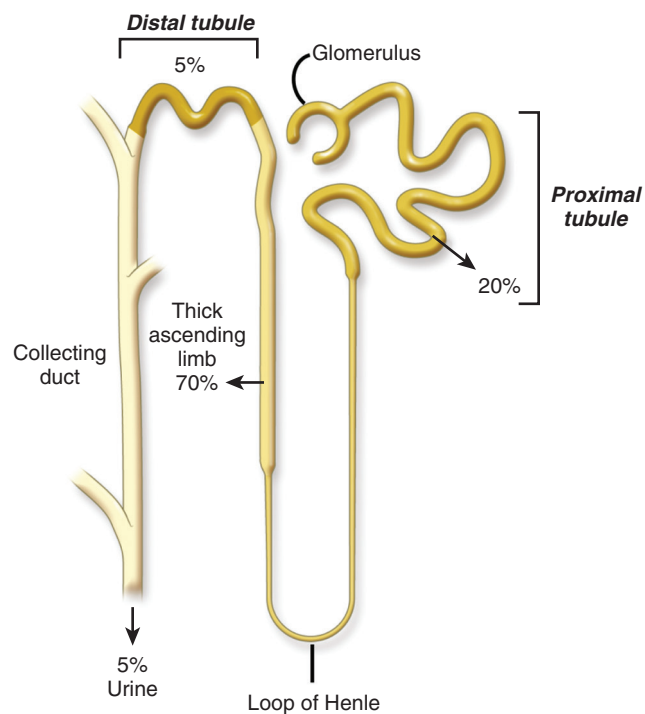


Fig. 7.10 Percentages of filtered magnesium reabsorbed along the tubule.

resulting from reabsorption of Na⁺ and water. However, magnesium permeability in this segment is likely to be quite low, as the tubular fluid-to-ultrafiltrate magnesium ratio can rise to 1.65 in the late PT.³⁵³

MG²⁺ REABSORPTION IN THE THICK ASCENDING LIMB

The bulk of the filtered magnesium is reabsorbed in the TALH, again by a paracellular mechanism of which claudin-16 is a critical component.^{199,201,354–361} As discussed earlier for Ca²⁺ transport, claudin-16 and claudin-19 form cation-selective paracellular channels^{199,200} that either directly mediate paracellular Mg²⁺ reabsorption or facilitate the generation of an NaCl diffusion potential that provides the driving force for paracellular Mg²⁺ reabsorption. Mutations of the *CLDN16* and *CLDN19* genes, and the *SLC12A1*, *KCNJ1*, and *CLCNKB* genes that encode proteins required for normal thick ascending limb function, result in excessive magnesium losses in the urine and hypomagnesemia. Claudin-10 is also highly expressed in the TALH. The predominant isoform, claudin-10b, acts as a paracellular Na⁺ channel and is spatially distinct from claudin-16/19, being expressed mainly in the medullary TALH.³⁶² Deletion of the *Cldn10* gene in mice is associated with decreased paracellular sodium reabsorption, hypermagnesemia, and nephrocalcinosis.³⁶³ In isolated perfused TAL tubules of claudin-10-deficient mice, paracellular permeability of sodium is decreased and the relative permeability of calcium and magnesium is increased. This suggests that claudin-10b uses the lumen-positive voltage in the early TALH to drive paracellular Na⁺ reabsorption and thereby reduces the electrical potential available for divalent cation reabsorption later on in the cortical TALH. Mutations in claudin-10, or specifically in claudin-10b, have recently been described in

several families with variable degrees of hypermagnesemia, hypocalciuria, and hypokalemic metabolic alkalosis, together with several unusual extrarenal manifestations, including anhidrosis, alacrims, xerostomia, and ichthyosis.^{364–366} Fig. 7.11 shows the mechanism by which magnesium is transported in the TALH.

Magnesium reabsorption in the TALH is inhibited by hypermagnesemia, presumably because it reduces the concentration gradient for paracellular diffusion.³⁶⁷ Conversely, hypomagnesemia and magnesium depletion stimulate magnesium reabsorption in the TALH.³⁶⁸ These are also the main physiological regulators of renal magnesium excretion.

Mg²⁺ REABSORPTION IN THE DISTAL TUBULE

Between 5% and 10% of filtered magnesium is reabsorbed transcellularly in the distal convoluted tubule. The rate-limiting step is thought to be apical entry of Mg²⁺ through an Mg²⁺ channel that is formed by a complex of TRPM6 and TRPM7.^{326,336,337} Epidermal growth factor (EGF) promotes TRPM6 trafficking to the plasma membrane.³⁶⁹ The driving force for apical Mg²⁺ entry is the lumen-negative electrical membrane potential, the set point of which is likely determined by the conductance of an apical voltage-gated potassium channel, Kv1.1.³⁷⁰ These explain why mutations in TRPM6, pro-EGF, and Kv1.1 are all genetic causes of hypomagnesemia (see Chapter 44 for a detailed discussion of inherited hypomagnesemia).

It is unclear as to the mode of basolateral exit of magnesium from the cell into the interstitial space.

CNNM2 is suspected to play a role because it encodes a transmembrane protein localized at the basolateral membrane that is regulated by Mg²⁺ deficiency and when mutated causes renal Mg²⁺ wasting.³⁷¹ It has been proposed to function as an Mg²⁺ channel or Mg²⁺-sensitive Na⁺ channel,^{372,373} but others have not found evidence that it transports Mg²⁺.³⁷⁴

Another intriguing possibility is SLC41A1, a homolog of bacterial MgtE Mg²⁺ transporters³⁷⁵ that functions as an Na⁺-Mg²⁺ exchanger when expressed in mammalian cells.³⁷⁶ Interestingly, mutations in SLC41A1 have recently been found to cause a form of nephronophthisis.³⁷⁷ Because basolateral extrusion of Mg²⁺ in the DT must involve energetically active transport, it is likely that the Na-K-ATPase plays a role, albeit indirectly. FXYP2 likely participates in this because it is the gamma subunit of the Na-K-ATPase and, when mutated, causes dominant isolated hypomagnesemia. Likewise, the transcription cofactors, hepatocyte nuclear factor 1B (HNF1B) and pterin-4 alpha-carbinolamine dehydratase (PCBD1) costimulate the promoter of FXYP2, and so mutations in either of them are associated with hypomagnesemia.^{378,379} Finally, mutations in the basolateral potassium channel in the DT, Kir4.1, cause a syndrome called SeSAME or EAST that is associated with hypomagnesemia.^{380,381} Kir4.1 is thought to facilitate Mg²⁺ reabsorption in the DT by recycling K⁺ across the basolateral membrane, thus enabling the Na-K-ATPase to transport Na⁺. Fig. 7.12 shows the cellular localization of these proteins in the distal convoluted tubule into the cell.

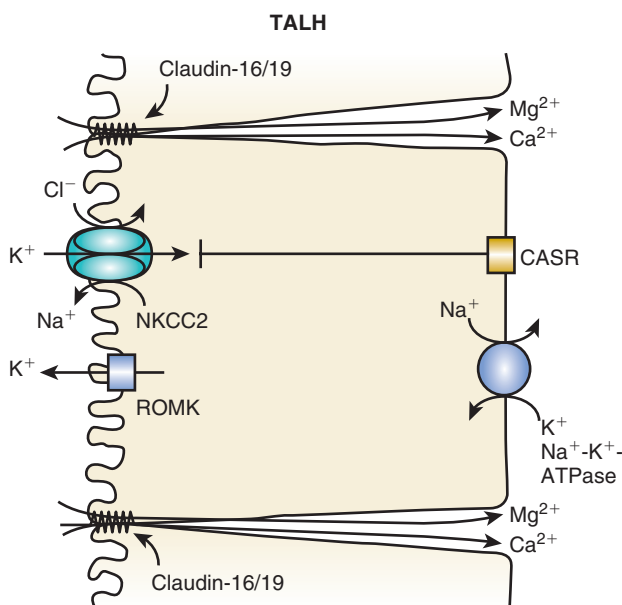


Fig. 7.11 Mechanism by which magnesium is transported in cells of the thick ascending limb of the loop of Henle (TALH). The majority of magnesium is reabsorbed by paracellular mechanisms. Claudin-16 and claudin-19 are depicted as directly transporting Ca²⁺ and Mg²⁺, but it has also been hypothesized that their primary role is to allow backleak of reabsorbed Na⁺ and thus establish an NaCl diffusion potential, thereby indirectly facilitating divalent cation reabsorption. CaSR, Calcium-sensing receptor; NKCC2, Na-K-Cl cotransporter; ROMK, renal outer medullary potassium channel.

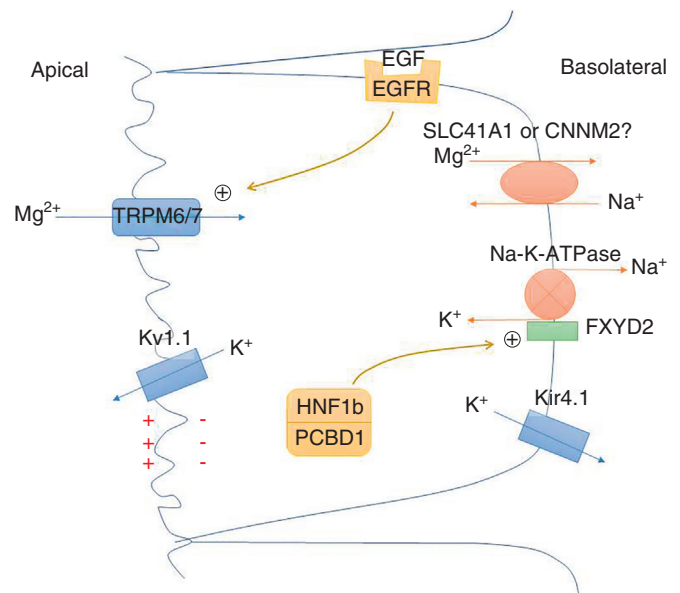


Fig. 7.12 Mechanism by which magnesium is transported in distal tubule cells. The majority of magnesium is reabsorbed by transcellular mechanisms. Mg²⁺ enters apically via the TRPM6/7 heteromeric channel, driven by the membrane voltage set by the K⁺ channel, Kv1.1. Its exit pathway is unknown but may be via CNNM2 or SLC41A1, perhaps acting as a basolateral Na-Mg exchanger. Active extrusion is likely driven by the Na⁺ gradient generated by the Na-K-ATPase alpha subunit and accessory subunit, FXYP2. The basolateral K⁺ channel Kir 4.1 recycles K⁺ that enters via the Na-K-ATPase. See text for role of other regulators. EGF, Epidermal growth factor; EGFR, epidermal growth factor receptor.

REGULATION OF MAGNESIUM TRANSPORT IN THE KIDNEY

A variety of factors alter magnesium reabsorption in the kidney (Table 7.3)*. With the exception of magnesium excess and depletion, it is unclear whether any of these are physiologically important regulators. Thus, although effects on magnesium excretion in the urine are noted following the infusion of various substances or following blockade of their activity, it is not clear that such changes occur with physiologic changes in concentrations of these factors in vivo. Furthermore, the concentrations of the effector substances do not change in the physiologically appropriate manner following changes in serum concentrations of magnesium. Thus, hormonal homeostasis, in which concentrations of a hormone (PTH, glucagon, arginine vasopressin, and so on) change following changes in the concentration of magnesium, and in turn, alter the retention or concentrations of magnesium, is difficult to demonstrate.

PHOSPHORUS TRANSPORT IN THE KIDNEY

THE ROLE OF PHOSPHORUS IN CELLULAR PROCESSES

Phosphorus is a key component of hydroxyapatite, the major component of bone mineral, nucleic acids, bioactive

Table 7.3 Factors Altering the Reabsorption of Magnesium in the Kidney

Substance	Effect
Peptide hormones	
Parathyroid hormone ^{205,383–387}	Increase
Calcitonin ^{387–395}	Increase
Glucagon ^{396,397}	Increase
Arginine vasopressin ³⁹⁸	Increase
Insulin ³⁹⁹	Increase
β-Adrenergic agonists	
Isoproterenol ³⁸²	Increase
Prostaglandins PGE₂ ⁴⁰⁰	
Decrease	
Mineralocorticoids	
Aldosterone	Increase
1, 25-dihydroxyvitamin D₃ ⁴⁰¹	
Decrease	
Magnesium	
Restriction ^{338–341,343}	Increase
Increase ^{348–350}	Decrease
Metabolic alkalosis ^{261,402,403}	
Decrease	
Metabolic acidosis ^{261,402,403}	
Decrease	
Hypercalcemia ⁴⁰⁴	
Decrease	
Phosphate depletion ^{405,406}	
Decrease	
Diuretics	
Furosemide	Decrease
Amiloride ^{408,409}	Increase
Chlorothiazide ^{407,410}	Increase

PGE₂, Prostaglandin E₂.

From Dai LJ, Ritchie G, Kerstan D, et al. Magnesium transport in the renal distal convoluted tubule. *Physiol Rev.* 2001;81:51–84.

signaling proteins, phosphorylated enzymes, and cellular membranes.^{411–414} Prolonged deficiency of phosphorus and inorganic phosphate results in serious biological problems, including impaired bone mineralization, resulting in osteomalacia or rickets, abnormal erythrocyte, leukocyte and platelet function, impaired cell membrane integrity that can result in rhabdomyolysis, and impaired cardiac function.^{415–417} Phosphate balance is maintained through a series of complex hormonally and locally regulated metabolic adjustments. In states of neutral phosphate balance, net intake equals net output. The major organs involved in the absorption, excretion, and reabsorption of phosphate are the intestine and the kidney (Fig. 7.13). A normal diet adequate in phosphorus normally contains ~1500 mg of phosphorus. Approximately 1100 mg of ingested dietary phosphate is absorbed in the proximal intestine predominantly in the jejunum. About 200 mg of phosphorus is secreted into the intestine via pancreatic and intestinal secretions, giving a net phosphorus absorption of approximately 900 mg/24 hr. Phosphorus that is not absorbed in the intestine or is secreted into the intestinal lumen eventually appears in the feces. Absorbed phosphorus enters the extracellular fluid pool and moves in and out of bone (and to a smaller extent in and out of soft tissues) as needed (~200 mg). Approximately 900 mg of phosphorus (equivalent to the amount absorbed in the intestine) is excreted in the urine.

PHOSPHORUS IS PRESENT IN BLOOD IN MULTIPLE FORMS

About 85% of phosphorus in the body is present in bones, 14% exists in cells from soft tissues, and 1% is present in extracellular fluids. In mammals, bone contains a substantial amount of phosphorus (approximately 10 g/100 g dry fat free tissue); in comparison, muscle contains 0.2 g/100 g fat free tissue, and the brain 0.33 g/100 g fresh tissue.⁴¹⁸ Phosphorus is present in virtually every bodily fluid. In human plasma

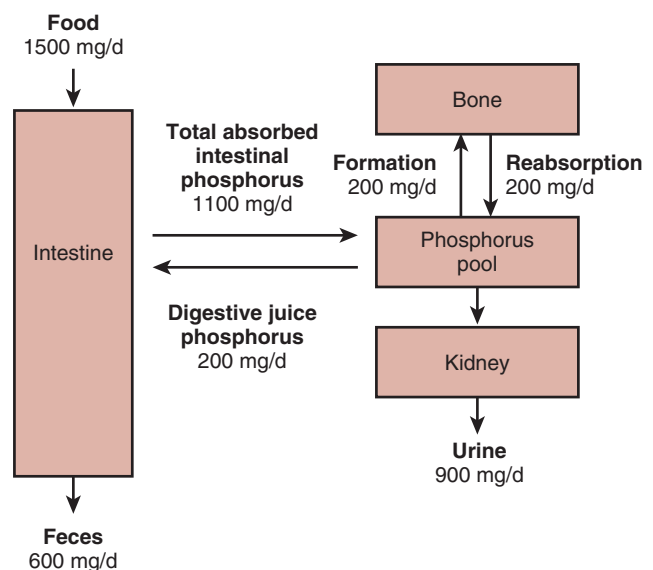


Fig. 7.13 Phosphorus homeostasis in humans. The major organs involved in the absorption, excretion, and reabsorption of phosphate are the intestine and the kidney.

*References 205, 261, 338–341, 343, 348–350, and 382–410.

Table 7.4 Distribution of and Concentrations of Phosphorus (mmol/L) in Adult Human Blood

Phosphorus Compounds	Erythrocytes	Plasma
Phosphate ester	12.3–19.0	0.86–1.45
Phospholipids	4.13–4.81	2.23–3.13
Inorganic phosphate	0.03–0.13	0.71–1.36

or serum, phosphorus exists in the form of inorganic phosphorus or phosphate (Pi), lipid phosphorus, and phosphoric ester phosphorus. Total serum phosphorus concentrations range between 8.9 and 14.9 mg/dL (2.87–4.81 mmol/L), inorganic phosphorus (phosphate, Pi) concentrations between 2.56 and 4.16 mg/dL (0.83–1.34 mmol/L) (this is what is usually measured clinically and referred to as the serum phosphorus, and the normal range changes with age),⁴¹⁹ phosphoric ester phosphorus concentrations between 2.5 and 4.5 mg/dL (0.81–1.45 mmol/L), and lipid phosphorus concentration between 6.9 and 9.7 mg/dL (2.23–3.13 mmol/L) (Table 7.4).⁴¹⁸

REGULATION OF PHOSPHATE HOMEOSTASIS—AN INTEGRATED VIEW

Intestinal feed-forward and hormonal feedback systems (PTH–vitamin D endocrine system and the phosphatonins) are likely to be responsible for the control of phosphorus homeostasis (Fig. 7.14). The short-term responses that occur within minutes to hours of feeding of a high-Pi meal are

important in regulating phosphorus homeostasis via feed-forward mechanisms, whereas the longer-term changes occur as a result of alterations in circulating concentrations of PTH, $1\alpha,25(\text{OH})_2\text{D}_3$, and the phosphatonins such as fibroblast growth factor 23.^{86,420–423} Intestinal signals have been shown in rodents to rapidly alter renal Pi excretion in response to changes in duodenal Pi concentrations.⁴²¹

PTH, $1\alpha,25(\text{OH})_2\text{D}_3$, and the phosphatonin FGF-23 control phosphorus homeostasis on longer-term basis (hours to days).^{85,86} Concentrations of these hormones and factors are regulated by phosphorus in a manner that is conducive to the maintenance of normal phosphorus concentrations. Fig. 7.15 shows the physiologic changes known to occur with low or high dietary intakes of phosphate. A decrease in serum phosphate concentrations, as would occur with a reduced intake of phosphorus, results in increased ionized calcium concentrations, decreased PTH secretion, and a subsequent decrease in renal phosphate excretion. At the same time, by PTH-independent mechanisms, there is an increase in renal 25-hydroxyvitamin D 1α -hydroxylase activity, increased $1\alpha,25(\text{OH})_2\text{D}_3$ synthesis, and increased phosphorus absorption in the intestine and reabsorption in the kidney.^{88,92,94,99–105} Conversely, with elevated phosphate intake, there are decreased calcium concentrations and increased PTH release from the parathyroid gland. PTH actually has two opposing effects: it increases urinary phosphate excretion but also increases the synthesis of $1\alpha,25(\text{OH})_2\text{D}_3$ by stimulating the activity of the renal 25-hydroxyvitamin D 1α -hydroxylase; the net effect is to increase renal phosphate excretion. Increased serum phosphate concentrations simultaneously inhibit renal 25-hydroxyvitamin D 1α -hydroxylase and decrease $1\alpha,25(\text{OH})_2\text{D}_3$ synthesis. Reduced $1\alpha,25(\text{OH})_2\text{D}_3$ concentrations decrease intestinal phosphorus absorption as well as renal

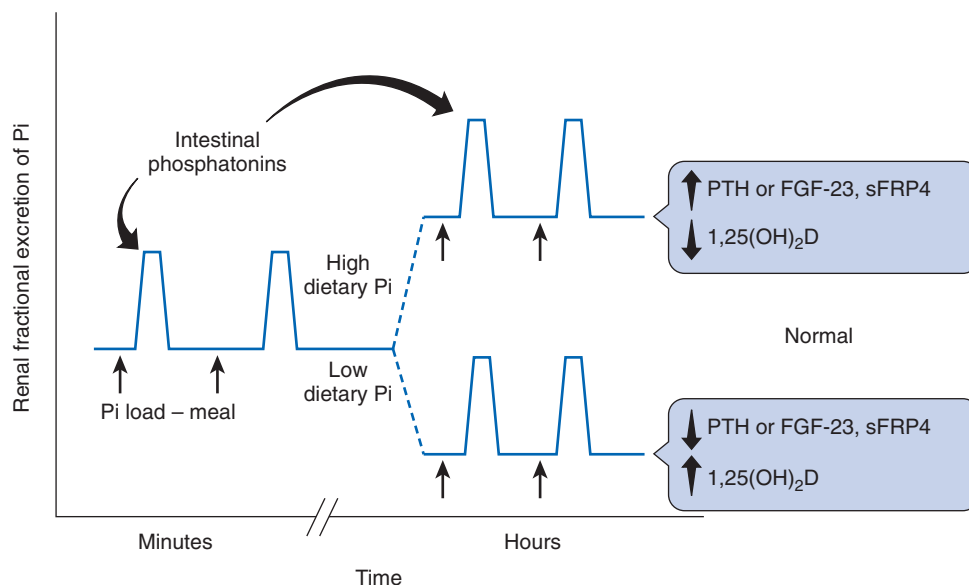


Fig. 7.14 Intestinal feed-forward and hormonal feedback systems are responsible for the control of phosphorus homeostasis. Changes in intestinal luminal phosphate concentrations (*Pi load – meal*) result in the elaboration of chemical signals (*Intestinal phosphatonins*) that alter the fractional excretion of phosphate in the kidney over a time frame of minutes. Long-term changes in the amount of phosphate in the diet result in changes in the concentrations of PTH, $1\alpha,25$ -dihydroxyvitamin D, and phosphatonins, which influence the fractional excretion of phosphate in the kidney over a time frame of hours, as shown. Short-term changes mediated by feed-forward intestinal signals are proposed to be superimposed on this chronic baseline. PTH, Parathyroid hormone.

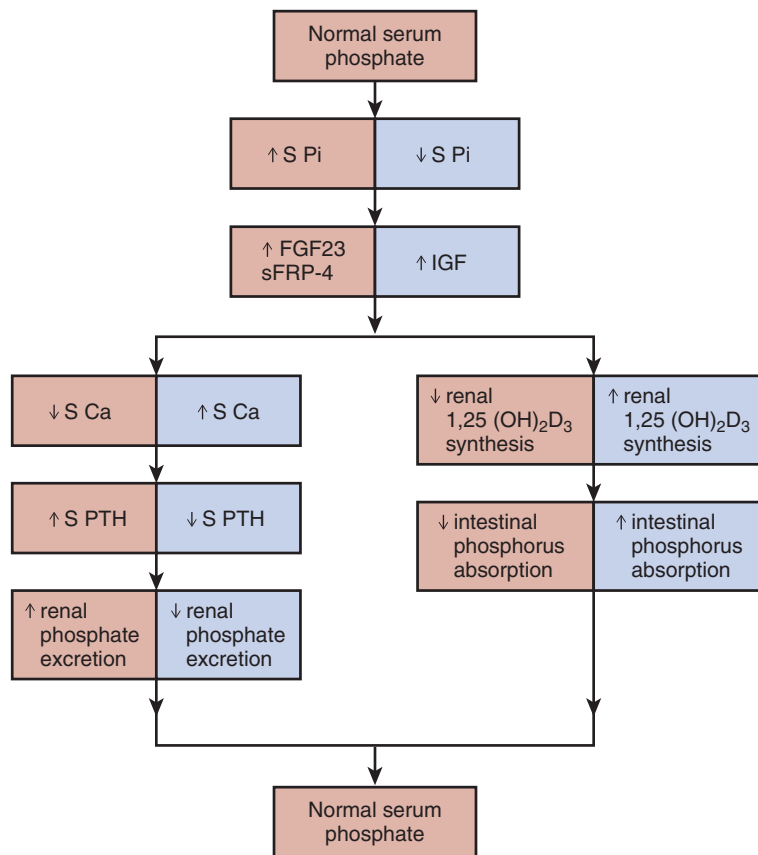


Fig. 7.15 Changes in growth factors (fibroblast growth factor 23 [FGF 23], sFRP-4 (secreted frizzled related protein 4) insulin-like growth factor (IGF), parathyroid hormone (PTH), and $1\alpha,25$ -dihydroxyvitamin D, and the subsequent physiologic changes in intestinal phosphate absorption or renal phosphate reabsorption following perturbations in serum phosphate.

phosphate reabsorption. All of these factors tend to bring serum phosphate concentrations back into the normal range.

The phosphatonins FGF-23 and sFRP-4 inhibit renal phosphate reabsorption.^{98,424–432} They also decrease,^{424,430,433–438} and IGF-1 increases⁹⁶ the activity of the 25-hydroxyvitamin D 1α -hydroxylase (“growth factors” in Fig. 7.15). FGF-23 induces renal phosphate wasting in patients with tumor-induced osteomalacia (TIO),^{427,439–441} autosomal dominant hypophosphatemic rickets (ADHR), X-linked hypophosphatemic rickets (XLH), and autosomal recessive hypophosphatemic rickets (ARHR).^{425,430,432,442} From a physiologic perspective, it would be appropriate for FGF-23 and sFRP-4 concentrations to be regulated by the intake of dietary phosphorus and by serum phosphate concentrations. In humans, in the short-term the feeding of meals containing increased amounts of phosphate does not increase serum FGF-23 concentrations despite the induction of a robust and dose-dependent phosphaturia.^{422,443} Other human studies conducted over a period of days or weeks, however, have shown changes in serum FGF-23 concentrations following alterations in the content of phosphate in the diet.^{444,445} In mice, Perwad et al. have shown that a high-phosphate diet increased and a low-phosphate diet decreased serum FGF-23 levels in these animals within 5 days of a changing dietary phosphate intake.⁴⁴⁶ The changes in serum FGF-23 correlated with changes in serum phosphate concentrations. Studies from our laboratory performed in rats fed a low-, normal, or high-phosphate diet demonstrate that serum FGF-23

levels significantly decrease in animals fed a low-phosphate diet, and increase in animals fed a high-phosphate diet within 24 hours of altering dietary phosphate intake but do not correlate with serum phosphate in the animals fed a high-phosphate diet.⁹⁸

REABSORPTION OF PHOSPHATE ALONG THE NEPHRON

Virtually all serum phosphate is filtered at the glomerulus.⁴⁴⁷ Under conditions of normal dietary phosphate intake, and in the presence of intact parathyroid glands, approximately 20% of the filtered phosphate load is excreted. The other 80% of the filtered load of phosphate is reabsorbed by the renal tubules. The PTs are the major sites of phosphate reabsorption along the nephron (Fig. 7.16).⁴⁴⁷ Little phosphate reabsorption occurs between the late PT and the early distal tubule in animals with intact parathyroid glands.^{448–456} In the absence of PTH, however, phosphate is avidly reabsorbed between the late PT and early distal tubule, reflecting phosphate reabsorption by the proximal straight tubule.⁴⁵¹ Phosphate transport rates are approximately three times higher in the proximal convoluted than in the proximal straight tubules.⁴⁵⁷ Renal phosphate handling is characterized by intranephronal heterogeneity, reflecting segmental differences in phosphate handling within an individual nephron as well as internephronal heterogeneity.^{448,452,457,458}

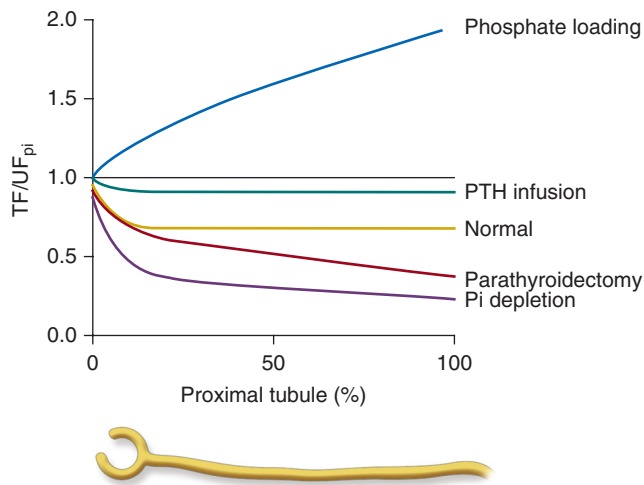


Fig. 7.16 The proximal tubule is the major site of phosphate reabsorption along the nephron. The effects of dietary phosphate loading or deprivation, parathyroid hormone (PTH) infusion, or parathyroidectomy on phosphate absorption along the proximal tubule are shown. *Proximal tubule %*, Distance along the proximal tubule as a percentage of total length; *PTH*, parathyroid hormone; *TF/UF_{pi}*, ratio of tubular fluid-to-ultrafiltrate phosphate concentration.

The uptake of phosphate is mediated by Na–phosphate cotransporters located at the apical border of PT cells (NaPi-IIa/Slc34A1 and NaPi IIc/Slc34a3).^{459–482} The structure and physiology of these phosphate transport molecules have been extensively reviewed, and the reader is directed to other publications in this regard.^{459–482} The Na–phosphate cotransporters are highly homologous and are predicted to have similar structures. Mice with ablation of the *NaPi-IIa/Slc34a1* gene exhibit renal phosphate wasting and reduced PT brush border membrane vesicle phosphate uptake (Fig. 7.17).⁴⁸³ In humans, *SLC34A1* mutations are associated with hypophosphatemia and urinary phosphate losses with urolithiasis or bone demineralization.⁴⁸⁴ It is estimated that the NaPi-IIa transporter is responsible for approximately 85% of proximal tubular phosphate transport and contributes to the adaptive increases in tubular phosphate transport in animals fed a low-phosphate diet.^{483,485} Mice with constitutive or renal-specific deletions of the *NaPi-IIc/Slc34a3* gene do not display abnormalities in phosphate excretion or phosphate serum concentrations.^{486,487} This is in contrast to humans, in whom *SLC34A3* mutations are associated with hypophosphatemic rickets with hypercalciuria.^{488,489} The extrusion of phosphate at the basolateral membrane of the proximal tubular cell may be mediated by the xenotropic and polytropic retroviral receptor (Xpr1).⁴⁹⁰ Mice with conditional deletions of *Xpr1* exhibited tubular dysfunction with glycosuria, amino-aciduria, hypercalciuria, and phosphaturia and developed hypophosphatemic rickets. In primary cultures of proximal tubular cells, Xpr1 deficiency significantly reduced phosphate uptake and decreased the expression of NaPi-IIa and NaPi-IIc cotransporters.

Interactions between the NaPi-IIa/Slc34A1 and the intracellular protein, the sodium-hydrogen exchanger regulatory factor-1 (NHERF-1), modulate the amount of NaPi-IIa/Slc34A1 and NaPi IIc/Slc34a3 present on the surface of the proximal tubular cell.^{491–510} By binding to the NaPi-IIa/Slc34A1 protein,

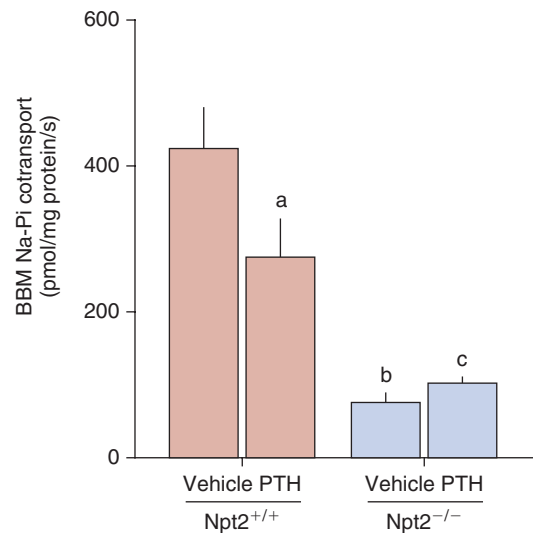


Fig. 7.17 Mice with ablation of the *NaPi-IIa* gene exhibit renal phosphate wasting and fail to respond to parathyroid hormone (PTH). The effect of PTH or vehicle on brush border membrane (BBM) Na-Pi cotransport in *Npt2^{+/+}* and *Npt2^{-/-}* mice is shown. ^aEffect of PTH in *Npt2^{+/+}* mice, $P < .0015$. ^bEffect of genotype in vehicle-treated mice, $P < .0001$; ^cEffect of genotype in PTH-treated mice, $P < .0041$. Reproduced from Zhao N, Tenenhouse HS. *Npt2* gene disruption confers resistance to the inhibitory action of parathyroid hormone on renal sodium-phosphate cotransport. *Endocrinology* 2000;141:2159–2165.

NHERF-1 functions to retain the NaPi-IIa/Slc34A1 protein on the surface of the proximal tubular cell; phosphate uptake diminishes as a consequence of endocytosis of the NaPi-IIa/Slc34A1 when it dissociates from NHERF-1, a process that is activated by the hormonal induction of protein kinase C and the phosphorylation of specific serine and threonine residues on the PDZ domain of NHERF-1.^{495,500,506,511–514} Ezrin, a protein that facilitates the association of NHERF-1 to the actin cytoskeleton, also plays a role in the regulation of proximal tubular phosphate transport and the expression of NaPi-IIa/Slc34A1 in proximal tubular cells.^{515,516} Ezrin knockdown mice exhibit hypophosphatemia and osteomalacia and a reduction in NaPi-IIa/Slc34A1 and NHERF-1 expression at the apical membrane of PTs. Cellular events associated with uptake of Pi into the cell and extrusion of Pi out of the cell are shown in Fig. 7.18.

REGULATION OF PHOSPHATE TRANSPORT IN THE KIDNEY

DIETARY PHOSPHATE

The influence of dietary phosphate intake on the urinary excretion of phosphate has been known for many years.^{448,517–532} The reabsorption of phosphate is decreased in animals fed a high-phosphate diet, whereas animals with a low intake of phosphate reabsorb almost 100% of the filtered load of phosphate.* These changes in phosphate reabsorption are associated with parallel changes in the abundance of NaPi-IIa and IIc.^{535,536} In infants and children, phosphate reabsorption is high so as to maintain a positive phosphate balance required for growth.^{537,538} Conversely, decreased phosphate reabsorption has been demonstrated in the elderly.⁵³⁹

*References 182, 219–228, 234, 240, 241, 354, 533, and 534.

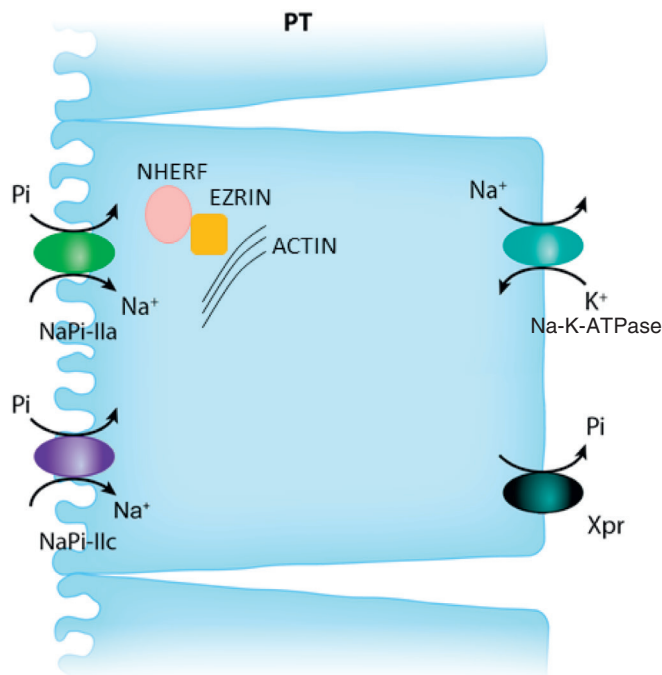


Fig. 7.18 Mechanisms by which phosphate is transported across the proximal tubular cell. Apical uptake is mediated by the sodium-phosphate cotransporters IIa and IIc. The Na-K ATPase located at the basolateral aspect of the cell provides a sodium gradient within the cell that permits these sodium-phosphate cotransporters to take up sodium and phosphate. By binding to the NaPi-IIa protein, NHERF-1 retains the NaPi-IIa protein on the surface of the proximal tubular cell thereby enhancing phosphate uptake; phosphate uptake diminishes as a consequence of endocytosis of the NaPi-IIa when it dissociates from NHERF-1, a process that is activated by the hormonal induction of protein kinase C and the phosphorylation of specific serine and threonine residues on the PDZ domain of NHERF-1. Ezrin, a protein that facilitates the association of NHERF-1 to the actin cytoskeleton also regulates proximal tubular phosphate transport. Ezrin knock down mice exhibit hypophosphatemia and osteomalacia and a reduction in NaPi-IIa/Slc34A1 and NHERF-1 expression at the apical membrane of proximal tubules. The xenotropic and polytropic retroviral receptor (Xpr1) plays a role in the extrusion of phosphate at the basolateral cell surface. *PT*, Proximal tubule.

Although dietary phosphate deprivation and excess results in marked changes in the plasma concentrations of several hormones (see Fig. 7.15) that contribute to the increase or decrease in renal phosphate reabsorption, acute changes in tubular reabsorption can also be demonstrated independent of changes in these hormones.^{421,540–543} When a bolus of phosphate is instilled into the duodenum of intact rats, renal phosphate excretion increases within 10 minutes without changes in serum Pi concentrations.⁴²¹ The change in Pi reabsorption in response to a high-Pi meal is independent of plasma Pi concentrations and filtered Pi load. Such changes are not elicited upon the administration of NaCl into the duodenum. The increase in renal phosphate excretion is independent of PTH as thyro-parathyroidectomy does not alter the process. Serum concentrations of PTH do not change, and serum concentrations of other phosphaturic peptides, such as FGF-23 and sFRP-4, are unchanged following the infusion of intraduodenal phosphate. Aqueous duodenal

extracts contain a phosphaturic substance that is likely to be a protein. The processes or pathways by which changes in luminal phosphate concentrations within the bowel are detected have not been defined, although the presence of a “phosphate sensor” has been postulated.⁵⁴⁴ A recent study, though, suggests that such an intestinal phosphate-sensing mechanism may be absent in humans.⁵⁴⁵

Studies using cultured renal proximal tubular cells provide evidence of an intrinsic ability of these cultured cells to increase phosphate transport when exposed to a low phosphate concentration in the medium.^{540–543} The mechanism of upregulation of Na/Pi cotransport in OK cells by low-Pi media involves two regulatory mechanisms: an immediate (early) increase (after 2 hours) in the expression of Na/Pi cotransporter, independent of mRNA synthesis or stability, and a delayed (late) effect (after 4–6 hours), resulting in an increase in NaPi-4 mRNA abundance.^{542,546} The enhanced Pi reabsorption of short-term Pi deprivation has been linked to decreased intrarenal synthesis of dopamine and/or stimulation of beta adrenoreceptors, because infusion of dopamine or propranolol restores the phosphaturic response to PTH in short-term (less than 3 days) Pi deprivation.^{547–549} Conversely, dopamine may also mediate the acute phosphaturic effect of a high-Pi diet.⁴⁹⁹ The NaPi-IIa transporter is expressed in the brain and is regulated by dietary Pi, suggesting that dietary Pi could regulate neural outputs and regulate renal Pi excretion.⁵⁵⁰ Increasing cerebrospinal fluid Pi concentrations in the presence of low plasma Pi concentrations reversed the adaptations to feeding a low-Pi diet, suggesting that the Pi concentration in the brain regulates not only central but also renal expression of NaPi-IIa transporters. It should be remembered that alterations in serum Pi concentrations also alter $1\alpha,25(\text{OH})_2\text{D}_3$ synthesis and serum concentrations.^{88,92,94,99–105} Infusions of $1\alpha,25(\text{OH})_2\text{D}_3$ increase the renal reabsorption Pi, predominantly in the proximal nephron.^{68,551–557}

PARATHYROID HORMONE

Parathyroidectomy decreases renal Pi excretion and, conversely, injection of PTH increases urinary Pi excretion^{558–562} by altering Pi reabsorption along the PT (see Fig. 7.16).^{450–454,563} The proximal straight tubule is an important site of PTH action with respect to Pi transport and may be critical in the final regulation of Pi excretion.^{449,455,458,564} PTH maintains Pi homeostasis by regulating NaPi cotransporters in the kidney. This is mediated by PTH/PTHrP receptors on the apical membrane that signal through protein kinase C (PKC), and on the basolateral membrane that signal through both cAMP/PKA and PKC. This leads to endocytosis of NaPi-IIa and -IIc cotransporters, which are degraded within the lysosomes.^{469,474,565,566} The transporters are reduced in number along the apical borders of proximal tubular cells following the administration of PTH 1-34 but not by the administration of PTH 3-34.^{479,480} Disruption of the *NaPi-IIa (Slc34a1)* gene in mice resulted in increased Pi excretion compared with wild-type mice and a resistance to the phosphaturic effect of PTH (see Fig. 7.17), although the cyclic adenosine monophosphate (cAMP) response is normal.⁵⁶⁷ It has been proposed that the primary mechanism for PTH action is PKC-mediated phosphorylation of a PDZ domain on NHERF-1. This leads to dissociation of NaPi-IIa/NHERF-1 complexes, freeing NaPi-IIa from the apical surface for internalization.^{500,506}

Under certain conditions, the phosphaturic effect of PTH is blunted or absent. These include short-term Pi deprivation or acute respiratory alkalosis. In these situations, the inhibitory effect of PTH on Pi reabsorption by the proximal convoluted tubule remains intact. However, the increased delivery of Pi leads to enhanced downstream reabsorption by the proximal straight tubule.^{455,458,564} These studies suggest that the regulation of Pi reabsorption by PTH in the proximal convoluted and proximal straight tubules may be mediated by different mechanisms. It should be noted that PTH has two opposing effects: PTH increases urinary Pi excretion but also increases the synthesis of $1\alpha,25(\text{OH})_2\text{D}_3$ by stimulating the activity of the $25(\text{OH})\text{D}_3$ 1α -hydroxylase enzyme in the kidney.^{88,92,94,99–105}

VITAMIN D AND VITAMIN D METABOLITES

Dietary Pi deprivation or hypophosphatemia induces 25-hydroxyvitamin D_3 1α -hydroxylase.^{88,92,94,99–105} Mice or rats, but not pigs, fed a low-Pi diet show a decrease in the activity of the 25-hydroxyvitamin D_3 24-hydroxylase (a renal enzyme involved in the catabolism of $1,25(\text{OH})_2\text{D}_3$) compared with rats fed a normal Pi diet within 24 hours of Pi restriction.^{83,568,569} $1,25(\text{OH})_2\text{D}_3$ decreases renal Pi excretion,^{62,68,551–554} but the mechanism remains unknown. VDR-mutant mice exhibit decreased serum Pi; however, Pi transport or by renal cortical brush border membranes, Pi excretion, or NaPi-IIa or NaPi IIc mRNA levels were not different between VDR-null or wild-type mice, whereas NaPi-IIa protein expression and NaPi-IIa cotransporter immunoreactive signals were slightly but significantly decreased in the VDR mice compared with the wild-type mice.⁵³⁶ When VDR knockout mice were fed a low-Pi diet, serum Pi concentrations were more markedly decreased in the VDR knockout mice than in the wild-type mice. Other studies performed in VDR and $25(\text{OH})\text{D}$ 1α -hydroxylase-null mutant mice show that both these knockout mice adapt to Pi deprivation with increased NaPi-IIa protein in a manner similar to that found in wild-type mice.⁵⁷⁰ However, when these mice were fed a high-Pi diet, Pi excretion was less in the VDR and 25-hydroxyvitamin D 1α -hydroxylase-null mutant mice compared with the wild-type mice. In vitamin D-deprived rats, NaPi-IIa transporter protein and mRNA were reported to be decreased in juxtamedullary but not superficial renal cortical tubules compared with normal rats.⁵⁷¹

INSULIN, GROWTH HORMONE, AND INSULIN-LIKE GROWTH FACTOR

Insulin decreases plasma Pi and Pi excretion in human and animal models.^{572–575} This enhanced renal Pi reabsorption can be demonstrated in the absence of changes in blood glucose, PTH, and Pi levels or urinary Na excretion. Micropuncture studies⁵⁷³ demonstrate enhanced Pi reabsorption in hyperinsulinemic dogs and somatostatin infusion, which decreases plasma insulin levels and increases Pi excretion.⁵⁷⁶ Growth hormone decreases Pi excretion and has been postulated to contribute to increased Pi reabsorption and positive Pi balance demonstrated in growing animals.^{577,578} Administration of a growth hormone antagonist for 4 days to immature rats is associated with increased Pi excretion and a decreased transport capacity for Pi reabsorption.^{579,580} In juvenile rats suppression of growth hormone is associated with an increase in Pi excretion as

a result of decreased NaPi-IIa expression.⁵⁸¹ Growth hormone administration increases Pi uptake by brush border membrane vesicles.⁵⁸² Because growth hormone increases renal insulin-like growth factor-1 (IGF-1 synthesis),⁵⁸³ the effects of growth hormone on Pi reabsorption may also be due to IGF-1.^{577,583–588}

RENAL NERVES, CATECHOLAMINES, DOPAMINE, AND SEROTONIN

Numerous studies have demonstrated that acute renal denervation or the administration of catecholamines alters Pi reabsorption regardless of PTH.^{547,589–601} The increase in urinary Pi excretion after acute renal denervation could be due to both increased production of dopamine and decreased α - or β -adrenoreceptor activity, because acute renal denervation has been shown to initially increase renal dopamine excretion and almost completely abolish renal norepinephrine and epinephrine levels.^{602,603} Epinephrine decreases plasma Pi, presumably by shifting Pi from the extracellular into the intracellular space. The hypophosphatemic response to isoproterenol infusion is blocked by propranolol, suggesting involvement of the beta adrenoreceptors. Infusion of isoproterenol markedly enhances renal Pi reabsorption in normal rats and in hypophosphatemic mice.^{600,604} The enhanced Pi reabsorption and attenuated phosphaturic response to PTH observed in acute respiratory alkalosis and Pi deprivation is blocked by infusion of propranolol, suggesting a possible role for stimulation of β -adrenoreceptors in these conditions. Stimulation of α -adrenoreceptors by the addition of epinephrine to OK cells blunts the PTH-induced increase in cAMP levels and the inhibition of Pi transport.⁶⁰⁵ Stimulation of α_2 -adrenoreceptors in vivo has also been demonstrated to attenuate the phosphaturic response to PTH.⁵⁴⁸ Dopamine infusion and the infusion of L-dopa or gludopa, or dopamine precursors, increase Pi excretion in the absence of PTH.^{606–608} Dopamine administration decreases Pi transport in OK cells and rabbit proximal straight tubules.^{599,609–614} Increasing dietary Pi intake increases urinary dopamine excretion and Pi excretion.⁶¹⁵ Inhibition of endogenous dopamine synthesis by the administration of carbidopa to rats results in decreased dopamine and Pi excretion, suggesting a role for endogenous dopamine in Pi regulation.^{595,603} A paracrine role for dopamine in Pi regulation is strengthened by studies in OK cells showing that the addition of dopamine or L-dopa selectively decreases Pi uptake. Furthermore, Pi-replete OK cells produce more dopamine from L-dopa than Pi-deprived cells.⁶¹¹ Dopamine inhibits Pi transport by multiple mechanisms, including activation of DA1 and DA2 receptors.^{610,613,614} Dopamine induces the internalization of NaPi-IIa cotransporter molecules by activation of luminal DA1 receptors.⁶⁰⁹ Renal PTs also synthesize serotonin from 5-hydroxytryptophan using the same enzyme that converts L-dopa to dopamine. Incubation of OK cells with either serotonin or 5-hydroxytryptophan enhances Pi transport and raises the possibility that serotonin may also be involved in the physiologic regulation of renal Pi transport.^{606,612,616,617}

PHOSPHATOMINS (FGF-23, sFRP-4)

The term “phosphatonin” was introduced to describe a factor or factors responsible for the inhibition of renal phosphate reabsorption and altered $25(\text{OH})\text{D}$ 1α -hydroxylase regulation

observed in patients with tumor-induced osteomalacia.⁴⁴⁰ Cai et al.⁴³⁹ described a patient with TIO in whom the biochemical characteristics of hypophosphatemia, renal phosphate wasting, and reduced serum $1\alpha,25(\text{OH})_2\text{D}$ disappeared following removal of the tumor. Several factors have been identified that are associated with phosphate wasting, including FGF-23 sFRP-4, fibroblast growth factor 7 (FGF-7), and matrix extracellular phosphoglycoprotein (MEPE).

The most extensively studied phosphatonin is FGF-23, a 251-amino acid–secreted protein.^{419,425,431,618} Recombinant FGF-23 administered intraperitoneally to mice or rats induces phosphaturia and inhibits 25-hydroxyvitamin D 1α -hydroxylase activity.^{419,425,431,618} The minimal sequence needed for phosphaturic activity resides between amino acids 176 and 210.⁴³¹ Transgenic animals overexpressing FGF-23 are hypophosphatemic, phosphaturic, and show the presence of rickets and reduced serum $1\alpha,25(\text{OH})_2\text{D}$ concentrations or 25-hydroxyvitamin D 1α -hydroxylase activity.^{433,434,619} Conversely, mice in which the *FGF-23* gene has been ablated demonstrate hyperphosphatemia, reduced phosphate excretion, markedly elevated serum $1\alpha,25(\text{OH})_2\text{D}$ concentrations and renal 25-hydroxyvitamin D 1α -hydroxylase mRNA expression, vascular calcification, and early mortality.^{434,620} The ablation of the VDR in FGF-23–null mice has been reported to rescue this phenotype, supporting an important role for vitamin D in the pathogenesis of the abnormal phenotype seen in FGF-23–null mice.⁶²¹

FGF-23 binds and signals through FGF receptors 1c, 3c, and FGFR4²⁶⁹; the role of *Fgfr3* and *Fgfr4* has not been established in mice in vivo.⁶²² Han et al. recently demonstrated that mice with deletion of *Fgfr1* in the PT had an increase in sodium-dependent phosphate cotransporter expression, hyperphosphatemia and refractoriness to the phosphaturic action of FGF-23, suggesting that FGFR1c plays a key role in its effects in the PT.⁶²³ Deletion of the *Fgfr1* in the distal tubule resulted in hypercalciuria and secondary hyperparathyroidism. A coreceptor, *klotho*, is necessary for FGF-23 to exhibit bioactivity.^{269,624} The role of *klotho* in FGF-23 signaling is supported by the observation that *klotho* knockout mice have a phenotype identical to that of FGF-23 knockout mice,⁶²⁵ whereas a human mutation that increases *klotho* levels phenocopies TIO and X-linked hypophosphatemic rickets.⁶²⁶

The mechanism for FGF-23 action is thought to involve downstream signaling through ERK1/2 and serum and glucocorticoid kinase-1 (SGK1).⁶²⁷ SGK1 in turn phosphorylates NHERF1, leading to the dissociation of NaPi-IIa transporters that become internalized and degraded, analogous to its regulation by PTH.⁶²⁸ This model is supported by the observation that FGF-23 is no longer phosphaturic when given to NHERF1–null mice.⁶²⁹ Recent evidence suggests that Jak3 may also be involved because Jak3–null mice have renal phosphate wasting and elevated FGF-23 levels.⁶³⁰

FGF-23 synthesis is regulated by $1\alpha,25(\text{OH})_2\text{D}$. Increasing doses of $1\alpha,25(\text{OH})_2\text{D}$ increase FGF-23 concentrations in the serum within 24 hours, but statistically significant changes are observed 4 hours after $1\alpha,25(\text{OH})_2\text{D}$ treatment.^{631,632} In the physiologic sense, it is possible that FGF-23 is a negative feedback regulator of the 25-hydroxyvitamin D 1α -hydroxylase enzyme.

The Wnt antagonist, sFRP-4, is highly expressed in tumors associated with renal phosphate wasting and osteomalacia.⁴²⁹

Recombinant sFRP-4 is phosphaturic in rats and prevents the upregulation of the 25-hydroxyvitamin D 1α -hydroxylase enzyme seen in the presence of hypophosphatemia.⁴²⁴ sFRP-4 decreases Na⁺-Pi cotransporter abundance in the brush border membrane of the PT, and reduces the surface expression of the Na⁺-Pi-IIa cotransporter in PTs of the kidney, as well as on the surface of OK cells.⁴³⁸ sFRP-4 expression is increased in bone samples and serum from X-linked hypophosphatemic mice in mice with a global knockout of the *phex* gene but not in mice in which the *phex* gene has been knocked out in bone alone.⁶³³ sFRP-4 protein concentrations are increased in the kidneys of rats fed a high-phosphate diet for 2 weeks but not in animals fed a low-phosphate diet, suggesting a possible role for sFRP-4 during increases in phosphate intake.⁶³⁴ This suggests in turn that sFRP-4 concentrations are altered in the kidney of animals fed a high-phosphate diet and could play a role in the long-term adaptations to high-phosphate intake.

MEPE is abundantly overexpressed in tumors associated with renal phosphate wasting and osteomalacia.⁶³⁵ Recombinant MEPE is phosphaturic and reduces serum phosphate concentrations when administered to mice in vivo.⁶³⁶ The protein has been shown to inhibit phosphate reabsorption in the proximal convoluted tubule,⁶³⁷ to inhibit Na-dependent phosphate uptake in opossum kidney cells, and to reduce PT expression of NaPi-IIa protein.⁶³⁸ The protein has also been demonstrated to reduce intestinal Pi absorption directly.⁶³⁸ MEPE also inhibits bone mineralization in vitro, and MEPE–null mice have increased bone mineralization.⁶³⁹ Thus, it is possible that MEPE is important in the pathogenesis of hypophosphatemia in renal phosphate wasting observed in patients with TIO. However, MEPE infusion does not recapitulate the defect in vitamin D metabolism seen in patients with TIO.⁶³⁶ Infusion of MEPE reduces serum phosphate concentrations, and serum $1\alpha,25(\text{OH})_2\text{D}$ concentrations increase following MEPE as would be expected in the face of hypophosphatemia. Thus, in patients with TIO, it is likely that MEPE contributes to the hypophosphatemia, but other products such as FGF-23 and sFRP-4 inhibit $1\alpha,25(\text{OH})_2\text{D}$ concentrations by inhibiting the activity of the 25-hydroxyvitamin D 1α -hydroxylase. MEPE may play a role in the pathogenesis of X-linked hypophosphatemic rickets, in which there is phosphate wasting, and evidence for a mineralization defect that is independent of low phosphate concentrations in the extracellular fluid.⁶³³ MEPE expression is increased in mice with the *Hyp* mutation, and mice with a global knockout of the *phex* gene but not in mice with a bone specific knockout of the *phex* gene. It is not known whether MEPE is regulated by phosphate concentrations although Jain et al. have demonstrated that it is correlated with serum Pi concentration in normal humans.⁶⁴⁰ Another growth factor, FGF-7, also known as keratinocyte growth factor, is overexpressed in tumors associated with phosphate wasting and osteomalacia.⁴⁸⁸ FGF-7 inhibits Na-dependent phosphate transport in OK cells, and we have demonstrated that FGF-7 inhibits renal phosphate reabsorption in vivo. FGF-7 is present in normal plasma and is significantly increased in patients with renal failure (personal observations). Whether or not FGF-7 is regulated by phosphate concentrations is unknown.

KEY REFERENCES

2. Brini M, Carafoli E. Calcium pumps in health and disease. *Physiol Rev.* 2009;89:1341–1378.
10. Marx SJ, Attie MF, Stock JL, et al. Maximal urine-concentrating ability: familial hypocalciuric hypercalcemia versus typical primary hyperparathyroidism. *J Clin Endocrinol Metab.* 1981;52:736–740.
14. Moore EW. Ionized calcium in normal serum, ultrafiltrates, and whole blood determined by ion-exchange electrodes. *J Clin Invest.* 1970;49:318–334.
15. DeLuca HF, Schnoes HK. Metabolism and mechanism of action of vitamin D. *Annu Rev Biochem.* 1976;45:631–666.
17. Wasserman RH, Smith CA, Brindak ME, et al. Vitamin D and mineral deficiencies increase the plasma membrane calcium pump of chicken intestine. *Gastroenterology.* 1992;102:886–894.
55. Ryan ZC, Ketha H, McNulty MS, et al. Sclerostin alters serum vitamin D metabolite and fibroblast growth factor 23 concentrations and the urinary excretion of calcium. *Proc Natl Acad Sci U S A.* 2013;110:6199–6204.
60. Brown EM, Pollak M, Hebert SC. The extracellular calcium-sensing receptor: its role in health and disease. *Annu Rev Med.* 1998;49:15–29.
145. Dimke H, Hoenderop JG, Bindels RJ. Molecular basis of epithelial Ca²⁺ and Mg²⁺ transport: insights from the TRP channel family. *J Physiol.* 2011;589:1535–1542.
159. Borke JL, Minami J, Verma A, et al. Monoclonal antibodies to human erythrocyte membrane Ca⁺⁺Mg⁺⁺ adenosine triphosphatase pump recognize an epitope in the basolateral membrane of human kidney distal tubule cells. *J Clin Invest.* 1987;80:1225–1231.
165. Lassiter WE, Gottschalk CW, Mylle M. Micropuncture study of renal tubular reabsorption of calcium in normal rodents. *Am J Physiol.* 1963;204:771–775.
168. Agus ZS, Gardner LB, Beck LH, et al. Effects of parathyroid hormone on renal tubular reabsorption of calcium, sodium, and phosphate. *Am J Physiol.* 1973;224:1143–1148.
175. Yu AS, Cheng MH, Coalson RD. Calcium inhibits paracellular sodium conductance through claudin-2 by competitive binding. *J Biol Chem.* 2010;285:37060–37069.
192. Gamba G, Miyanoshita A, Lombardi M, et al. Molecular cloning, primary structure, and characterization of two members of the mammalian electroneutral sodium-(potassium)-chloride cotransporter family expressed in kidney. *J Biol Chem.* 1994;269:17713–17722.
199. Konrad M, Schaller A, Seelow D, et al. Mutations in the tight-junction gene claudin 19 (CLDN19) are associated with renal magnesium wasting, renal failure, and severe ocular involvement. *Am J Hum Genet.* 2006;79:949–957.
203. Hebert SC. Bartter syndrome. *Curr Opin Nephrol Hypertens.* 2003;12:527–532.
206. Costanzo LS, Windhager EE. Calcium and sodium transport by the distal convoluted tubule of the rat. *Am J Physiol.* 1978;235:F492–F506.
208. Dimke H, Hoenderop JG, Bindels RJ. Hereditary tubular transport disorders: implications for renal handling of Ca²⁺ and Mg²⁺. *Clin Sci.* 2010;118:1–18.
210. Hoenderop JG, Nilius B, Bindels RJ. Calcium absorption across epithelia. *Physiol Rev.* 2005;85:373–422.
211. Hoenderop JG, van Leeuwen JP, van der Eerden BC, et al. Renal Ca²⁺ wasting, hyperabsorption, and reduced bone thickness in mice lacking TRPV5. *J Clin Invest.* 2003;112:1906–1914.
216. Magyar CE, White KE, Rojas R, et al. Plasma membrane Ca²⁺-ATPase and NCX1 Na⁺/Ca²⁺ exchanger expression in distal convoluted tubule cells. *Am J Physiol Renal Physiol.* 2002;283:F29–F40.
219. Yu AS, Hebert SC, Lee SL, et al. Identification and localization of renal Na⁽⁺⁾-Ca²⁺ exchanger by polymerase chain reaction. *Am J Physiol.* 1992;263:F680–F685.
246. Gamba G, Saltzberg SN, Lombardi M, et al. Primary structure and functional expression of a cDNA encoding the thiazide-sensitive, electroneutral sodium-chloride cotransporter. *Proc Natl Acad Sci U S A.* 1993;90:2749–2753.
270. Chang Q, Hoefs S, van der Kemp AW, et al. The beta-glucuronidase klotho hydrolyzes and activates the TRPV5 channel. *Science.* 2005;310:490–493.
298. Wiegmann T, Kaye M. Hypomagnesemic hypocalcemia. Early serum calcium and late parathyroid hormone increase with magnesium therapy. *Arch Intern Med.* 1977;137:953–955.
300. Sherwood LM, Herrman I, Bassett CA. Parathyroid hormone secretion in vitro: regulation by calcium and magnesium ions. *Nature.* 1970;225:1056–1058.
301. Chase LR, Slatopolsky E. Secretion and metabolic efficacy of parathyroid hormone in patients with severe hypomagnesemia. *J Clin Endocrinol Metab.* 1974;38:363–371.
308. Whang R, Chrysant S, Dillard B, et al. Hypomagnesemia and hypokalemia in 1,000 treated ambulatory hypertensive patients. *J Am Coll Nutr.* 1982;1:317–322.
326. Voets T, Nilius B, Hoefs S, et al. TRPM6 forms the Mg²⁺ influx channel involved in intestinal and renal Mg²⁺ absorption. *J Biol Chem.* 2004;279:19–25.
359. Simon DB, Lu Y, Choate KA, et al. Paracellin-1, a renal tight junction protein required for paracellular Mg²⁺ resorption. *Science.* 1999;285:103–106.
378. Ferre S, de Baaij JH, Ferreira P, et al. Mutations in PCBD1 cause hypomagnesemia and renal magnesium wasting. *J Am Soc Nephrol.* 2014;25:574–586.
416. Knochel JP. The pathophysiology and clinical characteristics of severe hypophosphatemia. *Arch Intern Med.* 1977;137:203–220.
419. Berndt T, Kumar R. Phosphatonins and the regulation of phosphate homeostasis. *Annu Rev Physiol.* 2007;69:341–359.
421. Berndt T, Thomas LF, Craig TA, et al. Evidence for a signaling axis by which intestinal phosphate rapidly modulates renal phosphate reabsorption. *Proc Natl Acad Sci U S A.* 2007;104:11085–11090.
427. Bowe AE, Finnegan R, Jan de Beur SM, et al. FGF-23 inhibits renal tubular phosphate transport and is a PHEX substrate. *Biochem Biophys Res Commun.* 2001;284:977–981.
428. De Beur SM, Finnegan RB, Vassiliadis J, et al. Tumors associated with oncogenic osteomalacia express genes important in bone and mineral metabolism. *J Bone Miner Res.* 2002;17:1102–1110.
430. Schiavi SC, Kumar R. The phosphatonin pathway: new insights in phosphate homeostasis. *Kidney Int.* 2004;65:1–14.
431. Berndt TJ, Craig TA, McCormick DJ, et al. Biological activity of FGF-23 fragments. *Pflugers Arch.* 2007;454:615–623.
439. Cai Q, Hodgson SF, Kao PC, et al. Brief report: inhibition of renal phosphate transport by a tumor product in a patient with oncogenic osteomalacia. *N Engl J Med.* 1994;330:1645–1649.
441. Shimada T, Mizutani S, Muto T, et al. Cloning and characterization of FGF23 as a causative factor of tumor-induced osteomalacia. *Proc Natl Acad Sci U S A.* 2001;98:6500–6505.
451. Greger R, Lang F, Marchand G, et al. Site of renal phosphate reabsorption. Micropuncture and microinfusion study. *Pflugers Arch.* 1977;369:111–118.
452. Haramati A, Haas JA, Knox FG. Nephron heterogeneity of phosphate reabsorption: effect of parathyroid hormone. *Am J Physiol.* 1984;246:F155–F158.
474. Murer H, Hernando N, Forster I, et al. Proximal tubular phosphate reabsorption: molecular mechanisms. *Physiol Rev.* 2000;80:1373–1409.
482. Werner A, Moore ML, Mantei N, et al. Cloning and expression of cDNA for a Na/Pi cotransport system of kidney cortex. *Proc Natl Acad Sci U S A.* 1991;88:9608–9612.
483. Beck L, Karaplis AC, Amizuka N, et al. Targeted inactivation of Npt2 in mice leads to severe renal phosphate wasting, hypercalciuria, and skeletal abnormalities. *Proc Natl Acad Sci U S A.* 1998;95:5372–5377.
618. ADHR Consortium. Autosomal dominant hypophosphataemic rickets is associated with mutations in FGF23. *Nat Genet.* 2000;26:345–348.
633. Yuan B, Takaiwa M, Clemens TL, et al. Aberrant PheX function in osteoblasts and osteocytes alone underlies murine X-linked hypophosphatemia. *J Clin Invest.* 2008.
635. Rowe PS, de Zoysa PA, Dong R, et al. MEPE, a new gene expressed in bone marrow and tumors causing osteomalacia. *Genomics.* 2000;67:54–68.

REFERENCES

- Clapham DE. Calcium signaling. *Cell*. 2007;131:1047–1058.
- Brini M, Carafoli E. Calcium pumps in health and disease. *Physiol Rev*. 2009;89:1341–1378.
- Carafoli E. Intracellular calcium homeostasis. *Annu Rev Biochem*. 1987;56:395–433.
- Hess AF. *Rickets Including Osteomalacia and Tetany*. Philadelphia: Lea and Febiger; 1929.
- Audran M, Gross M, Kumar R. The physiology of the vitamin D endocrine system. *Semin Nephrol*. 1986;6:4–20.
- Audran M, Kumar R. The physiology and pathophysiology of vitamin D. *Mayo Clin Proc*. 1985;60:851–866.
- Tebben PJ, Singh RJ, Kumar R. Vitamin D-mediated hypercalcemia: mechanisms, diagnosis, and treatment. *Endocr Rev*. 2016;37:521–547.
- Beck N, Singh H, Reed SW, et al. Pathogenic role of cyclic AMP in the impairment of urinary concentrating ability in acute hypercalcemia. *J Clin Invest*. 1974;54:1049–1055.
- Berl T, Erickson AE. Calcium-prostaglandin interaction on the action of antidiuretic hormone in the dog. *Am J Physiol*. 1982;242:F313–F320.
- Marx SJ, Attie MF, Stock JL, et al. Maximal urine-concentrating ability: familial hypocalciuric hypercalcemia versus typical primary hyperparathyroidism. *J Clin Endocrinol Metab*. 1981;52:736–740.
- Hebert SC, Brown EM, Harris HW. Role of the Ca(2+)-sensing receptor in divalent mineral ion homeostasis. *J Exp Biol*. 1997;200(Pt 2):295–302.
- Pak CY, Oata M, Lawrence EC, et al. The hypercalciurias. Causes, parathyroid functions, and diagnostic criteria. *J Clin Invest*. 1974;54:387–400.
- Sakhaee K, Maalouf NM, Sinnott B. Clinical review. Kidney stones 2012: pathogenesis, diagnosis, and management. *J Clin Endocrinol Metab*. 2012;97:1847–1860.
- Moore EW. Ionized calcium in normal serum, ultrafiltrates, and whole blood determined by ion-exchange electrodes. *J Clin Invest*. 1970;49:318–334.
- DeLuca HF, Schnoes HK. Metabolism and mechanism of action of vitamin D. *Annu Rev Biochem*. 1976;45:631–666.
- DeLuca HF, Schnoes HK. Vitamin D: recent advances. *Annu Rev Biochem*. 1983;52:411–439.
- Wasserman RH, Smith CA, Brindak ME, et al. Vitamin D and mineral deficiencies increase the plasma membrane calcium pump of chicken intestine. *Gastroenterology*. 1992;102:886–894.
- DeLuca HF. *Historical Overview of Vitamin D*. In: Feldman D, Pike JW, Adams JS, eds. *Vitamin D*. 3rd ed. Boston: Elsevier; 2011:3–12.
- DeLuca HF. Evolution of our understanding of vitamin D. *Nutr Rev*. 2008;66:S73–S87.
- Haussler MR, Whitfield GK, Kaneko I, et al. Molecular mechanisms of vitamin D action. *Calcif Tissue Int*. 2013;92:77–98.
- Mizwicki MT, Norman AW. The vitamin D sterol-vitamin D receptor ensemble model offers unique insights into both genomic and rapid-response signaling. *Sci Signal*. 2009;2:re4.
- McCullum EV, Simmonds N, Becker JE, et al. Studies on experimental rickets XXI. An experimental demonstration of the existence of a vitamin which promotes calcium deposition. *J Biol Chem*. 1922;53:293–312.
- Windaus A, Schenck F, von Weder F. Über das antirachitisch wirksame bestrahlungs-produkt aus 7-dehydro-cholesterin. *Hoppe Seylers Z Physiol Chem*. 1936;241:100–103 [in German].
- Steenbock H. The induction of growth promoting and calcifying properties in a ration by exposure to light. *Science*. 1924;60:224–225.
- Hess A, Weinstick M. Antirachitic properties imparted to lettuce and to growing wheat light ultraviolet irradiation. *Proc Soc Exp Biol Med*. 1924;22:5–6.
- DeLuca HF. The metabolism, physiology and function of vitamin D. In: Kumar R, ed. *Vitamin D*. Boston/The Hague/Dordrecht/Lancaster: Martinus Nijhoff Publishing; 1984.
- Esvelt RP, Schnoes HK, DeLuca HF. Vitamin D₃ from rat skins irradiated in vitro with ultraviolet light. *Arch Biochem Biophys*. 1978;188:282–286.
- Holick MF, Clark MB. The photobiogenesis and metabolism of vitamin D. *Fed Proc*. 1978;37:2567–2574.
- Holick MF, MacLaughlin JA, Clark MB, et al. Photosynthesis of previtamin D₃ in human skin and the physiologic consequences. *Science*. 1980;210:203–205.
- Holick MF, Richtand NM, McNeill SC, et al. Isolation and identification of previtamin D₃ from the skin of rats exposed to ultraviolet irradiation. *Biochemistry*. 1979;18:1003–1008.
- Green J. Studies on the analysis of vitamins D. 4. Studies on the irradiation of ergosterol and 7-dehydrocholesterol and the analysis of the products for calciferol, vitamin D₃, and component sterols. *Biochem J*. 1951;49:232–243.
- Rambeck WA, Weiser H, Zucker H. Biological activity of 1 alpha,25-dihydroxyergocalciferol in rachitic chicks and in rats. *Int J Vitam Nutr Res*. 1984;54:135–139.
- Blunt JW, DeLuca HF, Schnoes HK. 25-hydroxycholecalciferol. A biologically active metabolite of vitamin D₃. *Biochemistry*. 1968;7:3317–3322.
- Suda T, DeLuca HF, Schnoes H, et al. 25-hydroxyergocalciferol: a biologically active metabolite of vitamin D₂. *Biochem Biophys Res Commun*. 1969;35:182–185.
- Suda T, DeLuca HF, Schnoes HK, et al. The isolation and identification of 25-hydroxyergocalciferol. *Biochemistry*. 1969;8:3515–3520.
- Ponchon G, DeLuca HF. The role of the liver in the metabolism of vitamin D. *J Clin Invest*. 1969;48:1273–1279.
- Ponchon G, Kennan AL, DeLuca HF. “Activation” of vitamin D by the liver. *J Clin Invest*. 1969;48:2032–2037.
- Bhattacharyya MH, DeLuca HF. The regulation of rat liver calciferol-25-hydroxylase. *J Biol Chem*. 1973;248:2969–2973.
- Bhattacharyya MH, DeLuca HF. Subcellular location of rat liver calciferol-25-hydroxylase. *Arch Biochem Biophys*. 1974;160:58–62.
- Madhok TC, DeLuca HF. Characteristics of the rat liver microsomal enzyme system converting cholecalciferol into 25-hydroxycholecalciferol. Evidence for the participation of cytochrome p-450. *Biochem J*. 1979;184:491–499.
- Cheng JB, Levine MA, Bell NH, et al. Genetic evidence that the human CYP2R1 enzyme is a key vitamin D 25-hydroxylase. *Proc Natl Acad Sci U S A*. 2004;101:7711–7715.
- Zhu J, DeLuca HF, Vitamin D. 25-hydroxylase—four decades of searching, are we there yet? *Arch Biochem Biophys*. 2012;523:30–36.
- Zhu JG, Ochalek JT, Kaufmann M, et al. CYP2R1 is a major, but not exclusive, contributor to 25-hydroxyvitamin D production in vivo. *Proc Natl Acad Sci U S A*. 2013;110:15650–15655.
- Bilezikian JP, Canfield RE, Jacobs TP, et al. Response of 1alpha,25-dihydroxyvitamin D₃ to hypocalcemia in human subjects. *N Engl J Med*. 1978;299:437–441.
- Boyle IT, Gray RW, DeLuca HF. Regulation by calcium of in vivo synthesis of 1,25-dihydroxycholecalciferol and 21,25-dihydroxycholecalciferol. *Proc Natl Acad Sci U S A*. 1971;68:2131–2134.
- DeLuca HF. Regulation of vitamin D metabolism in the kidney. *Adv Exp Med Biol*. 1977;81:195–209.
- Kumar R. Metabolism of 1,25-dihydroxyvitamin D₃. *Physiol Rev*. 1984;64:478–504.
- Kumar R. Vitamin D metabolism and mechanisms of calcium transport. *J Am Soc Nephrol*. 1990;1:30–42.
- Holick MF, Schnoes HK, DeLuca HF. Identification of 1,25-dihydroxycholecalciferol, a form of vitamin D₃ metabolically active in the intestine. *Proc Natl Acad Sci U S A*. 1971;68:803–804.
- Holick MF, Schnoes HK, DeLuca HF, et al. Isolation and identification of 1,25-dihydroxycholecalciferol. A metabolite of vitamin D active in intestine. *Biochemistry*. 1971;10:2799–2804.
- Fraser DR, Kodicek E. Unique biosynthesis by kidney of a biological active vitamin D metabolite. *Nature*. 1970;228:764–766.
- Garabedian M, Holick MF, DeLuca HF, et al. Control of 25-hydroxycholecalciferol metabolism by parathyroid glands. *Proc Natl Acad Sci U S A*. 1972;69:1673–1676.
- Reeve L, Tanaka Y, DeLuca HF. Studies on the site of 1,25-dihydroxyvitamin D₃ synthesis in vivo. *J Biol Chem*. 1983;258:3615–3617.
- Shultz TD, Fox J, Heath H 3rd, et al. Do tissues other than the kidney produce 1,25-dihydroxyvitamin D₃ in vivo? A reexamination. *Proc Natl Acad Sci U S A*. 1983;80:1746–1750.
- Ryan ZC, Ketha H, McNulty MS, et al. Sclerostin alters serum vitamin D metabolite and fibroblast growth factor 23 concentrations and the urinary excretion of calcium. *Proc Natl Acad Sci U S A*. 2013;110:6199–6204.
- Kumar R, Vallon V. Reduced renal calcium excretion in the absence of sclerostin expression: evidence for a novel calcium-regulating bone kidney axis. *J Am Soc Nephrol*. 2014;25:2159–2168.
- Brown EM, Gamba G, Riccardi D, et al. Cloning and characterization of an extracellular Ca(2+)-sensing receptor from bovine parathyroid. *Nature*. 1993;366:575–580.

58. Brown EM, Hebert SC. A cloned Ca(2+)-sensing receptor: a mediator of direct effects of extracellular Ca²⁺ on renal function? *J Am Soc Nephrol*. 1995;6:1530–1540.
59. Brown EM, Hebert SC. A cloned extracellular Ca(2+)-sensing receptor: molecular mediator of the actions of extracellular Ca²⁺ on parathyroid and kidney cells? *Kidney Int*. 1996;49:1042–1046.
60. Brown EM, Pollak M, Hebert SC. The extracellular calcium-sensing receptor: its role in health and disease. *Annu Rev Med*. 1998;49:15–29.
61. Yamamoto M, Kawanobe Y, Takahashi H, et al. Vitamin D deficiency and renal calcium transport in the rat. *J Clin Invest*. 1984;74:507–513.
62. Hugi K, Bonjour JP, Fleisch H. Renal handling of calcium: influence of parathyroid hormone and 1,25-dihydroxyvitamin D₃. *Am J Physiol*. 1979;236:F349–F356.
63. Peacock M, Robertson WG, Nordin BE. Relation between serum and urinary calcium with particular reference to parathyroid activity. *Lancet*. 1969;1:384–386.
64. Berndt TJ, Thompson JR, Kumar R. The regulation of calcium, magnesium and phosphate excretion by the kidney. In: Skorecki K, Chertow GM, Marsden PA, et al, eds. *Brenner and Rector's The Kidney*. Philadelphia: Elsevier; 2016:185–203.
65. Bellido T. Downregulation of SOST/sclerostin by PTH: a novel mechanism of hormonal control of bone formation mediated by osteocytes. *J Musculoskelet Neuronal Interact*. 2006;6:358–359.
66. Omdahl J, Holick M, Suda T, et al. Biological activity of 1,25-dihydroxycholecalciferol. *Biochemistry*. 1971;10:2935–2940.
67. Puschett JB, Beck WS Jr, Jelonek A, et al. Study of the renal tubular interactions of thyrocalcitonin, cyclic adenosine 3',5'-monophosphate, 25-hydroxycholecalciferol, and calcium ion. *J Clin Invest*. 1974;53:756–767.
68. Puschett JB, Fernandez PC, Boyle IT, et al. The acute renal tubular effects of 1,25-dihydroxycholecalciferol. *Proc Soc Exp Biol Med*. 1972;141:379–384.
69. Bindels RJ, Hartog A, Timmermans J, et al. Active Ca²⁺ transport in primary cultures of rabbit kidney CCD: stimulation by 1,25-dihydroxyvitamin D₃ and PTH. *Am J Physiol*. 1991;261:F799–F807.
70. Hoenderop JG, Dardenne O, Van Abel M, et al. Modulation of renal Ca²⁺ transport protein genes by dietary Ca²⁺ and 1,25-dihydroxyvitamin D₃ in 25-hydroxyvitamin D₃-1 α -hydroxylase knockout mice. *FASEB J*. 2002;16:1398–1406.
71. Hoenderop JG, De Pont JJ, Bindels RJ, et al. Hormone-stimulated Ca²⁺ reabsorption in rabbit kidney cortical collecting system is cAMP-independent and involves a phorbol ester-insensitive PKC isotype. *Kidney Int*. 1999;55:225–233.
72. Albright F, Bauer W, Aub JC. Studies of Calcium and Phosphorus Metabolism: VIII. The influence of the thyroid gland and the parathyroid hormone upon the total acid-base metabolism. *J Clin Invest*. 1931;10:187–219.
73. Albright F, Bauer W, Ropes M, et al. Studies of Calcium and Phosphorus Metabolism: IV. The effect of the parathyroid hormone. *J Clin Invest*. 1929;7:139–181.
74. Ingalls TH, Donaldson G, Albright F. The locus of action of the parathyroid hormone: experimental studies with parathyroid extract on normal and nephrectomized rats. *J Clin Invest*. 1943;22:603–608.
75. Holick MF, Garabedian M, DeLuca HF. 1,25-dihydroxycholecalciferol: metabolite of vitamin D₃ active on bone in anephric rats. *Science*. 1972;176:1146–1147.
76. Raisz LG, Trummel CL, Holick MF, et al. 1,25-dihydroxycholecalciferol: a potent stimulator of bone resorption in tissue culture. *Science*. 1972;175:768–769.
77. Holick MF, Schnoes HK, DeLuca HF, et al. Isolation and identification of 24,25-dihydroxycholecalciferol, a metabolite of vitamin D made in the kidney. *Biochemistry*. 1972;11:4251–4255.
78. Lam HY, Schnoes HK, DeLuca HF, et al. 24,25-Dihydroxyvitamin D₃. Synthesis and biological activity. *Biochemistry*. 1973;12:4851–4855.
79. Tanaka Y, DeLuca HF, Ikekawa N, et al. Determination of stereochemical configuration of the 24-hydroxyl group of 24,25-dihydroxyvitamin D₃ and its biological importance. *Arch Biochem Biophys*. 1975;170:620–626.
80. Kumar R, Schnoes HK, DeLuca HF. Rat intestinal 25-hydroxyvitamin D₃- and 1 α ,25-dihydroxyvitamin D₃-24-hydroxylase. *J Biol Chem*. 1978;253:3804–3809.
81. Kumar R, Schaefer J, Grande JP, et al. Immunolocalization of calcitriol receptor, 24-hydroxylase cytochrome P-450, and calbindin D28k in human kidney. *Am J Physiol*. 1994;266:F477–F485.
82. Yang W, Friedman PA, Kumar R, et al. Expression of 25(OH)D₃ 24-hydroxylase in distal nephron: coordinate regulation by 1,25(OH)₂D₃ and cAMP or PTH. *Am J Physiol*. 1999;276:E793–E805.
83. Tanaka Y, DeLuca HF. Rat renal 25-hydroxyvitamin D₃ 1- and 24-hydroxylases: their in vivo regulation. *Am J Physiol*. 1984;246:E168–E173.
84. Kumar R, Schnoes HK, DeLuca HF. Rat intestinal 25-hydroxyvitamin D₃- and 1 α ,25-dihydroxyvitamin D₃-24-hydroxylase. *J Biol Chem*. 1978;253:3804–3809.
85. Popovtzer MM, Knochel JP, Kumar R. Disorders of calcium phosphorus, vitamin D, and parathyroid hormone activity. In: Schrier RW, ed. *Renal and Electrolyte Disorders*. 5th ed. Philadelphia: Lippincott-Raven; 1997:241–319.
86. Berndt TJ, Kumar R. Clinical disturbances of phosphate homeostasis. In: Alpern RJ, Caplan MJ, Moe OW, eds. *The Kidney: Physiology and Pathophysiology*. 5th ed. New York: Elsevier-Academic Press; 2013:2369–2391.
87. Berndt T, Thompson JR, Kumar R. The Regulation of calcium, magnesium, and phosphate excretion by the kidney. In: Skorecki K, Chertow G, Marsden P, et al, eds. *Brenner and Rector's The Kidney*. 10th ed. Elsevier; 2015:185–203.
88. Tanaka Y, Deluca HF. The control of 25-hydroxyvitamin D metabolism by inorganic phosphorus. *Arch Biochem Biophys*. 1973;154:566–574.
89. Baxter LA, DeLuca HF. Stimulation of 25-hydroxyvitamin D₃-1 α -hydroxylase by phosphate depletion. *J Biol Chem*. 1976;251:3158–3161.
90. Ribovich ML, DeLuca HF. 1,25-Dihydroxyvitamin D₃ metabolism. The effect of dietary calcium and phosphorus. *Arch Biochem Biophys*. 1978;188:164–171.
91. Dominguez JH, Gray RW, Lemann J Jr. Dietary phosphate deprivation in women and men: effects on mineral and acid balances, parathyroid hormone and the metabolism of 25-OH-vitamin D. *J Clin Endocrinol Metab*. 1976;43:1056–1068.
92. Gray RW, Wilz DR, Caldas AE, et al. The importance of phosphate in regulating plasma 1,25-(OH)₂-vitamin D levels in humans: studies in healthy subjects in calcium-stone formers and in patients with primary hyperparathyroidism. *J Clin Endocrinol Metab*. 1977;45:299–306.
93. Castillo L, Tanaka Y, DeLuca HF. The mobilization of bone mineral by 1,25-dihydroxyvitamin D₃ in hypophosphatemic rats. *Endocrinology*. 1975;97:995–999.
94. Steele TH, Engle JE, Tanaka Y, et al. Phosphatemic action of 1,25-dihydroxyvitamin D₃. *Am J Physiol*. 1975;229:489–495.
95. Tanaka Y, DeLuca HF. Role of 1,25-dihydroxyvitamin D₃ in maintaining serum phosphorus and curing rickets. *Proc Natl Acad Sci U S A*. 1974;71:1040–1044.
96. Condamine L, Mena C, Vrtovsnik F, et al. Local action of phosphate depletion and insulin-like growth factor I on in vitro production of 1,25-dihydroxyvitamin D by cultured mammalian kidney cells. *J Clin Invest*. 1994;94:1673–1679.
97. Mena C, Vrtovsnik F, Friedlander G, et al. Insulin-like growth factor I, a unique calcium-dependent stimulator of 1,25-dihydroxyvitamin D₃ production. Studies in cultured mouse kidney cells. *J Biol Chem*. 1995;270:25461–25467.
98. Sommer S, Berndt T, Craig T, et al. The phosphatonins and the regulation of phosphate transport and vitamin D metabolism. *J Steroid Biochem Mol Biol*. 2007;103:497–503.
99. Tanaka Y, Frank H, DeLuca HF. Intestinal calcium transport: stimulation by low phosphorus diets. *Science*. 1973;181:564–566.
100. Gray RW. Control of plasma 1,25-(OH)₂-vitamin D concentrations by calcium and phosphorus in the rat: effects of hypophysectomy. *Calcif Tissue Int*. 1981;33:485–488.
101. Gray RW. Effects of age and sex on the regulation of plasma 1,25-(OH)₂-D by phosphorus in the rat. *Calcif Tissue Int*. 1981;33:477–484.
102. Gray RW, Garthwaite TL. Activation of renal 1,25-dihydroxyvitamin D₃ synthesis by phosphate deprivation: evidence for a role for growth hormone. *Endocrinology*. 1985;116:189–193.
103. Gray RW, Garthwaite TL, Phillips LS. Growth hormone and triiodothyronine permit an increase in plasma 1,25(OH)₂D concentrations in response to dietary phosphate deprivation in hypophysectomized rats. *Calcif Tissue Int*. 1983;35:100–106.
104. Gray RW, Haasch ML, Brown CE. Regulation of plasma 1,25-(OH)₂-D₃ by phosphate: evidence against a role for total or acid-soluble renal phosphate content. *Calcif Tissue Int*. 1983;35:773–777.
105. Gray RW, Napoli JL. Dietary phosphate deprivation increases 1,25-dihydroxyvitamin D₃ synthesis in rat kidney in vitro. *J Biol Chem*. 1983;258:1152–1155.

106. Kido S, Kaneko I, Tatsumi S, et al. Vitamin D and type II sodium-dependent phosphate cotransporters. *Contrib Nephrol.* 2013;180:86–97.
107. Taketani Y, Segawa H, Chikamori M, et al. Regulation of type II renal Na⁺-dependent inorganic phosphate transporters by 1,25-dihydroxyvitamin D₃. Identification of a vitamin D-responsive element in the human NAPI-3 gene. *J Biol Chem.* 1998;273:14575–14581.
108. Wagner CA, Hernando N, Forster IC, et al. The SLC34 family of sodium-dependent phosphate transporters. *Pflugers Arch.* 2014;466:139–153.
109. Kumar R. The metabolism of dihydroxylated vitamin D metabolites. In: Kumar R, ed. *Vitamin D: Basic and clinical aspects*. Boston: Martinus Nijhoff; 1984:69–90.
110. Kumar R. The metabolism and mechanism of action of 1,25-dihydroxyvitamin D₃. *Kidney Int.* 1986;30:793–803.
111. Kumar R. Vitamin D metabolism and mechanisms of calcium transport. *J Am Soc Nephrol.* 1990;1:30–42.
112. Kumar R. Vitamin D and calcium transport. *Kidney Int.* 1991;40:1177–1189.
113. Kovacs CS. Maternal mineral and bone metabolism during pregnancy, lactation, and post-weaning recovery. *Physiol Rev.* 2016;96:449–547.
114. DeLuca HF. The kidney as an endocrine organ involved in the function of vitamin D. *Am J Med.* 1975;58:39–47.
115. Baker AR, McDonnell DP, Hughes M, et al. Cloning and expression of full-length cDNA encoding human vitamin D receptor. *Proc Natl Acad Sci U S A.* 1988;85:3294–3298.
116. Jehan F, DeLuca HF. Cloning and characterization of the mouse vitamin D receptor promoter. *Proc Natl Acad Sci U S A.* 1997;94:10138–10143.
117. Lu Z, Hanson K, DeLuca HF. Cloning and origin of the two forms of chicken vitamin D receptor. *Arch Biochem Biophys.* 1997;339:99–106.
118. Brumbaugh PF, Haussler MR. 1 α ,25-dihydroxyvitamin D₃ receptor: competitive binding of vitamin D analogs. *Life Sci.* 1973;13:1737–1746.
119. Rachez C, Lemon BD, Suldan Z, et al. Ligand-dependent transcription activation by nuclear receptors requires the DRIP complex. *Nature.* 1999;398:824–828.
120. Ciesielski F, Rochel N, Moras D. Adaptability of the vitamin D nuclear receptor to the synthetic ligand Gemini: remodelling the LBP with one side chain rotation. *J Steroid Biochem Mol Biol.* 2007;103:235–242.
121. Hourai S, Rodrigues LC, Antony P, et al. Structure-based design of a superagonist ligand for the vitamin D nuclear receptor. *Chem Biol.* 2008;15:383–392.
122. Rochel N, Hourai S, Perez-Garcia X, et al. Crystal structure of the vitamin D nuclear receptor ligand binding domain in complex with a locked side chain analog of calcitriol. *Arch Biochem Biophys.* 2007;460:172–176.
123. Rochel N, Wurtz JM, Mitschler A, et al. The crystal structure of the nuclear receptor for vitamin D bound to its natural ligand. *Mol Cell.* 2000;5:173–179.
124. Molnar F, Perakyla M, Carlberg C. Vitamin D receptor agonists specifically modulate the volume of the ligand-binding pocket. *J Biol Chem.* 2006;281:10516–10526.
125. Vaisanen S, Ryhanen S, Saarela JT, et al. Structurally and functionally important amino acids of the agonistic conformation of the human vitamin D receptor. *Mol Pharmacol.* 2002;62:788–794.
126. Yamada S, Shimizu M, Yamamoto K. Structure-function relationships of vitamin D including ligand recognition by the vitamin D receptor. *Med Res Rev.* 2003;23:89–115.
127. Yamamoto K, Masuno H, Choi M, et al. Three-dimensional modeling of and ligand docking to vitamin D receptor ligand binding domain. *Proc Natl Acad Sci U S A.* 2000;97:1467–1472.
128. Darwish H, DeLuca HF. Vitamin D-regulated gene expression. *Crit Rev Eukaryot Gene Expr.* 1993;3:89–116.
129. Haussler MR, Jurutka PW, Mizwicki M, et al. Vitamin D receptor (VDR)-mediated actions of 1 α ,25(OH)₂vitamin D₃: genomic and non-genomic mechanisms. *Best Pract Res Clin Endocrinol Metab.* 2011;25:543–559.
130. Jurutka PW, Whitfield GK, Hsieh JC, et al. Molecular nature of the vitamin D receptor and its role in regulation of gene expression. *Rev Endocr Metab Disord.* 2001;2:203–216.
131. Lowe KE, Maiyar AC, Norman AW. Vitamin D-mediated gene expression. *Crit Rev Eukaryot Gene Expr.* 1992;2:65–109.
132. Craig TA, Zhang Y, Magis AT, et al. Detection of 1 α ,25-dihydroxyvitamin D-regulated miRNAs in zebrafish by whole transcriptome sequencing. *Zebrafish.* 2014;11:207–218.
133. Craig TA, Zhang Y, McNulty MS, et al. Research resource: whole transcriptome RNA sequencing detects multiple 1 α ,25-dihydroxyvitamin D₃-sensitive metabolic pathways in developing zebrafish. *Mol Endocrinol.* 2012;26:1630–1642.
134. Ryan ZC, Craig TA, Folmes CD, et al. 1 α ,25-dihydroxyvitamin D₃ regulates mitochondrial oxygen consumption and dynamics in human skeletal muscle cells. *J Biol Chem.* 2016;291:1514–1528.
135. Shaffer PL, Gewirth DT. Structural basis of VDR-DNA interactions on direct repeat response elements. *EMBO J.* 2002;21:2242–2252.
136. Umesonon K, Giguere V, Glass CK, et al. Retinoic acid and thyroid hormone induce gene expression through a common responsive element. *Nature.* 1988;336:262–265.
137. Carlberg C, Bendik I, Wyss A, et al. Two nuclear signalling pathways for vitamin D. *Nature.* 1993;361:657–660.
138. Carlberg C, Polly P. Gene regulation by vitamin D₃. *Crit Rev Eukaryot Gene Expr.* 1998;8:19–42.
139. Schrader M, Bendik I, Becker-Andre M, et al. Interaction between retinoic acid and vitamin D signaling pathways. *J Biol Chem.* 1993;268:17830–17836.
140. DeLuca HF. Overview of general physiologic features and functions of vitamin D. *Am J Clin Nutr.* 2004;80:1689S–1696S.
141. Tebben PJ, Kumar R. The hormonal regulation of calcium metabolism. In: Alpern RJ, Moe OW, Caplan M, eds. *Seldin and Giebisch's The Kidney, Physiology and Pathophysiology*. New York: Academic Press; 2013:2273–2330.
142. Wasserman RH, Corradino RA, Fullmer CS, et al. Some aspects of vitamin D action; calcium absorption and the vitamin D-dependent calcium-binding protein. *Vitam Horm.* 1974;32:299–324.
143. Wasserman RH, Fullmer CS. Vitamin D and intestinal calcium transport: facts, speculations and hypotheses. *J Nutr.* 1995;125:1971S–1979S.
144. Wasserman RH, Chandler JS, Meyer SA, et al. Intestinal calcium transport and calcium extrusion processes at the basolateral membrane. *J Nutr.* 1992;122:662–671.
145. Dimke H, Hoenderop JG, Bindels RJ. Molecular basis of epithelial Ca²⁺ and Mg²⁺ transport: insights from the TRP channel family. *J Physiol.* 2011;589:1535–1542.
146. Brini M, Cali T, Ottolini D, et al. The plasma membrane calcium pump in health and disease. *FEBS J.* 2013.
147. Borke JL, Caride A, Verma AK, et al. Cellular and segmental distribution of Ca²⁺-pump epitopes in rat intestine. *Pflugers Arch.* 1990;417:120–122.
148. Philipson KD, Nicoll DA. Sodium-calcium exchange: a molecular perspective. *Annu Rev Physiol.* 2000;62:111–133.
149. Meyer MB, Zella LA, Nerenz RD, et al. Characterizing early events associated with the activation of target genes by 1,25-dihydroxyvitamin D₃ in mouse kidney and intestine in vivo. *J Biol Chem.* 2007;282:22344–22352.
150. Taylor AN, Wasserman RH. Vitamin D-induced calcium-binding protein: comparative aspects in kidney and intestine. *Am J Physiol.* 1972;223:110–114.
151. Wasserman RH, Brindak ME, Meyer SA, et al. Evidence for multiple effects of vitamin D₃ on calcium absorption: response of rachitic chicks, with or without partial vitamin D₃ repletion, to 1,25-dihydroxyvitamin D₃. *Proc Natl Acad Sci U S A.* 1982;79:7939–7943.
152. Wasserman RH, Taylor AN. Vitamin D₃-induced calcium-binding protein in chick intestinal mucosa. *Science.* 1966;152:791–793.
153. Cai Q, Chandler JS, Wasserman RH, et al. Vitamin D and adaptation to dietary calcium and phosphate deficiencies increase intestinal plasma membrane calcium pump gene expression. *Proc Natl Acad Sci U S A.* 1993;90:1345–1349.
154. Lee SM, Riley EM, Meyer MB, et al. 1,25-Dihydroxyvitamin D₃ controls a cohort of vitamin D receptor target genes in the proximal intestine that is enriched for calcium-regulating components. *J Biol Chem.* 2015;290:18199–18215.
155. Benn BS, Ajibade D, Porta A, et al. Active intestinal calcium transport in the absence of transient receptor potential vanilloid type 6 and calbindin-D9k. *Endocrinology.* 2008;149:3196–3205.
156. Kutuzova GD, Sundersingh F, Vaughan J, et al. TRPV6 is not required for 1 α ,25-dihydroxyvitamin D₃-induced intestinal calcium absorption in vivo. *Proc Natl Acad Sci U S A.* 2008;105:19655–19659.

157. Lieben L, Benn BS, Ajibade D, et al. Trpv6 mediates intestinal calcium absorption during calcium restriction and contributes to bone homeostasis. *Bone*. 2010;47:301–308.
158. Ryan ZC, Craig TA, Filoteo AG, et al. Deletion of the intestinal plasma membrane calcium pump, isoform 1, Atp2b1, in mice is associated with decreased bone mineral density and impaired responsiveness to 1, 25-dihydroxyvitamin D3. *Biochem Biophys Res Commun*. 2015;467:152–156.
159. Borke JL, Minami J, Verma A, et al. Monoclonal antibodies to human erythrocyte membrane Ca⁺⁺-Mg⁺⁺ adenosine triphosphatase pump recognize an epitope in the basolateral membrane of human kidney distal tubule cells. *J Clin Invest*. 1987;80:1225–1231.
160. Borke JL, Eriksen EF, Minami J, et al. Epitopes of the human erythrocyte Ca²⁺-Mg²⁺ ATPase pump in human osteoblast-like cell plasma membranes. *J Clin Endocrinol Metab*. 1988;67:1299–1304.
161. Borke JL, Penniston JT, Kumar R. Recent advances in calcium transport by the kidney. *Semin Nephrol*. 1990;10:15–23.
162. Kumar R, Penniston JT, Borke JL. Ca²⁺-Mg²⁺-ATPase calcium pumps in the kidney. *New Physiol Sci*. 1988;3:219–222.
163. Kumar R, Tebben PJ, Thompson JR. Vitamin D and the kidney. *Arch Biochem Biophys*. 2012;523:77–86.
164. Lambers TT, Bindels RJ, Hoenderop JG. Coordinated control of renal Ca²⁺ handling. *Kidney Int*. 2006;69:650–654.
165. Lassiter WE, Gottschalk CW, Mylle M. Micropuncture study of renal tubular reabsorption of calcium in normal rodents. *Am J Physiol*. 1963;204:771–775.
166. Harris CA, Baer PG, Dirks JH. Composition of mammalian glomerular filtrate. *Am J Physiol*. 1974;227:972–976.
167. Duarte CG, Watson JF. Calcium reabsorption in proximal tubule of the dog nephron. *Am J Physiol*. 1967;212:1355–1360.
168. Agus ZS, Gardner LB, Beck LH, et al. Effects of parathyroid hormone on renal tubular reabsorption of calcium, sodium, and phosphate. *Am J Physiol*. 1973;224:1143–1148.
169. Edwards BR, Baer PG, Sutton RA, et al. Micropuncture study of diuretic effects on sodium and calcium reabsorption in the dog nephron. *J Clin Invest*. 1973;52:2418–2427.
170. Edwards BR, Sutton RA, Dirks JH. Effect of calcium infusion on renal tubular reabsorption in the dog. *Am J Physiol*. 1974;227:13–18.
171. Agus ZS, Chiu PJ, Goldberg M. Regulation of urinary calcium excretion in the rat. *Am J Physiol*. 1977;232:F545–F549.
172. Sutton RAL, Wong NLM, Dirks JH. The hypercalciuria of metabolic acidosis—a specific impairment of distal calcium reabsorption. *Clin Res*. 1975;23:434A.
173. Nijenhuis T, Vallon V, van der Kemp AW, et al. Enhanced passive Ca²⁺ reabsorption and reduced Mg²⁺ channel abundance explains thiazide-induced hypocalciuria and hypomagnesemia. *J Clin Invest*. 2005;115:1651–1658.
174. Yu AS, Cheng MH, Angelow S, et al. Molecular basis for cation selectivity in claudin-2-based paracellular pores: identification of an electrostatic interaction site. *J Gen Physiol*. 2009;133:111–127.
175. Yu AS, Cheng MH, Coalson RD. Calcium inhibits paracellular sodium conductance through claudin-2 by competitive binding. *J Biol Chem*. 2010;285:37060–37069.
176. Ullrich KJ, Rumrich G, Kloss S. Active Ca²⁺ reabsorption in the proximal tubule of the rat kidney. Dependence on sodium- and buffer transport. *Pflugers Arch*. 1976;364:223–228.
177. Dominguez JH, Juhaszova M, Kleiboeker SB, et al. Na(+)-Ca²⁺ exchanger of rat proximal tubule: gene expression and subcellular localization. *Am J Physiol*. 1992;263:F945–F950.
178. Freeman TC, Howard A, Bentsen BS, et al. Cellular and regional expression of transcripts of the plasma membrane calcium pump PMCA1 in rabbit intestine. *Am J Physiol*. 1995;269:G126–G131.
179. Magosci M, Yamaki M, Penniston JT, et al. Localization of mRNAs coding for isozymes of plasma membrane Ca(2+)-ATPase pump in rat kidney. *Am J Physiol*. 1992;263:F7–F14.
180. Rocha AS, Magaldi JB, Kokko JP. Calcium and phosphate transport in isolated segments of rabbit Henle's loop. *J Clin Invest*. 1977;59:975–983.
181. Jamison RL, Frey NR, Lacy FB. Calcium reabsorption in the thin loop of Henle. *Am J Physiol*. 1974;227:745–751.
182. de Rouffignac C, Morel F, Moss N, et al. Micropuncture study of water and electrolyte movements along the loop of Henle in psammomys with special reference to magnesium, calcium and phosphorus. *Pflugers Arch*. 1973;344:309–326.
183. Bourdeau JE, Burg MB. Voltage dependence of calcium transport in the thick ascending limb of Henle's loop. *Am J Physiol*. 1979;236:F357–F364.
184. Bourdeau JE, Burg MB. Effect of PTH on calcium transport across the cortical thick ascending limb of Henle's loop. *Am J Physiol*. 1980;239:F121–F126.
185. Imai M. Calcium transport across the rabbit thick ascending limb of Henle's loop perfused in vitro. *Pflugers Arch*. 1978;374:255–263.
186. Imai M. Effects of parathyroid hormone and N6,O2'-dibutyryl cyclic AMP on Ca²⁺ transport across the rabbit distal nephron segments perfused in vitro. *Pflugers Arch*. 1981;390:145–151.
187. Shareghi GR, Stoner LC. Calcium transport across segments of the rabbit distal nephron in vitro. *Am J Physiol*. 1978;235:F367–F375.
188. Suki WN. Calcium transport in the pars recta and the loop of Henle. *Adv Exp Med Biol*. 1980;128:37–40.
189. Suki WN, Rouse D. Hormonal regulation of calcium transport in thick ascending limb renal tubules. *Am J Physiol*. 1981;241:F171–F174.
190. Suki WN, Rouse D, Ng RC, et al. Calcium transport in the thick ascending limb of Henle. Heterogeneity of function in the medullary and cortical segments. *J Clin Invest*. 1980;66:1004–1009.
191. Li J, Ananthapanyasut W, Yu AS. Claudins in renal physiology and disease. *Pediatr Nephrol*. 2011;26:2133–2142.
192. Gamba G, Miyanooshita A, Lombardi M, et al. Molecular cloning, primary structure, and characterization of two members of the mammalian electroneutral sodium-(potassium)-chloride cotransporter family expressed in kidney. *J Biol Chem*. 1994;269:17713–17722.
193. Kaplan MR, Plotkin MD, Brown D, et al. Expression of the mouse Na-K-2Cl cotransporter, mBSC2, in the terminal inner medullary collecting duct, the glomerular and extraglomerular mesangium, and the glomerular afferent arteriole. *J Clin Invest*. 1996;98:723–730.
194. Kaplan MR, Plotkin MD, Lee WS, et al. Apical localization of the Na-K-Cl cotransporter, rBSC1, on rat thick ascending limbs. *Kidney Int*. 1996;49:40–47.
195. Plata C, Mount DB, Rubio V, et al. Isoforms of the Na-K-2Cl cotransporter in murine TAL II. Functional characterization and activation by cAMP. *Am J Physiol*. 1999;276:F359–F366.
196. Greger R. Ion transport mechanisms in thick ascending limb of Henle's loop of mammalian nephron. *Physiol Rev*. 1985;65:760–797.
197. Ikari A, Hirai N, Shiroma M, et al. Association of paracellin-1 with ZO-1 augments the reabsorption of divalent cations in renal epithelial cells. *J Biol Chem*. 2004;279:54826–54832.
198. Will C, Breiderhoff T, Thumfart J, et al. Targeted deletion of murine Cldn16 identifies extra- and intrarenal compensatory mechanisms of Ca²⁺ and Mg²⁺ wasting. *Am J Physiol Renal Physiol*. 2010;298:F1152–F1161.
199. Konrad M, Schaller A, Seelow D, et al. Mutations in the tight-junction gene claudin 19 (CLDN19) are associated with renal magnesium wasting, renal failure, and severe ocular involvement. *Am J Hum Genet*. 2006;79:949–957.
200. Hou J, Renigunta A, Gomes AS, et al. Claudin-16 and claudin-19 interaction is required for their assembly into tight junctions and for renal reabsorption of magnesium. *Proc Natl Acad Sci U S A*. 2009;106:15350–15355.
201. Hou J, Paul DL, Goodenough DA. Paracellin-1 and the modulation of ion selectivity of tight junctions. *J Cell Sci*. 2005;118:5109–5118.
202. Hou J, Renigunta A, Konrad M, et al. Claudin-16 and claudin-19 interact and form a cation-selective tight junction complex. *J Clin Invest*. 2008;118:619–628.
203. Hebert SC. Barter syndrome. *Curr Opin Nephrol Hypertens*. 2003;12:527–532.
204. De Rouffignac C, Di Stefano A, Wittner M, et al. Consequences of differential effects of ADH and other peptide hormones on thick ascending limb of mammalian kidney. *Am J Physiol*. 1991;260:R1023–R1035.
205. Di Stefano A, Wittner M, Nitschke R, et al. Effects of parathyroid hormone and calcitonin on Na⁺, Cl⁻, K⁺, Mg²⁺ and Ca²⁺ transport in cortical and medullary thick ascending limbs of mouse kidney. *Pflugers Arch*. 1990;417:161–167.
206. Costanzo LS, Windhager EE. Calcium and sodium transport by the distal convoluted tubule of the rat. *Am J Physiol*. 1978;235:F492–F506.
207. Costanzo LS, Windhager EE, Ellison DH. Calcium and sodium transport by the distal convoluted tubule of the rat. 1978. *J Am Soc Nephrol*. 2000;11:1562–1580.
208. Dimke H, Hoenderop JG, Bindels RJ. Hereditary tubular transport disorders: implications for renal handling of Ca²⁺ and Mg²⁺. *Clin Sci*. 2010;118:1–18.

209. de Groot T, Bindels RJ, Hoenderop JG. TRPV5: an ingeniously controlled calcium channel. *Kidney Int.* 2008;74:1241–1246.
210. Hoenderop JG, Nilius B, Bindels RJ. Calcium absorption across epithelia. *Physiol Rev.* 2005;85:373–422.
211. Hoenderop JG, van Leeuwen JP, van der Eerden BC, et al. Renal Ca²⁺ wasting, hyperabsorption, and reduced bone thickness in mice lacking TRPV5. *J Clin Invest.* 2003;112:1906–1914.
212. Hsu YJ, Hoenderop JG, Bindels RJ. TRP channels in kidney disease. *Biochim Biophys Acta.* 2007;1772:928–936.
213. Nijenhuis T, Hoenderop JG, Loffing J, et al. Thiazide-induced hypocalciuria is accompanied by a decreased expression of Ca²⁺ transport proteins in kidney. *Kidney Int.* 2003;64:555–564.
214. van de Graaf SF, Hoenderop JG, Bindels RJ. Regulation of TRPV5 and TRPV6 by associated proteins. *Am J Physiol Renal Physiol.* 2006;290:F1295–F1302.
215. Johnson JA, Grande JP, Roche PC, et al. Immunohistochemical localization of the 1,25(OH)₂D₃ receptor and calbindin D28k in human and rat pancreas. *Am J Physiol.* 1994;267:E356–E360.
216. Magyar CE, White KE, Rojas R, et al. Plasma membrane Ca²⁺-ATPase and NCX1 Na⁺/Ca²⁺ exchanger expression in distal convoluted tubule cells. *Am J Physiol Renal Physiol.* 2002;283:F29–F40.
217. White KE, Gesek FA, Friedman PA. Structural and functional analysis of Na⁺/Ca²⁺ exchange in distal convoluted tubule cells. *Am J Physiol.* 1996;271:F560–F570.
218. White KE, Gesek FA, Reilly RF, et al. NCX1 Na/Ca exchanger inhibition by antisense oligonucleotides in mouse distal convoluted tubule cells. *Kidney Int.* 1998;54:897–906.
219. Yu AS, Hebert SC, Lee SL, et al. Identification and localization of renal Na⁺-Ca²⁺ exchanger by polymerase chain reaction. *Am J Physiol.* 1992;263:F680–F685.
220. de Groot T, Lee K, Langeslag M, et al. Parathyroid hormone activates TRPV5 via PKA-dependent phosphorylation. *J Am Soc Nephrol.* 2009;20:1693–1704.
221. Cha SK, Wu T, Huang CL. Protein kinase C inhibits caveolae-mediated endocytosis of TRPV5. *Am J Physiol Renal Physiol.* 2008;294:F1212–F1221.
222. Christakos S, Brunette MG, Norman AW. Localization of immunoreactive vitamin D-dependent calcium binding protein in chick nephron. *Endocrinology.* 1981;109:322–324.
223. Johnson JA, Kumar R. Renal and intestinal calcium transport: roles of vitamin D and vitamin D-dependent calcium binding proteins. *Semin Nephrol.* 1994;14:119–128.
224. Roth J, Thorens B, Hunziker W, et al. Vitamin D-dependent calcium binding protein: immunocytochemical localization in chick kidney. *Science.* 1981;214:197–200.
225. Schreiner DS, Jande SS, Parkes CO, et al. Immunocytochemical demonstration of two vitamin D-dependent calcium-binding proteins in mammalian kidney. *Acta Anat (Basel).* 1983;117:1–14.
226. Thomasset M, Desplan C, Warembourg M, et al. Vitamin-D dependent 9 kDa calcium-binding protein gene: cDNA cloning, mRNA distribution and regulation. *Biochimie.* 1986;68:935–940.
227. Thomasset M, Parkes CO, Cuisinier-Gleizes P. Rat calcium-binding proteins: distribution, development, and vitamin D dependence. *Am J Physiol.* 1982;243:E483–E488.
228. Caride AJ, Chini EN, Yamaki M, et al. Unique localization of mRNA encoding plasma membrane Ca²⁺ pump isoform 3 in rat thin descending loop of Henle. *Am J Physiol.* 1995;269:F681–F685.
229. Glendenning P, Ratajczak T, Dick IM, et al. Calcitriol upregulates expression and activity of the 1b isoform of the plasma membrane calcium pump in immortalized distal kidney tubular cells. *Arch Biochem Biophys.* 2000;380:126–132.
230. Kip SN, Strehler EE. Vitamin D₃ upregulates plasma membrane Ca²⁺-ATPase expression and potentiates apico-basal Ca²⁺ flux in MDCK cells. *Am J Physiol Renal Physiol.* 2004;286:F363–F369.
231. Stauffer TP, Guerini D, Carafoli E. Tissue distribution of the four gene products of the plasma membrane Ca²⁺ pump. A study using specific antibodies. *J Biol Chem.* 1995;270:12184–12190.
232. Bourdeau JE, Burg MB. Effect of PTH on calcium transport across the cortical thick ascending limb of Henle's loop. *Am J Physiol.* 1980;239:F121–F126.
233. Wittner M, Mandon B, Roinel N, et al. Hormonal stimulation of Ca²⁺ and Mg²⁺ transport in the cortical thick ascending limb of Henle's loop of the mouse: evidence for a change in the paracellular pathway permeability. *Pflügers Arch.* 1993;423:387–396.
234. Sato T, Courbebaisse M, Ide N, et al. Parathyroid hormone controls paracellular Ca²⁺ transport in the thick ascending limb by regulating the tight-junction protein claudin14. *Proc Natl Acad Sci U S A.* 2017;114:E3344–E3353.
235. Hebert SC, Brown EM, Harris HW. Role of the Ca²⁺-sensing receptor in divalent mineral ion homeostasis. *J Exp Biol.* 1997;200:295–302.
236. Toka HR, Al-Romaih K, Koshy JM, et al. Deficiency of the calcium-sensing receptor in the kidney causes parathyroid hormone-independent hypocalciuria. *J Am Soc Nephrol.* 2012;23:1879–1890.
237. Loupy A, Ramakrishnan SK, Wootla B, et al. PTH-independent regulation of blood calcium concentration by the calcium-sensing receptor. *J Clin Invest.* 2012;122:3355–3367.
238. Gong Y, Renigunta V, Himmerkus N, et al. Claudin-14 regulates renal Ca²⁺ transport in response to CaSR signalling via a novel microRNA pathway. *EMBO J.* 2012;31:1999–2012.
239. Dimke H, Desai P, Borovac J, et al. Activation of the Ca²⁺-sensing receptor increases renal claudin-14 expression and urinary Ca²⁺ excretion. *Am J Physiol Renal Physiol.* 2013;304:F761–F769.
240. Gong Y, Hou J. Claudin-14 underlies Ca²⁺-sensing receptor-mediated Ca²⁺ metabolism via NFAT-microRNA-based mechanisms. *J Am Soc Nephrol.* 2014;25:745–760.
241. Gong Y, Hou J. Claudins in barrier and transport function-the kidney. *Pflügers Arch.* 2017;469:105–113.
242. Lee CT, Chen HC, Lai LW, et al. Effects of furosemide on renal calcium handling. *Am J Physiol Renal Physiol.* 2007;293:F1231–F1237.
243. Brickman AS, Massry SG, Coburn JW. changes in serum and urinary calcium during treatment with hydrochlorothiazide: studies on mechanisms. *J Clin Invest.* 1972;51:945–954.
244. Costanzo LS, Moses AM, Rao KJ, et al. Dissociation of calcium and sodium clearances in patients with hypoparathyroidism by infusion of chlorothiazide. *Metabolism.* 1975;24:1367–1373.
245. Quamme GA, Wong NL, Sutton RA, et al. Interrelationship of chlorothiazide and parathyroid hormone: a micropuncture study. *Am J Physiol.* 1975;229:200–205.
246. Gamba G, Saltzberg SN, Lombardi M, et al. Primary structure and functional expression of a cDNA encoding the thiazide-sensitive, electroneutral sodium-chloride cotransporter. *Proc Natl Acad Sci U S A.* 1993;90:2749–2753.
247. Costanzo LS, Windhager EE. Calcium and sodium transport by the distal convoluted tubule of the rat. *Am J Physiol.* 1978;235:F492–F506.
248. Ellison DH. Divalent cation transport by the distal nephron: insights from Bartter's and Gitelman's syndromes. *Am J Physiol Renal Physiol.* 2000;279:F616–F625.
249. Bettinelli A, Bianchetti MG, Girardin E, et al. Use of calcium excretion values to distinguish two forms of primary renal tubular hypokalemic alkalosis: Bartter and Gitelman syndromes. *J Pediatr.* 1992;120:38–43.
250. Gitelman HJ, Graham JB, Welt LG. A new familial disorder characterized by hypokalemia and hypomagnesemia. *Trans Assoc Am Physicians.* 1966;79:221–235.
251. Loffing J, Vallon V, Loffing-Cueni D, et al. Altered renal distal tubule structure and renal Na⁺ and Ca²⁺ handling in a mouse model for Gitelman's syndrome. *J Am Soc Nephrol.* 2004;15:2276–2288.
252. Nordin BE, Need AG, Morris HA, et al. Evidence for a renal calcium leak in postmenopausal women. *J Clin Endocrinol Metab.* 1991;72:401–407.
253. McKane WR, Khosla S, Burritt MF, et al. Mechanism of renal calcium conservation with estrogen replacement therapy in women in early postmenopause—a clinical research center study. *J Clin Endocrinol Metab.* 1995;80:3458–3464.
254. Prince RL, Smith M, Dick IM, et al. Prevention of postmenopausal osteoporosis. A comparative study of exercise, calcium supplementation, and hormone-replacement therapy. *N Engl J Med.* 1991;325:1189–1195.
255. Van Abel M, Hoenderop JG, Dardenne O, et al. 1,25-dihydroxyvitamin D₃-independent stimulatory effect of estrogen on the expression of ECaCl₁ in the kidney. *J Am Soc Nephrol.* 2002;13:2102–2109.
256. Van Cromphaut SJ, Rummens K, Stockmans I, et al. Intestinal calcium transporter genes are upregulated by estrogens and the reproductive cycle through vitamin D receptor-independent mechanisms. *J Bone Miner Res.* 2003;18:1725–1736.
257. Lemann J Jr, Bushinsky DA, Hamm LL. Bone buffering of acid and base in humans. *Am J Physiol Renal Physiol.* 2003;285:F811–F832.
258. Marone CC, Wong NL, Sutton RA, et al. Acidosis and renal calcium excretion in experimental chronic renal failure. *Nephron.* 1981;28:294–296.

259. Marone CC, Wong NL, Sutton RA, et al. Effects of metabolic alkalosis on calcium excretion in the conscious dog. *J Lab Clin Med.* 1983;101:264–273.
260. Sutton RA, Wong NL, Dirks JH. Effects of metabolic acidosis and alkalosis on sodium and calcium transport in the dog kidney. *Kidney Int.* 1979;15:520–533.
261. Wong NL, Quamme GA, Dirks JH. Effects of acid-base disturbances on renal handling of magnesium in the dog. *Clin Sci.* 1986;70:277–284.
262. Nijenhuis T, Renkema KY, Hoenderop JG, et al. Acid-base status determines the renal expression of Ca²⁺ and Mg²⁺ transport proteins. *J Am Soc Nephrol.* 2006;17:617–626.
263. Yeh BI, Kim YK, Jabbar W, et al. Conformational changes of pore helix coupled to gating of TRPV5 by protons. *EMBO J.* 2005;24:3224–3234.
264. Yeh BI, Sun TJ, Lee JZ, et al. Mechanism and molecular determinant for regulation of rabbit transient receptor potential type 5 (TRPV5) channel by extracellular pH. *J Biol Chem.* 2003;278:51044–51052.
265. Vennekens R, Prenen J, Hoenderop JG, et al. Modulation of the epithelial Ca²⁺ channel ECaC by extracellular pH. *Pflugers Arch.* 2001;442:237–242.
266. Kuro-o M. Endocrine FGFs and Klotho: emerging concepts. *Trends Endocrinol Metab.* 2008;19:239–245.
267. Kuro-o M. Klotho. *Pflugers Arch.* 2010;459:333–343.
268. Kuro-o M, Matsumura Y, Aizawa H, et al. Mutation of the mouse klotho gene leads to a syndrome resembling ageing. *Nature.* 1997;390:45–51.
269. Kurosu H, Ogawa Y, Miyoshi M, et al. Regulation of fibroblast growth factor-23 signaling by klotho. *J Biol Chem.* 2006;281:6120–6123.
270. Chang Q, Hoefs S, van der Kemp AW, et al. The beta-glucuronidase klotho hydrolyzes and activates the TRPV5 channel. *Science.* 2005;310:490–493.
271. Brunkow ME, Gardner JC, Van Ness J, et al. Bone dysplasia sclerosteosis results from loss of the SOST gene product, a novel cystine knot-containing protein. *Am J Hum Genet.* 2001;68:577–589.
272. Beighton P, Barnard A, Hamersma H, et al. The syndromic status of sclerosteosis and van Buchem disease. *Clin Genet.* 1984;25:175–181.
273. Beighton P, Davidson J, Durr L, et al. Sclerosteosis—an autosomal recessive disorder. *Clin Genet.* 1977;11:1–7.
274. Beighton P, Durr L, Hamersma H. The clinical features of sclerosteosis. A review of the manifestations in twenty-five affected individuals. *Ann Intern Med.* 1976;84:393–397.
275. Balemans W, Patel N, Ebeling M, et al. Identification of a 52 kb deletion downstream of the SOST gene in patients with van Buchem disease. *J Med Genet.* 2002;39:91–97.
276. Li X, Ominsky MS, Niu QT, et al. Targeted deletion of the sclerostin gene in mice results in increased bone formation and bone strength. *J Bone Miner Res.* 2008;23:860–869.
277. Loots GG, Kneissel M, Keller H, et al. Genomic deletion of a long-range bone enhancer misregulates sclerostin in Van Buchem disease. *Genome Res.* 2005;15:928–935.
278. Lin C, Jiang X, Dai Z, et al. Sclerostin mediates bone response to mechanical unloading through antagonizing Wnt/ β -catenin signaling. *J Bone Miner Res.* 2009;24:1651–1661.
279. Epstein S, Hamersma H, Beighton P. Endocrine function in sclerosteosis. *S Afr Med J.* 1979;55:1105–1110.
280. Cooper AR, Forbes RM, Mitchell HH. Further studies on the gross composition and mineral elements of the adult human body. *J Biol Chem.* 1956;223:969–975.
281. Forbes GB, Lewis AM. Total sodium, potassium and chloride in adult man. *J Clin Invest.* 1956;35:596–600.
282. Forbes RM, Cooper AR, Mitchell HH. The composition of the adult human body as determined by chemical analysis. *J Biol Chem.* 1953;203:359–366.
283. Forbes RM, Cooper AR, Mitchell HH. On the occurrence of beryllium, boron, cobalt, and mercury in human tissues. *J Biol Chem.* 1954;209:857–865.
284. Widdowson EM, Mc CR, Spray CM. The chemical composition of the human body. *Clin Sci.* 1951;10:113–125.
285. Widdowson EM, Spray CM. Chemical development in utero. *Arch Dis Child.* 1951;26:205–214.
286. Rude RK, Shils ME. Magnesium. In: Shils ME, ed. *Modern Nutrition in Health and Disease.* Philadelphia: Lippincott, Williams & Wilkins; 2006.
287. Cowan JA. Structural and catalytic chemistry of magnesium-dependent enzymes. *Biometals.* 2002;15:225–235.
288. Maguire ME, Cowan JA. Magnesium chemistry and biochemistry. *Biometals.* 2002;15:203–210.
289. Sreedhara A, Cowan JA. Structural and catalytic roles for divalent magnesium in nucleic acid biochemistry. *Biometals.* 2002;15:211–223.
290. Rude RK. Renal cortical adenylate cyclase: characterization of magnesium activation. *Endocrinology.* 1983;113:1348–1355.
291. Alfrey AC. Normal and abnormal magnesium metabolism. In: Schrier RW, ed. *Renal and Electrolyte Disorders.* Philadelphia: Lippincott-Raven; 1997:320–348.
292. Smith RH. Calcium and magnesium metabolism in calves; plasma levels and retention in milk-fed calves. *Biochem J.* 1957;67:472–481.
293. Smith RH. Calcium and magnesium metabolism in calves. 4. Bone composition in magnesium deficiency and the control of plasma magnesium. *Biochem J.* 1959;71:609–614.
294. Miller ER, Ullrey DE, Zutaut CL, et al. Magnesium requirement of the baby pig. *J Nutr.* 1965;85:13–20.
295. Chiemchaisri Y, Phillips PH. Certain factors including fluoride which affect magnesium calcinosis in the dog and rat. *J Nutr.* 1965;86:23–28.
296. Dunn MJ. Magnesium depletion in the rhesus monkey: induction of magnesium-dependent hypocalcemia. *Clin Sci.* 1971;41:333–344.
297. MacMannus J, Heaton FW. Effective magnesium deficiency on calcium homeostasis in the rat. *Clin Sci.* 1969;36:297–306.
298. Wiegmann T, Kaye M. Hypomagnesemic hypocalcemia. Early serum calcium and late parathyroid hormone increase with magnesium therapy. *Arch Intern Med.* 1977;137:953–955.
299. Buckle RM, Care AD, Cooper CW, et al. The influence of plasma magnesium concentration on parathyroid hormone secretion. *J Endocrinol.* 1968;42:529–534.
300. Sherwood LM, Herrman I, Bassett CA. Parathyroid hormone secretion in vitro: regulation by calcium and magnesium ions. *Nature.* 1970;225:1056–1058.
301. Chase LR, Slatopolsky E. Secretion and metabolic efficacy of parathyroid hormone in patients with severe hypomagnesemia. *J Clin Endocrinol Metab.* 1974;38:363–371.
302. Connor TB, Toskes P, Mahaffey J, et al. Parathyroid function during chronic magnesium deficiency. *Johns Hopkins Med J.* 1972;131:100–117.
303. Anast CS, Winnacker JL, Forte LR, et al. Impaired release of parathyroid hormone in magnesium deficiency. *J Clin Endocrinol Metab.* 1976;42:707–717.
304. Mennes P, Rosenbaum R, Martin K, et al. Hypomagnesemia and impaired parathyroid hormone secretion in chronic renal disease. *Ann Intern Med.* 1978;88:206–209.
305. Hall RC, Hoffman RS, Beresford TP, et al. Refractory hypokalemia secondary to hypomagnesemia in eating-disorder patients. *Psychosomatics.* 1988;29:435–438.
306. Juan D. Clinical review: the clinical importance of hypomagnesemia. *Surgery.* 1982;91:510–517.
307. Whang R. Magnesium deficiency: pathogenesis, prevalence, and clinical implications. *Am J Med.* 1987;82:24–29.
308. Whang R, Chrysant S, Dillard B, et al. Hypomagnesemia and hypokalemia in 1,000 treated ambulatory hypertensive patients. *J Am Coll Nutr.* 1982;1:317–322.
309. Krasner BS, Girdwood R, Smith H. The effect of slow releasing oral magnesium chloride on the QTc interval of the electrocardiogram during open heart surgery. *Can Anaesth Soc J.* 1981;28:329–333.
310. Davis WH, Ziady F. The effect of oral magnesium chloride therapy on the QTc and QUc intervals of the electrocardiogram. *S Afr Med J.* 1978;53:591–593.
311. Walser M. Ion association. VI. Interactions between calcium, magnesium, inorganic phosphate, citrate and protein in normal human plasma. *J Clin Invest.* 1961;40:723–730.
312. Chutkow JG. Studies on the metabolism of magnesium in the magnesium-deficient rat. *J Lab Clin Med.* 1965;65:912–926.
313. Welt LG, Gitelman H. Disorders of magnesium metabolism. *Dis Mon.* 1965;47(1965):1–32.
314. Alfrey AC, Miller NL, Trow R. Effect of age and magnesium depletion on bone magnesium pools in rats. *J Clin Invest.* 1974;54:1074–1081.
315. Alfrey AC, Miller NL, Butkus D. Evaluation of body magnesium stores. *J Lab Clin Med.* 1974;84:153–162.
316. Elin RJ. Assessment of magnesium status. *Clin Chem.* 1987;33:1965–1970.
317. Elin RJ. Status of the mononuclear blood cell magnesium assay. *J Am Coll Nutr.* 1987;6:105–107.

318. Elin RJ, Hosseini J. Serum magnesium and mononuclear blood cell magnesium. *Am Heart J*. 1987;113:1534–1535.
319. Food and Nutrition Board IoM. *Dietary Reference Intakes for Calcium, Phosphorus, Magnesium, Vitamin D and Fluoride*. Washington, DC: National Academy Press; 1997.
320. Hardwick LL, Jones MR, Brautbar N, et al. Site and mechanism of intestinal magnesium absorption. *Miner Electrolyte Metab*. 1990;16:174–180.
321. Hardwick LL, Jones MR, Brautbar N, et al. Magnesium absorption: mechanisms and the influence of vitamin D, calcium and phosphate. *J Nutr*. 1991;121:13–23.
322. Hardwick LL, Jones MR, Buddington RK, et al. Comparison of calcium and magnesium absorption: in vivo and in vitro studies. *Am J Physiol*. 1990;259:G720–G726.
323. Kayne LH, Lee DB. Intestinal magnesium absorption. *Miner Electrolyte Metab*. 1993;19:210–217.
324. Norman DA, Fordtran JS, Brinkley LJ, et al. Jejunal and ileal adaptation to alterations in dietary calcium: changes in calcium and magnesium absorption and pathogenetic role of parathyroid hormone and 1,25-dihydroxyvitamin D. *J Clin Invest*. 1981;67:1599–1603.
325. Quamme GA. Recent developments in intestinal magnesium absorption. *Curr Opin Gastroenterol*. 2008;24:230–235.
326. Voets T, Nilius B, Hoefs S, et al. TRPM6 forms the Mg²⁺ influx channel involved in intestinal and renal Mg²⁺ absorption. *J Biol Chem*. 2004;279:19–25.
327. Clark K, Langeslag M, van Leeuwen B, et al. TRPM7, a novel regulator of actomyosin contractility and cell adhesion. *EMBO J*. 2006;25:290–301.
328. Jin J, Desai BN, Navarro B, et al. Deletion of *Trpm7* disrupts embryonic development and thymopoiesis without altering Mg²⁺ homeostasis. *Science*. 2008;322:756–760.
329. Liu W, Su LT, Khadka DK, et al. TRPM7 regulates gastrulation during vertebrate embryogenesis. *Dev Biol*. 2011;350:348–357.
330. Overton JD, Komiya Y, Mezzacappa C, et al. Hepatocystin is essential for TRPM7 function during early embryogenesis. *Sci Rep*. 2015;5:18395.
331. Runnels LW. TRPM6 and TRPM7: A Mul-TRP-PLIK-cation of channel functions. *Curr Pharm Biotechnol*. 2011;12:42–53.
332. Schmitz C, Dorovkov MV, Zhao X, et al. The channel kinases TRPM6 and TRPM7 are functionally nonredundant. *J Biol Chem*. 2005;280:37763–37771.
333. Schmitz C, Perraud AL, Johnson CO, et al. Regulation of vertebrate cellular Mg²⁺ homeostasis by TRPM7. *Cell*. 2003;114:191–200.
334. Su LT, Agapito MA, Li M, et al. TRPM7 regulates cell adhesion by controlling the calcium-dependent protease calpain. *J Biol Chem*. 2006;281:11260–11270.
335. Su LT, Liu W, Chen HC, et al. TRPM7 regulates polarized cell movements. *Biochem J*. 2011;434:513–521.
336. Chubanov V, Waldegger S, Mederos y Schnitzler M, et al. Disruption of TRPM6/TRPM7 complex formation by a mutation in the TRPM6 gene causes hypomagnesemia with secondary hypocalcemia. *Proc Natl Acad Sci U S A*. 2004;101:2894–2899.
337. Chubanov V, Ferioli S, Wisnowsky A, et al. Epithelium magnesium transport by TRPM6 is essential for prenatal development and adult survival. *eLife*. 2016;5:5. doi:10.7554/eLife.20914.
338. Whang R, Welt LG. Observations in experimental magnesium depletion. *J Clin Invest*. 1963;42:305–313.
339. Kruse HD, Orent ER, McCollum EV. Studies of magnesium deficiency and animals. I. Symptomatology resulting from magnesium deprivation. *J Biol Chem*. 1932;96:519.
340. Tufts EV, Greenberg DM. The biochemistry of magnesium deficiency. I. Chemical changes resulting from magnesium deprivation. *J Biol Chem*. 1937;38:122:693.
341. Greenberg DM, Lucia SP, Tufts EV. The effect of magnesium deprivation on renal function. *Am J Physiol*. 1938;121:424.
342. Barron GP, Brown SO, Pearson PB. Histological manifestations of a magnesium deficiency in rat and rabbit. *Proc Soc Exp Biol (NY)*. 1949;70:220.
343. Lowenhaupt E, Schulman MP, Greenberg DM. Basic histologic lesions of magnesium deficiency in the rat. *Am J Physiol*. 1950;49:427.
344. Cotlove E, Holliday MA, Schwartz R, et al. Effects of electrolyte depletion and acid-base disturbance on muscle cations. *Am J Physiol*. 1951;167:665–675.
345. Macintyre I, Davidsson D. The production of secondary potassium depletion, sodium retention, nephrocalcinosis and hypercalcaemia by magnesium deficiency. *Biochem J*. 1958;70:456–462.
346. O'Dell BL. Magnesium requirement and its relation to other dietary constituents. *Fed Proc*. 1960;19:648–654.
347. Barnes BA, Cope O, Harrison T. Magnesium conservation in the human being on a low magnesium diet. *J Clin Invest*. 1958;37:430–440.
348. Etteldorf JN, Clayton GW, Tuttle AH, et al. Renal function studies in pediatrics. II. Influence of magnesium sulfate on renal hemodynamics in normal children. *AMA Am J Dis Child*. 1952;83:301–305.
349. Harris JS, De MW. Effects of magnesium sulfate on the renal dynamics of normal dogs. *Am J Physiol*. 1951;166:199–201.
350. Heller BI, Hammarsten JF, Stutzman FL. Concerning the effects of magnesium sulfate on renal function, electrolyte excretion, and clearance of magnesium. *J Clin Invest*. 1953;32:858–861.
351. Shils ME, Rude RK. Deliberations and evaluations of the approaches, endpoints and paradigms for magnesium dietary recommendations. *J Nutr*. 1996;126:2398S–403S.
352. Ryan MF. The role of magnesium in clinical biochemistry: an overview. *Ann Clin Biochem*. 1991;28(Pt 1):19–26.
353. Brunette MG, Vigneault N, Carriere S. Micropuncture study of magnesium transport along the nephron in the young rat. *Am J Physiol*. 1974;227(4):891–896.
354. Gunzel D, Yu AS. Function and regulation of claudins in the thick ascending limb of Henle. *Pflugers Arch*. 2009;458:77–88.
355. Blanchard A, Jeunemaitre X, Coudol P, et al. Paracellin-1 is critical for magnesium and calcium reabsorption in the human thick ascending limb of Henle. *Kidney Int*. 2001;59:2206–2215.
356. Lee CT, Lien YH, Lai LW, et al. Increased renal calcium and magnesium transporter abundance in streptozotocin-induced diabetes mellitus. *Kidney Int*. 2006;69:1786–1791.
357. Lee DB, Huang E, Ward HJ. Tight junction biology and kidney dysfunction. *Am J Physiol Renal Physiol*. 2006;290:F20–F34.
358. Schmitz C, Deason F, Perraud AL. Molecular components of vertebrate Mg²⁺-homeostasis regulation. *Magnes Res*. 2007;20:6–18.
359. Simon DB, Lu Y, Choate KA, et al. Paracellin-1, a renal tight junction protein required for paracellular Mg²⁺ resorption. *Science*. 1999;285:103–106.
360. Staiger K, Staiger H, Haas C, et al. Hypomagnesemia and nephrocalcinosis in a patient with two heterozygous mutations in the *CLDN16* gene. *J Nephrol*. 2007;20:107–110.
361. Weber S, Schneider L, Peters M, et al. Novel paracellin-1 mutations in 25 families with familial hypomagnesemia with hypercalciuria and nephrocalcinosis. *J Am Soc Nephrol*. 2001;12:1872–1881.
362. Milatz S, Himmerkus N, Wulfmeyer VC, et al. Mosaic expression of claudins in thick ascending limbs of Henle results in spatial separation of paracellular Na⁺ and Mg²⁺ transport. *Proc Natl Acad Sci U S A*. 2017;114(2):E219–E227. 28028216. PMID:.
363. Breiderhoff T, Himmerkus N, Stuijver M, et al. Deletion of claudin-10 (*Cldn10*) in the thick ascending limb impairs paracellular sodium permeability and leads to hypermagnesemia and nephrocalcinosis. *Proc Natl Acad Sci U S A*. 2012;109:14241–14246.
364. Klar J, Piontek J, Milatz S, et al. Altered paracellular cation permeability due to a rare *CLDN10B* variant causes anhidrosis and kidney damage. *PLoS Genet*. 2017;13(7):e1006897. Jul 7, 28686597. PMID:.
365. Bongers EMHF, Shelton LM, Milatz S, et al. A novel hypokalemic-alkalotic salt-losing tubulopathy in patients with *CLDN10* mutations. *J Am Soc Nephrol*. 2017;28(10):3118–3128.
366. Hadj-Rabia S, Brideau G, Al-Sarraj Y, et al. Multiplex epithelium dysfunction due to *CLDN10* mutation: the HELIX syndrome. *Genet Med*. 2018;20(2):190–201.
367. Quamme GA, Dirks JH. Intraluminal and contraluminal magnesium on magnesium and calcium transfer in the rat nephron. *Am J Physiol*. 1980;238:F187–F198.
368. Carney SL, Wong NL, Quamme GA, et al. Effect of magnesium deficiency on renal magnesium and calcium transport in the rat. *J Clin Invest*. 1980;65:180–188.
369. Groenestege WM, Thebault S, van der Wijst J, et al. Impaired basolateral sorting of pro-EGF causes isolated recessive renal hypomagnesemia. *J Clin Invest*. 2007;117:2260–2267.
370. Glaudemans B, van der Wijst J, Scola RH, et al. A missense mutation in the *Kvl.1* voltage-gated potassium channel-encoding gene *KCNAL1* is linked to human autosomal dominant hypomagnesemia. *J Clin Invest*. 2009;119:936–942.
371. Stuijver M, Lainez S, Will C, et al. *CNNM2*, encoding a basolateral protein required for renal Mg²⁺ handling, is mutated in dominant hypomagnesemia. *Am J Hum Genet*. 2011;88:333–343.

372. Goytain A, Quamme GA. Functional characterization of ACDP2 (ancient conserved domain protein), a divalent metal transporter. *Physiol Genomics*. 2005;22:382.
373. Stuijver M, Lainez S, Will C, et al. CNNM2, encoding a basolateral protein required for renal Mg²⁺ handling, is mutated in dominant hypomagnesemia. *Am J Hum Genet*. 2011;88:333.
374. Sponder G, Mastrototaro L, Kurth K, et al. Human CNNM2 is not a Mg(2+) transporter per se. *Pflugers Arch*. 2016;468:1223–1240.
375. Goytain A, Quamme GA. Functional characterization of human SLC41A1, a Mg²⁺ transporter with similarity to prokaryotic MgtE Mg²⁺ transporters. *Physiol Genomics*. 2005;21:337–342.
376. Kolisek M, Nestler A, Vormann J, et al. Human gene SLC41A1 encodes for the Na⁺/Mg²⁺ exchanger. *Am J Physiol Cell Physiol*. 2012;302:C318–C326.
377. Hurd TW, Otto EA, Mishima E, et al. Mutation of the Mg²⁺ transporter SLC41A1 results in a nephronophthisis-like phenotype. *J Am Soc Nephrol*. 2013;24(6):967–977.
378. Ferre S, de Baaij JH, Ferreira P, et al. Mutations in PCBD1 cause hypomagnesemia and renal magnesium wasting. *J Am Soc Nephrol*. 2014;25:574–586.
379. Adalat S, Woolf AS, Johnstone KA, et al. HNF1B mutations associate with hypomagnesemia and renal magnesium wasting. *J Am Soc Nephrol*. 2009;20:1123–1131.
380. Bockenbauer D, Feather S, Stanescu HC, et al. Epilepsy, ataxia, sensorineural deafness, tubulopathy, and KCNJ10 mutations. *N Engl J Med*. 2009;360:1960–1970.
381. Scholl UI, Choi M, Liu T, et al. Seizures, sensorineural deafness, ataxia, mental retardation, and electrolyte imbalance (SeSAME syndrome) caused by mutations in KCNJ10. *Proc Natl Acad Sci U S A*. 2009;106:5842–5847.
382. Dai LJ, Ritchie G, Kerstan D, et al. Magnesium transport in the renal distal convoluted tubule. *Physiol Rev*. 2001;81:51–84.
383. Burnatowska MA, Harris CA, Sutton RA, et al. Effects of PTH and cAMP on renal handling of calcium, magnesium, and phosphate in the hamster. *Am J Physiol*. 1977;233:F514–F518.
384. Carney S, Thompson L. Effect of differing concentrations of parathyroid hormone on rat renal electrolyte excretion. *Am J Physiol*. 1982;243:F514–F517.
385. de Rouffignac C, Mandon B, Wittner M, et al. Hormonal control of renal magnesium handling. *Miner Electrolyte Metab*. 1993;19:226–231.
386. Wittner M, Mandon B, Roinel N, et al. Hormonal stimulation of Ca²⁺ and Mg²⁺ transport in the cortical thick ascending limb of Henle's loop of the mouse: evidence for a change in the paracellular pathway permeability. *Pflugers Arch*. 1993;423:387–396.
387. Carney SL. Comparison of parathyroid hormone and calcitonin on rat renal calcium and magnesium transport. *Clin Exp Pharmacol Physiol*. 1992;19:433–438.
388. Carney SL. Acute effect of endogenous calcitonin on rat renal function. *Miner Electrolyte Metab*. 1995;21:411–416.
389. Clark JD, Kenny AD. Hog thyrocalcitonin in the dog: urinary calcium, phosphorus, magnesium and sodium responses. *Endocrinology*. 1969;84:1199–1205.
390. Poujeol P, Touvay C, Roinel N, et al. Stimulation of renal magnesium reabsorption by calcitonin in the rat. *Am J Physiol*. 1980;239:F524–F532.
391. Quamme GA. Effect of calcitonin on calcium and magnesium transport in rat nephron. *Am J Physiol*. 1980;238:E573–E578.
392. Quamme GA. Renal handling of magnesium: drug and hormone interactions. *Magnesium*. 1986;5:248–272.
393. Quamme GA. Control of magnesium transport in the thick ascending limb. *Am J Physiol*. 1989;256:F197–F210.
394. Rasmussen H, Anast C, Arnaud C. Thyrocalcitonin, EGTA, and urinary electrolyte excretion. *J Clin Invest*. 1967;46:746–752.
395. Roy DR. Acute effect of salmon calcitonin on renal magnesium transport in the magnesium-loaded rat. *Can J Physiol Pharmacol*. 1986;64:66–71.
396. Bailly C, Amiel C. Effect of glucagon on magnesium renal reabsorption in the rat. *Pflugers Arch*. 1982;392:360–365.
397. Bailly C, Roinel N, Amiel C. PTH-like glucagon stimulation of Ca and Mg reabsorption in Henle's loop of the rat. *Am J Physiol*. 1984;246:F205–F212.
398. Carney SL, Gillies AH, Ray CD. Acute effect of physiological concentrations of vasopressin on rat renal function. *Clin Exp Pharmacol Physiol*. 1993;20:113–119.
399. Mandon B, Siga E, Chabardes D, et al. Insulin stimulates Na⁺, Cl⁻, Ca²⁺, and Mg²⁺ transports in TAL of mouse nephron: cross-potential with AVP. *Am J Physiol*. 1993;265:F361–F369.
400. Roman RJ, Skelton M, Lechene C. Prostaglandin-vasopressin interactions on the renal handling of calcium and magnesium. *J Pharmacol Exp Ther*. 1984;230:295–301.
401. Burnatowska MA, Harris CA, Sutton RA, et al. Effects of vitamin D on renal handling of calcium, magnesium and phosphate in the hamster. *Kidney Int*. 1985;27:864–870.
402. Marone CC, Sutton RA. Effects of acute metabolic acid-base changes and furosemide on magnesium excretion in rats. *Metabolism*. 1983;32:1033–1037.
403. Roy DR, Blouch KL, Jamison RL. Effects of acute acid-base disturbances on renal tubule reabsorption of magnesium in the rat. *Am J Physiol*. 1982;243:F197–F203.
404. Quamme GA. Effect of hypercalcemia on renal tubular handling of calcium and magnesium. *Can J Physiol Pharmacol*. 1982;60:1275–1280.
405. Dai LJ, Friedman PA, Quamme GA. Phosphate depletion diminishes Mg²⁺ uptake in mouse distal convoluted tubule cells. *Kidney Int*. 1997;51:1710–1718.
406. Wong NL, Quamme GA, O'Callaghan TJ, et al. Renal tubular transport in phosphate depletion: a micropuncture study. *Can J Physiol Pharmacol*. 1980;58:1063–1071.
407. Dai LJ, Friedman PA, Quamme GA. Cellular mechanisms of chlorothiazide and cellular potassium depletion on Mg²⁺ uptake in mouse distal convoluted tubule cells. *Kidney Int*. 1997;51:1008–1017.
408. Bundy JT, Connito D, Mahoney MD, et al. Treatment of idiopathic renal magnesium wasting with amiloride. *Am J Nephrol*. 1995;15:75–77.
409. Dai LJ, Raymond L, Friedman PA, et al. Mechanisms of amiloride stimulation of Mg²⁺ uptake in immortalized mouse distal convoluted tubule cells. *Am J Physiol*. 1997;272:F249–F256.
410. Quamme GA. Renal magnesium handling: new insights in understanding old problems. *Kidney Int*. 1997;52:1180–1195.
411. Neuman WF. Bone material and calcification mechanisms. In: Urist MR, ed. *Fundamental and Clinical Bone Physiology*. Philadelphia: Lippincott; 1980:83–107.
412. Cohen P. The structure and regulation of protein phosphatases. *Annu Rev Biochem*. 1989;58:453–508.
413. Hubbard SR, Till JH. Protein tyrosine kinase structure and function. *Annu Rev Biochem*. 2000;69:373–398.
414. Hunter T, Cooper JA. Protein-tyrosine kinases. *Annu Rev Biochem*. 1985;54:897–930.
415. Knochel JP. The clinical and physiological implications of phosphorus deficiency. In: Giebisch, ed. *The Kidney: Physiology and Pathophysiology*. New York: Raven Press, Ltd.; 1992:2533.
416. Knochel JP. The pathophysiology and clinical characteristics of severe hypophosphatemia. *Arch Intern Med*. 1977;137:203–220.
417. Knochel JP, Barcenas C, Cotton JR, et al. Hypophosphatemia and rhabdomyolysis. *Trans Assoc Am Physicians*. 1978;91:156–168.
418. Diem K, Lentner C. *Geigy Scientific Tables*. 7th ed. New York: Geigy Pharmaceuticals; 1970.
419. Berndt T, Kumar R. Phosphatonins and the regulation of phosphate homeostasis. *Annu Rev Physiol*. 2007;69:341–359.
420. Berndt T, Kumar R. Novel mechanisms in the regulation of phosphorus homeostasis. *Physiology (Bethesda)*. 2009;24:17–25.
421. Berndt T, Thomas LF, Craig TA, et al. Evidence for a signaling axis by which intestinal phosphate rapidly modulates renal phosphate reabsorption. *Proc Natl Acad Sci U S A*. 2007;104:11085–11090.
422. Nishida Y, Taketani Y, Yamanaka-Okumura H, et al. Acute effect of oral phosphate loading on serum fibroblast growth factor 23 levels in healthy men. *Kidney Int*. 2006;70:2141–2147.
423. Berndt TJ, Kumar R. Clinical disturbances of phosphate homeostasis. In: Alpern RJ, Hebert SC, eds. *Seldin and Giebisch's The Kidney*. New York: Academic Press/Elsevier; 2008:1989–2006.
424. Berndt T, Craig TA, Bowe AE, et al. Secreted frizzled-related protein 4 is a potent tumor-derived phosphaturic agent. *J Clin Invest*. 2003;112:785–794.
425. Berndt TJ, Bielez B, Craig TA, et al. Secreted frizzled-related protein-4 reduces sodium-phosphate co-transporter abundance and activity in proximal tubule cells. *Pflugers Arch*. 2006;451:579–587.
426. Berndt TJ, Schiavi S, Kumar R. "Phosphatonins" and the regulation of phosphorus homeostasis. *Am J Physiol Renal Physiol*. 2005;289:F1170–F1182.

427. Bowe AE, Finnegan R, Jan de Beur SM, et al. FGF-23 inhibits renal tubular phosphate transport and is a PHEX substrate. *Biochem Biophys Res Commun.* 2001;284:977–981.
428. De Beur SM, Finnegan RB, Vassiliadis J, et al. Tumors associated with oncogenic osteomalacia express genes important in bone and mineral metabolism. *J Bone Miner Res.* 2002;17:1102–1110.
429. Jan de Beur SM, Finnegan RB, Vassiliadis J, et al. Tumors associated with oncogenic osteomalacia express genes important in bone and mineral metabolism. *J Bone Miner Res.* 2002;17:1102–1110.
430. Schiavi SC, Kumar R. The phosphatonin pathway: new insights in phosphate homeostasis. *Kidney Int.* 2004;65:1–14.
431. Berndt TJ, Craig TA, McCormick DJ, et al. Biological activity of FGF-23 fragments. *Pflugers Arch.* 2007;454:615–623.
432. Shaikh A, Berndt T, Kumar R. Regulation of phosphate homeostasis by the phosphatonins and other novel mediators. *Pediatr Nephrol.* 2008.
433. Larsson T, Marsell R, Schipani E, et al. Transgenic mice expressing fibroblast growth factor 23 under the control of the alpha1(I) collagen promoter exhibit growth retardation, osteomalacia, and disturbed phosphate homeostasis. *Endocrinology.* 2004;145:3087–3094.
434. Shimada T, Hasegawa H, Yamazaki Y, et al. FGF-23 is a potent regulator of vitamin D metabolism and phosphate homeostasis. *J Bone Miner Res.* 2004;19:429–435.
435. Itami A, Kato M, Komoto I, et al. Human gastrinoma cells express calcium-sensing receptor. *Life Sci.* 2001;70:119–129.
436. Shimada T, Kakitani M, Hasegawa H, et al. Targeted ablation of FGF-23 causes hyperphosphatemia, increased 1,25-dihydroxyvitamin D levels and severe growth retardation. *J Bone Miner Res.* 2002;17(suppl 1):S168.
437. Perwad F, Zhang MY, Tenenhouse HS, et al. Fibroblast growth factor 23 impairs phosphorus and vitamin D metabolism in vivo and suppresses 25-hydroxyvitamin D-1alpha-hydroxylase expression in vitro. *Am J Physiol Renal Physiol.* 2007;293:F1577–F1583.
438. Berndt T, Bielez B, Craig TA, et al. Secreted frizzled-related protein-4 reduces sodium-phosphate co-transporter abundance and activity in proximal tubule cells. *Pflugers Arch.* 2006;451:579–587.
439. Cai Q, Hodgson SF, Kao PC, et al. Brief report: inhibition of renal phosphate transport by a tumor product in a patient with oncogenic osteomalacia. *N Engl J Med.* 1994;330:1645–1649.
440. Econs MJ, Drezner MK. Tumor-induced osteomalacia—unveiling a new hormone. *N Engl J Med.* 1994;330:1679–1681.
441. Shimada T, Mizutani S, Muto T, et al. Cloning and characterization of FGF23 as a causative factor of tumor-induced osteomalacia. *Proc Natl Acad Sci U S A.* 2001;98:6500–6505.
442. Kumar R. The phosphatonins and the regulation of phosphate homeostasis. *Ann Endocrinol (Paris).* 2006;67:142–146.
443. Jonsson KB, Zahradnik R, Larsson T, et al. Fibroblast growth factor 23 in oncogenic osteomalacia and X-linked hypophosphatemia. *N Engl J Med.* 2003;348:1656–1663.
444. Ferrari SL, Bonjour JP, Rizzoli R. FGF-23 relationship to dietary phosphate and renal phosphate handling in healthy young men. *J Clin Endocrinol Metab.* 2004.
445. Burnett SM, Gunawardene SC, Bringhurst FR, et al. Regulation of C-terminal and intact FGF-23 by dietary phosphate in men and women. *J Bone Miner Res.* 2006;21:1187–1196.
446. Perwad F, Azam N, Zhang MY, et al. Dietary and serum phosphorus regulate fibroblast growth factor 23 expression and 1,25-dihydroxyvitamin D metabolism in mice. *Endocrinology.* 2005;146:5358–5364.
447. Berndt T, Knox FG, eds. *Renal Regulation of Phosphate Excretion.* 2nd ed. New York: Raven Press, Ltd.; 1992.
448. Haramati A, Haas JA, Knox FG. Adaptation of deep and superficial nephrons to changes in dietary phosphate intake. *Am J Physiol.* 1983;244:F265–F269.
449. Awazu M, Berndt TJ, Knox FG. Effect of phosphate infusion on proximal tubule phosphate reabsorption in phosphate-depleted and respiratory alkalotic rats. *Miner Electrolyte Metab.* 1987;13:393–396.
450. Goldfarb S, Beck LH, Agus ZS, et al. Dissociation of tubular sites of action of saline, PTH and DbCAMP on renal phosphate reabsorption. *Nephron.* 1978;21:221–229.
451. Greger R, Lang F, Marchand G, et al. Site of renal phosphate reabsorption. Microperfusion and microinfusion study. *Pflugers Arch.* 1977;369:111–118.
452. Haramati A, Haas JA, Knox FG. Nephron heterogeneity of phosphate reabsorption: effect of parathyroid hormone. *Am J Physiol.* 1984;246:F155–F158.
453. Harris CA, Burnatowska MA, Seely JF, et al. Effects of parathyroid hormone on electrolyte transport in the hamster nephron. *Am J Physiol.* 1979;236:F342–F348.
454. Knox FG, Haas JA, Berndt T, et al. Phosphate transport in superficial and deep nephrons in phosphate-loaded rats. *Am J Physiol.* 1977;233:F150–F153.
455. Rybczynska A, Hoppe A, Knox FG. Effect of propranolol on phosphate reabsorption by superficial nephron segments in response to parathyroid hormone in phosphate-depleted rats. *J Am Soc Nephrol.* 1990;1:200–204.
456. Strickler JC, Thompson DD, Klose RM, et al. Micropuncture study of inorganic phosphate excretion in the rat. *J Clin Invest.* 1964;43:1596–1607.
457. Dennis VW, Woodhall PB, Robinson RR. Characteristics of phosphate transport in isolated proximal tubule. *Am J Physiol.* 1976;231:979–985.
458. Berndt TJ, Knox FG. Nephron site of resistance to phosphaturic effect of PTH during respiratory alkalosis. *Am J Physiol.* 1985;249:F919–F922.
459. Bacic D, Wagner CA, Hernando N, et al. Novel aspects in regulated expression of the renal type IIa Na/Pi-cotransporter. *Kidney Int Suppl.* 2004;S5–S12.
460. Biber J, Custer M, Magagnin S, et al. Renal Na/Pi-cotransporters. *Kidney Int.* 1996;49:981–985.
461. Biber J, Custer M, Werner A, et al. Localization of NaPi-1, a Na/Pi cotransporter, in rabbit kidney proximal tubules. II. Localization by immunohistochemistry. *Pflugers Arch.* 1993;424:210–215.
462. Biber J, Murer H. A molecular view of renal Na-dependent phosphate transport. *Ren Physiol Biochem.* 1994;17:212–215.
463. Biber J, Murer H, Forster I. The renal type II Na⁺/phosphate cotransporter. *J Bioenerg Biomembr.* 1998;30:187–194.
464. Custer M, Meier F, Schlatter E, et al. Localization of NaPi-1, a Na-Pi cotransporter, in rabbit kidney proximal tubules. I. mRNA localization by reverse transcription/polymerase chain reaction. *Pflugers Arch.* 1993;424:203–209.
465. Karim-Jimenez Z, Hernando N, Biber J, et al. A dibasic motif involved in parathyroid hormone-induced down-regulation of the type IIa NaPi cotransporter. *Proc Natl Acad Sci U S A.* 2000;97:12896–12901.
466. Lambert G, Traebert M, Hernando N, et al. Studies on the topology of the renal type II NaPi-cotransporter. *Pflugers Arch.* 1999;437:972–978.
467. Murer H. Homer Smith Award. Cellular mechanisms in proximal tubular Pi reabsorption: some answers and more questions. *J Am Soc Nephrol.* 1992;2:1649–1665.
468. Murer H, Biber J. Control of proximal tubular apical Na/Pi cotransport. *Exp Nephrol.* 1996;4:201–204.
469. Murer H, Biber J. Membrane traffic and control of proximal tubular sodium phosphate (Na/Pi)-cotransport. *Wien Klin Wochenschr.* 1997;109:441–444.
470. Murer H, Biber J. Molecular mechanisms of renal apical Na/phosphate cotransport. *Annu Rev Physiol.* 1996;58:607–618.
471. Murer H, Biber J. Renal sodium-phosphate cotransport. *Curr Opin Nephrol Hypertens.* 1994;3:504–510.
472. Murer H, Forster I, Hilfiker H, et al. Cellular/molecular control of renal Na/Pi-cotransport. *Kidney Int Suppl.* 1998;65:S2–S10.
473. Murer H, Hernando N, Forster I, et al. Molecular aspects in the regulation of renal inorganic phosphate reabsorption: the type IIa sodium/inorganic phosphate co-transporter as the key player. *Curr Opin Nephrol Hypertens.* 2001;10:555–561.
474. Murer H, Hernando N, Forster I, et al. Proximal tubular phosphate reabsorption: molecular mechanisms. *Physiol Rev.* 2000;80:1373–1409.
475. Murer H, Lotscher M, Kaissling B, et al. Molecular mechanisms in the regulation of renal proximal tubular Na/phosphate cotransport. *Kidney Blood Press Res.* 1996;19:151–154.
476. Pfister MF, Forgo J, Ziegler U, et al. cAMP-dependent and -independent downregulation of type II Na-Pi cotransporters by PTH. *Am J Physiol.* 1999;276:F720–F725.
477. Pfister MF, Lederer E, Forgo J, et al. Parathyroid hormone-dependent degradation of type II Na⁺/Pi cotransporters. *J Biol Chem.* 1997;272:20125–20130.

478. Pfister MF, Ruf I, Stange G, et al. Parathyroid hormone leads to the lysosomal degradation of the renal type II Na/Pi cotransporter. *Proc Natl Acad Sci U S A*. 1998;95:1909–1914.
479. Traebert M, Roth J, Biber J, et al. Internalization of proximal tubular type II Na-P(i) cotransporter by PTH: immunogold electron microscopy. *Am J Physiol Renal Physiol*. 2000;278:F148–F154.
480. Traebert M, Volkl H, Biber J, et al. Luminal and contraluminal action of 1-34 and 3-34 PTH peptides on renal type IIa Na-P(i) cotransporter. *Am J Physiol Renal Physiol*. 2000;278:F792–F798.
481. Werner A, Kempson SA, Biber J, et al. Increase of Na/Pi-cotransport encoding mRNA in response to low Pi diet in rat kidney cortex. *J Biol Chem*. 1994;269:6637–6639.
482. Werner A, Moore ML, Mantei N, et al. Cloning and expression of cDNA for a Na/Pi cotransport system of kidney cortex. *Proc Natl Acad Sci U S A*. 1991;88:9608–9612.
483. Beck L, Karaplis AC, Amizuka N, et al. Targeted inactivation of Npt2 in mice leads to severe renal phosphate wasting, hypercalciuria, and skeletal abnormalities. *Proc Natl Acad Sci U S A*. 1998;95:5372–5377.
484. Prie D, Huart V, Bakouh N, et al. Nephrolithiasis and osteoporosis associated with hypophosphatemia caused by mutations in the type 2a sodium-phosphate cotransporter. *N Engl J Med*. 2002;347:983–991.
485. Hoag HM, Martel J, Gauthier C, et al. Effects of Npt2 gene ablation and low-phosphate diet on renal Na(+)/phosphate cotransport and cotransporter gene expression. *J Clin Invest*. 1999;104:679–686.
486. Myakala K, Motta S, Murer H, et al. Renal-specific and inducible depletion of NaPi-IIc/Slc34a3, the cotransporter mutated in HHRH, does not affect phosphate or calcium homeostasis in mice. *Am J Physiol Renal Physiol*. 2014;306:F833–F843.
487. Segawa H, Onitsuka A, Furutani J, et al. Npt2a and Npt2c in mice play distinct and synergistic roles in inorganic phosphate metabolism and skeletal development. *Am J Physiol Renal Physiol*. 2009;297:F671–F678.
488. Bergwitz C, Roslin NM, Tieder M, et al. SLC34A3 mutations in patients with hereditary hypophosphatemic rickets with hypercalciuria predict a key role for the sodium-phosphate cotransporter NaPi-IIc in maintaining phosphate homeostasis. *Am J Hum Genet*. 2006;78:179–192.
489. Lorenz-Depiereux B, Benet-Pages A, Eckstein G, et al. Hereditary hypophosphatemic rickets with hypercalciuria is caused by mutations in the sodium-phosphate cotransporter gene SLC34A3. *Am J Hum Genet*. 2006;78:193–201.
490. Ansermet C, Moor MB, Centeno G, et al. Renal Fanconi syndrome and hypophosphatemic rickets in the absence of xenotropic and polytropic retroviral receptor in the nephron. *J Am Soc Nephrol*. 2017;28:1073–1078.
491. Capuano P, Bacic D, Roos M, et al. Defective coupling of apical PTH receptors to phospholipase C prevents internalization of the Na⁺-phosphate cotransporter NaPi-IIa in Nherf1-deficient mice. *Am J Physiol Cell Physiol*. 2007;292:C927–C934.
492. Cunningham R, Biswas R, Brazie M, et al. Signaling pathways utilized by PTH and dopamine to inhibit phosphate transport in mouse renal proximal tubule cells. *Am J Physiol Renal Physiol*. 2009;296:F355–F361.
493. Cunningham R, Steplock D, Wang F, et al. Defective parathyroid hormone regulation of NHE3 activity and phosphate adaptation in cultured NHERF-1^{-/-} renal proximal tubule cells. *J Biol Chem*. 2004;279:37815–37821.
494. Evan AP, Weinman EJ, Wu XR, et al. Comparison of the pathology of interstitial plaque in human ICSF stone patients to NHERF-1 and THP-null mice. *Urol Res*. 2010;38:439–452.
495. Hernando N, Deliot N, Gisler SM, et al. PDZ-domain interactions and apical expression of type IIa Na/P(i) cotransporters. *Proc Natl Acad Sci U S A*. 2002;99:11957–11962.
496. Shenolikar S, Voltz JW, Cunningham R, et al. Regulation of ion transport by the NHERF family of PDZ proteins. *Physiology (Bethesda)*. 2004;19:362–369.
497. Shenolikar S, Voltz JW, Minkoff CM, et al. Targeted disruption of the mouse NHERF-1 gene promotes internalization of proximal tubule sodium-phosphate cotransporter type IIa and renal phosphate wasting. *Proc Natl Acad Sci U S A*. 2002;99:11470–11475.
498. Wade JB, Welling PA, Donowitz M, et al. Differential renal distribution of NHERF isoforms and their colocalization with NHE3, ezrin, and ROMK. *Am J Physiol Cell Physiol*. 2001;280:C192–C198.
499. Weinman EJ, Biswas R, Steplock D, et al. Increased renal dopamine and acute renal adaptation to a high-phosphate diet. *Am J Physiol Renal Physiol*. 2011;300:F1123–F1129.
500. Weinman EJ, Biswas RS, Peng G, et al. Parathyroid hormone inhibits renal phosphate transport by phosphorylation of serine 77 of sodium-hydrogen exchanger regulatory factor-1. *J Clin Invest*. 2007;117:3412–3420.
501. Weinman EJ, Biswas RS, Peng G, et al. Parathyroid hormone inhibits renal phosphate transport by phosphorylation of serine 77 of sodium-hydrogen exchanger regulatory factor-1. *J Clin Invest*. 2007;117:3412–3420.
502. Weinman EJ, Boddeti A, Cunningham R, et al. NHERF-1 is required for renal adaptation to a low-phosphate diet. *Am J Physiol Renal Physiol*. 2003;285:F1225–F1232.
503. Weinman EJ, Eknayan G. Chronic effects of chlorothiazide on reabsorption by the proximal tubule of the rat. *Clin Sci Mol Med*. 1975;49:107–113.
504. Weinman EJ, Hall RA, Friedman PA, et al. The association of NHERF adaptor proteins with G protein-coupled receptors and receptor tyrosine kinases. *Annu Rev Physiol*. 2006;68:491–505.
505. Weinman EJ, Hall RA, Friedman PA, et al. The association of NHERF adaptor proteins with G protein-coupled receptors and receptor tyrosine kinases. *Annu Rev Physiol*. 2006;68:491–505.
506. Weinman EJ, Lederer ED. NHERF-1 and the regulation of renal phosphate reabsorption: a tale of three hormones. *Am J Physiol Renal Physiol*. 2012;303:F321–F327.
507. Weinman EJ, Shenolikar S. The Na-H exchanger regulatory factor. *Exp Nephrol*. 1997;5:449–452.
508. Weinman EJ, Shenolikar S, Cragoe EJ Jr, et al. Solubilization and reconstitution of renal brush border Na⁺-H⁺ exchanger. *J Membr Biol*. 1988;101:1–9.
509. Weinman EJ, Steplock D, Shenolikar S. NHERF-1 uniquely transduces the cAMP signals that inhibit sodium-hydrogen exchange in mouse renal apical membranes. *FEBS Lett*. 2003;536:141–144.
510. Weinman EJ, Steplock D, Tate K, et al. Structure-function of recombinant Na/H exchanger regulatory factor (NHE-RF). *J Clin Invest*. 1998;101:2199–2206.
511. Ketchem CJ, Khundmiri SJ, Gaweda AE, et al. Role of Na⁺/H⁺ exchanger regulatory factor 1 in forward trafficking of the type IIa Na⁺-Pi cotransporter. *Am J Physiol Renal Physiol*. 2015;309:F109–F119.
512. Khundmiri SJ, Ahmad A, Bennett RE, et al. Novel regulatory function for NHERF-1 in Npt2a transcription. *Am J Physiol Renal Physiol*. 2008;294:F840–F849.
513. Salyer S, Lesousky N, Weinman EJ, et al. Dopamine regulation of Na⁺-K⁺-ATPase requires the PDZ-2 domain of sodium hydrogen regulatory factor-1 (NHERF-1) in opossum kidney cells. *Am J Physiol Cell Physiol*. 2011;300:C425–C434.
514. Weinman EJ, Lederer ED. PTH-mediated inhibition of the renal transport of phosphate. *Exp Cell Res*. 2012;318:1027–1032.
515. Hatano R, Fujii E, Segawa H, et al. Ezrin, a membrane cytoskeletal cross-linker, is essential for the regulation of phosphate and calcium homeostasis. *Kidney Int*. 2013;83:41–49.
516. Kawaguchi K, Yoshida S, Hatano R, et al. Pathophysiological roles of ezrin/radixin/moesin proteins. *Biol Pharm Bull*. 2017;40:381–390.
517. Barrett PQ, Gertner JM, Rasmussen H. Effect of dietary phosphate on transport properties of pig renal microvillus vesicles. *Am J Physiol*. 1980;239:F352–F359.
518. Caverzasio J, Bonjour JP. Mechanism of rapid phosphate (Pi) transport adaptation to a single low Pi meal in rat renal brush border membrane. *Pflugers Arch*. 1985;404:227–231.
519. Caverzasio J, Danisi G, Straub RW, et al. Adaptation of phosphate transport to low phosphate diet in renal and intestinal brush border membrane vesicles: influence of sodium and pH. *Pflugers Arch*. 1987;409:333–336.
520. Caverzasio J, Murer H, Fleisch H, et al. Phosphate transport in brush border membrane vesicles isolated from renal cortex of young growing and adult rats. Comparison with whole kidney data. *Pflugers Arch*. 1982;394:217–221.
521. Haramati A, Knox FG. Relationship between plasma phosphate and renal handling of phosphate: studies with low phosphate diet and nicotinamide. *Adv Exp Med Biol*. 1982;151:41–46.
522. Levine BS, Ho K, Hodsman A, et al. Early renal brush border membrane adaptation to dietary phosphorus. *Miner Electrolyte Metab*. 1984;10:222–227.

523. Levine BS, Ho LD, Pasiecznik K, et al. Renal adaptation to phosphorus deprivation: characterization of early events. *J Bone Miner Res.* 1986;1:33–40.
524. Muhlbauer RC, Bonjour JP, Fleisch H. Tubular localization of adaptation to dietary phosphate in rats. *Am J Physiol.* 1977;233:F342–F348.
525. Pastoriza-Munoz E, Mishler DR, Lechene C. Effect of phosphate deprivation on phosphate reabsorption in rat nephron: role of PTH. *Am J Physiol.* 1983;244:F140–F149.
526. Shah SV, Kempson SA, Northrup TE, et al. Renal adaptation to a low phosphate diet in rats. *J Clin Invest.* 1979;64:955–966.
527. Steele TH. Interactions of starvation and selective phosphorus depletion on renal phosphate reabsorption. *Ren Physiol.* 1982;5:44–52.
528. Steele TH. Renal response to phosphorus deprivation: effect of the parathyroids and bicarbonate. *Kidney Int.* 1977;11:327–334.
529. Steele TH, DeLuca HF. Influence of dietary phosphorus on renal phosphate reabsorption in the parathyroidectomized rat. *J Clin Invest.* 1976;57:867–874.
530. Stoll R, Kinne R, Murer H, et al. Phosphate transport by rat renal brush border membrane vesicles: influence of dietary phosphate, thyroparathyroidectomy, and 1,25-dihydroxyvitamin D₃. *Pflugers Arch.* 1979;380:47–52.
531. Trohler U, Bonjour JP, Fleisch H. Inorganic phosphate homeostasis. Renal adaptation to the dietary intake in intact and thyroparathyroidectomized rats. *J Clin Invest.* 1976;57:264–273.
532. Wen SF, Boynar JW Jr, Stoll RW. Effect of phosphate deprivation on renal phosphate transport in the dog. *Am J Physiol.* 1978;234:F199–F206.
533. Dimke H, Desai P, Borovac J, et al. Activation of the Ca(2+)-sensing receptor increases renal claudin-14 expression and urinary Ca(2+) excretion. *Am J Physiol Renal Physiol.* 2013;304:F761–F769.
534. Gong Y, Renigunta V, Himmerkus N, et al. Claudin-14 regulates renal Ca(2+) transport in response to CaSR signalling via a novel microRNA pathway. *EMBO J.* 2012;31:1999–2012.
535. Ritthaler T, Traebert M, Lotscher M, et al. Effects of phosphate intake on distribution of type II Na/Pi cotransporter mRNA in rat kidney. *Kidney Int.* 1999;55:976–983.
536. Segawa H, Kaneko I, Yamanaka S, et al. Intestinal Na-P(i) cotransporter adaptation to dietary P(i) content in vitamin D receptor null mice. *Am J Physiol Renal Physiol.* 2004;287:F39–F47.
537. Brodehl J, Gellissen K, Weber HP. Postnatal development of tubular phosphate reabsorption. *Clin Nephrol.* 1982;17:163–171.
538. Vansel M. Tubular reabsorption of phosphate in normal children and in children with rickets. *Rev Eur Etud Clin Biol.* 1972;17:656–662.
539. Kiebzak GM, Sacktor B. Effect of age on renal conservation of phosphate in the rat. *Am J Physiol.* 1986;251:F399–F407.
540. Barac-Nieto M, Alfred M, Spitzer A. Phosphate depletion in opossum kidney cells: apical but not basolateral or transepithelial adaptations of Pi transport. *Exp Nephrol.* 2001;9:258–264.
541. Biber J, Forgo J, Murer H. Modulation of Na+Pi cotransport in opossum kidney cells by extracellular phosphate. *Am J Physiol.* 1988;255:C155–C161.
542. Markovich D, Verri T, Sorribas V, et al. Regulation of opossum kidney (OK) cell Na/Pi cotransport by Pi deprivation involves mRNA stability. *Pflugers Arch.* 1995;430:459–463.
543. Reshkin SJ, Forgo J, Biber J, et al. Functional asymmetry of phosphate transport and its regulation in opossum kidney cells: phosphate “adaptation”. *Pflugers Arch.* 1991;419:256–262.
544. Kumar R. Phosphate sensing. *Curr Opin Nephrol Hypertens.* 2009;18:281–284.
545. Scanni R, vonRotz M, Jehle S, et al. The human response to acute enteral and parenteral phosphate loads. *J Am Soc Nephrol.* 2014;25:2730–2739.
546. Murer H, Lotscher M, Kaissling B, et al. Renal brush border membrane Na/Pi-cotransport: molecular aspects in PTH-dependent and dietary regulation. *Kidney Int.* 1996;49:1769–1773.
547. Berndt TJ, Tucker RR, Kent PD, et al. Dopamine enhances the phosphaturic effect of PTH during acute respiratory alkalosis. *J Lab Clin Med.* 1999;134:616–622.
548. Isaac J, Berndt TJ, Chinnow SL, et al. Dopamine enhances the phosphaturic response to parathyroid hormone in phosphate-deprived rats. *J Am Soc Nephrol.* 1992;2:1423–1429.
549. Rybczynska A, Hoppe A, Knox FG. Propranolol restores phosphaturic effect of PTH in short-term phosphate deprivation. *Am J Physiol.* 1990;258:R120–R123.
550. Mulrone SE, Woda CB, Halaihel N, et al. Central control of renal sodium-phosphate (NaPi-2) transporters. *Am J Physiol Renal Physiol.* 2004;286:F647–F652.
551. Bonjour JP, Preston C, Fleisch H. Effect of 1,25-dihydroxyvitamin D₃ on the renal handling of Pi in thyroparathyroidectomized rats. *J Clin Invest.* 1977;60:1419–1428.
552. Muhlbauer RC, Bonjour JP, Fleisch H. Tubular handling of Pi: localization of effects of 1,25(OH)₂D₃ and dietary Pi in TPTX rats. *Am J Physiol.* 1981;241:F123–F128.
553. Puschett JB, Kuhrman MS. Renal tubular effects of 1,25-dihydroxy vitamin D₃: interactions with vasopressin and parathyroid hormone in the vitamin D-depleted rat. *J Lab Clin Med.* 1978;92:895–903.
554. Puschett JB, Egel J, Pfanstiel J. Brush border vesicle transport effects of 1,25-dihydroxy vitamin D₃. *Adv Exp Med Biol.* 1984;178:133–134.
555. Bonjour JP, Preston C, Troehler U, et al. Regulation of the tubular transport of phosphate in the rat: role of parathyroid hormone and 1,25-dihydroxyvitamin D₃. *Adv Exp Med Biol.* 1978;103:97–103.
556. Rizzoli R, Fleisch H, Bonjour JP. Role of 1,25-dihydroxyvitamin D₃ (1,25-(OH)₂D₃) on intestinal inorganic phosphate (Pi) absorption in rats with normal vitamin D supply. *Calcif Tissue Res.* 1977;22(suppl):561–562.
557. Rizzoli R, Fleisch H, Bonjour JP. Role of 1,25-dihydroxyvitamin D₃ on intestinal phosphate absorption in rats with a normal vitamin D supply. *J Clin Invest.* 1977;60:639–647.
558. Beutner EH, Munson PL. Time course of urinary excretion of inorganic phosphate by rats after parathyroidectomy and after injection of parathyroid extract. *Endocrinology.* 1960;66:610–616.
559. Foulks JG, Perry FA. Renal excretion of phosphate following parathyroidectomy in the dog. *Am J Physiol.* 1959;196:554–560.
560. Kuntziger H, Amiel C, Roinel N, et al. Effects of parathyroidectomy and cyclic AMP on renal transport of phosphate, calcium, and magnesium. *Am J Physiol.* 1974;227:905–911.
561. Talmage RV, Krantz FW. Progressive changes in renal phosphate and calcium excretion in rats following parathyroidectomy or parathyroid administration. *Proc Soc Exp Biol Med.* 1954;87:263–267.
562. Talmage RV, Krantz FW, Buchanan GD. Effect of parathyroid extract and phosphate salts on renal calcium and phosphate excretion after parathyroidectomy. *Proc Soc Exp Biol Med.* 1955;88:600–604.
563. Lorentz WB. Effect of parathyroid hormone on renal tubular permeability. *Am J Physiol.* 1976;231:1401–1407.
564. Rybczynska A, Berndt TJ, Hoppe A, et al. Site of restoration of the effect of PTH by propranolol in respiratory alkalosis. *Kidney Int.* 1990;38:258–262.
565. Hernando N, Forgo J, Biber J, et al. PTH-induced downregulation of the type IIa Na/P(i)-cotransporter is independent of known endocytic motifs. *J Am Soc Nephrol.* 2000;11:1961–1968.
566. Keusch I, Traebert M, Lotscher M, et al. Parathyroid hormone and dietary phosphate provoke a lysosomal routing of the proximal tubular Na/Pi-cotransporter type II. *Kidney Int.* 1998;54:1224–1232.
567. Zhao N, Tenenhouse HS. Npt2 gene disruption confers resistance to the inhibitory action of parathyroid hormone on renal sodium-phosphate cotransport. *Endocrinology.* 2000;141:2159–2165.
568. Engstrom GW, Horst RL, Reinhardt TA, et al. Effect of dietary phosphorus levels on porcine renal 25-hydroxyvitamin D-1 alpha- and 24R-hydroxylase activities and plasma 1,25-dihydroxyvitamin D₃ concentration. *J Anim Sci.* 1985;60:1005–1011.
569. Tenenhouse HS, Meyer RA Jr, Mandla S, et al. Renal phosphate transport and vitamin D metabolism in X-linked hypophosphatemic Gy mice: responses to phosphate deprivation. *Endocrinology.* 1992;131:51–56.
570. Capuano P, Radanovic T, Wagner CA, et al. Intestinal and renal adaptation to a low-Pi diet of type II NaPi cotransporters in vitamin D receptor- and 1alphaOHase-deficient mice. *Am J Physiol Cell Physiol.* 2005;288:C429–C434.
571. Taketani Y, Segawa H, Chikamori M, et al. Regulation of type II renal Na+-dependent inorganic phosphate transporters by 1,25-dihydroxyvitamin D₃. Identification of a vitamin D-responsive element in the human NAPI-3 gene. *J Biol Chem.* 1998;273:14575–14581.
572. DeFronzo RA, Cooke CR, Andres R, et al. The effect of insulin on renal handling of sodium, potassium, calcium, and phosphate in man. *J Clin Invest.* 1975;55:845–855.
573. DeFronzo RA, Goldberg M, Agus ZS. The effects of glucose and insulin on renal electrolyte transport. *J Clin Invest.* 1976;58:83–90.
574. Hammerman MR. Interaction of insulin with the renal proximal tubular cell. *Am J Physiol.* 1985;249:F1–F11.

575. Hammerman MR, Rogers S, Hansen VA, et al. Insulin stimulates Pi transport in brush border vesicles from proximal tubular segments. *Am J Physiol*. 1984;247:E616–E624.
576. Lau K, Guntupalli J, Eby B. Effects of somatostatin on phosphate transport: evidence for the role of basal insulin. *Kidney Int*. 1983;24:10–15.
577. Quigley R, Baum M. Effects of growth hormone and insulin-like growth factor I on rabbit proximal convoluted tubule transport. *J Clin Invest*. 1991;88:368–374.
578. Corvilain J, Abramow M, Bergans A. Some effects of human growth hormone on renal hemodynamics and on tubular phosphate transport in man. *J Clin Invest*. 1962;41:1230–1235.
579. Haramati A, Mulrone SE, Lumpkin MD. Regulation of renal phosphate reabsorption during development: implications from a new model of growth hormone deficiency. *Pediatr Nephrol*. 1990;4:387–391.
580. Mulrone SE, Lumpkin MD, Haramati A. Antagonist to GH-releasing factor inhibits growth and renal Pi reabsorption in immature rats. *Am J Physiol*. 1989;257:F29–F34.
581. Woda CB, Halaihel N, Wilson PV, et al. Regulation of renal NaPi-2 expression and tubular phosphate reabsorption by growth hormone in the juvenile rat. *Am J Physiol Renal Physiol*. 2004;287:F117–F123.
582. Hammerman MR, Karl IE, Hruska KA. Regulation of canine renal vesicle Pi transport by growth hormone and parathyroid hormone. *Biochim Biophys Acta*. 1980;603:322–335.
583. Caverzasio J, Bonjour JP. Growth factors and renal regulation of phosphate transport. *Pediatr Nephrol*. 1993;7:802–806.
584. Caverzasio J, Bonjour JP. [IGF-I and phosphate homeostasis during growth]. *Nephrologie*. 1992;13:109–113 [in French].
585. Caverzasio J, Bonjour JP. Influence of recombinant IGF-I (somatomedin C) on sodium-dependent phosphate transport in cultured renal epithelium. *Prog Clin Biol Res*. 1988;252:385–386.
586. Caverzasio J, Bonjour JP. Insulin-like growth factor I stimulates Na-dependent Pi transport in cultured kidney cells. *Am J Physiol*. 1989;257:F712–F717.
587. Caverzasio J, Montessuit C, Bonjour JP. Stimulatory effect of insulin-like growth factor-I on renal Pi transport and plasma 1,25-dihydroxyvitamin D₃. *Endocrinology*. 1990;127:453–459.
588. Hirschberg R, Ding H, Wanner C. Effects of insulin-like growth factor I on phosphate transport in cultured proximal tubule cells. *J Lab Clin Med*. 1995;126:428–434.
589. Mann KJ, Dousa DM, Kerrigan RJ, et al. Acute renal denervation decreases tubular phosphate reabsorption. *Miner Electrolyte Metab*. 1992;18:354–358.
590. Mann KJ, Rybczynska A, Berndt TJ, et al. Renal denervation enhances the phosphaturic effect of parathyroid hormone. *Miner Electrolyte Metab*. 1991;17:16–20.
591. Szalay L, Bencsath P, Takas L. Effect of splanchnicotomy on the renal excretion of inorganic phosphate in the anaesthetized dog. *Pflugers Arch*. 1977;367:283–286.
592. Szalay L, Colindres RE, Jackson R, et al. Effects of chronic renal denervation in conscious restrained rats. *Int Urol Nephrol*. 1986;18:3–18.
593. Szenasi G, Bencsath P, Lehoczy E, et al. Tubular transport and urinary excretion of phosphate after renal denervation in the anesthetized rat. *Am J Physiol*. 1981;240:F481–F486.
594. Cuche JL, Marchand GR, Greger RF, et al. Phosphaturic effect of dopamine in dogs. Possible role of intrarenally produced dopamine in phosphate regulation. *J Clin Invest*. 1976;58:71–76.
595. Debska-Slizien A, Ho P, Drangova R, et al. Endogenous renal dopamine production regulates phosphate excretion. *Am J Physiol*. 1994;266:F858–F867.
596. Goto F. The effects of dopamine on renal excretion of sodium, phosphate and cyclic AMP in thyroparathyroidectomized dogs. *Endocrinol Jpn*. 1979;26:649–654.
597. Isaac J, Berndt TJ, Knox FG. Role of dopamine in the exaggerated phosphaturic response to parathyroid hormone in the remnant kidney. *J Lab Clin Med*. 1995;126:470–473.
598. Isaac J, Berndt TJ, Thothathri V, et al. Catecholamines and phosphate excretion by the remnant kidney. *Kidney Int*. 1993;43:1021–1026.
599. Kameda Y, Bello-Reuss E. Effect of dopamine on phosphate reabsorption in isolated perfused rabbit proximal tubules. *Miner Electrolyte Metab*. 1983;9:147–150.
600. LeClaire M, Berndt TJ, Knox FG. Isoproterenol infusion increases the maximal tubular capacity of phosphate reabsorption. *Ren Physiol Biochem*. 1992;15:134–140.
601. Leme CE, Liberman B, Wajchenberg BL. Effect of norepinephrine, propranolol and phentolamine on the phosphaturic action of bovine parathyroid extract in man. *Nephron*. 1973;11:365–372.
602. Baines AD. Effects of salt intake and renal denervation on catecholamine catabolism and excretion. *Kidney Int*. 1982;21:316–322.
603. Debska-Slizien A, Ho P, Drangova R, et al. Endogenous dopamine regulates phosphate reabsorption but not NaK-ATPase in spontaneously hypertensive rat kidneys. *J Am Soc Nephrol*. 1994;5:1125–1132.
604. Thornton LR, Meyer MH, Meyer RA Jr. Isoproterenol increases renal tubular reabsorption of phosphate in X-linked hypophosphatemic (Hyp) mice. *Miner Electrolyte Metab*. 1999;25:204–209.
605. Cheng L, Liang CT, Precht P, et al. Alpha-2-adrenergic modulation of the parathyroid hormone-inhibition of phosphate uptake in cultured renal (OK) cells. *Biochem Biophys Res Commun*. 1988;155:74–82.
606. de Toledo FG, Beers KW, Berndt TJ, et al. Opposite paracrine effects of 5-HT and dopamine on Na(+)-Pi cotransport in opossum kidney cells. *Kidney Int*. 1997;52:152–156.
607. de Toledo FG, Thompson MA, Bolliger C, et al. gamma-L-glutamyl-L-DOPA inhibits Na(+)-phosphate cotransport across renal brush border membranes and increases renal excretion of phosphate. *Kidney Int*. 1999;55:1832–1842.
608. Sadiq S, Berndt TJ, Nath KA, et al. Effect of gamma-L-glutamyl-L-dopa on phosphate excretion. *J Lab Clin Med*. 2000;135:52–56.
609. Bacic D, Capuano P, Baum M, et al. Activation of dopamine D1-like receptors induces acute internalization of the renal Na+/phosphate cotransporter NaPi-IIa in mouse kidney and OK cells. *Am J Physiol Renal Physiol*. 2005;288:F740–F747.
610. Baines AD, Drangova R. Does dopamine use several signal pathways to inhibit Na-Pi transport in OK cells? *J Am Soc Nephrol*. 1998;9:1604–1612.
611. Glahn RP, Onsgard MJ, Tyce GM, et al. Autocrine/paracrine regulation of renal Na(+)-phosphate cotransport by dopamine. *Am J Physiol*. 1993;264:F618–F622.
612. Hafdi Z, Couette S, Comoy E, et al. Locally formed 5-hydroxytryptamine stimulates phosphate transport in cultured opossum kidney cells and in rat kidney. *Biochem J*. 1996;320(Pt 2):615–621.
613. Lederer ED, Sohi SS, McLeish KR. Dopamine regulates phosphate uptake by opossum kidney cells through multiple counter-regulatory receptors. *J Am Soc Nephrol*. 1998;9:975–985.
614. Perrichot R, Garcia-Ocana A, Couette S, et al. Locally formed dopamine modulates renal Na-Pi co-transport through DA1 and DA2 receptors. *Biochem J*. 1995;312(Pt 2):433–437.
615. Berndt TJ, MacDonald A, Walikonis R, et al. Excretion of catecholamines and metabolites in response to increased dietary phosphate intake. *J Lab Clin Med*. 1993;122:80–84.
616. Berndt TJ, Liang M, Tyce GM, et al. Intrarenal serotonin, dopamine, and phosphate handling in remnant kidneys. *Kidney Int*. 2001;59:625–630.
617. Gross JM, Berndt TJ, Knox FG. Effect of serotonin receptor antagonist on phosphate excretion. *J Am Soc Nephrol*. 2000;11:1002–1007.
618. ADHR Consortium. Autosomal dominant hypophosphataemic rickets is associated with mutations in FGF23. *Nat Genet*. 2000;26:345–348.
619. Bai X, Miao D, Li J, et al. Transgenic mice overexpressing human fibroblast growth factor 23 (R176Q) delineate a putative role for parathyroid hormone in renal phosphate wasting disorders. *Endocrinology*. 2004;145:5269–5279.
620. Sitara D, Razzaque MS, Hesse M, et al. Homozygous ablation of fibroblast growth factor-23 results in hyperphosphatemia and impaired skeletogenesis, and reverses hypophosphatemia in Phe-deficient mice. *Matrix Biol*. 2004;23:421–432.
621. Sitara D, Razzaque MS, St-Arnaud R, et al. Genetic ablation of vitamin D activation pathway reverses biochemical and skeletal anomalies in Fgf23-null animals. *Am J Pathol*. 2006;169:2161–2170.
622. Liu S, Vierthaler L, Tang W, et al. FGFR3 and FGFR4 do not mediate renal effects of FGF23. *J Am Soc Nephrol*. 2008;19:2342–2350.
623. Han X, Yang J, Li L, et al. Conditional deletion of Fgfr1 in the proximal and distal tubule identifies distinct roles in phosphate and calcium transport. *PLoS ONE*. 2016;11:e0147845.
624. Urakawa I, Yamazaki Y, Shimada T, et al. Klotho converts canonical FGF receptor into a specific receptor for FGF23. *Nature*. 2006;444:770–774.
625. Tsujikawa H, Kurotaki Y, Fujimori T, et al. Klotho, a gene related to a syndrome resembling human premature aging, functions in a negative regulatory circuit of vitamin D endocrine system. *Mol Endocrinol*. 2003;17:2393–2403.

626. Brownstein CA, Adler F, Nelson-Williams C, et al. A translocation causing increased alpha-klotho level results in hypophosphatemic rickets and hyperparathyroidism. *Proc Natl Acad Sci U S A*. 2008;105(9):3455–3460.
627. Andrukhova O, Zeitz U, Goetz R, et al. FGF23 acts directly on renal proximal tubules to induce phosphaturia through activation of the ERK1/2-SGK1 signaling pathway. *Bone*. 2012;51(3):621–628.
628. Sneddon WB, Ruiz GW, Gallo LI, et al. Convergent signaling pathways regulate parathyroid hormone and fibroblast growth factor-23 action on NPT2A-mediated phosphate transport. *J Biol Chem*. 2016;291(36):18632–18642.
629. Weinman EJ, Steplock D, Shenolikar S, et al. Fibroblast growth factor-23-mediated inhibition of renal phosphate transport in mice requires sodium-hydrogen exchanger regulatory factor-1 (NHERF-1) and synergizes with parathyroid hormone. *J Biol Chem*. 2011;286(43):37216–37221.
630. Umbach AT, Zhang B, Daniel C, et al. Janus kinase 3 regulates renal 25-hydroxyvitamin D 1 α -hydroxylase expression, calcitriol formation, and phosphate metabolism. *Kidney Int*. 2015;87(4):728–737.
631. Inoue Y, Segawa H, Kaneko I, et al. Role of the vitamin D receptor in FGF23 action on phosphate metabolism. *Biochem J*. 2005;390:325–331.
632. Kolek OI, Hines ER, Jones MD, et al. 1 α ,25-Dihydroxyvitamin D₃ upregulates FGF23 gene expression in bone: the final link in a renal-gastrointestinal-skeletal axis that controls phosphate transport. *Am J Physiol Gastrointest Liver Physiol*. 2005;289:G1036–G1042.
633. Yuan B, Takaiwa M, Clemens TL, et al. Aberrant Phex function in osteoblasts and osteocytes alone underlies murine X-linked hypophosphatemia. *J Clin Invest*. 2008.
634. Athanasopoulos AN, Schneider D, Keiper T, et al. Vascular endothelial growth factor (VEGF)-induced up-regulation of CCN1 in osteoblasts mediates proangiogenic activities in endothelial cells and promotes fracture healing. *J Biol Chem*. 2007;282:26746–26753.
635. Rowe PS, de Zoysa PA, Dong R, et al. MEPE, a new gene expressed in bone marrow and tumors causing osteomalacia. *Genomics*. 2000;67:54–68.
636. Rowe PS, Kumagai Y, Gutierrez G, et al. MEPE has the properties of an osteoblastic phosphatonin and minhibin. *Bone*. 2004;34:303–319.
637. Shirley DG. *Nephrol Dial Transplant*. 2010;25(10):3191–3195.
638. Marks J, Churchill LJ, Debnam ES, et al. Matrix extracellular phosphoglycoprotein inhibits phosphate transport. *J Am Soc Nephrol*. 2008;19:2313–2320.
639. Gowen LC, Petersen DN, Mansolf AL, et al. Targeted disruption of the osteoblast/osteocyte factor 45 gene (OF45) results in increased bone formation and bone mass. *J Biol Chem*. 2003;278:1998–2007.
640. Jain A, Fedarko NS, Collins MT, et al. Serum levels of matrix extracellular phosphoglycoprotein (MEPE) in normal humans correlate with serum phosphorus, parathyroid hormone and bone mineral density. *J Clin Endocrinol Metab*. 2004;89:4158–4161.

BOARD REVIEW QUESTIONS

1. A 35-year-old woman with intermittent diarrhea of 6 months' duration is referred to you for evaluation of bone pain. Previous evaluation has shown the presence of celiac disease. The following tests are available for evaluation of her symptoms.

Hemoglobin 10.5 g/dL, mean corpuscular volume 105 fL, leukocyte count $6.5 \times 10^9/L$, platelet count $165 \times 10^9/L$, serum folate 2.5 $\mu\text{g}/L$, serum sodium 135 mEq/L, potassium 3.7 mEq/L, chloride 105 mEq/L, bicarbonate 22 mEq/L, creatinine 0.9 mg/dL, blood urea nitrogen 12 mg/dL, total serum calcium 8.5 mg/dL, ionized calcium 4.0 mg/dL, phosphorus 2.5 mg/dL, alkaline phosphatase 200 U/L, parathyroid hormone 80 pg/mL, 25-hydroxyvitamin D 10 ng/mL, and 1,25-dihydroxyvitamin D 30 pg/mL. Urinalysis is normal. Urine microscopy is normal. Bone densitometry shows osteopenia.

A 24-hour urine sample is collected for measurement of calcium, phosphorus, and creatinine. In regard to her urinary analytes, one will anticipate that (select all correct answers):

- 24-hour urine calcium will be low.
- 24-hour urine calcium will be high.
- 24-hour urine phosphorus will be low.
- 24-hour urine phosphorus will be high.
- None of the above

Answers: a and d

- Fractional excretion of calcium will be low.
- Fractional excretion of calcium will be high.
- Fractional excretion of phosphorus will be low.
- Fractional excretion of phosphorus will be high.

Answers: a and d

Rationale: The patient has secondary hyperparathyroidism due to intestinal malabsorption of calcium. One would anticipate low urinary calcium excretion and a low fractional excretion of calcium as a result of elevated parathyroid hormone concentrations. One would expect urinary phosphorus to be elevated and fractional excretion of phosphorus to be high on account of secondary hyperparathyroidism.

2. The major effect of parathyroid hormone (PTH) on urinary calcium reabsorption occurs in the

- Proximal tubule
- Thick ascending limb of the loop of Henle

- Distal convoluted tubule
- Collecting duct
- All of the above

Answers: b and c

Rationale: The major sites of parathyroid hormone-mediated calcium absorption are in the thick ascending limb and the distal convoluted tubule. There is no effect of PTH on calcium absorption in the proximal tubule.

3. A 35-year-old female is referred to you for evaluation of bone pain. She was completely well 2 years ago when she started developing intermittent aches and pains. Family history is noncontributory. Examination is negative except for a 1×2 cm subcutaneous mass in the left popliteal fossa.

Laboratory values show the following: hemoglobin 12.8 g/dL, MCV 85 fL, leukocyte and platelet count. Serum sodium, potassium, chloride, and bicarbonate are normal. Serum calcium is 9.2 mg/dL, ionized calcium 4.6 mg/dL, phosphorus 2.0 mg/dL, alkaline phosphatase 150 U/L, 25-hydroxyvitamin D 22 ng/mL, 1,25-dihydroxy vitamin D 25 pg/mL, and PTH 30 pg/mL. Which one of the following tests will assist in making the diagnosis?

- Serum FGF-23
- 24-hour urine phosphorus and creatinine
- Bone density
- Sestamibi technician scan
- Magnetic resonance scan of the left tibial fossa
- All of the above

Answer: f

Rationale: The patient has tumor-induced osteomalacia based on the presence of a low serum phosphorus, normal serum 25-hydroxyvitamin D concentrations, and a low-normal 1,25-dihydroxyvitamin D and PTH concentration. Investigation will reveal an elevated 24-hour urine phosphorus and an increased fractional excretion of phosphorus. TmP/GFR will be suppressed. FGF-23 concentrations will be increased. Bone density will be reduced. A sestamibi technician scan will show uptake over the popliteal fossa. This will be confirmed by magnetic resonance spectroscopy.

8

Renal Handling of Organic Solutes

Volker Vallon | Stefan Broer | Sanjay K. Nigam

CHAPTER OUTLINE

GLUCOSE, 218

AMINO ACIDS, 239

ORGANIC CATIONS AND ANIONS, 230

KEY POINTS

- In a normoglycemic adult, the kidneys filter 160–180 g/day of glucose (~30% of daily energy expenditure), which is reabsorbed by the sodium glucose cotransporter SGLT2 (~97%) and SGLT1 (~3%) in the early and late proximal tubule, respectively.
- The basal overall glucose tubular reabsorption capacities for SGLT2 versus SGLT1 is in the range of 3:1 to 5:1. The transport capacity of tubular SGLT1 is unmasked (up to ~80 g/day) when more glucose is delivered to the late proximal tubule (e.g., in diabetes or with SGLT2 inhibition).
- The good correlation between the level of basolateral GLUT1 expression and the glycolytic activity of the different nephron segments indicates that the more distal tubule segments in particular are taking up glucose for energy supply via basolateral GLUT1.
- One of the major roles of organic anionic transporters, long considered mainly drug and toxin transporters, now appears to be to regulate many aspects of endogenous physiology.
- OAT1 and OAT3 appear to be the major renal basolateral transporters involved in the elimination of numerous uremic toxins originating in the gut microbiome, although OCT2 is likely the main route of TMAO elimination.
- The Remote Sensing and Signaling Hypothesis is a systems biology theory about the role of SLC and ABC transporters in the interorgan and interorganismal (e.g., host gut microbiome) “remote” communication via transporter-mediated movement of metabolites, signaling molecules, gut microbiome products, nutrients, uric acid, and uremic toxins into different body tissues and fluid compartments. It provides a framework for understanding uremia and hyperuricemia.
- Amino acid transporters often form heterodimers with ancillary subunits that are essential for trafficking of the transporters to the cell surface. Genetic complexity is observed in renal aminoacidurias due to heterodimer formation and transporter redundancy.
- Rare inherited aminoacidurias define four major routes of amino acid reabsorption. Amino acid antiporters play an important role in the apical and basolateral transport of cationic and neutral amino acids.

GLUCOSE

The kidneys are a major site of glucose handling. This includes the continuous glomerular filtration of large amounts of glucose, almost all of which is subsequently reabsorbed by the proximal tubule, such that the formed urine in a healthy individual is nearly glucose free. The glucose reabsorbed by

the proximal tubule is primarily taken up into the peritubular capillaries and provided as an energy source to further distal tubular segments or returned to the systemic circulation. Moreover and in addition to the liver, the kidneys contribute to the endogenous production of glucose or gluconeogenesis. Thus, the kidneys use glucose as fuel but also contribute to maintaining blood glucose levels and overall metabolic balance by reabsorbing filtered glucose and generating new glucose.

This is relevant in healthy individuals, in particular in the fasting state, and becomes pathophysiologically important in diabetes and hyperglycemic conditions. As a consequence, new antihyperglycemic drugs have been developed that target renal glucose reabsorption, induce urinary glucose loss, and have clinical efficacy with regard to lowering blood glucose, and even more importantly, they have protective effects on the kidney and cardiovascular system.

PHYSIOLOGY OF RENAL GLUCOSE TRANSPORT

In many organisms including human, the cellular uptake and metabolism of D-glucose serves as an important energy source.^{1,2} The brain primarily runs on glucose and depends on its continuous uptake, which alone requires ~125 g of glucose every day. As a consequence, glucose homeostasis is finely regulated, and blood glucose levels are maintained in a range of 4–9 mmol/L by various hormones, including insulin and glucagon, that regulate glucose uptake into target cells as well as glucose storage and endogenous glucose production.^{1,2}

Glucose is a small molecule that is freely filtered by the glomeruli of the kidneys. Under conditions of normal blood glucose levels (~5.5 mmol/L or 100 mg/dL) and normal glomerular filtration rate (GFR, ~180 L/day), the kidneys filter 160–180 g of glucose each day. This is equal to ~30% of the daily energy expenditure, which would be lost into the urine if not regained by the renal tubules. Instead, more than 99% of the filtered glucose is reabsorbed by the tubules, primarily in the proximal tubule (Fig. 8.1). As described in

more detail below, glucose reabsorption in the proximal tubule involves the two Na⁺-glucose cotransporters SGLT2 and SGLT1, which are expressed in the brush border membrane of the early and later proximal tubule, respectively. Na⁺-glucose cotransport is a saturable process and has a maximum transport capacity (T_{max}). The T_{max} of the kidneys for glucose can vary among individuals and averages ~430 g and ~500 g/day (300 and 350 mg/min) in female and male healthy human subjects, respectively.^{3,4} This equals ~threefold the normal tubular glucose load of 160–180 g/day so that the renal glucose reabsorption capacity is not saturated under conditions of normal blood glucose levels and GFR. Theoretically, at a normal GFR, the T_{max} should be reached, and glucose should begin to be excreted in the urine at a plasma glucose threshold of ~15.5 mmol/L (280 mg/dL). The T_{max} for glucose of individual nephrons is variable, however, and thus, low-level urinary glucose spilling begins in a normal, glucose-tolerant individual at modestly elevated plasma glucose levels of ~10–11 mmol/L (180–200 mg/dL; see “Splay,” Fig. 8.2). A robust and linear increase in urinary glucose excretion occurs when blood glucose levels rise above 15–16 mmol/L. GFR is a determinant of the filtered glucose load, and as a consequence, glucosuria can occur at lower plasma glucose concentrations when GFR is elevated (e.g., in pregnancy or in diabetes), or at higher blood glucose levels when GFR is reduced (e.g., in chronic kidney disease; CKD). In addition, changes in the transport activity and expression level of SGLT2 and SGLT1 (see later) are expected to further modify this relationship.

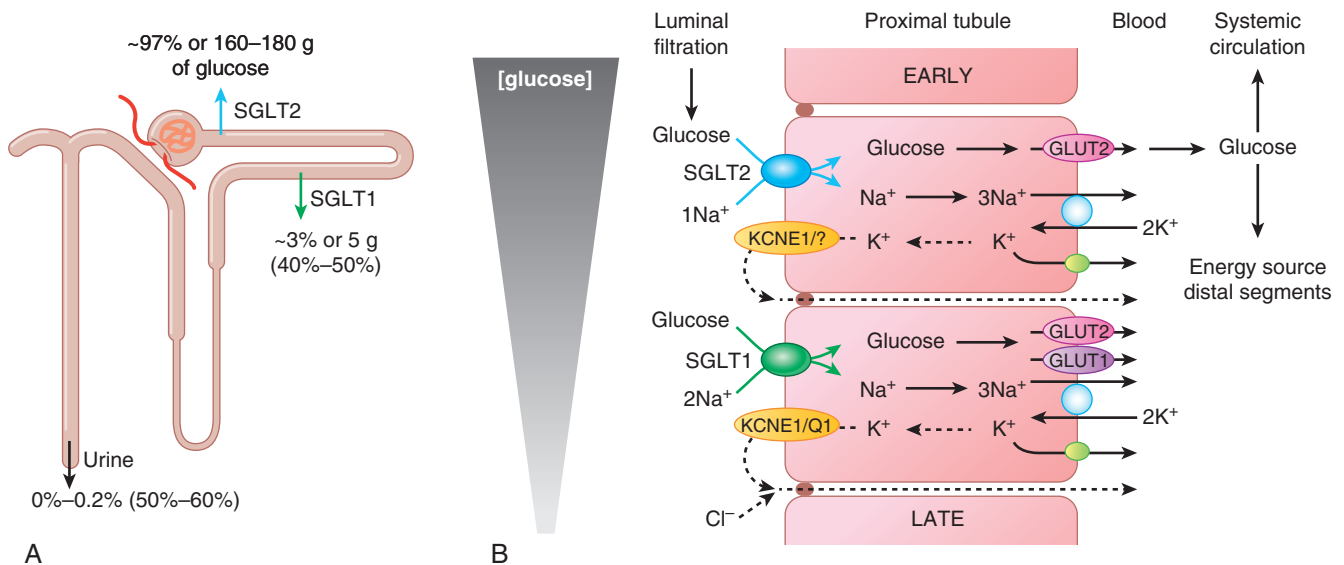


Fig. 8.1 Glucose transport in the kidney. (A) Under normoglycemia, ~97% of filtered glucose is reabsorbed via SGLT2 in the early segments of the proximal tubule. The remaining ~3% of glucose is reabsorbed by SGLT1 in the late proximal tubule such that the urine is nearly free of glucose. SGLT2 inhibition shifts glucose reabsorption downstream and unmasks the capacity of SGLT1 to reabsorb glucose (~40% of filtered glucose, depending on glucose load; see numbers in parentheses). (B) Cell model of glucose transport: The basolateral Na⁺-K⁺-ATPase lowers cytosolic Na⁺ concentrations and generates a negative interior voltage, thereby providing the driving force for Na⁺-coupled glucose uptake through SGLT2 and SGLT1 across the apical membrane. The facilitative glucose transporters GLUT2 and GLUT1 mediate glucose transport across the basolateral membrane down its chemical gradient. Na⁺-glucose cotransport is electrogenic and accompanied by paracellular Cl⁻ reabsorption or transcellular K⁺ secretion to stabilize membrane potential; K⁺ channels KCNE1/unknown α subunit and KCNE1/KCNQ1 in early and late proximal tubule, respectively. (This figure was modified with permission from Vallon V. Molecular determinants of renal glucose transport. *Am J Physiol Cell Physiol.* 2011;300:C6–C8.)

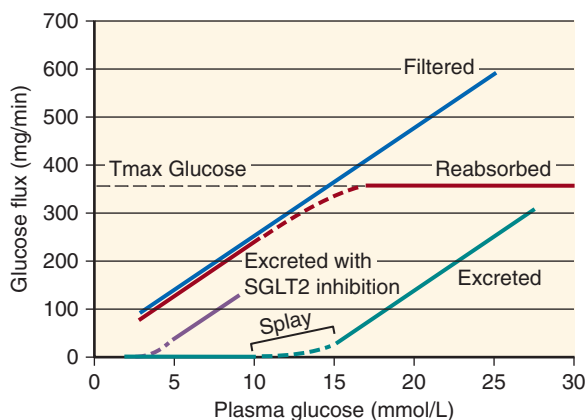


Fig. 8.2 Tubular reabsorption and urinary excretion of glucose as a function of filtered glucose. Tubular reabsorption of glucose increases linearly with the filtered glucose load until reabsorption reaches the tubular reabsorption capacity (*T_{max} Glucose*) and glucose starts appearing in the urine. Theoretically, a *T_{max}* of ~350 mg/min and normal glomerular filtration rate would result in a plasma glucose threshold of ~15.5 mmol/L. However, due to variability of *T_{max}* in individual nephrons, the plasma glucose concentration that results in glucosuria in a normal individual is ~10–11.1 mmol/L (see “*Splay*”). SGLT2 inhibition reduces the renal glucose reabsorption to the transport capacity of SGLT1 and shifts the function to the left—that is, it reduces the renal glucose threshold (~3 mM) and *T_{max}* (~150 mg/min).

A PRIMARY ROLE FOR SGLT2 IN RENAL GLUCOSE REABSORPTION

Experiments performed on isolated nephron segments of rabbit kidneys in the early 1980s identified differences in the rate of uptake and affinity for glucose between the early and late proximal tubule segments, respectively.⁵ Subsequent studies confirmed that the heterogeneity in glucose transport across the proximal tubule was attributed to the presence of two different glucose transporters in the brush border membrane.⁶ These studies and transport studies in membrane vesicles and analyses of mRNA expression in isolated nephron segments of rat and rabbit kidneys as well as the cloning of the responsible genes, performed largely between 1981 and 1995, identified the Na⁺–glucose cotransporters SGLT2 (SLC5A2) and SGLT1 (SLC5A1) as the primary genes and pathways for renal glucose reabsorption.^{5–14} These studies established the concept that the “bulk” of tubular glucose uptake across the apical membrane occurs in the “early” proximal tubule (S1/2 segment) and is mediated by the low-affinity and high-capacity SGLT2. In comparison, the higher-affinity and lower-capacity SGLT1 is thought to “clean up” most of the remaining luminal glucose in “later” parts of the proximal tubule (S2/S3 segment) (see Fig. 8.1). In accordance, SGLT2 and SGLT1 have been localized with the use of well-validated antibodies in both rodents and humans to the brush border membrane primarily of the early and late proximal tubule, respectively.^{15–18} In the mouse kidney, the levels of SGLT1 protein expression in the brush border were highest in S2 segments and somewhat lower in S3 segments in medullary rays and in the outer stripe.¹⁹ In the human kidney, the strongest expression of SGLT1 was found in the S3 segment.¹⁸ In accordance and demonstrating the functional role of SGLT2, free-flow renal micropuncture

showed that glucose reabsorption in the early proximal tubule is completely absent in mice lacking SGLT2¹⁵ (Fig. 8.3). In comparison, fractional glucose reabsorption along the proximal convoluted tubule (PCT) was only slightly reduced from 97% to 94% in mice lacking SGLT1.²⁰

The phenotype of humans carrying mutations in the genes for SGLT1 (*SLC5A1*) and SGLT2 (*SLC5A2*) demonstrated their distinct quantitative contribution to renal glucose reabsorption. Mutations in SGLT1 cause “Intestinal Glucose Galactose Malabsorption” [Online Mendelian Inheritance in Man (OMIM) 182380] because the active intestinal reabsorption of glucose is mediated by SGLT1.^{21,22} Newborns with mutations in SGLT1 as well as mice lacking SGLT1²⁰ can present with life-threatening diarrhea when exposed to dietary galactose or glucose; however, they show little or no glucosuria. In contrast, individuals with mutations in SGLT2 present persistent “Familial Renal Glucosuria” (OMIM 233100) ranging from 1 to >100 g per day, but they have no intestinal phenotype.²³ Although mutations in SGLT2 are rare and therefore the consequences are not well studied or fully understood, it is remarkable that no other complications (e.g., urinary infections or impaired kidney function) have been consistently observed in these subjects.^{21,23} This information added to the rationale of developing SGLT2 inhibitors as potentially safe antihyperglycemic drugs (see later). Consistent with the described phenotypes in humans, genetic and pharmacologic studies in mice showed that under normoglycemic conditions, SGLT2 reabsorbs ~97% of the filtered glucose, whereas SGLT1 mediates the reabsorption of the remaining ~2%–3%^{15,20,24} (see Figs. 8.1 and 8.3).

UNMASKING A SIGNIFICANT GLUCOSE TRANSPORT CAPACITY OF SGLT1 IN THE LATE PROXIMAL TUBULE

In healthy human subjects, similar to the phenotype in rodents, SGLT2 is thought to reabsorb >90% of filtered glucose, yet they maintain a fractional glucose reabsorption of 40%–50% following application of a selective SGLT2 inhibitor^{25–27} (see Fig. 8.1). This observation is mimicking the phenotype of normoglycemic mice lacking *Sglt2* (*Sglt2*^{–/–}), in which fractional renal glucose reabsorption varied between 10% and 60%, inversely with the amount of filtered glucose, with a mean value of ~40%¹⁵ (see Fig. 8.3). Follow-up studies demonstrated that the persisting glucose reabsorption is mediated in the downstream late proximal tubule by SGLT1, whose transport capacity is unmasked by SGLT2 inhibition (Figs. 8.1 and 8.3). First and indirect evidence came from micropuncture studies in *Sglt2*^{–/–} mice: these mice have no net glucose reabsorption in the early proximal tubule; however, their glucose reabsorption in the later parts of the PCT accessible to micropuncture, where SGLT1 is expressed in S2 segments, is increased compared with wild-type (WT) mice¹⁵ (Fig. 8.3). Metabolic cage studies further showed that the dose–response curve for glucosuria of a selective SGLT2 inhibitor was shifted leftward in *Sglt1*^{–/–} mice; that is, glucosuria initiated at lower doses, and the maximum glucosuric response doubled compared with WT mice²⁴ (Fig. 8.3). Renal clearance studies found that concentrations of the SGLT2 inhibitor in early proximal tubule fluid close to the reported half maximal inhibitory concentration (*IC*₅₀) for mouse SGLT2 were associated with fractional renal glucose reabsorption

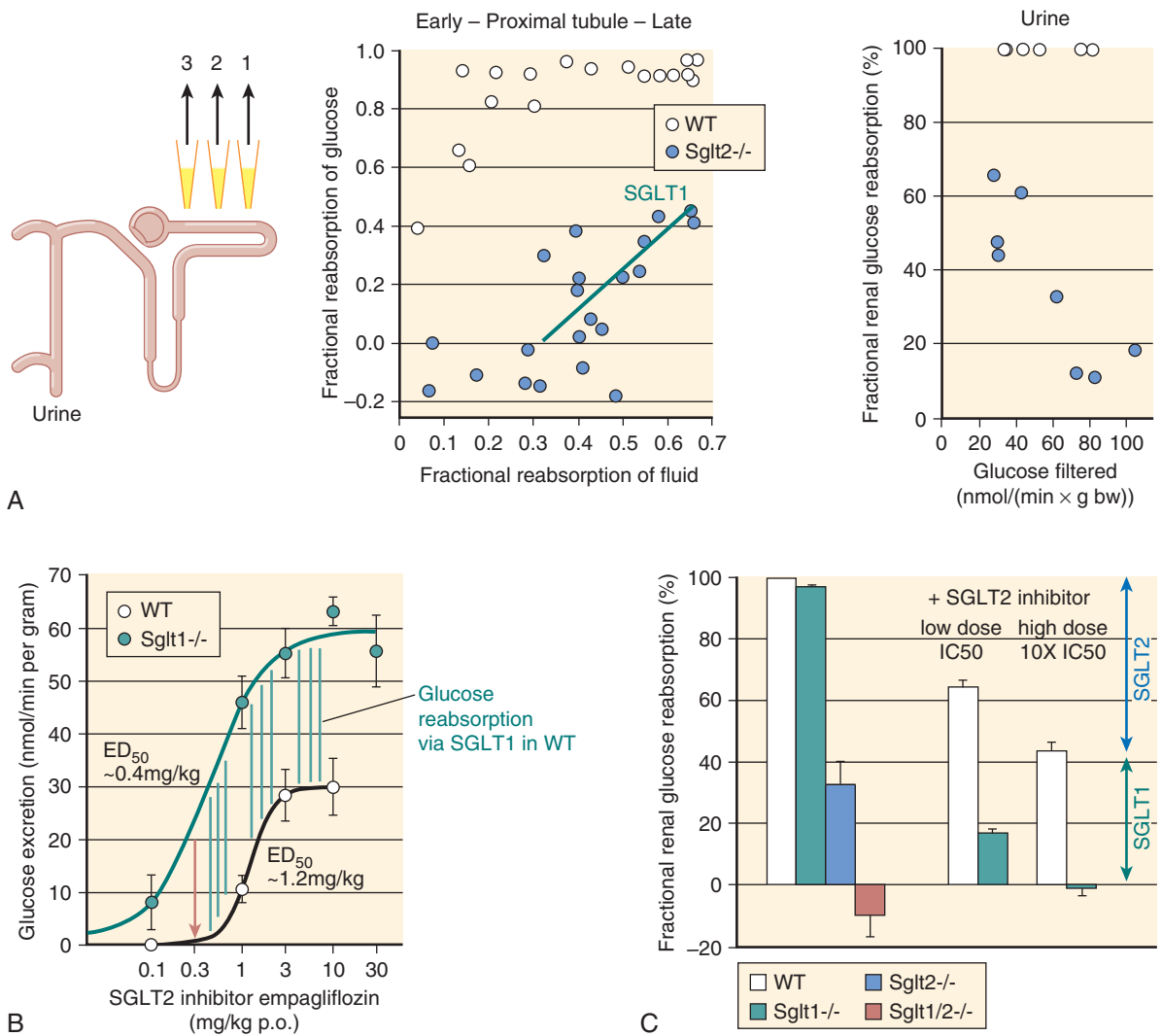


Fig. 8.3 Contribution of SGLT2 and SGLT1 to renal glucose reabsorption. (A) *Left panels:* Free-flow collections of tubular fluid performed by micropuncture to establish a profile for fractional reabsorption of glucose versus fluid along accessible proximal tubules at the kidney surface. Glucose reabsorption is absent in the early proximal tubule of *Sglt2*^{-/-} mice but enhanced in the later proximal tubule, potentially reflecting compensation by SGLT1-mediated transport. *Right panel:* Renal inulin clearance studies revealed that the reduction in fractional renal glucose reabsorption in *Sglt2*^{-/-} mice was inversely related to the amount of filtered glucose. (B) In metabolic cage studies, the SGLT2 inhibitor empagliflozin dose dependently increased glucose excretion in wild-type (*WT*) mice. The response curve was shifted leftward, and the maximum response doubled in *Sglt1*^{-/-} mice. The difference between dose-response curves, which reflects glucose reabsorption via SGLT1 in *WT* mice, was maintained for higher doses (all vertical lines have same length), consistent with selectivity of the inhibitor for SGLT2 versus SGLT1 in this dose range. Glucosuria is initiated in *WT* mice when SGLT1-mediated glucose uptake is saturate (red arrow). (C) Renal inulin clearance studies in mice lacking *Sglt1*, *Sglt2*, or both *Sglt1* and *Sglt2* indicated that the glucose reabsorption preserved in *Sglt2*^{-/-} (~40%) is mediated by SGLT1. Application of the SGLT2 inhibitor empagliflozin at low and high doses to establish free plasma concentrations (corresponding to early tubular concentrations) close to IC₅₀ for mouse SGLT2 (~1–2 nM) or 10-fold this concentration confirmed the role of SGLT1 during pharmacologic SGLT2 inhibition. (Data from Vallon V, Platt KA, Cunard R, et al. SGLT2 mediates glucose reabsorption in the early proximal tubule. *J Am Soc Nephrol.* 2011;22:104–112; and Rieg T, Masuda T, Gerasimova M, et al. Increase in SGLT1-mediated transport explains renal glucose reabsorption during genetic and pharmacological SGLT2 inhibition in euglycemia. *Am J Physiol Renal Physiol.* 2014;306:F188–F193.)

of 64% in *WT* and 17% in *Sglt1*^{-/-} mice. Dosing the SGLT2 inhibitor to fully inhibit SGLT2 reduced fractional renal glucose reabsorption to 44% in *WT* and eliminated net renal glucose reabsorption in *Sglt1*^{-/-} mice (Fig. 8.3). Finally, the absence of net renal glucose reabsorption was confirmed in male and female mice lacking both *Sglt1* and *Sglt2*²⁴ (Fig. 8.3). These studies demonstrated that SGLT1 provides a significant glucose transport capacity in the late proximal tubule, which, in the normal kidney, remains mostly unused

due to upstream glucose reabsorption by SGLT2. Inhibition of the latter, however, delivers more glucose downstream and unmasks the transport capacity of SGLT1 (Fig. 8.1). This is also consistent with a high maximal glucose transport rate proposed for human SGLT1 based on *in vitro* studies.²⁸ As a consequence, combined inhibition of renal SGLT2 and SGLT1 is more glucosuric than inhibition of SGLT2 alone. This has been observed in nondiabetic and diabetic mice^{24,29} and in studies using a potent dual SGLT2/SGLT1 inhibitor.³⁰

The studies further indicated that SGLT2 and SGLT1 can account for all net glucose reabsorption in the kidney under normoglycemic conditions²⁴ (Fig. 8.3). Moreover, the data allowed estimating that the basal overall glucose reabsorption capacities for SGLT2 versus SGLT1 in a nondiabetic mouse kidney is in the range of 3:1 to 5:1.³¹

Clinical Relevance

Inhibition of Renal Glucose Reabsorption as a New Antihyperglycemic Therapy

SGLT2 inhibitors are a new class of antihyperglycemic drugs that have been approved in T2DM, work independently of insulin, improve glycemic control in all stages of diabetes mellitus in the absence of clinically relevant hypoglycemia, and can be combined with other antidiabetic agents. SGLT2 inhibition lowers glomerular hyperfiltration by a blood glucose-independent mechanism. By acting as a diuretic and lowering blood pressure and diabetic glomerular hyperfiltration, SGLT2 inhibitors have the potential to induce protective effects on the kidney and cardiovascular system beyond blood glucose control.

MOLECULAR CHARACTERIZATION OF PROXIMAL TUBULAR GLUCOSE TRANSPORT

APICAL GLUCOSE TRANSPORTERS

Crane first proposed in 1960 that active glucose transport in the intestinal epithelium (which expresses SGLT1) was energized by the Na^+ gradient across cell membranes, the so-called Na^+ -glucose cotransport hypothesis (for review, see Wright et al.²¹). The Na^+/K^+ -ATPase located on the basolateral membrane is the primary active and ATP-consuming transport step, which lowers cytosolic Na^+ concentrations and establishes the concentration gradient that drives Na^+ uptake, and, secondary, the uptake of other molecules from the luminal surface into proximal tubule cells (Figs. 8.1 and 8.4). This concept was rapidly refined and extended to active transport processes of a diverse range of molecules and ions including Na^+ -glucose cotransport in the kidney.²¹

SGLT1 and SGLT2 have been the most intensively studied members of the human SLC5 solute carrier (SLC) family, which now includes 12 members. Six of these are named as SGLTs, varying in their preferences for binding of glucose, galactose, mannose, fructose, myoinositol, choline, short-chain fatty acids, and other anions.²¹ All SGLTs have 15 exons, spanning from 8 to 72 kb, which code for 60- to 80-kDa proteins composed of 580–718 amino acids.²¹ The molecular nature of SGLTs has been largely pioneered by studies in

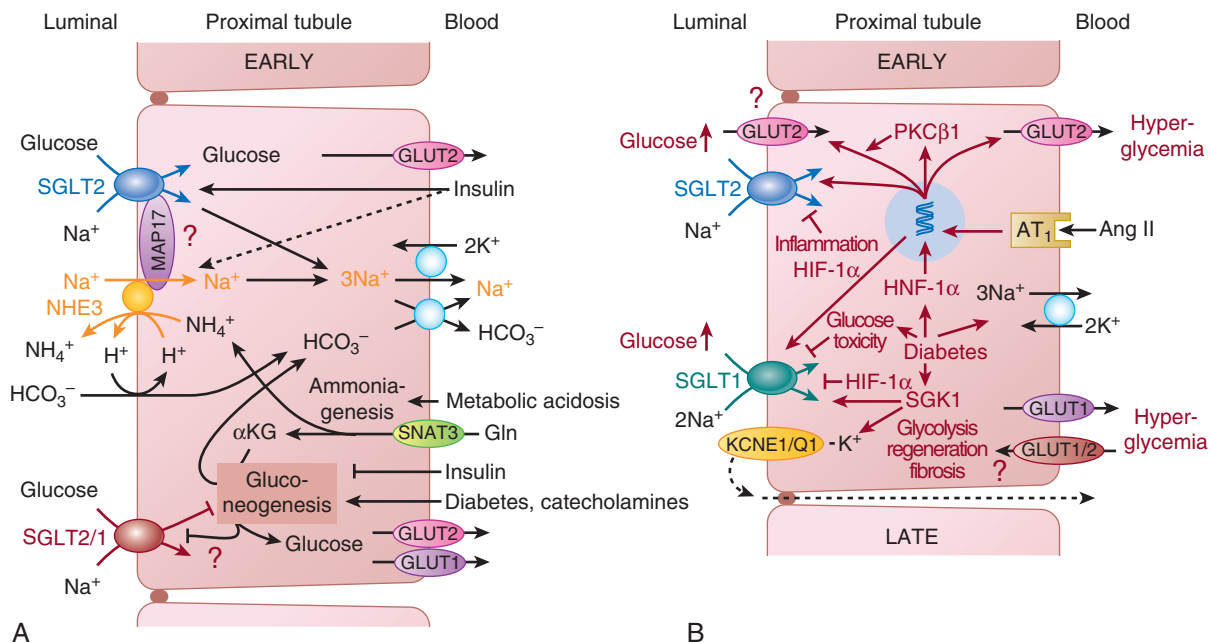


Fig. 8.4 Regulation of glucose transport in the proximal tubule. (A) Insulin is a physiologic stimulator of SGLT2, which may serve to maximize renal glucose reabsorption capacity in situations of increased blood glucose levels (e.g., after a meal). At the same time, enhanced Na^+ -glucose uptake and insulin suppress renal gluconeogenesis. The latter, in contrast, is stimulated by fasting, which may involve increased catecholamine levels. In metabolic acidosis, the increase in gluconeogenesis from glutamine (*Gln*) is linked to the formation of (1) ammonium (NH_4^+), a renally excreted acid equivalent, and (2) new bicarbonate, which is taken up into the circulation. The Na^+ - H^+ exchanger NHE3 contributes to apical H^+/NH_4^+ secretion and Na^+ /bicarbonate reabsorption. SGLT2 and NHE3 are both stimulated by insulin to enhance Na^+ and glucose reabsorption, and their functions may be positively linked through the scaffolding protein MAP17. (B) Diabetes increases luminal glucose delivery to both SGLT2- and SGLT1-expressing segments. Glucose transporters GLUT2 and GLUT1 mediate glucose transport across the basolateral membrane, but GLUT2 may also translocate to the apical membrane in diabetes. Angiotensin II (*Ang II*), serum, glucocorticoid-inducible kinase SGK1, hepatocyte nuclear factor HNF-1 α , and protein kinase C PKC β 1 promote glucose reabsorption in the diabetic kidney, whereas hypoxia-induced HIF-1 α , inflammation, and excessive intracellular glucose levels may be inhibitory. Basolateral glucose uptake via GLUT1/2 may be involved in glycolysis and tubule regeneration after injury as well as hyperglycemia-induced TGF- β .

the laboratory of Wright and colleagues (see Wright et al.²¹ for review). This involved identifying and cloning SGLT1, identifying that defects in SGLT1 were associated with intestinal malabsorption of glucose–galactose and cloning of SGLT2. Wright's group also defined the crystal structure of a sodium galactose bacterial isoform in *Vibrio parahaemolyticus* (vSGLT), which allowed better characterization of how Na⁺ and sugar transport is coupled: Na⁺ binds first to the outside of the transport protein to open the outside gate, thereby permitting outside sugar to bind and be trapped; this is followed by a conformational change and the subsequent opening of the inward gate releases the Na⁺ and sugar into the cell cytoplasm. The transport cycle is completed by the change in conformation from an inward-facing ligand-free state to an outward-facing ligand-free state.^{21,32}

The sugar selectivity and transport kinetics of cloned SGLTs were determined using electrophysiologic techniques in various expression systems. The affinity of SGLT1 is similar for glucose and galactose, whereas SGLT2 does not transport galactose, and neither transports fructose.²¹ More recent studies in transfected human embryonic kidney (HEK) 293T cells indicated that the apparent affinities (K_m) for D-glucose are rather similar for human SGLT1 and human SGLT2, with values of 2 mM and 5 mM, respectively.²⁸ Sugar binding occurs in a Na⁺-dependent manner, and the K_m values for Na⁺ transport by human SGLT1 and human SGLT2 are 70 mM and 25 mM, respectively.²⁸ Thus, under euglycemic conditions, the glucose concentration in the tubular fluid of the very early proximal tubule (reflecting blood glucose levels) is similar to the K_m of SGLT2, whereas the luminal Na⁺ concentration of ~140 mM is higher than the K_m of SGLT2 and not rate limiting.

SGLT1 and SGLT2 transport Na⁺ and glucose with an Na⁺–glucose coupling ratio of 2:1 and 1:1, respectively.²⁸ The greater Na⁺–glucose coupling ratio of SGLT1 enhances its glucose concentration power and thereby the ability of the late proximal tubule to effectively reabsorb glucose despite falling luminal glucose concentrations (see Fig. 8.1). Na⁺–glucose transport is electrogenic, and the membrane potential and driving force are maintained by paracellular Cl⁻ reabsorption or transcellular K⁺ secretion, the latter involving KCNE1/KCNQ1 channels in the luminal membrane of the proximal tubule^{33,34} (Fig. 8.1).

The mRNA expression of three other members of the SLC5 family that can transport glucose based on in vitro substrate studies has been detected in the kidney.³⁵ SGLT3 (*SLC5A4*) is not a glucose transporter, but glucose can depolarize the plasma membrane in its presence in a saturable, Na⁺-dependent manner, and this effect is inhibited by phlorizin. As such, it has been proposed to be a glucose sensor; however, its expression and function in the kidney remain unclear.³⁶ SGLT4 (*SLC5A9*) is expressed in the kidney, and transports glucose in COS-7 cells but with a lower apparent affinity than mannose (Ki 8 vs. 0.15 mM).³⁷ Thus, SGLT4 may primarily be involved in mannose homeostasis. SGLT5 (*SLC5A10*) is an Na⁺-dependent sugar transporter that has a relatively high affinity and capacity for mannose and fructose relative to glucose and galactose.^{38,39} SGLT5 mRNA is highly kidney abundant and expressed in kidney cortex,^{38,40} and recent studies in knockout mice indicated that SGLT5 is the major luminal transporter for fructose reabsorption in the kidney.⁴¹

BASOLATERAL GLUCOSE TRANSPORTERS

In the healthy kidney, the glucose that is being reabsorbed by proximal tubule cells is not linked to appreciable glucose metabolism in these cells. This is due to the fact that most glucose is reabsorbed in the early PCT (S1 segment), but these cells lack significant capacity for aerobic and anaerobic glycolysis.^{42–44} Thus, glucose that is taken up across the luminal membrane or formed within proximal tubule cells (see later) exits across the basolateral membrane into the interstitium by concentration–driven facilitative glucose transporters, GLUT2 and GLUT1 (see Fig. 8.1) and subsequently enters the peritubular capillaries by convection through fenestrated endothelial cells. GLUT2, the low-affinity (K_m ; 15–20 mM) “liver” transporter is primarily expressed in the PCT (S1/S2 segments), but GLUT2 mRNA has also been detected in the proximal straight tubule (PST) (S3 segment).⁴⁵ GLUT2 is thought to be the dominant transporter involved in basolateral exit of glucose derived from apical glucose uptake or gluconeogenesis in the PCT.^{46–48} In comparison, GLUT1, the high-affinity (1–2 mM) “erythroid/brain” transporter is expressed along the entire proximal tubule and has been implicated in transcellular glucose transport, particularly in the S3 segments.^{46–48} Notably, GLUT1 is also expressed in the basolateral membrane of further distal tubule segments and at higher levels than in S3 segments. This includes expression in the medullary thin and thick ascending limbs (TAL) of the rat kidney and at the highest levels in connecting segments and collecting ducts. In the latter, GLUT1 was expressed at the highest level in intercalated cells and to a lesser extent in principal cells.⁴⁸ These findings indicated a good correlation between the level of GLUT1 expression and the glycolytic activity of the different nephron segments, indicating that, in particular, the more distal tubule segments are taking up glucose for energy supply via basolateral GLUT1. Recent studies used positron emission tomography and α -methyl-4-[F-18]-fluoro-4-deoxy-d-glucopyranoside to monitor glucose transport in mouse kidneys lacking either SGLT1, SGLT2, or GLUT2. The studies confirmed prominent contributions of SGLT2 and SGLT1 to renal glucose uptake. Moreover, renal glucose reabsorption appeared absent in mice lacking GLUT2, consistent with a more prominent role of GLUT2 versus GLUT1 with regard to basolateral glucose exit of glucose in the proximal tubule⁴⁹ (Fig. 8.1). This is in line with the renal phenotype of patients with mutations in GLUT2 and GLUT1. Loss of function mutations in GLUT2 are the basis of the Fanconi–Bickel syndrome, which includes a renal Fanconi syndrome, a proximal tubulopathy consisting of glycosuria, phosphaturia, aminoaciduria, proteinuria, and hyperuricemia.^{50–52} The observed proximal tubulopathy may be due to intracellular glucose accumulation and glucotoxicity that occurs when basolateral glucose exit is blocked. In comparison, patients with GLUT1 mutations have primarily neurologic symptoms, and no renal phenotype has been documented.^{50,53}

In addition to GLUT1 and GLUT2, some of the other 12 members of the SLC2 gene family have been found in the kidney and may contribute to glucose transport, but little is known about their quantitative contribution.⁵⁴ For example, GLUT4 mRNA and immunoreactivity were focally localized in the TALH of the loop of Henle, coexpressed with IGF-I and increased by vasopressin treatment, indicating a potential

role in local fuel control.⁴⁵ GLUT5 is strongly expressed in the apical membrane of the S3 segment in the rat kidney but proposed to transport primarily fructose.^{45,55} GLUT12 can transport glucose, and an apical localization has been reported in distal tubules and collecting ducts, but its quantitative role remains to be determined.⁵⁶

RENAL FORMATION OF GLUCOSE

The kidneys not only reabsorb the filtered glucose and use glucose as an energy source, but they also generate new glucose. Gluconeogenesis involves the formation of glucose-6-phosphate from precursors such as lactate, glutamine, alanine, and glycerol with its subsequent hydrolysis by glucose-6-phosphatase to generate free glucose that can exit the cell. The healthy human kidneys produce ~15–55 g glucose per day by gluconeogenesis. In fact, the human liver and kidneys provide about equal amounts of glucose via gluconeogenesis in the postabsorptive state (i.e., 12–16 hours after the last meal).⁵⁷ Renal gluconeogenesis occurs along the entire proximal tubule, but its activity is usually higher in the earlier segments.^{43,58}

Renal gluconeogenesis is stimulated by epinephrine and inhibited by insulin⁵⁷ (see Fig. 8.4). Insulin-induced suppression of gluconeogenic gene expression in the proximal tubule was accompanied by phosphorylation and inactivation of forkhead box transcription factor 1 (FoxO1).⁵⁹ In contrast to the liver, renal gluconeogenesis is probably insensitive to glucagon.⁵⁷ Studies in humans indicated that in the postabsorptive state, renal gluconeogenesis uses primarily lactate as substrate, followed by glutamine, glycerol, and alanine.⁶⁰

In contrast to the uniform stimulation of gluconeogenesis along the entire proximal tubule by starvation, metabolic acidosis enhances gluconeogenesis primarily in S1 and S2 segments.^{43,58,61} Furthermore, gluconeogenesis in response to metabolic acidosis primarily uses glutamine as substrate. During the process of renal gluconeogenesis from glutamine, the conversion of glutamine to glutamate and α -ketoglutarate produces ammonium (NH_4^+), which is excreted into the urine as an acid equivalent. The subsequent pathway from α -ketoglutarate to glucose forms new bicarbonate, which is returned as buffer to the systemic circulation (see Fig. 8.4). The described link between proximal tubular ammonium, bicarbonate, and glucose formation explains why acidosis is a prominent stimulus for renal gluconeogenesis.^{57,60}

Apical glucose uptake via SGLT1 or SGLT2 can have an inhibitory influence on the expression of renal gluconeogenic genes (see Fig. 8.4). This effect may serve to prevent glucose overload in the cells of the proximal tubule, and has been proposed to involve glucose-induced and sirtuin 1–mediated deacetylation of peroxisome proliferator–activated receptor gamma coactivator 1- α , a coactivator of FoxO1.⁵⁹

In general, it is expected that cytosolic glucose in proximal tubule S3 segments is used for metabolism or leaves the cell via basolateral GLUT1. It has also been hypothesized that glucose generated from lactate in the medullary S3 segment forms part of an intrarenal Cori cycle⁶²; glucose enters the lumen by reversed transport through SGLT1 and is taken up by downstream tubular segments, where it is used as energy substrate for glycolysis (e.g., in medullary TAL), and the formed lactate is being returned to the neighboring S3 segment as a substrate for gluconeogenesis. Studies in human proximal tubule segments indicated that in contrast to S1

segments, lactate appears to be a better gluconeogenic precursor than glutamine in S2 and S3 segments.⁶³ Moreover, studies in mice indicated that the luminal membrane of the thick ascending limb in the outer stripe of the outer medulla and in the cortex (including the macula densa) express SGLT1.¹⁹ The rat appears to express SGLT1 also in the cortical TAL and macula densa.¹⁷ Further studies are needed to clarify whether the TAL (and macula densa) in human also express SGLT1, and determine the potential role of SGLT1 in these structures, including a proposed Cori cycle.

Taken together and under normal conditions, the PCT is the site of greatest renal glucose reabsorption and generation. The ability of early proximal tubular segments for gluconeogenesis but inability to metabolize glucose prevents a futile cycle. The reabsorption of filtered glucose and renal gluconeogenesis provide an energy source to distal tubular segments, primarily in the renal medulla, and returning the glucose to the systemic circulation helps to maintain blood glucose levels, particularly in the postabsorptive state. In addition, renal gluconeogenesis is closely linked to the renal response to metabolic acidosis. See Chapter 5 for additional discussion of the role of gluconeogenesis in renal metabolism.

RENAL GLUCOSE TRANSPORT IN DISEASE STATES

GLUCOSE TRANSPORT IS INCREASED IN THE DIABETIC KIDNEY

Lowering hyperglycemia is vital in diabetic patients to attenuate the progression of the underlying metabolic dysfunction⁶⁴ and to reduce the risk of diabetic complications including nephropathy and cardiovascular disease.⁶⁵ Current therapies for type 2 diabetes mellitus (T2DM) include drugs that target the liver, small intestine, adipose tissue, skeletal muscle, and/or pancreas. Many of these therapies, including insulin, have difficulties to establish adequate glycemic control without the potential for relevant unwanted side effects, including hypoglycemia and weight gain, and may not reduce cardiovascular complications.⁶⁶ The following sections outline how glucose transport changes in the diabetic kidney, its implications for diabetic kidney function, and how targeting renal glucose transport can serve as a new antihyperglycemic therapy.

Diabetes mellitus is associated with increased blood glucose levels. This enhances the amounts of glucose filtered by the kidneys, as long as GFR is preserved. In fact, the early phase of diabetes is often associated with an increase in GFR or glomerular hyperfiltration (see later), which further increases the tubular glucose load. At the same time, the tubular capacity to reabsorb glucose increases by ~20%–30% to ~500–600 g/day in patients with T2DM^{67,68} and type 1 diabetes (T1DM).³ Thus, diabetes often increases the glomerular filtration and tubular reabsorption of glucose. Moreover and despite increased blood glucose levels, diabetes also enhances renal gluconeogenesis.⁵⁷ The latter can be the consequence of diabetes-associated metabolic acidosis, and the induced gluconeogenesis involves metabolism of glutamine to glucose associated with the generation of ammonia and bicarbonate⁵⁷ (see Fig. 8.4). Other potential triggers for gluconeogenesis in diabetes include the activation of the sympathetic nervous system, the reduced insulin levels observed in T1DM, enhanced circulating fatty acids, or the kidneys receive another

signal from insulin-dependent cells that cannot take up glucose due to low insulin levels (T1DM) or insulin resistance (T2DM) and are glucose “starved.”

Increasing renal glucose reabsorption in response to a rise in filtered glucose makes sense with regard to energy substrate conservation. Moreover, the further distal segments may need/use more glucose as an energy substrate to reabsorb the load of salt and other compounds, which is increased due to glomerular hyperfiltration. Renal glucose retention and enhanced glucose formation become maladaptive in diabetes, however, when they sustain hyperglycemia (see Fig. 8.4). In this regard, the kidney provides a safety valve that can prevent extreme hyperglycemia. When blood glucose levels increase to the point that the filtered load exceeds the T_m or tubular transport capacity for glucose, then the surplus is excreted in the urine. The safety valve, however, only opens at rather high blood glucose levels (>15 mmol/L) (see Fig. 8.2) and only works as long as glomerular filtration is maintained, and its threshold depends on the level of expression and activity of the involved glucose transporter, and its functionality may thus vary from patient to patient.

GLUCOSE TRANSPORTERS IN THE DIABETIC KIDNEY

The levels of protein expression and activity of SGLT2, SGLT1, GLUT2, and potentially GLUT1 determine the capacity of renal glucose reabsorption, and their upregulation may explain the increased glucose transport maximum that can be observed in diabetes. The available preclinical and human studies reported increased, unchanged, or reduced renal glucose transporter expression and/or activity in diabetes or under high-glucose conditions.⁶⁹ The observed different responses may reflect different diabetes models, metabolic states, levels of kidney injury, other factors that regulate the expression of these transporters, the use of nonselective antibodies, or dissociations between mRNA and protein expression.

SGLT2 AND GLUT2

Using knockout mice as gold standard negative antibody controls, the renal protein expression of SGLT2 was found to be increased by 40%–80% in the early hyperglycemic stages of genetic mouse models of T2DM (db/db) and T1DM (Akita).^{70,71} The proximal tubule, like many nephron segments, expresses insulin receptors and binds insulin.⁷² Application of insulin to HEK-293T cells phosphorylated SGLT2 at Ser624, which increased Na^+ -glucose transport.⁷³ Thus, the insulin release following a meal may act on the PCT to enhance SGLT2 activity and conserve filtered glucose (see Fig. 8.4). Moreover, hyperinsulinemia associated with insulin resistance in obesity and T2DM may enhance renal SGLT2 activity⁷² (Fig. 8.4). This may be coordinated with a stimulatory effect of insulin on other Na^+ -coupled transporters in the proximal tubule, including the Na^+ -proton exchanger NHE3.^{72,74} Recent studies indicated that SGLT2 may be functionally linked to NHE3^{75–77} such that SGLT2 inhibition may, to some extent, inhibit NHE3 in the proximal tubule (Fig. 8.4). A similar interaction has been proposed for the coregulation of SGLT1 and NHE3 in the small intestine.

Consistent with a potential concerted regulation of luminal and basolateral glucose transport, upregulation of GLUT2 expression has been reported in renal proximal tubules in diabetic rats.^{78–81} Notably, studies in streptozotocin (STZ)-

induced T1DM in rats proposed targeting of GLUT2 (but not GLUT1) also to the brush border membrane of proximal tubules.^{82,83} The latter may be linked to protein kinase C $\text{PKC}\beta 1$ activation^{83–85} and may implicate facilitative glucose transport, together with SGLT2 and SGLT1 in the increased glucose reabsorption across the apical membrane of proximal tubules in the diabetic kidney (Fig. 8.4).

The available data on changes in glucose transporters in diabetic patients are sparse and also variable. Primary cultures of human exfoliated proximal tubular epithelial cells harvested from fresh urine of patients with T2DM showed an increased glucose uptake associated with increased protein expression of SGLT2 and GLUT2.⁸⁶ An increase in SGLT2 protein expression has also been reported in fresh kidney biopsies of patients with T2DM and advanced nephropathy.⁸⁷ On the other hand, the mRNA expression of SGLT2 and GLUT2 was slightly lower in 19 patients with T2DM and preserved kidney function as compared with 20 nondiabetic patients matched for age and estimated GFR (eGFR), all being subjected to nephrectomy.⁸⁸ Similar results were reported for SGLT2 and GLUT2 mRNA in another set of patients with T2DM, but the results did not reach statistical significance.⁸⁹

If an increase in SGLT2 expression occurs in the diabetic kidney, then it may simply reflect overall growth and hypertrophy of the diabetic proximal tubule and the associated increase in transport machinery,^{90,91} and this may be exaggerated with advanced nephropathy when nephrons are lost and the remaining nephrons aim to compensate. Moreover, upregulation of SGLT2 expression in diabetic rats has been linked to activation of Ang II AT1 receptors⁹² and the transcription factor, hepatocyte nuclear factor HNF-1 α .⁹³ The latter as well as HNF-3 β have also been implicated in renal GLUT2 upregulation⁷⁹ (see Fig. 8.4). Notably, pharmacologic inhibition of SGLT2 in normoglycemic mice also increased renal membrane SGLT2 protein expression,⁷¹ possibly reflecting a negative feedback regulation of SGLT2 expression by intracellular glucose levels. Along this line, if renal SGLT2 expression is reduced in the diabetic kidney, this may be due to enhanced diabetes-induced proximal tubular gluconeogenesis (Fig. 8.4) or reflect more severe tubular hypoxia or inflammation.^{94–96}

SGLT1 AND GLUT1

The renal expression of SGLT1 protein appears to vary among genetic mouse models of diabetes: renal SGLT1 protein expression was found to be increased in leptin-deficient ob/ob mice,⁹⁷ a model of T2DM, and reduced in Akita mice, a model of T1DM⁷⁰; the latter study used knockout mice as negative antibody control. In contrast to SGLT2 (see earlier), insulin stimulation slightly decreased SGLT1-mediated Na^+ -glucose transport in HEK-293T cells,⁷³ indicating differences in the regulation of these two transporters. In contrast to the strong increase in SGLT2 (see earlier), SGLT1 protein was not significantly changed in fresh kidney biopsies of patients with T2DM and nephropathy in comparison with nondiabetic controls.⁸⁷ The interpretation of renal SGLT1 mRNA expression data may be complicated by the observation that mRNA and protein expression can dissociate, at least in mouse kidney.⁹⁸

GLUT1 protein expression was downregulated in proximal tubules isolated from rat cortices at 2 and 4 weeks after STZ,⁸¹ but increased in kidneys of rats at 30 weeks after STZ.⁵⁶ A

study in patients with T2DM and preserved kidney function reported that in whole renal tissue, GLUT1 mRNA expression were slightly lower as compared with nondiabetic patients.⁸⁸

Why should diabetes reduce renal SGLT1 expression? Although this would make the renal glucose valve to open earlier (and make SGLT2 inhibitors more efficacious, see later), this may not be the kidneys' intention. A reduced renal SGLT1 protein expression was also observed in response to genetic or pharmacologic SGLT2 inhibition in nondiabetic mice.^{15,71} These conditions and diabetes share an enhanced glucose load to the late proximal tubule. In vitro studies in proximal tubule cells indicated that high glucose can reduce SGLT expression and Na⁺-glucose cotransport activity via enhanced oxidative stress.⁹⁹ Studies in a model of pig epithelial tubular cells (LLC-PK1) showed that hypoxia can diminish SGLT1 (and SGLT2) protein expression by activation of hypoxia-inducible factor-1 α (HIF-1 α).⁹⁵ Thus, an increased glucose load to the outer medullary S3 segment enhances Na⁺-glucose reabsorption and thereby hypoxia, which may downregulate SGLT1 to limit oxygen-consuming transport work and glucotoxicity in this segment, which has a high sensitivity to acute injury⁹⁴ (see Fig. 8.4).

In comparison, an increase in SGLT1 expression in the diabetic kidney would further increase the renal glucose reabsorption capacity but may put the S3 segment at risk of hypoxia and enhanced glucotoxicity. Studies in Akita diabetic mice indicated that the serum and glucocorticoid-inducible kinase SGK1 may stimulate SGLT1 activity and glucose reabsorption in PSTs.¹⁰⁰ SGK1 could also promote proximal tubular glucose reabsorption by enhancing the activity of luminal K⁺ channels (KCNE1/KCNQ1), which maintain the electrical driving force during electrogenic Na⁺-glucose cotransport^{33,34,101} (see Fig. 8.4). SGK1 was upregulated in proximal tubules in patients with diabetic nephropathy.¹⁰²

Transport functions in proximal tubules require high turnover of ATP, which, under normal conditions, is derived primarily through mitochondrial oxidative phosphorylation.^{43,103} This may change in pathophysiologic situations with impaired mitochondrial function, when glycolysis may be enhanced and contribute to maintaining ATP. For example, a shift to glycolysis has been proposed in proximal tubules regenerating from acute kidney injury (AKI) as well as proximal tubules undergoing atrophy.¹⁰⁴ This metabolic switch to glycolysis occurred early during proximal tubule regeneration and was reversed during successful tubular recovery, but persisted and became progressively more severe in tubule cells that failed to redifferentiate. Tubular upregulation of HIF-1 α in mice enhanced renal GLUT1 mRNA expression; this was associated with less oxygen consumption and increased glycolysis.¹⁰⁵ Thus, hypoxia may increase basolateral GLUT1-mediated facilitative uptake of glucose, which is then used for glycolysis and recovery. Hypoxia-induced GLUT1 likely applies to distal tubule segments but may also be relevant for medullary S3 segments.¹⁰⁴ In this regard, studies in the proximal tubular cell line LLC-PK1, which was cultured and polarized on porous tissue culture inserts, showed that basolateral exposure to 25 mmol/L D-glucose enhanced glucose uptake via GLUT1 and the subsequent intracellular metabolism of glucose enhanced TGF- β 1 synthesis and secretion; this was not observed in response to apical glucose exposure.¹⁰⁶ These in vitro studies suggest that it may be the hyperglycemia-induced persistent uptake of glucose via

basolateral GLUT1 (or GLUT2), rather than the filtered glucose, that affects the tubular synthesis of TGF- β 1 and thereby the development of tubulointerstitial fibrosis and tubular growth (Fig. 8.4).

INHIBITION OF RENAL GLUCOSE REABSORPTION AS A NEW ANTIHYPERGLYCEMIC THERAPY

When blood glucose levels increase to the point that the filtered load exceeds the transport capacity of the tubular system, then the surplus is excreted in the urine. This renal safety valve can prevent extreme hyperglycemia. As outlined earlier, most capacity for renal glucose reabsorption is provided by SGLT2 in the early proximal tubule. When SGLT2 is inhibited, the reabsorptive capacity for glucose declines to the residual capacity of SGLT1, which equals ~80 g/day. In other words, SGLT2 inhibition causes the renal safety valve to open at a lower threshold (see Fig. 8.2) and makes it also relevant to glucose homeostasis in the euglycemic and moderately hyperglycemic range. Several SGLT2 inhibitors have now been approved as glucose-lowering agents for subjects with T2DM and preserved kidney function. Previously, the presence of glucosuria in a diabetic patient indicated inappropriate blood glucose control, as it showed that blood glucose was so high that the filtered glucose overwhelmed the glucose reabsorption capacity. In contrast and with the use of SGLT2 inhibitors, glucosuria is purposely induced to improve blood glucose control. The following sections discuss the role of SGLT2 in the pathophysiology of renal glucose reabsorption and outline the unexpected logic of inhibiting SGLT2 in the diabetic kidney.⁹⁰ This includes the counterproductive enhancement of renal glucose reabsorption via SGLT2 in diabetes as well as a brief discussion of the basic mechanisms that link a primary inhibition of Na⁺-glucose cotransport in the kidney to secondary beneficial consequences on the metabolism, the kidneys, and the cardiovascular system.

Long-term access to excessive exogenous energy resources is not part of human evolution. As a consequence, it may not come as a surprise that the body's responses to excess exogenous energy resources can be maladaptive. In contrast, the body's responses to environments with scarce energy resources have been intensively tested and refined during evolution for the survival of the organism. Therefore, targeting metabolism in the "periphery" by inhibiting renal glucose reabsorption and spilling glucose as an energy resource into the urine and then using the central metabolic counterregulatory mechanisms to readjust the metabolism, may provide unique benefits as an antihyperglycemic approach.⁹⁰ This is supported by clinical outcome studies using an SGLT2 inhibitor on top of standard of care in patients with high cardiovascular risk that demonstrated protective effects with regard to clinically relevant renal and cardiovascular outcomes.¹⁰⁷⁻¹⁰⁹

Phlorizin is a flavonoid contained in the bark of various fruit trees and was discovered to cause glucosuria more than 100 years ago.¹¹⁰ Phlorizin competitively inhibits SGLT2 and SGLT1, the former with a 10-fold higher affinity.^{21,28} SGLT1 is expressed in many other organs and is the primary pathway for glucose reabsorption in the intestine.¹¹¹ As a consequence, oral administration of phlorizin is burdened by extrarenal side effects, most prominently diarrhea. In comparison and in healthy subjects, SGLT2 appears to be expressed only in

kidney proximal tubule,^{18,98} with a proposed expression and function in α cells of the pancreas¹¹² needing confirmation. Inhibition of renal glucose transport became practical when phlorizin derivatives were developed that are specific for SGLT2, have good oral bioavailability, and are suitable for once-daily dosing.¹¹³ Three members in this class, dapagliflozin (Forxiga or Farxiga in the United States), canagliflozin (Invokana), and empagliflozin (Jardiance) are approved in the United States and Europe for use in T2DM with preserved kidney function. Others, including ipragliflozin (Suglat), luseogliflozin (Lusefi), and tofogliflozin (0) are approved in Japan. SGLT2 inhibitors are under clinical investigation as add-on therapies to insulin in T1DM.

SGLT2 inhibitors act on their target from the extracellular surface of the cell membrane¹¹⁴ and reach their target by glomerular filtration and, as indicated for empagliflozin, also by tubular secretion.¹¹⁵ SGLT2 inhibitors induce a sustained urinary glucose loss of 40–80 g/day.^{113,116,117} In patients with T2DM, this is associated with a decrease in Hb A1C levels by 0.5%–0.7% at 12 weeks of treatment, and this effect persisted for up to 52 weeks.¹¹⁸ The higher the blood glucose level and GFR, the more glucose is filtered and reabsorbed and, as a consequence, can be excreted in response to SGLT2 blockade. Thus, SGLT2 blockers naturally have a greater efficacy when it is desirable for them to be more efficacious.^{15,119,120} By lowering blood glucose levels and body weight, SGLT2 inhibitors improve β -cell function and sensitivity to insulin in patients and rodent models with T2DM.^{119,121–124} Because the renal mechanism of action of SGLT2 inhibitors is independent of insulin, their efficacy is not declining with progressive β -cell dysfunction and/or insulin resistance, and SGLT2 inhibitors act synergistically with other blood glucose-lowering agents.¹¹³

Two SGLT2 inhibitors have now been evaluated in major clinical trials in patients with T2DM: empagliflozin in the 7,020-patient EMPA-REG OUTCOME trial^{107,109} and, more recently, canagliflozin in 10,142 patients in the CANVAS program.¹⁰⁸ In addition to cardiovascular endpoints, both trials also included measurement of albuminuria and eGFR. The outcomes of the EMPA-REG OUTCOME and the CANVAS program are similar in most regards. Both went beyond the requisite safety parameters to show ~35% reductions in the incidence of heart failure. Both trials also reported beneficial effects on the kidney, including 40%–50% reductions in the hazard ratios for albuminuria or decline in eGFR. The relative risk of cardiovascular death was significantly reduced by SGLT2 inhibition in the EMPA-REG OUTCOME trial but not in the CANVAS program. This difference might be due to the higher prevalence of cardiovascular disease in the EMPA-REG OUTCOME cohort at baseline. The main cardiovascular effect of SGLT2 inhibition was on heart failure, rather than ischemic events, and both trials showed tangible benefits on heart failure outcomes. These benefits occurred when added to standard care, which included ~80% of patients being treated with an angiotensin-converting enzyme inhibitor or angiotensin AT1 receptor antagonist. The main side effect of SGLT2 inhibitors is an increased risk of genitourinary infections due to the glucosuric effect.¹²⁵

How can inhibition of renal glucose transport protect the kidney and cardiovascular system? By reducing hyperglycemia, SGLT2 inhibitors have the potential to reduce glucotoxicity in the kidney and extrarenal organs.^{126,127} In accordance,

studies in diabetic rodents have shown that SGLT2 inhibition can reduce growth, lipid accumulation, inflammation, and injury of the diabetic kidney secondary to a strong blood glucose-lowering effect^{70,71,87,97,128–131} (Fig. 8.5). The observed small effect of SGLT2 inhibitors on blood glucose control in the EMPA-REG OUTCOME trial and the CANVAS program alone, however, appears insufficient to fully explain the rapid beneficial effect on heart failure detectable within a few months. Although other mechanisms are likely to contribute (see later), it is also possible that, in contrast to SGLT2 inhibitors, these other agents have simultaneous countervailing effects that offset the benefits of better glycemic control, including increased obesity or an increased hypoglycemia risk.

SGLT2 inhibition lowers body weight and has a low hypoglycemia risk. In patients with T2DM, including those in the EMPA-REG OUTCOME trial and the CANVAS program, the glucosuric effect of SGLT2 inhibition was associated with a 2- to 3-kg lower body weight. Although the diuretic effect and fluid loss may contribute to the initial weight loss, the majority of the steady-state weight loss with SGLT2 inhibitor treatment is due to fat loss, including lesser visceral and subcutaneous fat^{132–134} (see Fig. 8.5), due to a shift in substrate utilization from carbohydrates to lipids.^{119,135,136} The released free fatty acids are used by the liver to form ketone bodies and thus increase ketogenesis.¹³⁷ SGLT2 inhibitors may improve cardiac outcomes in part by increasing plasma levels of ketone bodies like β -hydroxybutyrate, which are used as energy substrate to improve the performance of cardiac myocytes (or the kidney) in diabetes mellitus^{138,139} (Fig. 8.5). SGLT2 inhibitors can increase the risk of diabetic ketoacidosis,¹³⁷ particularly when the drugs are used off-label in patients with T1DM.¹³⁷

SGLT2 inhibitors do not increase the incidence of hypoglycemia.^{107–109,118} This is because they become ineffective at lowering blood glucose any further once the filtered glucose load falls to ~80 g/day, which can be handled by renal SGLT1 (see Fig. 8.1). In addition, SGLT2 inhibitors leave the metabolic counterregulation intact and increase plasma glucagon concentrations and subsequently endogenous hepatic glucose production (gluconeogenesis) in patients with T2DM.^{119,122} This is potentially relevant for cardiovascular outcome, because episodes of hypoglycemia can impair the cardioprotective effects of antihyperglycemic therapy.¹⁴⁰

SGLT2 inhibition lowers blood pressure and improves hyperuricemia. A meta-analysis of patients with T2DM treated with SGLT2 inhibitors found a consistent decrease in systolic blood pressure of 3–6 mm Hg,¹¹⁸ similar to preclinical data and the EMPA-REG OUTCOME trial and the CANVAS program. The magnitude of this blood pressure effect is expected to have cardiovascular protective consequences, particularly in high-risk patients.¹⁴¹ The blood pressure-lowering effect of SGLT2 inhibition relates to the reduction in body weight and a modest glucose-based osmotic diuresis (100–470 mL/day) and a small natriuretic effect.^{126,142–145} The lower blood pressure and an associated modest reduction in plasma volume¹⁴⁶ may quickly reduce cardiac pre- and afterload and thereby contribute to the rapid beneficial effects in heart failure patients¹⁰⁷ (see Fig. 8.5).

Beneficial renal and cardiovascular effects of SGLT2 inhibition may also be due to a plasma uric acid-lowering effect.¹⁴⁷ The uricosuric effect of SGLT2 inhibitors is positively

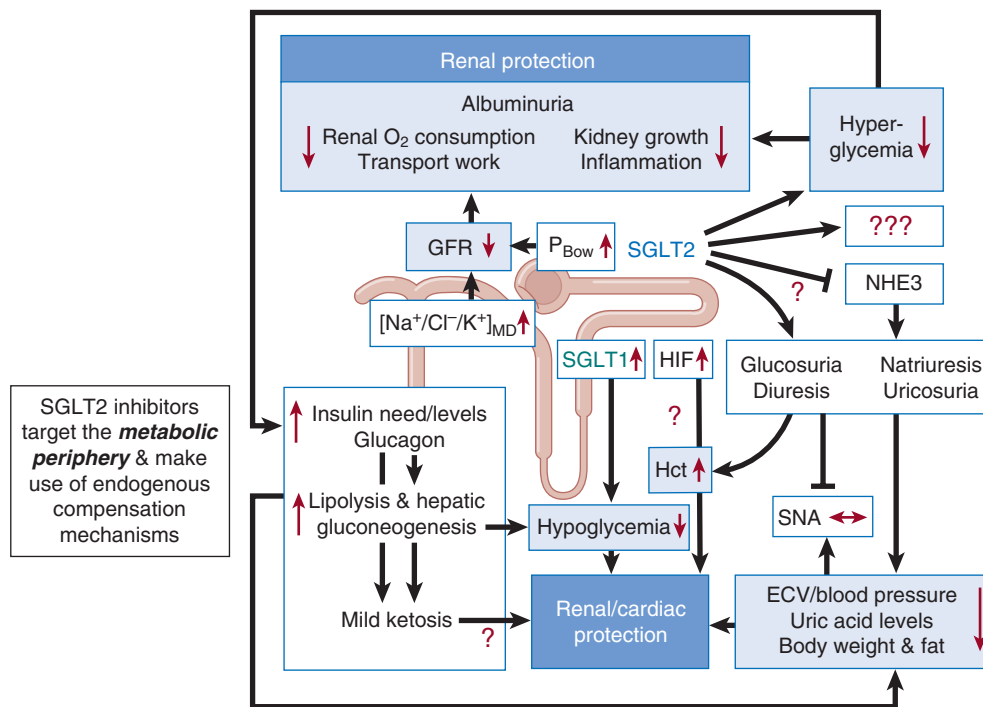


Fig. 8.5 Proposed mechanisms of kidney and heart protection by SGLT2 inhibition in type 1 and type 2 diabetes. SGLT2 inhibition attenuates the primary proximal tubular hyperreabsorption in the diabetic kidney, which increases/restores (1) the signal of the tubuloglomerular feedback at the macula densa ($[Na^+/Cl^-/K^+]_{MD}$) and (2) the hydrostatic pressure in the Bowman space (P_{Bow}). This lowers glomerular hyperfiltration with beneficial effects on tubular transport work and thus oxygen consumption and the filtration of albumin. By lowering blood glucose, SGLT2 inhibitors can reduce kidney growth and inflammation and albuminuria. SGLT2 inhibitors have a modest osmotic diuretic, natriuretic, and uricosuric effect, which can reduce extracellular volume (ECV), blood pressure, serum uric acid levels, and body weight. SGLT2 inhibition blunts an expected reactive increase in sympathetic nerve activity (SNA). SGLT2 may be functionally linked to the Na^+-H^+ -exchanger 3 (NHE3) such that SGLT2 inhibition may also inhibit NHE3 in the proximal tubule. SGLT2 inhibition lowers insulin levels (therapeutic need and/or endogenous) and increases glucagon levels, which increases lipolysis and hepatic gluconeogenesis. These metabolic adaptations reduce fat tissue/body weight and the hypoglycemia risk and induce a mild ketosis, which all may be beneficial for the kidney and cardiovascular system. The hypoglycemia risk is further reduced by SGLT1-mediated glucose reabsorption. SGLT2 enhances active glucose and Na^+ reabsorption in the outer medulla; this may enhance hypoxia-inducible factor (HIF)-induced genes and have kidney and cardiac protective effects through enhancing erythropoietin, hematocrit, and oxygen transport. *Black arrows* indicate consequences of SGLT2 inhibition, and *red arrows* demonstrate direction of changes in the associated variables. “?” indicates hypotheses that need further confirmation. (This figure was modified with permission from Vallon V, Thomson SC. Targeting renal glucose reabsorption to treat hyperglycaemia: the pleiotropic effects of SGLT2 inhibition. *Diabetologia* 2017;60:215–225.)

related to the increase in tubular and urinary glucose delivery, as observed in healthy subjects and patients with T2DM^{148,149} (see Fig. 8.5) and may involve an interaction with the luminal urate transporter URAT1.¹⁴⁹

SGLT2 inhibition lowers diabetic glomerular hyperfiltration. Glomerular hyperfiltration, which is observed in a subset of patients at the onset of T1DM and T2DM, can increase the risk for developing diabetic nephropathy later on.¹⁵⁰ Less than 1% of filtered Na^+ is excreted in the urine in normal human subjects to match urinary excretion to dietary Na^+ intake (i.e., almost all the filtered Na^+ is reabsorbed). As a consequence, GFR, as the primary determinant of filtered Na^+ , also becomes the primary determinant of renal Na^+ reabsorption. The latter, however, determines transport work and, thereby, renal oxygen consumption and requirement. Therefore, glomerular hyperfiltration increases transport work and oxygen consumption in the diabetic kidney, and lowering GFR has opposite effects.¹⁴²

According to the “tubular hypothesis,” glomerular hyperfiltration in diabetes is explained by primary tubular hyperreabsorption (for review, see Vallon and Thomson⁶⁹). Moderate levels of hyperglycemia increase proximal tubular

reabsorption by providing more substrate for Na^+ -glucose cotransport via SGLT2 and SGLT1 and by causing the tubule to grow, which enhances the transport machinery and capacity. The increased reabsorption reduces the $NaCl$ and fluid delivery to the downstream macula densa, which senses this reduction and causes GFR to increase through the normal physiologic action of tubuloglomerular feedback (TGF) (Fig. 8.6). The primary effect of the TGF is to adjust the tone of the afferent arteriole and thereby GFR of the same nephron to stabilize the $NaCl$ and fluid delivery downstream of the macula densa. This facilitates the fine regulation of $NaCl$ and fluid balance in the distal nephron by neurohumoral control. A secondary consequence of this TGF physiology is that the mechanism contributes to the autoregulation of GFR and renal blood flow. Moreover, it makes GFR responsive to primary changes in tubular transport upstream of the macula densa, like in the diabetic kidney. A primary increase in proximal reabsorption also reduces distal tubular flow rate, which increases GFR by lowering tubular back pressure—i.e., the hydrostatic pressure in Bowman space—and thereby increasing the effective glomerular filtration pressure (Fig. 8.6). Mathematical modeling indicates that TGF and the

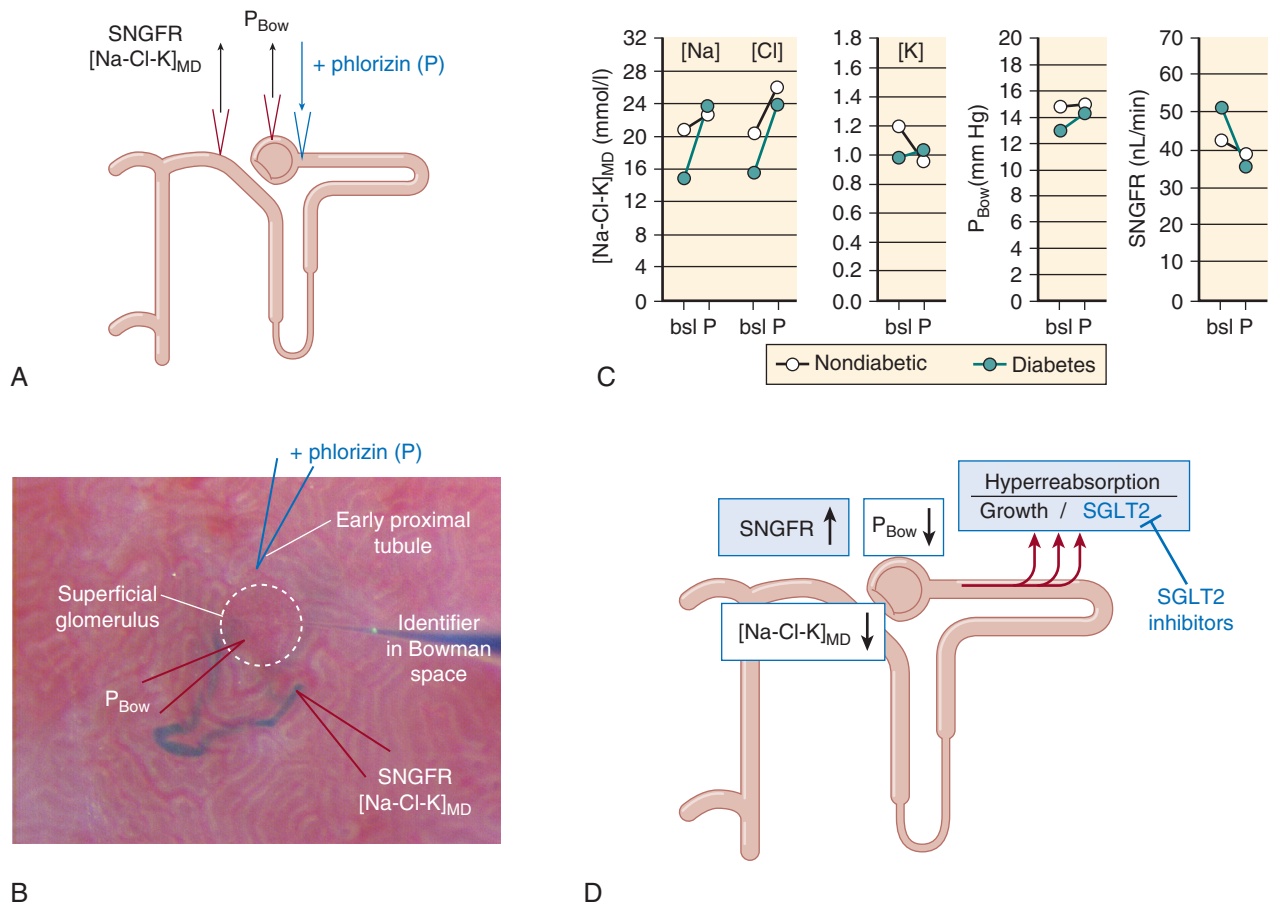


Fig. 8.6 The tubular hypothesis of diabetic glomerular hyperfiltration: effect of SGLT2 inhibition. (A, B) In vivo micropuncture studies in rats with superficial glomeruli were performed in nondiabetic and streptozotocin diabetic rats.¹⁵² Small amounts of blue dye were injected into the Bowman space to determine nephron configuration, including the first proximal tubular loop and the early distal tubule close to the macula densa. Tubular fluid was collected close to the macula densa to determine (1) the tubuloglomerular feedback signal ($[Na-CI-K]_{MD}$), and (2) single-nephron glomerular filtration rate (SNGFR) by inulin clearance. The Bowman space was punctured to determine the hydrostatic pressure (P_{Bow}). Measurements were performed under control conditions and following application of the SGLT2/SGLT1 inhibitor phlorizin into the early proximal tubule (i.e., without changing systemic blood glucose levels). (C) Basal measurements (bsl) revealed that glomerular hyperfiltration in diabetes was associated with reductions in $[Na-CI-K]_{MD}$ and P_{Bow} . Adding phlorizin (P) had a small effect in nondiabetic rats but normalized $[Na-CI-K]_{MD}$, P_{Bow} , and SNGFR in diabetes. (D) Diabetes induces a primary hyperreabsorption in the proximal tubule due to tubular growth and enhanced Na^+ -glucose cotransport, which, through tubuloglomerular feedback ($[Na-CI-K]_{MD}$) and reducing tubular back pressure (P_{Bow}), causes glomerular hyperfiltration. SGLT2 contributes to the tubular hyperreabsorption, and as a consequence, SGLT2 inhibition mitigates these changes and lowers glomerular hyperfiltration. (This figure was modified with permission from Vallon V, Thomson SC. Targeting renal glucose reabsorption to treat hyperglycaemia: the pleiotropic effects of SGLT2 inhibition. *Diabetologia* 2017;60:215–225.)

changes in tubular back pressure contribute equally to the increase in GFR in diabetes.¹⁵¹

Vice versa, SGLT2 inhibition attenuates proximal tubule hyperreabsorption in the diabetic kidney and thereby lowers diabetic glomerular hyperfiltration (see Figs. 8.5 and 8.6). This has been shown in micropuncture studies in rats using direct application of phlorizin into the Bowman space¹⁵² and by acute or chronic systemic application of selective SGLT2 inhibitors.¹⁵³ In accordance, pharmacologic or genetic inhibition of SGLT2 suppressed hyperfiltration on the whole-kidney level in diabetic mice.^{70,71} Consistent with the proposed local mechanism, the suppression of diabetic hyperfiltration in response to SGLT2 inhibition was associated with an increase in the NaCl concentration at the macula densa^{152,153} and in the hydrostatic pressure in the Bowman space,¹⁵² and was independent of effects on blood glucose^{70,152,153} (Fig. 8.5). The GFR-lowering effect has more recently been confirmed

in humans. The SGLT2 inhibitor empagliflozin decreased GFR by 19% in T1DM patients with baseline hyperfiltration independently of lowering blood glucose levels.¹²⁰ The SGLT2 inhibitor canagliflozin initially lowered eGFR in patients with T2DM and basal eGFR of ≥ 55 mL/min/1.73 m². Following this initial dip, eGFR increased over the following weeks and months in the canagliflozin-treated group such that eGFR was better preserved after 2 years of follow-up and associated with reduced urinary albumin-to-creatinine ratios than in the control group, which had been treated with glimepiride to achieve similar blood glucose control.¹⁵⁴

Surviving nephrons in advanced stages of CKD are assumed to hyperfilter as a way of compensation for the reduced nephron number and thus maintain a high glucose load on the level of the single nephron. This should preserve the acute GFR-lowering effect of SGLT2 inhibition, even if the effect on overall glucose homeostasis was attenuated. In

accordance, the SGLT2 inhibitor canagliflozin modestly reduced eGFR together with proteinuria within 3 weeks in patients with T2DM and basal eGFR values between 30 and 50 mL/min/1.73 m² (CKD3).¹⁵⁵ Empagliflozin also induced a small decline in eGFR in patients with T2DM and CKD2 and CKD3; this effect was maintained at 52 weeks, associated with reduced urine albumin-to-creatinine ratios and, most importantly, full reversibility after a 3-week washout period, indicating a functional GFR reduction.¹⁵⁶

Lowering single-nephron glomerular hyperfiltration in CKD and thereby the oxygen-consuming transport work may help to preserve the integrity of the remaining nephrons and overall kidney function in the long term (see Fig. 8.5). This has been proposed for blockers of angiotensin II¹⁵⁷ and may also apply to SGLT2 inhibitors. Because ~80% of patients were also treated with a form of angiotensin II blockade, the EMPA-REG OUTCOME trial and CANVAS program provided evidence that the two strategies are additive and apply to patients with initial GFRs of at least 30 mL/min/1.73 m² of body surface area.^{108,109} The additive effect is consistent with the concept that angiotensin II blockade is primarily dilating the efferent arteriole, whereas SGLT2 inhibition primarily constricts the afferent arteriole.

SGLT2 inhibition has distinct effects on renal cortical and medullary O₂ requirements. Mathematical modeling predicted that inhibition of SGLT2 in the diabetic kidney reduces oxygen consumption in the PCT and renal cortex, in part by lowering GFR^{142,143} (Fig. 8.5). The predicted increase in cortical O₂ pressure and availability has been observed in a diabetic rat model using phlorizin, a dual SGLT1/SGLT2 inhibitor.¹⁵⁸ Interestingly, preserving renal cortical oxygenation may be important to preserve kidney function in patients with CKD.¹⁵⁹

SGLT2 inhibition also shifts glucose uptake downstream to the S3 segments (see earlier) and enhances transcellular Na⁺ reabsorption in distal segments, including the S3 segment and medullary TAL. This may further reduce the already physiologically low O₂ availability in the renal outer medulla. The latter has been proposed for SGLT2 inhibition using mathematical modeling^{142,143} and was shown in vivo in rats in response to acute dual SGLT2/SGLT1 inhibition by phlorizin in nondiabetic and diabetic rats.¹⁵⁸ The effect on medullary transport and oxygenation would be attenuated by the reduction in blood glucose and GFR in response to SGLT2 inhibition.^{142,143} Moreover, the proposed SGLT2 inhibitor-induced reduction in oxygen pressure in the deep cortex and outer medulla may stimulate hypoxia-inducible factors HIF-1 and HIF-2 (see Fig. 8.5). Gene knockout of SGLT2 increased the renal mRNA expression of hemoxygenase,^{1,7} a tissue-protective gene that is induced by HIF-1 α . On the other hand, activation of HIF-2 may explain an enhanced erythropoietin release from renal interstitial cells in response to SGLT2 inhibition.¹⁶⁰ Together with the diuretic effect, the latter may contribute to the observed modest increase in hematocrit and hemoglobin in response to SGLT2 inhibition. This may improve the oxygenation of the kidney outer medulla and cortex but also facilitate oxygen delivery to the heart and other organs (Fig. 8.5). Notably, changes in hematocrit and hemoglobin from baseline explained 51.8% and 48.9%, respectively, of the effect of the SGLT2 inhibitor empagliflozin versus placebo on the risk of cardiovascular death.¹⁶¹ In other words and in addition to its volume effect, SGLT2 inhibition may simulate systemic hypoxia to the oxygen

sensor in the deep cortex and outer medulla of the kidney, and the induced response then helps the failing heart and also the kidney. In accordance with an overall nephroprotective effect, SGLT2 inhibitor use reduced the risk of AKI in an analysis of >3000 patients with T2DM by ~50%.¹⁶² Nevertheless, caution is warranted, as excessive volume depletion and the transport shift to the outer medulla may increase the AKI risk in individual sensitive patients.

Preservation of blood pressure-lowering and heart failure-protective effects of SGLT2 inhibitors in CKD despite attenuated antihyperglycemic effects. The amount of filtered glucose determines the glucosuric and blood glucose-lowering effect of SGLT2 inhibition. As a consequence, the antihyperglycemic effects of SGLT2 inhibitors are attenuated in patients with reduced GFR. In contrast, the blood pressure-lowering and heart failure-protective effects are preserved in patients with CKD and reduced GFR (eGFR \geq 30 mL/min 1.73 m²).^{163,164} Modeling studies of CKD and nephron loss predicted that the increase in single-nephron GFR in remaining nephrons and the reduction of glucose reabsorption by SGLT2 inhibition increase paracellular Na⁺ secretion in the proximal tubule.¹⁶⁵ Thus, the model predicted that the chronic natriuretic and diuretic effects of SGLT2 inhibition persist in CKD. The modeling approach also predicted that the SGLT2 inhibition-induced changes in the oxygen signal at the renal sensor are preserved in CKD.¹⁶⁵

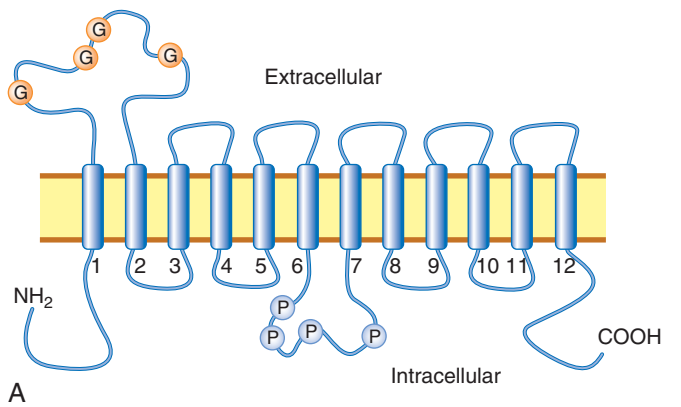
Ongoing trials with different SGLT2 inhibitors, also including studies in nondiabetic patients with heart failure and/or CKD, will provide further data for comparison between SGLT2 inhibitors and are expected to further refine our understanding of the therapeutic potential and safety of SGLT2 inhibition.

ORGANIC CATIONS AND ANIONS

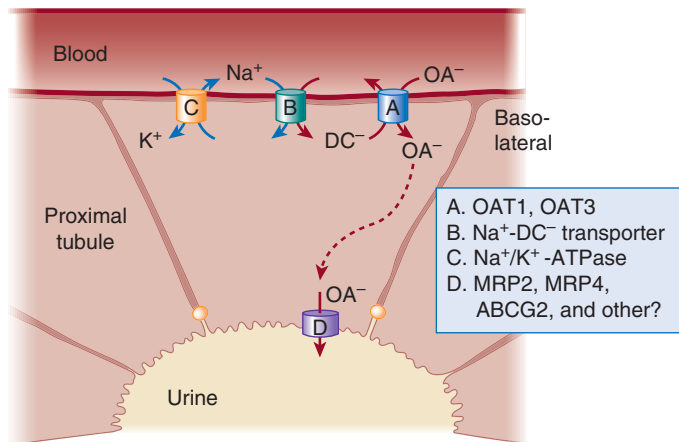
ORGANIC ANION TRANSPORTERS AND ORGANIC CATION TRANSPORTERS

Historically, the renal organic anion transport system has been one of the best studied in physiology.¹⁶⁶⁻¹⁷³ Essentially, it has been operationally characterized as the probenecid-sensitive para-aminohippurate (PAH) transport system. Classically, it is described as a proximal tubule transport system of small organic anions (e.g., PAH) bound with low affinity to plasma proteins (mainly albumin). Because, with an intact glomerular filtration barrier, albumin-bound molecules would not be filtered, they move into the peritubular capillaries. Molecules like PAH are efficiently extracted on a “first pass” by a high-capacity transport system with selectivity for organic anions. This explains why PAH clearance can be used as a measure of renal plasma flow. Operationally, the system can be blocked by the organic anion drug probenecid, which has seen considerable clinical use in the setting of hyperuricemia and to increase blood levels of other organic anion drugs like penicillins and cidofovir.¹⁷⁴⁻¹⁷⁶

The main gene responsible for this probenecid-inhibited PAH transport is a SLC transporter known as OAT1 (SLC22A6) and was originally called NKT (novel kidney transporter).^{177,178} Like most other members of the mammalian SLC family, it has 12 membrane-spanning segments (Fig. 8.7A). At the time of its discovery, NKT was proposed to function as either



A



B

Fig. 8.7 Topology of OAT1 and schematic of OAT1-mediated organic anion influx uptake as a “tertiary” transport process.

(A) An intracellular loop links two six-transmembrane domains yielding 12 membrane-spanning regions similar to many other SLC transporters (G, glycosylation sites; P, PKC, phosphorylation sites). (B) Schematic depicting a proximal tubule cell showing OAT-mediated influx of organic anions (OA^-) from the plasma to the lumen. OAT1 (A), OA^- influx by OAT1 at the basolateral membrane via antiport of dicarboxylates (DC^-) down a gradient. OAT-mediated influx is connected to the transmembrane gradient of dicarboxylates created as a result Na^+ /dicarboxylate cotransporter and mitochondrial TCA cycle (B). This “tertiary” process depends upon the ATP hydrolyzed by the Na^+ - K^+ -ATPase to create an extracellular-to-intracellular sodium gradient (C). Transport of OA^- into urinary space (D) probably occurs through a number of apical membrane transporters, including the MRPs. (Modified from Nigam SK, Bush KT, Martovetsky G, et al. The organic anion transporter (OAT) family: a systems biology perspective. *Physiol Rev.* 2015;95:83–123; and Eraly SA, Bush KT, Sampogna RV, et al. The molecular pharmacology of organic anion transporters: from DNA to FDA? *Mol. Pharmacol.* 2004;65:479–487.)

an organic anion or organic cation transporter; numerous studies have since confirmed that, although OAT1 and other members of the OAT subfamily are predominantly organic anion transporters, they can also transport organic cations and zwitterions.^{179,180}

The current view of how a prototypical organic anion—PAH in this case—is taken up across the basolateral membrane (blood side) of the proximal tubule cell involves three different transporters: OAT1, the sodium–dicarboxylate cotransporter (NaDC3, SLC13A3), and the sodium–potassium ATPase (Fig. 8.7B). This “tertiary” transport system is believed to operate

through the following mechanisms: (1) exchange (antiport) of PAH in the plasma with α -ketoglutarate by OAT1; (2) cotransport (symport) of sodium and α -ketoglutarate into the cell by NaDC3; and (3) extrusion of sodium into the plasma, creating a sodium gradient, through the ATP-dependent action of the sodium–potassium ATPase (Na-K-ATPase). Thus, organic anion transport is ATP dependent only in an indirect way and depends on two other gradients: (1) a sodium gradient generated by the Na-K-ATPase, among other factors, that enables cotransport of sodium with α -ketoglutarate into the cell by NaDC3; and (2) a high intracellular α -ketoglutarate level that is partly due to the aforementioned NaDC3 cotransport and partly contributed by aerobic mitochondrial metabolism resulting in the generation of tricarboxylic acid (TCA) cycle intermediates such as α -ketoglutarate. Blocking any of these processes, for example, ouabain inhibition of the Na-K-ATPase, lithium inhibition of NaDC3, or probenecid inhibition of OAT1, markedly diminishes or even completely abolishes PAH transport via OAT1. In general, OAT3 appears to function via an analogous tertiary transport system, although it is not entirely clear that the linkage to α -ketoglutarate exchange is as tight.

When OAT1 was originally discovered (as NKT), two other homologous transporters, NLT (now OAT2, SLC22A7)¹⁸¹ and OCT1, organic cation transporter 1 (SLC22A1)¹⁸² were also found in the sequence database, and it was proposed that this was a new family of SLC transporters, which is now known as SLC22.¹⁷⁸ Since then, the SLC22 family has grown to roughly 30 transporters in humans and mice.^{183,184}

A new evolutionary-based classification of SLC22 has been proposed, which divides the family into a major OAT clade and a major OCT clade, which further divide into six subclades (Fig. 8.8). The assumption is that the various SLC22 subclades defined by phylogenetic relationships will lead to a better functional classification and help deorphanize SLC22 transporters of unclear function. Accordingly, subclades within the OAT clade include the OAT subclade, the OAT-like subclade, and the OAT-related subclade; within the OCT clade is the OCT subclade, OCT-like (OCTN) subclade, and the OCT-related subclade.^{183,185} The specific details of many of these transporters are beyond the scope of this chapter, and, indeed, many remain “orphans” with respect to endogenous substrate preference. Nevertheless, it is important to point out that, with the exception of certain subclades, the predominant expression for most of the other SLC22 transporters tends to be in the kidney proximal tubule, choroid plexus, or the liver. Even so, SLC22 transporters are expressed throughout the body, and there are even members with highly selective localization to the olfactory epithelium and brain substructures (OAT6, SLC22A20).¹⁸⁶ SLC22 is thus a very interesting SLC family involved in the transport of anionic, cationic, and zwitterionic drugs; toxins; metabolites; signaling molecules; antioxidants; dietary components; vitamins; gut microbiome products; and uremic toxins.¹⁸³

Here we focus on OAT1 (SLC22A6) and OAT3 (SLC22A8), which are the major renal metabolite, drug, and toxin (including uremic toxin) organic anion transporters (Table 8.1); OCT2 (SLC22A2), the major transporter of cationic drugs and metabolites; and URAT1 (SLC22A12), the latter being the most extensively studied of several urate transporters in the OAT subclade. Along with a number of other SLC and ABC transporters, these SLC22 transporters are the most

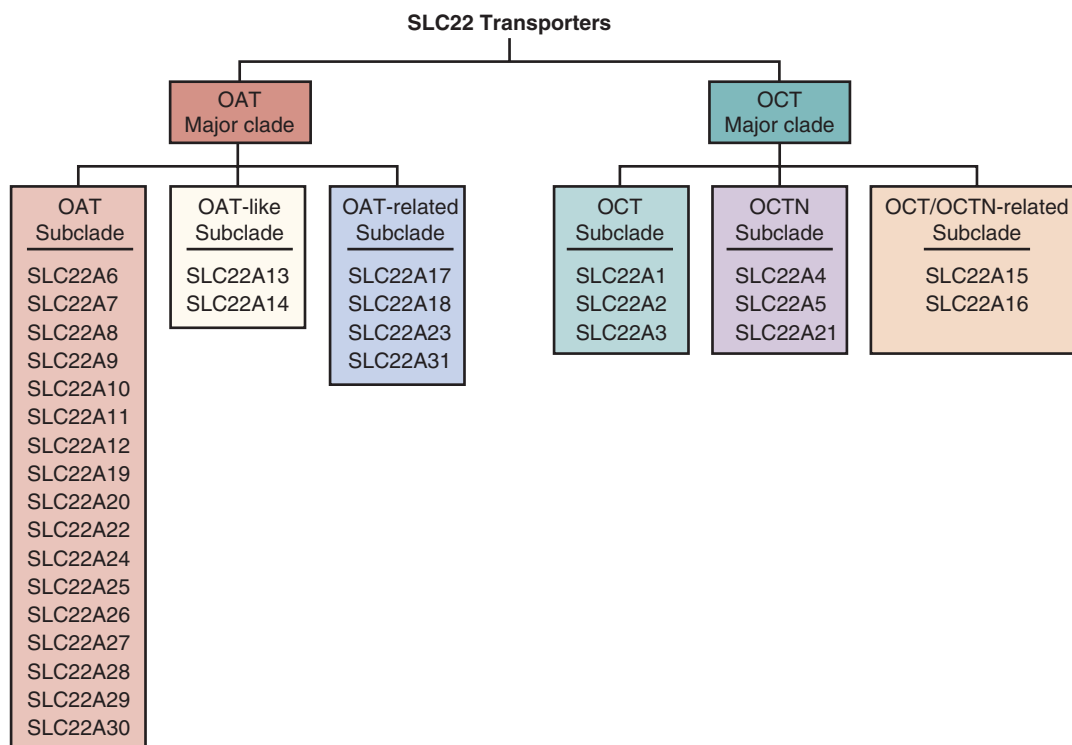


Fig. 8.8 The six subfamilies of SLC22 transporters. Evolutionary analysis indicates that SLC22 transporters are highly conserved and found in fly, worm, sea urchin, and other organisms. The SLC22 family is composed of two major clades, which are the organic anion transporter (OAT) major clade and organic cation transporter (OCT) major clade. Each of these clades is divided into three subclades, designated as OAT, OAT-like, OAT-related, OCT, OCTN (organic cation/carnitine transporter), and OCT/OCTN-related. (Modified from Nigam SK. The SLC22 transporter family: a paradigm for the impact of drug transporters on metabolic pathways, signaling, and disease. *Ann Rev Pharmacol Toxicol.* 2018;58:32.31–32.25; and Zhu C, Nigam KB, Date RC, et al. Evolutionary analysis and classification of OATS, OCTS, OCTNS, and other SLC22 transporters: structure-function implications and analysis of sequence motifs. *PLoS ONE.* 2015;10:e0140569.)

clinically relevant and quantitatively important organic anion and organic cation transporters in the proximal tubule of the kidney.^{184,187}

OAT1 (SLC22A6) AND OAT3 (SLC22A8)

Both OAT1 and OAT3 were among the original seven drug transporters that regulatory agencies identified as important for analysis of the possibility of transport of new drug entities.¹⁸⁸ This regulatory attention has perpetuated the notion that these transporters primarily transport drugs. Although it is true that the OATs transport drugs (e.g., antibiotics, antivirals, nonsteroidal antiinflammatory drugs, diuretics) and toxins (e.g., organic mercurials, aristolochic acid), it is now clear that they, as well as the other five SLC and ABC transporters highlighted by regulatory agencies, transport many endogenous metabolites, signaling molecules, vitamins, gut microbiome, and dietary products.¹⁸⁴

Indeed, there is a growing appreciation that the primary function of these multispecific transporters may not be the handling of drugs and toxins but rather the modulation of local and systemic metabolism and signaling.^{189,190} Much of this change in our understanding of “what drug transporters really do” is the result of “omics” analyses of knockout mice, human genome-wide association studies (GWAS), and the identification of heritable mutations that cause or modulate well-known metabolic diseases.¹⁸⁴

According to this new systems biology view (explained in more detail later), the multispecificity of these transporters for

endogenous substrates enables a range of drugs and toxins to coopt these transporters expressed in the gut, liver, kidney, and many other tissues. But the pharmaceutical and commercial relevance of these transporters can create the misconception that these widely expressed and evolutionarily conserved genes primarily exist to handle synthetic drugs. Although this is apparently their key role from the perspective of clinical pharmacology and pharmacokinetics, it is becoming clear that this lens is extremely limited even from the clinical point of view, because it is now evident that OAT1, OAT3, and other “drug” transporters are central to endogenous physiology and are important for understanding the pathophysiology of uremia, hyperuricemia, and a number of genetic conditions.

OAT1 KNOCKOUT AND OAT3 KNOCKOUT MICE

Our understanding of in vivo OAT function has changed with the application of omics (e.g., metabolomics, transcriptomics) analyses to *Oat* knockout mice. The *Oat1* and *Oat3* knockout mice were first analyzed over a decade ago and have continued to yield considerable insight into the in vivo function of these two major organic anion transporters, particularly their endogenous function.^{191–196}

As expected, the *Oat1* knockout mouse tissue has defective uptake of the classic organic anion transporter probe PAH, whereas the *Oat3* knockout mouse tissue has defective uptake of estrone sulfate.^{191,197} Consistent with in vitro data, the *Oat1* and/or *Oat3* knockout mice have altered in vivo or ex vivo (e.g., embryonic kidney organ cultures) handling of diuretics

Table 8.1 Some SLC22 Transporter Substrates

Substrate	SLC22 Transporter			
	SLC22A6 OAT1	SLC22A8 OAT3	SLC22A1 OCT1	SLC22A2 OCT2
Nonsteroidal antiinflammatory drugs	✓	✓		
Ibuprofen				
Naproxen				
Antivirals	✓	✓		
Tenofovir				
Adefovir				
Cidofovir				
β-lactam antibiotics	✓	✓		
Ampicillin				
Benzylpenicillin				
Diuretics	✓	✓		
Bumetanide				
Furosemide				
TCA cycle intermediates	✓	✓		
Short-chain fatty acids	✓	✓		
Bile acids				
Flavonoids	✓	✓		
Gut microbiome products	✓	✓	✓	✓
Organic mercurials	✓	✓		
Cisplatin			✓	✓
Metformin			✓	✓
Cimetidine		✓	✓	✓
Thiamine			✓	✓

TCA, Tricarboxylic acid.

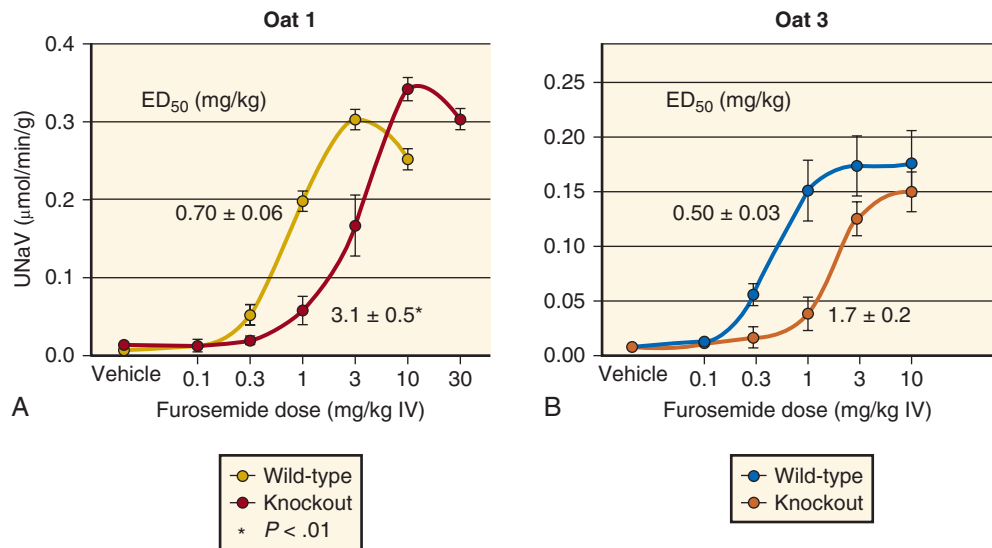


Fig. 8.9 Marked attenuation of thiazide and loop diuretic effects in *Oat1* and *Oat3* knockout mice. In *Oat1* or *Oat3* knockout, which transport diuretics (Table 8.1), luminal sodium elimination is markedly attenuated. ED₅₀, Half-maximal effective dose; IV, intravenous; UNaV, urinary sodium excretion. (Modified from Eraly SA, Vallon V, Vaughn DA, et al. Decreased renal organic anion secretion and plasma accumulation of endogenous organic anions in OAT1 knock-out mice. *J Biol Chem* 2006;281:5072–5083; and Vallon V, Rieg T, Ahn SY, et al. Overlapping in vitro and in vivo specificities of the organic anion transporters OAT1 and OAT3 for loop and thiazide diuretics. *Am J Physiol Renal Physiol.* 2008;294:F867–F873.)

(e.g., loop, thiazides), antibiotics (e.g., penicillin, ciprofloxacin), a wide range of antiviral agents, and methotrexate.^{198–204}

Knockout mice responses to loop and thiazide diuretics provide a useful illustration (Fig. 8.9). These albumin-bound drugs in the peritubular capillaries must be transported by

basolateral uptake transporters OAT1 and OAT3 in the proximal tubule, transit the cell, and exit through apical transporters (including members of the ABCC or MRP families)—all before flowing down the luminal (urinary) space to be excreted or, for the loop and thiazide diuretics, to inhibit

salt reabsorption in later nephron segments. Three to five times more diuretic is required to achieve the same degree of natriuresis after deletion of either *Oat1* or *Oat3* in mice.^{191,198}

OATs are implicated in renal organic mercurial toxicity because mercury binds to glutathione and other thiol-containing compounds, many of which are “effectively” seen as organic anions by the transporter.²⁰⁵ When the *Oat1* knockout mouse was treated with high-dose mercury, the kidneys were surprisingly well protected from injury (histologically and by renal indices), consistent with the inability of the organic mercurial to be taken up by the proximal tubule due to the absence of *Oat1*.²⁰⁶

Perhaps most interesting, and somewhat unexpected, have been the results from performing metabolomics analyses on the plasma of the *Oat* knockout animals^{191,193–195,207} (Fig. 8.10). These have revealed a somewhat surprising range of endogenous OAT substrates.

Generally speaking, both OAT1 and OAT3 appear to play a key role in regulating the flow of organic anions through the so-called gut–liver–kidney axis.¹⁹⁴ This includes the renal handling of many compounds derived from the gut microbiome—either products of the gut microbiome or due to the action of the gut microbiome on dietary components such as phytochemicals. For example, in the *Oat3* knockout, among the greatest changes are in flavonoids that have been acted upon by phase 2 liver enzymes (e.g., glucuronidation). This highlights the important connection between OATs (especially OAT3) with liver metabolism (via so-called drug-metabolizing enzymes) of endogenous compounds as well as drugs and toxins.

Other groups of metabolites elevated in the *Oat3* knockout include primary and secondary bile acids.¹⁹⁴ In *Oat1* and *Oat3* knockouts, fatty acids, TCA cycle intermediates, and vitamins are also elevated. Nevertheless, unlike the case of FDA-approved drugs—where it is difficult to distinguish

molecular properties of drug substrates that predispose to interaction with OAT1 or OAT3²⁰⁸—the sets of metabolites appear fairly distinct, although there is still much overlap.¹⁹⁴

These chemical properties of drugs and metabolites interacting with OAT1 versus OAT3 deserve further mention. With respect to drugs, OAT1 and OAT3 strongly favor anionic drug substrates, but both transporters (especially OAT3) can bind a limited number of cationic/zwitterionic drugs.¹⁸⁰ Cimetidine is an example.¹⁷⁹ Importantly, chemical properties of metabolites interacting with the OATs appear substantially different from the drug data. This could partly be due to a selection factor related to which drugs make it to market. However, it remains that, more than for drugs, the molecular and chemical properties of metabolites appear to distinguish, in a general way, between OAT1 and OAT3 substrates—with OAT3 substrates being larger, less polar, more chemically complex, and containing more ring structures.¹⁹⁴ Nevertheless, it is worth mentioning again that there is overlap between OAT1 and OAT3 metabolite substrates.

In addition, metabolic reconstructions based on changes in gene expression in the knockouts have been performed.^{207–209} These metabolic reconstructions are generally consistent with metabolomics data; the reconstructions indicate that OATs regulate many systemic biochemical pathways as well as those in the proximal tubule (Table 8.2). For example, among the top biochemical pathways revealed in reconstructions are purine metabolism, TCA cycle, fatty acid metabolism, eicosanoid metabolism, amino acid metabolism (tryptophan, tyrosine, arginine), and a variety of vitamin-dependent pathways. Together, the reconstructions and the metabolomics data support the view that OATs are not simply “drug” transporters but impact many aspects of systemic and proximal tubule physiology.

Together, the metabolic reconstructions based on knockout omics data and the analysis of endogenous substrates (e.g.,

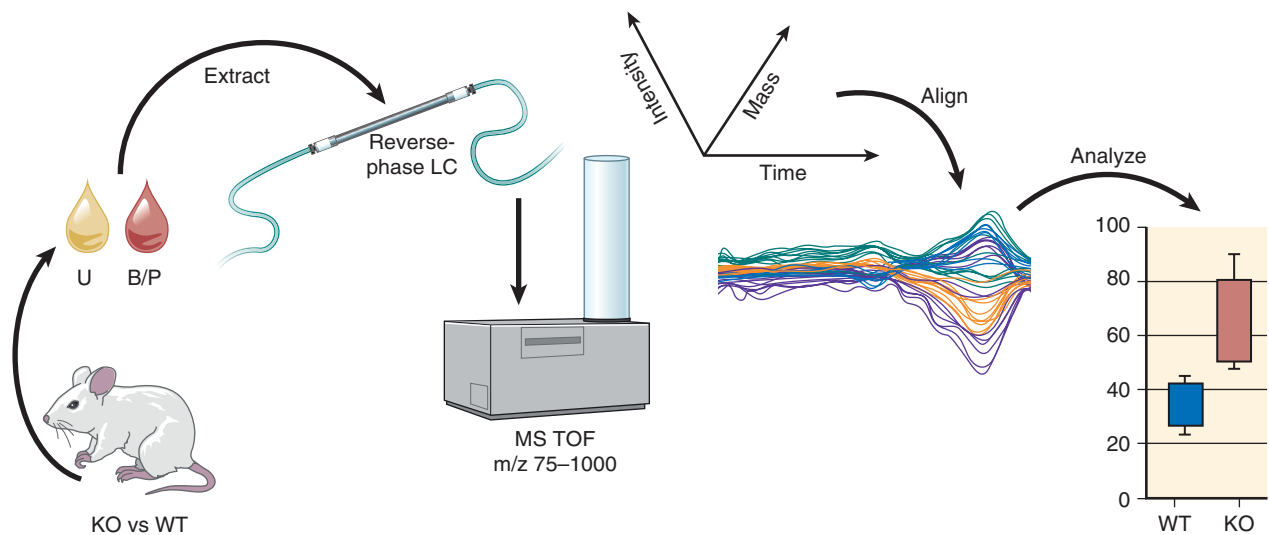


Fig. 8.10 Schematic of approach to metabolomic analysis of *Oat1* knockout mice. Schematic of strategy for untargeted metabolomic analysis of metabolites, gut microbiome (enterobiome) products, vitamins, and signaling molecules, many of which have been shown to directly interact with *Oat1* as determined by *in vitro* assays. Wild-type and *Oat1*^{−/−} mice plasma and urine were profiled using liquid chromatography with tandem mass spectrometry (LC/MS/MS). Importantly, untargeted metabolomics identifies gut microbiome and uremic toxins 1 (*Oat1*). Subsequently, *Oat3* knockouts were also profiled; gut microbiome products and uremic toxins were also identified, as well as a number of bile acids and flavonoid metabolites. *KO*, Knockout; *WT*, wild-type. (Modified from Wikoff WR, Nagle MA, Kouznetsova VL, et al. Untargeted metabolomics identifies enterobiome metabolites and putative uremic toxins as substrates of organic anion transporter 1 (*Oat1*). *J Proteome Res.* 2011;10:2842–2851.)

Table 8.2 Top Pathways Affected by Oat1 Loss in Knockout Mice

TCA cycle
 Tyrosine metabolism
 Alanine, aspartate, and glutamate metabolism
 Butanoate metabolism
 Arginine and proline metabolism
 Tryptophan metabolism
 Nicotinate and nicotinamide metabolism
 Valine, leucine, and isoleucine degradation
 Nitrogen metabolism
 Glyoxylate and dicarboxylate metabolism
 Propanoate metabolism
 Glycine, serine, and threonine metabolism
 Purine metabolism
 Pyrimidine metabolism

TCA, Tricarboxylic acid.

Adapted from Liu HC, Jamshidi N, Chen Y, et al. An organic anion transporter 1 (OAT1)-centered metabolic network. *J Biol Chem.* 2016;291:19474-19486.

metabolites, signaling molecules) from the perspective of chemical properties calls into question the oft-discussed “redundancy” of OAT1 and OAT3 in the proximal tubule. From a practical pharmacokinetic perspective, this view may still be a useful first approximation for many drugs that can interact with both OAT1 and OAT3. But considering the endogenous metabolite preferences alone (without considering drugs), a more appropriate view might be that the two transporters have distinct roles in many metabolic processes, although they work together to handle certain substrates like uric acid. Based on current data, OAT1 appears more linked to local and systemic aerobic metabolism, whereas OAT3 appears more linked to flow of metabolites that originate in the gut or liver (e.g., primary and secondary bile acids). There is also some evidence to suggest that OAT3 could modify phenotypes, for instance, in diabetic disease,²¹⁰ blood pressure,¹⁹² and in the setting of treatment with SGLT2 inhibitors.¹¹⁵

OAT1 AND OAT3 SINGLE-NUCLEOTIDE POLYMORPHISMS

Nonsynonymous coding region single-nucleotide polymorphisms (SNPs) in the OATs are uncommon compared with noncoding region SNPs.²¹¹ Although SNPs in OATs have received less attention than OCT SNPs—because OCTs appear to be more polymorphic in humans—associations have, in recent years, been reported that affect diuretic responsiveness, mercury toxicity, antibiotic levels, and hyperuricemia.^{212–216} A noncoding SNP in the OAT1 gene appears to be associated with the progression of renal disease; whether or not this is related to altered handling of one or more uremic or other toxins is not clear.²¹⁷ Based on animal and human data, it would not be surprising if OAT3 SNPs are found to be associated with glucose homeostasis or diabetic renal disease. Because there is considerable overlap in drugs transported by OAT1 and OAT3, it may be that SNPs in both OATs (or in an OAT and the “corresponding” apical transporter such as MRP2 or MRP4) are required for pronounced drug, toxin, and metabolite phenotypes.²¹⁸ This question needs to be examined in more detail.

OCT2 (SLC22A2)

Unlike the OAT subclade (of the SLC22 OAT major clade), which is large, the OCT subclade (one of three subclades of the SLC22 OCT major clade) consists of three highly homologous (both protein sequence and function) transporters: OCT1, OCT2, and OCT3.¹⁸³ OCTs are generally held to be electrogenic uniporters.²¹⁹ Organic cation transporter 2 (OCT2) is the main renal uptake transporter on the basolateral membrane (blood side) of the proximal tubule cell that is involved in the elimination of organic cationic drugs such as metformin and *cis*-platinum.^{220,221} On the luminal (apical, urine side) of the cell, it appears that MATE (SLC47) transporter family members efflux organic cations into the urinary space.²²² Recently, the primary liver OCT, OCT1—one of the drug transporters that, along with OAT1 and OAT3, has been highlighted by regulatory agencies as important for new drug testing to identify transport mechanisms—has been shown to be a thiamine transporter.²²³

Thus, as with the OATs, OCTs may function primarily in regulating metabolite flow into and out of tissues, and as with OATs, the best *in vivo* functional information regarding endogenous function comes from analysis of metabolites altered in the knockout mice. On the whole, the known drug and metabolite substrates for the OCTs appear less diverse than for the OATs, and it appears that, based on molecular property analysis of drug substrates, OCT1 and OCT2 have largely overlapping specificities, at least for drugs.¹⁸⁰

OCT2 SINGLE NUCLEOTIDE POLYMORPHISMS

The OCTs appear more polymorphic than the OATs; SNPs in OCT2 have received considerable clinical attention because, consistent with *in vitro* studies, they can affect levels of the antidiabetic agent metformin and the chemotherapeutic agent *cis*-platinum.^{224–227} These associations are much better established than the SNP associations mentioned above for the OATs.²²⁸ Because metformin and *cis*-platinum have been so widely used, and because of the potential for toxicity, it is important for the clinician to be aware of the possibility that SNPs in OCT2 can affect drug levels.

Clinical Relevance

The Remote Sensing and Signaling Hypothesis: A Framework for Understanding Hyperuricemia and Uremia

The OATs and OCTs have recently garnered a great deal of attention because of regulatory concerns due to transporter-mediated drug–drug interactions. Much more is likely on the way regarding drug-metabolite interactions (DMI) with the advent of better techniques to analyze metabolites in tissues and body fluids. With new approaches to uremia and hyperuricemia (especially in CKD) being considered, one expects more clinical studies and trials aimed at decreasing the burden of uremic toxins and uric acid—and prolonging time to severe CKD and dialysis. In this regard, the Remote Sensing and Signaling Hypothesis should be useful for considering approaches to ameliorate perturbed inter-organ and interorganismal communication via metabolites and signaling molecules, including those derived from the gut microbiome.

APICAL MEMBRANE PROXIMAL TUBULE TRANSPORTERS INVOLVED IN THE HANDLING OF ORGANIC ANIONS, ORGANIC CATIONS, AND ORGANIC ZWITTERIONS

In the proximal tubule, the OAT1, OAT3, and OCT2 function in basolateral side uptake (influx) of organic anions and cations from the blood. Although what happens to these charged organic molecules inside the cell remains poorly defined, their exit, usually in unchanged form, has become better understood in recent years. Many of the organic anions taken up by OAT1 and OAT3, for example, are effluxed across the apical membrane by members of the ABCC family, MRP2 (ABCC2) and MRP4 (ABCC4).¹⁶⁸ These are not the only apical transporters of organic anions in the proximal tubule; for example, OAT4 and the well-known ABC transporters, P-glycoprotein and ABCG2, appear to play a role for certain substrates.¹⁶⁸ Although in simplified representations, there is a tendency to match basolateral OAT1 and OAT3 with apical MRP2 and MRP4, it is likely that, depending on the anionic substrate taken up by OAT1 and OAT3, one or several apical transporters are involved in apical efflux into the proximal tubule lumen.

With respect to the apical efflux of organic cations, in recent years, MATEs, particularly MATE-2K, have received attention.^{168,222} MATEs are members of the SLC47 family, and it is well established that they transport many cationic drugs taken up by OCT2. Other apical transporters might also transport some OCT2 substrates, but their contribution is not well defined. It is also important to mention the organic cation/zwitterion transporters OCTN1 (SLC22A4) and OCTN2 (SLC22A5). Although they are sometimes listed along with drug transporters, their endogenous substrates—ergothioneine and carnitine, respectively—are well established.^{229,230} Indeed, mutations in OCTN2 cause systemic carnitine deficiency, which can lead to severe cardiac and skeletal myopathy. Ergothioneine, on the other hand, is considered an important antioxidant. Nevertheless, OCTNs have some ability to interact with cation drugs.

RENAL TRANSPORT OF SPECIFIC ORGANIC SUBSTRATES IN DISEASE

UREMIC TOXIN TRANSPORT

The importance of OATs in renal handling of gut microbiome-derived metabolites merits further discussion. Many of the metabolites accumulating in the *Oat* knockouts, such as indoxyl sulfate, kynurenine, p-cresol sulfate, and hippurate, are among the sets of gut microbiome-derived small molecules (organic anions); they are also frequently implicated as “uremic toxins”^{193,195} (Table 8.3).

The list of small molecules implicated in uremic toxicity is long and much debated.^{231,232} These uremic toxins are thought to play a role in many tissue and organ toxicities and dysfunctions that occur in the uremic syndrome associated with severe CKD. It is unlikely that any single uremic toxin on the list is the key to all the manifestations of the uremic syndrome, although there is growing evidence that certain uremic toxins play a role in particular tissue toxicities. These include TMAO (trimethylamine-N-oxide), which has been implicated in cardiovascular toxicity,^{233,234} and indoxyl sulfate, which has been implicated in multiple aspects of the uremic syndrome.²³⁵

Table 8.3 Uremic Toxins Accumulating in *Oat1* and/or *Oat3* Knockout Mice

Indoxyl sulfate	Indolelactate
p-Cresol sulfate	Kynurenate
Hippurate	Putrescine
CMPF	Uric acid
Phenyl sulfate	Creatinine
Xanthurenate	

CMPF, 3-Carboxy-4-methyl-5-propyl-2-furanpropanoate.

Adapted from Wikoff WR, Nagle MA, Kouznetsova VL, et al.

Untargeted metabolomics identifies enterobiome metabolites and putative uremic toxins as substrates of organic anion transporter 1 (*Oat1*). *J Proteome Res.* 2011;10:2842-2851; and Wu W, Bush KT, Nigam SK. Key role for the organic anion transporters, *OAT1* and *OAT3*, in the in vivo handling of uremic toxins and solutes. *Sci Rep.* 2017;7:4939.

Some of these uremic toxins (e.g., indoxyl sulfate) may play a role in the actual progression of renal disease, presumably via OAT-mediated uptake into proximal tubule cells.^{195,236} The pathophysiology of uremia is beyond the scope of this chapter, and readers are referred instead to Chapter 52. But it is important to emphasize the growing appreciation of the role of OAT1 and OAT3 in regulating levels of many molecules considered uremic toxins. Thus, it will be interesting to determine whether SNPs, or other factors that affect the expression or function of OAT1 and OAT3, alter the time at which the uremic syndrome develops or the progression of renal disease.

OCT2 also appears to be a transporter of certain cationic uremic toxins, notably TMAO, a molecule accumulating in CKD that is associated with cardiovascular disease.²³⁷ The apical transporters of organic anions, the MATEs, appear to be involved in the efflux of TMAO. Of note, the deletion in mice of OAT3, which can transport a few organic cations despite being an organic anion transporter, results in elevated levels of TMAO, although it is not clear whether TMAO is actually transported by OAT3.¹⁹⁵

URIC ACID TRANSPORT

Uric acid is an antioxidant that also has deleterious effects.²³⁸ It is also on the list of “uremic toxins.” Apart from gout and kidney stones, hyperuricemia has been associated with cardiovascular disease, metabolic syndrome, hypertension, and progression of renal disease.²³⁹ Metabolism of purines by enzymes primarily in the liver (e.g., xanthine oxidase) results in uric acid formation. On the other hand, uric acid elimination and retention in the body is largely determined by the kidney and, to a lesser extent (in the absence of kidney disease), by the intestine.

One of the unexpected results of GWAS and knockout mouse studies from the perspective of uric acid homeostasis was the number of SLC and ABC “drug” transporters that were implicated in regulating serum uric acid levels and then shown to transport urate.^{238,240} These transporters include ABCG2 (also known as BCRP), URAT1 (a close relative of OAT1 and OAT3), OAT1 and OAT3, as well as other OATs. In murine knockouts of OAT1, OAT3, and URAT1 (SLC22A12, originally discovered as *Rst* in mice²⁴¹), there are alterations in renal urate handling, although they are not as great as

might have been expected if these genes were, as was thought by many at the time, the major contributors to renal urate handling.¹⁹⁶ Subsequently, another SLC transporter, related to the glucose transporters, known as GLUT9 (SLC2A9), was found to be very important for renal urate handling.²⁴² Other transporters implicated in uric acid transport are MRP2 (ABCC2), MRP4 (ABCC4), NPT1 (SLC17A1), NPT4 (SLC17A3), OAT4 (SLC22A11), and OAT10 (SLC22A13).²⁴³ The list of associated genes, which includes nontransporters as well, continues to grow as more analyses are done in different ethnic groups. Indeed, based on GWAS and other studies, it appears that different subsets of the aforementioned genes may be more or less important in urate handling, depending on ethnicity and gender.

Together, these transporters are responsible for the complex handling of uric acid by the kidney, but it is important to emphasize that ABCG2 is increasingly perceived as the main intestinal uric acid efflux transporter.²⁴⁴ Intestinal extrusion of urate becomes particularly important in the setting of severe renal insufficiency, and in this regard, it has been found that SNPs in ABCG2 become more highly associated with uric acid levels in CKD patients²¹⁵ (Fig. 8.11). This seems

to be an example of remote organ communication (i.e., between injured kidney to intestine; see also later) with the apparent “objective” of optimizing uric acid levels as transport in another organ (intestinal efflux) takes over from the declining kidney, thereby reducing the plasma uric acid levels. From studies in animal models, it is believed that the high uric acid level itself in CKD leads to increased expression and/or function of intestinal ABCG2, and if so, this may be a case of substrate induction of the transporter.²⁴⁵

CREATININE TRANSPORT

Although new measures may soon become routinely used in hospitals, serum creatinine continues to be considered an index of renal function both in primary care and hospital settings. A number of members of the SLC22 family (containing OATs and OCTs) transport creatinine. These include OCT2, OAT2, OAT3, and possibly OAT1.^{246–248} All of these are considered key transporters of organic cation drugs, organic anion drugs, and zwitterionic drugs. Their relative importance in renal creatinine handling is debated, but it is likely that all play some role in the renal handling of creatinine, with OCT2 and OAT2 being particularly important, at least based on more recent

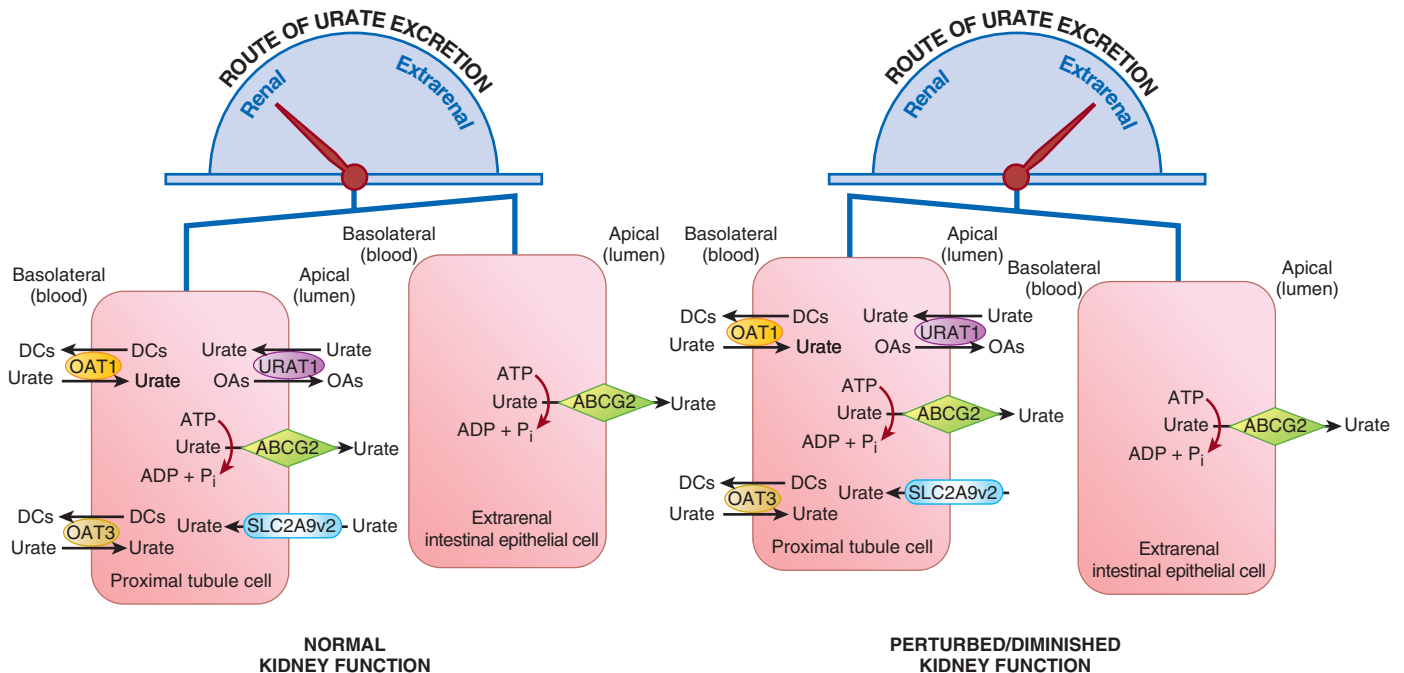


Fig. 8.11 In chronic kidney disease, the intestinal role of uric acid transporters (mainly ABCG2) becomes much more important. Schematic of urate excretion in the setting of normal renal function versus that in which there is diminished renal function. In the normal situation, the majority of urate excretion (~70%) is performed mainly in the proximal tubule of the kidney and is mediated by a number of transporters found on the apical and basolateral membranes of the proximal tubule cell. The illustration depicts only some of the transporters involved and includes members of the SLC and ABC families of membrane transporters. On the basolateral surface, the uptake of uric acid from the blood is mediated mainly by OAT1 (SLC22A6) and OAT3 (SLC22A8). These solute carrier transporters exchange dicarboxylates (DCs) for urate resulting in the net movement of this organic anion into the proximal tubular cell. At the apical surface, a number of transporters, including ABCG2 (depicted here), NPT1 (SLC17A1), and NPT4 (SLC17A3), as well as ABCC family members, work to secrete urate into the tubular lumen for excretion via the urine. The relative importance of the aforementioned apical transporters in urate secretion remains unclear. Transport of urate via ABCG2 is driven through ATP hydrolysis. Several other apical membrane transporters are well established in the reabsorption of urate, including URAT1 and SLC2A9v2. URAT1, or SLC22A12, exchanges intercellular organic anions for urate, resulting in the movement of uric acid back into the proximal tubule cell. Meanwhile, under normal physiologic conditions, up to 30% of uric acid is excreted via extrarenal transporters, believed to largely be driven by ABCG2 expressed in intestinal epithelial cells. The results of the analysis of human data—as well as physiologic data from rodent models with renal dysfunction—support the view that urate transport by ABCG2, most likely in intestine, compensates for poor renal urate handling in the setting of diminished kidney function. (Modified from Bhatnagar V, Richard EL, Wu W, et al. Analysis of ABCG2 and other urate transporters in uric acid homeostasis in chronic kidney disease: potential role of remote sensing and signaling. *Clin Kidney J.* 2016;9:444–453.)

studies. The issue is clinically relevant, because a number of drugs (e.g., trimethoprim) are thought to “artificially” create the impression of renal dysfunction when creatinine is the primary measure used because of drug–metabolite interactions at the level of the transporter.¹⁶⁸

THE REMOTE SENSING AND SIGNALING HYPOTHESIS: A FRAMEWORK FOR UNDERSTANDING HYPERURICEMIA AND UREMIA

It is evident from *in vitro* transport studies, metabolomics analyses of knockout animals, GWAS studies, and metabolic diseases due to transporter mutations that multispecific “drug” transporters of both the SLC and ABC transporter family are critical in the local and systemic regulation of levels of a huge array of metabolites.^{183,184,189,190,249}

The Remote Sensing and Signaling Hypothesis—which began to be formulated in 2004–2007¹⁸⁶—argues that the physiologic role of multispecific “drug” transporters and their close (often mono- or oligo-specific) relatives is the regulation of “remote” interorgan and interorganismal communication via metabolites and signaling molecules by these SLC and ABC transporters (Fig. 8.12).

The system is hypothesized to be actively regulated through transcriptional mechanisms (e.g., nuclear receptors) and posttranslational mechanisms (e.g., kinases regulating

transporter internalization or PDZ domain association). It is envisioned to work in parallel with the neuroendocrine, growth factor cytokine, and autonomic systems. The argument is that this type of SLC and ABC transporter-mediated remote interorgan and remote interorganismal communication via small molecules of “high informational content” (e.g., rate-limiting metabolites, signaling molecules, antioxidants, vitamins) is as critical as these other homeostatic systems and, as such, deserves comparable consideration for understanding health and disease states.

The hypothesis seems to be particularly relevant to renal disease. Consider, for instance, the previously discussed example of apparent interorgan remote communication—in order to reestablish uric acid homeostasis.²⁴³ An injured organ—the malfunctioning kidney in CKD—is involved in a kind of “organ cross-talk” with the intestine, whereby intestinal ABCG2 transporters, and possibly others, appear to “take over” from many renal SLC uric acid transporters as tubular function declines. As discussed earlier, high urate, certain uremic toxins, or both—accumulating as a consequence of renal disease—are thought to induce expression of intestinal transporters.

More generally, considering the uremic syndrome as partly due to “pathologic” transporter-mediated remote interorgan and interorganismal communication of uremic toxins—which includes signaling molecules that bind G-protein-coupled

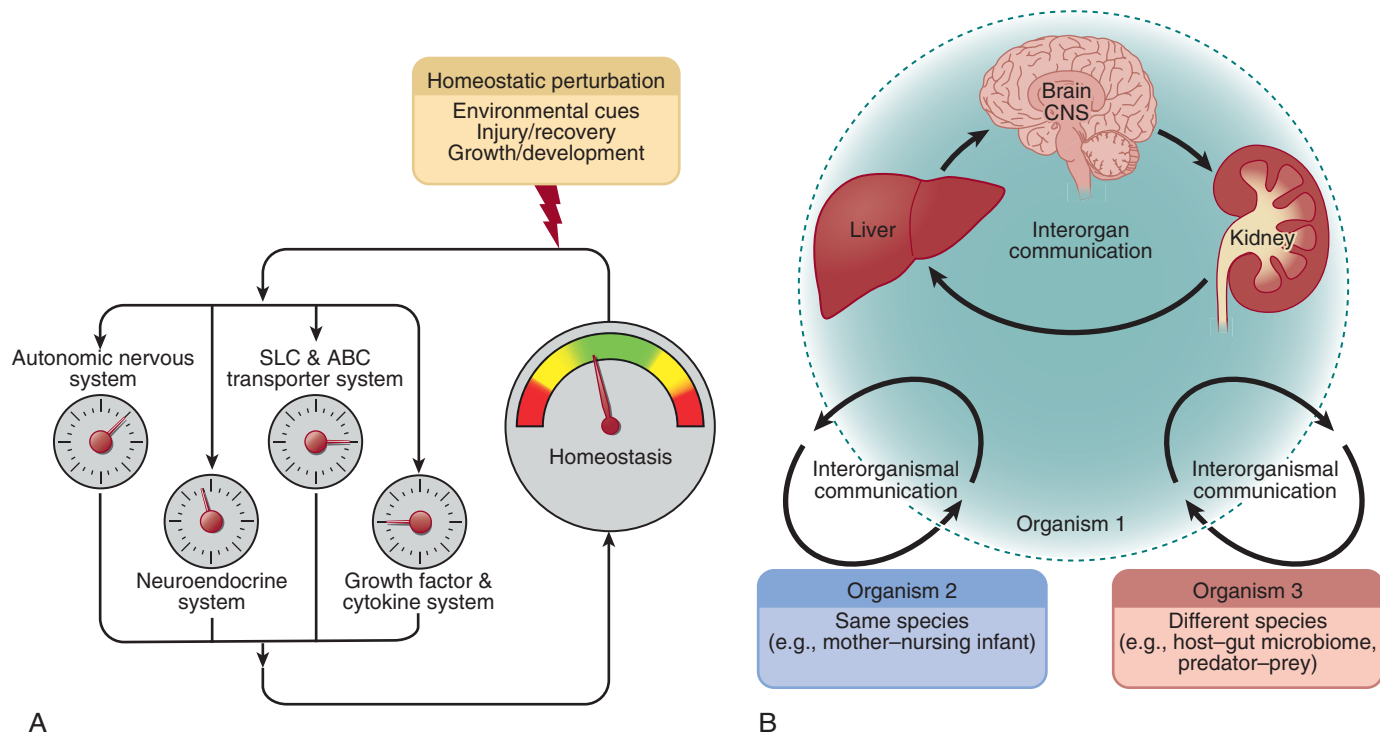


Fig. 8.12 The Remote Sensing and Signaling Hypothesis as it relates to multispecific and more selective SLC and ABC transporters as well as drug-metabolizing enzymes (DMEs) in different tissues communicating “remotely” (interorgan and interorganismal) in part due to differentially expressed transporters via the gut–liver–kidney axis in health and disease. The Remote Sensing and Signaling Hypothesis emphasizes the role of multispecific (“drug” transporters like OAT1, OAT3, ABCG2, and MRPs) and more selective SLC22 transporters as well as other SLC and ABC drug and DMEs in a remote interorgan and interorganismal communication network involving transporters and DMEs in epithelial and nonepithelial tissues as well as various body fluid spaces, such as cerebrospinal fluid, breast milk, and urine. This remote sensing and signaling system works in concert with more classic systems involved in homeostasis and resetting homeostasis in the setting of diseases like hyperuricemia and uremia. These other systems include the neuroendocrine, growth factor cytokine, autonomic nervous systems, and increasing evidence indicates that it is intertwined with these classic homeostatic systems. CNS, Central nervous system. (Adapted from Nigam SK. What do drug transporters really do? *Nat Rev Drug Discov.* 2015;14:29–44.)

receptors (e.g., kynurenine) and nuclear receptors (e.g., indoxyl sulfate)—provides a different lens on the numerous biochemical and cellular aberrations found in the uremic syndrome, which affect many tissues and body compartments. Moreover, the source of many uremic toxins in the body is the gut microbiome—the result of interorganismal communication—and these toxins affect signaling and metabolism in multiple organs before, in many cases, being eliminated by proximal tubule multispecific “drug” transporters, such as the OAT1, OAT3, OCT2, and the MATEs.

The Remote Sensing and Signaling Hypothesis provides a systems pathophysiology framework for thinking about the many metabolic and signaling aberrations of the uremic syndrome in the context of remote interorgan and interorganismal small molecule communication. Such a systems-level view may lead to the consideration of new therapeutic approaches aimed at altering remote sensing and signaling mechanisms as they become better understood—with the hope of ameliorating some of the many harmful manifestations of the uremic syndrome.

DRUG–METABOLITE INTERACTIONS

As more is learned about the endogenous substrates of OATs, OCTs, and other drug transporters, and as more is learned through metabolomics and metabolic reconstructions (such as those described above) regarding the regulation of tissue-specific metabolism by these transporters, it will become possible to consider new ways to modulate complex metabolic diseases like uremia and to understand the implications of drug–metabolite interactions (DMI) beyond simple competition at the level of the transporter itself.^{168,208} For example, currently the thinking on DMI is largely limited to looking at the transporter-level competition between the drug trimethoprim, which binds OCT2 and thereby raises the plasma concentration of a single OCT2-transported metabolite such as creatinine. But in the case of OAT1, it is now well established from knockout studies that loss of OAT1 function affects many metabolic pathways.^{208,209} The implication is that a drug that competes for OAT1 binding with endogenous metabolites normally transported by OAT1 (e.g., probenecid) will have broad effects on metabolism, affecting metabolites and signaling molecules that may themselves not be direct OAT1 substrates. This type of DMI may help partly explain the broad metabolic syndrome–like effects seen in the setting of chronic use of certain OAT-transported drugs, such as diuretics and HIV antivirals.^{250,251} Much work needs to be done in this area of DMI where competition for transport by the drug may affect a wide range of metabolic pathways; this would seem particularly relevant in the setting of moderate CKD where the affected metabolites would likely include certain uremic toxins.¹⁶⁸

AMINO ACIDS

PHYSIOLOGY OF RENAL AMINO ACID TRANSPORT

Rare inherited defects of renal amino acid transport have been instrumental for our understanding of renal metabolite reabsorption.^{252,253} Four disorders associated with apical amino

acid transporters define four major renal transport pathways, namely, a transporter for neutral amino acids (mutated in Hartnup disorder), a transporter for cationic amino acids and cystine (mutated in cystinuria), a transporter for anionic amino acids (mutated in dicarboxylic aminoaciduria), and a transporter for glycine and proline (mutated in iminoglycinuria)²⁵⁴ (see Chapter 44 for a detailed discussion of these inherited disorders). With the exception of iminoglycinuria, aminoacidurias also affect intestinal transport. Genetic complexity is observed in cystinuria and iminoglycinuria, demonstrating the involvement of more than one gene in the transport process. Apart from intestinal transport, aminoacidurias affecting apical transport have little effect on other organs, indicating that expression of these transporters is largely specific to the apical membrane in the kidney and intestine, although some renal amino acid transporters are also found in the brain. The four major amino acid transport activities were verified further by *in vitro* studies using a variety of methods such as microperfusion studies, brush border membrane vesicles, cortical slices, and cell lines.^{254,255} *In vitro* studies, in addition, identified a fifth transport activity, namely for β -amino acids, for which no corresponding disorder exists. Transport across the basolateral membrane has been more challenging to delineate, and it is unclear whether the five apical pathways are matched by five basolateral exit routes. A clear pathway for the release of cationic amino acids has been genetically identified through the rare amino aciduria lysinuric protein intolerance (LPI) and through functional studies.^{256,257} A release pathway for neutral amino acids was defined functionally using vesicles derived from the basolateral membrane.²⁵⁸ Release of anionic amino acids is difficult to measure, due to significant metabolism of glutamate by epithelial cells²⁵⁹ (see also Fig. 8.4). Glycine is likely to join other neutral amino acids for efflux, but the efflux pathways for proline and β -amino acids remain unclear. More than 98% of all filtered amino acids are reabsorbed in the proximal tubule; other parts of the tubule thus do not significantly contribute to amino acid reabsorption and are not discussed here.²⁶⁰ Some differences in transporter expression are observed between the PCT and the PST; these are illustrated in Fig. 8.13. Species differences may occur in the kidney and are mentioned where relevant.

MOLECULAR BIOLOGY OF RENAL AMINO ACID TRANSPORTERS

Molecular cloning, human genetics, and mouse models have helped to identify almost all amino acid transporters in the apical and basolateral membrane.^{254,261} Renal epithelial amino acid transporters are found in a variety of SLC families (Table 8.4). The SLC nomenclature is generally used for the genes, whereas acronyms are typically used for the proteins that describe some of the properties of the transporter. Expression cloning using *Xenopus laevis* oocytes or mammalian cell lines has been instrumental in the identification of renal amino acid transporters.²⁶² Additional transporters were identified by sequence similarity. As a result of these efforts, the amino acid transporter endowment of renal epithelial cells is now well understood, and an overview is depicted in Fig. 8.13. In the following, transporters for each group of amino acids are described in detail.

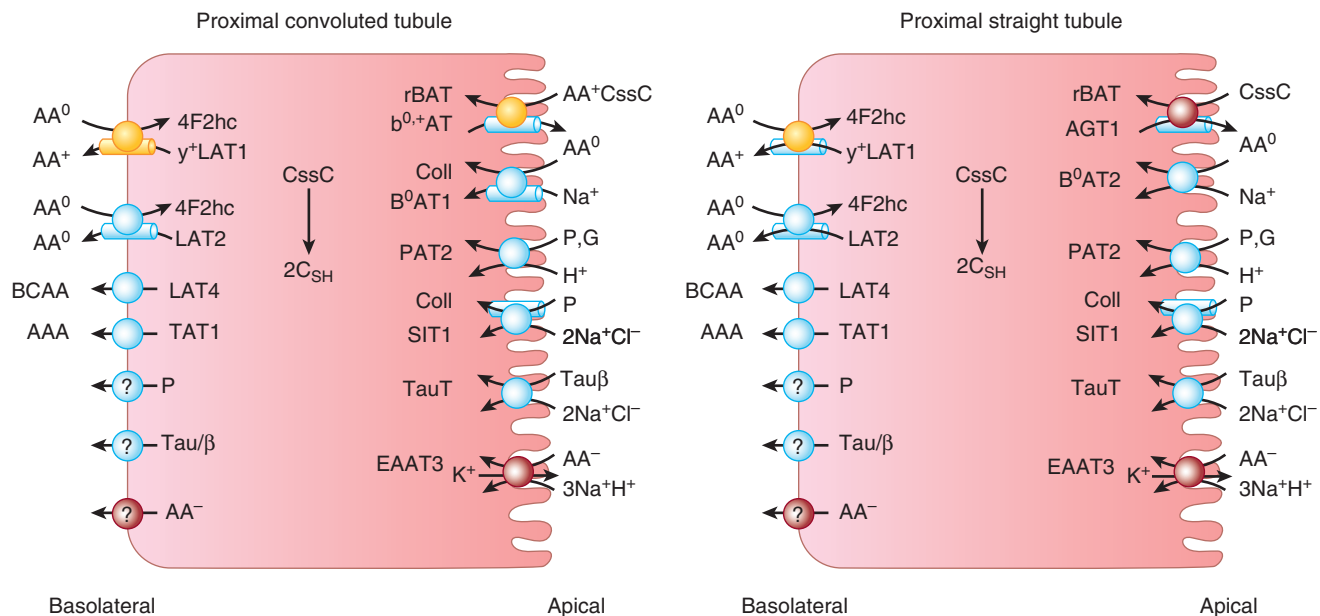


Fig. 8.13 Amino acid transporters in the proximal tubule. The common name of amino acid transporters in the proximal convoluted tubule and proximal straight tubule are shown next to each transporter. Transporter requirement for ancillary subunits are indicated by a tubelike structure. Transporters for anionic amino acids are shown in red; transporters for cationic amino acid are shown in yellow. AA^0 , neutral amino acids; AA^+ , cationic amino acids; AA^- , anionic amino acids; AAA, aromatic amino acids; BCAA, branched-chain amino acids; C_{SH} , cystine; CysC, cystine; G, glycine; P, proline; Tau/β , taurine and β -amino acids.

Table 8.4 Human Tubular Amino Acid Transporters Properties and Distribution of Human Renal Tubular Transporters

Amino Acid Transporter	SLC	PCT/PST	Substrates	Affinities	Disease	Structure class
Apical						
B^0AT1	SLC6A19	PCT	All neutral	800–15,000 μM	Hartnup disorder (OMIM 234500)	LeuT
B^0AT2	SLC6A15	PCT	BCAA, Met, Pro	50–200 μM	n.r.	LeuT
Collectrin	TMEM27	PCT	N/A	Ancillary	n.r.	1TM
rBAT	SLC3A1	PCT < PST	N/A	Ancillary	Cystinuria (OMIM 220100)	1TM
b^0+AT	SLC7A9	PCT > PST	Arg, Lys, Orn, CysC, Met, Leu, Ala	100 μM	Cystinuria (OMIM 220100), isolated cystinuria (OMIM 238200)	LeuT
EAAT3	SLC1A1	PCT < PST	Glu, Asp, CysC	20–80 μM	Dicarboxylic amino aciduria (OMIM 222730)	Git
AGT1	SLC7A13	PCT = PST	Glu, Asp, CysC	20–60 μM	n.r.	LeuT
PAT2	SLC36A2	PCT			Iminoglycinuria (OMIM 242600), Hyperglycinuria (OMIM138500)	LeuT
SIT	SLC36A2	PCT < PST			Iminoglycinuria (modifier) (OMIM 242600)	LeuT
TauT	SLC6A6	PCT, PST			n.r.	LeuT
Basolateral						
LAT2	SLC7A8	PCT			n.r.	LeuT
4F2hc	SLC3A2	PCT = PST		Ancillary	Lethal	1TM
y^+LAT1	SLC7A7	PCT = PST			Lysinuric protein intolerance (OMIM 222700)	LeuT
TAT1	SLC16A10	PCT			n.r.	MFS
LAT4	SLC43A2	PCT = PST	BCAA, Met, Phe	5000 μM	n.r.	MFS

BCAA, Branched-chain amino acids; CysC, cystine; 1TM, single transmembrane-helix protein; MFS, multifacilitator superfamily; n.r., not reported; OMIM, Online Mendelian Inheritance in Man; PCT, proximal convoluted tubule; PST, proximal straight tubule. Links to Diseases Refer to the OMIM Database.

TRANSPORTERS FOR NEUTRAL AMINO ACIDS

APICAL TRANSPORTERS

The presence of a dominant transporter for neutral amino acids can be inferred from the aminoaciduria observed in Hartnup disorder, which is restricted to neutral amino acids, but affecting every member of this group.²⁶³ This transporter was identified as the amino acid transporter B⁰AT1 (Broad neutral (0) Amino acid Transporter 1, SLC6A19).^{264,265} Although Hartnup disorder shows simple recessive inheritance and therefore is monogenic, the transporter protein requires association with ancillary proteins to traffic to the apical membrane and to be fully functional.²⁶⁶ In the kidney, this is facilitated by collectrin (TMEM27),²⁶⁷ whereas in the intestine, this role is served by angiotensin-converting enzyme 2 (ACE2).²⁶⁸ Both proteins are type I transmembrane (TM) proteins with a single TM domain. Although ACE2 is expressed in the kidney, its expression levels in the proximal tubule are too small to make a significant contribution to B⁰AT1 surface expression. B⁰AT1 and TMEM27 are both expressed in the PCT.²⁶⁷ Consistent with the monogenic inheritance, mutations in TMEM27 have not been observed in Hartnup disorder and would be expected to show an amino acid transporter defect in the kidney but not intestine. Thus far, more than 20 different causative mutations have been identified in the *SLC6A19* gene.²⁶⁹ Interestingly, rare variants in *SLC6A19* have been associated with low serum creatinine levels and may have a kidney protective effect or affect creatinine synthesis.²⁷⁰ B⁰AT1 transports all neutral amino acids in symport with 1Na⁺; in contrast to many other members of the SLC6 family, chloride ions are not cotransported.²⁷¹ Substrate affinities range from 1–12 mM, with a preference for branched-chain amino acids (BCAA) and methionine, followed by large hydrophilic and aromatic amino acids.²⁷² In *in vitro* systems proline and tryptophan are very poor substrates of B⁰AT1,

but *in vivo* data suggest a significant contribution to the transport of both amino acids.²⁷³ Mice lacking B⁰AT1 replicate the human aminoaciduria of Hartnup disorder but do not show any additional pathology (Table 8.5). In addition to the low-affinity B⁰AT1 transporter in the PCT, functional studies suggest the presence of a high-affinity transporter for neutral amino acids in the PST. A candidate could be B⁰AT2 (SLC6A15), which is expressed at low levels in the proximal tubule.²⁷⁴ B⁰AT2 has a narrower substrate specificity than B⁰AT1, showing a strong preference for BCAA and methionine with substrate affinities <100 μM. Like B⁰AT1, the transporter is Na⁺ dependent and chloride independent.²⁷⁵

Specific Apical Transporters for Proline and Glycine

Proline and glycine have unusual physicochemical properties, which cause these amino acids to be inefficiently transported by more broadly specific amino acid transporters. Glycine is lacking a side chain, reducing its affinity to side-chain binding pockets, whereas proline has a secondary amino group and restricted flexibility. As a result, proline is a poor substrate for B⁰AT1 and is not recognized by the basolateral neutral amino acid transporter LAT2 (see later). A common transporter for glycine, proline, and hydroxyproline in humans is supported by two lines of evidence. First, in the rare disorder iminoglycinuria, all three amino acids are found in the urine.²⁷³ Second, prolinemia, when passing the renal threshold, causes prolinuria, hydroxyprolinuria, and glycinuria.²⁷⁶ Although iminoglycinuria is an autosomal recessive disorder, it shows clear signs of genetic complexity.²⁷⁷ For instance, some cases of iminoglycinuria show malabsorption of proline in the intestine. Moreover, in some cases, heterozygotes are normal, whereas in other pedigrees, hyperglycinuria is observed. These cases can all be explained by the combined action of proton-amino acid transporter 2 (PAT2, SLC36A2), the system IMINO

Table 8.5 Physiologic Characteristics of Knockout Mice of Renal Amino Acid Transporters

Transporter	Plasma AA	Urine AA	Renal Pathology	Other Features
rBAT	Normal	+++ Lys, Arg, Orn, CysC	Nephritis, kidney stones	None
b ⁰ +AT	+: His, Ser, Glu/n	+++ Lys, Arg, Orn, CysC, + Glu/n	Glomerular fibrosis, nephritis, kidney stones	None
B ⁰ AT1	Normal	+++ Neutral AA	None	Propensity for colitis, improved glycemic control
B ⁰ AT3	Normal	+++ Gly ++: Ala, Val, Leu, Ile, Met, Ser, Thr, Gln, Phe, Tyr	Reduced serum creatinine	Stress-induced increase of blood pressure
TAT1	+: Phe, Tyr, Trp -: Gly, Ala, Met, Ser, Thr, Asn, Gln HPD +: Phe, Tyr, Trp	+: Phe, Tyr, Trp HPD +: Val, Ile, Leu, Thr, Gln, His, Phe, Tyr, Trp	None	None
LAT4	-: Ala, Pro, His, Ser	Not available	None reported	Liver inflammation, malnutrition
LAT2	+: Gly, Ala, Ser, Thr, Gln, Val, Lys	+: Gly, Ser, Thr, Gln, Leu, Val	None	None
y ⁻ LAT1	Not available	+++ Lys, Arg, Orn	None	Failure to thrive, intrauterine growth restriction
TauT	-: Taurine -: Glu	+++ Taurine	Enlarged kidney, glomerulosclerosis, nephropathy	Muscle weakness, cardiomyopathy, retinal degeneration, hearing loss, chronic liver disease

CssC, Cystine; *Glu/n*, glutamate or glutamine; *HPD*, high-protein diet; +, elevated, ++ significantly elevated, +++ highly elevated; -, reduced, -, significantly reduced.

transporter SIT1 (SLC6A20), and the general neutral amino acid transporter B⁰AT1 (SLC6A19).²⁷³ Homozygous mutations in PAT2 account for iminoglycinuria, whereas heterozygous mutations cause selective hyperglycinuria. SIT1 mutations contribute to the iminoglycinuria phenotype and also explain a sporadically observed reduced proline absorption in the intestine. B⁰AT1 provides the baseload for proline and glycine reabsorption, explaining why the extent of aminoaciduria is well below the filtered amounts.²⁷³ The related glycine and alanine transporter B⁰AT3 (SLC6A18) is only functional in mouse^{278,279} (Table 8.5) but not in higher mammalian species, where its function has been replaced by PAT2.

PAT2 (SLC36A2) has been identified as the specific transporter for small neutral amino acids, specifically alanine, glycine, and proline. Single N-methylation of amino acids is tolerated such as in sarcosine or proline. PAT2 is mutated in all cases of iminoglycinuria and is expressed in the proximal tubule of the kidney.²⁷³ The K_M values for its substrates range from 0.1–0.6 mM.²⁸⁰

SIT1 (SLC6A20) accepts only amino acids with secondary, tertiary, or quaternary amines, such as proline, sarcosine, betaine, and methylaminoisobutyric acid.^{281,282} SIT1 is an Na⁺ and Cl⁻ dependent transporter, transporting 1 substrate, 2Na⁺ and 1Cl⁻ ion. This generates a net positive transporter current, which can be observed when expressed heterologously. Expression of the transporter at the cell surface requires collectrin (TMEM27).²⁸³

B⁰AT3 (SLC6A18) preferentially transports alanine and glycine.²⁷⁹ SLC6A18 knockout mice have hyperglycinuria and slightly elevated urine levels of other neutral amino acids,²⁷⁸ but humans with homozygous mutations in SLC6A18 are normal because even the normal allele is nonfunctional.^{273,284} The mouse transporter requires collectrin coexpression for trafficking and also for its catalytic function.²⁸⁴

Specific Apical Transporters for B-Amino Acids

This group of amino acids consists of taurine, β-alanine, and its homolog gamma-aminobutyric acid (GABA). Plasma concentration of GABA is very low (about 0.1 μM), while taurine levels are significantly higher (about 50 μM). Both amino acids are often accepted by the same transporters, but in the kidney, specific GABA transporters are observed as well. Reabsorption of these amino acids is mainly mediated by the taurine transporter TauT (SLC6A6).²⁸⁵ PAT2 shows weak affinity for these substrates but is probably physiologically irrelevant. TauT translocates taurine with a K_M of 20 μM in a process that involves the cotransport of 2Na⁺ and 1Cl⁻. Urinary taurine excretion in TauT-deficient mice reaches the filtered amounts.²⁸⁶

BASOLATERAL TRANSPORTERS

Functional studies identified an Na⁺-independent transporter broadly specific for neutral amino acids also in the basolateral membrane. The heteromeric amino acid transporter 4F2hc-LAT2 (SLC3A2-SLC7A8) matches with regard to the substrate specificity but mechanistically is an antiporter.^{287–289} A uniporter has been identified for aromatic amino acids (TAT1, SLC16A10),²⁹⁰ but this transporter cannot explain the net flux of amino acids across the renal epithelium as illustrated by *Tat1* knockout mice.²⁹¹ These mice show elevated levels of aromatic amino acids in the urine but normal levels of other amino acids. Only on a high-protein diet, a more general

aminoaciduria was observed, suggesting cooperation between LAT2 and TAT1. LAT4 (SLC43A2) allows efflux of BCAA, methionine, and phenylalanine, thus covering large neutral amino acids.²⁹² A specific efflux pathway for small neutral amino acids has not been identified and thus is likely to occur through cooperation between LAT2, TAT1, and LAT4: efflux of small neutral AA in exchange for large neutral AA or aromatic AA, which is supported by the appearance of small neutral amino acids in the urine of *Lat2* knockout mice.²⁹³

LAT2 (SLC3A2-SLC7A8) shows a distinct asymmetry with regard to affinity on the two faces of the membrane. The K_M values on the outside range from 40–200 μM, while on the inside, K_M values range from 3–30 mM.²⁹⁴ The transporter accepts all neutral amino acids except proline. TAT1 (SLC16A10) shows very low affinity for its substrates, ranging from 3–7 mM.²⁹⁵ Although the transporter is related to monocarboxylate transporters, it does not cotransport protons.²⁹⁰ Apart from aromatic amino acids, TAT1 also transports the N-methylated derivatives of these amino acids and L-dopa.

LAT4 (SLC43A2) belongs to a separate transporter family than 4F2hc-LAT2. It does not require additional subunits and transports its substrates with low affinity (K_M for phenylalanine is 5 mM) on both sides of the membrane.²⁹⁶

The kidney contributes to gluconeogenesis and pH regulation. The glutamine, asparagine, and histidine transporter SNAT3 (SLC38A3) is located in the basolateral membrane but is typically expressed at low levels. During chronic acidosis, it is upregulated and glutamine imported for deamination by phosphate-activated glutaminase.²⁹⁷ The resulting glutamate is further deaminated to 2-oxoglutarate, which serves as a substrate for gluconeogenesis²⁹⁸ (see also Fig. 8.4). Ammonia is released into the urine, thereby disposing of protons. Upregulation of SNAT3 mRNA during chronic metabolic acidosis involves promoter regulation and mRNA stability.²⁹⁹ The related transporter SNAT (SLC38A5) is also expressed in the kidney and may contribute to glutamine uptake.³⁰⁰ Its subcellular localization is unknown.

There is no clear pathway for the basolateral exit of proline. Although glycine is inefficiently transported by many neutral amino acid transporters, including 4F2hc-LAT2, the latter does not accept proline. Release of taurine also remains unclear. The GABA/betaine transporter BGT1 (SLC6A12) has been identified in the basolateral membrane of renal epithelial cells but accumulates its substrates in the cytosol and therefore is not a feasible efflux pathway.

TRANSPORTERS FOR CATIONIC AMINO ACIDS AND CYSTINE

APICAL TRANSPORTERS

The presence of a transporter for cationic amino acids that is shared with cystine can be deduced from the aminoaciduria observed in cystinuria, which includes both groups of amino acids.³⁰¹ Renal cystine clearance is close to GFR in cystinuria, whereas cationic amino acids remain partially reabsorbed. Cationic amino acids and cystine are transported in the proximal tubule by the heteromeric transporter rBAT/b⁰+AT (broad neutral and cationic amino acid transporter).³⁰² Cystinuria is an autosomal recessive disorder. Homozygous (or compound heterozygous) mutations in the rBAT encoding gene SLC3A1 are classified as type A cystinuria, whereas homozygous (or compound heterozygous) mutations in the b⁰+AT encoding

gene SLC7A9 are classified as type B.³⁰³ This genetic heterogeneity can be detected in the heterozygous state, where rBAT heterozygotes do not show residual aminoaciduria, while b⁰⁺AT heterozygotes show some release of cystine and lysine into the urine. Cystinuria causes formation of kidney stones due to the low solubility of cystine.³⁰¹ The distribution of rBAT along the proximal tubule shows increasing expression toward the PST, whereas b⁰⁺AT shows the opposite trend. This suggested that rBAT may have a different partner in the PST, which was shown to be the aspartate/glutamate transporter AGT1.³⁰⁴ Initially AGT1 was thought to have a basolateral localization; however, follow-up studies using more specific antibodies demonstrated an apical localization. Functionally, AGT1 operates as a cystine transporter, exchanging cystine for glutamate. Interestingly, this suggests that cystine is transported as a neutral amino acid in the PCT and as an anionic amino acid in the PST. In b⁰⁺AT knockout mice fractional excretion of arginine reaches 80%, while only 11% of the tubular cystine load is excreted.³⁰⁵ This is consistent with the presence of additional cystine transporters, such as AGT1 and EAAT3 (see anionic amino acid transporters later). The rBAT protein is a highly glycosylated type II membrane protein that is connected by a disulfide bridge to the transporter subunit b⁰⁺AT just outside the membrane.³⁰⁶ Heterodimer formation is essential for the exit of the complex from the endoplasmic reticulum.³⁰⁷ Transport properties of rbat/b⁰⁺AT have been largely elucidated using the oocyte endogenous transporter that associates with rbat when its cRNA is expressed in this system.³⁰⁸ These experiments show that rbat/b⁰⁺AT is an obligatory antiporter that preferentially takes up cationic amino acids from the lumen in exchange for neutral amino acids. This directionality is imposed by the inside-negative cell membrane potential, and it is also confirmed by the lack of neutral amino acids in cystinuria.³⁰⁹ Affinities for cationic amino acids and cystine are approximately 100 μM ; neutral amino acids have slightly higher apparent K_M values.³¹⁰ The acidic amino acid–cystine exchanger AGT1 transports cystine with a K_M of 68 μM .³⁰⁴ In mice, the gene is only expressed in males and thus is unlikely to be essential for renal cystine reabsorption. In humans, isolated cystinuria, a rare disorder in which only cystine is elevated in urine, is caused by selected mutations in b⁰⁺AT that affect the substrate selectivity of the transport subunit.³¹¹ Mutations in AGT1 have not been identified thus far.

Clinical Relevance

Transporters for Cationic Amino Acids and Cystine Apical Transporters

Urolithiasis occurs in most cases of cystinuria. The generation of kidney stones is managed through the combination of several treatments. Tiopronin (α -mercaptopropionylglycine) is administered to form adducts with cysteine, which have a higher solubility than cystine. Potassium citrate is used to increase the pH of urine >7.5 . Reduction of animal protein intake and nocturnal fluid intakes are recommended. All treatments are aimed to reduce cysteine formation and precipitation.

BASOLATERAL TRANSPORTERS

A basolateral exit pathway for cationic amino acids is defined by the disease LPI.^{256,312} LPI is caused by mutations in the

SLC7A7 light chain of the heteromeric transporter 4F2hc-SLC7A7.^{313,314} The disease is very rare, with less than 200 cases reported, mainly from the Finnish population, where a founder mutation exists. In contrast to apical transport disorders, which are often benign, LPI can be a very severe disease, although clinical symptoms vary widely.²⁵⁶ It also has a number of extrarenal pathologies, such as alveolar proteinosis and immune defects, which are not well understood. Plasma levels of cationic amino acids are reduced, which affects urea cycle function, causing the adverse reaction to protein ingestion. Urine levels of cationic amino acids are very high, particularly that of lysine. Intestinal absorption of cationic amino acids is also affected. Although a functionally redundant transporter exists (4F2hc-SLC7A6), its expression is low and cannot replace malfunction of SLC7A7.³¹⁵ Functionally, SLC7A6 and SLC7A7 are characterized as system y⁺L, indicating a transporter that exchanges neutral and cationic amino acids, which was initially discovered in placenta and erythrocytes.³¹⁶ The y⁺LAT1 (SLC7A7) transporter accepts neutral and cationic amino acids with high affinity (K_M values about 20 μM), but the affinity for neutral amino acids is two orders of magnitude lower in the absence of Na⁺.³¹⁷ As a result, the preferential mode of operation is an efflux of cationic amino acids in exchange for extracellular neutral amino acids. The y⁺LAT1 transporter is widely expressed in the basolateral membrane of the proximal tubulus.

The prevalence of exchangers for the transport of cationic and neutral amino acids sets these mechanisms apart from the paradigm set by glucose reabsorption. One possible reason could be the maintenance of cytosolic amino acid pools that are significantly higher than those observed in blood plasma and which are required for protein biosynthesis and amino acid homeostasis.³¹⁸ In the presence of basolateral facilitators, cytosolic amino acid pools would be close to those observed in the blood.

TRANSPORTERS FOR ANIONIC AMINO ACIDS

The main apical transporter for anionic amino acids in the proximal tubule is EAAT3 (named EAAC1 in rodents, SLC1A3).³¹⁹ EAAT3 transports both glutamate ($K_M = 14 \mu\text{M}$) and aspartate and shows a preference for D-aspartate over L-aspartate.³²⁰ As pointed out earlier, EAAT3 also contributes to cystine transport,³²¹ but cystine is only marginally elevated in individuals with dicarboxylic aminoaciduria.³²² The latter is a rare condition caused by mutations in EAAT3.³²² It is readily detected by highly elevated urine levels of aspartate and glutamate; excretion can reach or even exceed the filtered amounts. In addition to the kidney, EAAT3 is expressed in neurons and the intestine and allows high cytosolic accumulation due to the cotransport of 3Na⁺ and 1H⁺ and the antiport of 1K⁺.³²³ Despite expression of EAAT3 in neurons, dicarboxylic aminoaciduria is considered a benign disorder.³²⁴ However, an association of EAAT3 mutations with obsessive-compulsive disorder has been reported.³²⁵ Expression of EAAT3 is relatively low in the PCT, increases toward the PST, and is also observed in the distal parts of the tubule.³¹⁹ Nevertheless, 90% of the filtered anionic amino acid load is reabsorbed in the PCT. The transporter is regulated by osmolarity and amino acid deprivation.³²⁶ A dedicated efflux pathway for glutamate in renal epithelial cells has not been identified. In fact, there is evidence for an accumulative glutamate

transporter in the basolateral membrane, which would prevent efflux.²⁵⁹ In accordance, glutamate is intensively metabolized in epithelial cells, and efflux may be limited. Moreover, members of the SLC22 family are nonspecific anion transporters, and those located in the basolateral membrane may serve as efflux pathways for glutamate.³²⁷

STRUCTURAL INFORMATION OF AMINO ACID TRANSPORTERS

Plasma membrane amino acid transporters thus far fall into three different protein folds, namely the LeuT-fold, the Glt-fold, and the multifacilitator superfamily (MFS)-fold³²⁸ (see Table 8.4). Functionally, it has long been established that transporters must be able to adopt an inward-facing and an outward-facing conformation.^{329,330} All transporters analyzed thus far operate in an alternating access mode in which the substrate and cosubstrates (if applicable) bind on one side

of the membrane (e.g., outside). Subsequently, weak interactions between substrate and the transporter cause the transporter to enclose the substrate, resulting in the occluded conformation. The transporter transitions further into an inside–open conformation to release the substrate.³²⁸ In the case of antiporters, the energy barrier for a substrate-less translocation is too high; thus, the return to the initial conformation is only possible in a substrate-bound state. In the case of symporters and uniporters, the empty transporter can transition back through a substrate-free occluded state, back to the outside–open conformation, thereby closing the catalytic cycle. However, at least in the case of the LeuT protein fold, a pseudosubstrate in the form of a leucine side chain residing close to the substrate binding site occupies the empty binding site, thereby facilitating the transition back to the outside conformation.³³¹

For the LeuT-fold, high-resolution structures have been identified for all but one stage of the transport cycle (Fig.

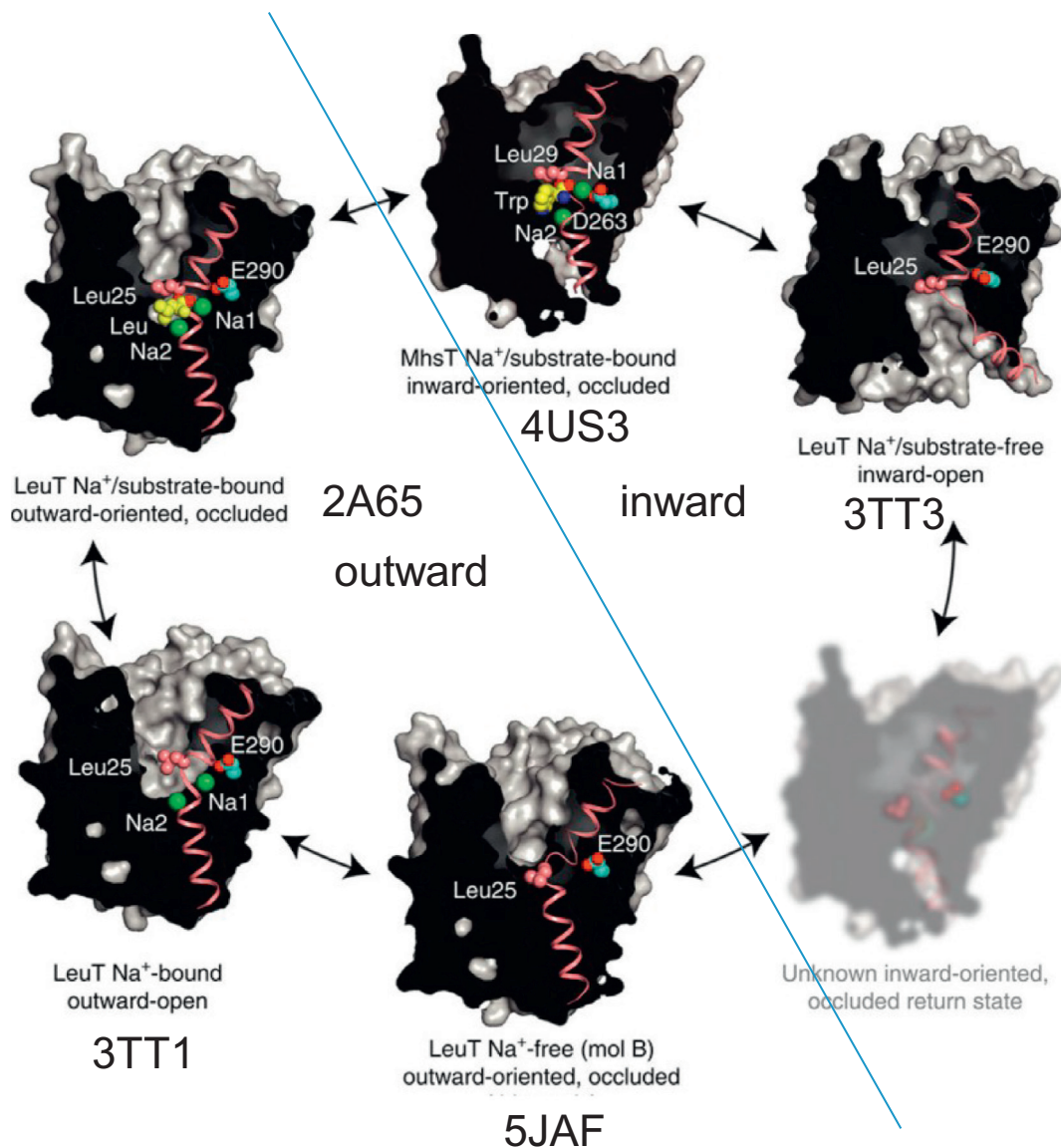


Fig. 8.14 Transport cycle of LeuT-fold proteins. TM1 helix and pseudosubstrate Leu25 (Leu29^{MhsT}) are shown in pink, the Na⁺ ions are shown as green spheres, and Glu290 (or Asp263^{MhsT}) as cyan, and substrate at the binding site as yellow spheres. (Reused from Malinauskaitė L, Said S, Sahin C, et al. A conserved leucine occupies the empty substrate site of LeuT in the Na(+)-free return state. *Nat Commun.* 2016;7:11673, under creative common license.)

8.14). The first structure of LeuT revealed an internal symmetry, whereby helix 1-5 can be superimposed onto helix 1-6 in a twofold rotation.³³² This internal symmetry provides the structural basis for the adoption of an inward- and outward-facing conformation.³³³ Further investigation of this protein fold revealed that part of the protein remains rather immobile—an arrangement of helices 3,5 and 7,8 named the hash (#)—whereas others move significantly—the bundle—composed of helices 1,2 and 6,7.³³³ The hydrogen bond network is interrupted in the center of helices 1 and 6, allowing the helix to bend and to use these hydrogen bonds to interact with substrates and cotransported ions. A key feature in most transporters with a LeuT-fold is a motion of the bundle relative to the hash or vice versa, thereby alternatively closing and opening alternating sites of the transporter.³²⁸ Another common feature is the presence of one or more aromatic amino acids adjacent to the substrate binding site, which insulate the substrate during the transition to the occluded state. These residues are referred to as “thin” gates in contrast to subsequent enclosure of the substrate by more substantial parts of the protein (thick gates).

The transport process in Na⁺-driven glutamate transporters is quite different, as it involves an elevator-like movement of the transport domain relative to a rigid scaffold domain.³³⁴ Glt_{ph} is composed of eight TM segments and two helical hairpins (HP1 and HP2).³³⁵ The six N-terminal helices form a large bracket that holds TM7, TM8, HP1, and HP2. Two large loops, one connecting TM2 and TM3 and the other TM5 and TM6, serve as the hinge to allow elevator-like movement of the substrate binding domain.³³⁶ Reminiscent of similar features in LeuT, the structure and ions are bound by unwound regions of TM7, TM8, HP1, and HP2. Alternating access is mediated by opening of helical HPs on the respective side of the membrane. Glutamate transporters form trimers, which are likely to be important to stabilize the scaffold against the movement of the elevator domain.

In the MFS fold, the protein has a symmetry axis perpendicular to the membrane between helices 1–6 and 7–12.^{337,338} During the transport cycle, the two halves of the protein move against each other. This rocker-switch mode needs to be modified to accommodate initial occlusion of the substrate by the bending of the outer ends of helices 1 and 7 on the outside or 4 and 10 on the inside. Binding of amino acids remains unclear due to the lack of high-resolution structures of amino acid-translocating members.

As pointed out earlier, several renal amino acid transporters form heterodimers with ancillary proteins—for instance, SLC7 transporters with 4F2hc and rBAT and SLC6 transporter B⁰AT1 with collectrin. The main role of ancillary subunits is to facilitate the exit of the complex from the endoplasmic reticulum.³⁰⁷ Collectrin, in addition, is also essential for the catalytic activity of the transporter.²⁸⁴ The structure of the ectodomains of transporter ancillary proteins is known for 4F2hc,³³⁹ but the precise heteromeric arrangement is only partially understood.³⁴⁰ The structure of the 4F2hc ectodomain, which is related to bacterial α -amylases, is composed of two subdomains, namely domain A, a triphosphate isomerase barrel domain ($\alpha\beta$)₈, and domain C, made up of eight antiparallel β -strands.³³⁹ However, neither 4F2hc nor rBAT has glycosidase activity and they both lack conservation of critical catalytic residues. The glycosylation of the ancillary proteins could be important to help with quality control in the endoplasmic reticulum. In addition to its role in amino

acid transport, collectrin is thought to be involved in kidney development and vesicle exocytosis, but these functions are mechanistically less well understood.³⁴¹ The 4F2 heavy chain has additional functions in integrin signaling, which are well understood in cancer cells but not in epithelial cells.^{266,306,342}



Complete reference list available at ExpertConsult.com.

KEY REFERENCES

- Barfuss DW, Schafer JA. Differences in active and passive glucose transport along the proximal nephron. *Am J Physiol*. 1981;241:F322–F332.
- Turner RJ, Moran A. Heterogeneity of sodium-dependent D-glucose transport sites along the proximal tubule: evidence from vesicle studies. *Am J Physiol*. 1982;242:F406–F414.
- Wells RG, Pajor AM, Kanai Y, et al. Cloning of a human kidney cDNA with similarity to the sodium-glucose cotransporter. *Am J Physiol*. 1992;263:F459–F465.
- Hediger MA, Coady MJ, Ikeda TS, et al. Expression cloning and cDNA sequencing of the Na⁺/glucose co-transporter. *Nature*. 1987;330:379–381.
- Vallon V, Platt KA, Cunard R, et al. SGLT2 mediates glucose reabsorption in the early proximal tubule. *J Am Soc Nephrol*. 2011;22:104–112.
- Gorboulev V, Schurmann A, Vallon V, et al. Na(+)-D-glucose cotransporter SGLT1 is pivotal for intestinal glucose absorption and glucose-dependent incretin secretion. *Diabetes*. 2012;61:187–196.
- Wright EM, Loo DD, Hirayama BA. Biology of human sodium glucose transporters. *Physiol Rev*. 2011;91:733–794.
- Martin MG, Turk E, Lostao MP, et al. Defects in Na⁺/glucose cotransporter (SGLT1) trafficking and function cause glucose-galactose malabsorption. *Nat Genet*. 1996;12:216–220.
- Rieg T, Masuda T, Gerasimova M, et al. Increase in SGLT1-mediated transport explains renal glucose reabsorption during genetic and pharmacological SGLT2 inhibition in euglycemia. *Am J Physiol Renal Physiol*. 2014;306:F188–F193.
- Hummel CS, Lu C, Loo DD, et al. Glucose transport by human renal Na⁺/D-glucose cotransporters SGLT1 and SGLT2. *Am J Physiol Cell Physiol*. 2011;300:C14–C21.
- Faham S, Watanabe A, Besserer GM, et al. The crystal structure of a sodium galactose transporter reveals mechanistic insights into Na⁺/sugar symport. *Science*. 2008;321:810–814.
- Fukuzawa T, Fukazawa M, Ueda O, et al. SGLT5 reabsorbs fructose in the kidney but its deficiency paradoxically exacerbates hepatic steatosis induced by fructose. *PLoS ONE*. 2013;8:e56681.
- Gerich JE. Role of the kidney in normal glucose homeostasis and in the hyperglycaemia of diabetes mellitus: therapeutic implications. *Diabet Med*. 2010;27:136–142.
- Vallon V, Thomson SC. Targeting renal glucose reabsorption to treat hyperglycaemia: the pleiotropic effects of SGLT2 inhibition. *Diabetologia*. 2017;60:215–225.
- Wanner C, Inzucchi SE, Lachin JM, et al. Empagliflozin and progression of kidney disease in type 2 diabetes. *N Engl J Med*. 2016;375:323–334.
- Cherney DZ, Perkins BA, Soleymanlou N, et al. Renal hemodynamic effect of sodium-glucose cotransporter 2 inhibition in patients with type 1 diabetes mellitus. *Circulation*. 2014;129:587–597.
- Vallon V, Richter K, Blantz RC, et al. Glomerular hyperfiltration in experimental diabetes mellitus: potential role of tubular reabsorption. *J Am Soc Nephrol*. 1999;10:2569–2576.
- Inzucchi SE, Zinman B, Fitchett D, et al. How does empagliflozin reduce cardiovascular mortality? Insights from a mediation analysis of the EMPA-REG OUTCOME trial. *Diabetes Care*. 2018;41:356–363.
- You G. Structure, function, and regulation of renal organic anion transporters. *Med Res Rev*. 2002;22:602–616.
- Emami RA, Nies AT, Schaeffeler E, et al. Organic anion transporters and their implications in pharmacotherapy. *Pharmacol Rev*. 2012;64:421–449.
- Saito H. Pathophysiological regulation of renal SLC22A organic ion transporters in acute kidney injury: pharmacological and toxicological implications. *Pharmacol Ther*. 2010;125:79–91.
- Lopez-Nieto CE, You G, Bush KT, et al. Molecular cloning and characterization of NKT, a gene product related to the organic cation transporter family that is almost exclusively expressed in the kidney. *J Biol Chem*. 1997;272:6471–6478.

182. Grundemann D, Gorboulev V, Gambaryan S, et al. Drug excretion mediated by a new prototype of polyspecific transporter. *Nature*. 1994;372:549–552.
183. Nigam SK. The SLC22 transporter family: a paradigm for the impact of drug transporters on metabolic pathways, signaling, and disease. *Annu Rev Pharmacol Toxicol*. 2018;58:663–687.
184. Nigam SK. What do drug transporters really do? *Nat Rev Drug Discov*. 2015;14:29–44.
187. U.S. Food and Drug Administration. *Guidance for Industry: Drug Interaction Studies—Study Design, Data Analysis, Implications for Dosing, and Labeling Recommendations*. Silver Spring, MD: US Department of Health and Human Services, Food Drug Administration Center for Drug Evaluation and Research CDER; 2012. <http://www.fda.gov/downloads/Drugs/GuidanceComplianceRegulatoryInformation/Guidances/UCM292362.pdf>.
193. Wikoff WR, Nagle MA, Kouznetsova VL, et al. Untargeted metabolomics identifies enterobiome metabolites and putative uremic toxins as substrates of organic anion transporter 1 (Oat1). *J Proteome Res*. 2011;10:2842–2851.
194. Bush KT, Wu W, Lun C, et al. The drug transporter OAT3 (SLC22A8) and endogenous metabolite communication via the gut-liver-kidney axis. *J Biol Chem*. 2017;292:15789–15803.
195. Wu W, Bush KT, Nigam SK. Key role for the organic anion transporters, OAT1 and OAT3, in the in vivo handling of uremic toxins and solutes. *Sci Rep*. 2017;7:4939.
198. Vallon V, Rieg T, Ahn SY, et al. Overlapping in vitro and in vivo specificities of the organic anion transporters OAT1 and OAT3 for loop and thiazide diuretics. *Am J Physiol Renal Physiol*. 2008;294:F867–F873.
199. Vanwert AL, Bailey RM, Sweet DH. Organic anion transporter 3 (Oat3/Slc22a8) knockout mice exhibit altered clearance and distribution of penicillin G. *Am J Physiol Renal Physiol*. 2007;293:F1332–F1341.
203. Miyajima M, Kusuhara H, Fujishima M, et al. Organic anion transporter 3 mediates the efflux transport of an amphipathic organic anion, dehydroepiandrosterone sulfate, across the blood-brain barrier in mice. *Drug Metab Dispos*. 2011;39:814–819.
206. Torres AM, Dnyanmote AV, Bush KT, et al. Deletion of multispecific organic anion transporter Oat1/Slc22a6 protects against mercury-induced kidney injury. *J Biol Chem*. 2011;286:26391–26395.
208. Liu HC, Jamshidi N, Chen Y, et al. An organic anion transporter 1 (OAT1)-centered metabolic network. *J Biol Chem*. 2016;291:19474–19486.
215. Bhatnagar V, Richard EL, Wu W, et al. Analysis of ABCG2 and other urate transporters in uric acid homeostasis in chronic kidney disease: potential role of remote sensing and signaling. *Clin Kidney J*. 2016;9:444–453.
222. Nies AT, Koepsell H, Damme K, et al. Organic cation transporters (OCTs, MATEs), in vitro and in vivo evidence for the importance in drug therapy. *Handb Exp Pharmacol*. 2011;105–167.
223. Chen L, Shu Y, Liang X, et al. OCT1 is a high-capacity thiamine transporter that regulates hepatic steatosis and is a target of metformin. *Proc Natl Acad Sci U. S. A.* 2014;111:9983–9988.
238. Mandal AK, Mount DB. The molecular physiology of uric acid homeostasis. *Annu Rev Physiol*. 2015;77:323–345.
257. Rajantie J, Simell O, Perheentupa J. Lysinuric protein intolerance. Basolateral transport defect in renal tubuli. *J Clin Invest*. 1981;67:1078–1082.
264. Seow HF, Broer S, Broer A, et al. Hartnup disorder is caused by mutations in the gene encoding the neutral amino acid transporter SLC6A19. *Nat Genet*. 2004;36:1003–1007.
265. Kleta R, Romeo E, Ristic Z, et al. Mutations in SLC6A19, encoding B0AT1, cause Hartnup disorder. *Nat Genet*. 2004;36:999–1002.
267. Danilczyk U, Sarao R, Remy C, et al. Essential role for collectrin in renal amino acid transport. *Nature*. 2006;444:1088–1091.
273. Broer S, Bailey CG, Kowalczyk S, et al. Iminoglycinuria and hyperglycinuria are discrete human phenotypes resulting from complex mutations in proline and glycine transporters. *J Clin Invest*. 2008;118:3881–3892.
301. Chillaron J, Font-Llitjos M, Fort J, et al. Pathophysiology and treatment of cystinuria. *Nat Rev Nephrol*. 2010;6:424–434.
304. Nagamori S, Wiriyasermkul P, Guarch ME, et al. Novel cystine transporter in renal proximal tubule identified as a missing partner of cystinuria-related plasma membrane protein rBAT/SLC3A1. *Proc Natl Acad Sci U. S. A.* 2016;113:775–780.
313. Torrents D, Mykkanen J, Pineda M, et al. Identification of SLC7A7, encoding γ -LAT-1, as the lysinuric protein intolerance gene. *Nat Genet*. 1999;21:293–296.
314. Borsani G, Bassi MT, Sperandeo MP, et al. SLC7A7, encoding a putative permease-related protein, is mutated in patients with lysinuric protein intolerance. *Nat Genet*. 1999;21:297–301.
322. Bailey CG, Ryan RM, Thoeng AD, et al. Loss-of-function mutations in the glutamate transporter SLC1A1 cause human dicarboxylic aminoaciduria. *J Clin Invest*. 2011;121:446–453.

REFERENCES

- Zierler K. Whole body glucose metabolism. *Am J Physiol*. 1999;276:E409–E426.
- Kowalski GM, Bruce CR. The regulation of glucose metabolism: implications and considerations for the assessment of glucose homeostasis in rodents. *Am J Physiol Endocrinol Metab*. 2014;307:E859–E871.
- Mogensen CE. Maximum tubular reabsorption capacity for glucose and renal hemodynamics during rapid hypertonic glucose infusion in normal and diabetic subjects. *Scand J Clin Lab Invest*. 1971;28:101–109.
- Farber SJ, Berger EY, Earle DP. Effect of diabetes and insulin on the maximum capacity of the renal tubules to reabsorb glucose. *J Clin Invest*. 1951;30:125–129.
- Barfuss DW, Schafer JA. Differences in active and passive glucose transport along the proximal nephron. *Am J Physiol*. 1981;241:F322–F332.
- Turner RJ, Moran A. Heterogeneity of sodium-dependent D-glucose transport sites along the proximal tubule: evidence from vesicle studies. *Am J Physiol*. 1982;242:F406–F414.
- Wells RG, Pajor AM, Kanai Y, et al. Cloning of a human kidney cDNA with similarity to the sodium-glucose cotransporter. *Am J Physiol*. 1992;263:F459–F465.
- Hediger MA, Coady MJ, Ikeda TS, et al. Expression cloning and cDNA sequencing of the Na⁺/glucose co-transporter. *Nature*. 1987;330:379–381.
- Wright EM. Renal Na⁽⁺⁾-glucose cotransporters. *Am J Physiol Renal Physiol*. 2001;280:F10–F18.
- Wright EM, Turk E. The sodium/glucose cotransport family SLC5. *Pflugers Arch*. 2004;447:510–518.
- Quamme GA, Freeman HJ. Evidence for a high-affinity sodium-dependent D-glucose transport system in the kidney. *Am J Physiol*. 1987;253:F151–F157.
- Kanai Y, Lee WS, You G, et al. The human kidney low affinity Na⁺/glucose cotransporter SGLT2. Delineation of the major renal reabsorptive mechanism for D-glucose. *J Clin Invest*. 1994;93:397–404.
- You G, Lee WS, Barros EJ, et al. Molecular characteristics of Na⁽⁺⁾-coupled glucose transporters in adult and embryonic rat kidney. *J Biol Chem*. 1995;270:29365–29371.
- Lee WS, Kanai Y, Wells RG, et al. The high affinity Na⁺/glucose cotransporter. Re-evaluation of function and distribution of expression. *J Biol Chem*. 1994;269:12032–12039.
- Vallon V, Platt KA, Cunard R, et al. SGLT2 mediates glucose reabsorption in the early proximal tubule. *J Am Soc Nephrol*. 2011;22:104–112.
- Sabolic I, Vrhovac I, Eror DB, et al. Expression of Na⁺-D-glucose cotransporter SGLT2 in rodents is kidney-specific and exhibits sex and species differences. *Am J Physiol Cell Physiol*. 2012;302:C1174–C1188.
- Balen D, Ljubojevic M, Breljak D, et al. Revised immunolocalization of the Na⁺-D-glucose cotransporter SGLT1 in rat organs with an improved antibody. *Am J Physiol Cell Physiol*. 2008;295:C475–C489.
- Vrhovac I, Balen ED, Klessen D, et al. Localizations of Na⁺-D-glucose cotransporters SGLT1 and SGLT2 in human kidney and of SGLT1 in human small intestine, liver, lung, and heart. *Pflugers Arch*. 2015;467:1881–1898.
- Madunic IV, Breljak D, Karaica D, et al. Expression profiling and immunolocalization of Na⁽⁺⁾-D-glucose-cotransporter 1 in mice employing knockout mice as specificity control indicate novel locations and differences between mice and rats. *Pflugers Arch*. 2017;469:1545–1565.
- Gorboulev V, Schurmann A, Vallon V, et al. Na⁽⁺⁾-D-glucose cotransporter SGLT1 is pivotal for intestinal glucose absorption and glucose-dependent incretin secretion. *Diabetes*. 2012;61:187–196.
- Wright EM, Loo DD, Hirayama BA. Biology of human sodium glucose transporters. *Physiol Rev*. 2011;91:733–794.
- Martin MG, Turk E, Lostao MP, et al. Defects in Na⁺/glucose cotransporter (SGLT1) trafficking and function cause glucose-galactose malabsorption. *Nat Genet*. 1996;12:216–220.
- Santer R, Calado J. Familial renal glucosuria and SGLT2: from a Mendelian trait to a therapeutic target. *Clin J Am Soc Nephrol*. 2010;5:133–141.
- Rieg T, Masuda T, Gerasimova M, et al. Increase in SGLT1-mediated transport explains renal glucose reabsorption during genetic and pharmacological SGLT2 inhibition in euglycemia. *Am J Physiol Renal Physiol*. 2014;306:F188–F193.
- Komoroski B, Vachharajani N, Boulton D, et al. Dapagliflozin, a novel SGLT2 inhibitor, induces dose-dependent glucosuria in healthy subjects. *Clin Pharmacol Ther*. 2009;85:520–526.
- Heise T, Seewaldt-Becker E, Macha S, et al. Safety, tolerability, pharmacokinetics and pharmacodynamics following 4 weeks' treatment with empagliflozin once daily in patients with type 2 diabetes. *Diabetes Obes Metab*. 2013;15:613–621.
- Sha S, Devineni D, Ghosh A, et al. Canagliflozin, a novel inhibitor of sodium glucose co-transporter 2, dose dependently reduces calculated renal threshold for glucose excretion and increases urinary glucose excretion in healthy subjects. *Diabetes Obes Metab*. 2011;13:669–672.
- Hummel CS, Lu C, Loo DD, et al. Glucose transport by human renal Na⁺/D-glucose cotransporters SGLT1 and SGLT2. *Am J Physiol Cell Physiol*. 2011;300:C14–C21.
- Powell DR, DaCosta CM, Gay J, et al. Improved glycemic control in mice lacking SglT1 and SglT2. *Am J Physiol Endocrinol Metab*. 2013;304:E117–E130.
- Powell DR, DaCosta CM, Smith M, et al. Effect of LX4211 on glucose homeostasis and body composition in preclinical models. *J Pharmacol Exp Ther*. 2014;350:232–242.
- Gallo LA, Wright EM, Vallon V. Probing SGLT2 as a therapeutic target for diabetes: basic physiology and consequences. *Diab Vasc Dis Res*. 2015;12:78–89.
- Faham S, Watanabe A, Besserer GM, et al. The crystal structure of a sodium galactose transporter reveals mechanistic insights into Na⁺/sugar symport. *Science*. 2008;321:810–814.
- Vallon V, Grahmmer F, Volkl H, et al. KCNQ1-dependent transport in renal and gastrointestinal epithelia. *Proc Natl Acad Sci U. S. A*. 2005;102:17864–17869.
- Vallon V, Grahmmer F, Richter K, et al. Role of KCNE1-dependent K⁺ fluxes in mouse proximal tubule. *J Am Soc Nephrol*. 2001;12:2003–2011.
- Wright EM. Glucose transport families SLC5 and SLC50. *Mol Aspects Med*. 2013;34:183–196.
- Sotak M, Marks J, Unwin RJ. Putative tissue location and function of the SLC5 family member SGLT3. *Exp Physiol*. 2017;102:5–13.
- Tazawa S, Yamato T, Fujikura H, et al. SLC5A9/SGLT4, a new Na⁺-dependent glucose transporter, is an essential transporter for mannose, 1,5-anhydro-D-glucitol, and fructose. *Life Sci*. 2005;76:1039–1050.
- Grempler R, Augustin R, Froehner S, et al. Functional characterisation of human SGLT-5 as a novel kidney-specific sodium-dependent sugar transporter. *FEBS Lett*. 2012;586:248–253.
- Ghezzi C, Gorraitz E, Hirayama BA, et al. Fingerprints of hSGLT5 sugar and cation selectivity. *Am J Physiol Cell Physiol*. 2014;306:C864–C870.
- Chen J, Williams S, Ho S, et al. Quantitative PCR tissue expression profiling of the human SGLT2 gene and related family members. *Diabetes Ther*. 2010;1:57–92.
- Fukuzawa T, Fukazawa M, Ueda O, et al. SGLT5 reabsorbs fructose in the kidney but its deficiency paradoxically exacerbates hepatic steatosis induced by fructose. *PLoS ONE*. 2013;8:e56681.
- Uchida S, Endou H. Substrate specificity to maintain cellular ATP along the mouse nephron. *Am J Physiol*. 1988;255:F977–F983.
- Guder WG, Ross BD. Enzyme distribution along the nephron. *Kidney Int*. 1984;26:101–111.
- Klein KL, Wang MS, Torikai S, et al. Substrate oxidation by isolated single nephron segments of the rat. *Kidney Int*. 1981;20:29–35.
- Chin E, Zhou J, Bondy C. Anatomical and developmental patterns of facilitative glucose transporter gene expression in the rat kidney. *J Clin Invest*. 1993;91:1810–1815.
- Wood IS, Trayhurn P. Glucose transporters (GLUT and SGLT): expanded families of sugar transport proteins. *Br J Nutr*. 2003;89:3–9.
- Dominguez JH, Camp K, Maianu L, et al. Glucose transporters of rat proximal tubule: differential expression and subcellular distribution. *Am J Physiol*. 1992;262:F807–F812.
- Thorens B, Lodish HF, Brown D. Differential localization of two glucose transporter isoforms in rat kidney. *Am J Physiol*. 1990;259:C286–C294.
- Sala-Rabanal M, Hirayama BA, Ghezzi C, et al. Revisiting the physiological roles of SGLTs and GLUTs using positron emission tomography in mice. *J Physiol*. 2016;594:4425–4438.
- Pascual JM, Wang D, Lecumberri B, et al. GLUT1 deficiency and other glucose transporter diseases. *Eur J Endocrinol*. 2004;150:627–633.

51. Santer R, Groth S, Kinner M, et al. The mutation spectrum of the facilitative glucose transporter gene SLC2A2 (GLUT2) in patients with Fanconi-Bickel syndrome. *Hum Genet.* 2002;110:21–29.
52. Santer R, Schneppenheim R, Suter D, et al. Fanconi-Bickel syndrome—the original patient and his natural history, historical steps leading to the primary defect, and a review of the literature. *Eur J Pediatr.* 1998;157:783–797.
53. Seidner G, Alvarez MG, Yeh JI, et al. GLUT-1 deficiency syndrome caused by haploinsufficiency of the blood-brain barrier hexose carrier. *Nat Genet.* 1998;18:188–191.
54. Mueckler M, Thorens B. The SLC2 (GLUT) family of membrane transporters. *Mol Aspects Med.* 2013;34:121–138.
55. Sugawara-Yokoo M, Suzuki T, Matsuzaki T, et al. Presence of fructose transporter GLUT5 in the S3 proximal tubules in the rat kidney. *Kidney Int.* 1999;56:1022–1028.
56. Linden KC, DeHaan CL, Zhang Y, et al. Renal expression and localization of the facilitative glucose transporters GLUT1 and GLUT2 in animal models of hypertension and diabetic nephropathy. *Am J Physiol Renal Physiol.* 2006;290:F205–F213.
57. Gerich JE. Role of the kidney in normal glucose homeostasis and in the hyperglycaemia of diabetes mellitus: therapeutic implications. *Diabet Med.* 2010;27:136–142.
58. Burch HB, Narins RG, Chu C, et al. Distribution along the rat nephron of three enzymes of gluconeogenesis in acidosis and starvation. *Am J Physiol.* 1978;235:F246–F253.
59. Sasaki M, Sasako T, Kubota N, et al. Dual regulation of gluconeogenesis by insulin and glucose in the proximal tubules of the kidney. *Diabetes.* 2017;66:2339–2350.
60. Gerich JE, Meyer C, Woerle HJ, et al. Renal gluconeogenesis: its importance in human glucose homeostasis. *Diabetes Care.* 2001;24:382–391.
61. Drownowski KD, Craig MR, Digiovanni SR, et al. PEPCK mRNA localization in proximal tubule and gene regulation during metabolic acidosis. *J Physiol Pharmacol.* 2002;53:3–20.
62. Bankir L, Yang B. New insights into urea and glucose handling by the kidney, and the urine concentrating mechanism. *Kidney Int.* 2012;81:1179–1198.
63. Conjard A, Martin M, Guitton J, et al. Gluconeogenesis from glutamine and lactate in the isolated human renal proximal tubule: longitudinal heterogeneity and lack of response to adrenaline. *Biochem J.* 2001;360:371–377.
64. DeFronzo RA. Banting lecture. From the triumvirate to the ominous octet: a new paradigm for the treatment of type 2 diabetes mellitus. *Diabetes.* 2009;58:773–795.
65. The Diabetes Control and Complications Trial Research Group. The effect of intensive treatment of diabetes on the development and progression of long-term complications in insulin-dependent diabetes mellitus. *N Engl J Med.* 1993;329:977–986.
66. Gerstein HC, Miller ME, Byington RP, et al. Effects of intensive glucose lowering in type 2 diabetes. *N Engl J Med.* 2008;358:2545–2559.
67. Farber SJ, Berger EY, Earle DP. Effect of diabetes and insulin of the maximum capacity of the renal tubules to reabsorb glucose. *J Clin Invest.* 1951;30:125–129.
68. Burckhardt BC, Burckhardt G. Transport of organic anions across the basolateral membrane of proximal tubule cells. *Rev Physiol Biochem Pharmacol.* 2003;146:95–158.
69. Vallon V, Thomson SC. Renal function in diabetic disease models: the tubular system in the pathophysiology of the diabetic kidney. *Annu Rev Physiol.* 2012;74:351–375.
70. Vallon V, Rose M, Gerasimova M, et al. Knockout of Na-glucose transporter SGLT2 attenuates hyperglycemia and glomerular hyperfiltration but not kidney growth or injury in diabetes mellitus. *Am J Physiol Renal Physiol.* 2013;304:F156–F167.
71. Vallon V, Gerasimova M, Rose MA, et al. SGLT2 inhibitor empagliflozin reduces renal growth and albuminuria in proportion to hyperglycemia and prevents glomerular hyperfiltration in diabetic Akita mice. *Am J Physiol Renal Physiol.* 2014;306:F194–F204.
72. Tiwari S, Riazi S, Ecelbarger CA. Insulin's impact on renal sodium transport and blood pressure in health, obesity, and diabetes. *Am J Physiol Renal Physiol.* 2007;293:F974–F984.
73. Ghezzi C, Wright EM. Regulation of the human Na⁺-dependent glucose cotransporter hSGLT2. *Am J Physiol Cell Physiol.* 2012;303:C348–C354.
74. Vallon V, Komers R. Pathophysiology of the diabetic kidney. *Compr Physiol.* 2011;1:1175–1232.
75. Pessoa TD, Campos LC, Carraro-Lacroix L, et al. Functional role of glucose metabolism, osmotic stress, and sodium-glucose cotransporter isoform-mediated transport on Na⁺/H⁺ exchanger isoform 3 activity in the renal proximal tubule. *J Am Soc Nephrol.* 2014;25:2028–2039.
76. Coady MJ, El TA, Santer R, et al. MAP17 is a necessary activator of renal Na⁺/glucose cotransporter SGLT2. *J Am Soc Nephrol.* 2017;28:85–93.
77. Fu Y, Gerasimova M, Mayoux E, et al. SGLT2 inhibitor empagliflozin increases renal NHE3 phosphorylation in diabetic Akita mice: possible implications for the prevention of glomerular hyperfiltration. *Diabetes.* 2014;63(suppl 1):A132.
78. Kamran M, Peterson RG, Dominguez JH. Overexpression of GLUT2 gene in renal proximal tubules of diabetic Zucker rats. *J Am Soc Nephrol.* 1997;8:943–948.
79. Freitas HS, Schaan BD, David-Silva A, et al. SLC2A2 gene expression in kidney of diabetic rats is regulated by HNF-1alpha and HNF-3beta. *Mol Cell Endocrinol.* 2009;305:63–70.
80. Chin E, Zamah AM, Landau D, et al. Changes in facilitative glucose transporter messenger ribonucleic acid levels in the diabetic rat kidney. *Endocrinology.* 1997;138:1267–1275.
81. Dominguez JH, Camp K, Maianu L, et al. Molecular adaptations of GLUT1 and GLUT2 in renal proximal tubules of diabetic rats. *Am J Physiol.* 1994;266:F283–F290.
82. Marks J, Carvou NJ, Debnam ES, et al. Diabetes increases facilitative glucose uptake and GLUT2 expression at the rat proximal tubule brush border membrane. *J Physiol.* 2003;553:137–145.
83. Goestemeyer AK, Marks J, Srail SK, et al. GLUT2 protein at the rat proximal tubule brush border membrane correlates with protein kinase C (PKC)-beta1 and plasma glucose concentration. *Diabetologia.* 2007;50:2209–2217.
84. Pfaff IL, Vallon V. Protein kinase C beta isoenzymes in diabetic kidneys and their relation to nephroprotective actions of the ACE inhibitor lisinopril. *Kidney Blood Press Res.* 2002;25:329–340.
85. Pfaff IL, Wagner HJ, Vallon V. Immunolocalization of protein kinase C isoenzymes alpha, beta1 and betaII in rat kidney. *J Am Soc Nephrol.* 1999;10:1861–1873.
86. Rahmoune H, Thompson PW, Ward JM, et al. Glucose transporters in human renal proximal tubular cells isolated from the urine of patients with non-insulin-dependent diabetes. *Diabetes.* 2005;54:3427–3434.
87. Wang XX, Levi J, Luo Y, et al. SGLT2 expression is increased in human diabetic nephropathy: SGLT2 inhibition decreases renal lipid accumulation, inflammation and the development of nephropathy in diabetic mice. *J Biol Chem.* 2017;292:5335–5348.
88. Solini A, Rossi C, Mazzanti CM, et al. Sodium-glucose co-transporter (SGLT)2 and SGLT1 renal expression in patients with type 2 diabetes. *Diabetes Obes Metab.* 2017;19:1289–1294.
89. Norton L, Shannon CE, Fourcaudot M, et al. Sodium-glucose co-transporter (SGLT) and glucose transporter (GLUT) expression in the kidney of type 2 diabetic subjects. *Diabetes Obes Metab.* 2017;19:1322–1326.
90. Vallon V, Thomson SC. Targeting renal glucose reabsorption to treat hyperglycaemia: the pleiotropic effects of SGLT2 inhibition. *Diabetologia.* 2017;60:215–225.
91. Vallon V. The proximal tubule in the pathophysiology of the diabetic kidney. *Am J Physiol Regul Integr Comp Physiol.* 2011;300:R1009–R1022.
92. Osorio H, Bautista R, Rios A, et al. Effect of treatment with losartan on salt sensitivity and SGLT2 expression in hypertensive diabetic rats. *Diabetes Res Clin Pract.* 2009;86:e46–e49.
93. Freitas HS, Anhe GF, Melo KF, et al. Na⁺(+)-glucose transporter-2 messenger ribonucleic acid expression in kidney of diabetic rats correlates with glycemic levels: involvement of hepatocyte nuclear factor-1alpha expression and activity. *Endocrinology.* 2008;149:717–724.
94. Vallon V. Tubular transport in acute kidney injury: relevance for diagnosis, prognosis and intervention. *Nephron.* 2016;134:160–166.
95. Zapata-Morales JR, Galicia-Cruz OG, Franco M, et al. Hypoxia-inducible factor-1alpha (HIF-1alpha) protein diminishes sodium glucose transport 1 (SGLT1) and SGLT2 protein expression in renal epithelial tubular cells (LLC-PK1) under hypoxia. *J Biol Chem.* 2014;289:346–357.
96. Schmidt C, Hoehlerl K, Schweda F, et al. Regulation of renal sodium transporters during severe inflammation. *J Am Soc Nephrol.* 2007;18:1072–1083.
97. Gembardt F, Bartaun C, Jarzewska N, et al. The SGLT2 inhibitor empagliflozin ameliorates early features of diabetic nephropathy in

- BTBR ob/ob type 2 diabetic mice with and without hypertension. *Am J Physiol Renal Physiol.* 2014;307:F317–F325.
98. Vallon V. The mechanisms and therapeutic potential of SGLT2 inhibitors in diabetes mellitus. *Annu Rev Med.* 2015;66:255–270.
 99. Han HJ, Lee YJ, Park SH, et al. High glucose-induced oxidative stress inhibits Na⁺/glucose cotransporter activity in renal proximal tubule cells. *Am J Physiol Renal Physiol.* 2005;288:F988–F996.
 100. Ackermann TF, Boini KM, Volk H, et al. SGK1-sensitive renal tubular glucose reabsorption in diabetes. *Am J Physiol Renal Physiol.* 2009;296:F859–F866.
 101. Embark HM, Bohmer C, Vallon V, et al. Regulation of KCNE1-dependent K(+) current by the serum and glucocorticoid-inducible kinase (SGK) isoforms. *Pflugers Arch.* 2003;445:601–606.
 102. Lang F, Gorlach A, Vallon V. Targeting SGK1 in diabetes. *Expert Opin Ther Targets.* 2009;13:1303–1311.
 103. Weinberg JM, Molitoris BA. Illuminating mitochondrial function and dysfunction using multiphoton technology. *J Am Soc Nephrol.* 2009;20:1164–1166.
 104. Lan R, Geng H, Singha PK, et al. Mitochondrial pathology and glycolytic shift during proximal tubule atrophy after ischemic AKI. *J Am Soc Nephrol.* 2016;27:3356–3367.
 105. Farsijani NM, Liu Q, Kobayashi H, et al. Renal epithelium regulates erythropoiesis via HIF-dependent suppression of erythropoietin. *J Clin Invest.* 2016;126:1425–1437.
 106. Phillips AO, Steadman R, Morrisey K, et al. Polarity of stimulation and secretion of transforming growth factor-beta 1 by cultured proximal tubular cells. *Am J Pathol.* 1997;150:1101–1111.
 107. Zimman B, Wanner C, Lachin JM, et al. Empagliflozin, cardiovascular outcomes, and mortality in type 2 diabetes. *N Engl J Med.* 2015;373:2117–2128.
 108. Neal B, Perkovic V, Mahaffey KW, et al. Canagliflozin and cardiovascular and renal events in type 2 diabetes. *N Engl J Med.* 2017;377:644–657.
 109. Wanner C, Inzucchi SE, Lachin JM, et al. Empagliflozin and progression of kidney disease in type 2 diabetes. *N Engl J Med.* 2016;375:323–334.
 110. Ehrenkranz JR, Lewis NG, Kahn CR, et al. Phlorizin: a review. *Diabetes Metab Res Rev.* 2005;21:31–38.
 111. Song P, Onishi A, Koepsell H, et al. Sodium glucose cotransporter SGLT1 as a therapeutic target in diabetes mellitus. *Expert Opin Ther Targets.* 2016;20:1109–1125.
 112. Bonner C, Kerr-Conte J, Gmyr V, et al. Inhibition of the glucose transporter SGLT2 with dapagliflozin in pancreatic alpha cells triggers glucagon secretion. *Nat Med.* 2015;21:512–517.
 113. Washburn WN, Poucher SM. Differentiating sodium-glucose cotransporter-2 inhibitors in development for the treatment of type 2 diabetes mellitus. *Expert Opin Investig Drugs.* 2013;22:463–486.
 114. Ghezzi C, Hirayama BA, Gorraitz E, et al. SGLT2 inhibitors act from the extracellular surface of the cell membrane. *Physiol Rep.* 2014;2:pii: e12058.
 115. Fu Y, Breljak D, Onishi A, et al. The organic anion transporter OAT3 enhances the glucosuric effect of the SGLT2 inhibitor empagliflozin. *Am J Physiol Renal Physiol.* 2018;doi:10.1152/ajprenal.00503.2017.
 116. Abdul-Ghani MA, DeFronzo RA. Lowering plasma glucose concentration by inhibiting renal sodium-glucose co-transport. *J Intern Med.* 2014;276:352–363.
 117. Hasan FM, Alsahli M, Gerich JE. SGLT2 inhibitors in the treatment of type 2 diabetes. *Diabetes Res Clin Pract.* 2014;104:297–322.
 118. Monami M, Nardini C, Mannucci E. Efficacy and safety of sodium glucose co-transport-2 inhibitors in type 2 diabetes: a meta-analysis of randomized clinical trials. *Diabetes Obes Metab.* 2014;16:457–466.
 119. Ferrannini E, Muscelli E, Frascerra S, et al. Metabolic response to sodium-glucose cotransporter 2 inhibition in type 2 diabetic patients. *J Clin Invest.* 2014;124:499–508.
 120. Cherney DZ, Perkins BA, Soleymanlou N, et al. Renal hemodynamic effect of sodium-glucose cotransporter 2 inhibition in patients with type 1 diabetes mellitus. *Circulation.* 2014;129:587–597.
 121. Jurczak MJ, Lee HY, Birkenfeld AL, et al. SGLT2 deletion improves glucose homeostasis and preserves pancreatic beta-cell function. *Diabetes.* 2011;60:890–898.
 122. Merovci A, Solis-Herrera C, Daniele G, et al. Dapagliflozin improves muscle insulin sensitivity but enhances endogenous glucose production. *J Clin Invest.* 2014;124:509–514.
 123. Hansen HH, Jelsing J, Hansen CF, et al. The sodium glucose cotransporter type 2 inhibitor empagliflozin preserves beta-cell mass and restores glucose homeostasis in the male Zucker diabetic fatty rat. *J Pharmacol Exp Ther.* 2014;350:657–664.
 124. Macdonald FR, Peel JE, Jones HB, et al. The novel sodium glucose transporter 2 inhibitor dapagliflozin sustains pancreatic function and preserves islet morphology in obese, diabetic rats. *Diabetes Obes Metab.* 2010;12:1004–1012.
 125. Geerlings S, Fonseca V, Castro-Diaz D, et al. Genital and urinary tract infections in diabetes: impact of pharmacologically-induced glucosuria. *Diabetes Res Clin Pract.* 2014;103:373–381.
 126. Guthrie RM. Sodium-glucose co-transporter 2 inhibitors and the potential for cardiovascular risk reduction in patients with type 2 diabetes mellitus. *Postgrad Med.* 2013;125:21–32.
 127. Basile JN. The potential of sodium glucose cotransporter 2 (SGLT2) inhibitors to reduce cardiovascular risk in patients with type 2 diabetes (T2DM). *J Diabetes Complications.* 2013;27:280–286.
 128. Nagata T, Fukuzawa T, Takeda M, et al. Tofogliflozin, a novel sodium-glucose co-transporter 2 inhibitor, improves renal and pancreatic function in db/db mice. *Br J Pharmacol.* 2013;170:519–531.
 129. Terami N, Ogawa D, Tachibana H, et al. Long-term treatment with the sodium glucose cotransporter 2 inhibitor, dapagliflozin, ameliorates glucose homeostasis and diabetic nephropathy in db/db mice. *PLoS ONE.* 2014;9:e100777.
 130. Gangadharan KM, Gross S, Mudaliar H, et al. Inhibition of kidney proximal tubular glucose reabsorption does not prevent against diabetic nephropathy in type 1 diabetic eNOS knockout mice. *PLoS ONE.* 2014;9:e108994.
 131. Kojima N, Williams JM, Takahashi T, et al. Effects of a new SGLT2 inhibitor, luseogliflozin, on diabetic nephropathy in T2DN rats. *J Pharmacol Exp Ther.* 2013;345:464–472.
 132. Bolinder J, Ljunggren O, Johansson L, et al. Dapagliflozin maintains glycaemic control while reducing weight and body fat mass over 2 years in patients with type 2 diabetes mellitus inadequately controlled on metformin. *Diabetes Obes Metab.* 2014;16:159–169.
 133. Bolinder J, Ljunggren O, Kullberg J, et al. Effects of dapagliflozin on body weight, total fat mass, and regional adipose tissue distribution in patients with type 2 diabetes mellitus with inadequate glycemic control on metformin. *J Clin Endocrinol Metab.* 2012;97:1020–1031.
 134. Cefalu WT, Leiter LA, Yoon KH, et al. Efficacy and safety of canagliflozin versus glimepiride in patients with type 2 diabetes inadequately controlled with metformin (CANTATA-SU): 52 week results from a randomised, double-blind, phase 3 non-inferiority trial. *Lancet.* 2013;382:941–950.
 135. Yokono M, Takasu T, Hayashizaki Y, et al. SGLT2 selective inhibitor ipragliflozin reduces body fat mass by increasing fatty acid oxidation in high-fat diet-induced obese rats. *Eur J Pharmacol.* 2014;727:66–74.
 136. Suzuki M, Takeda M, Kito A, et al. Tofogliflozin, a sodium/glucose cotransporter 2 inhibitor, attenuates body weight gain and fat accumulation in diabetic and obese animal models. *Nutr Diabetes.* 2014;4:e125.
 137. Qiu H, Novikov A, Vallon V. Ketosis and diabetic ketoacidosis in response to SGLT2 inhibitors: basic mechanisms and therapeutic perspectives. *Diabetes Metab Res Rev.* 2017;33(5):doi:10.1002/dmrr.2886. [Epub 2017 Feb 23].
 138. Mudaliar S, Aljo S, Henry RR. Can a shift in fuel energetics explain the beneficial cardiorenal outcomes in the EMPA-REG OUTCOME study? A unifying hypothesis. *Diabetes Care.* 2016;39:1115–1122.
 139. Ferrannini E, Mark M, Mayoux E. CV protection in the EMPA-REG OUTCOME trial: a “thrifty substrate” hypothesis. *Diabetes Care.* 2016;39:1108–1114.
 140. Khunti K, Davies M, Majeed A, et al. Hypoglycemia and risk of cardiovascular disease and all-cause mortality in insulin-treated people with type 1 and type 2 diabetes: a cohort study. *Diabetes Care.* 2015;38:316–322.
 141. Foote C, Perkovic V, Neal B. Effects of SGLT2 inhibitors on cardiovascular outcomes. *Diab Vasc Dis Res.* 2012;9:117–123.
 142. Layton AT, Vallon V, Edwards A. Predicted consequences of diabetes and SGLT inhibition on transport and oxygen consumption along a rat nephron. *Am J Physiol Renal Physiol.* 2016;310:F1269–F1283.
 143. Layton AT, Vallon V, Edwards A. Modeling oxygen consumption in the proximal tubule: effects of NHE and SGLT2 inhibition. *Am J Physiol Renal Physiol.* 2015;308:F1343–F1357.
 144. Baker WL, Smyth LR, Riche DM, et al. Effects of sodium-glucose co-transporter 2 inhibitors on blood pressure: a systematic review and meta-analysis. *J Am Soc Hypertens.* 2014;8:262–275.
 145. Oliva RV, Bakris GL. Blood pressure effects of sodium-glucose co-transport 2 (SGLT2) inhibitors. *J Am Soc Hypertens.* 2014;8:330–339.

146. Lambers Heerspink HJ, de Zeeuw D, Wie L, et al. Dapagliflozin a glucose-regulating drug with diuretic properties in subjects with type 2 diabetes. *Diabetes Obes Metab*. 2013;15:853–862.
147. Kanbay M, Jensen T, Solak Y, et al. Uric acid in metabolic syndrome: from an innocent bystander to a central player. *Eur J Intern Med*. 2016;29:3–8.
148. Lytvyn Y, Skrtic M, Yang GK, et al. Glycosuria-mediated urinary uric acid excretion in patients with uncomplicated type 1 diabetes mellitus. *Am J Physiol Renal Physiol*. 2015;308:F77–F83.
149. Novikov A, Fu Y, Huang W, et al. SGLT2 inhibition and renal urate excretion: the role of luminal glucose, GLUT9 and URAT1. *Am J Physiol Renal Physiol*. 2018;doi:10.1152/ajprenal.00462.2018. [Epub ahead of print].
150. Magee GM, Bilous RW, Cardwell CR, et al. Is hyperfiltration associated with the future risk of developing diabetic nephropathy? A meta-analysis. *Diabetologia*. 2009;52:691–697.
151. Hallow KM, Gebremichael Y, Helmlinger G, et al. Primary proximal tubule hyperreabsorption and impaired tubular transport counterregulation determine glomerular hyperfiltration in diabetes: a modeling analysis. *Am J Physiol Renal Physiol*. 2017;312:F819–F835.
152. Vallon V, Richter K, Blantz RC, et al. Glomerular hyperfiltration in experimental diabetes mellitus: potential role of tubular reabsorption. *J Am Soc Nephrol*. 1999;10:2569–2576.
153. Thomson SC, Rieg T, Miracle C, et al. Acute and chronic effects of SGLT2 blockade on glomerular and tubular function in the early diabetic rat. *Am J Physiol Regul Integr Comp Physiol*. 2012;302:R75–R83.
154. Heerspink HJ, Desai M, Jardine M, et al. Canagliflozin slows progression of renal function decline independently of glycemic effects. *J Am Soc Nephrol*. 2018;28:368–375.
155. Yale JF, Bakris G, Cariou B, et al. Efficacy and safety of canagliflozin in subjects with type 2 diabetes and chronic kidney disease. *Diabetes Obes Metab*. 2013;15:463–473.
156. Barnett AH, Mithal A, Manassie J, et al. Efficacy and safety of empagliflozin added to existing antidiabetes treatment in patients with type 2 diabetes and chronic kidney disease: a randomised, double-blind, placebo-controlled trial. *Lancet Diabetes Endocrinol*. 2014;2:369–384.
157. Holtkamp FA, de Zeeuw D, Thomas MC, et al. An acute fall in estimated glomerular filtration rate during treatment with losartan predicts a slower decrease in long-term renal function. *Kidney Int*. 2011;80:282–287.
158. Neill O, Fasching A, Pihl L, et al. Acute SGLT inhibition normalizes oxygen tension in the renal cortex but causes hypoxia in the renal medulla in anaesthetized control and diabetic rats. *Am J Physiol Renal Physiol*. 2015;309:F227–F234.
159. Pruijm M, Milani B, Pivin E, et al. Reduced cortical oxygenation predicts a progressive decline of renal function in patients with chronic kidney disease. *Kidney Int*. 2018;93:932–940.
160. Sano M, Takei M, Shiraishi Y, et al. Increased hematocrit during sodium-glucose cotransporter 2 inhibitor therapy indicates recovery of tubulointerstitial function in diabetic kidneys. *J Clin Med Res*. 2016;8:844–847.
161. Inzucchi SE, Zinman B, Fitchett D, et al. How does empagliflozin reduce cardiovascular mortality? Insights from a mediation analysis of the EMPA-REG OUTCOME trial. *Diabetes Care*. 2018;41:356–363.
162. Nadkarni GN, Ferrandino R, Chang A, et al. Acute kidney injury in patients on SGLT2 inhibitors: a propensity-matched analysis. *Diabetes Care*. 2017;40:1479–1485.
163. Wanner C, Lachin JM, Inzucchi SE, et al. Empagliflozin and clinical outcomes in patients with type 2 diabetes mellitus, established cardiovascular disease, and chronic kidney disease. *Circulation*. 2018;137:119–129.
164. Petrykiv S, Sjostrom CD, Greasley PJ, et al. Differential effects of dapagliflozin on cardiovascular risk factors at varying degrees of renal function. *Clin J Am Soc Nephrol*. 2017;12:751–759.
165. Layton AT, Vallon V. SGLT2 inhibition in a kidney with reduced nephron number: modeling and analysis of solute transport and metabolism. *Am J Physiol Renal Physiol*. 2018;doi:10.1152/ajprenal.00551.2017.
166. Sweet DH, Bush KT, Nigam SK. The organic anion transporter family: from physiology to ontogeny and the clinic. *Am J Physiol Renal Physiol*. 2001;281:F197–F205.
167. You G. Structure, function, and regulation of renal organic anion transporters. *Med Res Rev*. 2002;22:602–616.
168. Nigam SK, Wu W, Bush KT, et al. Handling of drugs, metabolites, and uremic toxins by kidney proximal tubule drug transporters. *Clin J Am Soc Nephrol*. 2015;10:2039–2049.
169. Emami RA, Nies AT, Schaeffeler E, et al. Organic anion transporters and their implications in pharmacotherapy. *Pharmacol Rev*. 2012;64:421–449.
170. Burckhardt G. Drug transport by organic anion transporters (OATs). *Pharmacol Ther*. 2012;136:106–130.
171. Vanwert AL, Gionfriddo MR, Sweet DH. Organic anion transporters: discovery, pharmacology, regulation and roles in pathophysiology. *Biopharm Drug Dispos*. 2010;31:1–71.
172. Saito H. Pathophysiological regulation of renal SLC22A organic ion transporters in acute kidney injury: pharmacological and toxicological implications. *Pharmacol Ther*. 2010;125:79–91.
173. Wright SH, Dantzler WH. Molecular and cellular physiology of renal organic cation and anion transport. *Physiol Rev*. 2004;84:987–1049.
174. Kampmann J, Hansen JM, Siersboek-Nielsen K, et al. Effect of some drugs on penicillin half-life in blood. *Clin Pharmacol Ther*. 1972;13:516–519.
175. Neu HC, Garvey GJ. Comparative in vitro activity and clinical pharmacology of ticarcillin and carbenicillin. *Antimicrob Agents Chemother*. 1975;8:457–462.
176. Cihlar T, Lin DC, Pritchard JB, et al. The antiviral nucleotide analogs cidofovir and adefovir are novel substrates for human and rat renal organic anion transporter 1. *Mol Pharmacol*. 1999;56:570–580.
177. Lopez-Nieto CE, You G, Barros EJG, et al. Molecular cloning and characterization of a novel transport protein with very high expression in the kidney (abstract). *J Am Soc Nephrol*. 1996;7:1301.
178. Lopez-Nieto CE, You G, Bush KT, et al. Molecular cloning and characterization of NKT, a gene product related to the organic cation transporter family that is almost exclusively expressed in the kidney. *J Biol Chem*. 1997;272:6471–6478.
179. Ahn SY, Eraly SA, Tsigelny I, et al. Interaction of organic cations with organic anion transporters. *J Biol Chem*. 2009;284:31422–31430.
180. Liu HC, Goldenberg A, Chen Y, et al. Molecular properties of drugs interacting with SLC22 transporters OAT1, OAT3, OCT1, and OCT2: a machine-learning approach. *J Pharmacol Exp Ther*. 2016;359:215–229.
181. Simonson G, Vincent A, Roberg K, et al. Molecular cloning and characterization of a novel liver-specific transport protein. *J Cell Sci*. 1994;107:1065–1072.
182. Grundemann D, Gorboulev V, Gambaryan S, et al. Drug excretion mediated by a new prototype of polyspecific transporter. *Nature*. 1994;372:549–552.
183. Nigam SK. The SLC22 transporter family: a paradigm for the impact of drug transporters on metabolic pathways, signaling, and disease. *Annu Rev Pharmacol Toxicol*. 2018;58:663–687.
184. Nigam SK. What do drug transporters really do? *Nat Rev Drug Discov*. 2015;14:29–44.
185. Zhu C, Nigam KB, Date RC, et al. Evolutionary analysis and classification of OATs, OCTs, OCTNs, and other SLC22 transporters: structure-function implications and analysis of sequence motifs. *PLoS ONE*. 2015;10:e0140569.
186. Monte JC, Nagle MA, Eraly SA, et al. Identification of a novel murine organic anion transporter family member, OAT6, expressed in olfactory mucosa. *Biochem Biophys Res Commun*. 2004;323:429–436.
187. U.S. Food and Drug Administration. *Guidance for industry: drug interaction studies—study design, data analysis, implications for dosing, and labeling recommendations*. Silver Spring, MD: US Department of Health and Human Services; 2017. <http://www.fda.gov/downloads/Drugs/GuidanceComplianceRegulatoryInformation/Guidances/UCM292362.pdf>.
188. FDA. *Clinical Drug Interaction Studies—Study Design, Data Analysis, and Clinical Implications Guidance for Industry*. Silver Spring, MD: U.S. Department of Health and Human Services Food and Drug Administration Center for Drug Evaluation and Research (CDER); 2017. <http://www.fda.gov/downloads/Drugs/GuidanceComplianceRegulatoryInformation/Guidances/UCM292362.pdf>.
189. Ahn SY, Nigam SK. Toward a systems level understanding of organic anion and other multispecific drug transporters: a remote sensing and signaling hypothesis. *Mol Pharmacol*. 2009;76:481–490.
190. Wu W, Dnyanmote AV, Nigam SK. Remote communication through solute carriers and ATP binding cassette drug transporter pathways: an update on the remote sensing and signaling hypothesis. *Mol Pharmacol*. 2011;79:795–805.

191. Eraly SA, Vallon V, Vaughn DA, et al. Decreased renal organic anion secretion and plasma accumulation of endogenous organic anions in OAT1 knock-out mice. *J Biol Chem.* 2006;281:5072–5083.
192. Vallon V, Eraly SA, Wikoff WR, et al. Organic anion transporter 3 contributes to the regulation of blood pressure. *J Am Soc Nephrol.* 2008;19:1732–1740.
193. Wikoff WR, Nagle MA, Kouznetsova VL, et al. Untargeted metabolomics identifies enterobiome metabolites and putative uremic toxins as substrates of organic anion transporter 1 (Oat1). *J Proteome Res.* 2011;10:2842–2851.
194. Bush KT, Wu W, Lun C, et al. The drug transporter OAT3 (SLC22A8) and endogenous metabolite communication via the gut-liver-kidney axis. *J Biol Chem.* 2017;292:15789–15803.
195. Wu W, Bush KT, Nigam SK. Key role for the organic anion transporters, OAT1 and OAT3, in the in vivo handling of uremic toxins and solutes. *Sci Rep.* 2017;7:4939.
196. Eraly SA, Vallon V, Rieg T, et al. Multiple organic anion transporters contribute to net renal excretion of uric acid. *Physiol Genomics.* 2008;33:180–192.
197. Sweet DH, Miller DS, Pritchard JB, et al. Impaired organic anion transport in kidney and choroid plexus of organic anion transporter 3 (Oat3 (Slc22a8)) knockout mice. *J Biol Chem.* 2002;277:26934–26943.
198. Vallon V, Rieg T, Ahn SY, et al. Overlapping in vitro and in vivo specificities of the organic anion transporters OAT1 and OAT3 for loop and thiazide diuretics. *Am J Physiol Renal Physiol.* 2008;294:F867–F873.
199. Vanwert AL, Bailey RM, Sweet DH. Organic anion transporter 3 (Oat3/Slc22a8) knockout mice exhibit altered clearance and distribution of penicillin G. *Am J Physiol Renal Physiol.* 2007;293:F1332–F1341.
200. Truong DM, Kaler G, Khandelwal A, et al. Multi-level analysis of organic anion transporters 1, 3, and 6 reveals major differences in structural determinants of antiviral discrimination. *J Biol Chem.* 2008;283:8654–8663.
201. Vanwert AL, Srimaroeng C, Sweet DH. Organic anion transporter 3 (oat3/slc22a8) interacts with carboxyfluoroquinolones, and deletion increases systemic exposure to ciprofloxacin. *Mol Pharmacol.* 2008;74:122–131.
202. Vanwert AL, Sweet DH. Impaired clearance of methotrexate in organic anion transporter 3 (Slc22a8) knockout mice: a gender specific impact of reduced folates. *Pharm Res.* 2008;25:453–462.
203. Miyajima M, Kusuhara H, Fujishima M, et al. Organic anion transporter 3 mediates the efflux transport of an amphipathic organic anion, dehydroepiandrosterone sulfate, across the blood-brain barrier in mice. *Drug Metab Dispos.* 2011;39:814–819.
204. Nagle MA, Truong DM, Dnyanmote AV, et al. Analysis of three-dimensional systems for developing and mature kidneys clarifies the role of OAT1 and OAT3 in antiviral handling. *J Biol Chem.* 2011;286:243–251.
205. Zalups RK, Ahmad S. Handling of cysteine S-conjugates of methylmercury in MDCK cells expressing human OAT1. *Kidney Int.* 2005;68:1684–1699.
206. Torres AM, Dnyanmote AV, Bush KT, et al. Deletion of multispecific organic anion transporter Oat1/Slc22a6 protects against mercury-induced kidney injury. *J Biol Chem.* 2011;286:26391–26395.
207. Wu W, Jamshidi N, Eraly SA, et al. Multispecific drug transporter Slc22a8 (Oat3) regulates multiple metabolic and signaling pathways. *Drug Metab Dispos.* 2013;41:1825–1834.
208. Liu HC, Jamshidi N, Chen Y, et al. An organic anion transporter 1 (OAT1)-centered metabolic network. *J Biol Chem.* 2016;291:19474–19486.
209. Ahn SY, Jamshidi N, Mo ML, et al. Linkage of organic anion transporter-1 to metabolic pathways through integrated “omics”-driven network and functional analysis. *J Biol Chem.* 2011;286:31522–31531.
210. Prentice KJ, Luu L, Allister EM, et al. The furan fatty acid metabolite CMPF is elevated in diabetes and induces beta cell dysfunction. *Cell Metab.* 2014;19:653–666.
211. Bhatnagar V, Xu G, Hamilton BA, et al. Analyses of 5′-regulatory region polymorphisms in human SLC22A6 (OAT1) and SLC22A8 (OAT3). *J Hum Genet.* 2006;51:575–580.
212. Engstrom K, Ameer S, Bernaudat L, et al. Polymorphisms in genes encoding potential mercury transporters and urine mercury concentrations in populations exposed to mercury vapor from gold mining. *Environ Health Perspect.* 2012;121:85–91.
213. Han YF, Fan XH, Wang XJ, et al. Association of intergenic polymorphism of organic anion transporter 1 and 3 genes with hypertension and blood pressure response to hydrochlorothiazide. *Am J Hypertens.* 2011;24:340–346.
214. Yee SW, Nguyen AN, Brown C, et al. Reduced renal clearance of cefotaxime in Asians with a low-frequency polymorphism of OAT3 (SLC22A8). *J Pharm Sci.* 2013;102:3451–3457.
215. Bhatnagar V, Richard EL, Wu W, et al. Analysis of ABCG2 and other urate transporters in uric acid homeostasis in chronic kidney disease: potential role of remote sensing and signaling. *Clin Kidney J.* 2016;9:444–453.
216. Vormfelde SV, Burckhardt G, Zirk A, et al. Pharmacogenomics of diuretic drugs: data on rare monogenic disorders and on polymorphisms and requirements for further research. *Pharmacogenomics.* 2003;4:701–734.
217. Sun CY, Wu MS, Lee CC, et al. A novel SNP in the 5′ regulatory region of organic anion transporter 1 is associated with chronic kidney disease. *Sci Rep.* 2018;8:8085.
218. Xu G, Bhatnagar V, Wen G, et al. Analyses of coding region polymorphisms in apical and basolateral human organic anion transporter (OAT) genes [OAT1 (NKT), OAT2, OAT3, OAT4, URAT (RST)]. *Kidney Int.* 2005;68:1491–1499.
219. Koepsell H. Substrate recognition and translocation by polyspecific organic cation transporters. *Biol Chem.* 2011;392:95–101.
220. Shu Y, Brown C, Castro RA, et al. Effect of genetic variation in the organic cation transporter 1, OCT1, on metformin pharmacokinetics. *Clin Pharmacol Ther.* 2008;83:273–280.
221. Ciarimboli G, Deuster D, Knief A, et al. Organic cation transporter 2 mediates cisplatin-induced oto- and nephrotoxicity and is a target for protective interventions. *Am J Pathol.* 2010;176:1169–1180.
222. Nies AT, Koepsell H, Damme K, et al. Organic cation transporters (OCTs, MATEs), in vitro and in vivo evidence for the importance in drug therapy. *Handb Exp Pharmacol.* 2011;105:167.
223. Chen L, Shu Y, Liang X, et al. OCT1 is a high-capacity thiamine transporter that regulates hepatic steatosis and is a target of metformin. *Proc Natl Acad Sci U. S. A.* 2014;111:9983–9988.
224. Roth M, Obaidat A, Hagenbuch B. OATPs, OATs and OCTs: the organic anion and cation transporters of the SLC0 and SLC22A gene superfamilies. *Br J Pharmacol.* 2012;165:1260–1287.
225. Choi MK, Song IS. Organic cation transporters and their pharmacokinetic and pharmacodynamic consequences. *Drug Metab Pharmacokinet.* 2008;23:243–253.
226. Zolk O. Current understanding of the pharmacogenomics of metformin. *Clin Pharmacol Ther.* 2009;86:595–598.
227. McKusick-Nathans Institute of Genetic Medicine. *Online Mendelian Inheritance in Man.* Baltimore, MD: Johns Hopkins University; 2018. <https://omim.org/>.
228. Lozano E, Briz O, Macias RIR, et al. Genetic heterogeneity of SLC22 family of transporters in drug disposition. *J Pers Med.* 2018;8.
229. Tamai I. Pharmacological and pathophysiological roles of carnitine/organic cation transporters (OCTNs: SLC22A4, SLC22A5 and Slc22a21). *Biopharm Drug Dispos.* 2013;34:29–44.
230. Grundemann D. The ergothioneine transporter controls and indicates ergothioneine activity—a review. *Prev Med.* 2012;54(suppl): S71–S74.
231. Vanholder R, Abou-Deif O, Argiles A, et al. The role of EUTox in uremic toxin research. *Semin Dial.* 2009;22:323–328.
232. Ramezani A, Raj DS. The gut microbiome, kidney disease, and targeted interventions. *J Am Soc Nephrol.* 2014;25:657–670.
233. Tang WH, Hazen SL. Microbiome, trimethylamine N-oxide, and cardiometabolic disease. *Transl Res.* 2017;179:108–115.
234. Cosola C, Rocchetti MT, Cupisti A, et al. Microbiota metabolites: pivotal players of cardiovascular damage in chronic kidney disease. *Pharmacol Res.* 2018.
235. Ellis RJ, Small DM, Vesey DA, et al. Indoxyl sulphate and kidney disease: causes, consequences and interventions. *Nephrology (Carlton).* 2016;21:170–177.
236. Motojima M, Hosokawa A, Yamato H, et al. Uraemic toxins induce proximal tubular injury via organic anion transporter 1-mediated uptake. *Br J Pharmacol.* 2002;135:555–563.
237. Teft WA, Morse BL, Leake BF, et al. Identification and characterization of trimethylamine-N-oxide uptake and efflux transporters. *Mol Pharm.* 2017;14:310–318.
238. Mandal AK, Mount DB. The molecular physiology of uric acid homeostasis. *Annu Rev Physiol.* 2015;77:323–345.
239. Chen C, Lu JM, Yao Q. Hyperuricemia-related diseases and xanthine oxidoreductase (XOR) inhibitors: an overview. *Med Sci Monit.* 2016;22:2501–2512.
240. Xu L, Shi Y, Zhuang S, et al. Recent advances on uric acid transporters. *Oncotarget.* 2017;8:100852–100862.

241. Mori K, Ogawa Y, Ebihara K, et al. Kidney-specific expression of a novel mouse organic cation transporter-like protein. *FEBS Lett.* 1997;417:371–374.
242. Vitart V, Rudan I, Hayward C, et al. SLC2A9 is a newly identified urate transporter influencing serum urate concentration, urate excretion and gout. *Nat Genet.* 2008;40:437–442.
243. Nigam SK, Bhatnagar V. The systems biology of uric acid transporters: the role of remote sensing and signaling. *Curr Opin Nephrol Hypertens.* 2018;27:305–313.
244. Ichida K, Matsuo H, Takada T, et al. Decreased extra-renal urate excretion is a common cause of hyperuricemia. *Nat Commun.* 2012;3:764.
245. Chen M, Lu X, Lu C, et al. Soluble uric acid increases PDZK1 and ABCG2 expression in human intestinal cell lines via the TLR4-NLRP3 inflammasome and PI3K/Akt signaling pathway. *Arthritis Res Ther.* 2018;20:20.
246. Ciaramboli G, Lancaster CS, Schlatter E, et al. Proximal tubular secretion of creatinine by organic cation transporter OCT2 in cancer patients. *Clin Cancer Res.* 2012;18:1101–1108.
247. Vallon V, Eraly SA, Rao SR, et al. A role for the organic anion transporter OAT3 in renal creatinine secretion in mice. *Am J Physiol Renal Physiol.* 2012;302:F1293–F1299.
248. Shen H, Liu T, Morse BL, et al. Characterization of organic anion transporter 2 (SLC22A7): a highly efficient transporter for creatinine and species-dependent renal tubular expression. *Drug Metab Dispos.* 2015;43:984–993.
249. Nigam SK, Bush KT, Martovetsky G, et al. The organic anion transporter (OAT) family: a systems biology perspective. *Physiol Rev.* 2015;95:83–123.
250. Bradbury RA, Samaras K. Antiretroviral therapy and the human immunodeficiency virus—improved survival but at what cost? *Diabetes Obes Metab.* 2008;10:441–450.
251. Cooper-DeHoff RM, Pacanowski MA, Pepine CJ. Cardiovascular therapies and associated glucose homeostasis: implications across the dysglycemia continuum. *J Am Coll Cardiol.* 2009;53:S28–S34.
252. Scriver CR, Tenenhouse HS. *Mendelian Phenotypes as Probes of Renal Transport Systems for Amino Acids and Phosphate.* 11th ed. Windhager EE, ed. Oxford: Oxford University Press; 1992.
253. Milne MD. Genetic aspects of renal disease. *Prog Med Genet.* 1970;7:112–162.
254. Broer S. Amino acid transport across mammalian intestinal and renal epithelia. *Physiol Rev.* 2008;88:249–286.
255. Silbernagl S. The renal handling of amino acids and oligopeptides. *Physiol Rev.* 1988;68:911–1007.
256. Palacin M, Bertran J, Chillaron J, et al. Lysinuric protein intolerance: mechanisms of pathophysiology. *Mol Genet Metab.* 2004;81(suppl):27–37.
257. Rajantie J, Simell O, Perheentupa J. Lysinuric protein intolerance. Basolateral transport defect in renal tubuli. *J Clin Invest.* 1981;67:1078–1082.
258. Evers J, Murer H, Kinne R. Phenylalanine uptake in isolated renal brush border vesicles. *Biochim Biophys Acta.* 1976;426:598–615.
259. Welbourne TC, Matthews JC. Glutamate transport and renal function. *Am J Physiol.* 1999;277:F501–F505.
260. Young JA, Freedman BS. Renal tubular transport of amino acids. *Clin Chem.* 1971;17:245–266.
261. Verrey F, Singer D, Ramadan T, et al. Kidney amino acid transport. *Pflugers Arch.* 2009;458:53–60.
262. Romero MF, Kanai Y, Gunshin H, et al. Expression cloning using *Xenopus laevis* oocytes. *Methods Enzymol.* 1998;296:17–52.
263. Levy LL. Hartnup disorder. In: Scriver CR, Beaudet AL, Sly SW, et al., eds. *The Online Metabolic & Molecular Bases of Inherited Disease.* 3rd ed. New York: McGraw-Hill; 2001.
264. Seow HF, Broer S, Broer A, et al. Hartnup disorder is caused by mutations in the gene encoding the neutral amino acid transporter SLC6A19. *Nat Genet.* 2004;36:1003–1007.
265. Kleta R, Romeo E, Ristic Z, et al. Mutations in SLC6A19, encoding B0AT1, cause Hartnup disorder. *Nat Genet.* 2004;36:999–1002.
266. Broer S. The role of the neutral amino acid transporter B0AT1 (SLC6A19) in Hartnup disorder and protein nutrition. *IUBMB Life.* 2009;61:591–599.
267. Danilczyk U, Sarao R, Remy C, et al. Essential role for collectrin in renal amino acid transport. *Nature.* 2006;444:1088–1091.
268. Kowalczyk S, Broer A, Tietze N, et al. A protein complex in the brush-border membrane explains a Hartnup disorder allele. *FASEB J.* 2008;22:2880–2887.
269. Broer S. Diseases associated with general amino acid transporters of the solute carrier 6 family (SLC6). *Curr Mol Pharmacol.* 2013;6:74–87.
270. Sveinbjornsson G, Mikalsdottir E, Palsson R, et al. Rare mutations associating with serum creatinine and chronic kidney disease. *Hum Mol Genet.* 2014;23:6935–6943.
271. Broer A, Klingel K, Kowalczyk S, et al. Molecular cloning of mouse amino acid transport system B0, a neutral amino acid transporter related to Hartnup disorder. *J Biol Chem.* 2004;279:24467–24476.
272. Bohmer C, Broer A, Munzinger M, et al. Characterization of mouse amino acid transporter B0AT1 (slc6a19). *Biochem J.* 2005;389:745–751.
273. Broer S, Bailey CG, Kowalczyk S, et al. Iminoglycinuria and hyperglycinuria are discrete human phenotypes resulting from complex mutations in proline and glycine transporters. *J Clin Invest.* 2008;118:3881–3892.
274. Tietze N. *Physiology and Pathology of Neutral Amino Acid Transporters in Renal and Intestinal Epithelial Cells.* [dissertation]. Canberra, Australian National University Research School of Biology, 2010.
275. Broer A, Tietze N, Kowalczyk S, et al. The orphan transporter v7-3 (slc6a15) is a Na⁺-dependent neutral amino acid transporter (B0AT2). *Biochem J.* 2006;393:421–430.
276. Scriver CR, Efron ML, Schafer IA. Renal tubular transport of proline, hydroxyproline, and glycine in health and in familial hyperprolinemia. *J Clin Invest.* 1964;43:374–385.
277. Broer S, Chesney RW. Immunoglycinuria. In: *The Online Metabolic & Molecular Bases of Inherited Disease 21.* New York: McGraw-Hill; 2010.
278. Singer D, Camargo SM, Huggel K, et al. Orphan transporter SLC6A18 is renal neutral amino acid transporter B0AT3. *J Biol Chem.* 2009;284:19953–19960.
279. Vanslambrouck JM, Broer A, Thavyogarahaj T, et al. Renal imino acid and glycine transport system ontogeny and involvement in developmental iminoglycinuria. *Biochem J.* 2010;428:397–407.
280. Boll M, Foltz M, Rubio-Aliaga I, et al. Functional characterization of two novel mammalian electrogenic proton-dependent amino acid cotransporters. *J Biol Chem.* 2002;277:22966–22973.
281. Kowalczyk S, Broer A, Munzinger M, et al. Molecular cloning of the mouse IMINO system: an Na⁺- and Cl⁻-dependent proline transporter. *Biochem J.* 2005;386:422.
282. Takanaga H, Mackenzie B, Suzuki Y, et al. Identification of mammalian proline transporter SIT1 (SLC6A20) with characteristics of classical system imino. *J Biol Chem.* 2005;280:8974–8984.
283. Vuille-dit-Bille RN, Camargo SM, Emmenegger L, et al. Human intestine luminal ACE2 and amino acid transporter expression increased by ACE-inhibitors. *Amino Acids.* 2015;47:693–705.
284. Fairweather SJ, Broer A, Subramanian N, et al. Molecular basis for the interaction of the mammalian amino acid transporters B(0)AT1 and B(0)AT3 with their ancillary protein collectrin. *J Biol Chem.* 2015;290:24308–24325.
285. Uchida S, Kwon HM, Yamauchi A, et al. Molecular cloning of the cDNA for an MDCK cell Na⁽⁺⁾- and Cl⁽⁻⁾-dependent taurine transporter that is regulated by hypertonicity. *Proc Natl Acad Sci U. S. A.* 1992;89:8230–8234.
286. Huang DY, Boini KM, Lang PA, et al. Impaired ability to increase water excretion in mice lacking the taurine transporter gene TAUT. *Pflugers Arch.* 2006;451:668–677.
287. Segawa H, Fukasawa Y, Miyamoto K, et al. Identification and functional characterization of a Na⁺-independent neutral amino acid transporter with broad substrate selectivity. *J Biol Chem.* 1999;274:19745–19751.
288. Rossier G, Meier C, Bauch C, et al. LAT2, a new basolateral 4F2hc/CD98-associated amino acid transporter of kidney and intestine. *J Biol Chem.* 1999;274:34948–34954.
289. Pineda M, Fernandez E, Torrents D, et al. Identification of a membrane protein, LAT-2, that co-expresses with 4F2 heavy chain, an L-type amino acid transport activity with broad specificity for small and large zwitterionic amino acids. *J Biol Chem.* 1999;274:19738–19744.
290. Kim DK, Kanai Y, Chairoungdua A, et al. Expression cloning of a Na⁺-independent aromatic amino acid transporter with structural similarity to H⁺/monocarboxylate transporters. *J Biol Chem.* 2001;276:17221–17228.

291. Mariotta L, Ramadan T, Singer D, et al. T-type amino acid transporter TAT1 (Slc16a10) is essential for extracellular aromatic amino acid homeostasis control. *J Physiol*. 2012;590:6413–6424.
292. Guetg A, Mariotta L, Bock L, et al. Essential amino acid transporter Lat4 (Slc43a2) is required for mouse development. *J Physiol*. 2015;593:1273–1289.
293. Braun D, Wirth EK, Wohlgegmuth F, et al. Aminoaciduria, but normal thyroid hormone levels and signalling, in mice lacking the amino acid and thyroid hormone transporter Slc7a8. *Biochem J*. 2011;439:249–255.
294. Meier C, Ristic Z, Klauser S, et al. Activation of system L heterodimeric amino acid exchangers by intracellular substrates. *EMBO J*. 2002;21:580–589.
295. Ramadan T, Camargo SM, Summa V, et al. Basolateral aromatic amino acid transporter TAT1 (Slc16a10) functions as an efflux pathway. *J Cell Physiol*. 2006;206:771–779.
296. Bodoy S, Fotiadis D, Stoeger SM, et al. The small SLC43 family: facilitator system I amino acid transporters and the orphan EEG1. *Mol Aspects Med*. 2013;34:638–645.
297. Karinch AM, Lin CM, Wolfgang CL, et al. Regulation of expression of the SN1 transporter during renal adaptation to chronic metabolic acidosis in rats. *Am J Physiol Renal Physiol*. 2002;283:F1011–F1019.
298. Curthoys NP. Role of mitochondrial glutaminase in rat renal glutamine metabolism. *J Nutr*. 2001;131:2496S–2497S.
299. Balkrishna S, Broer A, Welford SM, et al. Expression of glutamine transporter Slc38a3 (SNAT3) during acidosis is mediated by a different mechanism than tissue-specific expression. *Cell Physiol Biochem*. 2014;33:1591–1606.
300. Nakanishi T, Kekuda R, Fei YJ, et al. Cloning and functional characterization of a new subtype of the amino acid transport system N. *Am J Physiol Cell Physiol*. 2001;281:C1757–C1768.
301. Chillaron J, Font-Llitjos M, Fort J, et al. Pathophysiology and treatment of cystinuria. *Nat Rev Nephrol*. 2010;6:424–434.
302. Palacin M, Bertran J, Zorzano A. Heteromeric amino acid transporters explain inherited aminoacidurias. *Curr Opin Nephrol Hypertens*. 2000;9:547–553.
303. Dello Strologo L, Pras E, Pontesilli C, et al. Comparison between SLC3A1 and SLC7A9 cystinuria patients and carriers: a need for a new classification. *J Am Soc Nephrol*. 2002;13:2547–2553.
304. Nagamori S, Wiriyasakul P, Guarch ME, et al. Novel cystine transporter in renal proximal tubule identified as a missing partner of cystinuria-related plasma membrane protein rBAT/SLC3A1. *Proc Natl Acad Sci U. S. A*. 2016;113:775–780.
305. Di Giacomo A, Rubio-Aliaga I, Cantone A, et al. Differential cystine and dibasic amino acid handling after loss of function of the amino acid transporter b₀,+AT (Slc7a9) in mice. *Am J Physiol Renal Physiol*. 2013;305:F1645–F1655.
306. Chillaron J, Roca R, Valencia A, et al. Heteromeric amino acid transporters: biochemistry, genetics, and physiology. *Am J Physiol Renal Physiol*. 2001;281:F995–F1018.
307. Bartoccioni P, Rius M, Zorzano A, et al. Distinct classes of trafficking rBAT mutants cause the type I cystinuria phenotype. *Hum Mol Genet*. 2008;17:1845–1854.
308. Busch AE, Herzer T, Waldegger S, et al. Opposite directed currents induced by the transport of dibasic and neutral amino acids in *Xenopus* oocytes expressing the protein rBAT. *J Biol Chem*. 1994;269:25581–25586.
309. Pineda M, Wagner CA, Broer A, et al. Cystinuria-specific rBAT(R365W) mutation reveals two translocation pathways in the amino acid transporter rBAT-b₀,+AT. *Biochem J*. 2004;377:665–674.
310. Chillaron J, Estevez R, Mora C, et al. Obligatory amino acid exchange via systems b₀,+like and y⁺L-like. A tertiary active transport mechanism for renal reabsorption of cystine and dibasic amino acids. *J Biol Chem*. 1996;271:17761–17770.
311. Eggermann T, Elbracht M, Haverkamp F, et al. Isolated cystinuria (OMIM 238200) is not a separate entity but is caused by a mutation in the cystinuria gene SLC7A9. *Clin Genet*. 2007;71:597–598.
312. Simell O. Lysinuric protein intolerance and other cationic aminoacidurias. In: Scriver CR, Beaudet AL, Sly SW, et al., eds. *The Online Metabolic & Molecular Bases of Inherited Disease*. New York: McGraw Hill; 2001.
313. Torrents D, Mykkanen J, Pineda M, et al. Identification of SLC7A7, encoding y⁺LAT-1, as the lysinuric protein intolerance gene. *Nat Genet*. 1999;21:293–296.
314. Borsani G, Bassi MT, Sperandeo MP, et al. SLC7A7, encoding a putative permease-related protein, is mutated in patients with lysinuric protein intolerance. *Nat Genet*. 1999;21:297–301.
315. Sperandeo MP, Paladino S, Maiuri L, et al. A y⁺LAT-1 mutant protein interferes with y⁺LAT-2 activity: implications for the molecular pathogenesis of lysinuric protein intolerance. *Eur J Hum Genet*. 2005;13:628–634.
316. Deves R, Boyd CA. Transporters for cationic amino acids in animal cells: discovery, structure, and function. *Physiol Rev*. 1998;78:487–545.
317. Kanai Y, Fukasawa Y, Cha SH, et al. Transport properties of a system y⁺L neutral and basic amino acid transporter. Insights into the mechanisms of substrate recognition. *J Biol Chem*. 2000;275:20787–20793.
318. Broer S, Broer A. Amino acid homeostasis and signalling in mammalian cells and organisms. *Biochem J*. 2017;474:1935–1963.
319. Shayakul C, Kanai Y, Lee WS, et al. Localization of the high-affinity glutamate transporter EAAC1 in rat kidney. *Am J Physiol*. 1997;273:F1023–F1029.
320. Kanai Y, Hediger MA. Primary structure and functional characterization of a high-affinity glutamate transporter [see comments]. *Nature*. 1992;360:467–471.
321. Hayes D, Wiessner M, Rauen T, et al. Transport of L-[14C]cystine and L-[14C]cysteine by subtypes of high affinity glutamate transporters over-expressed in HEK cells. *Neurochem Int*. 2005;46:585–594.
322. Bailey CG, Ryan RM, Thoeng AD, et al. Loss-of-function mutations in the glutamate transporter SLC1A1 cause human dicarboxylic aminoaciduria. *J Clin Invest*. 2011;121:446–453.
323. Kanai Y, Clemencon B, Simonin A, et al. The SLC1 high-affinity glutamate and neutral amino acid transporter family. *Mol Aspects Med*. 2013;34:108–120.
324. Wilcken B, Smith A, Brown DA. Urine screening for aminoacidopathies: is it beneficial? Results of a long-term follow-up of cases detected by screening one million babies. *J Pediatr*. 1980;97:492–497.
325. Arnold PD, Sicard T, Burroughs E, et al. Glutamate transporter gene SLC1A1 associated with obsessive-compulsive disorder. *Arch Gen Psychiatry*. 2006;63:769–776.
326. McGivan JD, Nicholson B. Regulation of high-affinity glutamate transport by amino acid deprivation and hyperosmotic stress. *Am J Physiol*. 1999;277:F498–F500.
327. Otani N, Ouchi M, Hayashi K, et al. Roles of organic anion transporters (OATs) in renal proximal tubules and their localization. *Anat Sci Int*. 2017;92:200–206.
328. Shi Y. Common folds and transport mechanisms of secondary active transporters. *Annu Rev Biophys*. 2013;42:51–72.
329. Erdelt H, Weidemann MJ, Buchholz M, et al. Some principle effects of bongkreic acid on the binding of adenine nucleotides to mitochondrial membranes. *Eur J Biochem*. 1972;30:107–122.
330. Widdas WF. Facilitated transfer of hexoses across the human erythrocyte membrane. *J Physiol*. 1954;125:163–180.
331. Malinauskaitė L, Said S, Sahin C, et al. A conserved leucine occupies the empty substrate site of LeuT in the Na⁺-free return state. *Nat Commun*. 2016;7:11673.
332. Yamashita A, Singh SK, Kawate T, et al. Crystal structure of a bacterial homologue of Na⁺/Cl⁻-dependent neurotransmitter transporters. *Nature*. 2005;437:215–223.
333. Forrest LR, Rudnick G. The rocking bundle: a mechanism for ion-coupled solute flux by symmetrical transporters. *Physiology (Bethesda)*. 2009;24:377–386.
334. Vandenberg RJ, Ryan RM. Mechanisms of glutamate transport. *Physiol Rev*. 2013;93:1621–1657.
335. Yernool D, Boudker O, Jin Y, et al. Structure of a glutamate transporter homologue from *Pyrococcus horikoshii*. *Nature*. 2004;431:811–818.
336. Drew D, Boudker O. Shared molecular mechanisms of membrane transporters. *Annu Rev Biochem*. 2016;85:543–572.
337. Yan N. A Glimpse of membrane transport through structures—advances in the structural biology of the GLUT glucose transporters. *J Mol Biol*. 2017;429:2710–2725.
338. Quistgaard EM, Low C, Guettou F, et al. Understanding transport by the major facilitator superfamily (MFS): structures pave the way. *Nat Rev Mol Cell Biol*. 2016;17:123–132.

339. Fort J, de la Ballina LR, Burghardt HE, et al. The structure of human 4F2hc ectodomain provides a model for homodimerization and electrostatic interaction with plasma membrane. *J Biol Chem.* 2007;282:31444–31452.
340. Rosell A, Meury M, Alvarez-Marimon E, et al. Structural bases for the interaction and stabilization of the human amino acid transporter LAT2 with its ancillary protein 4F2hc. *Proc Natl Acad Sci U. S. A.* 2014;111:2966–2971.
341. Zhang H, Wada J, Hida K, et al. Collectrin, a collecting duct-specific transmembrane glycoprotein, is a novel homolog of ACE2 and is developmentally regulated in embryonic kidneys. *J Biol Chem.* 2001;276:17132–17139.
342. Wagner CA, Lang F, Broer S. Function and structure of heterodimeric amino acid transporters. *Am J Physiol Cell Physiol.* 2001;281:C1077–C1093.

BOARD REVIEW QUESTION

1. What statement about the sodium glucose cotransporter SGLT2 in the kidney is incorrect?
- SGLT2 reabsorbs >90% of the filtered glucose in an euglycemic individual with normal kidney function
 - SGLT2 is expressed in the early proximal tubule
 - SGLT2 inhibition enhances GFR in short term
 - SGLT2 inhibition excretes only ~50% of the filtered glucose in an euglycemic individual with normal kidney function
 - SGLT2 inhibition is uricosuric

Answer: c

Rationale: SGLT2 is expressed in the brush border of the early proximal tubule. SGLT2 reabsorbs >90% of the filtered

glucose in an euglycemic individual with normal kidney function. SGLT2 inhibition excretes only ~50% of the filtered glucose in an euglycemic individual with normal kidney function, because SGLT1 in the downstream later part of the proximal tubule can compensate when more glucose is delivered to that site. SGLT2 inhibition is uricosuric and can lower blood urate levels. SGLT2 inhibition reduces GFR in short term through the tubuloglomerular feedback mechanism and by increasing tubular back pressure. SGLT2 inhibition can preserve or maintain higher GFR in the long term in type 2 diabetic patients.

Renal Acidification Mechanisms

I. David Weiner | Jill W. Verlander

CHAPTER OUTLINE

BICARBONATE REABSORPTION, 247
BICARBONATE GENERATION, 260
ACID-BASE SENSORS, 271

DIURNAL VARIATION IN ACID
EXCRETION, 272

KEY POINTS

- Proximal tubule filtered bicarbonate reabsorption involves apical H^+ secretion by NHE3 and H^+ -ATPase, and in the neonatal kidney NHE8 substitutes for NHE3.
- Proximal tubule bicarbonate reabsorption is regulated by peritubular HCO_3^- and CO_2 , but not directly by peritubular pH.
- Proximal tubule basolateral NBCe1 is necessary for bicarbonate reabsorption and regulates both ammonia metabolism and citrate reabsorption.
- Aquaporins transport CO_2 and NH_3 in addition to H_2O .
- Renal ammonia transport involves selective transport of NH_3 and NH_4^+ by specific membrane proteins that exhibit significant axial and apical versus basolateral plasma membrane heterogeneity along the nephron and collecting duct.
- Ammonia metabolism involves both ammonia generation (ammoniogenesis) and ammonia recycling; the latter occurs through the protein glutamine synthetase.
- Renal interstitial sulfatides, probably by reversibly binding interstitial NH_4^+ , are necessary for normal ammonia metabolism.
- The bicarbonate secreting anion exchanger, pendrin, which is necessary for recovery from metabolic alkalosis, has a critical role in volume homeostasis and blood pressure regulation through roles both as a Cl^- reabsorbing protein and through indirect interactions with the Na^+ -reabsorbing protein, ENaC.

Maintaining normal acid–base homeostasis is critical for normal health. Acid–base disorders can lead to a number of clinical problems, such as growth retardation, nausea, and vomiting; increased susceptibility to cardiac arrhythmias; decreased cardiovascular catecholamine sensitivity; bone disorders, including osteoporosis and osteomalacia; recurrent nephrolithiasis, skeletal muscle atrophy; paresthesia; and coma.²⁶⁶ In people with chronic kidney disease (CKD), metabolic acidosis leads to more rapid progression of worsened renal function and increased risk of requiring renal replacement therapy.^{97,216} Finally, the presence of either metabolic acidosis or metabolic alkalosis correlates with increased mortality in patients both with and without CKD.^{214,289,327}

Acid–base homeostasis involves two separate but related processes, bicarbonate reabsorption and new bicarbonate generation. The first relates to the reabsorption of bicarbonate

filtered by the glomerulus. The second relates to the need to generate “new bicarbonate” to replenish bicarbonate that neutralizes endogenous and exogenous fixed acid loads. Finally, a number of pathophysiologic conditions generate acid or alkali loads to which the kidneys must respond to in order to maintain acid–base homeostasis.

BICARBONATE REABSORPTION

Bicarbonate reabsorption involves coordinated transport events in multiple nephron segments (Fig. 9.1). The proximal tubule reabsorbs the majority of filtered bicarbonate. Little-to-no bicarbonate reabsorption occurs in the thin descending limb of the loop of Henle, moderate reabsorption occurs in the thick ascending limb (TAL) of Henle loop, and the

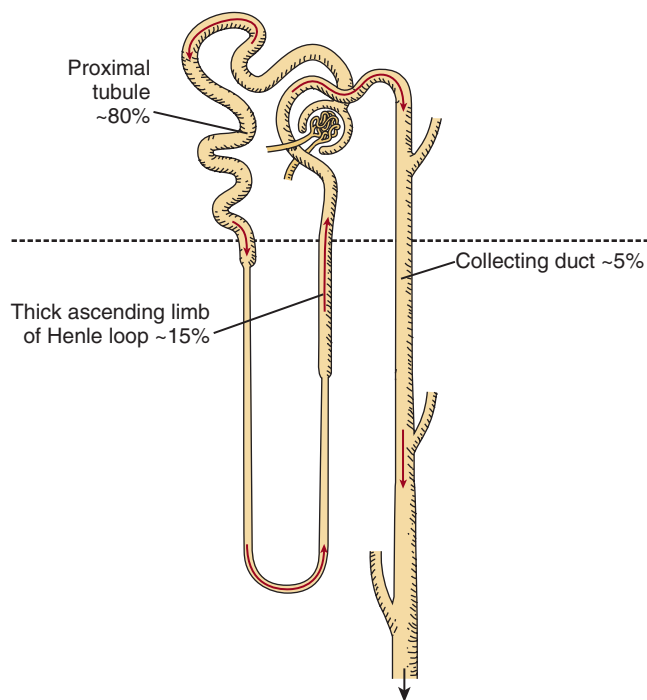


Fig. 9.1 Summary of sites of bicarbonate reabsorption. The proximal tubule is the primary site quantitatively for filtered bicarbonate reabsorption. Minimal reabsorption occurs in the thin limb of the loop of Henle. The thick ascending limb of the loop of Henle reabsorbs the majority of the bicarbonate not reabsorbed in the proximal tubule. The collecting duct is the primary site for reabsorption of the remaining filtered bicarbonate.

remaining filtered bicarbonate is reabsorbed in the distal convoluted tubule (DCT), connecting segment (CNT), initial collecting tubule (ICT), and the collecting duct.

PROXIMAL TUBULE

GENERAL TRANSPORT MECHANISMS

Proximal tubule bicarbonate reabsorption involves several distinct, but interconnected, processes (Fig. 9.2). First, protons (H^+) are secreted into the luminal fluid. Multiple proteins mediate H^+ secretion; the apical Na^+/H^+ exchanger, NHE3, and an apical H^+ -ATPase are the primary mechanisms of proton secretion in the adult kidney. In the neonatal kidney, the Na^+/H^+ exchanger, NHE8, appears to substitute for NHE3 as the primary Na^+/H^+ exchanger (NHE) isoform.³⁰ In the adult kidney, NHE3 is responsible for 60%–70% of H^+ secretion and H^+ -ATPase accounts for the majority of the remainder.

Secreted H^+ combines with luminal HCO_3^- to form carbonic acid (H_2CO_3). Luminal carbonic acid dissociates to water (H_2O) and carbon dioxide (CO_2). Although this can occur spontaneously, the spontaneous dehydration rate is inadequate to support normal rates of proximal tubule bicarbonate reabsorption. The dehydration reaction is catalyzed by carbonic anhydrase IV (CA IV), a membrane-bound carbonic anhydrase isoform present in the proximal tubule brush border.

Luminal CO_2 then moves across the apical plasma membrane into the cell. Although this process has traditionally

been thought to occur through lipid-phase diffusion, the integral membrane protein, aquaporin 1 (AQP1), may mediate ~50% of CO_2 transport across the apical plasma membrane.⁴⁶ Cytosolic CO_2 is then hydrated, forming carbonic acid, through a process accelerated by the cytosolic carbonic anhydrase, carbonic anhydrase II (CA II). Cytosolic carbonic acid spontaneously dissociates to H^+ and HCO_3^- . This “replenishes” the H^+ secreted across the apical plasma membrane by apical NHE3 and H^+ -ATPase.

Cytosolic HCO_3^- is transported across the basolateral plasma membrane. In the S1 and S2 segments of the proximal tubule the primary HCO_3^- transport mechanism is a sodium-coupled, electrogenic bicarbonate cotransporter, NBCe1-A.^{1,256} Because NBCe1-A is electrogenic, generation and regulation of the transmembrane voltage between cytoplasm and interstitium is important, and appears to be related to extracellular pH-dependent activation of the basolateral TWIK-related acid-sensitive K^+ channel, TASK2.⁴⁴⁵ In the S3 segment, an Na^+ -dependent, Cl^-/HCO_3^- exchanger appears to be the primary mechanism of basolateral HCO_3^- transport,²¹⁷ although NBCe1 may also contribute.²⁸⁴

In addition to active H^+ secretion-mediated luminal bicarbonate reabsorption, the proximal tubule also exhibits passive H^+ and bicarbonate transport. Because bicarbonate reabsorption decreases the luminal bicarbonate concentration and increases the luminal H^+ concentration relative to the peritubular space, passive bicarbonate transport results in bicarbonate secretion, which limits net bicarbonate reabsorption. The molecular mechanisms of bicarbonate backleak are unclear, but several functional aspects are known. It is quantitatively less in the newborn than in the adult kidney,³²³ is decreased by angiotensin II (AngII),²⁴² involves both paracellular and transcellular components, and involves membrane proteins, but not NHE3.^{158,315} Quantitatively, the bicarbonate backleak rate is less than that of bicarbonate reabsorption in the initial portions of the proximal tubule. However, in more distal portions, particularly when luminal bicarbonate concentrations have decreased as a result of more proximal bicarbonate reabsorption, bicarbonate backleak rates are greater as a result of the greater transepithelial bicarbonate gradient. Simultaneously, the lower luminal pH limits NHE3-mediated proton secretion and bicarbonate reabsorption. This can result in the bicarbonate backleak rate becoming equivalent to the bicarbonate reabsorption rate. When this occurs, there is no further net bicarbonate reabsorption. Under typical circumstances, this occurs when luminal bicarbonate concentrations have decreased to approximately 6 mmol/L, corresponding to a luminal pH of 6.8.

Proteins Involved in Proximal Tubule Bicarbonate Reabsorption

Na^+/H^+ Exchangers. Na^+/H^+ exchangers are expressed widely in the kidney, where they function in intracellular pH regulation, transepithelial bicarbonate reabsorption, and vacuolar acidification. All use the extracellular-to-intracellular H^+ gradient to enable secondary active, electroneutral H^+ secretion. Although the preferred ions are Na^+ and H^+ , Li^+ can substitute for Na^+ and NH_4^+ can substitute for H^+ .²⁰⁴ The latter process, which enables Na^+/NH_4^+ exchange, appears to be important for proximal tubule NH_4^+ secretion.²⁷⁴

NHE3 (SLC9A3) is the primary apical Na^+/H^+ exchanger in the proximal tubule and mediates the majority of

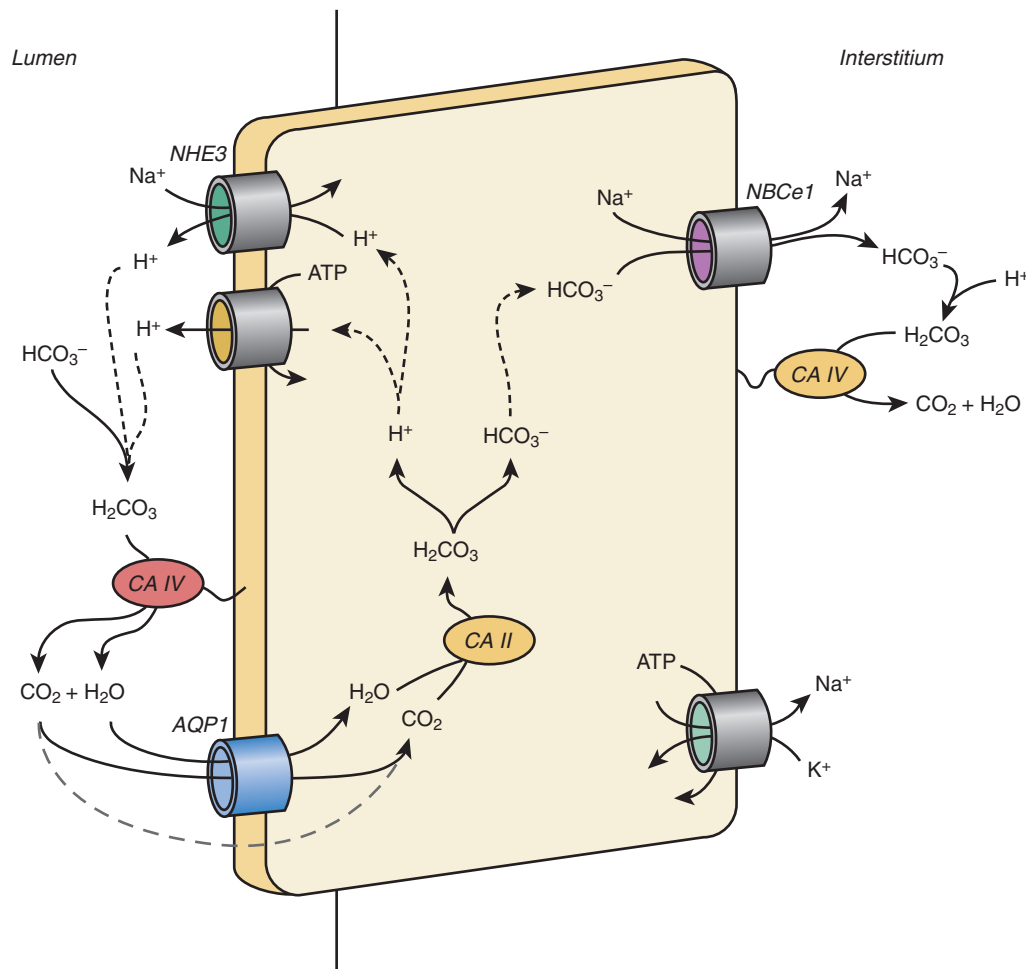


Fig. 9.2 Bicarbonate reabsorption in the proximal tubule. Proximal tubule HCO_3^- reabsorption involves integrated function of multiple proteins. Protons are secreted by the Na^+/H^+ exchanger, *NHE3*, and by H^+ -ATPase, and titrate luminal HCO_3^- to H_2CO_3 . Luminal H_2CO_3 dehydration to H_2O and CO_2 is accelerated by luminal carbonic anhydrase activity mediated by *CA IV*. CO_2 enters the cell via aquaporin I (*AQP1*) and most likely also via passive lipid-phase diffusion, where its hydration to H_2CO_3 is accelerated by cytoplasmic *CA II*. H_2CO_3 rapidly dissociates to H^+ and HCO_3^- , thereby “replenishing” the secreted cytosolic H^+ . Cytosolic HCO_3^- exits across the basolateral plasma membrane primarily by the electrogenic sodium-bicarbonate cotransporter, *NBCe1-A*. In the *PST*, a basolateral $\text{Cl}^-/\text{HCO}_3^-$ exchange activity (not shown) is the primary basolateral HCO_3^- exit mechanism. *ATP*, Adenosine triphosphate; *CA IV*, carbonic anhydrase 4; *PST*, proximal straight tubule.

luminal bicarbonate reabsorption. Multiple mechanisms regulate *NHE3*; the best studied are parathyroid hormone (PTH), dopamine, and AngII. Both PTH and dopamine inhibit *NHE3* activity, whereas AngII has a biphasic effect, stimulatory at low concentrations and inhibitory at high concentrations. Both PTH and dopamine increase intracellular cyclic adenosine monophosphate (cAMP) levels, leading to decreased *NHE3* activity,⁸⁷ and dopamine also has protein kinase C- (PKC)-dependent effects.¹³⁷ AngII decreases cAMP levels and activates PKC, tyrosine kinase, and phosphatidylinositol-3-kinase.¹⁷⁸

NHE3 phosphorylation is an important regulatory mechanism. Serine-552 (in the rat sequence) is a consensus protein kinase A (PKA) phosphorylation site, and phosphorylation of this site causes localization to the coated pit region of the brush-border membrane, where *NHE3* cannot contribute to bicarbonate reabsorption.²¹¹ Similarly, phosphorylation of serine-719 regulates insertion into the plasma membrane.³⁴⁵ This phosphorylation affects interactions of multiple signaling proteins with *NHE3*, alters the size of the *NHE3* protein

binding complex, and alters *NHE3* lipid raft distribution, which cause changes in specific aspects of basal as well as acutely regulated *NHE* exchange activity.³⁴⁶ Dephosphorylation, mediated by the serine/threonine phosphatase PP1, but not PP2, at serines 552 and 605, and at other novel phosphorylation sites, stimulates *NHE3* activity.¹⁰⁵ Ang II counteracts the effects of cAMP/PKA by dephosphorylating *NHE3* at serine 552, which may be a key event in the regulation of renal proximal tubule sodium handling.⁸⁹

Movement of *NHE3* between different subcellular locations, including microvilli, intermicrovillar clefts, endosomes, and the cytoplasm, is an important regulatory mechanism. Only *NHE3* in microvilli contributes to bicarbonate reabsorption. Redistribution within these domains is regulated by a variety of factors, including renal sympathetic nerve activity, glucocorticoids, insulin, AngII, dopamine, and PTH.^{22,39,87,260,334} This process involves a number of cellular proteins, including dynamin, NHERF-1, clathrin-coated vesicles, calcineurin homologous protein-1, ezrin phosphorylation, G-protein alpha subunits, and G-protein beta-gamma dimers.^{8,100,179}

NHE8 (SLC9A8) is a second Na^+/H^+ exchanger found in the proximal tubule.¹⁴⁹ Under normal conditions in the adult kidney, NHE8 is mostly intracellular,³⁸ but in the absence of NHE3 and during acid-loading in normal mice, NHE8 protein expression increases in brush border membrane fractions and contributes to bicarbonate reabsorption.³⁰ In the neonatal kidney, brush border membrane NHE8 expression is increased and NHE3 expression is decreased compared with adult kidneys, suggesting that NHE8 is the primary mechanism of apical NHE activity in the neonatal kidney.^{30,31,309,406}

NHE1 (SLC9A1) is a third member of the NHE family that is present in the proximal tubule. NHE1 is a ubiquitous sodium hydrogen exchanger present in essentially all cells in mammalian organs and is located in the proximal tubule in the basolateral plasma membrane.³⁴ Its role in the proximal tubule appears to be acute intracellular pH regulation.⁶⁰

H^+ -ATPase. A second mechanism of proximal tubule apical H^+ secretion involves the vacuolar H^+ -ATPase.⁴⁴³ H^+ -ATPase is expressed in the brush border microvilli, the base of the brush border, and apical invaginations between clathrin-coated domains.⁵² H^+ -ATPase also acidifies proximal tubule endosomes and lysosomes, senses endosomal pH, and is involved in recruiting trafficking proteins to acidified vesicles, thereby ensuring appropriate progression from early endosomes to lysosomes.⁵⁴ Proximal tubule H^+ -ATPase activity is increased by AngII, increased axial flow, and chronic metabolic acidosis.^{74,103,427} H^+ -ATPase has a direct binding interaction with aldolase, which may underlie the development of proximal RTA in individuals with hereditary fructose intolerance.²⁴⁷ In addition, PKA stimulates and the adenosine monophosphate-activated protein kinase (AMPK) inhibits apical plasma membrane H^+ -ATPase insertion and activity.⁷

NBCe1 (SLC4A4). Basolateral bicarbonate exit largely is mediated by the electroneutral sodium-bicarbonate cotransporter, NBCe1. In humans, three splice variants of the NBCe1 gene are known; NBCe1-A, also known as kNBC1, is the primary splice variant expressed in the kidney, where it is found exclusively in the basolateral plasma membrane in the proximal convoluted tubule.^{61,256} In mice, there are a total of five known splice variants.²¹⁹ NBCe1-A has large cytoplasmic amino- and carboxy-termini tails, 14 transmembrane domains, and two glycosylation sites.^{45,244,335,490}

NBCe1-A in the proximal tubule mediates the coupled net movement of Na^+ and HCO_3^- . The majority of evidence suggests this involves a 1:3 ratio of Na^+ and HCO_3^- equivalents.^{151,336} Because the cytoplasm is negatively charged relative to the peritubular compartment, this electrical gradient provides the driving gradient to enable the coupled movement of Na^+ and HCO_3^- out of the cell, against their concentration gradient. The coupling ratio of Na^+ and HCO_3^- is likely to be critically important: a 1:3 coupling mediates net HCO_3^- efflux, whereas with a 1:2 ratio, depending on the assumptions of intracellular Na^+ and HCO_3^- concentration and of basolateral membrane voltage, the net electrochemical gradient may favor HCO_3^- influx. Indeed, some proximal renal tubular acidosis (RTA) cases may result from NBCe1 mutations that alter the coupling ratio.⁴⁹¹ However, the specific molecular mechanisms of this 1:3 coupling ratio are only partially understood. In nonrenal cells, NBCe1-A appears to have a

1:2 coupling ratio.^{151,173,232} Moreover, it appears that when NBCe1-A is expressed in a proximal tubule cell line, Ser-982 phosphorylation shifts the stoichiometry from 1:3 to 1:2.¹⁵² Two aspartate residues near Ser-982 are necessary for this stoichiometry shift.¹⁵³ Thus, the coupling ratio of 1:3 appears to be important for NBCe1-A to facilitate bicarbonate exit and to be determined, at least in part, by phosphorylation-dephosphorylation of specific amino acid residues.

Proximal tubule NBCe1-A-mediated bicarbonate transport is regulated by physiologic conditions. Transport activity increases in response to metabolic acidosis and to a variety of stimuli that increase bicarbonate reabsorption.^{130,314,373} However, changes in steady-state protein expression do not appear to be an important regulatory mechanism, as metabolic acidosis does not appear to alter NBCe1-A expression.²²⁰ Other factors known to regulate NBCe1-A activity include intracellular ATP, possibly through an as yet unidentified kinase,¹⁷³ and a regulated recycling pathway involving PKC³⁰⁵ and calcium/calmodulin-dependent protein kinase II.³⁰⁶ Although Ste20/SPS1-related proline-alanine-rich kinase (SPAK)-dependent Ser65 phosphorylation and IRBIT- and SPAK-dependent Thr49 phosphorylation regulate NBCe1-B activity,¹⁷⁶ as a result of alternative splicing these residues are not present in NBCe1-A. Moreover, because of differential splicing, the auto-inhibitory domain present in NBCe1-B and NBCe1-C is not present in NBCe1-A, which results in approximately fourfold greater basal activity of NBCe1-A compared with the -B and -C variants.²⁵⁹

Defects in NBCe1 are the most common cause of autosomal recessive proximal RTA (pRTA).^{186,219,491} In addition to causing severe pRTA, NBCe1 defects can cause growth and mental retardation, basal ganglia calcification, cataracts, corneal opacities (band keratopathy), glaucoma, elevated serum amylase and lipase, and defects in the enamel suggestive of amelogenesis imperfecta.^{186,219} In mice, homozygous NBCe1 deletion causes a very severe phenotype, with severe metabolic acidosis, marked volume depletion, and death within a few weeks after birth. Heterozygous deletion causes a milder phenotype but still causes development of pRTA.^{129,167}

NBCe1, in addition to its role in proximal tubule bicarbonate reabsorption, also has a critical role regulating other proximal tubule acid-base functions. NBCe1 gene deletion causes abnormal renal ammonia and organic anion metabolism, and these effects appear to be mediated through alterations in proximal tubule proteins involved in the metabolism and/or transport of these acid-base components.^{167,293} This critical role of NBCe1 appears to be due, at least in part, to the A splice variant, NBCe1-A. Recent studies show that mice with NBCe1-A-specific deletion live to adulthood, have spontaneous metabolic acidosis without increased ammonia excretion, an abnormal physiologic response, and have greatly impaired ammonia metabolism and excretion response to acid loading.²²⁸ The abnormal ammonia excretion correlates with abnormal expression of critical proteins involved in ammoniogenesis, including PDG, PEPCK, and GS.²²⁸

Carbonic Anhydrase. Carbonic anhydrases are a family of zinc metalloenzymes that catalyze the reversible hydration of CO_2 to form carbonic acid (H_2CO_3), reaction A in the equation:



In the absence of carbonic anhydrase, the hydration/dehydration reaction (reaction A) is rate limiting, whereas reaction B occurs essentially instantaneously.

CA II. CA II is the predominant carbonic anhydrase in the kidney and in the proximal tubule. It is located in the cytoplasm of the proximal tubule, in addition to multiple other sites in the kidney, including thin descending limb, thick ascending limb of the loop of Henle (TAL), and intercalated cells. In the mouse kidney, CA II is also expressed in collecting duct principal cells.

CA IV. CA IV is found in the proximal tubule and in intercalated cells in the collecting duct.³⁵² CA IV is linked to the plasma membrane via a glycosylphosphatidylinositol (GPI) anchor and extends into the extracellular compartment; the active site is thus extracellular, not intracellular.⁴⁹² In the proximal tubule, CA IV is expressed in both apical and basolateral plasma membranes where, by facilitating HCO_3^- interconversion with CO_2 , it contributes to transepithelial bicarbonate reabsorption.⁵³

REGULATION OF PROXIMAL TUBULE BICARBONATE REABSORPTION

Systemic Acid-Base

Changes in extracellular acid-base status profoundly alter proximal tubule bicarbonate reabsorption. Both metabolic and respiratory acidosis increase bicarbonate reabsorption, and alkalosis decreases it. This occurs with both acute and chronic pH changes, although the effects are substantially greater with chronic changes. It is important to note that these effects are mediated through changes in interstitial (i.e., peritubular) HCO_3^- , and pCO_2 . Changes in luminal HCO_3^- have the opposite effect on proximal tubule bicarbonate transport, a manifestation of glomerular-tubular balance.

Recent studies have begun to elucidate the mechanisms through which extracellular bicarbonate and CO_2 regulate proximal tubule bicarbonate reabsorption. Changes in either peritubular CO_2 or HCO_3^- concentration, but not pH when the other two components are constant, alter bicarbonate reabsorption.⁴⁸⁹ These effects are specific to bicarbonate reabsorption, as fluid reabsorption rates do not change. The basolateral plasma membrane protein, protein-tyrosine phosphatase, receptor-type, gamma (PTPRG), is necessary for this molecular sensing.⁴⁸⁸ PTPRG may couple to the ErbB tyrosine kinases, ErbB1 and ErbB2, as inhibitors of these proteins block these responses, and phosphorylation of ErbB1 and ErbB2 is regulated by both bicarbonate and CO_2 concentration.³⁷⁰ An additional mechanism may involve the intrarenal angiotensin system, as peritubular CO_2 stimulates intracellular AngII production and luminal secretion, which acts through an apical AT_1 receptor to stimulate bicarbonate reabsorption.^{485,487}

Chronic metabolic acidosis increases proximal tubule bicarbonate reabsorption more than acute metabolic acidosis. This adaptive increase involves increased NHE3 expression and activity and increased H^+ -ATPase activity,^{16,74,314} but not detectable changes in NBCe1 or NBCe1-A expression.^{220,228} Glucocorticoid levels rise with chronic metabolic acidosis,⁴⁶⁴ and glucocorticoid receptor activation enhances acidosis-induced increases in NHE3 expression and apical trafficking.¹⁴

Luminal Flow Rate. Renal bicarbonate reabsorption changes in parallel with glomerular filtration rate and luminal flow.³¹⁰

Increased luminal flow enhances apical plasma membrane NHE3 activity.³¹² In addition, increased flow minimizes changes in the luminal bicarbonate concentration, thereby maintaining a higher mean luminal bicarbonate concentration, which facilitates bicarbonate reabsorption.¹³ Proximal tubule brush border microvilli may function as flow sensors, with drag force transmitted through the actin filament, altering cytoskeletal elements and regulating transport.¹⁰³

AngII. AngII is an important regulator of proximal tubule ion transport, including bicarbonate reabsorption. Low AngII concentrations increase but high concentrations inhibit bicarbonate reabsorption.^{78,442} Both luminal and peritubular low-dose AngII stimulate bicarbonate reabsorption, mediated predominantly through apical and basolateral AT_1 receptors. Acidosis increases AT_1 receptor expression, which may contribute to adaptive changes in bicarbonate reabsorption.²⁷⁹

Potassium. Chronic hypokalemia stimulates and hyperkalemia inhibits proximal tubule bicarbonate reabsorption.³²⁸ This is associated with parallel changes in apical Na^+/H^+ exchange and basolateral sodium-bicarbonate cotransport activity,³⁷² and involves increased apical and basolateral plasma membrane AT_1 receptor expression.¹²⁶ Acute changes in extracellular potassium concentration, however, do not alter proximal tubule bicarbonate transport.⁷⁷

Endothelin. Endothelin has important and direct effects on ion transport in a variety of renal epithelial cells, including the proximal tubule. Endothelin can be produced in the proximal tubule and exhibits an autocrine effect to stimulate NHE3.²⁴⁰ In particular, metabolic acidosis-induced increases in NHE3 expression may require endothelin B (ET-B) receptor activation.²²²

PTH. PTH acutely inhibits proximal tubule bicarbonate reabsorption through activation of adenylyl cyclase and increased intracellular cAMP production.²⁶³ Systemic PTH administration leads acutely to metabolic acidosis, but chronically leads to metabolic alkalosis.¹⁸³ The acute effect is due primarily to increased urinary bicarbonate excretion, likely due to changes in proximal tubule bicarbonate reabsorption; the chronic effect is due to increased titratable acid excretion, which is likely due to increased excretion of dihydrogen and hydrogen phosphate.¹⁸³

Calcium Sensing Receptor. The calcium sensing receptor (CaSR) is present in the apical membrane in the proximal tubule. CaSR activation, either by increased luminal calcium or through calcimimetic agents, increases bicarbonate reabsorption through a mechanism likely involving the activation of apical NHE3.⁶⁶ CaSR activation may modulate the effects of PTH in proximal tubule bicarbonate reabsorption; hypercalcemia resulting from excess PTH has the opposite effect of PTH alone on bicarbonate transport.

LOOP OF HENLE

The TAL of the loop of Henle reabsorbs ~15% of the filtered bicarbonate load. The overall schema is fundamentally similar to that in the proximal tubule. Apical Na^+/H^+ exchange and vacuolar H^+ -ATPase secrete H^+ . Quantitatively, apical Na^+/H^+ exchange activity is the major H^+ secretory mechanism;

vacuolar H⁺-ATPase activity is present, but has at most a minor role in bicarbonate reabsorption.^{67,148} Two Na⁺/H⁺ exchanger isoforms are present in the TAL, NHE2, and NHE3, and NHE3 appears to be the predominant isoform.^{409,444} Secreted H⁺ reacts with luminal HCO₃⁻, forming H₂CO₃, which dissociates to CO₂ and H₂O. Whether luminal CA IV is present is unclear, with conflicting reports in the literature.^{53,402} Luminal CO₂ moves down its concentration gradient across the apical plasma membrane into the cell cytoplasm. Cytoplasmic CA II catalyzes CO₂ hydration to form H₂CO₃, which dissociates to H⁺ and HCO₃⁻, thereby regenerating the H⁺ secreted across the apical plasma membrane. Several basolateral bicarbonate exit mechanisms are present. These include basolateral Cl⁻/HCO₃⁻ exchange, possibly AE2,¹¹ and a coupled K⁺-HCO₃⁻ cotransport activity that may be mediated by KCC4.²⁷⁰ Although an electroneutral sodium–bicarbonate cotransporter (NBCn1) is present,⁴²⁴ electrochemical gradients for its transport favor bicarbonate uptake, not extrusion, suggesting that it is unlikely to contribute significantly to basolateral bicarbonate exit.

Several plasma membrane proteins either directly or indirectly alter bicarbonate reabsorption. Inhibiting the apical Na⁺-K⁺-2Cl⁻ cotransporter, NKCC2, increases bicarbonate reabsorption.⁶⁷ This may occur because inhibiting NKCC2 decreases Na⁺ entry, which decreases intracellular Na⁺, increasing the Na⁺ uptake gradient for apical Na⁺/H⁺ exchange and thereby increasing bicarbonate reabsorption. Inhibiting basolateral Na⁺/H⁺ exchange activity decreases bicarbonate reabsorption through cytoskeletal alterations that decrease apical NHE3 expression.^{145,447}

Regulation of TAL Bicarbonate Reabsorption

A variety of stimuli regulate TAL bicarbonate reabsorption. Metabolic acidosis increases TAL bicarbonate reabsorption,^{69,138} but whether the effects are specific to metabolic acidosis or due to other mechanisms is not clear. One study reported that metabolic acidosis induced with NH₄Cl and that chloride loading with NaCl had similar effects on bicarbonate transport, raising the possibility that chloride loads, not acid loads, regulate TAL bicarbonate transport.¹³⁸ Data in favor of acidosis regulating TAL bicarbonate transport are that NH₄Cl-induced metabolic acidosis, but not equivalent chloride loading with NaCl, increases TAL NHE3 expression.¹⁹⁸ Further supporting a role of the TAL in acid–base regulation is that experimental models of metabolic alkalosis decrease bicarbonate reabsorption.¹⁴¹

Several hormones regulate bicarbonate reabsorption. AngII stimulates TAL bicarbonate reabsorption, likely through activation of AT₁ receptors.^{68,272} Glucocorticoid receptors are present in the TAL and glucocorticoids are necessary for normal bicarbonate reabsorption.⁴⁰⁸ Mineralocorticoids, at high concentrations, stimulate bicarbonate reabsorption,¹⁴¹ but their absence does not alter basal transport.⁴⁰⁸ Arginine vasopressin (AVP) inhibits bicarbonate reabsorption through prostaglandin E₂-mediated inhibition of apical Na⁺/H⁺ exchange activity.^{44,139} PTH inhibits bicarbonate reabsorption, but the effect is less than the effect of AVP.¹³⁹

Cytokines also regulate bicarbonate transport. Lipopolysaccharide (LPS) inhibits transport; this effect involves the cytokine receptor, TLR4, and separate pathways activated by luminal and peritubular LPS. Luminal LPS involves the mTOR pathway, whereas peritubular LPS functions through the

mitogen-activated protein kinase kinase (MAP) extracellular signal-related kinase (ERK) pathway.^{146,448} High-mobility group box 1 (HMGB1) is a nuclear protein released extracellularly in response to infection or injury, where it interacts with toll-like receptor 4 (TLR4) and other receptors to mediate inflammation. It inhibits TAL bicarbonate reabsorption through a receptor for advanced glycation end products (RAGE)-dependent mechanism that involves signaling through Rho and Rho-associated kinase (ROCK).^{147,446}

Another important regulatory factor is medullary osmolality. Increased tonicity inhibits and decreased tonicity stimulates bicarbonate reabsorption; this occurs through phosphatidylinositol 3-kinase-mediated changes in apical Na⁺/H⁺ exchange activity.^{140,144} In addition, AVP, which contributes to the development of the medullary osmotic gradient, discussed elsewhere in this textbook, inhibits bicarbonate reabsorption.¹³⁹

ACID–BASE TRANSPORTERS IN THE TAL

Many of the major H⁺ and HCO₃⁻ transporters were discussed earlier in relation to the proximal tubule and are not repeated here.

NBCn1 (SLC4A7)

NBCn1 facilitates the electroneutral, coupled transport of Na⁺ and HCO₃⁻ in a 1:1 ratio. In the kidney, NBCn1 is found in the basolateral plasma membrane in the TAL, outer medullary collecting duct (OMCD) intercalated cells, and terminal inner medullary collecting duct (IMCD).^{220,311} Because the concentrations of Na⁺ and HCO₃⁻ are generally lower in the cytoplasm than in the interstitium, basolateral NBCn1 likely mediates peritubular HCO₃⁻ uptake. Moreover, both metabolic acidosis and hypokalemia increase TAL NBCn1 expression.^{189,220} Thus, NBCn1 is unlikely to mediate a critical role in bicarbonate reabsorption. Instead, it is likely to contribute to ammonia reabsorption, which will be discussed later.

DISTAL CONVOLUTED TUBULE

The DCT consists of two cell types, DCT cells and intercalated cells, and the mechanisms involved in bicarbonate reabsorption appear to differ between DCT and intercalated cells. DCT cells express apical NHE2⁷⁵ and NHE2 inhibitors decrease bicarbonate reabsorption.⁴⁴⁴ Basolateral HCO₃⁻ exit likely involves AE2.¹¹ A basolateral Cl⁻ channel that has limited HCO₃⁻ permeability may also contribute.⁴⁶³ Cytosolic CA II is present, but not apical CA IV.⁵³ In the late DCT intercalated cells are present.²⁵¹ Quantitatively, intercalated cells constitute only a very small proportion of all cells in the DCT, ~4% and 7% in the mouse and rat kidneys, respectively.²⁰¹ The majority of intercalated cells in the DCT are type A and non-A, non-B intercalated cells.²⁰¹

COLLECTING DUCT

The renal collecting duct is the final site of bicarbonate reabsorption and both reabsorbs and secretes luminal bicarbonate.²⁶¹ Specific proteins in specific epithelial cell types, which vary in type and frequency in different collecting duct segments, mediate these processes.

Collecting Duct Segments

Technically, the collecting duct begins with the ICT, immediately distal to the CNT, and extends through the IMCD. The

CNT arises from a different embryonic origin than the ICT and the remainder of the collecting duct. However, the CNT is included in the discussion of the role of the collecting duct in acid–base regulation because it has cell types and acid–base transport mechanisms similar to the collecting duct. Different portions of the collecting duct are identified by where they reside: ICT, cortical collecting duct (CCD), outer medullary collecting duct in the outer stripe (OMCDo), outer medullary collecting duct in the inner stripe (OMCDi), and the IMCD.

Cell Composition

Collecting duct segments contain several distinct epithelial cell types, and the cellular composition differs in the various collecting duct segments. Two distinct cell types, intercalated cells and principal cells, are present. Principal cells account for ~60%–65% of cells and intercalated cells account for the remainder in the ICT, CCD, and OMCD. In the IMCD, the proportion of intercalated cells is less, about 10% of cells in the initial portion of the rat IMCD, and it decreases progressively from the outer medullary–inner medullary junction distally, completing disappearing by the middle of the papilla. In the terminal IMCD, the epithelium is composed of IMCD cells, a cell distinct from both intercalated cells and principal cells. The CNT contains both intercalated cells and a cell type specific to the CNT, termed the CNT cell; in some species, principal cells are also present.

At least three distinct intercalated cell subtypes exist: the type A (or α) intercalated cell, the type B (or β) intercalated cell, and the non-A, non-B intercalated cell (Fig. 9.3). In the CNT, both type A and non-A, non-B intercalated cells are present, and type B intercalated cells are infrequent. In the CCD, both type A and type B intercalated cells are present, and the non-A, non-B cell is infrequent. In the OMCD and IMCD, only the type A intercalated cell is present under normal conditions.

Type A Intercalated Cell

The type A intercalated cell is involved in H^+ secretion, HCO_3^- reabsorption, and ammonia secretion. The proteins involved in these processes are, in general, different from those in the proximal tubule and TAL (Fig. 9.4).

Both vacuolar H^+ -ATPase and P-type H^+ - K^+ -ATPases are involved in apical H^+ secretion. H^+ -ATPase is abundant in the apical plasma membrane and in apical cytoplasmic tubulovesicles in type A intercalated cells. H^+ -ATPase undergoes trafficking between the cytoplasmic compartment and the apical plasma membrane; this mechanism, rather than changes in total protein expression, appears to be the major adaptive response to acid–base disturbances.²⁷ In addition to having a major role in H^+ secretion, H^+ -ATPase also has an essential role in cell volume regulation and maintenance of intracellular electronegativity, replacing the Na^+ - K^+ -ATPase that provides these functions in most other cell types.⁷³

A second means of H^+ secretion involves electroneutral, K^+ -dependent H^+ - K^+ -ATPase activity that is mediated by P-type H^+ - K^+ -ATPase proteins.¹⁵⁵ At least two H^+ - K^+ -ATPase α -isoforms are present. One, $HK\alpha_1$, is similar to the α -isoform involved in gastric acid secretion. The other, $HK\alpha_2$, is similar to the α -isoform in the colon. K^+ reabsorbed via apical H^+ - K^+ -ATPase can either recycle across the apical plasma membrane or exit the cell across the basolateral plasma membrane, and relative movement across the apical versus basolateral plasma membranes is regulated by dietary K^+ intake.⁴⁸⁴

A truncated isoform of the erythrocyte anion exchanger, termed $kAE1$, is present in the basolateral plasma membrane and mediates basolateral bicarbonate exit.⁹ Cl^- that enters the cell via basolateral Cl^-/HCO_3^- exchange exits via the KCl cotransporter, $KCC4$ ^{41,264}; a basolateral Cl^- channel, presumably $ClC-Kb$ in humans and $ClC-K2$ in rodents, also contributes to Cl^- recycling.²¹⁰

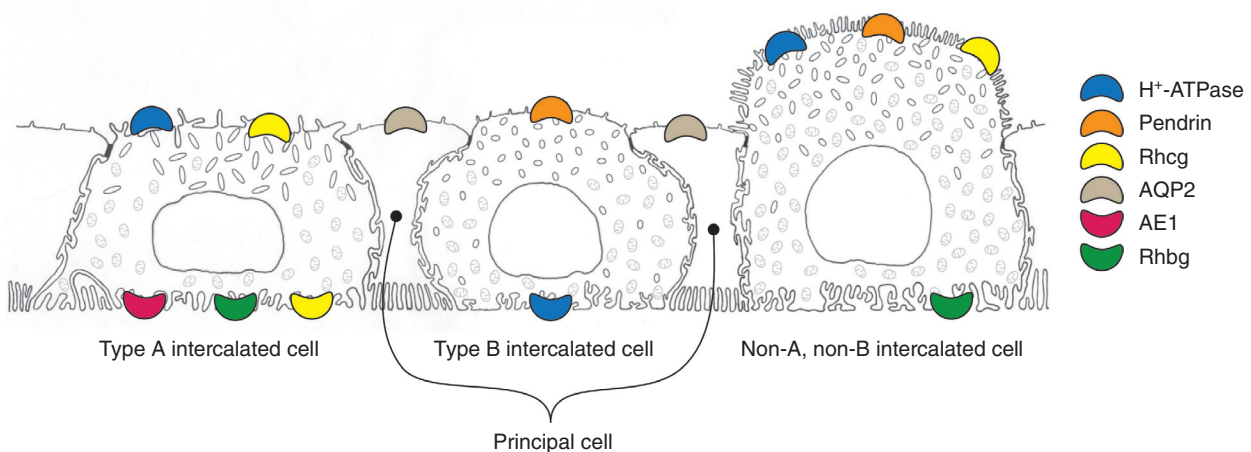
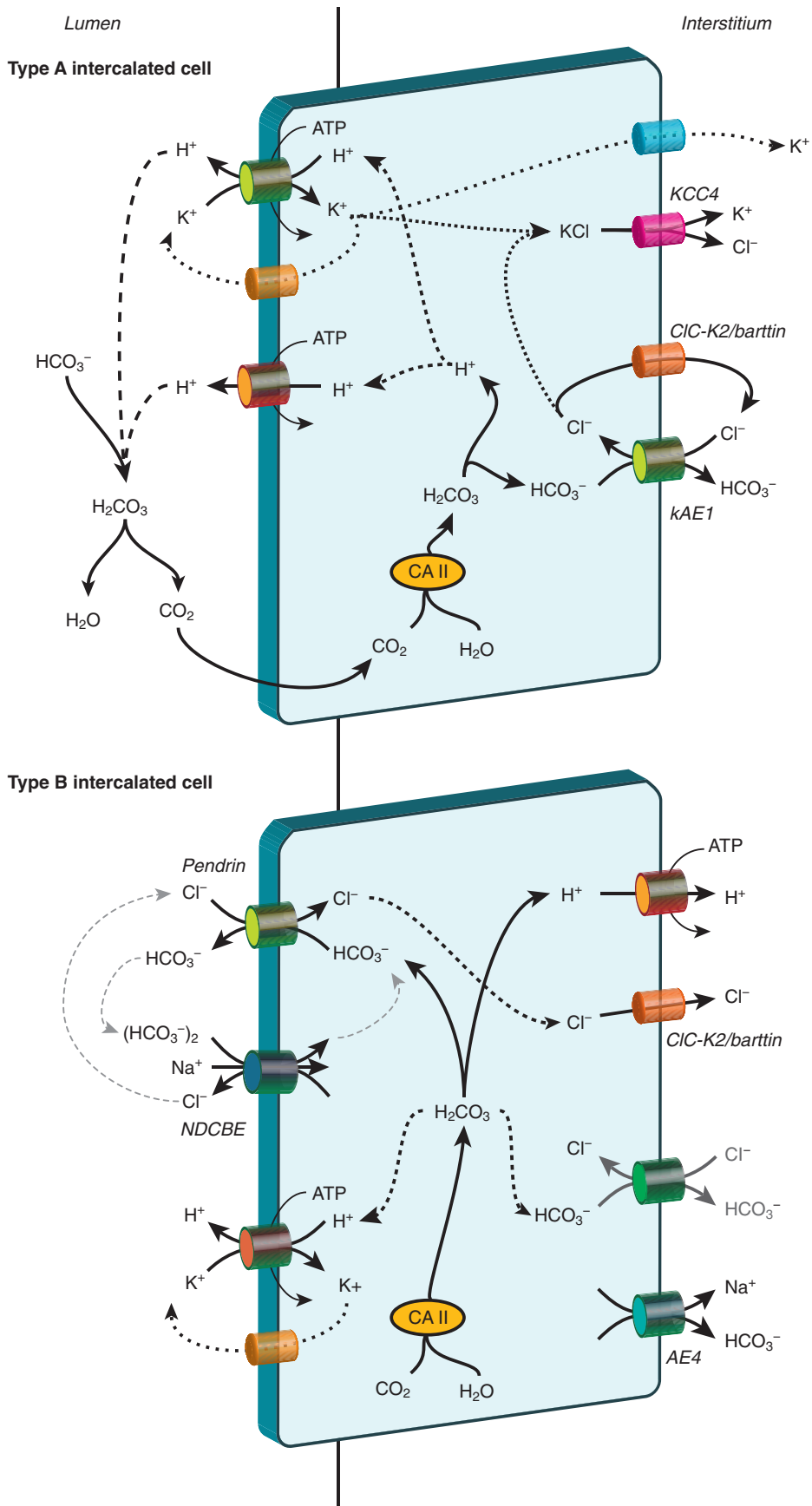


Fig. 9.3 Intercalated cell subtypes in the distal nephron and collecting duct. The late DCT, connecting segment, initial collecting tubule, CCD, OMCD, and IMCD have multiple distinct cell types. Three intercalated cell types can be distinguished based on ultrastructural features and differential expression in plasma membrane domains of several proteins involved in renal acid–base transport, including H^+ -ATPase, AE1, pendrin, Rhbg, and Rhcg. H^+ -ATPase is present in the apical portion of the type B intercalated cell, where it is found in cytoplasmic vesicles; ultrastructural analysis shows it is not in the apical plasma membrane. These specific intercalated cell subtypes occur at different frequencies specific to the various tubule segments. *CCD*, Collecting duct system; *DCT*, distal convoluted tubule; *IMCD*, inner medullary collecting duct; *OMCD*, outer medullary collecting duct.



Cytoplasmic CA II is abundant in type A intercalated cells and enables intracellular generation of H^+ for apical secretion and HCO_3^- for basolateral transport. In addition, membrane-associated carbonic anhydrases are present in the apical region (CA IV) and, at least in mouse and rabbit, in the basolateral region (CA XII) of intercalated cells.³¹⁶

Type B Intercalated Cell

The type B intercalated cell mediates a major role in HCO_3^- secretion and luminal Cl^- reabsorption. It contains basolateral H^+ -ATPase and an apical Cl^-/HCO_3^- exchanger, pendrin.¹⁰ H^+ -ATPase is also present in vesicles throughout the cell, but it is not present in the apical plasma membrane. Similar to the type A intercalated cell, H^+ -ATPase, rather than Na^+ - K^+ -ATPase, maintains intracellular electronegativity and prevents cell swelling.⁷³ Type B intercalated cells also express H^+ - K^+ -ATPase.^{421,473} In the rabbit and mouse an apical H^+ - K^+ -ATPase activity is present,^{250,456} whereas in the rat a basolateral H^+ - K^+ -ATPase activity may be present.¹³³ The type B cell also has cytoplasmic CA II, which facilitates intracellular H^+ and HCO_3^- production. Fig. 9.4 summarizes the proteins involved in type B intercalated cell acid–base transport.

There is functional evidence that pendrin-mediated apical Cl^-/HCO_3^- exchange works in concert with an apical Na^+ -dependent Cl^-/HCO_3^- exchanger, NDCBE (*Slc4a8*), to mediate net $NaCl$ absorption,²³⁷ and NDCBE protein and mRNA have been reported in renal cortical homogenates.^{237,468} However, in recent studies using single-cell RNA-seq NDCBE transcripts were virtually undetectable in type B intercalated cells.⁸⁰ Basolateral Na^+ and Cl^- exits are mediated by the basolateral $NaHCO_3$ cotransporter, AE4,⁷³ and a Cl^- channel, ClC -K2/Barttin, or ClC -Kb.¹⁷⁰

The type B intercalated cell also has the ability to secrete H^+ and reabsorb luminal HCO_3^- . As noted earlier, most studies indicate the type B intercalated cell has an apical H^+ - K^+ -ATPase activity that may mediate proton secretion, and functional studies have shown that CCD intercalated cells with apical Cl^-/HCO_3^- exchange activity (i.e., all type B intercalated cells) also have basolateral Cl^-/HCO_3^- exchange activity that is functionally distinct from the $kAE1$ activity that present in type A intercalated cells.⁴⁵⁹

The type B intercalated cell has several roles in acid–base and ion transport homeostasis. Genetic deletion of the apical Cl^-/HCO_3^- exchanger, pendrin, impairs HCO_3^- secretion, luminal Cl^- reabsorption, and, through a mechanism involving coordinated function with principal cell luminal Na^+ reabsorption.^{203,339,413} The type B intercalated cell may also contribute

to H^+ secretion and luminal HCO_3^- reabsorption. Ammonia, which is increased in metabolic acidosis and hypokalemia, increases type B intercalated cell apical H^+ - K^+ -ATPase and basolateral Cl^-/HCO_3^- exchange activity, which would result in increased net HCO_3^- reabsorption.¹²¹

Non-A, Non-B, or Type C Intercalated Cell

A third intercalated cell subtype, generally termed the non-A, non-B cell, is present in the CNT and ICT.^{201,391} This cell has several features that distinguish it from both the type A intercalated cell and the type B intercalated cell. These differences include the expression of both pendrin and H^+ -ATPase in the apical plasma membrane and in apical cytoplasmic vesicles, the absence of basolateral plasma membrane H^+ -ATPase and AE1, the presence of apical, but not basolateral Rhcg, and the absence of basolateral Rhbg (see Fig. 9.3). Thus, it differs significantly from both type A and type B intercalated cells. Studies of the developing kidney show that non-A, non-B cells and type B intercalated cells arise simultaneously, but from different foci.^{164,374} This cell type was termed “non-A, non-B cell” in early studies. However, its unique transporter expression, distribution, and developmental origin suggest this is a third distinct intercalated cell subtype.

Principal Cells

Principal cells have indirect and direct roles in acid secretion. Indirectly, principal cell–mediated Na^+ reabsorption leads to luminal electronegativity; this facilitates H^+ secretion by the electrogenic, and thus voltage-sensitive, H^+ -ATPase. In addition, principal cells have direct roles. Functional studies show that principal cells have apical H^+ secretory and basolateral Cl^-/HCO_3^- exchange activities,^{452,460} and they express H^+ -ATPase^{102,425} and both the $HK\alpha_1$ and $HK\alpha_2$ isoforms of H^+ - K^+ -ATPase.¹⁵⁵ In the mouse and rat kidney, principal cells in the OMCDi and initial IMCD express both carbonic anhydrase activity and CA II protein.^{101,205} Finally, the ammonia transporters, Rhcg and Rhbg, are both present in principal cells in the rat and mouse CCD and OMCD.¹⁹⁹

IMCD Cell

The IMCD cell is a distinct cell type and is the predominant cell present in the terminal IMCD. It exhibits carbonic anhydrase activity,²⁰⁵ both H^+ -ATPase and H^+ - K^+ -ATPase activity,^{155,435} and basolateral Cl^-/HCO_3^- exchange.⁴⁴⁹ In vitro microperfusion studies have demonstrated directly that the IMCD secretes H^+ and reabsorbs luminal HCO_3^- .⁴³⁷

Fig. 9.4 Bicarbonate transport by the type A and the type B intercalated cell. *Top panel* shows a model of acid–base transport by the type A intercalated cell. Two families of H^+ transporters, H^+ -ATPase and H^+ - K^+ -ATPase, are present in the apical plasma membrane. Secreted H^+ titrates luminal HCO_3^- to form H_2CO_3 , which dehydrates to water (H_2O) and carbon dioxide (CO_2). Luminal carbonic anhydrase activity, most likely mediated by CA IV, is variably present in the collecting duct (see text for details). Cytosolic H^+ and HCO_3^- are formed from CA II-accelerated hydration of CO_2 and rapid dissociation of H_2CO_3 . Cytosolic HCO_3^- exits across the basolateral plasma membrane via the anion exchanger, $kAE1$. Cl^- that enters via $kAE1$ recycles via a basolateral Cl^- channel. K^+ that enters via apical H^+ - K^+ -ATPase can either recycle via an apical, Ba^{2+} -sensitive K^+ channel or be reabsorbed via a basolateral Ba^{2+} -sensitive K^+ channel. A basolateral Na^+/H^+ exchanger is present but does not contribute to bicarbonate reabsorption and is not shown. *Bottom panel* shows a model of acid–base transport by the type B intercalated cell. Apical pendrin is the primary mechanism of bicarbonate secretion. Chloride enters the cell via pendrin and exits across a basolateral chloride channel, ClC -K2/barttin. Basolateral H^+ -ATPase extrudes protons into the peritubular compartment. Cytoplasmic bicarbonate and protons are produced from CO_2 and water in a CA II-catalyzed reaction. In addition, an apical H^+ - K^+ -ATPase in series with a basolateral Cl^-/HCO_3^- exchange activity is present and may contribute to bicarbonate reabsorption by the type B intercalated cell. Apical NDCBE is present and mediates $Na^+-(HCO_3^-)_2$ exchange for Cl^- . When coupled with pendrin this can enable coupled Na^+-Cl^- reabsorption. CA II, Carbonic anhydrase II.

FUNCTIONAL ROLE OF DIFFERENT COLLECTING DUCT SEGMENTS

CNT-ICT

Relatively little information is available on the functional role of the CNT and ICT in acid–base homeostasis. Morphologic and immunolocalization studies suggest that the CNT and ICT contain type A and type B intercalated cell types and non-A, non-B cells.^{201,391,419} Under basal conditions, the CNT, at least in the rabbit, secretes bicarbonate through a Cl^- , carbonic anhydrase–, and H^+ -ATPase–dependent mechanism⁴⁰⁴; this likely involves apical pendrin, cytosolic CA II, and basolateral H^+ -ATPase.

CCD

Unlike the OMCD and IMCD, which can secrete only acid (i.e., reabsorb bicarbonate), the CCD both reabsorbs and secretes bicarbonate. The basal direction of bicarbonate transport varies among species, but both bicarbonate absorption and secretion can be induced in response to systemic acid or alkali loading.^{18,245,261} The ability to secrete bicarbonate, which is not found in the OMCD or IMCD, correlates with the presence of type B intercalated cells in the CCD, but not in the OMCD or IMCD. Mineralocorticoids stimulate CCD bicarbonate secretion, likely related to generation of metabolic alkalosis and to stimulation of pendrin expression^{128,413}; however, mineralocorticoid receptors are present in type B intercalated cells,^{288,363} and thus direct stimulation of type B cell ion transport by mineralocorticoids is possible.

OMCD

The OMCD is responsible for approximately 40%–50% of the net acid secretion that occurs in the collecting duct. Both intercalated cells and principal cells contribute to acid secretion, although intercalated cells are believed to be the primary cell responsible for OMCD acid secretion.^{452,460}

IMCD

The IMCD secretes H^+ and reabsorbs luminal bicarbonate.⁴³³ However, the number of type A intercalated cells is substantially less than in other collecting duct segments. In the rat they account for only 10% of cells in IMCD1⁸⁶ and in all species examined the prevalence diminishes distally such that almost no intercalated cells exist in the distal portion of IMCD (IMCD3). Nonetheless, bicarbonate reabsorption occurs in the terminal IMCD and basolateral $\text{Cl}^-/\text{HCO}_3^-$ exchange is present in cultured IMCD cells.⁴⁴⁹ H^+ secretion is partly mediated by H^+ - K^+ -ATPase.⁴³⁹ In rats fed a potassium-deficient diet, H^+ - K^+ -ATPase activities were upregulated,⁴³⁵ but H^+ - K^+ -ATPase accounted for only ~50% of bicarbonate reabsorption in the IMCD, indicating that other mechanisms of luminal acidification also contribute, likely including H^+ -ATPase. The IMCD expresses CA IV and luminal, cytoplasmic, and lateral membrane–associated carbonic anhydrase activity has been reported.^{205,432}

PROTEINS INVOLVED IN COLLECTING DUCT H^+ /BICARBONATE TRANSPORT

Collecting duct H^+ and HCO_3^- transport involves the coordinated activity of multiple transporters in conjunction with specific carbonic anhydrase isoforms. Later in this chapter we review the specific proteins involved.

H^+ -ATPase

Electrogenic apical H^+ secretion in acid-secreting intercalated cells and basolateral proton transport by bicarbonate-secreting intercalated cells is mediated by the vacuolar H^+ -ATPase. Intercalated cells in the OMCD and initial IMCD, type A intercalated cells in the CCD, and non-A, non-B intercalated cells in the CNT and CCD, contain H^+ -ATPase in the apical plasma membrane and in an apical cytoplasmic vesicle pool, and redistribution between the cytoplasmic vesicle pool and the apical plasma membrane is a major mechanism regulating H^+ secretion. H^+ -ATPase is also present in the apical region of principal cells and CNT cells, but expression is much less than in intercalated cells. In Type B intercalated cells, H^+ -ATPase is present in the basolateral plasma membrane and in sub-apical vesicles, but not in the apical plasma membrane. The role of apical H^+ -ATPase in nonintercalated cells has not been clearly defined; it may be involved in endosomal trafficking and fusion,¹⁸⁴ and in the OMCDi it can also mediate apical H^+ secretion.⁴⁵²

Vacuolar H^+ -ATPase is an assembly of multiple subunits that form two main domains, the V_1 domain, which is extramembranous and hydrolyzes ATP, and the V_0 domain, which is a transmembranous portion and transports protons. The V_0 domain is composed of six subunits; the V_1 domain is composed of eight subunits and is linked to the V_0 domain via a stalk region composed of subunits from both V_0 and V_1 . Distinct isoforms and splice variants have been identified for many of these H^+ -ATPase subunits and their cell-specific distribution may contribute to cell-specific regulation of proton and bicarbonate transport.

Genetic defects in several H^+ -ATPase subunits have been shown to cause distal RTA (dRTA), also known as Type I RTA, in humans. Defects in the B1 subunit of the hydrolytic V_1 domain resulting from ATP6V1B1 gene mutations can produce early-onset hearing loss in combination with autosomal recessive, severe dRTA.^{194,195,382} Mice with B1 subunit deletion have incomplete distal RTA.¹¹⁶ In these mice, the B2 subunit appears to substitute partially for the B1 subunit, enabling partial compensation.³⁰¹ Mutations in the a4 subunit (ATP6V0A4) in the H^+ -translocating V_0 domain also produce recessive, severe early onset of dRTA, with variable onset of hearing loss.^{371,382,411}

Normal H^+ -ATPase function appears to involve coexpression of the Atp6ap2/(pro)renin receptor. This is a type 1 transmembrane protein and an accessory subunit of H^+ -ATPase and may also function in the renin-angiotensin system. Its deletion results in decreased H^+ -ATPase activity and impaired renal acid–base homeostasis.³⁹⁹ Although Atp6ap2 is a cell surface protein capable of binding and nonproteolytically activating prorenin, prorenin does not acutely regulate H^+ -ATPase activity.⁹⁶ Atp6ap2 also appears to regulate NKCC2 and AQP2 expression, and this may occur through the autophagosomal substrate p62.³⁹⁹

H^+ - K^+ -ATPase

The second mechanism of collecting duct H^+ secretion involves electroneutral H^+ - K^+ exchange.¹⁵⁵ The active protein is a heterodimer composed of α - and β -subunits. The α -subunit is an integral membrane protein with multiple membrane spanning domains and contains the catalytic portion of the enzyme. Two α -subunit isoforms have been identified. HK α_1 , also termed the gastric isoform, was identified originally in

the stomach. $\text{HK}\alpha_1$ forms heterodimers with its specific β -subunit, $\text{HK}\beta$. The β -subunit has only a single membrane-spanning region and is necessary for targeting of the α -subunit to the plasma membrane and for transport function.¹⁵⁵ $\text{HK}\alpha_2$ was identified originally in the colon and is sometimes referred to as the colonic isoform. Three splice variants of $\text{HK}\alpha_2$ have been identified in the kidney. $\text{HK}\alpha_2$ forms heterodimers with the β_1 -subunit of $\text{Na}^+\text{-K}^+\text{-ATPase}$.

$\text{HK}\alpha_1$, $\text{HK}\alpha_2$, and $\text{HK}\beta$ are expressed throughout the collecting duct, with greater expression in intercalated cells than in principal cells.^{4,6,64} Functional studies suggest that both $\text{HK}\alpha_1$ and $\text{HK}\alpha_2$ are present in type A as well as type B intercalated cells.^{250,265,456} However, immunohistochemistry studies have yielded variable results with respect to the precise cellular distribution of the $\text{HK}\alpha_1$ and $\text{HK}\alpha_2$ isoforms. $\text{HK}\alpha_1$ immunoreactivity was found in both AE1-positive (type A) and AE1-negative intercalated cells in both rat and rabbit collecting ducts,⁴⁷³ but in human kidneys, diffuse $\text{HK}\alpha_1$ immunoreactivity was present in both intercalated and principal cells.²¹⁵ $\text{HK}\alpha_2$ immunoreactivity was consistently apical, but in different cell types in different studies. It was found exclusively in the CNT cell in rabbits in one study¹¹⁴ and exclusively in the OMCD principal cell in rats in another.³⁴³ A third study found the splice variant, $\text{HK}\alpha_{2c}$, in intercalated cells, principal cells, and CNT cells from the CNT through the initial IMCD in rabbit kidney.⁴²¹ In situ hybridization studies have shown both intercalated cell and principal cell expression of $\text{HK}\alpha_1$, $\text{HK}\alpha_2$, and $\text{HK}\beta$ mRNA in the rat kidney, although principal cell signal was less intense than intercalated cell signal.^{5,64}

Multiple physiologic conditions alter $\text{H}^+\text{-K}^+\text{-ATPase}$ expression and activity. Metabolic acidosis increases $\text{H}^+\text{-K}^+\text{-ATPase}$ activity in the CCD and $\text{HK}\alpha_1$ and $\text{HK}\alpha_2$ mRNA expression in the OMCD, suggesting that $\text{H}^+\text{-K}^+\text{-ATPase}$ contributes to H^+ secretion.¹⁵⁵ Specific studies have identified apical, but not basolateral, $\text{H}^+\text{-K}^+\text{-ATPase}$ activity in both types A and B intercalated cells in mouse and rabbit kidneys.^{265,456,483} Extracellular ammonia, which increases with both metabolic acidosis and hypokalemia, enhances apical $\text{H}^+\text{-K}^+\text{-ATPase}$ -mediated H^+ secretion in both type A and type B intercalated cells in the CCD.^{121,123}

Pendrin (SLC26A4)

Pendrin is an electroneutral $\text{Cl}^-/\text{HCO}_3^-$ exchanger present in the kidney exclusively in type B and non-A, non-B intercalated cells. It is found in the apical plasma membrane and in apical cytoplasmic vesicles in type B and non-A, non-B intercalated cells in the CNT, ICT, and CCD. Under basal conditions, pendrin is predominantly expressed in the apical plasma membrane in non-A, non-B intercalated cells and in subapical cytoplasmic vesicles in type B intercalated cells, and redistribution between these two subcellular sites is an important regulatory mechanism.⁴⁴¹ Pendrin is regulated by AngII, nitric oxide, and cAMP.^{393,414} In addition to bicarbonate secretion, pendrin also mediates an important role in extracellular fluid volume and blood pressure regulation. This appears to involve roles in both transcellular Cl^- reabsorption and, through luminal alkalization due to HCO_3^- secretion, activation of the principal cell epithelial Na^+ transporter, ENaC ^{108,436} and involving the Na^+ -dependent, chloride-bicarbonate exchanger (NDCBE, SLC4A8).²³⁷

Carbonic Anhydrase

Three carbonic anhydrase isoforms, CA II, CA IV, and CA XII, are present in the collecting duct. CA II is cytosolic in proximal tubule cells, discussed earlier, in intercalated cells, and in principal cells in the collecting ducts of mice.⁴²⁰ CA II is present in all intercalated cell types, but expression is generally greater in the type A than in type B intercalated cells.

CA IV is an extracellular, membrane-associated carbonic anhydrase tethered to the membrane through a glycosylphosphatidylinositol lipid (GPI) anchoring protein. It is expressed apically in the majority of cells in rabbit OMCD and IMCD and in type A intercalated cells in the CCD.³⁵⁶ In the OMCDi, luminal carbonic anhydrase inhibition decreases bicarbonate absorption, suggesting an important role for CA IV in acid-base homeostasis.⁴⁰³

Carbonic anhydrase XII (CA XII) is another extracellular, membrane-associated carbonic anhydrase found in the collecting duct.³¹⁶ In contrast to CA IV, CA XII is an integral membrane protein with a single transmembrane spanning region.³¹⁶ Basolateral CA XII immunoreactivity has been reported in principal cells in the human kidney, and in the mouse, basolateral CA XII immunoreactivity is found in type A intercalated cells in the CCD and OMCD.^{316,319}

kAE1

The major basolateral anion exchanger in type A intercalated cells is kAE1, a truncated form of the erythrocyte anion exchanger AE1. In the human, rat, and mouse kidneys, kAE1 is expressed almost entirely in the basolateral plasma membrane. In the rabbit kidney under basal conditions, kAE1 is present in intracytoplasmic multivesicular bodies, as well as in the basolateral plasma membrane; metabolic acidosis decreases intracellular kAE1 and increases basolateral kAE1, suggesting regulated trafficking contributes to bicarbonate reabsorption.⁴¹⁶

Several mutations in AE1 cause human autosomal dominant and autosomal recessive dRTA. Autosomal dominant dRTA can be caused by a trafficking defect leading either to mistargeting to the apical plasma membrane or failure of plasma membrane insertion.^{324,362} Autosomal recessive dRTA due to defective AE1 is commonly due to mutations that lead to intracellular protein retention.³⁸⁸

KCC4

KCC4 is a member of the SLC12 family of solute transporters and mediates electroneutral, coupled transport of K^+ and Cl^- . Basolateral KCC4 expression has been shown in the proximal convoluted tubule (PCT), TAL, DCT, CNT, and type A intercalated cells.^{41,412} In the type A intercalated cell, KCC4 likely contributes to basolateral Cl^- recycling. Metabolic acidosis increases KCC4 expression in type A intercalated cells in the OMCD, suggesting a role in the response to metabolic acidosis²⁶⁴ by facilitating basolateral $\text{Cl}^-/\text{HCO}_3^-$ exchange, and KCC4 deletion causes development of distal RTA,⁴¹ suggesting KCC4 is necessary for both basal and acidosis-stimulated acid-base homeostasis.

Cl^- Channel

Cl^- entry via basolateral kAE1 recycles across the basolateral plasma membrane. In addition to KCC4, the Cl^- channel, ClC-K2 , is present in the basolateral plasma membrane of type A intercalated cells and likely contributes to this recycling.²⁹⁶

Other Anion Exchangers

Several other anion transporters, including anion exchangers and sodium bicarbonate cotransporters (NBCs), are present in the collecting duct, but their roles in acid–base homeostasis are less completely understood. AE2 is expressed in collecting ducts, particularly in the basolateral plasma membrane of IMCD cells.¹²⁵ Another $\text{Cl}^-/\text{HCO}_3^-$ exchanger, Slc26a7, is found in the basolateral plasma membrane of OMCD intercalated cells.³⁰⁷ Slc26a7 mRNA and protein expression increases with acid loading, suggesting it may contribute to regulated bicarbonate reabsorption.³⁸⁴ AE4 (Slc4a9) is present in the collecting duct, but both its location and function are in question. Although originally thought to be an anion exchanger, other evidence suggests AE4 functions in type B intercalated cells as a NaHCO_3 cotransporter.⁷³ Studies of the rabbit kidney have variously reported that AE4 immunoreactivity is exclusively apical in type B intercalated cells,⁴⁰¹ apical and lateral in type A intercalated cells,²⁰⁹ and exclusively lateral in type B intercalated cells.³¹⁸ In both rat and mouse kidneys, only basolateral AE4 protein expression has been detected in both type A^{80,209} and type B intercalated cells.^{73,80,209} In the mouse, both mRNA and basolateral protein expression are significantly stronger in type B than in type A intercalated cells.⁸⁰

Sodium Bicarbonate Cotransporters

Several NBCs are expressed in the collecting duct. NBC3 (Slc4a7) is found in the apical region of OMCD intercalated cells and type A intercalated cells in the CCD and in the basolateral region of type B intercalated cells.^{221,320} It appears to contribute to intracellular pH regulation, but not to transepithelial bicarbonate transport.⁴⁸² NBCn1, another SLC4A7 gene product, is an electroneutral NBC, and basolateral expression is found in the terminal IMCD and in OMCD intercalated cells.³¹¹ Finally, recent evidence indicates AE4 (SLC4A9), discussed earlier, functions as a $\text{Na}^+\text{-HCO}_3^-$ cotransporter.⁷³

NBCe2 (SLC4A5)

The electrogenic, $\text{Na}^+\text{-HCO}_3^-$ cotransporter, isoform 2 (NBCe2, SLC4A5) appears to contribute to acid–base homeostasis, but its specific cellular expression remains unclear. An initial study suggested there was only apical expression in collecting duct intercalated cells in the CCD and OMCD,⁹⁵ whereas a different study identified NBCe2 in microdissected mouse CNT segments.⁴⁶⁶ Genetic deletion in one study induced metabolic acidosis,¹⁵⁰ whereas in a second study, NBCe2 deletion did not alter basal acid–base homeostasis, but did impair the ability to respond to exogenous acid loading.⁴⁶⁶ The mechanism through which NBCe2 contributes to acid–base homeostasis, given the evidence for its apical localization, is unclear. There is evidence that NBCe2 deletion leads to increased pendrin expression, which could, by increasing HCO_3^- secretion, contribute to the acid–base phenotype observed.⁹⁵ NBCe2 deletion is also associated with increased expression of the β_1 -subunit of $\text{H}^+\text{-ATPase}$, which may serve as an adaptive response that minimizes the extent of the acid–base disturbance.⁴⁶⁶ However, the possibility of additional mechanisms through which NBCe2 contributes to acid–base homeostasis cannot be excluded at present.

Other studies suggest NBCe2 is present in the proximal tubule, not the distal nephron. In a study examining the

human kidney under basal conditions, NBCe2 mRNA was found in the proximal tubule by *in situ* hybridization, and protein expression was observed in subcellular fractionation enriched for apical brush-border proteins.¹³⁵

REGULATION OF COLLECTING DUCT ACID–BASE TRANSPORT

The collecting duct is the final site controlling renal acid–base regulation. It responds quickly to physiologic conditions to increase acid or bicarbonate excretion as needed to maintain systemic acid–base homeostasis.

ACIDOSIS

The collecting duct response to metabolic acidosis includes adaptations in all segments of the collecting duct and the CNT. Increased acid secretion in the collecting duct during acidosis is mediated primarily by $\text{H}^+\text{-ATPase}$. Both metabolic and respiratory acidosis increase apical plasma membrane $\text{H}^+\text{-ATPase}$ expression and activity in acid-secreting collecting duct intercalated cells. Redistribution of $\text{H}^+\text{-ATPase}$ from a subapical vesicle pool to the apical plasma membrane is the primary means of activation of proton secretion, and involves vesicular trafficking that requires soluble NSF-attachment protein receptor (SNARE) proteins and Rab GTPases.^{102,425} In most models of metabolic acidosis, total renal $\text{H}^+\text{-ATPase}$ mRNA and protein expression do not change,^{379,425} but a study examining OMCD segments from acid-loaded mice found increased mRNA expression of several $\text{H}^+\text{-ATPase}$ subunits, including the B1 and a4 subunits.⁸²

During chronic metabolic acidosis, AE1 mRNA and AE1 protein expression in the basolateral plasma membrane in OMCD and CCD type A intercalated cells is increased.^{181,341} In rats and mice, AE1 is present in the basolateral plasma membrane under basal conditions, and the subcellular distribution does not change with metabolic acidosis.^{181,341} In rabbits fed a normal diet, AE1 is in both intracellular multivesicular bodies and the basolateral plasma membrane in type A intercalated cells. Metabolic acidosis increases the basolateral plasma membrane boundary length and the amount of AE1 immunoreactivity in the basolateral plasma membrane and reduces intracellular AE1.⁴¹⁶

During metabolic acidosis, both net HCO_3^- secretion and type B intercalated cell-mediated unidirectional HCO_3^- secretion decrease. This is associated with decreased pendrin expression in type B and non-A, non-B cells as well as decreased apical $\text{Cl}^-/\text{HCO}_3^-$ exchange activity in type B intercalated cells in the CCD.^{124,426,475} Reduced bicarbonate secretion by B cells during acid loading thus contributes to increased net bicarbonate reabsorption.

Carbonic anhydrase activity and the expression of CA II and CA IV in the collecting duct are increased by metabolic acidosis.³¹⁶ CA IV expression is upregulated in the OMCD, whereas CA II expression is upregulated in the CNT, CCD, and OMCD.

The collecting duct response to respiratory acidosis appears to be similar to that of metabolic acidosis. Respiratory acidosis stimulates structural changes in OMCD and CCD type A intercalated cells consistent with translocation of $\text{H}^+\text{-ATPase}$ -bearing membrane from the apical vesicle pool to the apical plasma membrane.⁴¹⁸ Respiratory acidosis also stimulates N-ethylmaleimide-sensitive ATPase activity, a measure of $\text{H}^+\text{-ATPase}$ activity^{106,425} and bicarbonate reabsorption in isolated

CCDs,²⁶² consistent with activation of H⁺-ATPase mediated proton secretion. In addition, chronic respiratory acidosis increases kAE1 mRNA.⁹⁴ Pendrin expression decreases during respiratory acidosis,⁹⁸ which likely mediates decreased bicarbonate secretion.

ALKALOSIS

Metabolic alkalosis induces coordinated changes in acid–base transport throughout the collecting duct. In the OMCD of bicarbonate-loaded animals, bicarbonate reabsorption is decreased compared with control animals²⁴⁵ and in the IMCD, bicarbonate loading abolishes acid secretion.³² In the CCD, bicarbonate loading in animals produces net bicarbonate secretion.²⁶¹ However, no studies have shown the development of HCO₃⁻ secretion by the OMCD or the IMCD in response to metabolic alkalosis, and this correlates with the lack of pendrin-expressing type B and non-A, non-B intercalated cells in these segments.

The cellular response to alkalosis in OMCD and CCD type A cells entails essentially the reverse of processes that occur to stimulate acid secretion. H⁺-ATPase is redistributed from the apical plasma membrane into the apical vesicle pool, and basolateral AE1 immunoreactivity decreases.^{26,341,417} Depending on the animal model, alkalosis increases pendrin expression and its apical distribution in type B and non-A, non-B intercalated cells and increases pendrin-mediated CCD bicarbonate secretion.^{124,426} However, pendrin expression, subcellular location, and functional activity are regulated by other factors independent of acid–base status, including pregnancy, aldosterone, AngII, activation of AT1a and AT1b receptors, nitric oxide, and cAMP,* in addition to chloride balance and luminal chloride delivery.^{321,415}

HORMONAL REGULATION OF COLLECTING DUCT ACID–BASE TRANSPORT

In addition to extracellular pH, multiple other factors regulate collecting duct acid–base transport. Importantly, in vivo acid–base changes cause greater adaptations than equivalent in vitro changes, suggesting that in vivo regulatory mechanisms mediate a critical role in the response to acid–base disturbances.¹³⁴ Several hormones and receptors regulate bicarbonate transport in the collecting duct, particularly aldosterone and its analogs, and AngII.

Aldosterone is an important regulator of collecting duct bicarbonate transport.³⁸¹ Both in vivo and in vitro mineralocorticoids increase OMCD bicarbonate reabsorption.³⁸¹ This involves, at least when studied in vitro, increased H⁺-ATPase activity and apical translocation in OMCD intercalated cells, stimulated through a non-genomic pathway not inhibited by mineralocorticoid receptor blockade.⁴⁷⁴ Mineralocorticoids also increase CCD bicarbonate secretion; this is dependent on luminal chloride, mediated by pendrin, and involves increased pendrin mRNA and protein expression and pendrin redistribution from cytoplasmic vesicles to the apical plasma membrane in type B intercalated cells.^{339,413} Likely because of parallel stimulation of both acid and bicarbonate secretion, mineralocorticoid therapy usually has modest effects on systemic acid–base homeostasis.

AngII exerts effects on the proximal tubule, TAL, DCT and collecting ducts. The collecting duct expresses apical

AT1 (AT1a) receptors in both principal cells and intercalated cells.³³⁸ In mouse OMCD and CCD, AngII in vitro increases H⁺-ATPase activity in acid-secreting intercalated cells by trafficking H⁺-ATPase to the apical plasma membrane.^{304,338} In mouse OMCD, AngII stimulates H⁺-ATPase activity through a G-protein–coupled phosphokinase C pathway.³³⁸ However, in other studies, in vivo and in vitro AngII decreased bicarbonate reabsorption in rat OMCD and in vitro AngII decreased H⁺-ATPase activity via AT1 receptors^{394,440}; this apparent discrepancy has not been resolved. AngII also increases pendrin-dependent Cl⁻ absorption,³⁰² apical Cl⁻/HCO₃⁻ exchange in type B intercalated cells,⁴⁵⁷ and pendrin protein expression in the apical plasma membrane in non-A, non-B intercalated cells in the CNT, an effect mediated through activation of the angiotensin type 1a receptor (Agtr1a).⁴¹⁴

Endothelin has important effects on collecting duct acid–base transport that are mediated partly by nitric oxide. Dietary protein intake stimulates urinary acidification through a process involving H⁺-ATPase activation, mediated by endothelin and nitric oxide.⁴⁶⁷ Endothelin-1 (ET-1) is synthesized by the collecting duct,^{364,383} and endothelin receptors A and B (ET-A and ET-B) are present in the collecting duct.²¹² ET-B activation regulates both type A and type B intercalated cell responses to metabolic acidosis.⁴⁰⁵

The CaSR is apical in IMCD cells and in type A intercalated cells³³¹ and mediates luminal Ca⁺²-stimulation of H⁺-ATPase.³³⁰ Luminal acidification stimulated by this pathway may inhibit calcium precipitation and minimize development of nephrolithiasis.³³⁰

Activation of the vasopressin type 1A (V1a) receptor is an additional regulatory mechanism. The V1a receptor is expressed in the medullary TAL (mTAL) and throughout the collecting duct,^{70,481} with expression in both intercalated cells and principal cells in the CCD and only in intercalated cells in the OMCD.⁷⁰ Metabolic acidosis increases V1a receptor expression in the mTAL and the OMCD in the inner stripe.^{70,389} Genetic deficiency of the V1a receptor causes development of type IV RTA and diminishes mineralocorticoid stimulation of H⁺-K⁺-ATPase and Rhcg.¹⁸⁷

Several other hormones and drugs also alter collecting duct acid–base transport. Kallikrein inhibits bicarbonate secretion.²⁵³ Calcitonin stimulates H⁺-ATPase-dependent bicarbonate reabsorption in the rabbit CCD.³⁶⁵ Isoproterenol stimulates bicarbonate secretion by type B intercalated cells.³⁵¹

PARACRINE REGULATION

Several compounds produced and/or transported in the proximal tubule and TAL have downstream effects that regulate collecting duct acid–base transport. Presumably, this enables these segments, which exist in an area with very high blood flow and thus rapid exposure to changes in systemic acid–base and potassium, to regulate transport in collecting duct segments in the outer medulla and inner medulla, sites of low blood flow and thus reduced exposure to changes in systemic acid–base and potassium homeostasis. The paracrine molecules most extensively studied are ammonia and alpha-ketoglutarate.

Ammonia, discussed in detail later regarding its role in net acid excretion, also appears to function as an intrarenal, paracrine signaling molecule that regulates collecting duct transport.⁴⁵¹ It is produced primarily in the proximal tubule and undergoes regulated transport in both the proximal

*References 302, 303, 393, 413, 414, 468.

tubule and the TAL in response to both acid loading and hypokalemia. In addition to its roles in bicarbonate generation, ammonia stimulates CCD bicarbonate reabsorption in a concentration-dependent fashion.¹²³ Ammonia stimulates type A intercalated cell acid secretion and inhibits type B intercalated cell bicarbonate secretion.^{121,123} Its stimulation of proton secretion involves stimulation of H⁺-K⁺-ATPase, not H⁺-ATPase, activity.^{122,123}

The Krebs cycle intermediate, 2-oxoglutarate (alpha-ketoglutarate), may have an important role in acid–base homeostasis. Changes in acid–base loading change the net direction of transport in the proximal tubule and the loop of Henle from reabsorption, seen with acid loading, to net secretion, seen with alkali loading.^{79,115,395} In the CNT and CCD, luminal 2-oxoglutarate enhances net bicarbonate and sodium chloride reabsorption, acting through its receptor, Oxgr1, in type B and non-A, non-B intercalated cells.³⁹⁵ Thus, 2-oxoglutarate can function as a paracrine mediator enabling functional coordination of the proximal tubule and the TAL with the collecting duct.

CELLULAR ADAPTATIONS TO ACID–BASE PERTURBATIONS

In addition to changes in the abundance and subcellular distribution of membrane transporters, adaptive responses to some physiologic disturbances may involve changes in the numbers of intercalated cells. Several studies have shown that chronic metabolic acidosis and chronic hypokalemia increase intercalated cell numbers in medullary collecting ducts,* whereas others find no change in intercalated cell number in these conditions.^{168,181,419} Chronic administration of lithium and acetazolamide also increases intercalated cell numbers in the OMCD.^{23,85,398}

Increases in intercalated cell numbers could result from intercalated cell proliferation or from principal cell proliferation followed by conversion into intercalated cells. Studies using proliferation markers show that metabolic acidosis, hypokalemia, and lithium administration are each associated with increased proliferation of collecting duct cells,^{84,297,465} some showing increased proliferation in type A intercalated cells,^{410,465} and others showing the proliferating cells are principal cells.^{84,202,297,398} The latter studies suggested that principal cells and OMCD intercalated cells may interconvert based on observations of rare cells with immunohistochemical and ultrastructural characteristics of both cell types^{84,297,398} and through genetic studies that irreversibly identify principal cells as cells that express genes under the control of the AQP2 promoter.²⁰² The histone H3 K79 methyltransferase, Dot1L, may be involved in preventing transformation of principal cells into intercalated cells; Dot1L deletion decreases the number of principal cells and increases the number of collecting duct intercalated cells.⁴⁷⁹ Other studies show that principal cells respond to acid by producing the cytokine SDF1, also known as CXCL12, which then acts on adjacent intercalated cells via its receptor, CXCR4.³⁵⁵ SDF1 is transcriptionally regulated and is a target of the hypoxia-sensing transcription factor HIF1 α in principal cells.³⁵⁵

With respect to the CCD, some studies suggested there may be interconversion of type A and type B intercalated cells. An early paper examining the rabbit isolated perfused

CCD equated apical endocytosis with alpha (type A) intercalated cells and used apical peanut lectin binding as a marker of beta (type B) intercalated cells. Chronic NH₄Cl loading in vivo increased the number of intercalated cells exhibiting apical endocytosis in microperfused CCDs and decreased the number of cells that bound peanut lectin; the interpretation was that intercalated cell subtypes in the CCD could interconvert, with the type B intercalated cells reversing polarity to meet the physiologic demand for increased acid secretion.³⁵³ Subsequently, some studies reported that acidosis, lithium administration, and carbonic anhydrase inhibition each alter the relative numbers of intercalated cells identifiable as type A or type B, although none have shown cells in native tissue with either apical AE1, basolateral pendrin, or coexpression of these two transporters.^{23,85,124,317,465} Other studies of acid–base disturbances find regulation of the abundance and distribution of transport proteins specific to the A and B intercalated cell types and changes in cell morphology, but no change in the relative or absolute numbers of specific intercalated cell subtypes.^{27,341,418,419} The explanation for these different findings could include differences in the experimental models, species examined, sensitivity and specificity of intercalated cell identification, and cell quantitation methods.

In vitro studies have implicated the extracellular matrix protein, hensin, and the prolyl isomerase activity of cyclophilin in the process of intercalated cell remodeling.^{354,387} In mice with intercalated cell-specific hensin deletion there is development of a distal RTA, lack of type A intercalated cells, and an increased number of type B intercalated cells.¹²⁷ Hensin's effects on type A intercalated cell development appears to require the activation of beta-1 integrin.¹²⁷

BICARBONATE GENERATION

Acid–base homeostasis requires not only reabsorption of filtered bicarbonate, but also the generation of new bicarbonate to replace the bicarbonate used for buffering of endogenous and exogenous fixed acids. There are two major components of bicarbonate generation, titratable acid excretion and ammonia excretion. In addition, organic anion excretion is biologically important. Organic anions can be metabolized to form HCO₃⁻; accordingly, their excretion is physiologically equivalent to bicarbonate excretion.

TITRATABLE ACID EXCRETION

Titratable acids are urinary solutes that buffer secreted protons, enabling H⁺ excretion without substantial changes in urine pH. Titratable acid excretion constitutes ~40% of net acid excretion under basal conditions. Metabolic acidosis increases titratable acid excretion by as much as 50% above baseline^{159,347} (Fig. 9.5).

Multiple buffers contribute to titratable acid excretion. An ideal urinary buffer has a pK_a lower than systemic pH, so that the majority of the filtered component is in the base form, and a pK_a higher than urine pH, so that the majority of the urinary form is in the acid form. Phosphate is the predominant titratable acid and typically accounts for more than 50% of total titratable acid.^{159,478} Citrate and creatinine also contribute to titratable acid excretion, but to a lesser

*References 23, 85, 297, 398, 410, and 465.

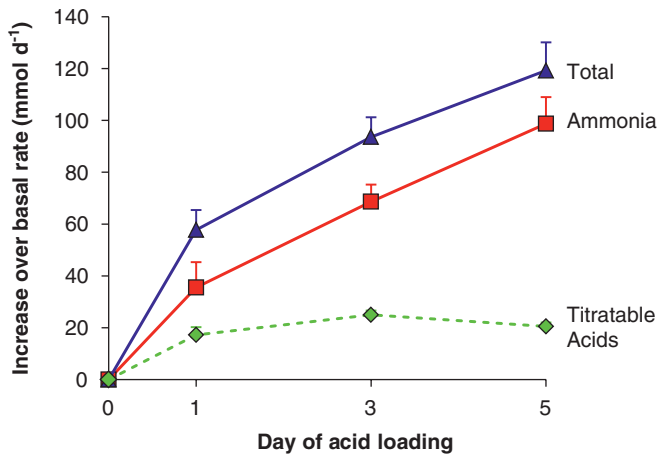


Fig. 9.5 Relative contribution of titratable acid and ammonia excretion in the response to metabolic acidosis. Normal human volunteers were acid-loaded with ~2 mmol/kg of ammonium chloride and changes in urinary ammonia and titratable acid excretion were quantified. Data recalculated from Elkinton et al.¹⁰⁹

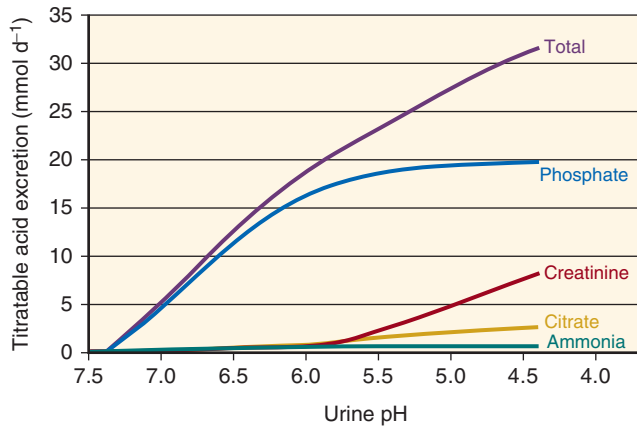


Fig. 9.6 Relative contribution of various urinary buffers to titratable acid excretion. Ability of various urinary buffers to contribute to titratable acid excretion depends on the amount excreted in the urine, their pK_a , and final urine pH. Figure shows titratable acid excretion accounted for by each of the four major urinary buffers, phosphate, creatinine, citrate, and ammonia, at differing urine pH. Rates were calculated with daily excretion rate and pK_a , respectively, for phosphate, 25 mmol/d and 6.8; creatinine, 11 mmol/d and 4.9; citrate, 3 mmol/d and 5.6; and ammonia, 40 mmol/d and 9.15.

extent. Although ammonia is frequently termed a urinary buffer, because of its high pK_a it does not contribute substantially to titratable acid excretion. The role of ammonia in new bicarbonate generation is considered separately later in the chapter. Fig. 9.6 shows the relative contributions of major urinary buffers to titratable acid excretion and shows the effect of changes in urine pH after taking into account the amount excreted under normal conditions and the pK_a of each buffer.

PHOSPHATE AS A TITRATABLE ACID

Titratable acid excretion in the form of phosphate is the amount of HPO_4^{2-} that is filtered, not reabsorbed, and that

buffers secreted H^+ , forming $H_2PO_4^-$. Phosphate exists, under physiologically relevant conditions, in equilibrium between two forms: $H_2PO_4^-$ and HPO_4^{2-} .² The relative amount of these two forms is given by

$$10^{pH-6.8} = \frac{[HPO_4^{2-}]}{[H_2PO_4^-]}$$

The amount of $H_2PO_4^-$ in the urine ($H_2PO_4^-_{Urine}$) at any given pH can be calculated as

$$H_2PO_4^-_{Urine} = \frac{U_{Phos}V}{10^{(pH_U-6.8)} + 1},$$

where U_{Phos} is the urinary concentration of total phosphate. Filtered phosphate, at the typical serum pH of 7.4, is ~80% in the form of HPO_4^{2-} and 20% in the form of $H_2PO_4^-$. Thus, at any urine pH (pH_U), titratable acid excretion in the form of phosphate (TA_{Phos}) is given by the formula

$$TA_{Phos} = U_{Phos}V * \left(\frac{1}{10^{(pH_U-6.8)} + 1} - 0.2 \right).$$

These considerations indicate that titratable acid excretion as phosphoric acid is determined by phosphate excretion and by the ability to lower urine pH. Phosphate excretion is determined by the difference between the filtered load of phosphate and tubular phosphate reabsorption. Regulation of renal tubular phosphate transport is a complex process and is discussed in detail elsewhere in this text. Here, we review only the factors that regulate this process in response to acid-base disorders.

The proximal tubule is the primary site of phosphate reabsorption and is where metabolic acidosis and other acid-base disorders regulate phosphate transport. Acid loading decreases proximal tubule phosphate reabsorption, leading to increased excretion. However, absolute changes in urinary phosphate excretion are usually rather modest, less than a twofold increase. The decrease involves decreased NaPi-IIa protein and mRNA expression and changes in its subcellular distribution.^{15,15,156} Acid loading alters NaPi-IIa expression even if the acid load is completely compensated and there are no changes in systemic pH, suggesting that factors that precede changes in systemic pH regulate this response.⁴²³ Metabolic acidosis also lowers luminal pH in the proximal tubule, which directly inhibits phosphate uptake.^{174,407} Finally, metabolic acidosis increases PTH release, which also inhibits phosphate reabsorption.

Other phosphate transporters besides NaPi-IIa, such as NaPi-IIc and Pit-2, are present in the proximal tubule apical plasma membrane. Whether NaPi-IIc changes with metabolic acidosis is unclear as some studies find decreased expression⁴²³ and others do not.²⁹² Pit-2 expression, although regulated by dietary phosphate availability, is not altered in metabolic acidosis in phosphate replete conditions, but does increase in response to metabolic acidosis in conditions of phosphate depletion.⁴²³

Acidosis-induced changes in phosphate excretion depend on systemic phosphate availability. In the presence of dietary phosphate restriction, basal phosphate excretion is reduced, and the increase in urinary phosphate excretion in response to metabolic acidosis is blunted.⁴²³ Similarly, changes in NaPi-IIa abundance are blunted.¹⁵ In contrast to NaPi-IIa, and to their response to metabolic acidosis in

phosphate-replete animals, NaPi-IIc and Pit-2 expression actually increase in phosphate-restricted animals exposed to metabolic acidosis.⁴²³

Increased renal phosphate excretion with metabolic acidosis is balanced by parallel increases in extrarenal phosphate transport. Metabolic acidosis increases small intestinal Na⁺-dependent phosphate transport, and this is associated with increased expression of NaPi-IIb.³⁷⁸ There is also increased phosphate release from bone in response to both acute and chronic metabolic acidosis.²³⁴ These extrarenal effects minimize the changes in systemic phosphate levels that could otherwise develop from the increased phosphate excretion.

OTHER URINARY BUFFERS

Creatinine, which is used typically to assess glomerular filtration, has a pK_a of ~4.9 and is excreted in sufficient amounts, ~11 mmol d⁻¹, that it can contribute to titratable acid excretion. This is particularly true in conditions when urinary pH is 5.5 or less.¹⁵⁹ Uric acid, although it can function as a buffer, is typically excreted in such small amounts, ~4 mmol d⁻¹, as to limit its role as a titratable acid. In ketoacidosis, β-hydroxybutyric acid and acetoacetic acid excretion increases, which increases titratable acid excretion. However, because ketoacids can be metabolized to bicarbonate, their loss in the urine has no net effect on acid–base homeostasis.

ORGANIC ANION EXCRETION

Multiple organic anions in the urine can contribute to acid–base homeostasis. At least 95 different urinary organic anions have been identified, and many, including hippuric, erythronic, threonic, tartaric, and uric acids, are excreted in substantial quantities.⁷² In general, their role in acid–base homeostasis is not as a titratable acid. Instead, because their metabolism produces bicarbonate, their excretion enables alkali excretion without altering urine pH.

CITRATE EXCRETION

Citrate plays an important role in both acid–base homeostasis and preventing calcium nephrolithiasis. The latter function relates to citrate's ability to form reversible, noncovalent complexes with urinary and luminal calcium, thereby decreasing ionized calcium and decreasing the rate of calcium deposition into renal stones. Citrate may also inhibit calcium oxalate nucleation by colloidal stabilization of early-stage calcium oxalate complexes.³⁴⁰ A complete description of citrate's role in nephrolithiasis can be found elsewhere in this text. In this chapter we discuss citrate's role in acid–base homeostasis.

Citrate has two roles in acid–base homeostasis: (1) as a urinary buffer contributing to titratable acid excretion, and (2) as a substrate in the tricarboxylic acid cycle. The two primary molecular forms of citrate, citrate⁻³ and citrate⁻², exist in equilibrium with each other:



The pK_a of this buffer reaction is ~6.4. Other molecular forms, citrate⁻¹ and citrate⁰, because of the pK_a of the appropriate buffer reactions, are at such sufficiently low concentrations that they appear to not be transported to a significant extent. Thus, at a normal physiologic pH of 7.4, ~91% of total citrate is in the form of citrate⁻³ and only ~9% is citrate⁻². Because

glomerular filtrate has a pH essentially identical to systemic arterial pH, essentially all filtered citrate is in the form of citrate⁻³. In contrast, only 29% of urinary citrate at a typical urine pH of ~6.0 is in the form of citrate⁻³, meaning that ~71% has been protonated and converted to citrate⁻². This difference in citrate⁻² between filtrate and final urine enables citrate to serve as a titratable acid (see Fig. 9.6).

The second mechanism through which citrate contributes to acid–base homeostasis relates to its function as a metabolic substrate for the tricarboxylic acid cycle. Its complete metabolism, as occurs in the proximal tubule, results in HCO₃⁻ generation. Thus, citrate excretion, which is the difference between its filtration and its reabsorption, with subsequent metabolism that forms HCO₃⁻, is functionally equivalent to HCO₃⁻ excretion. Citrate excretion thereby enables base excretion without altering urine pH, which may be beneficial for minimization of pH-dependent calcium nucleation and calcium-containing stone growth.

Multiple factors regulate renal citrate excretion. Metabolic acidosis decreases and alkalosis increases citrate excretion.²⁵ Hypokalemia reduces citrate excretion.^{2,120} This effect is likely independent of systemic pH. The carbonic anhydrase inhibitor, acetazolamide, and a high dietary intake of either NaCl or protein decrease citrate excretion.^{157,213} Lithium chloride administered at therapeutic doses in animal models increases citrate excretion,⁴² but studies in humans have not confirmed this finding.⁴³

Renal tubular citrate transport is the primary determinant of citrate excretion. In humans, plasma citrate levels average ~0.1 mM, and changes in plasma levels are not an important regulatory mechanism. The proximal tubule reabsorbs a variable proportion, typically 65%–90%, of filtered citrate, and reabsorption parallels the filtered load. Citrate transported into proximal tubule cells, whether across apical or basolateral plasma membranes, is fully metabolized, enabling citrate to serve as a significant component of renal oxidative metabolism.¹⁵⁷ There does not appear to be significant transepithelial citrate transport, and there does not appear to be significant citrate transport in other renal sites.

Apical citrate transport is mediated primarily by the sodium–dicarboxylate cotransporter, NaDC1, an integral membrane protein highly expressed in the apical plasma membrane in the proximal tubule.^{223,294,357} This conclusion is based on the finding that NaDC1 expression parallels citrate reabsorption in metabolic acidosis,¹⁷ by the similarity of NaDC1 transport activity to the transport activity identified in brush border membrane vesicles,^{294,357} and by results of NaDC1 gene deletion studies. Specifically, NaDC1 deletion increases citrate excretion, along with excretion of several other Krebs cycle intermediates known to be transported by NaDC1.¹⁷¹

However, NaDC1 may not be the only protein involved in filtered citrate reabsorption. Preliminary studies report the presence of a residual citrate reabsorption process in NaDC1-knockout mice.³⁹² This additional citrate transport activity may be the calcium-regulated transport activity that has been identified in cultured proximal tubule cells.^{171,172} At present, the gene and gene product responsible for this citrate transport activity have not been identified.

Multiple mechanisms regulate proximal tubule citrate transport. First, the transported citrate form is citrate⁻², not citrate⁻³. Because the pK_a of the citrate buffer reaction is 6.4, luminal acidification, resulting from increased apical H⁺

secretion, directly increases luminal citrate⁻² concentration, which increases citrate reabsorption. Because many conditions stimulate luminal acidification, this provides a mechanism to increase filtered citrate reabsorption without altering the number or activity of citrate transporters. Second, metabolic acidosis increases apical citrate transport capacity,¹⁹⁰ most likely by increasing NaDC-1 expression.¹⁷ Both hypokalemia and starvation decrease citrate excretion, likely through stimulation of proximal tubule citrate transport.^{236,472} Several cellular signaling proteins regulate NaDC1. One is the calcineurin inhibitor target protein, cyclophilin,³³ which likely mediates the effects of calcineurin inhibitors to increase citrate reabsorption.³⁷⁵ Others include protein kinase C, sodium–hydrogen exchanger regulating factor 2, serum and glucocorticoid-inducible kinase, and protein kinase B.^{40,295} Finally, recent studies have implicated the proximal tubule basolateral bicarbonate transporter, NBCe1, as a critical determinant of NaDC1 expression.²⁹³

Basolateral citrate transport in the proximal tubule has different characteristics than apical transport. Uptake is pH-independent, Na⁺-dependent, and electroneutral, appears to involve 3 Na⁺ and 1 citrate⁻,^{157,191} and appears to be mediated by NaDC3.⁵⁹ Approximately 20% of proximal tubule citrate uptake appears to be mediated by basolateral uptake. However, because the proximal tubule does not secrete citrate, basolateral citrate uptake does not regulate renal citrate excretion.

OTHER ORGANIC ANIONS

Humans excrete 26–52 mEq d⁻¹ of organic anions other than citrate. Because organic anions can be metabolized to bicarbonate, organic anion excretion is functionally equivalent to alkali excretion and thereby can contribute to acid–base regulation. The extent of change in these organic anions with acid–base disturbances is not clear. Some studies show acid or alkali loading does not alter urinary organic anion excretion,²³⁵ whereas other studies show alkali loading increases and acid loading decreases organic anion excretion.¹⁷⁷

Quantitatively, there are important species-dependent differences in the magnitude of organic anion excretion. In humans, basal organic anion excretion averages 0.3–0.7 mEq kg⁻¹ d⁻¹,²³⁵ whereas in the rat organic anion excretion is 2–8 mEq kg⁻¹ d⁻¹.^{56,333} Studies in the dog report 1–2 mEq kg⁻¹ d⁻¹²⁹⁰ and in the rabbit average 4 mEq kg⁻¹ d⁻¹.³³³ This species-dependent variation may in part reflect differences in intestinal organic anion absorption³³³ or in the intestinal biome.

AMMONIA METABOLISM

Renal ammonia metabolism and transport is a predominant mechanism of the renal response to most acid–base disorders (see Fig. 9.5). Ammonia metabolism involves integrated function of multiple portions of the kidney. Only a minimal amount of urinary ammonia derives from glomerular filtration, making urinary ammonia excretion unique among the major compounds present in the urine. Instead, the kidney produces ammonia, which is then selectively transported either into the urine or the renal vein, where it is transported to the systemic circulation. Importantly, renal vein ammonia content exceeds arterial content, indicating the kidney is a net producer of ammonia, even when there is significant

urinary ammonia excretion. Selective ammonia transport involves integrated transport in the proximal tubule, TAL of the loop of Henle, and the collecting duct (Fig. 9.7).

AMMONIA CHEMISTRY

Ammonia exists in two molecular forms, NH₃ and NH₄⁺. The relative amounts of each are governed by the buffer reaction: NH₃ + H⁺ ↔ NH₄⁺. This reaction occurs essentially instantaneously and has a pK_a under biologically relevant conditions of ~9.15. Accordingly, the majority of ammonia is present as NH₄⁺; at pH 7.4 only ~1.7% is present as NH₃. Because most biological fluids exist at a pH substantially below this pK_a, small changes in pH cause exponential changes in NH₃ concentration, but almost no change in NH₄⁺ concentration (Fig. 9.8).

NH₃, although uncharged, has an asymmetric arrangement of positively charged hydrogen nuclei around a central nitrogen; this results in significant polarity (Fig. 9.9). As a consequence, NH₃ has limited lipid permeability. Consequently, diffusion across plasma membranes is limited, and NH₃ transporters both accelerate NH₃ transport and provide important regulatory control.

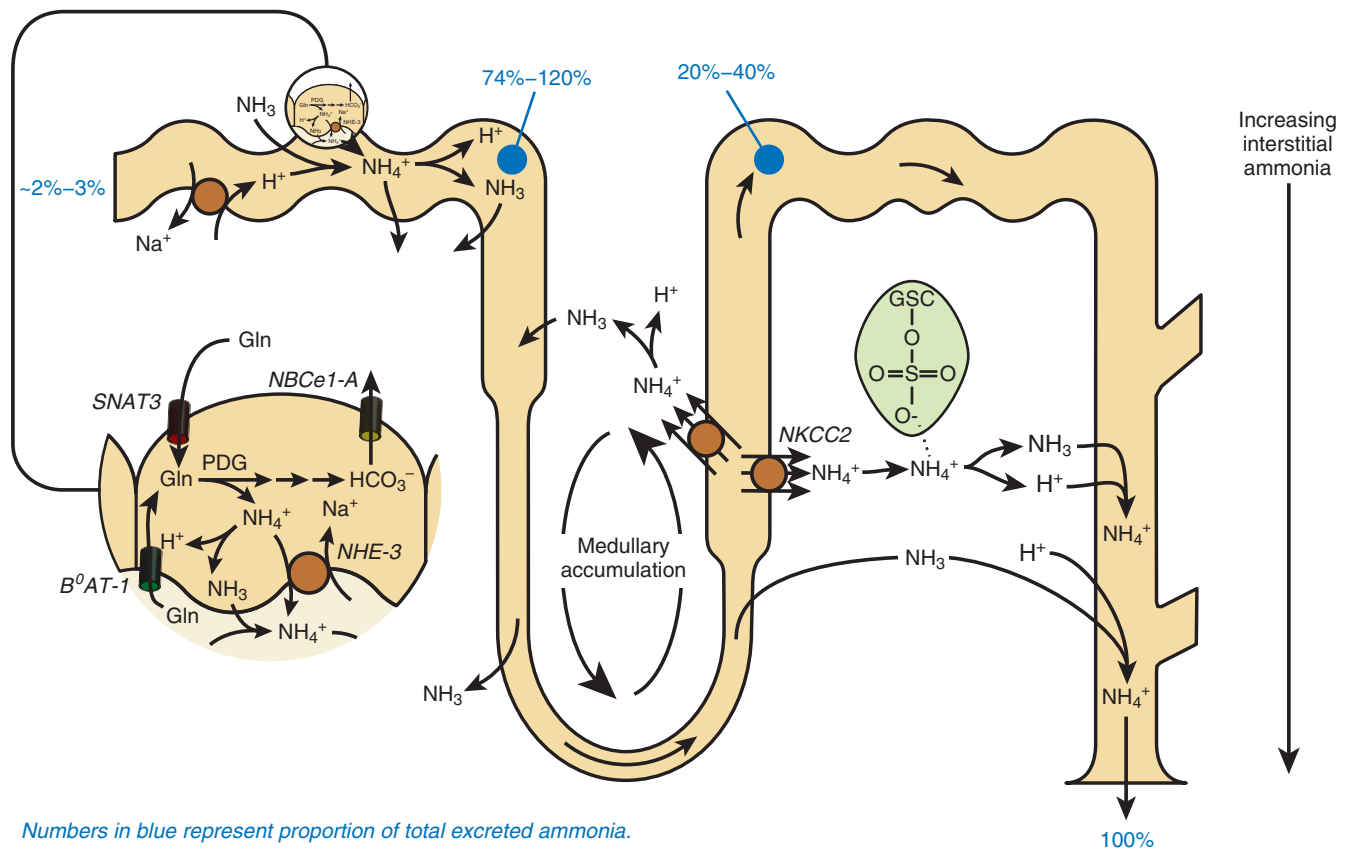
NH₄⁺ also has limited permeability across lipid bilayers in the absence of specific transport proteins. However, in aqueous solutions NH₄⁺ and K⁺ have nearly identical biophysical characteristics, which enables NH₄⁺ to be transported at the K⁺-transport site of essentially all K⁺ transporters.⁴⁵³ Several Na⁺/H⁺ exchanger (NHE) family members also appear to transport NH₄⁺ at the H⁺ binding site, resulting in Na⁺/NH₄⁺ exchange activity.

AMMONIA PRODUCTION

Almost all renal epithelial cells can produce ammonia, but the proximal tubule is the primary site for physiologically relevant ammoniogenesis.¹⁴³ The renal isoform of glutaminase (KGA), also known as phosphate-dependent glutaminase (PDG), is involved in this process.⁹¹ The proximal tubule accounts for 60%–70% of total renal ammonia production under basal conditions and at least 70%–80% in response to metabolic acidosis¹⁴³ (Fig. 9.10).

Although multiple pathways for ammoniogenesis are present in the proximal tubule (Fig. 9.11), the predominant pathway involves PDG.^{92,461} PDG is an inner mitochondrial membrane-bound enzyme that metabolizes glutamine to glutamate, producing NH₄⁺. Glutamate then undergoes further metabolism through multiple pathways. The major pathways involve glutamate dehydrogenase (GDH) with production of α-ketoglutarate (α-KG, also known as 2-oxoglutarate) and release of NH₄⁺. GDH-mediated metabolism is regulated in parallel with changes in total renal ammoniogenesis. Because glutamate is a negative regulator of PDG activity, changes in GDH activity, by changing mitochondrial glutamate levels, indirectly regulates PDG functional activity.

Glutamate can be converted back to glutamine via the enzyme glutamine synthetase. This reaction uses NH₄⁺ as a cosubstrate, decreasing net NH₄⁺ formation. Glutamine synthetase is expressed in the proximal tubule and in intercalated cells, and its expression decreases in response to metabolic acidosis^{88,226} and, in the proximal tubule, with hypokalemia.⁴²² Dietary protein restriction, which decreases ammonia excretion, increases glutamine synthetase expression, likely resulting in increased ammonia recycling and thereby



Numbers in blue represent proportion of total excreted ammonia.

Fig. 9.7 Integrated overview of renal ammonia metabolism. Renal ammoniagenesis occurs primarily in the proximal tubule, involving glutamine uptake by SNAT3 (SN1) and B⁰AT-1, glutamine metabolism forming ammonium and bicarbonate, and apical NH₄⁺ secretion involving NHE3 and parallel H⁺ and NH₃ transport. Ammonia reabsorption in the thick ascending limb, involving apical NKCC2-mediated uptake, results in medullary ammonia accumulation. Medullary sulfatides (*highlighted in green*) reversibly bind NH₄⁺, contributing to medullary accumulation. Ammonia is secreted in the collecting duct via parallel H⁺ and NH₃ secretion. Numbers in blue represent the proportion of total excreted ammonia at each location. GSC, Galactosylceramide backbone.

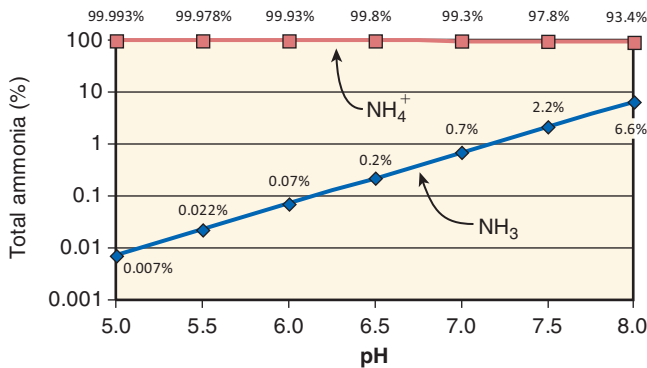


Fig. 9.8 Relative changes in NH₃ and NH₄⁺ concentration as pH changes. NH₃ and NH₄⁺ contributions to total ammonia were determined from the buffer reaction, NH₃ + H⁺ ↔ NH₄⁺. A pK_a of 9.15 was used for calculations. Amounts shown are proportion of total ammonia present as NH₃ and NH₄⁺. Note that the y-axis log transformed. Reprinted from Weiner ID, JW Verlander. Renal ammonia metabolism and transport. *Compr. Physiol.* 2013;3:201–220 with permission.

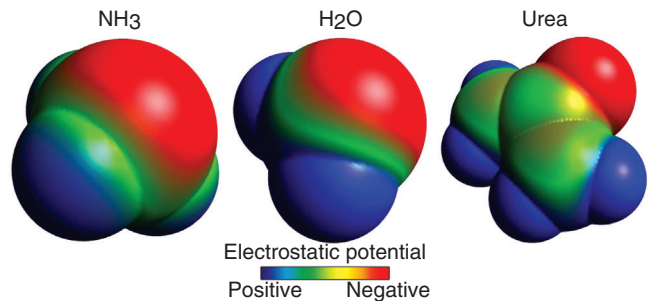


Fig. 9.9 Electrostatic charge distribution in NH₃, H₂O, and urea molecules. Models of NH₃, H₂O, and urea showing space-filling representation and surface pseudocolored to show surface charge. Each molecule, although an uncharged molecule, is polar. This polarity results in limited permeability across plasma membranes. Models generated using Avogadro software (Avogadro Chemistry, Inc.) v1.0.3.

diminishing net ammoniagenesis. Proximal tubule-specific glutamine synthetase deletion blunts the decrease in ammonia excretion in response to dietary protein restriction.²²⁷ Thus, glutamine synthetase-mediated ammonia recycling, which exhibits regulation counter to that of PDG in conditions

that alter ammonia excretion, is an important component of renal ammonia metabolism.

α-KG can be metabolized through α-KG dehydrogenase and succinate dehydrogenase to form oxaloacetic acid (OAA). OAA can serve as a substrate for phosphoenolpyruvate carboxykinase (PEPCK) to form phosphoenolpyruvate (PEP), which can be used as a substrate for gluconeogenesis.

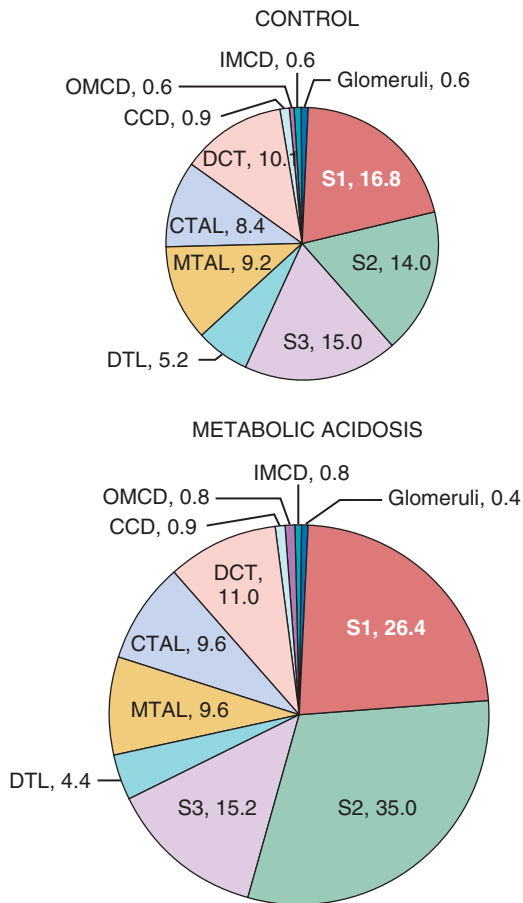


Fig. 9.10 Ammonia production in various renal segments. Ammonia production rates in different renal components measured in microdissected components from rats on control diets and after inducing metabolic acidosis. All segments tested produced ammonia. Metabolic acidosis increases total renal ammoniogenesis, but only through increased production in proximal tubule segments (S1, S2, and S3). Rates (pmol/mm) were calculated from measured ammonia production rates and mean length per segment as described in Good and Burg.¹⁴³ The size of the pie graph is proportional to total renal ammoniogenesis rates. CCD, Cortical collecting duct; CTAL, cortical thick ascending limb of Henle loop; DCT, distal convoluted tubule; DTL, descending thin limb of Henle loop; IMCD, inner medullary collecting duct; MTAL, medullary thick ascending limb of Henle loop; OMCD, outer medullary collecting duct.

Conditions that increase ammonia increase flux through this pathway and stimulate renal gluconeogenesis. Alternatively, PEP can be converted to pyruvate in an ATP-dependent reaction by pyruvate kinase. Pyruvate can then enter the TCA cycle, where its metabolism leads to ATP generation. The net result is that complete glutamine metabolism results in production of 2 NH_4^+ and 2 HCO_3^- molecules per glutamine molecule in association with a variable extent of glucose production. Conversion of PEP to pyruvate with subsequent entry into the TCA cycle results in more ATP production than utilization of PEP for gluconeogenesis.⁴⁵⁸

GLUTAMINE TRANSPORT IN AMMONIAGENESIS

Glutamine is the primary substrate for renal ammoniogenesis. Under normal acid–base balance conditions, the kidneys

extract less than 3% of the glutamine present in arterial blood flow to the kidneys. Acute metabolic acidosis induces a rapid, ~twofold increase in plasma glutamine levels; this results primarily from increased skeletal muscle and hepatic glutamine release.³⁹⁰ In parallel, renal glutamine uptake increases to as much as 20% of delivered glutamine.^{182,390} With chronic metabolic acidosis, renal extraction can increase to as much as 50% of delivered glutamine.¹⁸² Because glutamine uptake can exceed filtered glutamine, the presence of and ability to increase basolateral glutamine uptake is an important component of the regulation of ammoniogenesis.

Filtered glutamine is almost completely reabsorbed in the PCT.³⁶⁶ Multiple glutamine transporters are expressed in the apical membrane in the proximal tubule, including the Na^+ -dependent neutral amino acid transporters $\text{B}^0\text{AT1}$ (SLC6A19) and $\text{B}^0\text{AT3}$ (SLC6A18). Under basal conditions, luminal glutamine reabsorbed in the proximal tubule not used for ammoniogenesis can be transported across the basolateral plasma membrane. This appears to involve LAT2-4F2hc (SLC7A8-SLC3A2) and $\text{Y}^+\text{LAT1-4F2hc}$ (SLC7A7-SLC3A2).^{29,308,337} LAT2-4F2hc and $\text{Y}^+\text{LAT1-4F2hc}$ are obligatory amino acid exchangers, and the amino acid transported into the cell likely exits via basolateral TAT1 (Slc16a10), a facilitated aromatic amino acid transporter.^{29,325,326}

Basolateral glutamine uptake into proximal tubule cells appears to occur through the Na^+ -coupled, neutral amino acid transporter, SN1 (SLC38A3, also known as SNAT3).¹⁹⁶ Under basal conditions, basolateral SN1 is detectable only in the S3 proximal tubule segments, conditions that increase ammoniogenesis, such as metabolic acidosis and hypokalemia, increase S3 segment expression and induce expression in the S2 proximal tubule segment.^{62,269}

Because the initial enzyme involved in ammonia, PDG, is a mitochondrial enzyme, glutamine movement across the mitochondrial membrane is necessary. This process involves a specific transporter-mediated mechanism, is trans-stimulated and cis-inhibited by alanine, and is stimulated by metabolic acidosis.³⁴⁸ The gene and the gene product that mediate this activity are unknown at present.

AMMONIA TRANSPORT

Ammonia produced in the proximal tubule is secreted preferentially into the tubule lumen. Preferential apical secretion is due to multiple factors, including NHE3-mediated $\text{Na}^+/\text{NH}_4^+$ exchange and luminal acidification, which facilitates “trapping” of secreted NH_3 as NH_4^+ .^{275,368} However, a recent study examining the effect of proximal tubule NHE3 deletion on acid–base homeostasis found no alteration in renal ammonia excretion.²³⁸

The proximal tubule also can reabsorb luminal ammonia; this appears to occur primarily in the late proximal tubule.¹⁶⁰ These portions of the proximal tubule express glutamine synthetase, which catalyzes the reaction of NH_4^+ with glutamate to form glutamine.⁵⁷ Metabolic acidosis converts late proximal tubule ammonia transport from net reabsorption to net secretion¹⁶⁰; the molecular mechanisms that underlie this conversion involve decreased glutamine synthetase-mediated NH_4^+ metabolism.^{88,329}

The TAL reabsorbs luminal ammonia. The apical $\text{Na}^+\text{-K}^+\text{-2Cl}^-$ cotransporter, NKCC2, mediates the majority of ammonia reabsorption.¹⁹ Metabolic acidosis increases both TAL ammonia reabsorption and NKCC2 expression.²⁰ Intracellular

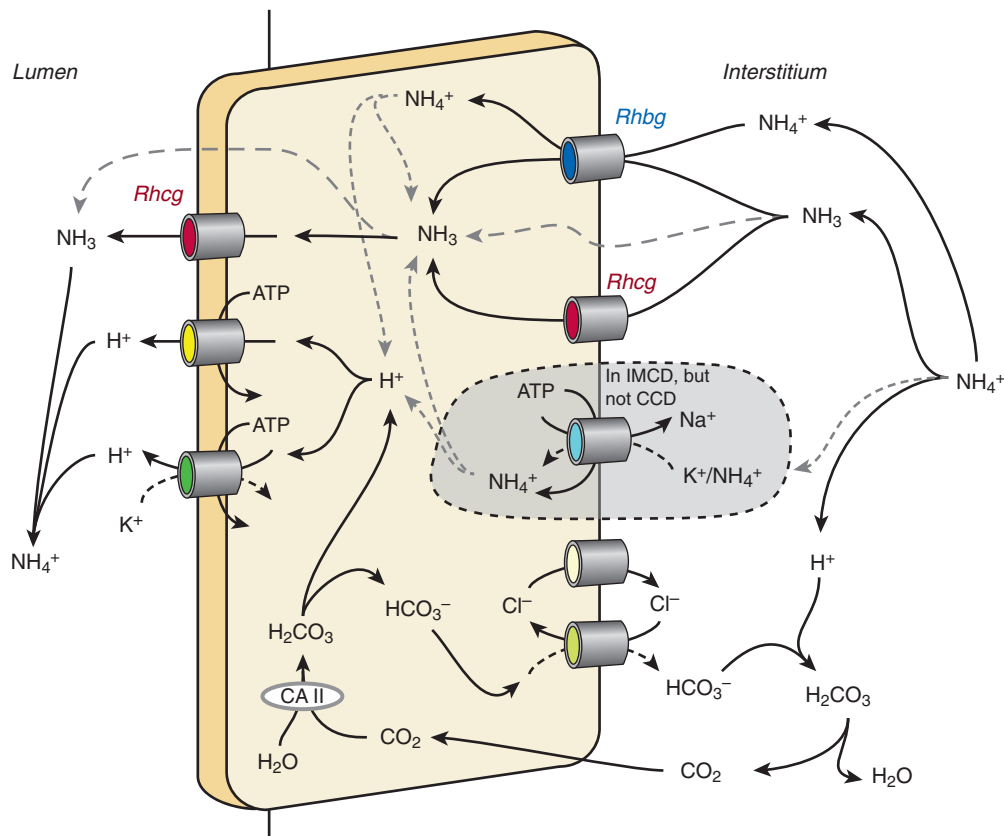


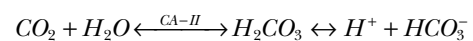
Fig. 9.12 Mechanisms of collecting duct ammonia secretion. Rhbg and Rhcg likely both contribute to basolateral ammonia uptake. As described in the text, whether Rhbg transports ammonia in the molecular form of NH_4^+ or NH_3 , or even both, remains controversial, but the likely electrochemical gradients result in uptake of both ammonia molecular species across the basolateral membrane. Rhcg mediates electroneutral NH_3 uptake across the basolateral plasma membrane. NH_3 is then secreted across the apical plasma membrane down its electrochemical gradient through processes involving both apical Rhcg transport and through a separate, undefined mechanism that may reflect lipid-phase diffusion. H^+ ions are secreted across the apical plasma membrane by both H^+ -ATPase and H^+ - K^+ -ATPase. Cytoplasmic H^+ is supplied either by dissociation of NH_4^+ or via a carbonic anhydrase II (CA II)-dependent bicarbonate shuttle mechanism involving basolateral chloride–bicarbonate exchange and basolateral chloride channel—mediated bicarbonate shuttling. Also shown is NH_4^+ uptake by basolateral Na^+ - K^+ -ATPase, which contributes to ammonia secretion in the IMCD where the majority of cells do not express Rh glycoproteins. IMCD, Inner medullary collecting duct.

collecting duct location. In the CCD and OMCD, the Rhesus glycoproteins, Rhbg (SLC42A2) and Rhcg (SLC42A3), appear to be the primary transport mechanisms. A hyperpolarization-activated cyclic nucleotide-gated HCN2 channel may also enable basolateral NH_4^+ uptake.⁷¹ In the IMCD basolateral Na^+ - K^+ -ATPase contributes to basolateral NH_4^+ uptake.^{428,429,438} In contrast, in the CCD inhibiting Na^+ - K^+ -ATPase does not alter ammonia secretion, suggesting either that it is uninvolved in ammonia secretion in this region of the collecting duct or that other transport mechanisms compensate when it is inhibited.²⁰⁷ Another possible NH_4^+ transport mechanism involves NKCC1. Basolateral NKCC1, which can transport NH_4^+ at the K^+ binding site, is present in both OMCD intercalated cells and IMCD cells.^{136,193} However, inhibiting NKCC1 does not alter OMCD ammonia secretion, suggesting either NKCC1 does not contribute to transepithelial ammonia secretion or that alternative transport mechanisms compensate in its absence.⁴³⁰ There may also be a component of NH_3 -gradient driven, diffusive NH_3 uptake, at least as has been identified in cultured IMCD cells.¹⁶⁵

Apical ammonia secretion appears to occur only by NH_3 movement. The primary protein involved is Rhcg. In studies

of CCD and OMCD from acid-loaded mice examined with *in vitro* microperfusion, Rhcg deletion decreased apical NH_3 transport by ~65%.³⁷ A significant component of the remaining NH_3 permeability may involve diffusive NH_3 transport.¹⁶⁶ Additionally, some studies have raised the possibility that, at least in response to dietary K^+ restriction, the colonic isoform of H^+ - K^+ -ATPase, HK α 2, secretes NH_4^+ .²⁸²

A substantial component of collecting duct ammonia secretion appears to involve cytosolic HCO_3^- production by CA II. Studies using microperfused collecting duct segments show that inhibiting CA-II essentially abolishes ammonia secretion.⁴³⁰ Presumably, CA II-mediated acceleration of the reaction



provides the H^+ needed for the apical H^+ secretion. The HCO_3^- is transported across the basolateral plasma membrane, in most cases likely by a basolateral $\text{Cl}^-/\text{HCO}_3^-$ exchanger. This results either in the generation of “new” HCO_3^- or, if cytosolic NH_3 resulted from basolateral NH_3 uptake, buffering of the H^+ released from NH_4^+ as a result of the decrease in peritubular NH_3 concentration.

The absence or presence of carbonic anhydrase activity at the apical membrane also impacts collecting duct ammonia secretion. In the absence of luminal carbonic anhydrase, H⁺ secretion increases the luminal [H⁺] above equilibrium because of relatively slow spontaneous dehydration of H₂CO₃ to CO₂ and H₂O. This is termed a luminal “disequilibrium pH.” This increased luminal acidification shifts the H⁺ + NH₃ ↔ NH₄⁺ reaction toward NH₄⁺, thereby decreasing luminal [NH₃]. The decreased luminal [NH₃] increases the gradient for NH₃ secretion and increases net ammonia secretion. A luminal disequilibrium pH has been found and shown to accelerate ammonia secretion in the rat OMCD and terminal IMCD^{119,432} and in the rabbit CCD and OMCD_o,^{207,376,377} but not in the rabbit OMCDi.³⁷⁶

SPECIFIC PROTEINS INVOLVED IN RENAL AMMONIA METABOLISM

Phosphate-Dependent Glutaminase

PDG is the initial enzymatic step in renal ammoniogenesis. It is located in mitochondria and catalyzes the reaction, L-glutamine + H₂O → L-glutamate + NH₄⁺. In the kidney, PDG activity is found primarily in the proximal tubule, although a lesser degree of activity is found in essentially all renal epithelial cells.^{91,197,477} The physiologic role of this activity outside of the proximal tubule is unclear. Some studies have found that metabolic acidosis increases PDG activity in the DTL, mTAL in the outer stripe, and DCT,¹⁹⁷ whereas others have found no change in activity in sites other than the proximal tubule.⁴⁷⁷ Quantitative analyses suggest that the proximal tubule is the primary site of ammonia production, and accounts for the majority of the increase in ammoniogenesis with metabolic acidosis.^{92,461}

Multiple PDG isoforms exist. In humans, the gene for the kidney-type isoform gives rise to at least two transcripts, human kidney-type glutaminase (KGA) and the glutaminase C splice variant (GAC).²⁵⁵ A separate gene gives rise to a liver-type glutaminase isoform (LGA). The KGA protein is expressed ubiquitously in the kidney, including the renal proximal tubule, and is the source of the majority of renal PDG.

Metabolic acidosis increases proximal tubule PDG activity; these increases derive from multiple mechanisms. There is increased protein expression, and this appears to be transcriptionally mediated.^{396,397} The increase in PDG mRNA results from mRNA stabilization, not increased transcription rates.¹⁸⁵ A second regulatory mechanism likely involves changes in intra-mitochondrial glutamate. Glutamate is a competitive inhibitor of PDG,³⁶⁰ and decreases in intra-mitochondrial glutamate concentration, which occur during metabolic acidosis as a consequence of increased glutamate dehydrogenase activity, increase PDG activity.³

Glutamate Dehydrogenase (GDH)

GDH is a mitochondrial enzyme that catalyzes the reaction, L-glutamate + H₂O + NAD⁺ (or NADP⁺) → α-KG⁻² + NH₄⁺ + NADH (or NADPH) + H⁺. Two GDH isoforms exist and are products of two different genes; GLUD1 is widely expressed, including in the kidney, whereas GLUD2 appears to be a neural and testicular-specific isoform.^{257,361}

Metabolic acidosis stimulates renal GDH activity,⁴⁷⁶ both by altering its affinity for glutamate and by increasing protein and mRNA (GLUD1) expression.^{3,90,93} Acidosis also decreases

intramitochondrial α-ketoglutarate (α-KG) concentration, which contributes to increased GDH activity.³⁶⁰ Decreased α-KG accelerates GDH activity by relieving α-KG-mediated competitive inhibition of the enzymatic reaction and by inhibiting the reverse reaction.^{349,350} Changes in mRNA expression occur through changes in mRNA stability, not transcription rate.¹⁹²

Phosphoenolpyruvate Carboxykinase (PEPCK)

Renal PEPCK is a cytosolic enzyme that is the product of the PCK1 gene. In the kidney, as in extrarenal sites, including liver, adipose tissue, and small intestine, PEPCK is a key enzyme in gluconeogenesis through its role in conversion of oxaloacetate into PEP and CO₂. It also mediates an important role in the renal response to metabolic acidosis,⁵⁸ coincident with increased renal gluconeogenesis. The adaptive increase in PEPCK activity and protein expression result from increased protein synthesis and mRNA expression.⁹⁰ In contrast to PDG and GDH, the increased PEPCK mRNA expression appears to result from increased gene transcription.¹⁶⁹

γ-GT

γ-GT accounts for phosphate-independent glutaminase activity identified in many early enzymatic studies of renal ammoniogenesis. However, γ-GT is expressed primarily in the proximal straight tubule (PST),⁹¹ and micropuncture studies suggest that glutamine is completely reabsorbed in the PCT, making PST ammoniogenesis via γ-GT unlikely to contribute significantly to renal ammoniogenesis.

NHE3

Multiple lines of evidence suggest that the apical Na⁺/H⁺ exchanger, NHE3, secretes NH₄⁺ through binding of NH₄⁺ at the H⁺ binding site. These data include evidence that proximal tubule brush border membrane vesicles exhibit NH₄⁺/Na⁺ exchange activity,²⁰⁴ that combining a low luminal Na⁺ concentration with Na⁺/H⁺ exchange inhibitor, amiloride, decreases ammonia secretion;²⁷⁴ and that the Na⁺/H⁺ exchange inhibitor, EIPA, blunts ammonia secretion when alternative secretory pathways are blocked.³⁶⁸ Against a role of NHE3 in ammonia secretion, however, is that proximal tubule-specific NHE3 deletion does not alter either basal or acidosis-stimulated ammonia excretion.²³⁸

Changes in NHE3 expression and activity during metabolic acidosis may be an important component of ammonia regulation and may be regulated by AngII and ET-1. Specific studies show that NHE3 expression and activity parallel changes in ammonia secretion in response to chronic metabolic acidosis, changes in extracellular potassium and exposure to AngII.^{16,110,276,280} In S2 and S3 segments, chronic metabolic acidosis increases AT1 receptor-mediated stimulation of NHE3.^{277,278,281} ET-1 expression increases during metabolic acidosis and subsequent activation of the ET-B receptor increases NHE3 expression and renal ammonia excretion.²²²

NHE3 is also present in the apical plasma membrane of the TAL. However, because NHE3 secretes NH₄⁺ and the TAL reabsorbs NH₄⁺, NHE3 appears unlikely to mediate an important role in loop of Henle ammonia transport.

POTASSIUM CHANNELS

At a molecular level, K⁺ and NH₄⁺ have nearly identical biophysical characteristics. This enables essentially all K⁺

transporters to also transport NH_4^+ , albeit at transport rates that are often 10%–20% of that observed for K^+ .⁴⁵³ The primary evidence that apical K^+ channels contribute to proximal tubule ammonia transport comes from in vitro microperfusion studies showing that barium, a nonspecific K^+ channel inhibitor, inhibits proximal tubule ammonia transport.³⁶⁸ Multiple K^+ channels are present in the apical plasma membrane of the proximal tubule, including KCNA10, TWIK-1, and KCNQ1; it is not known currently which of these mediates ammonia transport. In the TAL, K^+ channels can contribute to luminal NH_4^+ uptake when apical $\text{Na}^+\text{-K}^+\text{-2Cl}^-$ cotransport is inhibited.¹⁹ However, NKCC2 inhibitors completely inhibit TAL ammonia transport, suggesting that apical K^+ channels are unlikely to mediate a quantitatively important role in TAL ammonia transport.¹⁴²

$\text{Na}^+\text{-K}^+\text{-2Cl}^-$ Cotransport

NKCC1 (SLC12A2), also known as $\text{Na}^+\text{-K}^+\text{-2Cl}^-$ cotransporter, isoform 1, is present in the basolateral plasma membrane of intercalated cells in the OMCD and IMCD and in IMCD cells.^{83,136,193} However pharmacologic inhibitors do not alter either OMCD ammonia secretion or IMCD basolateral ammonia uptake.^{429,430} Thus, NKCC1 appears unlikely to mediate a substantial role in ammonia secretion.

NKCC2 (SLC12A1), also known as $\text{Na}^+\text{-K}^+\text{-2Cl}^-$ cotransporter, isoform 2, is a kidney-specific isoform expressed in the apical plasma membrane of the TAL and is the major mechanism for ammonia reabsorption in the TAL of the loop of Henle.¹⁴² Luminal NH_4^+ competes for binding with K^+ to the K^+ -transport site, enabling alterations in luminal K^+ in hypokalemia and in hyperkalemia to alter net NH_4^+ transport and leading to alterations in medullary interstitial ammonia concentration in conditions of altered potassium homeostasis. Metabolic acidosis increases NKCC2 expression, which likely contributes to the increased ammonia reabsorption observed.^{20,138} Acidosis-induced increases in glucocorticoid levels appear to mediate increased NKCC2 expression and activity.²¹

$\text{Na}^+\text{-K}^+\text{-ATPase}$

$\text{Na}^+\text{-K}^+\text{-ATPase}$ is present in the basolateral plasma membrane of essentially all renal epithelial cells. NH_4^+ binds to and is transported at the K^+ -binding site, enabling Na^+ for NH_4^+ exchange.^{218,434} In the IMCD, $\text{Na}^+\text{-K}^+\text{-ATPase}$ -mediated basolateral NH_4^+ uptake is critical for IMCD ammonia and acid secretion.^{218,434} Decreases in interstitial K^+ levels during hypokalemia facilitate increased basolateral NH_4^+ uptake by $\text{Na}^+\text{-K}^+\text{-ATPase}$, and contribute to increased NH_4^+ secretion rates.⁴³¹ In the CCD, in contrast, basolateral $\text{Na}^+\text{-K}^+\text{-ATPase}$ does not appear to contribute to CCD ammonia secretion.²⁰⁷

$\text{H}^+\text{-K}^+\text{-ATPase}$

$\text{H}^+\text{-K}^+\text{-ATPase}$ proteins are members of the P-type ATPase family and transport NH_4^+ . The majority of evidence suggests NH_4^+ is transported at the K^+ binding site, such that these proteins mediate H^+/NH_4^+ exchange. Thus, $\text{H}^+\text{-K}^+\text{-ATPase}$ is unlikely to contribute to collecting duct ammonia secretion. However, potassium deficiency increases expression of the colonic $\text{H}^+\text{-K}^+\text{-ATPase}$ and it has been postulated that this mediates increased NH_4^+ secretion via transport at the H^+ binding site.²⁸²

Aquaporins

H_2O and NH_3 have a similar molecular size and charge distribution. This has led to several studies examining whether aquaporin water channels transport NH_3 . These studies have demonstrated that some, but not all, aquaporin-family members can transport ammonia. Table 9.1 summarizes the results of these studies. With the exception of AQP8, discussed later, experimental evidence regarding the role of these proteins in renal ammonia metabolism is not available.

Substantial evidence, but not without a degree of controversy, indicates that AQP8 contributes to renal ammonia metabolism. It is found in intracellular sites in the proximal tubule, CCD, and OMCD in the kidney, but not the plasma membrane.¹¹¹ The majority of ammonia generation occurs inside mitochondria in the proximal tubule. Thus, ammonia must be transported from mitochondria to cytoplasm. Several studies using heterologous expression show AQP8 can transport ammonia^{132,175,243,344} and it is able to complement ammonia transport defects in yeast lacking endogenous ammonia transporters.¹⁸⁸ In cultured proximal tubule cells, AQP8 is located in the inner mitochondrial membrane and AQP8 knockdown decreases ammonia secretion.²⁶⁸ In vivo, metabolic acidosis increases AQP8 expression.²⁶⁸ All of these findings suggest AQP8 has an important role in proximal tubule mitochondrial ammonia transport. However, studies examining mice with AQP8 gene deletion found normal ammonia excretion, under basal conditions and following acute or chronic acid loading.⁴⁸⁰

CARBONIC ANHYDRASE

Carbonic anhydrase, in addition to its role in bicarbonate reabsorption, also contributes to ammonia secretion. Direct studies have shown that carbonic anhydrase inhibition, presumably through effects on CA II, blocks OMCD ammonia secretion.⁴³⁰ Fig. 9.12 shows the putative role of cytoplasmic CA II in facilitating transepithelial ammonia secretion.

CA IV, although functioning to increase bicarbonate reabsorption, likely decreases collecting duct ammonia secretion because it prevents a luminal disequilibrium pH. Apical CA IV expression has been demonstrated in the

Table 9.1 Ammonia Transport by Aquaporins

Aquaporin	Finding	Citation
AQP1	NH_3 transport	132, 285
	No transport	175
AQP2	No transport	132
AQP3	NH_3 transport	132
	Both NH_3 and NH_4^+ transport	175
AQP4	No transport	132, 273
AQP5	No transport	132, 273
AQP6	NH_3 transport	132
AQP7	NH_3 transport	132
AQP8	NH_3 transport	132, 344
	Both NH_3 and NH_4^+ transport	175
	Transport present, NH_3 vs. NH_4^+ not differentiated	243
AQP9	NH_3 transport	132
	NH_3 and NH_4^+ transport	175
AQP0	No transport	132

rabbit CCD type A intercalated cell, in the rabbit OMCD and IMCD,³⁵⁶ in the human CCD and OMCD,²⁴⁶ but not in the rat collecting duct.⁵³ This pattern is inconsistent with evidence of luminal disequilibrium pH in the rat CCD and OMCD,^{119,208} but is consistent with the evidence of luminal disequilibrium pH in the rabbit CCD and OMCD outer stripe segments.^{376,377}

Rh GLYCOPROTEINS

Rh glycoproteins are mammalian orthologs of Mep/AMT proteins, ammonia transporter family proteins present in yeast, plants, bacteria, and many other organisms. Three mammalian Rh glycoproteins are known: Rh A glycoprotein (RhAG/Rhag), Rh B glycoprotein (RhBG/Rhbg), and Rh C glycoprotein (RhCG/Rhcg).

Rhag/RhAG (SLC42A1)

Rhag is an essential component of the erythrocyte “Rhesus complex,” which consists of Rhag in association with RhD and RhCE subunits in what appears to be a 1:1:1 stoichiometric ratio.¹⁵⁴ Rhag transports ammonia in the form of NH₃, whereas RhD and RhCE do not.^{254,470} In humans, RhAG deficiency leads to Rh_{null} disease, which is characterized by hemolytic anemia, spherocytosis, and lack of erythrocyte expression of RhAG, RhD, and RhCE.^{180,469} Rhag protein is present in erythrocytes and in erythrocyte precursor cells present in the bone marrow and in rodent spleen, but does not appear to be expressed in nonerythroid tissues. In particular, Rhag is not found in the kidney, except in residual erythrocytes.^{450,455}

Rhbg/RhBG (SLC42A2)

Rhbg in the kidney is found exclusively in distal epithelial cell populations, with low-level basolateral expression in the DCT, and higher-level basolateral expression in the CNT, CCD, OMCD, and IMCD.^{162,322,420} The CNT and the collecting duct have heterogeneous epithelial cell populations; type A and non-A, non-B intercalated cells, principal cells, and CNT cells express Rhbg, but expression is greater in intercalated cells. Type B intercalated cells do not express detectable Rhbg immunolabel. Although an initial study detected Rhbg mRNA but not Rhbg protein in the human kidney,⁵¹ subsequent studies identified Rhbg protein expression in a pattern nearly identical to that observed in the studies of the rat and mouse kidney.¹⁶²

The majority of evidence indicates that Rhbg contributes significantly to renal ammonia excretion during basal conditions and conditions that increase ammonia excretion. Intercalated cell-specific Rhbg deletion, while not altering ammonia excretion, induces adaptive changes in other enzymes involved in ammonia metabolism that appear to compensate for its absence, indicating a role for Rhbg under basal conditions.³⁶ Both metabolic acidosis and hypokalemia, common conditions associated with increased ammonia excretion, increase Rhbg protein expression, and genetic deletion of Rhbg from intercalated cells impairs changes in ammonia excretion in response to these stimuli.^{35,36} However, a study that used a different method of acid loading, which produced less stimulation of ammonia excretion, found no effect of Rhbg deletion.⁷⁶ This suggests that other mechanisms can compensate for the lack of Rhbg, such as those identified by Bishop et al,³⁶ if only modest increases in ammonia

Table 9.2 NH₃ and NH₄⁺ Transport Characteristics of Rhbg and Rhcg

	Electroneutral		Electrogenic		Citation
	NH ₃ Transport	CH ₃ NH ₂ transport	NH ₄ ⁺ Transport	CH ₃ NH ₃ ⁺ Transport	
Rhbg	Absent		Present		287
		Present		Absent	248
	Present		Absent		493
		Present		Absent	252
		Present	Present	Present	283
	Absent	Present	Present	Present	286
Rhcg	Present				131
	Present		Present		65
	Present		Present		24
		Present		Absent	493
		Present		Absent	252
		Present		Absent	258
		Present		Absent	37
		Present		Absent	271
	Present		Absent		154
	Present		Absent		48
Present				131	
Absent		Present		65	

excretion are needed, whereas greater degrees of adaptation require Rhbg expression.

A number of studies have addressed the issue as to whether Rhbg transports NH₃, NH₄⁺, or both, and have resulted in conflicting results. Table 9.2 summarizes these studies. The more recent studies suggest that Rhbg can transport both NH₃ and NH₄⁺. The molecular mechanism through which NH₄⁺ is transported has not been identified, but is likely to be a form of NH₃-H⁺ cotransport rather than direct transport of the molecular species NH₄⁺. Importantly, the electrochemical gradient across the basolateral plasma membrane is such that both electroneutral NH₃ transport and electrogenic NH₄⁺ transport modes will result in ammonia transport from the interstitium into the cell cytoplasm.⁴⁶²

Rhcg/RhCG

Rhcg is expressed in the kidney exclusively in epithelial cells of distal segments.^{107,161,358,359,420} Rhcg expression is prominent in the CNT, ICT, CCD, OMCD, and IMCD, weakly expressed in late DCT cells, and exhibits both apical and basolateral expression.^{161,199,358,359} Rhcg expression differs among renal epithelial cell types. In general, type A intercalated cells express higher levels of Rhcg than do principal cells. Rhcg is not detectable by immunohistochemistry in type B intercalated cells. In the CNT, non-A, non-B intercalated cells express apical Rhcg but have very little or no basolateral Rhcg immunolabel. IMCD cells do not express detectable Rhcg.

Rhcg has an important role in renal ammonia excretion in a wide variety of conditions, including basal acid–base homeostasis, metabolic acidosis, hypokalemia, and several other conditions. Gene deletion studies show that the absence of Rhcg impairs basal ammonia excretion.^{37,224} Metabolic acidosis, hypokalemia, and high dietary protein intake increase Rhcg expression, and Rhcg expression is necessary for the

normal increase in ammonia excretion.* In contrast to high dietary protein intake, during dietary protein restriction Rhcg expression is not needed for the decreased ammonia excretion that occurs.²²⁵ With reduced renal mass there is increased single-nephron ammonia excretion, and this increase involves increased polarization of Rhcg to the apical and basolateral plasma membrane.²⁰⁰ Cyclosporine A can induce renal tubular acidosis, and this involves altered Rhcg expression.²⁴¹ Aldosterone and chronic lithium administration increase renal ammonia excretion, and both are associated with increased Rhcg expression.^{187,454} Finally, the critical role of Rhcg in collecting duct ammonia secretion has been shown in studies using in vitro microperfusion that show that Rhcg deletion, at least in CCD and OMCD from mice with chronic metabolic acidosis, impairs transepithelial ammonia secretion and impairs both apical and basolateral plasma membrane NH₃ transport.^{37,48}

Rhcg expression appears to be regulated through a variety of mechanisms. There are changes in total protein expression in a variety of conditions, as detailed earlier. In metabolic acidosis, this increase is not associated with changes in steady-state mRNA expression, indicating at least a component of posttranscriptional regulation.³⁵⁸ During a high protein diet there is a transient increase in Rhcg mRNA expression, indicating that there can also be a component of transcriptional regulation.⁴⁷ In addition, Rhcg is found in both the apical and basolateral plasma membrane and in subapical cytoplasmic vesicles, and changes in subcellular distribution and expression are a prominent component of the response to metabolic acidosis, hypokalemia, and reduced renal mass.^{35,163,200,359}

Rhcg may regulate collecting duct ammonia secretion in part through effects on H⁺-ATPase expression. Recent studies show that Rhcg and H⁺-ATPase are located within the same cellular protein complex and that Rhcg may modulate H⁺-ATPase activity and expression.⁴⁹ However, H⁺-ATPase does not appear to affect Rhcg function. This mechanism may help to coordinate ammonia and proton secretion beyond physicochemical driving forces.

Multiple studies have addressed the molecular form of ammonia that Rhcg transports. Table 9.2 summarizes the results of these studies. Essentially all studies have found that Rhcg transports ammonia in the form of NH₃. This selective transport of NH₃ is critical for Rhcg to facilitate ammonia secretion across the apical plasma membrane in the collecting duct. Under normal conditions, the high luminal NH₄⁺ concentrations present throughout the collecting duct in combination with intracellular electronegativity relative to the luminal fluid result in a substantial electrochemical gradient for electrogenic NH₄⁺ transport from the lumen to the cytoplasm. Thus, if Rhcg were an electrogenic NH₄⁺ transporter, it would facilitate collecting duct NH₄⁺ reabsorption, and would be highly unlikely to contribute to collecting duct ammonia secretion.

CO₂ Transport by Rh Glycoproteins

Rhesus glycoproteins can transport molecules other than ammonia, specifically CO₂. Quantitative studies using human erythrocytes deficient in RhAG show that the absence of RhAG decreases CO₂ transport.^{112,113} Studies using heterolo-

gous expression in *Xenopus* oocytes show all Rh glycoproteins can transport CO₂.^{131,273} However, the physiologic role of Rhbg- or Rhcg-mediated CO₂ transport in the kidney is not clear. Intercalated cells use cytoplasmic CO₂ to generate, through a CA II-catalyzed process, the intracellular H⁺ used for urinary acidification. Several studies using Rhbg and/or Rhcg deletion show that Rhbg and Rhcg expression are not necessary for urine acidification.[†] However, these studies cannot exclude the possibility of either altered intrarenal CO₂ concentrations, which enable diffusive CO₂ movement in the absence of Rhbg and Rhcg, or adaptive changes in other CO₂ transport mechanisms.

SULFATIDES

Sulfatides, highly charged anionic glycosphingolipids, appear to have an important role in renal ammonia metabolism. Sulfatides can reversibly bind NH₄⁺. They are expressed throughout the kidney, but levels are highest in the outer and inner medulla and metabolic acidosis increases medullary interstitial sulfatide content.³⁸⁰ Sulfatides appear to have an important role in maintaining the high inner medullary ammonia and increase in urinary acid elimination that develop during metabolic acidosis. Disruption of renal sulfatide synthesis, by a genetic approach along the entire renal tubule, led to lower urinary pH accompanied by lower ammonium excretion.³⁸⁰ After acid loading, mice deficient in renal sulfatide synthesis showed impaired ammonia excretion, decreased ammonia accumulation in the papilla, and chronic hyperchloremic metabolic acidosis.³⁸⁰ Thus, sulfatides, likely through their ability to reversibly bind interstitial NH₄⁺, have an important role in renal ammonia, handling, urinary acidification, and acid–base homeostasis.

ACID–BASE SENSORS

Several studies have begun to elucidate the molecular mechanisms through which the kidney recognizes altered systemic pH. Candidate molecular sensors have included acid-/alkali-sensing receptors, tyrosine kinases, and bicarbonate-stimulated adenylyl cyclase.

ACID-/ALKALI-SENSING RECEPTORS

GPR4

Several G-protein–coupled receptors are sensitive to extracellular pH, which results in pH-dependent intracellular cAMP or IP₃ production.²⁴⁹ Of these, GPR4 has been studied most extensively. It is expressed in the kidney, and GPR4 deletion results in mild metabolic acidosis, less acidic urine, and decreased ability to excrete an acid load.³⁸⁶ In acid-loaded mice, GPR4 deletion blunted the ability to increase expression of the intercalated cell basolateral protein AE1, and it blunted the acidosis-induced increase in type A and decrease in type B cells that were detectable in the CCD.³⁸⁵ Which renal cells express GPR4 has not been determined, but a preliminary report suggests that GPR4 is expressed in renal interstitial cells, not tubule epithelial cells.²⁶⁷

*References 37, 47, 224, 230, 358, and 359.

†References 36, 37, 76, 224, 229, 231.

INSULIN RECEPTOR–RELATED RECEPTOR (InsR-RR)

InsR-RR is a member of the insulin receptor family and may have a role regulating collecting duct acid–base transport. It is found in the kidney in the basolateral plasma membrane of type B cell and non-A, non-B intercalated cells,²⁸ and is activated by alkaline pH.⁹⁹ InsR-RR–deficient mice express lower levels of pendrin and have decreased ability to excrete an alkali load.⁹⁹

KINASES

Pyk2/ETB RECEPTOR PATHWAY

The nonreceptor tyrosine kinase, Pyk2, may function as a pH sensor in renal epithelial cells.²³⁹ In cultured proximal tubule cells, Pyk2 is activated by extracellular acidosis, and through activation of c-Src, leads to NHE3 activation.^{239,400} A parallel pathway for proximal tubule NHE3 activation exists, involving ERK1/2 and c-fos activation, but does not involve Pyk2.⁵⁵ These two pathways both increase expression of the endothelin gene, ET-1, which in turn activates the ETB receptor and increases apical plasma membrane NHE3 expression.³¹³ In cultured OMCD cells, Pyk2 is required for acidosis-induced activation of H⁺-ATPase through a signaling mechanism that involves the MAPK signaling pathway ERK1/2.¹¹⁷

RECEPTOR TYROSINE KINASE

The proximal tubule responds to changes in peritubular HCO₃⁻ and CO₂ with altered rates of luminal HCO₃⁻ reabsorption. This activation involves a receptor tyrosine kinase, possibly a member of the ErbB family,⁴⁸⁶ and may involve ErbB1/2 heterodimerization and activation of receptor tyrosine phosphatase-γ.⁵⁵ Acute acidosis increases tyrosine phosphorylation of ErbB1 and ErbB2, consistent with a role in a signaling cascade regulating HCO₃⁻ reabsorption.³⁷⁰

BICARBONATE-STIMULATED ADENYLYL CYCLASE

Another mechanism regulating renal acid–base homeostasis involves the soluble adenylyl cyclase (sAC). Its production of cAMP is directly stimulated by increases in cytoplasmic HCO₃⁻,⁸¹ and cAMP stimulates collecting duct H⁺ secretion.³⁰⁰ sAC is widely expressed in the kidney, including the TAL, DCT, and collecting duct.^{298,299} In collecting duct intercalated cells, sAC colocalizes with H⁺-ATPase in both the type A and type B intercalated cell and it coimmunoprecipitates with H⁺-ATPase, implicating it in regulation of H⁺ secretion.²⁹⁹ In clear cells of the epididymis, used as a model system of collecting duct intercalated cells, sAC regulates apical H⁺-ATPase expression through changes in cAMP production.²⁹⁸ Changes in cAMP levels also alter the expression of pendrin protein in type B and non-A, non-B intercalated cells in cultured CCD and CNT.³⁹³ Increased cAMP increases pendrin expression in these cells, whereas nitric oxide reduces pendrin expression through hydrolysis of intracellular cAMP.

DIURNAL VARIATION IN ACID EXCRETION

There is a diurnal variation in renal acid excretion, which involves ammonia and titratable acid excretion and urine

pH.³⁶⁹ Circadian changes in NHE3 expression have been identified, particularly in the TAL in the outer medulla,²⁹¹ and are likely mediated by Clock and BMAL1 genes.³⁴² There are also circadian changes in ENaC expression,³³² which by altering luminal electronegativity may alter voltage-sensitive H⁺ secretion and urine acidification. Diurnal variation in net acid excretion is altered in uric acid stone formers and may contribute to the pathogenesis of nephrolithiasis in this condition.⁶³

ACKNOWLEDGMENTS

The authors thank the many talented investigators with whom we have been fortunate to work; the superb mentors who have supported, encouraged, and enabled our scientific endeavors; and our wonderful spouses and families who have supported all aspects of our lives. The preparation of this chapter was supported by funds from NIH R01-DK-045788 and R01-DK107798.



Complete reference list available at ExpertConsult.com.

KEY REFERENCES

- Baum M, Twombly K, Gattineni J, et al. Proximal tubule Na⁺/H⁺ exchanger activity in adult NHE8^{-/-}, NHE3^{-/-}, and NHE3^{-/-}/NHE8^{-/-} mice. *Am J Physiol Renal Physiol*. 2012;303:F1495–F1502.
- Bishop JM, Verlander JW, Lee HW, et al. Role of the rhesus glycoprotein, Rh B glycoprotein, in renal ammonia excretion. *Am J Physiol Renal Physiol*. 2010;299:F1065–F1077.
- Biver S, Belge H, Bourgeois S, et al. A role for Rhesus factor rhcg in renal ammonium excretion and male fertility. *Nature*. 2008;456:339–343.
- Bobulescu IA, Moe OW. Luminal Na⁺/H⁺ exchange in the proximal tubule. *Pflugers Arch*. 2009;458:5–21.
- Boettger T, Hubner CA, Maier H, et al. Deafness and renal tubular acidosis in mice lacking the K-CL co-transporter Kcc4. *Nature*. 2002;416:874–878.
- Bourgeois S, Meer LV, Wootla B, et al. NHE4 is critical for the renal handling of ammonia in rodents. *J Clin Invest*. 2010;120:1895–1904.
- Brown D, Hirsch S, Gluck SL. Localization of a proton-pumping ATPase in rat kidney. *J Clin Invest*. 1988;82:2114–2126.
- Brown D, Paunescu TG, Breton S, et al. Regulation of the v-ATPase in kidney epithelial cells: dual role in acid–base homeostasis and vesicle trafficking. *J Exp Biol*. 2009;212:1762–1772.
- Busque SM, Wagner CA. Potassium restriction, high protein intake, and metabolic acidosis increase expression of the glutamine transporter SNAT3 (Slc38a3) in mouse kidney. *Am J Physiol Renal Physiol*. 2009;297:F440–F450.
- Chambrey R, Kurth I, Peti-Peterdi J, et al. Renal intercalated cells are rather energized by a proton than a sodium pump. *Proc Natl Acad Sci U S A*. 2013;110:7928–7933.
- Chen L, Lee JW, Chou CL, et al. Transcriptomes of major renal collecting duct cell types in mouse identified by single-cell RNA-seq. *Proc Natl Acad Sci U S A*. 2017;114:E9989–E9998.
- Chen Y, Cann MJ, Litvin TN, et al. Soluble adenylyl cyclase as an evolutionarily conserved bicarbonate sensor. *Science*. 2000;289:625–628.
- Christensen BM, Kim YH, Kwon TH, et al. Lithium treatment induces a marked proliferation of primarily principal cells in rat kidney inner medullary collecting duct. *Am J Physiol Renal Physiol*. 2006;291:F39–F48.
- Curthoys NP, Moe OW. Proximal tubule function and response to acidosis. *Clin J Am Soc Nephrol*. 2014;9:1627–1638.
- de Brito-Ashurst I, Varagunam M, Raftery MJ, et al. Bicarbonate supplementation slows progression of CKD and improves nutritional status. *J Am Soc Nephrol*. 2009;20:2075–2084.
- Finberg KE, Wagner CA, Bailey MA, et al. The B1-subunit of the H⁺ ATPase is required for maximal urinary acidification. *Proc Natl Acad Sci U S A*. 2005;102:13616–13621.
- Geyer RR, Musa-Aziz R, Qin X, et al. Relative CO₂/NH₃ selectivities of mammalian aquaporins 0–9. *Am J Physiol Cell Physiol*. 2013;304:C985–C994.

154. Gruswitz F, Chaudhary S, Ho JD, et al. Function of human Rh based on structure of RhCG at 2.1 Å. *Proc Natl Acad Sci U S A*. 2010; 107:9638–9643.
155. Gumz ML, Lynch IJ, Greenlee MM, et al. The renal H⁺-K⁺-ATPases: physiology, regulation, and structure. *Am J Physiol Renal Physiol*. 2010;298:F12–F21.
167. Handlogten ME, Osis G, Lee HW, et al. NBCe1 expression is required for normal renal ammonia metabolism. *Am J Physiol Renal Physiol*. 2015;309:F658–F666.
186. Igarashi T, Inatomi J, Sekine T, et al. Mutations in SLC4a4 cause permanent isolated proximal renal tubular acidosis with ocular abnormalities. *Nat Genet*. 1999;23:264–266.
189. Jakobsen JK, Odgaard E, Wang W, et al. Functional up-regulation of basolateral Na⁺-dependent HCO₃⁻-transporter NBCn1 in medullary thick ascending limb of K⁺-depleted rats. *Pflugers Arch*. 2004;448:571–578.
195. Karet FE, Finberg KE, Nelson RD, et al. Mutations in the gene encoding B1 subunit of H⁺-ATPase cause renal tubular acidosis with sensorineural deafness. *Nat Genet*. 1999;21:84–90.
202. Kim WY, Nam S, Choi A, et al. Aquaporin 2-labeled cells differentiate to intercalated cells in response to potassium depletion. *Histochem Cell Biol*. 2016;145:17–24.
216. Kraut JA, Madias NE. Metabolic acidosis of CKD: an update. *Am J Kidney Dis*. 2016;67:307–317.
219. Kurtz I, Zhu Q. Structure, function, and regulation of the SLC4 NBCe1 transporter and its role in causing proximal renal tubular acidosis. *Curr Opin Nephrol Hypertens*. 2013;22:572–583.
226. Lee HW, Osis G, Handlogten ME, et al. Proximal tubule-specific glutamine synthetase deletion alters basal and acidosis-stimulated ammonia metabolism. *Am J Physiol Renal Physiol*. 2016; 310:F1229–F1242.
228. Lee HW, Osis G, Harris AN, et al. NBCe1-A regulates proximal tubule ammonia metabolism under basal conditions and in response to metabolic acidosis. *J Am Soc Nephrol*. 2018;29:1182–1187.
273. Musa-Aziz R, Chen LM, Pelletier MF, et al. Relative CO₂/NH₃ selectivities of AQP1, AQP4, AQP5, AmtB, and RhAG. *Proc Natl Acad Sci U S A*. 2009;106:5406–5411.
293. Osis G, Handlogten ME, Lee H-W, et al. Effect of NBCe1 deletion on renal citrate and 2-oxoglutarate handling. *Physiol Rep*. 2016;4:e12778.
302. Pech V, Kim YH, Weinstein AM, et al. Angiotensin II increases chloride absorption in the cortical collecting duct in mice through a pendrin-dependent mechanism. *Am J Physiol Renal Physiol*. 2007; 292:F914–F920.
303. Pech V, Thumova M, Dikalov SI, et al. Nitric oxide reduces Cl⁻-absorption in the mouse cortical collecting duct through an ENaC-dependent mechanism. *Am J Physiol Renal Physiol*. 2013; 304:F1390–F1397.
339. Royaux IE, Wall SM, Karniski LP, et al. Pendrin, encoded by the pendred syndrome gene, resides in the apical region of renal intercalated cells and mediates bicarbonate secretion. *Proc Natl Acad Sci U S A*. 2001;98:4221–4226.
342. Saifur RM, Emoto N, Nonaka H, et al. Circadian clock genes directly regulate expression of the Na⁽⁺⁾/H⁽⁺⁾ exchanger NHE3 in the kidney. *Kidney Int*. 2005;67:1410–1419.
355. Schwartz GJ, Gao X, Tsuruoka S, et al. SDF1 induction by acidosis from principal cells regulates intercalated cell subtype distribution. *J Clin Invest*. 2015;125:4365–4374.
380. Stettner P, Bourgeois S, Marsching C, et al. Sulfatides are required for renal adaptation to chronic metabolic acidosis. *Proc Natl Acad Sci U S A*. 2013;110:9998–10003.
386. Sun X, Yang LV, Tiegs BC, et al. Deletion of the pH sensor GPR4 decreases renal acid excretion. *J Am Soc Nephrol*. 2010;21:1745–1755.
395. Tokonami N, Morla L, Centeno G, et al. α-ketoglutarate regulates acid-base balance through an intrarenal paracrine mechanism. *J Clin Invest*. 2013;123:3166–3171.
413. Verlander JW, Hassell KA, Royaux IE, et al. Deoxycorticosterone upregulates PDS (Slc26a4) in mouse kidney: role of pendrin in mineralocorticoid-induced hypertension. *Hypertension*. 2003;42: 356–362.
418. Verlander JW, Madsen KM, Tisher CC. Effect of acute respiratory acidosis on two populations of intercalated cells in rat cortical collecting duct. *Am J Physiol*. 1987;253:F1142–F1156.
420. Verlander JW, Miller RT, Frank AE, et al. Localization of the ammonium transporter proteins, Rh B glycoprotein and rh C glycoprotein, in the mouse kidney. *Am J Physiol Renal Physiol*. 2003;284:F323–F337.
436. Wall SM, Pech V. The interaction of pendrin and the epithelial sodium channel in blood pressure regulation. *Curr Opin Nephrol Hypertens*. 2008;17:18–24.
447. Watts BA III, George T, Good DW. The basolateral NHE1 Na⁺/H⁺ exchanger regulates transepithelial HCO₃⁻-absorption through actin cytoskeleton remodeling in renal thick ascending limb. *J Biol Chem*. 2005;280:11439–11447.
458. Weiner ID, Verlander JW. Ammonia transporters and their role in acid-base balance. *Physiol Rev*. 2017;97:465–494.
466. Wen D, Yuan Y, Cornelius RJ, et al. Deficient acid handling with distal RTA in the NBCe2 knockout mouse. *Am J Physiol Renal Physiol*. 2015;309:F523–F530.
467. Wesson DE. Regulation of kidney acid excretion by endothelins. *Kidney Int*. 2006;70:2066–2073.
470. Westhoff CM, Ferreri-Jacobia M, Mak DO, et al. Identification of the erythrocyte Rh-blood group glycoprotein as a mammalian ammonium transporter. *J Biol Chem*. 2002;277:12499–12502.
479. Wu H, Chen L, Zhou Q, et al. Aqp2-expressing cells give rise to renal intercalated cells. *J Am Soc Nephrol*. 2013;24:243–252.
481. Yasuoka Y, Kobayashi M, Sato Y, et al. The intercalated cells of the mouse kidney OMCD are the target of the vasopressin V1a receptor axis for urinary acidification. *Clin Exp Nephrol*. 2013;17: 783–792.
489. Zhou Y, Zhao J, Bouyer P, et al. Evidence from renal proximal tubules that HCO₃⁻ and solute reabsorption are acutely regulated not by pH but by basolateral HCO₃⁻ and CO₂. *Proc Natl Acad Sci U S A*. 2005;102:3875–3880.

REFERENCES

- Abuladze N, Lee I, Newman D, et al. Axial heterogeneity of sodium-bicarbonate cotransporter expression in the rabbit proximal tubule. *Am J Physiol*. 1998;274:F628–F633.
- Adler S, Zett B, Anderson B. Renal citrate in the potassium-deficient rat: role of potassium and chloride ions. *J Lab Clin Med*. 1974;84:307–316.
- Adroge HJ. Glucose homeostasis and the kidney. *Kidney Int*. 1992;42:1266–1282.
- Ahn KY, Kone BC. Expression and cellular localization of mRNA encoding the “gastric” isoform of the H⁺-K⁺-ATPase alpha-subunit in rat kidney. *Am J Physiol*. 1995;268:F99–F109.
- Ahn KY, Madsen KM, Tisher CC, et al. Differential expression and cellular distribution of mRNAs encoding alpha- and beta-isoforms of Na⁺-K⁺-ATPase in rat kidney. *Am J Physiol*. 1993;265:F792–F801.
- Ahn KY, Turner PB, Madsen KM, et al. Effects of chronic hypokalemia on renal expression of the “gastric” H⁺-K⁺-ATPase α -subunit gene. *Am J Physiol*. 1996;270:F557–F566.
- Al bataineh MM, Gong F, Marciszyn AL, et al. Regulation of proximal tubule vacuolar H(+)-ATPase by PKA and AMP-activated protein kinase. *Am J Physiol Renal Physiol*. 2014;306:F981–F995.
- Albrecht FE, Xu J, Moe OW, et al. Regulation of NHE3 activity by G protein subunits in renal brush-border membranes. *Am J Physiol Regul Integr Comp Physiol*. 2000;278:R1064–R1073.
- Alper SL. Molecular physiology and genetics of Na⁺-independent SLC4 anion exchangers. *J Exp Biol*. 2009;212:1672–1683.
- Alper SL, Natale J, et al. Subtypes of intercalated cells in rat kidney collecting duct defined by antibodies against erythroid band 3 and renal vacuolar H⁺-ATPase. *Proc Natl Acad Sci U S A*. 1989;86:5429–5433.
- Alper SL, Stuart-Tilley AK, Biemesderfer D, et al. Immunolocalization of AE2 anion exchanger in rat kidney. *Am J Physiol*. 1997;273:F601–F614.
- Alpern RJ, Cogan MG, Rector FC Jr. Effect of luminal bicarbonate concentration on proximal acidification in the rat. *Am J Physiol*. 1982;243:F53–F59.
- Alpern RJ, Cogan MG, Rector FC Jr. Flow dependence of proximal tubular bicarbonate absorption. *Am J Physiol*. 1983;245:F478–F484.
- Ambuhl PA, Yang X, Peng Y, et al. Glucocorticoids enhance acid activation of the Na⁺/H⁺ exchanger 3 (NHE3). *J Clin Invest*. 1999;103:429–435.
- Ambuhl PA, Zajicek HK, Wang H, et al. Regulation of renal phosphate transport by acute and chronic metabolic acidosis in the rat. *Kidney Int*. 1998;53:1288–1298.
- Ambuhl PM, Amemiya M, Danczkay M, et al. Chronic metabolic acidosis increases NHE3 protein abundance in rat kidney. *Am J Physiol*. 1996;271:F917–F925.
- Aruga S, Wehrli S, Kaissling B, et al. Chronic metabolic acidosis increases NaDC-1 mRNA and protein abundance in rat kidney. *Kidney Int*. 2000;58:206–215.
- Atkins JL, Burg MB. Bicarbonate transport by isolated perfused rat collecting ducts. *Am J Physiol*. 1985;249:F485–F489.
- Attmane-Elakeb A, Amlal H, Bichara M. Ammonium carriers in medullary thick ascending limb. *Am J Physiol Renal Physiol*. 2001;280:F1–F9.
- Attmane-Elakeb A, Mount DB, Sibella V, et al. Stimulation by in vivo and in vitro metabolic acidosis of expression of rBSC-1, the Na⁺-K⁺-(NH₄⁺)-2Cl⁻ cotransporter of the rat medullary thick ascending limb. *J Biol Chem*. 1998;273:33681–33691.
- Attmane-Elakeb A, Sibella V, Vernimmen C, et al. Regulation by glucocorticoids of expression and activity of rBSC1, the Na⁺-K⁺-(NH₄⁺)-2Cl⁻ cotransporter of medullary thick ascending limb. *J Biol Chem*. 2000;275:33548–33553.
- Bacic D, Kaissling B, McLeroy P, et al. Dopamine acutely decreases apical membrane Na/H exchanger NHE3 protein in mouse renal proximal tubule. *Kidney Int*. 2003;64:2133–2141.
- Bagnis C, Marshansky V, Breton S, et al. Remodeling the cellular profile of collecting ducts by chronic carbonic anhydrase inhibition. *Am J Physiol Renal Physiol*. 2001;280:F437–F448.
- Bakouh N, Benjelloun F, Hulin P, et al. NH₃ is involved in the NH₄⁺ transport induced by the functional expression of the human Rh C glycoprotein. *J Biol Chem*. 2004;279:15975–15983.
- Balagura-Baruch S, Burich RL, King VF. Effects of alkalosis on renal citrate metabolism in dogs infused with citrate. *Am J Physiol*. 1973;225:385–388.
- Bastani B, McEnaney S, Yang L, et al. Adaptation of inner medullary collecting duct vacuolar H-adenosine triphosphatase to chronic acid or alkali loads in the rat. *Exp Nephrol*. 1994;2:171–175.
- Bastani B, Purcell H, Hemken P, et al. Expression and distribution of renal vacuolar proton-translocating adenosine triphosphatase in response to chronic acid and alkali loads in the rat. *J Clin Invest*. 1991;88:126–136.
- Bates CM, Merenmies JM, Kelly-Spratt KS, et al. Insulin receptor-related receptor expression in non-A intercalated cells in the kidney. *Kidney Int*. 1997;52:674–681.
- Bauch C, Forster N, Loffing-Cueni D, et al. Functional cooperation of epithelial heteromeric amino acid transporters expressed in Madin-Darby canine kidney cells. *J Biol Chem*. 2003;278:1316–1322.
- Baum M, Twombly K, Gattineni J, et al. Proximal tubule Na⁺/H⁺ exchanger activity in adult NHE8^{-/-}, NHE3^{-/-}, and NHE3^{-/-}/NHE8^{-/-} mice. *Am J Physiol Renal Physiol*. 2012;303:F1495–F1502.
- Becker AM, Zhang J, Goyal S, et al. Ontogeny of NHE8 in the rat proximal tubule. *Am J Physiol Renal Physiol*. 2007;293:F255–F261.
- Bengele HH, McNamara ER, Schwartz JH, et al. Suppression of acidification along inner medullary collecting duct. *Am J Physiol*. 1988;255:F307–F312.
- Bergeron MJ, Bürzle M, Kovacs G, et al. Synthesis, maturation, and trafficking of human Na⁺-dicarboxylate cotransporter NaDC1 requires the chaperone activity of cyclophilin B. *J Biol Chem*. 2011;286:11242–11253.
- Biemesderfer D, Reilly RF, Exner M, et al. Immunocytochemical characterization of Na(+)-H+ exchanger isoform NHE-1 in rabbit kidney. *Am J Physiol*. 1992;263:F833–F840.
- Bishop JM, Lee HW, Handlogten ME, et al. Intercalated cell-specific Rh B glycoprotein deletion diminishes renal ammonia excretion response to hypokalemia. *Am J Physiol Renal Physiol*. 2013;304:F422–F431.
- Bishop JM, Verlander JW, Lee HW, et al. Role of the Rhesus glycoprotein, Rh B glycoprotein, in renal ammonia excretion. *Am J Physiol Renal Physiol*. 2010;299:F1065–F1077.
- Biver S, Belge H, Bourgeois S, et al. A role for Rhesus factor Rhcg in renal ammonium excretion and male fertility. *Nature*. 2008;456:339–343.
- Bobulescu IA, Moe OW. Luminal Na⁺/H⁺ exchange in the proximal tubule. *Pflugers Arch*. 2009;458:5–21.
- Bobulescu IA, Dwarakanath V, Zou L, et al. Glucocorticoids acutely increase cell surface Na⁺/H⁺ exchanger-3 (NHE3) by activation of NHE3 exocytosis. *Am J Physiol Renal Physiol*. 2005;289:F685–F691.
- Boehmer C, Embark HM, Bauer A, et al. Stimulation of renal Na⁺-dicarboxylate cotransporter 1 by Na⁺/H⁺ exchanger regulating factor 2, serum and glucocorticoid inducible kinase isoforms, and protein kinase B. *Biochem Biophys Res Commun*. 2004;313:998–1003.
- Boettger T, Hubner CA, Maier H, et al. Deafness and renal tubular acidosis in mice lacking the K-Cl co-transporter KCC4. *Nature*. 2002;416:874–878.
- Bond PA, Jenner FA. The effect of lithium and related metal ions on the urinary excretion of 2-oxoglutarate and citrate in the rat. *Br J Pharmacol*. 1974;50:283–289.
- Bond PA, Jenner FA, Lee CR, et al. The effect of lithium salts on the urinary excretion of α -oxoglutarate in man. *Br J Pharmacol*. 1972;46:116–123.
- Borensztein P, Juvin P, Vernimmen C, et al. cAMP-dependent control of Na⁺/H⁺ antiport by AVP, PTH, and PGE₂ in rat medullary thick ascending limb cells. *Am J Physiol Renal Physiol*. 1993;264:F354–F364.
- Boron WF, Chen L, Parker MD. Modular structure of sodium-coupled bicarbonate transporters. *J Exp Biol*. 2009;212:1697–1706.
- Boron WF. Acid-base transport by the renal proximal tubule. *J Am Soc Nephrol*. 2006;17:2368–2382.
- Bounoure L, Ruffoni D, Muller R, et al. The role of the renal ammonia transporter Rhcg in metabolic responses to dietary protein. *J Am Soc Nephrol*. 2014;25:2040–2052.
- Bourgeois S, Bounoure L, Christensen EL, et al. Haploinsufficiency of the ammonia transporter rhcg predisposes to chronic acidosis: Rhcg is critical for apical and basolateral ammonia transport in the mouse collecting duct. *J Biol Chem*. 2012;288:5518–5529.
- Bourgeois S, Bounoure L, Mouro-Chanteloup I, et al. The ammonia transporter RhCG modulates urinary acidification by interacting with the vacuolar proton-ATPases in renal intercalated cells. *Kidney Int*. 2018;93:390–402.
- Bourgeois S, Meer LV, Wooda B, et al. NHE4 is critical for the renal handling of ammonia in rodents. *J Clin Invest*. 2010;120:1895–1904.

51. Brown ACN, Hallouane D, Mawby WJ, et al. RhCG is the major putative ammonia transporter expressed in human kidney and RhBG is not expressed at detectable levels. *Am J Physiol Renal Physiol*. 2009;296:F1279–F1290.
52. Brown D, Hirsch S, Gluck S. Localization of a proton-pumping ATPase in rat kidney. *J Clin Invest*. 1988;82:2114–2126.
53. Brown D, Zhu XL, Sly WS. Localization of membrane-associated carbonic anhydrase type IV in kidney epithelial cells. *Proc Natl Acad Sci U S A*. 1990;87:7457–7461.
54. Brown D, Paunescu TG, Breton S, et al. Regulation of the V-ATPase in kidney epithelial cells: dual role in acid-base homeostasis and vesicle trafficking. *J Exp Biol*. 2009;212:1762–1772.
55. Brown D, Wagner CA. Molecular mechanisms of acid-base sensing by the kidney. *J Am Soc Nephrol*. 2012;23:774–780.
56. Brown JC, Packer RK, Knepper MA. Role of organic anions in renal response to dietary acid and base loads. *Am J Physiol*. 1989;257:F170–F176.
57. Burch HB, Choi S, McCarthy WZ, et al. The location of glutamine synthetase within the rat and rabbit nephron. *Biochem Biophys Res Commun*. 1978;82:498–505.
58. Burch HB, Narins RG, Chu C, et al. Distribution along the rat nephron of three enzymes of gluconeogenesis in acidosis and starvation. *Am J Physiol*. 1978;235:F246–F253.
59. Burckhardt BC, Burckhardt G. Transport of organic anions across the basolateral membrane of proximal tubule cells. *Rev Physiol Biochem Pharmacol*. 2003;146:95–158.
60. Burckhardt G, Di Sole F, Helmle-Kolb C. The Na⁺/H⁺ exchanger gene family. *J Nephrol*. 2002;15:S3–S21.
61. Burnham CE, Amlal H, Wang Z, et al. Cloning and functional expression of a human kidney Na⁺/HCO₃⁻ cotransporter. *J Biol Chem*. 1997;272:19111–19114.
62. Busque SM, Wagner CA. Potassium restriction, high protein intake, and metabolic acidosis increase expression of the glutamine transporter SNAT3 (Slc38a3) in mouse kidney. *Am J Physiol Renal Physiol*. 2009;297:F440–F450.
63. Cameron M, Maalouf NM, Poindexter J, et al. The diurnal variation in urine acidification differs between normal individuals and uric acid stone formers. *Kidney Int*. 2012;81:1123–1130.
64. Campbell-Thompson ML, Verlander JW, Curran KA, et al. In situ hybridization of H-K-ATPase beta-subunit mRNA in rat and rabbit kidney. *Am J Physiol*. 1995;269:F345–F354.
65. Caner T, Abdunour-Nakhoul S, Brown K, et al. Mechanisms of ammonia and ammonium transport by Rhesus associated glycoproteins. *Am J Physiol Cell Physiol*. 2015;309:C747–C758.
66. Capasso G, Geibel PJ, Damiano S, et al. The calcium sensing receptor modulates fluid reabsorption and acid secretion in the proximal tubule. *Kidney Int*. 2013;84:277–284.
67. Capasso G, Unwin R, Agulian S, et al. Bicarbonate transport along the loop of Henle. I. Microperfusion studies of load and inhibitor sensitivity. *J Clin Invest*. 1991;88:430–437.
68. Capasso G, Unwin R, Ciani F, et al. Bicarbonate transport along the loop of Henle. II. Effects of acid-base, dietary, and neurohumoral determinants. *J Clin Invest*. 1994;94:830–838.
69. Capasso G, Unwin R, Rizzo M, et al. Bicarbonate transport along the loop of Henle: molecular mechanisms and regulation. *J Nephrol*. 2002;15(suppl 5):S88–S96.
70. Carmosino M, Brooks HL, Cai Q, et al. Axial heterogeneity of vasopressin-receptor subtypes along the human and mouse collecting duct. *Am J Physiol Renal Physiol*. 2007;292:F351–F360.
71. Carrisoza-Gaytan R, Rangel C, Salvador C, et al. The hyperpolarization-activated cyclic nucleotide-gated HCN2 channel transports ammonium in the distal nephron. *Kidney Int*. 2011;80:832–840.
72. Chalmers RA, Lawson AM. *Organic Acids in Man*. London: Chapman and Hall; 1982:163–208.
73. Chambrey R, Kurth I, Peti-Peterdi J, et al. Renal intercalated cells are rather energized by a proton than a sodium pump. *Proc Natl Acad Sci U S A*. 2013;110:7928–7933.
74. Chambrey R, Paillard M, Podevin RA. Enzymatic and functional evidence for adaptation of the vacuolar H⁽⁺⁾-ATPase in proximal tubule apical membranes from rats with chronic metabolic acidosis. *J Biol Chem*. 1994;269:3243–3250.
75. Chambrey R, Warnock DG, Podevin RA, et al. Immunolocalization of the Na⁺/H⁺ exchanger isoform NHE2 in rat kidney. *Am J Physiol*. 1998;275:F379–F386.
76. Chambrey R, Goossens D, Bourgeois S, et al. Genetic ablation of rhbg in mouse does not impair renal ammonium excretion. *Am J Physiol Renal Physiol*. 2005;289:F1281–F1290.
77. Chan YL, Biagi B, Giebisch G. Control mechanisms of bicarbonate transport across the rat proximal convoluted tubule. *Am J Physiol Renal Physiol*. 1982;242:F532–F543.
78. Chatsudhipong V, Chan YL. Inhibitory effect of angiotensin II on renal tubular transport. *Am J Physiol Renal Physiol*. 1991;260:F340–F346.
79. Cheema-Dhadli S, Lin SH, Halperin ML. Mechanisms used to dispose of progressively increasing alkali load in rats. *Am J Physiol Renal Physiol*. 2002;282:F1049–F1055.
80. Chen L, Lee JW, Chou CL, et al. Transcriptomes of major renal collecting duct cell types in mouse identified by single-cell RNA-seq. *Proc Natl Acad Sci U S A*. 2017;114:E9989–E9998.
81. Chen Y, Cann MJ, Litvin TN, et al. Soluble adenylyl cyclase as an evolutionarily conserved bicarbonate sensor. *Science*. 2000;289:625–628.
82. Cheval L, Morla L, Elalouf JM, et al. Kidney collecting duct acid-base “regulon.” *Physiol Genomics*. 2006;27:271–281.
83. Chou CL, Yu MJ, Kassai EM, et al. Roles of basolateral solute uptake via NKCC1 and of myosin II in vasopressin-induced cell swelling in inner medullary collecting duct. *Am J Physiol Renal Physiol*. 2008;295:F192–F201.
84. Christensen BM, Kim YH, Kwon TH, et al. Lithium treatment induces a marked proliferation of primarily principal cells in rat kidney inner medullary collecting duct. *Am J Physiol Renal Physiol*. 2006;291:F39–F48.
85. Christensen BM, Marples D, Kim YH, et al. Changes in cellular composition of kidney collecting duct cells in rats with lithium-induced NDI. *Am J Physiol Cell Physiol*. 2004;286:C952–C964.
86. Clapp WL, Madsen KM, Verlander JW, et al. Intercalated cells of the rat inner medullary collecting duct. *Kidney Int*. 1987;31:1080–1087.
87. Collazo R, Fan L, Hu MC, et al. Acute regulation of Na⁺/H⁺ exchanger NHE3 by parathyroid hormone via NHE3 phosphorylation and dynamin-dependent endocytosis. *J Biol Chem*. 2000;275:31601–31608.
88. Conjard A, Komaty O, Delage H, et al. Inhibition of glutamine synthetase in the mouse kidney: a novel mechanism of adaptation to metabolic acidosis. *J Biol Chem*. 2003;278:38159–38166.
89. Crajoinas RO, Polidoro JZ, Carneiro de Moraes CPA, et al. Angiotensin II counteracts the effects of cAMP/PKA on NHE3 activity and phosphorylation in proximal tubule cells. *Am J Physiol Cell Physiol*. 2016;311:C768–C776.
90. Curthoys NP, Gstraunthaler G. Mechanism of increased renal gene expression during metabolic acidosis. *Am J Physiol Renal Physiol*. 2001;281:F381–F390.
91. Curthoys NP, Lowry OH. The distribution of glutaminase isoenzymes in the various structures of the nephron in normal, acidotic, and alkalotic rat kidney. *J Biol Chem*. 1973;248:162–168.
92. Curthoys NP, Moe OW. Proximal tubule function and response to acidosis. *Clin J Am Soc Nephrol*. 2014;9:1627–1638.
93. Curthoys NP, Taylor L, Hoffert JD, et al. Proteomic analysis of the adaptive response of rat renal proximal tubules to metabolic acidosis. *Am J Physiol Renal Physiol*. 2007;292:F140–F147.
94. Da-Silva-Junior JC, Perrone RD, Johns CA, et al. Rat kidney band 3 mRNA modulation in chronic respiratory acidosis. *Am J Physiol*. 1991;260:F204–F209.
95. Damkier HH, Nielsen S, Praetorius J. Molecular expression of SLC4-derived Na⁺-dependent anion transporters in selected human tissues. *Am J Physiol Regul Integr Comp Physiol*. 2007;293:R2136–R2146.
96. Daryadel A, Bourgeois S, Figueiredo MFL, et al. Colocalization of the (Pro)renin Receptor/atp6ap2 with H⁺-ATPases in mouse kidney but prorenin does not acutely regulate intercalated cell H⁺-ATPase activity. *PLoS One*. 2016;11:e0147831.
97. de Brito-Ashurst I, Varagunam M, Raftery MJ, et al. Bicarbonate supplementation slows progression of CKD and improves nutritional status. *J Am Soc Nephrol*. 2009;20:2075–2084.
98. de Seigneux S, Malte H, Dimke H, et al. Renal compensation to chronic hypoxic hypercapnia: downregulation of pendrin and adaptation of the proximal tubule. *Am J Physiol Renal Physiol*. 2007;292:F1256–F1266.
99. Deyev IE, Sohet F, Vassilenko KP, et al. Insulin receptor-related receptor as an extracellular alkali sensor. *Cell Metab*. 2011;13:679–689.
100. DiSole F, Babich V, Moe OW. The calcineurin homologous protein-1 increases na⁽⁺⁾/H⁽⁺⁾-exchanger 3 trafficking via ezrin phosphorylation. *J Am Soc Nephrol*. 2009;20:1776–1786.

101. Dobyan DC, Magill LS, Friedman PA, et al. Carbonic anhydrase histochemistry in rabbit and mouse kidneys. *Anat Rec.* 1982;204:185–197.
102. Donadio JV Jr, Burgess JH, Holley KE. Membranous lupus nephropathy: a clinicopathologic study. *Medicine (Baltimore).* 1977;56:527–536.
103. Du Z, Yan Q, Duan Y, et al. Axial flow modulates proximal tubule NHE3 and H-ATPase activities by changing microvillus bending moments. *Am J Physiol Renal Physiol.* 2006;290:F289–F296.
104. DuBose TD, Good DW, Hamm LL, et al. Ammonium transport in the kidney: new physiological concepts and their clinical implications. *J Am Soc Nephrol.* 1991;1:1193–1203.
105. Dymia DW, Steinmetz AG, Kocinsky HS. NHE3 function and phosphorylation are regulated by a calyculin A-sensitive phosphatase. *Am J Physiol Renal Physiol.* 2009;298:F745–F753.
106. Eiamong S, Laski ME, Kurtzman NA, et al. Effect of respiratory acidosis and respiratory alkalosis on renal transport enzymes. *Am J Physiol.* 1994;267:F390–F399.
107. Eladari D, Cheval L, Quentin F, et al. Expression of RhCG, a new putative $\text{NH}_3/\text{NH}_4^+$ transporter, along the rat nephron. *J Am Soc Nephrol.* 2002;13:1999–2008.
108. Eladari D, Chambrey R, Frische S, et al. Pendrin as a regulator of ECF and blood pressure. *Curr Opin Nephrol Hypertens.* 2009;18:356–362.
109. Elkinton JR, Huth EJ, Webster GD Jr, et al. The renal excretion of hydrogen ion in renal tubular acidosis. *Am J Med.* 1960;36:554–575.
110. Elkjar ML, Kwon TH, Wang W, et al. Altered expression of renal NHE3, TSC, BSC-1, and ENaC subunits in potassium-depleted rats. *Am J Physiol Renal Physiol.* 2002;283:F1376–F1388.
111. Elkjar ML, Nejsum LN, Gresz V, et al. Immunolocalization of aquaporin-8 in rat kidney, gastrointestinal tract, testis, and airways. *Am J Physiol Renal Physiol.* 2001;281:F1047–F1057.
112. Endeward V, Cartron JP, Ripoche P, et al. Red cell membrane CO_2 permeability in normal human blood and in blood deficient in various blood groups, and effect of DIDS. *Transfus Clin Biol.* 2006;13:123–127.
113. Endeward V, Cartron JP, Ripoche P, et al. RhAG protein of the rhesus complex is a CO_2 channel in the human red cell membrane. *FASEB J.* 2007;22:64–73.
114. Fejes-Toth G, Naray-Fejes-Toth A. Immunohistochemical localization of colonic H-K-ATPase to the apical membrane of connecting tubule cells. *Am J Physiol Renal Physiol.* 2001;281:F318–F325.
115. Ferrier B, Martin M, Baverel G. Reabsorption and secretion of alpha-ketoglutarate along the rat nephron: a micropuncture study. *Am J Physiol.* 1985;248:F404–F412.
116. Finberg KE, Wagner CA, Bailey MA, et al. The B1-subunit of the H⁺-ATPase is required for maximal urinary acidification. *Proc Natl Acad Sci U S A.* 2005;102:13616–13621.
117. Fisher KD, Codina J, Petrovic S, et al. Pyk2 regulates H⁺-ATPase-mediated proton secretion in the outer medullary collecting duct via an ERK1/2 signaling pathway. *Am J Physiol Renal Physiol.* 2012;303:F1353–F1362.
118. Flessner MF, Mejia R, Knepper MA. Ammonium and bicarbonate transport in isolated perfused rodent long-loop thin descending limbs. *Am J Physiol.* 1993;264:F388–F396.
119. Flessner MF, Wall SM, Knepper MA. Ammonium and bicarbonate transport in rat outer medullary collecting ducts. *Am J Physiol.* 1992;262:F1–F7.
120. Fourman P, Robinson JR. Diminished urinary excretion of citrate during deficiencies of potassium in man. *Lancet.* 1953;265:656–657.
121. Frank AE, Weiner ID. Effects of ammonia on acid-base transport by the B-type intercalated cell. *J Am Soc Nephrol.* 2001;12:1607–1614.
122. Frank AE, Wingo CS, Andrews PM, et al. Mechanisms through which ammonia regulates cortical collecting duct net proton secretion. *Am J Physiol Renal Physiol.* 2002;282:F1120–F1128.
123. Frank AE, Wingo CS, Weiner ID. Effects of ammonia on bicarbonate transport in the cortical collecting duct. *Am J Physiol Renal Physiol.* 2000;278:F219–F226.
124. Frische S, Kwon TH, Frokiaer J, et al. Regulated expression of pendrin in rat kidney in response to chronic NH_4Cl or NaHCO_3 loading. *Am J Physiol Renal Physiol.* 2003;284:F584–F593.
125. Frische S, Zolotarev AS, Kim YH, et al. AE2 isoforms in rat kidney: immunohistochemical localization and regulation in response to chronic NH_4Cl loading. *Am J Physiol Renal Physiol.* 2004;286:F1163–F1170.
126. Fryer JN, Burns KD, Ghorbani M, et al. Effect of potassium depletion on proximal tubule AT1 receptor localization in normal and remnant rat kidney. *Kidney Int.* 2001;60:1792–1799.
127. Gao X, Eladari D, Levie F, et al. Deletion of *hensin/DMBT1* blocks conversion of β to α -intercalated cells and induces distal renal tubular acidosis. *Proc Natl Acad Sci U S A.* 2010;107:21872–21877.
128. Garcia-Aust J, Good DW, Burg MB, et al. Deoxycorticosterone-stimulated bicarbonate secretion in rabbit cortical collecting ducts: effects of luminal chloride removal and in vivo acid loading. *Am J Physiol.* 1985;249:F205–F212.
129. Gawenis LR, Bradford EM, Prasad V, et al. Colonic anion secretory defects and metabolic acidosis in mice lacking the NBC1 cotransporter. *J Biol Chem.* 2007;282:9042–9052.
130. Geibel J, Giebisch G, Boron WF. Angiotensin II stimulates both Na^+H^+ exchange and $\text{Na}^+/\text{HCO}_3^-$ cotransport in the rabbit proximal tubule. *Proc Natl Acad Sci U S A.* 1990;87:7917–7920.
131. Geyer RR, Parker MD, Toye AM, et al. Relative CO_2/NH_3 permeabilities of human RhAG, RhBG and RhCG. *J Membr Biol.* 2013;246:915–926.
132. Geyer RR, Musa-Aziz R, Qin X, et al. Relative CO_2/NH_3 selectivities of mammalian aquaporins 0–9. *Am J Physiol Cell Physiol.* 2013;304:C985–C994.
133. Gifford JD, Rome L, Galla JH. H^+K^+ -ATPase activity in rat collecting duct segments. *Am J Physiol.* 1992;262:F692–F695.
134. Gifford JD, Ware MW, Luke RG, et al. HCO_3^- transport in rat CCD: rapid adaptation by in vivo but not in vitro alkalosis. *Am J Physiol.* 1993;264:F435–F440.
135. Gildea JJ, Xu P, Carlson JM, et al. The sodium-bicarbonate cotransporter NBCe2 (slc4a5) expressed in human renal proximal tubules shows increased apical expression under high-salt conditions. *Am J Physiol Regul Integr Comp Physiol.* 2015;309:R1447–R1459.
136. Ginns SM, Knepper MA, Ecelbarger CA, et al. Immunolocalization of the secretory isoform of Na-K-Cl cotransporter in rat renal intercalated cells. *J Am Soc Nephrol.* 1996;7:2533–2542.
137. Gomes P, Soares-da-Silva P. Dopamine acutely decreases type 3 Na^+H^+ exchanger activity in renal OK cells through the activation of protein kinases A and C signalling cascades. *Eur J Pharmacol.* 2004;488:51–59.
138. Good DW. Adaptation of HCO_3^- and NH_4^+ transport in rat MTAL: effects of chronic metabolic acidosis and Na^+ intake. *Am J Physiol.* 1990;258:F1345–F1353.
139. Good DW. Inhibition of bicarbonate absorption by peptide hormones and cyclic adenosine monophosphate in rat medullary thick ascending limb. *J Clin Invest.* 1990;85:1006–1013.
140. Good DW. Effects of osmolality on bicarbonate absorption by medullary thick ascending limb of the rat. *J Clin Invest.* 1992;89:184–190.
141. Good DW. The thick ascending limb as a site of renal bicarbonate reabsorption. *Semin Nephrol.* 1993;13:225–235.
142. Good DW. Ammonium transport by the thick ascending limb of Henle's loop. *Annu Rev Physiol.* 1994;56:623–647.
143. Good DW, Burg MB. Ammonia production by individual segments of the rat nephron. *J Clin Invest.* 1984;73:602–610.
144. Good DW, Di Mari JF, Watts BA III. Hyposmolality stimulates Na^+/H^+ exchange and HCO_3^- absorption in thick ascending limb via PI 3-kinase. *Am J Physiol Cell Physiol.* 2000;279:C1443–C1454.
145. Good DW, George T, Watts BA III. Basolateral membrane Na^+/H^+ exchange enhances HCO_3^- absorption in rat medullary thick ascending limb: evidence for functional coupling between basolateral and apical membrane Na^+/H^+ exchangers. *Proc Natl Acad Sci U S A.* 1995;92:12525–12529.
146. Good DW, George T, Watts BA III. Lipopolysaccharide directly alters renal tubule transport through distinct TLR4-dependent pathways in basolateral and apical membranes. *Am J Physiol Renal Physiol.* 2009;297:F866–F874.
147. Good DW, George T, Watts BA III. High-mobility group box 1 inhibits HCO_3^- absorption in medullary thick ascending limb through a basolateral receptor for advanced glycation end products pathway. *Am J Physiol Renal Physiol.* 2015;309:F720–F730.
148. Good DW, Watts BA III. Functional roles of apical membrane Na^+/H^+ exchange in rat medullary thick ascending limb. *Am J Physiol Renal Physiol.* 1996;270:F691–F699.
149. Goyal S, Vanden Heuvel G, Aronson PS. Renal expression of novel Na^+/H^+ exchanger isoform NHE8. *Am J Physiol Renal Physiol.* 2003;284:F467–F473.
150. Groger N, Vitzthum H, Fröhlich H, et al. Targeted mutation of SLC4A5 induces arterial hypertension and renal metabolic acidosis. *Hum Mol Genet.* 2012;21:1025–1036.

151. Gross E, Hawkins K, Abuladze N, et al. The stoichiometry of the electrogenic sodium bicarbonate cotransporter NBC1 is cell-type dependent. *J Physiol*. 2001;531:597–603.
152. Gross E, Hawkins K, Pushkin A, et al. Phosphorylation of Ser982 in the sodium bicarbonate cotransporter kNBC1 shifts the HCO₃⁻:Na⁺ stoichiometry from 3:1 to 2:1 in murine proximal tubule cells. *J Physiol*. 2001;537:659–665.
153. Gross E, Pushkin A, Abuladze N, et al. Regulation of the sodium bicarbonate cotransporter kNBC1 function: role of Asp986, Asp988 and kNBC1-carbonic anhydrase II binding. *J Physiol*. 2002;544:679–685.
154. Gruswitz F, Chaudhary S, Ho JD, et al. Function of human rh based on structure of RhCG at 2.1 Å. *Proc Natl Acad Sci U S A*. 2010;107:9638–9643.
155. Gumz ML, Lynch JJ, Greenlee MM, et al. The renal H⁺-K⁺-ATPases: physiology, regulation, and structure. *Am J Physiol Renal Physiol*. 2010;298:F12–F21.
156. Guntupalli J, Eby B, Lau K. Mechanism for the phosphaturia of NH₄Cl: dependence on acidemia but not on diet PO₄ or PTH. *Am J Physiol*. 1982;242:F552–F560.
157. Hamm LL. Renal handling of citrate. *Kidney Int*. 1990;38:728–735.
158. Hamm LL, Pucacco LR, Kokko JP, et al. Hydrogen ion permeability of the rabbit proximal convoluted tubule. *Am J Physiol*. 1984;246:F3–F11.
159. Hamm LL, Simon EE. Roles and mechanisms of urinary buffer excretion. *Am J Physiol*. 1987;253:F595–F605.
160. Hamm LL, Simon EE. Ammonia transport in the proximal tubule in vivo. *Am J Kidney Dis*. 1989;14:253–257.
161. Han KH, Croker BP, Clapp WL, et al. Expression of the ammonia transporter, Rh C glycoprotein, in normal and neoplastic human kidney. *J Am Soc Nephrol*. 2006;17:2670–2679.
162. Han K-H, Lee HW, Handlogten ME, et al. Expression of the ammonia transporter family member, Rh B glycoprotein, in the human kidney. *Am J Physiol Renal Physiol*. 2013;304:F972–F981.
163. Han KH, Lee HW, Handlogten ME, et al. Effect of hypokalemia on renal expression of the ammonia transporter family members, Rh B glycoprotein and Rh C glycoprotein, in the rat kidney. *Am J Physiol Renal Physiol*. 2011;301:F823–F832.
164. Han KH, Lee SY, Kim WY, et al. Expression of the ammonia transporter family members, Rh B glycoprotein and Rh C glycoprotein, in the developing rat kidney. *Am J Physiol Renal Physiol*. 2010;299:F187–F198.
165. Handlogten ME, Hong SP, Westhoff CM, et al. Basolateral ammonium transport by the mouse inner medullary collecting duct cell (mIMCD-3). *Am J Physiol Renal Physiol*. 2004;287:F628–F638.
166. Handlogten ME, Hong SP, Westhoff CM, et al. Apical ammonia transport by the mouse inner medullary collecting duct cell (mIMCD-3). *Am J Physiol Renal Physiol*. 2005;289:F347–F358.
167. Handlogten ME, Osis G, Lee HW, et al. NBCe1 expression is required for normal renal ammonia metabolism. *Am J Physiol Renal Physiol*. 2015;309:F658–F666.
168. Hansen GP, Tisher CC, Robinson RR. Response of the collecting duct to disturbances of acid-base and potassium balance. *Kidney Int*. 1980;17:326–337.
169. Hanson RW, Reshef L. Regulation of phosphoenolpyruvate carboxykinase (GTP) gene expression. *Annu Rev Biochem*. 1997;66:581–611.
170. Hennings JC, Andrini O, Picard N, et al. The ClC-K2 chloride channel is critical for salt handling in the distal nephron. *J Am Soc Nephrol*. 2017;28:209–217.
171. Hering-Smith KS, Mao W, Schiro FR, et al. Localization of the calcium-regulated citrate transport process in proximal tubule cells. *Urolithiasis*. 2014;42:209–219.
172. Hering-Smith KS, Schiro FR, Pajor AM, et al. Calcium sensitivity of dicarboxylate transport in cultured proximal tubule cells. *Am J Physiol Renal Physiol*. 2011;300:F425–F432.
173. Heyer M, Müller-Berger S, Romero MF, et al. Stoichiometry of the rat kidney Na⁺-HCO₃⁻ cotransporter expressed in *Xenopus laevis* oocytes. *Pflügers Arch*. 1999;438:322–329.
174. Hoffmann N, Thees M, Kinne R. Phosphate transport by isolated renal brush border vesicles. *Pflügers Arch*. 1976;362:147–156.
175. Holm LM, Jahn TP, Moller AL, et al. NH₃ and NH₄⁺ permeability in aquaporin-expressing *Xenopus* oocytes. *Pflügers Arch*. 2005;450:415–428.
176. Hong JH, Yang D, Shcheynikov N, et al. Convergence of IRBIT, phosphatidylinositol (4,5) bisphosphate, and WNK/SPAK kinases in regulation of the Na⁺-HCO₃⁻ cotransporters family. *Proc Natl Acad Sci U S A*. 2013;110:4105–4110.
177. Hood VL. pH regulation of endogenous acid production in subjects with chronic ketoacidosis. *Am J Physiol Renal Physiol*. 1985;249:F220–F226.
178. Houillier P, Chambrey R, Achard JM, et al. Signaling pathways in the biphasic effect of angiotensin II on apical Na⁺/H antiport activity in proximal tubule. *Kidney Int*. 1996;50:1496–1505.
179. Hu MC, Fan L, Crowder LA, et al. Dopamine acutely stimulates Na⁺/H⁺ exchanger (NHE3) endocytosis via clathrin-coated vesicles: dependence on protein kinase A-mediated NHE3 phosphorylation. *J Biol Chem*. 2001;276:26906–26915.
180. Huang CH. The human Rh50 glycoprotein gene. Structural organization and associated splicing defect resulting in Rh(null) disease. *J Biol Chem*. 1998;273:2207–2213.
181. Huber S, Asan E, Jons T, et al. Expression of rat kidney anion exchanger 1 in type A intercalated cells in metabolic acidosis and alkalosis. *Am J Physiol*. 1999;277:F841–F849.
182. Hughey RP, Rankin BB, Curthoys NP. Acute acidosis and renal arteriovenous differences of glutamine in normal and adrenalectomized rats. *Am J Physiol Renal Physiol*. 1980;238:F199–F204.
183. Hulter HN, Peterson JC. Acid-base homeostasis during chronic PTH excess in humans. *Kidney Int*. 1985;28:187–192.
184. Hurtado-Lorenzo A, Skinner M, Annan JE, et al. V-ATPase interacts with ARNO and Arf6 in early endosomes and regulates the protein degradative pathway. *Nat Cell Biol*. 2006;8:124–136.
185. Hwang JJ, Perera S, Shapiro RA, et al. Mechanism of altered renal glutaminase gene expression in response to chronic acidosis. *Biochemistry*. 1991;30:7522–7526.
186. Igarashi T, Inatomi J, Sekine T, et al. Mutations in SLC4a4 cause permanent isolated proximal renal tubular acidosis with ocular abnormalities. *Nat Genet*. 1999;23:264–266.
187. Izumi Y, Hori K, Nakayama Y, et al. Aldosterone requires vasopressin V1a receptors on intercalated cells to mediate acid-base homeostasis. *J Am Soc Nephrol*. 2011;22:673–680.
188. Jahn TP, Moller AL, Zeuthen T, et al. Aquaporin homologues in plants and mammals transport ammonia. *FEBS Lett*. 2004;574:31–36.
189. Jakobsen JK, Odgaard E, Wang W, et al. Functional up-regulation of basolateral Na⁺-dependent HCO₃⁻ transporter NBCn1 in medullary thick ascending limb of K⁺-depleted rats. *Pflügers Arch*. 2004;448:571–578.
190. Jenkins AD, Dousa TP, Smith LH. Transport of citrate across renal brush border membrane: effects of dietary acid and alkali loading. *Am J Physiol Renal Physiol*. 1985;249:F590–F595.
191. Jorgensen KE, Kragh-Hansen U, Roigaard-Petersen H, et al. Citrate uptake by basolateral and luminal membrane vesicles from rabbit kidney cortex. *Am J Physiol Renal Physiol*. 1983;244:F686–F695.
192. Kaiser S, Hwang JJ, Smith H, et al. Effect of altered acid-base balance and of various agonists on levels of renal glutamate dehydrogenase mRNA. *Am J Physiol Renal Physiol*. 1992;262:F507–F512.
193. Kaplan MR, Plotkin MD, Brown D, et al. Expression of the mouse Na-K-2Cl cotransporter, mBSC2, in the terminal inner medullary collecting duct, the glomerular and extraglomerular mesangium, and the glomerular afferent arteriole. *J Clin Invest*. 1996;98:723–730.
194. Karet FE, Finberg KE, Nayir A, et al. Localization of a gene for autosomal recessive distal renal tubular acidosis with normal hearing (rdRTA2) to 7q33-34. *Am J Hum Genet*. 1999;65:1656–1665.
195. Karet FE, Finberg KE, Nelson RD, et al. Mutations in the gene encoding B1 subunit of H⁺-ATPase cause renal tubular acidosis with sensorineural deafness. *Nat Genet*. 1999;21:84–90.
196. Karinch AM, Lin CM, Wolfgang CL, et al. Regulation of expression of the SN1 transporter during renal adaptation to chronic metabolic acidosis in rats. *Am J Physiol Renal Physiol*. 2002;283:F1011–F1019.
197. Karnovsky MJ, Himmelhoch SR. Histochemical localization of glutaminase I activity in kidney. *Am J Physiol*. 1961;201:786–790.
198. Kim GH, Ecelbarger C, Knepper MA, et al. Regulation of thick ascending limb ion transporter abundance in response to altered acid/base intake. *J Am Soc Nephrol*. 1999;10:935–942.
199. Kim HY, Verlander JW, Bishop JM, et al. Basolateral expression of the ammonia transporter family member, Rh C glycoprotein, in the mouse kidney. *Am J Physiol Renal Physiol*. 2009;296:F545–F555.
200. Kim HY, Baylis C, Verlander JW, et al. Effect of reduced renal mass on renal ammonia transporter family, Rh C glycoprotein and Rh B glycoprotein, expression. *Am J Physiol Renal Physiol*. 2007;293:F1238–F1247.
201. Kim J, Kim YH, Cha JH, et al. Intercalated cell subtypes in connecting tubule and cortical collecting duct of rat and mouse. *J Am Soc Nephrol*. 1999;10:1–12.

202. Kim WY, Nam S, Choi A, et al. Aquaporin 2-labeled cells differentiate to intercalated cells in response to potassium depletion. *Histochem Cell Biol.* 2016;145:17–24.
203. Kim YH, Pech V, Spencer KB, et al. Reduced ENaC protein abundance contributes to the lower blood pressure observed in pendrin-null mice. *Am J Physiol Renal Physiol.* 2007;293:F1314–F1324.
204. Kinsella JL, Aronson PS. Interaction of NH_4^+ and Li^+ with the renal microvillus membrane $\text{Na}^+\text{-H}^+$ exchanger. *Am J Physiol.* 1981;241:C220–C226.
205. Kleinman JG, Bain JL, Fritsche C, et al. Histochemical carbonic anhydrase in rat inner medullary collecting duct. *J Histochem Cytochem.* 1992;40:1535–1545.
206. Knepper MA. NH_4^+ transport in the kidney. *Kidney Int.* 1991;40:S95–S102.
207. Knepper MA, Good DW, Burg MB. Mechanism of ammonia secretion by cortical collecting ducts of rabbits. *Am J Physiol.* 1984;247:F729–F738.
208. Knepper MA, Good DW, Burg MB. Ammonia and bicarbonate transport by rat cortical collecting ducts perfused in vitro. *Am J Physiol.* 1985;249:F870–F877.
209. Ko SB, Luo X, Hager H, et al. AE4 is a DIDS-sensitive $\text{I}(-)/\text{HCO}(-)$ (3) exchanger in the basolateral membrane of the renal CCD and the SMG duct. *Am J Physiol Cell Physiol.* 2002;283:C1206–C1218.
210. Kats K, Uchida S, Mizutani S, et al. Intrarenal and cellular localization of CLC-k2 protein in the mouse kidney. *J Am Soc Nephrol.* 2001;12:1327–1334.
211. Kocinsky HS, Girardi AC, Biemesderfer D, et al. Use of phospho-specific antibodies to determine the phosphorylation of endogenous Na^+/H^+ exchanger NHE3 at PKA consensus sites. *Am J Physiol Renal Physiol.* 2005;289:F249–F258.
212. Kohan DE. Biology of endothelin receptors in the collecting duct. *Kidney Int.* 2009;76:481–486.
213. Kok DJ, Iestra JA, Doorenbos CJ, et al. The effects of dietary excesses in animal protein and sodium on the composition and the crystallization kinetics of calcium oxalate monohydrate in urines of healthy men. *J Clin Endocrinol Metab.* 1990;71:861–867.
214. Kovesdy CP, Anderson JE, Kalantar-Zadeh K. Association of serum bicarbonate levels with mortality in patients with non-dialysis-dependent CKD. *Nephrol Dial Transplant.* 2009;24:1232–1237.
215. Kraut JA, Helander KG, Helander HF, et al. Detection and localization of H^+/K^+ -ATPase isoforms in human kidney. *Am J Physiol Renal Physiol.* 2001;281:F763–F768.
216. Kraut JA, Madias NE. Metabolic acidosis of CKD: an update. *Am J Kidney Dis.* 2016;67:307–317.
217. Kurtz I. Basolateral membrane Na^+/H^+ antiport, Na^+/base cotransport and Na^+ -independent Cl^-/base exchange in the rabbit S_3 proximal tubule. *J Clin Invest.* 1989;83:616–622.
218. Kurtz I, Balaban RS. Ammonium as a substrate for Na^+/K^+ -ATPase in rabbit proximal tubules. *Am J Physiol.* 1986;250:F497–F502.
219. Kurtz I, Zhu Q. Structure, function, and regulation of the SLC4 NBCe1 transporter and its role in causing proximal renal tubular acidosis. *Curr Opin Nephrol Hypertens.* 2013;22:572–583.
220. Kwon TH, Fulton C, Wang W, et al. Chronic metabolic acidosis upregulates rat kidney Na^+/HCO cotransporters NBCn1 and NBC3 but not NBC1. *Am J Physiol Renal Physiol.* 2002;282:F341–F351.
221. Kwon TH, Pushkin A, Abuladze N, et al. Immunoelectron microscopic localization of NBC3 sodium-bicarbonate cotransporter in rat kidney. *Am J Physiol Renal Physiol.* 2000;278:F327–F336.
222. Laghmani K, Preisig PA, Moe OW, et al. Endothelin-1/endothelin-B receptor-mediated increases in NHE3 activity in chronic metabolic acidosis. *J Clin Invest.* 2001;107:1563–1569.
223. Lee HW, Handlogten ME, Osis G, et al. Expression of sodium-dependent dicarboxylate transporter 1 ($\text{NaDC1}/\text{SLC13A2}$) in normal and neoplastic human kidney. *Am J Physiol Renal Physiol.* 2017;312:F427–F435.
224. Lee HW, Verlander JW, Bishop JM, et al. Collecting duct-specific Rh C glycoprotein deletion alters basal and acidosis-stimulated renal ammonia excretion. *Am J Physiol Renal Physiol.* 2009;296:F1364–F1375.
225. Lee HW, Osis G, Handlogten ME, et al. Effect of dietary protein restriction on renal ammonia metabolism. *Am J Physiol Renal Physiol.* 2015;308:F1463–F1473.
226. Lee HW, Osis G, Handlogten ME, et al. Proximal tubule-specific glutamine synthetase deletion alters basal and acidosis-stimulated ammonia metabolism. *Am J Physiol Renal Physiol.* 2016;310:F1229–F1242.
227. Lee HW, Osis G, Handlogten ME, et al. Proximal tubule glutamine synthetase expression is necessary for the normal response to dietary protein restriction. *Am J Physiol Renal Physiol.* 2017;313:F116–F125.
228. Lee HW, Osis G, Harris AN, et al. NBCe1-A regulates proximal tubule ammonia metabolism under basal conditions and in response to metabolic acidosis. *J Am Soc Nephrol.* 2018;29:1182–1197.
229. Lee HW, Verlander JW, Bishop JM, et al. Effect of intercalated cell-specific Rh C glycoprotein deletion on basal and metabolic acidosis-stimulated renal ammonia excretion. *Am J Physiol Renal Physiol.* 2010;299:F369–F379.
230. Lee HW, Verlander JW, Bishop JM, et al. Renal ammonia excretion in response to hypokalemia: effects of collecting duct-specific Rh C glycoprotein deletion. *Am J Physiol Renal Physiol.* 2013;304:F410–F421.
231. Lee HW, Verlander JW, Handlogten ME, et al. Effect of collecting duct-specific deletion of both Rh B glycoprotein (Rhbg) and Rh C glycoprotein (Rhcg) on renal response to metabolic acidosis. *Am J Physiol Renal Physiol.* 2014;306:F389–F400.
232. Lee SK, Boron WF, Parker MD. Substrate specificity of the electrogenic sodium/bicarbonate cotransporter NBCe1-a (SLC4a4, variant A) from humans and rabbits. *Am J Physiol Renal Physiol.* 2013;304:F883–F899.
233. Lee S, Lee HJ, Yang HS, et al. $\text{Na}^+/\text{bicarbonate}$ cotransporter NBCn1 in the kidney medullary thick ascending limb cell line is upregulated under acidic conditions and enhances ammonium transport. *Exp Physiol.* 2010;95:926–937.
234. Lemann J Jr, Bushinsky DA, Hamm LL. Bone buffering of acid and base in humans. *Am J Physiol Renal Physiol.* 2003;285:F811–F832.
235. Lemann J Jr, Lennon EJ, Goodman AD, et al. The net balance of acid in subjects given large loads of acid or alkali. *J Clin Invest.* 1965;44:507–517.
236. Levi M, McDonald LA, Preisig PA, et al. Chronic K depletion stimulates rat renal brush-border membrane Na^+ -citrate cotransporter. *Am J Physiol Renal Physiol.* 1991;261:F767–F773.
237. Levief F, Hubner CA, Houillier P, et al. The $\text{Na}^+(\text{+})$ -dependent chloride-bicarbonate exchanger SLC4A8 mediates an electroneutral $\text{Na}^+(\text{+})$ reabsorption process in the renal cortical collecting ducts of mice. *J Clin Invest.* 2010;120:1627–1635.
238. Li HC, Du Z, Barone S, et al. Proximal tubule specific knockout of the Na^+/H^+ exchanger NHE3: effects on bicarbonate absorption and ammonium excretion. *J Mol Med.* 2013;91:951–963.
239. Li S, Sato S, Yang X, et al. Pyk2 activation is integral to acid stimulation of sodium/hydrogen exchanger 3. *J Clin Invest.* 2004;114:1782–1789.
240. Licht C, Laghmani K, Yanagisawa M, et al. An autocrine role for endothelin-1 in the regulation of proximal tubule NHE3. *Kidney Int.* 2004;65:1320–1326.
241. Lim SW, Ahn KO, Kim WY, et al. Expression of ammonia transporters, Rhbg and Rhcg, in chronic cyclosporine nephropathy in rats. *Nephron Exp Nephrol.* 2008;110:e49–e58.
242. Liu FY, Cogan MG. Angiotensin II stimulation of hydrogen ion secretion in the rat early proximal tubule. Modes of action, mechanism, and kinetics. *J Clin Invest.* 1988;82:601–607.
243. Liu K, Nagase H, Huang CG, et al. Purification and functional characterization of aquaporin-8. *Biol Cell.* 2006;98:153–161.
244. Liu Y, Xu JY, Wang DK, et al. Cloning and identification of two novel NBCe1 splice variants from mouse reproductive tract tissues: a comparative study of NCBT genes. *Genomics.* 2011;98:112–119.
245. Lombard WE, Kokko JP, Jacobson HR. Bicarbonate transport in cortical and outer medullary collecting tubules. *Am J Physiol.* 1983;244:F289–F296.
246. Lonnerholm G, Wistrand PJ. Membrane-bound carbonic anhydrase CA IV in the human kidney. *Acta Physiol Scand.* 2008;141:231–234.
247. Lu M, Holliday LS, Zhang L, et al. Interaction between aldolase and vacuolar H^+/ATPase : evidence for direct coupling of glycolysis to the ATP -hydrolyzing proton pump. *J Biol Chem.* 2001;276:30407–30413.
248. Ludewig U. Electroneutral ammonium transport by basolateral rhesus B glycoprotein. *J Physiol.* 2004;559:751–759.
249. Ludwig MG, Vanek M, Guerini D, et al. Proton-sensing G-protein-coupled receptors. *Nature.* 2003;425:93–98.
250. Lynch IJ, Rudin A, Xia SL, et al. Impaired acid secretion in cortical collecting duct intercalated cells from H,K-ATPase -deficient mice: role of HK isoforms. *Am J Physiol Renal Physiol.* 2008;294:F621–F627.
251. Madsen KM, Tisher CC. Structural-functional relationship along the distal nephron. *Am J Physiol.* 1986;250:F1–F15.

252. Mak DO, Dang B, Weiner ID, et al. Characterization of transport by the kidney Rh glycoproteins, RhBG and RhCG. *Am J Physiol Renal Physiol.* 2006;290:F297–F305.
253. Manucha W, Valles P. Effect of glandular kallikrein on distal bicarbonate transport. Role of basolateral Cl⁻/HCO₃⁻ exchanger and vacuolar H⁽⁺⁾-ATPase. *Biochem J.* 1999;23:161–170.
254. Marini AM, Matassi G, Raynal V, et al. The human Rhesus-associated RhAG protein and a kidney homologue promote ammonium transport in yeast. *Nat Genet.* 2000;26:341–344.
255. Marquez J, Lopez de la Oliva A, Mates JM, et al. Glutaminase: a multifaceted protein not only involved in generating glutamate. *Neurochem Int.* 2005;48:465–471.
256. Maunsbach AB, Vorum H, Kwon TH, et al. Immunoelectron microscopic localization of the electrogenic Na/HCO₃ cotransporter in rat and amblyoma kidney. *J Am Soc Nephrol.* 2000;11:2179–2189.
257. Mavrothalassitis G, Tzimogiorgis G, Mitsialis A, et al. Isolation and characterization of cDNA clones encoding human liver glutamate dehydrogenase: evidence for a small gene family. *Proc Natl Acad Sci U S A.* 1988;85:3494–3498.
258. Mayer M, Schaaf G, Mouro I, et al. Different transport mechanisms in plant and human AMT/Rh-type ammonium transporters. *J Gen Physiol.* 2006;127:133–144.
259. McAlear SD, Liu X, Williams JB, et al. Electrogenic Na/HCO₃ cotransporter (NBCe1) variants expressed in *Xenopus* oocytes: functional comparison and roles of the amino and carboxy termini. *J Gen Physiol.* 2006;127:639–658.
260. McDonough AA, Biemesderfer D. Does membrane trafficking play a role in regulating the sodium/hydrogen exchanger isoform 3 in the proximal tubule? *Curr Opin Nephrol Hypertens.* 2003;12:533–541.
261. McKinney TD, Burg MB. Bicarbonate transport by rabbit cortical collecting tubules. Effect of acid and alkali loads in vivo on transport in vitro. *J Clin Invest.* 1977;60:766–768.
262. McKinney TD, Davidson KK. Effects of respiratory acidosis on HCO₃⁻ transport by rabbit collecting tubules. *Am J Physiol.* 1988;255:F656–F665.
263. McKinney TD, Myers P. Bicarbonate transport by proximal tubules: effect of parathyroid hormone and dibutyl cyclic AMP. *Am J Physiol.* 1980;238:F166–F174.
264. Melo Z, Cruz-Rangel S, Bautista R, et al. Molecular evidence for a role for K⁽⁺⁾-Cl⁽⁻⁾ cotransporters in the kidney. *Am J Physiol Renal Physiol.* 2013;305:F1402–F1411.
265. Milton AE, Weiner ID. Intracellular pH regulation in the rabbit cortical collecting duct A-type intercalated cell. *Am J Physiol.* 1997;273:F340–F347.
266. Mitch WE. Metabolic and clinical consequences of metabolic acidosis. *J Nephrol.* 2006;19:S70–S75.
267. Molina DP, Sun X, Marrs GS, et al. Mapping of pH sensor, GPR4, to peritubular capillaries. *J Am Soc Nephrol.* 2013;24:243A [abstract].
268. Molinas SM, Trumper L, Marinelli RA. Mitochondrial aquaporin-8 in renal proximal tubule cells: evidence for a role in the response to metabolic acidosis. *Am J Physiol Renal Physiol.* 2012;303:F458–F466.
269. Moret C, Dave MH, Schulz N, et al. Regulation of renal amino acid transporters during metabolic acidosis. *Am J Physiol Renal Physiol.* 2007;292:F555–F566.
270. Mount DB. Thick ascending limb of the loop of Henle. *Clin J Am Soc Nephrol.* 2014;9:1974–1986.
271. Mouro-Chanteloup I, Cochet S, Chami M, et al. Functional reconstitution into liposomes of purified human RhCG ammonia channel. *PLoS ONE.* 2010;5:e8921.
272. Mujais SK, Kauffman S, Katz AI. Angiotensin II binding sites in individual segments of the rat nephron. *J Clin Invest.* 1986;77:315–318.
273. Musa-Aziz R, Chen LM, Pelletier MF, et al. Relative CO₂/NH₃ selectivities of AQP1, AQP4, AQP5, AmtB, and RhAG. *Proc Natl Acad Sci U S A.* 2009;106:5406–5411.
274. Nagami GT. Luminal secretion of ammonia in the mouse proximal tubule perfused in vitro. *J Clin Invest.* 1988;81:159–164.
275. Nagami GT. Ammonia production and secretion by the proximal tubule. *Am J Kidney Dis.* 1989;14:258–261.
276. Nagami GT. Effect of bath and luminal potassium concentration on ammonia production and secretion by mouse proximal tubules perfused in vitro. *J Clin Invest.* 1990;86:32–39.
277. Nagami GT. Enhanced ammonia secretion by proximal tubules from mice receiving NH₄Cl: role of angiotensin II. *Am J Physiol Renal Physiol.* 2002;282:F472–F477.
278. Nagami GT. Ammonia production and secretion by S3 proximal tubule segments from acidotic mice: role of ANG II. *Am J Physiol Renal Physiol.* 2004;287:F707–F712.
279. Nagami GT, Kraut JA. Acid-base regulation of angiotensin receptors in the kidney. *Curr Opin Nephrol Hypertens.* 2010;19:91–97.
280. Nagami GT, Sonu CM, Kurokawa K. Ammonia production by isolated mouse proximal tubules perfused in vitro: effect of metabolic acidosis. *J Clin Invest.* 1986;78:124–129.
281. Nagami GT. Role of angiotensin II in the enhancement of ammonia production and secretion by the proximal tubule in metabolic acidosis. *Am J Physiol Renal Physiol.* 2008;294:F874–F880.
282. Nakamura S, Amlal H, Galla JH, et al. NH₄⁺ secretion in inner medullary collecting duct in potassium deprivation: role of colonic H⁺-K⁺-ATPase. *Kidney Int.* 1999;56:2160–2167.
283. Nakhoul NL, Abdunour-Nakhoul SM, Schmidt E, et al. pH sensitivity of ammonium transport by rhbg. *Am J Physiol Cell Physiol.* 2010;299:C1386–C1397.
284. Nakhoul NL, Chen LK, Boron WF. Intracellular pH regulation in rabbit S3 proximal tubule: basolateral Cl⁻/HCO₃⁻ exchange and Na/HCO₃ cotransport. *Am J Physiol.* 1990;258:F371–F381.
285. Nakhoul NL, Hering-Smith KS, Abdunour-Nakhoul SM, et al. Transport of NH₃/NH₄⁺ in oocytes expressing aquaporin-1. *Am J Physiol Renal Physiol.* 2001;281:F255–F263.
286. Nakhoul NL, Abdunour-Nakhoul SM, Boulpaep EL, et al. Substrate specificity of Rhbg: ammonium and methyl ammonium transport. *Am J Physiol Cell Physiol.* 2010;299:C695–C705.
287. Nakhoul NL, DeJong H, Abdunour-Nakhoul SM, et al. Characteristics of renal Rhbg as an NH₄⁺ transporter. *Am J Physiol Renal Physiol.* 2004;288:F170–F181.
288. Naray-Fejes-Toth A, Rusvai E, Fejes-Toth G. Mineralocorticoid receptors and 11 beta-steroid dehydrogenase activity in renal principal and intercalated cells. *Am J Physiol Renal Physiol.* 1994;266:F76–F80.
289. Navaneethan SD, Schold JD, Arrigain S, et al. Serum bicarbonate and mortality in stage 3 and stage 4 chronic kidney disease. *Clin J Am Soc Nephrol.* 2011;6:2395–2402.
290. Needle MA, Kaloyanides GJ, Schwartz WB. The effects of selective depletion of hydrochloric acid on acid-base and electrolyte equilibrium. *J Clin Invest.* 1964;43:1836–1846.
291. Nishinaga H, Komatsu R, Doi M, et al. Circadian expression of the Na⁺/H⁺ exchanger NHE3 in the mouse renal medulla. *Biomed Res.* 2009;30:87–93.
292. Nowik M, Picard N, Stange G, et al. Renal phosphaturia during metabolic acidosis revisited: molecular mechanisms for decreased renal phosphate reabsorption. *Pflugers Arch.* 2008;457:539–549.
293. Osis G, Handlogten ME, Lee H-W, et al. Effect of NBCe1 deletion on renal citrate and 2-oxoglutarate handling. *Physiol Rep.* 2016;4:e12778.
294. Pajor AM. Molecular cloning and functional expression of a sodium-dicarboxylate cotransporter from human kidney. *Am J Physiol.* 1996;270:F642–F648.
295. Pajor AM, Sun N. Protein kinase C-mediated regulation of the renal Na⁽⁺⁾/dicarboxylate cotransporter, NaDC-1. *Biochim Biophys Acta.* 1999;1420:223–230.
296. Palmer LG, Frindt G. Cl⁻ channels of the distal nephron. *Am J Physiol Renal Physiol.* 2006;291:F1157–F1168.
297. Park EY, Kim WY, Kim YM, et al. Proposed mechanism in the change of cellular composition in the outer medullary collecting duct during potassium homeostasis. *Histol Histopathol.* 2012;27:1559–1577.
298. Pastor-Soler N, Beaulieu VR, Litvin TN, et al. Bicarbonate-regulated adenylyl cyclase (sAC) is a sensor that regulates pH-dependent v-ATPase recycling. *J Biol Chem.* 2003;278:49523–49529.
299. Paunescu TG, Da Silva N, Russo LM, et al. Association of soluble adenylyl cyclase with the V-ATPase in renal epithelial cells. *Am J Physiol Renal Physiol.* 2008;294:F130–F138.
300. Paunescu TG, Ljubojevic M, Russo LM, et al. cAMP stimulates apical V-ATPase accumulation, microvillar elongation, and proton extrusion in kidney collecting duct A-intercalated cells. *Am J Physiol Renal Physiol.* 2010;298:F643–F654.
301. Paunescu TG, Russo LM, Da Silva N, et al. Compensatory membrane expression of the V-ATPase B2 subunit isoform in renal medullary intercalated cells of B1-deficient mice. *Am J Physiol Renal Physiol.* 2007;293:F1915–F1926.
302. Pech V, Kim YH, Weinstein AM, et al. Angiotensin II increases chloride absorption in the cortical collecting duct in mice through a pendrin-dependent mechanism. *Am J Physiol Renal Physiol.* 2007;292:F914–F920.

303. Pech V, Thumova M, Dikalov SI, et al. Nitric oxide reduces Cl(-) absorption in the mouse cortical collecting duct through an ENaC-dependent mechanism. *Am J Physiol Renal Physiol.* 2013;304:F1390–F1397.
304. Pech V, Zheng W, Pham TD, et al. Angiotensin II activates H⁺-ATPase in type A intercalated cells. *J Am Soc Nephrol.* 2008;19:84–91.
305. Perry C, Baker OJ, Reyland ME, et al. PKC[alpha]{beta}{gamma}- and PKC[delta]-dependent endocytosis of NBCe1-A and NBCe1-B in salivary parotid acinar cells. *Am J Physiol Cell Physiol.* 2009;297:C1409–C1423.
306. Perry C, Le H, Grichchenko II. ANG II and calmodulin/CaMKII regulate surface expression and functional activity of NBCe1 via separate means. *Am J Physiol Renal Physiol.* 2007;293:F68–F77.
307. Petrovic S, Barone S, Xu J, et al. SLC26a7: a basolateral Cl⁻/HCO₃⁻-exchanger specific to intercalated cells of the outer medullary collecting duct. *Am J Physiol Renal Physiol.* 2004;286:F161–F169.
308. Pfeiffer R, Rossier G, Spindler B, et al. Amino acid transport of γ -L-type by heterodimers of 4D2hc/CD98 and members of the glycoprotein-associated amino acid transporter family. *EMBO J.* 1999;18:49–57.
309. Pirojsakul K, Gattineni J, Dwarakanath V, et al. Renal NHE expression and activity in neonatal NHE3- and NHE8-null mice. *Am J Physiol Renal Physiol.* 2015;308:F31–F38.
310. Pitts RF, Lotspeich WD. Bicarbonate and the renal regulation of acid base balance. *Am J Physiol.* 1946;147:138–154.
311. Praetorius J, Kim YH, Bouzina E, et al. NBCn1 is a basolateral Na⁺-HCO₃⁻ cotransporter in rat kidney inner medullary collecting ducts. *Am J Physiol Renal Physiol.* 2004;286:F903–F912.
312. Preisig PA. Luminal flow rate regulates proximal tubule H-HCO₃ transporters. *Am J Physiol.* 1992;262:F47–F54.
313. Preisig PA. The acid-activated signaling pathway: starting with pyk2 and ending with increased NHE3 activity. *Kidney Int.* 2007;72:1324–1329.
314. Preisig PA, Alpern RJ. Chronic metabolic acidosis causes an adaptation in the apical membrane Na/H antiporter and basolateral membrane na(HCO₃)₃ symporter in the rat proximal convoluted tubule. *J Clin Invest.* 1988;82:1445–1453.
315. Preisig PA, Alpern RJ. Contributions of cellular leak pathways to net NaHCO₃ and NaCl absorption. *J Clin Invest.* 1989;83:1859–1867.
316. Purkerson JM, Schwartz GJ. The role of carbonic anhydrases in renal physiology. *Kidney Int.* 2007;71:103–115.
317. Purkerson JM, Tsuruoka S, Suter DZ, et al. Adaptation to metabolic acidosis and its recovery are associated with changes in anion exchanger distribution and expression in the cortical collecting duct. *Kidney Int.* 2010;78:993–1005.
318. Purkerson JM, Heintz EV, Nakamori A, et al. Insights into acidosis-induced regulation of SLC26A4 (pendrin) and SLC4A9 (AE4) transporters using three-dimensional morphometric analysis of β -intercalated cells. *Am J Physiol Renal Physiol.* 2014;307:F601–F611.
319. Purkerson JM, Schwartz GJ. Expression of membrane-associated carbonic anhydrase isoforms IV, IX, XII, and XIV in the rabbit: induction of CA IV and IX during maturation. *Am J Physiol Regul Integr Comp Physiol.* 2005;288:R1256–R1263.
320. Pushkin A, Yip KP, Clark I, et al. NBC3 expression in rabbit collecting duct: colocalization with vacuolar H⁺-ATPase. *Am J Physiol Renal Physiol.* 1999;277:F974–F981.
321. Quentin F, Chambrey R, Trinh-Trang-Tan MM, et al. The Cl⁻/HCO₃⁻-exchanger pendrin in the rat kidney is regulated in response to chronic alterations in chloride balance. *Am J Physiol Renal Physiol.* 2004;287:F1179–F1188.
322. Quentin F, Eladari D, Cheval L, et al. RhBG and RhCG, the putative ammonia transporters, are expressed in the same cells in the distal nephron. *J Am Soc Nephrol.* 2003;14:545–554.
323. Quigley R, Baum M. Developmental changes in rabbit proximal straight tubule paracellular permeability. *Am J Physiol Renal Physiol.* 2002;283:F525–F531.
324. Quilty JA, Li J, Reithmeier RA. Impaired trafficking of distal renal tubular acidosis mutants of the human kidney anion exchanger kAE1. *Am J Physiol Renal Physiol.* 2002;282:F810–F820.
325. Ramadan T, Camargo SMR, Herzog B, et al. Recycling of aromatic amino acids via TAT1 allows efflux of neutral amino acids via LAT2-4F2hc exchanger. *Pflugers Arch.* 2007;454:507–516.
326. Ramadan T, Camargo SMR, Summa V, et al. Basolateral aromatic amino acid transporter TAT1 (Slc16a10) functions as an efflux pathway. *J Cell Physiol.* 2006;206:771–779.
327. Raphael KL, Murphy RA, Shlipak MG, et al. Bicarbonate concentration, acid-base status, and mortality in the health, aging, and body composition study. *Clin J Am Soc Nephrol.* 2016;11:308–316.
328. Rector FC Jr, Bloomer HA, Seldin DW. Effect of potassium deficiency on the reabsorption of bicarbonate in the proximal tubule of the rat kidney. *J Clin Invest.* 1976;43:1964.
329. Rector FC Jr, Orloff J. The effect of the administration of sodium bicarbonate and ammonium chloride on the excretion and production of ammonia. The absence of alterations in the activity of renal ammonia-producing enzymes in the dog. *J Clin Invest.* 1959;38:366–372.
330. Renkema KY, Velic A, Dijkman HB, et al. The calcium-sensing receptor promotes urinary acidification to prevent nephrolithiasis. *J Am Soc Nephrol.* 2009;20:1705–1713.
331. Riccardi D, Brown EM. Physiology and pathophysiology of the calcium-sensing receptor in the kidney. *Am J Physiol Renal Physiol.* 2010;298:F485–F499.
332. Richards J, Greenlee MM, Jeffers LA, et al. Inhibition of α ENaC expression and ENaC activity following blockade of the circadian clock-regulatory kinases CK1 δ /e. *Am J Physiol Renal Physiol.* 2012;303:F918–F927.
333. Richardson RM, Goldstein MB, Stinebaugh BJ, et al. Influence of diet and metabolism on urinary acid excretion in the rat and the rabbit. *J Lab Clin Med.* 1979;94:510–518.
334. Riquier-Brisson ADM, Leong PKK, Pihakaski-Maunsbach K, et al. Angiotensin II stimulates trafficking of NHE3, NaPi2, and associated proteins into the proximal tubule microvilli. *Am J Physiol Renal Physiol.* 2010;298:F177–F186.
335. Romero MF. Molecular pathophysiology of SLC4 bicarbonate transporters. *Curr Opin Nephrol Hypertens.* 2005;14:495–501.
336. Romero MF, Fulton CM, Boron WF. The SLC4 family of HCO₃⁻ transporters. *Pflugers Arch.* 2004;447:495–509.
337. Rossier G, Meier C, Bauch C, et al. LAT2, a new basolateral 4F2hc/CD98-associated amino acid transporter of kidney and intestine. *J Biol Chem.* 1999;274:34948–34954.
338. Rothenberger F, Velic A, Stehberger PA, et al. Angiotensin II stimulates vacuolar H(+)-ATPase activity in renal acid-secretory intercalated cells from the outer medullary collecting duct. *J Am Soc Nephrol.* 2007;18:2085–2093.
339. Royaux IE, Wall SM, Karniski LP, et al. Pendrin, encoded by the pendred syndrome gene, resides in the apical region of renal intercalated cells and mediates bicarbonate secretion. *Proc Natl Acad Sci U S A.* 2001;98:4221–4226.
340. Ruiz-Agudo E, Burgos-Cara A, Ruiz-Agudo C, et al. A non-classical view on calcium oxalate precipitation and the role of citrate. *Nat Commun.* 2017;8:768.
341. Sabolic I, Brown D, et al. Regulation of AE1 anion exchanger and H(+)-ATPase in rat cortex by acute metabolic acidosis and alkalosis. *Kidney Int.* 1997;51:125–137.
342. Saifur RM, Emoto N, Nonaka H, et al. Circadian clock genes directly regulate expression of the Na(+)/H(+) exchanger NHE3 in the kidney. *Kidney Int.* 2005;67:1410–1419.
343. Sangan P, Kolla SS, Rajendran VM, et al. Colonic H-K-ATPase beta-subunit: identification in apical membranes and regulation by dietary K depletion. *Am J Physiol.* 1999;276:C350–C360.
344. Saparov SM, Liu K, Agre P, et al. Fast and selective ammonia transport by aquaporin-8. *J Biol Chem.* 2007;282:5296–5301.
345. Sarker R, Gronborg M, Cha B, et al. Casein kinase 2 binds to the C terminus of Na⁺/H⁺ exchanger 3 (NHE3) and stimulates NHE3 basal activity by phosphorylating a separate site in NHE3. *Mol Biol Cell.* 2008;19:3859.
346. Sarker R, Cha B, Kovbasnjuk O, et al. Phosphorylation of NHE3-S719 regulates NHE3 activity through the formation of multiple signaling complexes. *Mol Biol Cell.* 2017;28:1754–1767.
347. Sartorius OW, Roemmelt JC, Pitts RF. The renal regulation of acid-base balance in man. IV. The nature of the renal compensations in ammonium chloride acidosis. *J Clin Invest.* 1949;28:423–439.
348. Sastrasinh S, Sastrasinh M. Glutamine transport in submitochondrial particles. *Am J Physiol Renal Physiol.* 1989;257:F1050–F1058.
349. Schoolwerth AC, Strzelecki T, LaNoue KF, et al. Effect of pH and alpha-ketoglutarate on mitochondrial ammonia production. *Contrib Nephrol.* 1982;31:127–133.
350. Schoolwerth AC. Regulation of renal ammoniogenesis in metabolic acidosis. *Kidney Int.* 1991;40:961–973.

351. Schuster VL. Cyclic adenosine monophosphate-stimulated bicarbonate secretion in the rabbit cortical collecting tubule. *J Clin Invest.* 1985;75:2056–2064.
352. Schwartz GJ. Physiology and molecular biology of renal carbonic anhydrase. *J Nephrol.* 2002;15(suppl 5):S61–S74.
353. Schwartz GJ, Barasch J, Al-Awqati Q. Plasticity of functional epithelial polarity. *Nature.* 1985;318:368–371.
354. Schwartz GJ, Tsuruoka S, Vijayakumar S, et al. Acid incubation reverses the polarity of intercalated cell transporters, an effect mediated by hensin. *J Clin Invest.* 2002;109:89–99.
355. Schwartz GJ, Gao X, Tsuruoka S, et al. SDF1 induction by acidosis from principal cells regulates intercalated cell subtype distribution. *J Clin Invest.* 2015;125:4365–4374.
356. Schwartz GJ, Kittelberger AM, Barnhart DA, et al. Carbonic anhydrase IV is expressed in H⁺-secreting cells of rabbit kidney. *Am J Physiol Renal Physiol.* 2000;278:F894–F904.
357. Sekine T, Cha SH, Hosoyamada M, et al. Cloning, functional characterization, and localization of a rat renal Na⁺-dicarboxylate transporter. *Am J Physiol.* 1998;275:F298–F305.
358. Seshadri RM, Klein JD, Kozlowski S, et al. Renal expression of the ammonia transporters, Rhbg and Rhcg, in response to chronic metabolic acidosis. *Am J Physiol Renal Physiol.* 2006;290:F397–F408.
359. Seshadri RM, Klein JD, Smith T, et al. Changes in the subcellular distribution of the ammonia transporter Rhcg, in response to chronic metabolic acidosis. *Am J Physiol Renal Physiol.* 2006;290:F1443–F1452.
360. Shapiro RA, Morehouse RF, Curthoys NP. Inhibition by glutamate of phosphate-dependent glutaminase of rat kidney. *Biochem J.* 1982;207:561–566.
361. Shashidharan P, Huntley GW, Meyer T, et al. Neuron-specific human glutamate transporter: molecular cloning, characterization and expression in human brain. *Brain Res.* 1994;662:245–250.
362. Shayakul C, Alper SL. Defects in processing and trafficking of the AE1 Cl⁻/HCO₃⁻ exchanger associated with inherited distal renal tubular acidosis. *Clin Exp Nephrol.* 2004;8:1–11.
363. Shibata S, Rinehart J, Zhang J, et al. Mineralocorticoid receptor phosphorylation regulates ligand binding and renal response to volume depletion and hyperkalemia. *Cell Metab.* 2013;18:660–671.
364. Shiraishi N, Kitamura K, Kohda Y, et al. Increased endothelin-1 expression in the kidney in hypercalcemic rats. *Kidney Int.* 2003;63:845–852.
365. Siga E, Houillier P, Mandon B, et al. Calcitonin stimulates H⁺ secretion in rat kidney intercalated cells. *Am J Physiol.* 1996;40:F1217–F1223.
366. Silbernagl S. Tubular reabsorption of l-glutamine studied by free-flow micropuncture and micropfusion of rat kidney. *Int J Biochem.* 1980;12:9–16.
367. Simon E, Martin D, Buerkert J. Contribution of individual superficial nephron segments to ammonium handling in chronic metabolic acidosis in the rat. Evidence for ammonia disequilibrium in the renal cortex. *J Clin Invest.* 1985;76:855–864.
368. Simon EE, Merli C, Herndon J, et al. Effects of barium and 5-(N-ethyl-Nisopropyl)-amiloride on proximal tubule ammonia transport. *Am J Physiol.* 1992;262:F36–F39.
369. Simpson GE. Diurnal variations in the rate of urine excretion for two hour intervals: some associated factors. *J Biol Chem.* 1924;59:107–122.
370. Skelton LA, Boron WF. Effect of acute acid-base disturbances on ErbB1/2 tyrosine phosphorylation in rabbit renal proximal tubules. *Am J Physiol Renal Physiol.* 2013;305:F1747–F1764.
371. Smith AN, Skaug J, Choate KA, et al. Mutations in ATP6n1b, encoding a new kidney vacuolar proton pump 116-kD subunit, cause recessive distal renal tubular acidosis with preserved hearing. *Nat Genet.* 2000;26:71–75.
372. Soleimani M, Bergman JA, Hosford MA, et al. Potassium depletion increases luminal Na⁺/H⁺ exchange and basolateral Na⁺:CO₃⁺:HCO₃⁻ cotransport in rat renal cortex. *J Clin Invest.* 1990;86:1076–1083.
373. Soleimani M, Bizal GL, McKinney TD, et al. Effect of in vitro metabolic acidosis on luminal Na⁺/H⁺ exchange and basolateral Na⁺:HCO₃⁻ cotransport in rabbit kidney proximal tubules. *J Clin Invest.* 1992;90:211–218.
374. Song HK, Kim WY, Lee HW, et al. Origin and fate of pendrin-positive intercalated cells in developing mouse kidney. *J Am Soc Nephrol.* 2007;18:2672–2682.
375. Stapenhorst L, Sassen R, Beck B, et al. Hypocitraturia as a risk factor for nephrocalcinosis after kidney transplantation. *Pediatr Nephrol.* 2005;20:652–656.
376. Star RA, Burg MB, Knepper MA. Luminal disequilibrium pH and ammonia transport in outer medullary collecting duct. *Am J Physiol.* 1987;252:F1148–F1157.
377. Star RA, Kurtz I, Mejia R, et al. Disequilibrium pH and ammonia transport in isolated perfused cortical collecting ducts. *Am J Physiol.* 1987;253:F1232–F1242.
378. Stauber A, Radanovic T, Stange G, et al. Regulation of intestinal phosphate transport II. Metabolic acidosis stimulates Na⁺-dependent phosphate absorption and expression of the Na⁺-Pi cotransporter NaPi-IIb in small intestine. *Am J Physiol Gastrointest Liver Physiol.* 2005;288:G501–G506.
379. Stehberger PA, Schulz N, Finberg KE, et al. Localization and regulation of the ATP6V0A4 (a4) vacuolar H⁺-ATPase subunit defective in an inherited form of distal renal tubular acidosis. *J Am Soc Nephrol.* 2003;14:3027–3038.
380. Stettner P, Bourgeois S, Marsching C, et al. Sulfatides are required for renal adaptation to chronic metabolic acidosis. *Proc Natl Acad Sci U S A.* 2013;110:9998–10003.
381. Stone DK, Seldin DW, Kokko JP, et al. Mineralocorticoid modulation of rabbit medullary collecting duct acidification. A sodium-independent effect. *J Clin Invest.* 1983;72:77–83.
382. Stover EH, Borthwick KJ, Bavalia C, et al. Novel ATP6V1B1 and ATP6V0A4 mutations in autosomal recessive distal renal tubular acidosis with new evidence for hearing loss. *J Med Genet.* 2002;39:796–803.
383. Strait KA, Stricklett PK, Kohan JL, et al. Calcium regulation of endothelin-1 synthesis in rat inner medullary collecting duct. *Am J Physiol Renal Physiol.* 2007;293:F601–F606.
384. Sun X, Petrovic S. Increased acid load and deletion of AE1 increase Slc26a7 expression. *Nephron Physiol.* 2008;109:29–35.
385. Sun X, Stephens L, DuBose TD, et al. Adaptation by the collecting duct to an exogenous acid load is blunted by deletion of the proton-sensing receptor GPR4. *Am J Physiol Renal Physiol.* 2015;309:F120–F136.
386. Sun X, Yang LV, Tiegs BC, et al. Deletion of the pH sensor GPR4 decreases renal acid excretion. *J Am Soc Nephrol.* 2010;21:1745–1755.
387. Takito J, Hikita C, Al-Awqati Q. Hensin, a new collecting duct protein involved in the in vitro plasticity of intercalated cell polarity. *J Clin Invest.* 1996;98:2324–2331.
388. Tanphaichitr VS, Sumbtoonnanonda A, Ideguchi H, et al. Novel AE1 mutations in recessive distal renal tubular acidosis. Loss-of-function is rescued by glycoprotein A. *J Clin Invest.* 1998;102:2173–2179.
389. Tashima Y, Kohda Y, Nonoguchi H, et al. Intranephron localization and regulation of the V1a vasopressin receptor during chronic metabolic acidosis and dehydration in rats. *Pflugers Arch.* 2001;442:652–661.
390. Taylor L, Curthoys NP. Glutamine metabolism: role in acid-base balance. *Biochem Mol Biol Educ.* 2004;32:291–304.
391. Tengunnay P, Verlander JW, Yuan W, et al. Identification of distinct subpopulations of intercalated cells in the mouse collecting duct. *J Am Soc Nephrol.* 1996;7:260–274.
392. Teran FJ, Huang W, Hamm LL, et al. NaDC1 knockout: effects on blood pressure and urine pH. *J Am Soc Nephrol.* 2015;26:382A [abstract].
393. Thumova M, Pech V, Froehlich O, et al. Pendrin protein abundance in the kidney is regulated by nitric oxide and cAMP. *Am J Physiol Renal Physiol.* 2012;303:F812–F820.
394. Tojo A, Tisher CC, Madsen KM. Angiotensin II regulates H⁺-ATPase activity in rat cortical collecting duct. *Am J Physiol.* 1994;267:F1045–F1051.
395. Tokonami N, Morla L, Centeno G, et al. α -Ketoglutarate regulates acid-base balance through an intrarenal paracrine mechanism. *J Clin Invest.* 2013;123:3166–3171.
396. Tong J, Harrison G, Curthoys NP. The effect of metabolic acidosis on the synthesis and turnover of rat renal phosphate-dependent glutaminase. *Biochem J.* 1986;233:139–144.
397. Tong J, Shapiro RA, Curthoys NP. Changes in the levels of translatable glutaminase mRNA during onset and recovery from metabolic acidosis. *Biochemistry.* 1987;26:2773–2777.
398. Trepiccione F, Capasso G, Nielsen S, et al. Evaluation of cellular plasticity in the collecting duct during the recovery of lithium-induced nephrogenic diabetes insipidus. *Am J Physiol Renal Physiol.* 2013;305:F919–F929.
399. Trepiccione F, Gerber SD, Grahammer F, et al. Renal Atp6ap2/(Pro)renin receptor is required for normal vacuolar H⁺-ATPase

- function but not for the renin-angiotensin system. *J Am Soc Nephrol*. 2016;27:3320–3330.
400. Tsuganezawa H, Sato S, Yamaji Y, et al. Role of c-SRC and ERK in acid-induced activation of NHE3. *Kidney Int*. 2002;62:41–50.
 401. Tsuganezawa H, Kobayashi K, Iyori M, et al. A new member of the HCO₃⁻ transporter superfamily is an apical anion exchanger of beta-intercalated cells in the kidney. *J Biol Chem*. 2001;276:8180–8189.
 402. Tsuruoka S, Kittelberger AM, Schwartz GJ. Carbonic anhydrase II and IV mRNA in rabbit nephron segments: stimulation during metabolic acidosis. *Am J Physiol*. 1998;274:F259–F267.
 403. Tsuruoka S, Schwartz GJ. HCO₃⁻ absorption in rabbit outer medullary collecting duct: role of luminal carbonic anhydrase. *Am J Physiol*. 1998;274:F139–F147.
 404. Tsuruoka S, Schwartz GJ. Mechanisms of HCO₃⁻ secretion in the rabbit connecting segment. *Am J Physiol*. 1999;277:F567–F574.
 405. Tsuruoka S, Watanabe S, Purkerson JM, et al. Endothelin and nitric oxide mediate adaptation of the cortical collecting duct to metabolic acidosis. *Am J Physiol Renal Physiol*. 2006;291:F866–F873.
 406. Twombly K, Gattineni J, Bobulescu IA, et al. Effect of metabolic acidosis on neonatal proximal tubule acidification. *Am J Physiol Regul Integr Comp Physiol*. 2010;299:R1360–R1368.
 407. Ullrich KJ, Rummich G, Klöss S. Phosphate transport in the proximal convolution of the rat kidney. *Pflugers Arch*. 1978;377:33–42.
 408. Unwin R, Capasso G, Giebisch G. Bicarbonate transport along the loop of Henle effects of adrenal steroids. *Am J Physiol*. 1995;268:F234–F239.
 409. Vallon V, Schwark JR, Richter K, et al. Role of Na⁺/H⁺ exchanger NHE3 in nephron function: micropuncture studies with s3226, an inhibitor of NHE3. *Am J Physiol Renal Physiol*. 2000;278:F375–F379.
 410. Van Huyen JPD, Cheval L, Bloch-Faure M, et al. GDF15 triggers homeostatic proliferation of acid-secreting collecting duct cells. *J Am Soc Nephrol*. 2008;19:1965–1974.
 411. Vargas-Poussou R, Houillier P, Le Pottier N, et al. Genetic investigation of autosomal recessive distal renal tubular acidosis: evidence for early sensorineural hearing loss associated with mutations in the ATP6V0A4 gene. *J Am Soc Nephrol*. 2006;17:1437–1443.
 412. Velazquez H, Silva T. Cloning and localization of KCC4 in rabbit kidney: expression in distal convoluted tubule. *Am J Physiol Renal Physiol*. 2003;285:F49–F58.
 413. Verlander JW, Hassell KA, Royaux IE, et al. Deoxycorticosterone upregulates PDS (Slc26a4) in mouse kidney: role of pendrin in mineralocorticoid-induced hypertension. *Hypertension*. 2003;42:356–362.
 414. Verlander JW, Hong S, Pech V, et al. Angiotensin II acts through the angiotensin 1a receptor to upregulate pendrin. *Am J Physiol Renal Physiol*. 2011;301:F1314–F1325.
 415. Verlander JW, Kim YH, Shin W, et al. Dietary Cl⁻ restriction upregulates pendrin expression within the apical plasma membrane of type B intercalated cells. *Am J Physiol Renal Physiol*. 2006;291:F833–F839.
 416. Verlander JW, Madsen KM, Cannon JK, et al. Activation of acid-secreting intercalated cells in rabbit collecting duct with ammonium chloride loading. *Am J Physiol*. 1994;266:F633–F645.
 417. Verlander JW, Madsen KM, Galla JH, et al. Response of intercalated cells to chloride depletion metabolic alkalosis. *Am J Physiol*. 1992;262:F309–F319.
 418. Verlander JW, Madsen KM, Tisher CC. Effect of acute respiratory acidosis on two populations of intercalated cells in rat cortical collecting duct. *Am J Physiol*. 1987;253:F1142–F1156.
 419. Verlander JW, Madsen KM, Tisher CC. Axial distribution of band 3-positive intercalated cells in the collecting duct of control and ammonium chloride-loaded rabbits. *Kidney Int*. 1996;57:S137–S147, S137–S147.
 420. Verlander JW, Miller RT, Frank AE, et al. Localization of the ammonium transporter proteins, Rh B glycoprotein and Rh C glycoprotein, in the mouse kidney. *Am J Physiol Renal Physiol*. 2003;284:F323–F337.
 421. Verlander JW, Moudy RM, Campbell WG, et al. Immunohistochemical localization of H-K-ATPase alpha(2c)-subunit in rabbit kidney. *Am J Physiol Renal Physiol*. 2001;281:F357–F365.
 422. Verlander JW, Chu D, Lee HW, et al. Expression of glutamine synthetase in the mouse kidney: localization in multiple epithelial cell types and differential regulation by hypokalemia. *Am J Physiol Renal Physiol*. 2013;305:F701–F713.
 423. Villa-Bellosta R, Sorribas V. Compensatory regulation of the sodium/phosphate cotransporters NaPi-IIc (SCL34A3) and Pit-2 (SLC20A2) during Pi deprivation and acidosis. *Pflugers Arch*. 2009;459:499–508.
 424. Vorum H, Kwon TH, Fulton C, et al. Immunolocalization of electroneutral Na-HCO₃⁻ cotransporter in rat kidney. *Am J Physiol Renal Physiol*. 2000;279:F901–F909.
 425. Wagner CA, Finberg KE, Breton S, et al. Renal vacuolar H⁺-ATPase. *Physiol Rev*. 2004;84:1263–1314.
 426. Wagner CA, Finberg KE, Stehberger PA, et al. Regulation of the expression of the Cl⁻/anion exchanger pendrin in mouse kidney by acid-base status. *Kidney Int*. 2002;62:2109–2117.
 427. Wagner CA, Giebisch G, Lang F, et al. Angiotensin II stimulates vesicular H⁺-ATPase in rat proximal tubular cells. *Proc Natl Acad Sci U S A*. 1998;95:9665–9668.
 428. Wall SM. NH₄⁺ augments net acid-secretion by a ouabain-sensitive mechanism in isolated-perfused inner medullary collecting ducts. *Am J Physiol*. 1996;270:F432–F439.
 429. Wall SM. Ouabain reduces net acid secretion and increases pH_i by inhibiting NH₄⁺ uptake on rat tMCD Na⁽⁺⁾-K⁽⁺⁾-ATPase. *Am J Physiol*. 1997;273:F857–F868.
 430. Wall SM, Fischer MP. Contribution of the Na⁺-K⁺-2Cl⁻ cotransporter (NKCC1) to transepithelial transport of H⁺, NH₄⁺, K⁺, and Na⁺ in rat outer medullary collecting duct. *J Am Soc Nephrol*. 2002;13:827–835.
 431. Wall SM, Fischer MP, Kim GH, et al. In rat inner medullary collecting duct, NH₄⁺ uptake by the Na,K-ATPase is increased during hypokalemia. *Am J Physiol Renal Physiol*. 2002;282:F91–F102.
 432. Wall SM, Flessner MF, Knepper MA. Distribution of luminal carbonic anhydrase activity along rat inner medullary collecting duct. *Am J Physiol*. 1991;260:F738–F748.
 433. Wall SM, Knepper MA. Acid-base transport in the inner medullary collecting duct. *Semin Nephrol*. 1990;10:148–158.
 434. Wall SM, Koger LM. NH₄⁺ transport mediated by Na⁺-K⁺-ATPase in rat inner medullary collecting duct. *Am J Physiol*. 1994;267:F660–F670.
 435. Wall SM, Mehta P, DuBose TD. Dietary K⁺ restriction upregulates total and Sch-28080-sensitive bicarbonate absorption in rat tMCD. *Am J Physiol*. 1998;275:F543–F549.
 436. Wall SM, Pech V. The interaction of pendrin and the epithelial sodium channel in blood pressure regulation. *Curr Opin Nephrol Hypertens*. 2008;17:18–24.
 437. Wall SM, Sands JM, Flessner MF, et al. Net acid transport by isolated perfused inner medullary collecting ducts. *Am J Physiol*. 1990;258:F75–F84.
 438. Wall SM, Trinh HN, Woodward KE. Heterogeneity of NH₄⁺ transport in mouse inner medullary collecting duct cells. *Am J Physiol*. 1995;269:F536–F544.
 439. Wall SM, Truong AV, DuBose TD. H⁽⁺⁾-K⁽⁺⁾-ATPase mediates net acid secretion in rat terminal inner medullary collecting duct. *Am J Physiol*. 1996;271:F1037–F1044.
 440. Wall SM, Fischer MP, Glapion DM, et al. ANG II reduces net acid secretion in rat outer medullary collecting duct. *Am J Physiol Renal Physiol*. 2003;285:F930–F937.
 441. Wall SM, Hassell KA, Royaux IE, et al. Localization of pendrin in mouse kidney. *Am J Physiol Renal Physiol*. 2003;284:F229–F241.
 442. Wang T, Chan YL. Mechanism of angiotensin II action on proximal tubular transport. *J Pharmacol Exp Ther*. 1990;252:689–695.
 443. Wang T, Yang CL, Abbiati T, et al. Mechanism of proximal tubule bicarbonate absorption in NHE3 null mice. *Am J Physiol*. 1999;277:F298–F302.
 444. Wang T, Hropot M, Aronson PS, et al. Role of NHE isoforms in mediating bicarbonate reabsorption along the nephron. *Am J Physiol Renal Physiol*. 2001;281:F1117–F1122.
 445. Warth R, Barriere H, Meneton P, et al. Proximal renal tubular acidosis in TASK2 K⁺ channel-deficient mice reveals a mechanism for stabilizing bicarbonate transport. *Proc Natl Acad Sci U S A*. 2004;101:8215–8220.
 446. Watts BA III, George T, Badalamenti A, et al. High-mobility group box 1 inhibits HCO₃⁻ absorption in the medullary thick ascending limb through RAGE-rho-ROCK-mediated inhibition of basolateral Na⁺/H⁺ exchange. *Am J Physiol Renal Physiol*. 2016;311:F600–F613.
 447. Watts BA III, George T, Good DW. The basolateral NHE1 Na⁺/H⁺ exchanger regulates transepithelial HCO₃⁻ absorption through actin cytoskeleton remodeling in renal thick ascending limb. *J Biol Chem*. 2005;280:11439–11447.
 448. Watts BA III, George T, Good DW. Lumen LPS inhibits HCO₃⁻ absorption in the medullary thick ascending limb through TLN4-PI3k-akt-mTOR-dependent inhibition of basolateral Na⁺/H⁺ exchange. *Am J Physiol Renal Physiol*. 2013;305:F451–F462.

449. Weill AE, Tisher CC, Conde MF, et al. Mechanisms of bicarbonate transport by cultured rabbit inner medullary collecting duct cells. *Am J Physiol*. 1994;266:F466–F476.
450. Weiner ID. The Rh gene family and renal ammonium transport. *Curr Opin Nephrol Hypertens*. 2004;13:533–540.
451. Weiner ID. Roles of renal ammonia metabolism other than in acid-base homeostasis. *Pediatr Nephrol*. 2016;32:933–942.
452. Weiner ID, Frank AE, Wingo CS. Apical proton secretion by the inner stripe of the outer medullary collecting duct. *Am J Physiol Renal Physiol*. 1999;276:F606–F613.
453. Weiner ID, Hamm LL. Molecular mechanisms of renal ammonia transport. *Annu Rev Physiol*. 2007;69:317–340.
454. Weiner ID, Leader JP, Bedford JJ, et al. Effects of chronic lithium administration on renal acid excretion in humans and rats. *Physiol Rep*. 2014;doi:10.14814/phy2.12242.
455. Weiner ID, Miller RT, Verlander JW. Localization of the ammonium transporters, Rh B glycoprotein and Rh C glycoprotein in the mouse liver. *Gastroenterology*. 2003;124:1432–1440.
456. Weiner ID, Milton AE. H⁺-K⁺-ATPase in rabbit cortical collecting duct B-type intercalated cell. *Am J Physiol*. 1996;270:F518–F530.
457. Weiner ID, New AR, Milton AE, et al. Regulation of luminal alkalization and acidification in the cortical collecting duct by angiotensin II. *Am J Physiol*. 1995;269:F730–F738.
458. Weiner ID, Verlander JW. Ammonia transporters and their role in acid-base balance. *Physiol Rev*. 2017;97:465–494.
459. Weiner ID, Weill AE, New AR. Distribution of Cl⁻/HCO₃⁻ exchange and intercalated cells in the rabbit cortical collecting duct. *Am J Physiol*. 1994;267:F952–F964.
460. Weiner ID, Wingo CS, Hamm LL. Regulation of intracellular pH in two cell populations of the inner stripe of the rabbit outer medullary collecting duct. *Am J Physiol Renal Physiol*. 1993;265:F406–F415.
461. Weiner ID, Verlander JW. Renal ammonia metabolism and transport. *Compr Physiol*. 2013;3:201–220.
462. Weiner ID, Verlander JW. Ammonia transport in the kidney by Rhesus glycoproteins. *Am J Physiol Renal Physiol*. 2014;306:F1107–F1120.
463. Weinstein AM. A mathematical model of rat distal convoluted tubule. I. Cotransporter function in early DCT. *Am J Physiol Renal Physiol*. 2005;289:F699–F720.
464. Welbourne TC. Acidosis activation of the Pituitary-adrenal-renal glutaminase I axis. *Endocrinology*. 1976;99:1071–1079.
465. Welsh-Bacic D, Nowik M, Kaissling B, et al. Proliferation of acid-secretory cells in the kidney during adaptive remodelling of the collecting duct. *PLoS ONE*. 2011;6:e25240.
466. Wen D, Yuan Y, Cornelius RJ, et al. Deficient acid handling with distal RTA in the NBCe2 knockout mouse. *Am J Physiol Renal Physiol*. 2015;309:F523–F530.
467. Wesson DE. Regulation of kidney acid excretion by endothelins. *Kidney Int*. 2006;70:2066–2073.
468. West CA, Verlander JW, Wall SM, et al. The chloride-bicarbonate exchanger pendrin is increased in the kidney of the pregnant rat. *Exp Physiol*. 2015;100:1177–1186.
469. Westhoff CM. The structure and function of the Rh antigen complex. *Semin Hematol*. 2007;44:42–50.
470. Westhoff CM, Ferreri-Jacobia M, Mak DO, et al. Identification of the erythrocyte Rh-blood group glycoprotein as a mammalian ammonium transporter. *J Biol Chem*. 2002;277:12499–12502.
471. Wilcox CS, Granges F, Kirk G, et al. Effects of saline infusion on titratable acid generation and ammonia secretion. *Am J Physiol*. 1984;247:F506–F519.
472. Windus DW, Cohn DE, Heifets M. Effects of fasting on citrate transport by the brush-border membrane of rat kidney. *Am J Physiol Renal Physiol*. 1986;251:F678–F682.
473. Wingo CS, Madsen KM, Smolka A, et al. H-K-ATPase immunoreactivity in cortical and outer medullary collecting duct. *Kidney Int*. 1990;38:985–990.
474. Winter C, Schulz N, Giebisch G, et al. Nongenomic stimulation of vacuolar H⁺-ATPases in intercalated renal tubule cells by aldosterone. *Proc Natl Acad Sci U S A*. 2004;101:2636–2641.
475. Wood GS, Warnke R. Suppression of endogenous avidin-binding activity in tissues and its relevance to biotin-avidin detection systems. *J Histochem Cytochem*. 1981;29:1196–1204.
476. Wright PA, Knepper MA. Glutamate dehydrogenase activities in microdissected rat nephron segments: effects of acid-base loading. *Am J Physiol*. 1990;259:F53–F59.
477. Wright PA, Knepper MA. Phosphate-dependent glutaminase activity in rat renal cortical and medullary tubule segments. *Am J Physiol*. 1990;259:F961–F970.
478. Wrong O, Davies HE. The excretion of acid in renal disease. *Q J Med*. 1959;28:259–313.
479. Wu H, Chen L, Zhou Q, et al. Aqp2-expressing cells give rise to renal intercalated cells. *J Am Soc Nephrol*. 2013;24:243–252.
480. Yang B, Zhao D, Solenov E, et al. Evidence from knockout mice against physiologically significant aquaporin 8-facilitated ammonia transport. *Am J Physiol Cell Physiol*. 2006;291:C417–C423.
481. Yasuoka Y, Kobayashi M, Sato Y, et al. The intercalated cells of the mouse kidney OMCD are the target of the vasopressin V1a receptor axis for urinary acidification. *Clin Exp Nephrol*. 2013;17:783–792.
482. Yip KP, Tsuruoka S, Schwartz GJ, et al. Apical H(+)/base transporters mediating bicarbonate absorption and pH(i) regulation in the OMCD. *Am J Physiol Renal Physiol*. 2002;283:F1098–F1104.
483. Zheng W, Verlander JW, Cash M, et al. Cellular distribution of the potassium channel, KCNQ1, in normal mouse kidney. *Am J Physiol Renal Physiol*. 2007;292:F456–F466.
484. Zhou X, Lynch IJ, Xia SL, et al. Activation of H⁺-K⁺-ATPase by CO₂ requires a basolateral Ba(2+)-sensitive pathway during K restriction. *Am J Physiol Renal Physiol*. 2000;279:F153–F160.
485. Zhou Y, Boron WF. Role of endogenously secreted angiotensin II in the CO₂-induced stimulation of HCO₃⁻ reabsorption by renal proximal tubules. *Am J Physiol Renal Physiol*. 2008;294:F245–F252.
486. Zhou Y, Bouyer P, Boron WF. Role of a tyrosine kinase in the CO₂-induced stimulation of HCO₃⁻ reabsorption by rabbit S2 proximal tubules. *Am J Physiol Renal Physiol*. 2006;291:F358–F367.
487. Zhou Y, Bouyer P, Boron WF. Role of the AT1a receptor in the CO₂-induced stimulation of HCO₃⁻ reabsorption by renal proximal tubules. *Am J Physiol Renal Physiol*. 2007;293:F110–F120.
488. Zhou Y, Skelton LA, Xu L, et al. Role of receptor protein tyrosine phosphatase γ in sensing extracellular CO₂ and HCO₃⁻. *J Am Soc Nephrol*. 2016;27:2616–2621.
489. Zhou Y, Zhao J, Bouyer P, et al. Evidence from renal proximal tubules that HCO₃⁻ and solute reabsorption are acutely regulated not by pH but by basolateral HCO₃⁻ and CO₂. *Proc Natl Acad Sci U S A*. 2005;102:3875–3880.
490. Zhu Q, Kao L, Azimov R, et al. Topological location and structural importance of the NBCe1-A residues mutated in proximal renal tubular acidosis. *J Biol Chem*. 2010;285:13416–13426.
491. Zhu Q, Shao XM, Kao L, et al. Missense mutation alters T485S NBCe1-A electrogenicity causing proximal renal tubular acidosis. *Am J Physiol Cell Physiol*. 2013;305:C392–C405.
492. Zhu XL, Sly WS. Carbonic anhydrase IV from human lung. Purification, characterization, and comparison with membrane carbonic anhydrase from human kidney. *J Biol Chem*. 1990;265:8795–8801.
493. Zidi-Yahiaoui N, Mouro-Chanteloup I, D'Ambrosio AM, et al. Human Rhesus B and Rhesus C glycoproteins: properties of facilitated ammonium transport in recombinant kidney cells. *Biochem J*. 2005;391:33–40.

BOARD REVIEW QUESTIONS

- Proximal tubule bicarbonate reabsorption increases in response to acidotic conditions. This effect occurs as a direct effect of
 - Changes in luminal fluid composition
 - Changes in intracellular pH
 - Changes in peritubular HCO_3^- and Pco_2 but not pH
 - Changes in proximal tubule cellular composition
 - Changes in extracellular K^+ , which then alter proximal tubule bicarbonate reabsorption

Answer: c

Rationale: Studies using “out of equilibrium” solutions, which enabled separate evaluation of the roles of pH, bicarbonate, and Pco_2 , show that peritubular pH does not have a direct effect on proximal tubule bicarbonate reabsorption, whereas peritubular bicarbonate and CO_2 do. Moreover, the effect of peritubular bicarbonate and CO_2 on bicarbonate reabsorption is dissociated from the effects on intracellular pH. The effect of peritubular bicarbonate and CO_2 appears to be mediated through the basolateral membrane protein, receptor protein tyrosine kinase gamma. Changes in the luminal fluid are not a major regulatory mechanism, and with decreases in the luminal bicarbonate, as occur in metabolic acidosis, a decrease bicarbonate reabsorption may indirectly stimulate peritubular bicarbonate backleak. Whereas there is increasing evidence for changes in the collecting duct cellular composition in acid–base conditions, this does not occur in the proximal tubule. Acid–base alterations in proximal tubule bicarbonate reabsorption are independent of changes in extracellular potassium concentration.

- Citrate excretion is regulated primarily through:
 - Changes in filtered load that result from changes in serum citrate levels
 - Changes in proximal tubule citrate reabsorption
 - Changes in loop of Henle citrate reabsorption
 - Changes in collecting duct citrate reabsorption
 - Changes in collecting duct citrate secretion.

Answer: b

Rationale: Citrate excretion is regulated almost entirely by changes in proximal tubule citrate reabsorption. Changes that occur in response to acid–base and electrolyte disorders are independent of plasma citrate concentrations and of filtered citrate load. There is no known regulation of citrate reabsorption in segments distal to the proximal tubule.

- The regulation of renal ammonia handling involves
 - Changes only in filtered ammonia load
 - Changes only in proximal tubule ammonia generation
 - Ammonia transport that involves only diffusive NH_3 movement and trapping
 - Specific integral membrane proteins that transport NH_3 or NH_4^+
 - Changes in ammonia recycling and glutamine regeneration in the loop of Henle

Answer: d

Rationale: A major advance in the understanding of ammonia metabolism has been the identification that specific integral membrane proteins transport NH_3 or NH_4^+ . Examples of these proteins include NHE3 in the proximal tubule, and NKCC2 and NHE4 in the thick ascending limb of the loop of Henle, and the ammonia transporter family members, Rhbg and Rhcg, in the collecting duct. This model has now essentially replaced the previous model of diffusion equilibrium for NH_3 and NH_4^+ trapping. In contrast to other urinary solutes, very little of urinary ammonia derives directly from arterial delivery; intrarenal ammonia generation is the primary source of urinary ammonia excretion. Changes in plasma ammonia levels, and thereby of filtered load for ammonia, are not a regulatory mechanism altering renal ammonia excretion. Although proximal tubule ammonia generation is involved in response to acid–base and electrolyte disorders, it is not the only regulatory mechanism, as changes in the expression and regulation of ammonia transporting proteins are also critical components of the response. Although there are changes in ammonia recycling and glutamine regeneration, which occurs via the enzyme glutamine synthetase, this occurs in the proximal tubule, and not in the loop of Henle.

- Transport of gas molecules, CO_2 , and NH_3 , that have critical roles in the maintenance of acid–base homeostasis across plasma membranes involves
 - Diffusive movement only
 - Interaction with specific lipid molecule components of the lipid bilayer
 - Peritubular transport only
 - Transport by integral membrane proteins with no selectivity between different gas molecules
 - Transport by integral membrane proteins that have varying specificity for different gas molecules.

Answer: e

Rationale: Members both of the aquaporin family and the Rhesus glycoproteins family transport both CO_2 and NH_3 . Different members have different selectivity for CO_2 or NH_3 , in some cases transporting one, but not the other. Although there is a component of diffusive movement of both CO_2 and NH_3 , increasing evidence indicates that transporter-mediated movement is a critical component of acid–base regulation. There is no evidence that interaction of CO_2 or NH_3 with specific bilayer phospholipids is a critical component of their transmembrane movement. There currently is no evidence of peritubular CO_2 or NH_3 transport in acid–base homeostasis.

Urine Concentration and Dilution

Jeff M. Sands | Harold E. Layton | Robert Andrew Fenton

CHAPTER OUTLINE

INDEPENDENT REGULATION OF WATER AND SALT EXCRETION, 275

ORGANIZATION OF STRUCTURES IN THE KIDNEY RELEVANT TO URINARY CONCENTRATING AND DILUTING PROCESS, 275

VASOPRESSIN AND THE TYPE 2 VASOPRESSIN RECEPTOR, 283

VASOPRESSIN-REGULATED WATER TRANSPORT, 285

VASOPRESSIN-REGULATED UREA TRANSPORT IN THE INNER MEDULLA, 291

URINE CONCENTRATION AND DILUTION PROCESSES ALONG THE MAMMALIAN NEPHRON, 296

KEY POINTS

- Nephron segments and vasculature in the renal medulla are arranged in complex but specific anatomic relationships, both in terms of which segment leads to the next segment and in terms of which segments are adjacent to one another, that play an important role in the concentrating and diluting process. The recently discovered interstitial nodal spaces in the inner medulla may participate in this three-dimensional architecture.
- The urinary concentrating mechanism is dependent on two independent processes: (1) generation of a hypertonic medullary interstitium by concentration of NaCl and urea via countercurrent multiplication processes; and (2) osmotic equilibration of the tubule fluid within the medullary collecting ducts with the hypertonic medullary interstitium under the control of vasopressin.
- Vasopressin and the type 2 vasopressin receptor (V_2R) play a central role in the urinary concentrating mechanism. V_2R activation stimulates NaCl reabsorption by the thick ascending limbs of Henle, urea transport in terminal portions of the inner medullary collecting duct (IMCD), and accumulation of the water channel, AQP2, on the apical plasma membrane of collecting duct principal cells.
- Vasopressin binding to V_2R stimulates adenylyl cyclase, predominantly isoform 6, to increase cytosolic cyclic adenosine monophosphate (cAMP) levels as well as intracellular calcium. This stimulates AQP2 accumulation at the apical plasma membrane by inducing depolymerization of the actin cytoskeleton, and by protein phosphorylation, with S256 being an essential site.
- Vasopressin stimulates phosphorylation of the urea transporters (UTs), UT-A1 (at serines 486 and 499), and UT-A3, and their apical plasma membrane accumulation in the inner medullary collecting duct (IMCD) through two cAMP-dependent pathways: protein kinase A (PKA) and Epac (exchange protein activated by cAMP). This leads to increased urea permeability in the IMCD, which facilitates urea reabsorption, increasing medullary interstitial osmolality and the osmotic gradient promoting water reabsorption through AQP2.
- Urea is lost from the inner medullary interstitium, largely via the vasa recta, but urea recycling pathways play a major role in limiting this loss.
- Metformin, an AMP-activated kinase (AMPK) activator, increases UT-A1 and AQP2 phosphorylation and urine-concentrating ability in rodents. Thus, drugs that activate AMPK may be a future therapy for nephrogenic diabetes insipidus.
- Controversy persists as to the nature of the mechanism that generates the inner medullary osmolality, particularly the NaCl gradient, because there is no active NaCl transport in the thin ascending limb. Several recent and ingenious hypotheses have been advanced that depend on the peristalsis of the renal pelvis and the compressibility of the hyaluronan matrix that constitutes the medullary interstitial matrix as integral components of the concentrating mechanism.

INDEPENDENT REGULATION OF WATER AND SALT EXCRETION

The kidney is responsible for numerous homeostatic functions. For example, body fluid tonicity is tightly controlled by the regulation of water excretion, extracellular fluid volume is controlled by regulation of NaCl excretion, systemic acid–base balance is controlled by regulation of net acid excretion, systemic K⁺ balance is controlled by regulation of K⁺ excretion, and body nitrogen balance¹ is maintained through regulation of urea excretion.

The independent regulation of water and solute excretion is essential for the homeostatic functions of the kidney to be performed simultaneously. This means that in the absence of changes in solute intake or in the metabolic production of waste solutes, the kidney is able to excrete different volumes of water upon changes in water intake. This ability to excrete the appropriate amount of water without marked perturbations in solute excretion (without disturbing the other homeostatic functions of the kidney) is dependent on renal concentrating and diluting mechanisms and forms the basis of this chapter.

Renal water excretion is tightly regulated by the peptide hormone arginine vasopressin (AVP; also named antidiuretic hormone, ADH). Under normal circumstances, the circulating vasopressin level is determined by osmoreceptors in the hypothalamus that trigger increases in vasopressin secretion (by the posterior pituitary gland) when the osmolality of the blood rises above a threshold value, about 292 mOsm/kg H₂O (reviewed by Sands et al.²). This mechanism can be modulated when other inputs to the hypothalamus (e.g., arterial underfilling, severe fatigue, or physical stress) override the osmotic mechanism. Upon an increase in plasma osmolality, vasopressin is secreted from the posterior pituitary gland into the peripheral plasma. The kidney responds to the variable vasopressin levels by varying urine flow (i.e., water excretion). For example, during extreme antidiuresis (high vasopressin), water excretion is greater than 100-fold lower than during major water diuresis (low vasopressin). These major changes in water excretion are obtained without substantial changes in steady-state solute excretion (Fig. 10.1). This phenomenon is dependent on the kidney's ability to concentrate and dilute the urine. During low circulating vasopressin levels, urine osmolality is less than that of plasma (290 mOsm/kg H₂O): the diluting function of the kidney. In contrast, when the circulating vasopressin level is high, urine osmolality is much higher than that of plasma: the concentrating function of the kidney.

ORGANIZATION OF STRUCTURES IN THE KIDNEY RELEVANT TO URINARY CONCENTRATING AND DILUTING PROCESS

The kidney's ability to vary water excretion over a wide physiologic range, without altering steady-state solute excretion, cannot be simply explained as a consequence of the sequential transport processes along the nephron.³ The independent regulation of water and sodium excretion occurs in the renal medulla, where the nephron segments and

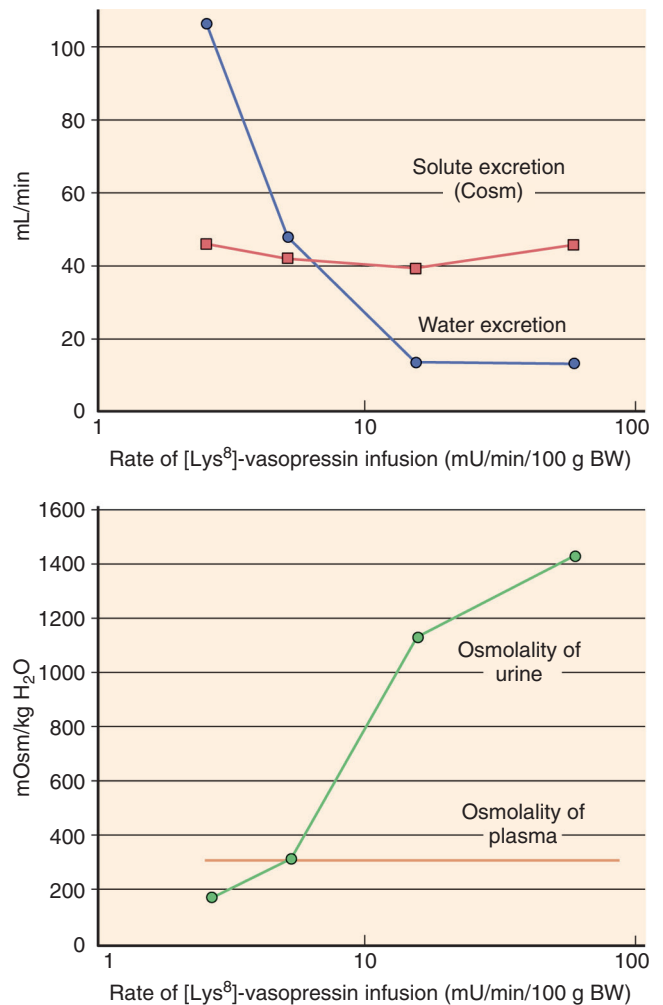


Fig. 10.1 Steady-state renal response to varying rates of vasopressin infusion in conscious rats. A water load (4% of body weight) was maintained throughout the experiments to suppress endogenous vasopressin secretion. Although the urine flow rate was markedly reduced at higher vasopressin infusion rates, the osmolar clearance (solute excretion) changed little. Concordantly, at higher vasopressin infusion rates, the osmolality of the urine increases significantly, whereas plasma osmolality remains constant. *BW*, Body weight. Data from Atherton JC, Hai MA, Thomas S. The time course of changes in renal tissue composition during water diuresis in the rat. *J Physiol.* 1068; 197:429–443.

vasculature (vasa recta) are arranged in complex but specific anatomic relationships, both in terms of which segments connect to which segments and their three-dimensional configuration. Thus, it is necessary to consider the parallel interactions between nephron segments that occur as a result of its looped or hairpin structure. Fig. 10.2 illustrates the regional architecture of the renal medulla and medullary rays.⁴

Fig. 10.3 shows a schematic representation of the mammalian nephron with the localization of major water channels (aquaporins; AQP), urea transporters (UTs), and ion transporters important to the urinary concentrating process. Fig. 10.4 shows which of these transporters and channels are molecular targets for regulated vasopressin action, either in abundance or activity, and thus likely to play a role in urine

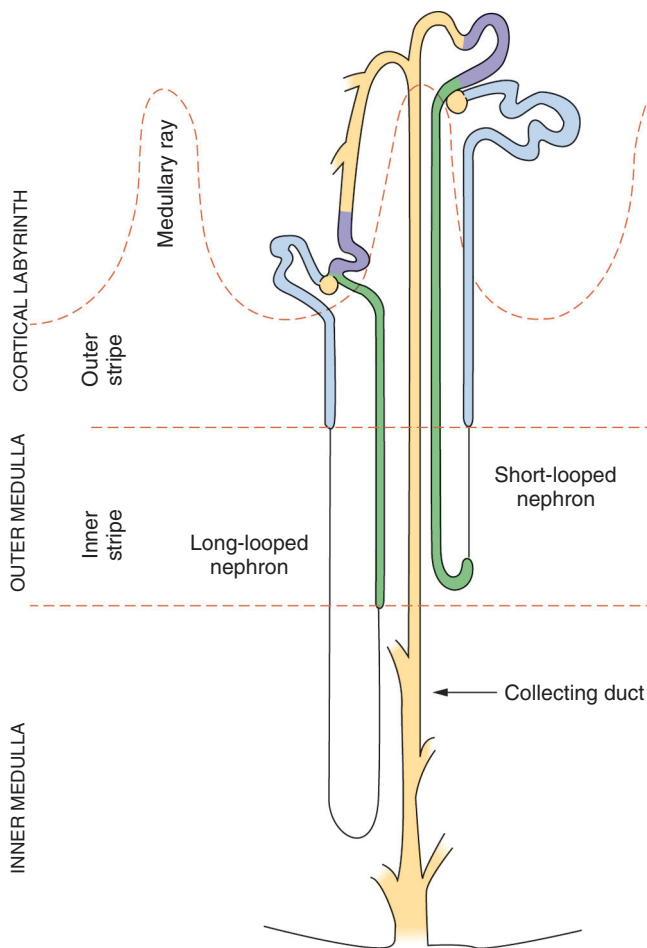


Fig. 10.2 Mammalian renal structure. Major regions of the kidney are shown on the left. Configurations of a long-looped and a short-looped nephron are depicted. The major portions of the nephron are proximal tubules (medium blue), thin limbs of loops of Henle (single line), thick ascending limbs of loops of Henle (green), distal convoluted tubules (lavender), and the collecting duct system (yellow). Modified from Knepper MA, Stephenson JL. Urinary concentrating and diluting processes. In: Andreoli TE, Fanestil DD, Hoffman JF, Schultz SG, eds. *Physiology of Membrane Disorders*. New York: Plenum; 1986:713–726.

concentration. The functions of several of the transporters and channels shown in Fig. 10.3 have been evaluated in mice using gene deletion techniques (reviewed by Fenton et al.⁵). The phenotypes of these mice have been informative with regard to the role of these proteins and their nephron segments in the urinary concentrating and diluting mechanisms.

RENAL TUBULE

LOOPS OF HENLE

The kidney generally contains two populations of nephrons, long-looped and short-looped, which merge to form a common collecting duct system (see Fig. 10.2). Both types of nephrons have loops of Henle that are arranged in a folded or hairpin configuration. Short-looped nephrons generally have glomeruli that are located more superficially in the cortex and have loops that bend in the outer medulla. Long-looped nephrons generally have glomeruli that are located more deeply within the cortex and have loops that

bend at various levels of the inner medulla. Long-looped nephrons also contain a thin ascending limb, a segment that is not present in short-looped nephrons. Thin ascending limbs are found only in the inner medulla. The inner-outer medullary border is defined by the transition from thin to thick ascending limbs. Thus, the outer medulla contains only thick ascending limbs, regardless of the type of loop. The long-looped nephrons bend at various levels of the inner medulla from the inner-outer medullary border to the papillary tip. Thus, progressively fewer loops of Henle extend to deeper levels of the inner medulla. Some mammalian kidneys, such as human kidneys, also contain cortical nephrons, which are nephrons whose loops of Henle do not reach into the medulla.

The loops of Henle receive tubular fluid from the proximal convoluted tubules. Tubular fluid exits the thick ascending limbs of both long- and short-looped nephrons, and from cortical nephrons in species that have them, and flows into distal convoluted tubules. Thus, the descending and ascending limbs of the loops of Henle have a countercurrent flow configuration and are composed of several different nephron segments (see Fig. 10.2). The descending portion of the loop of Henle consists of the S2 proximal straight tubule in the medullary ray, the S3 proximal straight tubule (or pars recta) in the outer stripe of the outer medulla, and the thin descending limb in the inner stripe of the outer medulla and the inner medulla. The descending thin limb of short-looped nephrons differs structurally and functionally from the descending thin limb of long-looped nephrons.^{6,7}

The location of the descending thin limb of short-looped nephrons within the outer medulla is illustrated in Fig. 10.5 (labeled in green).⁸ The descending thin limbs of short-looped nephrons surround the vascular bundles in the outer medulla and tend to be organized in a ring-like pattern (see Fig. 10.5, inset). Thin descending limbs of long-looped nephrons in the outer medulla differ morphologically and functionally from thin descending limbs of long-looped nephrons in the inner medulla.^{9–12} The histologic transition from the outer medullary to the inner medullary type of thin descending limbs of long-looped nephrons is gradual and often occurs at some distance into the inner medulla, rather than strictly at the inner-outer medullary border as is the case for the transition between thin and thick ascending limbs.

Pannabecker and coworkers used immunohistochemical labeling and computer-assisted reconstruction to provide new detail about the functional architecture of the rat inner medulla.^{13–15} Fig. 10.6 shows a computerized reconstruction of the inner medullary portion of several long-looped nephrons from rats that are labeled using antibodies to the water channel aquaporin-1 (AQP1, shown in red) and the chloride channel ClC-K1 (shown in green) (reviewed by Pannabecker et al.^{13–16}). AQP1 is a marker of thin descending limbs of long-looped nephrons in the outer medulla, and it is detected in thin descending limbs of long-looped nephrons in the inner medulla for a variable distance. However, AQP1 was not found in the thin descending limbs of the loops of Henle that turn within the upper millimeter of the inner medulla. Correspondingly, Zhai and colleagues determined that AQP1 was not detectable along the entire length of thin descending limbs of short-looped rat nephrons.¹⁷ In contrast, the upper 40% of thin descending limbs that turn below the first millimeter express AQP1, whereas the lower 60% do

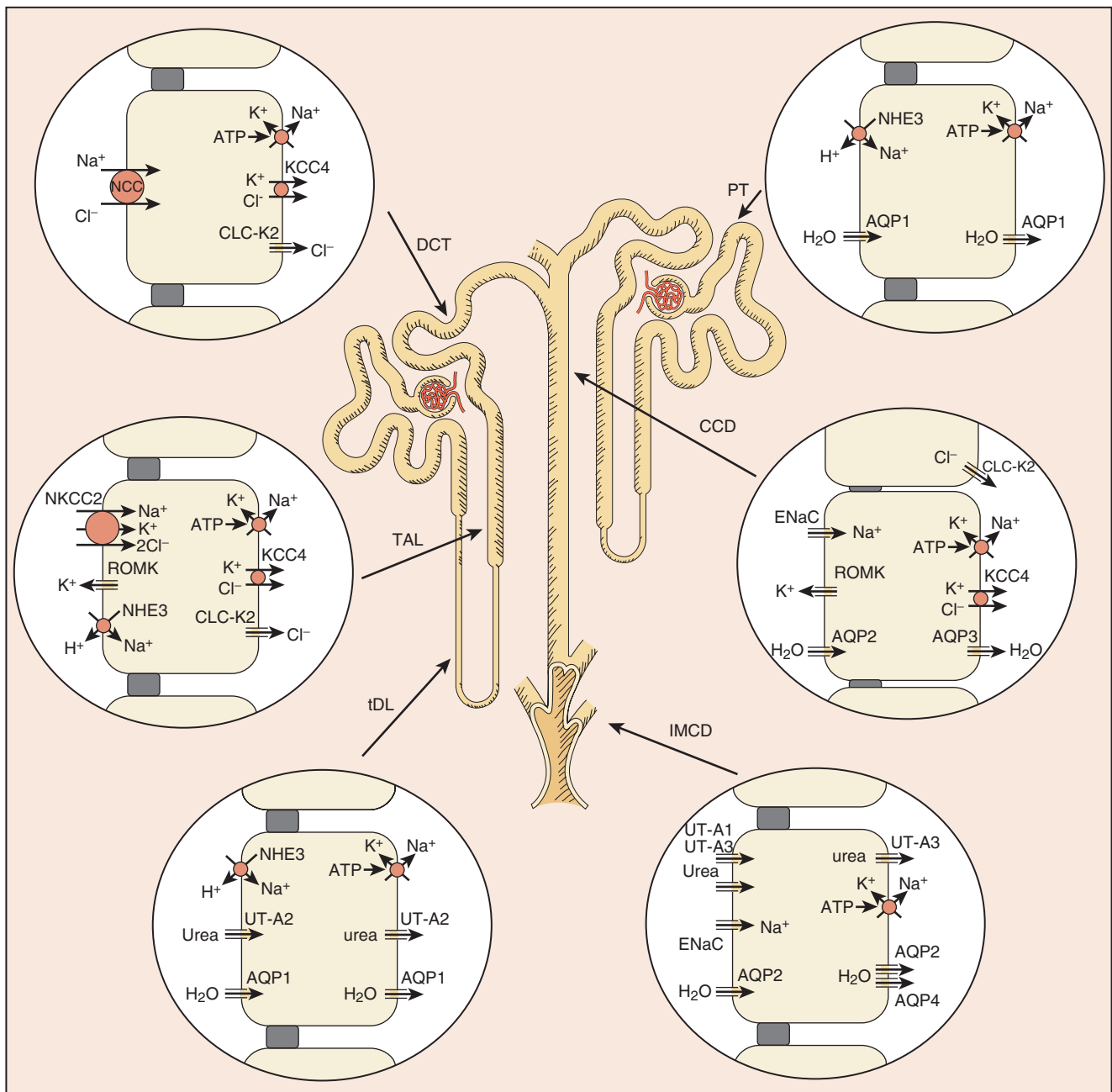


Fig. 10.3 Major aquaporins, urea transporters, and ion transporters/channels that are important to the urinary concentrating and diluting process. Figure depicts a schematic overview of a mammalian kidney tubule, showing the solute and water transport pathways in the proximal tubule (PT), thin descending limb of Henle loop (tDL), thick ascending limb (TAL), distal convoluted tubule (DCT), cortical collecting duct (CCD), and inner medullary collecting duct (IMCD). Tubule lumen side is always on the left-hand side of the cell, whereas the interstitium is on the right-hand side. Arrows represent direction of movement. Adapted from Fenton RA, Knepper MA. Mouse models and the urinary concentrating mechanism in the new millennium. *Physiol Rev.* 2007;87:1083–1112.

not. CIC-K1 is a marker of the thin ascending limb-type epithelium. It is first detected just before the bend of the loops of Henle, consistent with several morphologic studies demonstrating that the descending limb to ascending limb demarcation occurs before the loop bend. A substantial portion of the inner medullary thin descending limb of long-looped nephrons did not express either AQP1 or CIC-K1, as indicated in gray in Fig. 10.6.

The deepest portions of descending thin limbs have low water permeability and reduced AQP1.¹⁸ It has been proposed,

but not demonstrated experimentally, that urine concentration would be improved by the presence of a urea- Na^+ or urea- Cl^- cotransporter in the AQP1-null portion of the thin descending limb.¹⁹ These deep AQP1-null, prebend segments and thin ascending limbs lie equally near the collecting ducts.¹⁸ However, the distal 30% of thin ascending limbs of the longest loops of Henle lie distant from collecting ducts.¹⁸ Urea permeability is lower in the upper portion of thin descending limbs than in the lower portion or in thin ascending limbs in Munich-Wistar rats.²⁰ Because phloretin does not inhibit urea

	LDL-OM	LDL-IM	SDL (early)	SDL (late)	ATL	MTAL	CTAL	DCT	CNT	ICT	CCD	OMCD	IMCD (initial)	IMCD (terminal)
Aquaporin-1	Expressed, not regulated by vasopressin	Expressed, not regulated by vasopressin	Expressed, not regulated by vasopressin											
Aquaporin-2									Expressed, regulated by vasopressin					
Aquaporin-3									Expressed, regulated by vasopressin					
Aquaporin-4												Expressed, not regulated by vasopressin	Expressed, not regulated by vasopressin	Expressed, not regulated by vasopressin
Urea transporter UT-A1														Expressed, regulated by vasopressin
Urea transporter UT-A2		Expressed, regulated by vasopressin		Expressed, regulated by vasopressin										
Urea transporter UT-A3														Expressed, regulated by vasopressin
Na-H exchanger (NHE3)	Expressed, not regulated by vasopressin	Expressed, not regulated by vasopressin				Expressed, regulated by vasopressin	Expressed, regulated by vasopressin							
Na-K-2Cl cotransporter (NKCC2)						Expressed, regulated by vasopressin	Expressed, regulated by vasopressin							
Na-K-2Cl cotransporter (NKCC1)													Expressed, not regulated by vasopressin	Expressed, not regulated by vasopressin
Na-Cl cotransporter (NCC)								Expressed, regulated by vasopressin						
Epithelial Na channel (ENaC)									Expressed, regulated by vasopressin	Expressed, not regulated by vasopressin	Expressed, not regulated by vasopressin			
Cl channel CIC-K1					Expressed, regulated by vasopressin									
Cl channel CIC-K2						Expressed, not regulated by vasopressin								
Potassium channel (ROMK)						Expressed, regulated by vasopressin	Expressed, regulated by vasopressin		Expressed, regulated by vasopressin	Expressed, regulated by vasopressin	Expressed, regulated by vasopressin			
K-Cl cotransporter (KCC4)						Expressed, not regulated by vasopressin								

Fig. 10.4 Grid showing sites of expression of water channels, urea transporters, and ion transporters important to the urinary concentrating process. (See text for details).

permeability, urea transport is not mediated by the UT-A2 urea transporter in these segments.²⁰ Two novel variants of UT-A2, UT-A2c, and UT-A2d, and a variant of the sodium-glucose cotransporter 1, SGLT1a, are expressed in the lower portion of thin descending and thin ascending limb segments, and may mediate urea transport.²¹

Pannabecker and Dantzer²² identified three population groups of loops of Henle in Munich-Wistar rats that can be

distinguished by the position of the thin ascending limb at the base of the inner medulla and by differing loop length (Fig. 10.7). Group 1 loops have thin ascending limbs that are interposed between collecting ducts; group 2 loops have thin ascending limbs that are adjacent to just one collecting duct; and group 3 loops have thin ascending limbs that lie more than 0.5 tubule diameters from a collecting duct. As the collecting ducts coalesce and the shorter loops of Henle

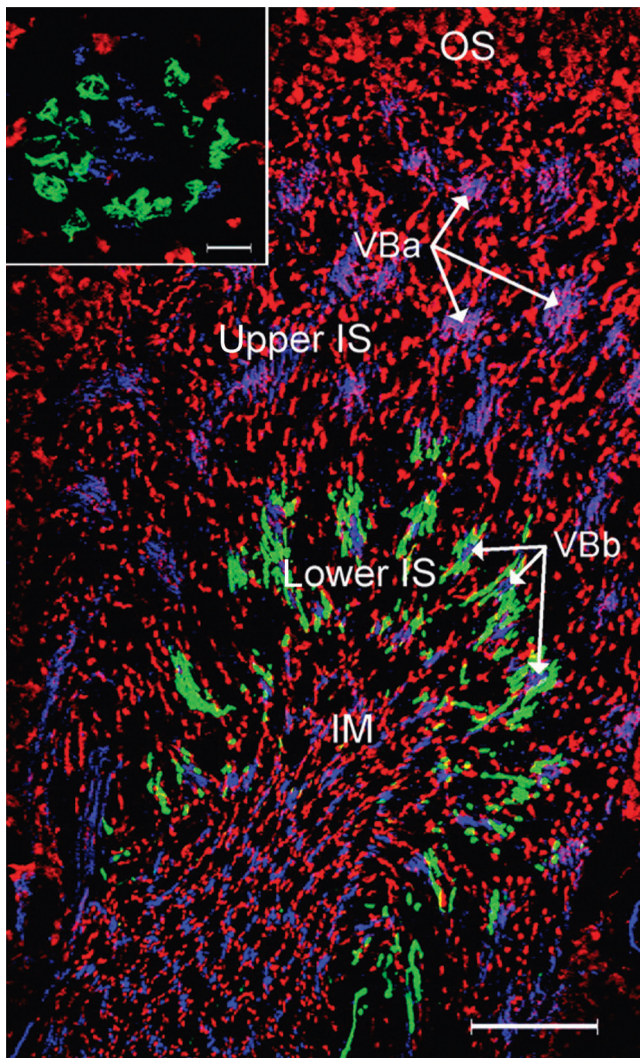


Fig. 10.5 Triple immunolabeling of rat renal medulla showing localization of UT-A2 (green), marking late thin descending limbs from short-looped nephrons, von Willebrand factor (blue) marking endothelial cells of vasa recta, and aquaporin-1 (red) marking thin descending limbs from outer medullary long-looped nephrons and early short-looped nephrons. Inset shows a cross-section of a vascular bundle demonstrating that UT-A2-positive thin descending limbs from short-looped nephrons surround the vascular bundles in the deep part of the outer medulla. *IM*, Inner medulla; *IS*, inner stripe of outer medulla; *OS*, outer stripe of outer medulla; *VBa*, vascular bundles in outer part of inner stripe; *VBb*, vascular bundles in inner part of inner stripe. Reproduced with permission from Wade JB, Lee AJ, Liu J, et al. UT-A2. A 55 kDa urea transporter protein in thin descending limb of Henle loop whose abundance is regulated by vasopressin. *Am J Physiol Renal Physiol.* 2002;278:F52–F62.

disappear, the originating portions of the longer thin ascending limbs run alongside the collecting ducts for a substantial distance.²²

Detailed studies of inner medullary structure, both by Kriz and colleagues^{23–26} and more recently by Pannabecker and colleagues,^{16,19,22,27–30} found that the inner medullary collecting ducts in the inner medullary base (initial inner medullary collecting ducts) form clusters that coalesce along the cortico-medullary axis. The thin descending limbs are

predominantly present at the periphery of these clusters and appear to form an asymmetric ring around each collecting duct cluster, whereas the thin ascending limbs are distributed relatively uniformly among the collecting ducts and thin descending limbs.^{27,31}

In the rat, each collecting duct is surrounded by approximately four ascending vasa recta.³² One or two thin ascending limbs lie between each ascending vasa recta, and opposite to the collecting duct.³² Pannabecker and colleagues hypothesized that descending and ascending thin limbs enter and exit collecting duct clusters in a manner that is important for the generation and maintenance of the osmolality gradient within the inner medulla.¹⁸ These structures form an interstitial nodal space that runs axially through the inner medulla and that may carry water, urea, and NaCl.³² These anatomic relationships may facilitate the preferential mixing of solutes and fluid within the interstitial nodal space.³³ In humans, interstitial nodal spaces are relatively infrequent.³⁰

Kidney-Specific Chloride Channel 1 (ClC-K1)

ClC-K1 localizes to both the apical and basolateral plasma membranes of thin ascending limbs.³⁴ Additionally, ClC-K1 mRNA has been detected in both the thick ascending limb and distal convoluted tubule.³⁵ In isolated perfused tubules, the chloride conductance of thin ascending limbs is increased by vasopressin exposure: either as a result of increased unit conductance or altered cellular localization of ClC-K1 chloride channels.³⁶ Microperfusion studies of ClC-K1 null mice (*Clcnk1*^{−/−}) determined that there was drastically reduced transepithelial chloride transport in the thin ascending limbs of knockout mice.³⁷ *Clcnk1*^{−/−} mice had significantly greater urine volume and lower urine osmolality compared with controls, and even after water deprivation or vasopressin administration, knockout mice were unable to concentrate their urine. This observed polyuria was due to water diuresis and not osmotic diuresis. Inner medullary concentrations of Na⁺ and Cl[−] from *Clcnk1*^{−/−} mice were approximately half those of controls, resulting in a significantly reduced osmolality of the papilla. These studies demonstrate that ClC-K1 is necessary for maintenance of maximal osmolality in the inner medullary tissue. The findings in the *Clcnk1*^{−/−} mice emphasize the importance of rapid chloride exit (and presumably sodium exit) from thin ascending limbs in the inner medullary concentrating process and provide support for the “passive mechanism” (see later).

Na⁺-K-2Cl Cotransporter Type 2 (NKCC2) and Na⁺-H⁺-Exchanger Isoform Type 3 (NHE3)

NKCC2 and NHE3 are the major apical transporters mediating Na⁺ entry in the thick ascending limb.^{38–41} However, knockout of NKCC2 or NHE3 results in drastically different effects on the urinary concentrating mechanism.^{42,43} Total NHE3 knockout mice have a marked reduction in proximal tubule fluid absorption, with a compensatory decrease in glomerular filtration rate owing to an intact tubuloglomerular feedback mechanism.⁴⁴ On *ad libitum* water intake, total NHE3 knockout mice manifest a moderate increase in water intake associated with lower urinary osmolality.⁴⁵ In addition, renal tubule-selective NHE3 knockout mice have only small increases in fluid intake and urinary flow under basal conditions and a minor urinary concentrating defect.⁴⁶ In contrast, NKCC2 knockout mice die before weaning due to renal fluid wasting

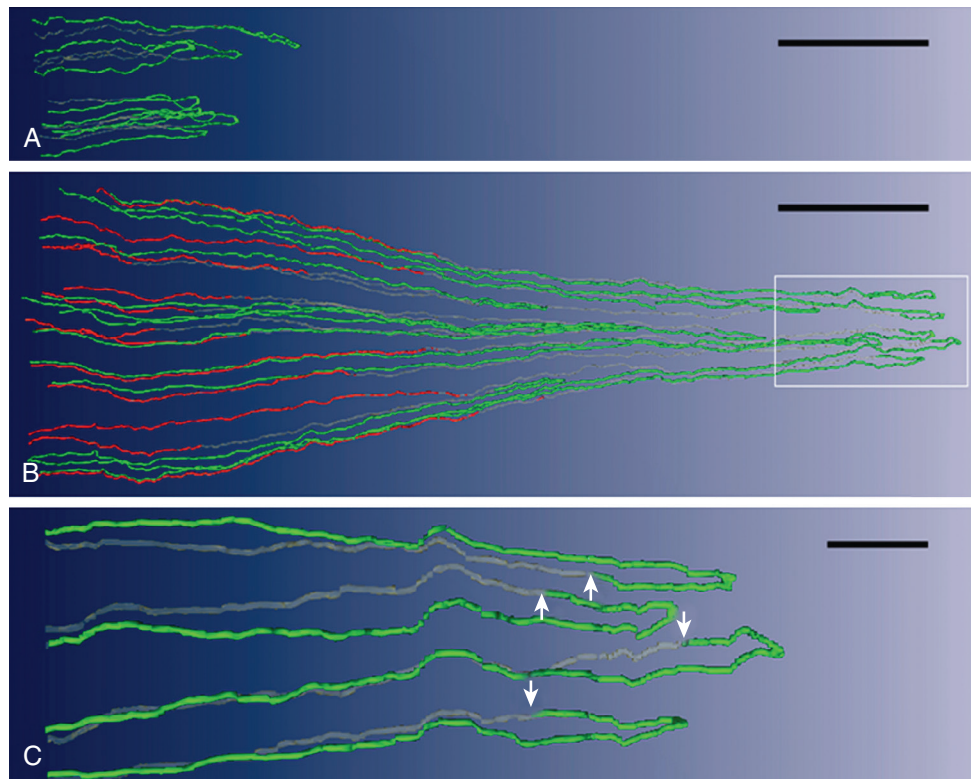


Fig. 10.6 Computer-assisted reconstruction of loops of Henle from rat inner medulla showing expression of aquaporin-1 (AQP1; red) and CIC-K1 (green); gray regions (B-crystallin) express undetectable levels of AQP1 and CIC-K1. Loops are oriented along the corticopapillary axis, with the left edge of each image nearer the base of the inner medulla. (A) Thin limbs that have their bends within the first millimeter beyond the outer-inner medullary boundary. Descending segments lack detectable AQP1. CIC-K1 is expressed continuously along the prebend segment and the thin ascending limb. (B) Loops that have their bends beyond the first millimeter of the inner medulla. AQP1 is expressed along the initial 40% of each thin descending limb and is absent from the remainder of each loop. CIC-K1 is expressed continuously along the prebend segment and the thin ascending limb. Boxed area is enlarged in (C). (C) Enlargement of near-bend regions of four thin limbs from box in (B). CIC-K1 expression, corresponding to thin descending limb prebend segment, begins, on average, 165 μm before the loop bend (arrows). Scale bars, 500 μm (A) and (B) and 100 μm (C). Reproduced with permission from: Pannabecker TL, Dantzier WH, Layton HE, et al. Role of three-dimensional architecture in the urine concentrating mechanism of the rat renal inner medulla. *Am J Physiol Renal Physiol.* 2008;295:F1271–F1285.

and dehydration,⁴³ highlighting the essential role of NKCC2 in the urinary concentrating mechanism.

Why does the deletion of NKCC2 result in such a severe phenotype, when the deletion of NHE3, a transporter responsible for reabsorption of far more Na^+ , results in a viable mouse capable of maintaining extracellular fluid volume? The answer appears to be in the special role that NKCC2 plays in the macula densa in the mediation of tubuloglomerular feedback. Tubuloglomerular feedback allows NHE3 knockout mice to maintain a relatively normal distal delivery through a decrease in glomerular filtration rate, whereas NKCC2 mice cannot compensate in this manner because the transporter is necessary for tubuloglomerular feedback to occur.^{47,48}

Renal Outer Medullary Potassium Channel (ROMK, Kir 1.1)

ROMK is an ATP-sensitive inwardly rectifier potassium channel that localizes to the thick ascending limb, distal convoluted tubule, connecting tubule, and collecting duct system, where it is predominantly associated with the apical plasma membrane.^{49–53} Chronic vasopressin treatment increases

ROMK abundance in thick ascending limbs, thus contributing to vasopressin's long-term effect to increase NaCl transport in this segment.^{54,55} The majority of ROMK knockout mice die before weaning due to hydronephrosis and severe dehydration.⁵⁶ Although 5% of these mice survive the perinatal period, adult mice manifest polydipsia, polyuria, impaired urinary concentrating ability, hypernatremia, and reduced blood pressure, consistent with the known role of ROMK in active NaCl absorption in the thick ascending limb. From these animals, a line of mice has been derived that has a greater survival rate and no hydronephrosis in adult animals; yet the urine concentrating defect persists.

DISTAL TUBULE SEGMENTS IN THE CORTICAL LABYRINTH

After tubular fluid exits the loop of Henle through the cortical thick ascending limb, it enters the distal convoluted tubule, which is located in the cortical labyrinth. In most mammalian species, several distal tubules merge to form a connecting tubule arcade.⁵⁷ The connecting tubule cells express both the vasopressin-regulated water channel, aquaporin-2 (AQP2), and the type 2 vasopressin receptor (V_2R),⁵⁸ suggesting that

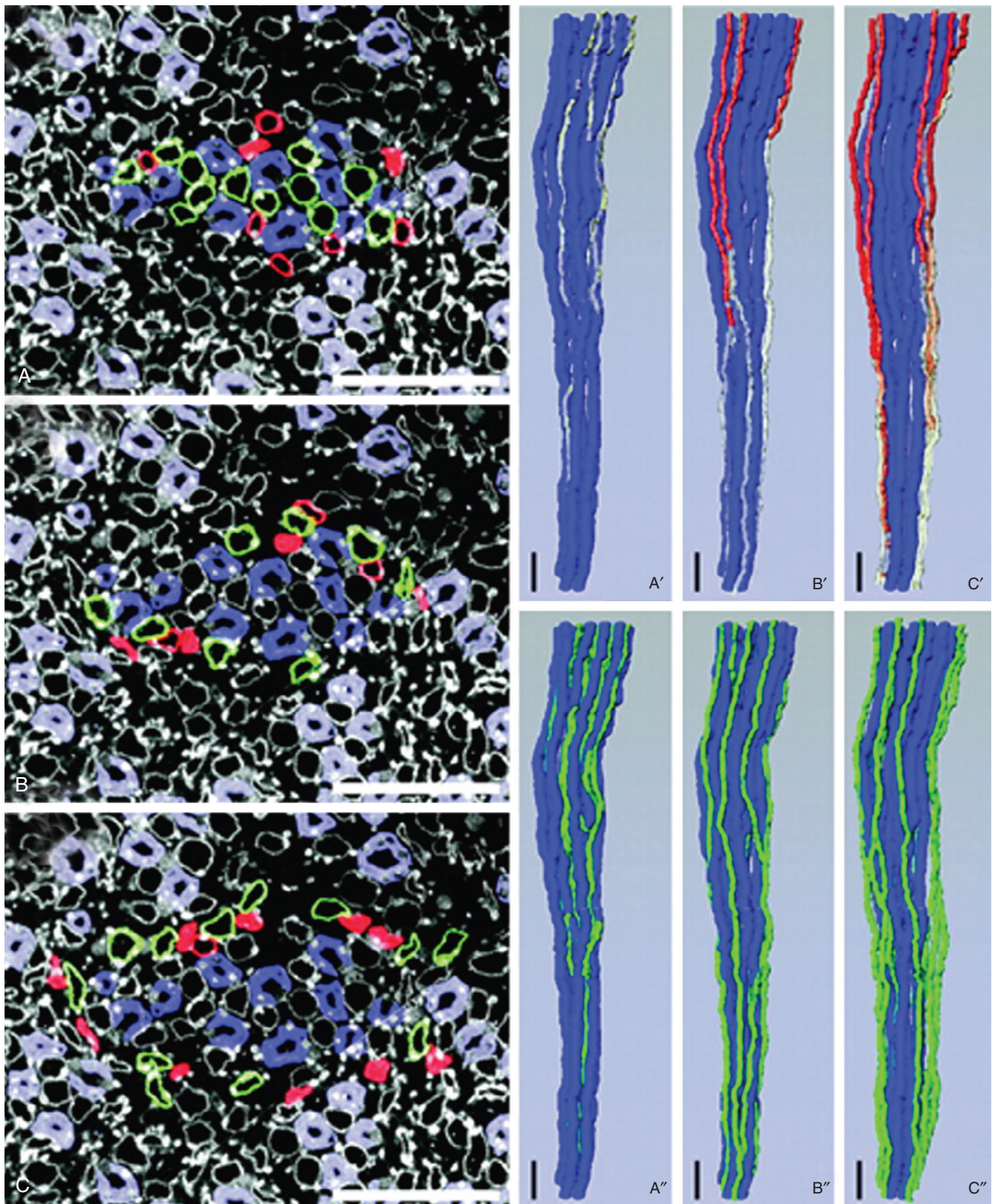


Fig. 10.7 Spatial relationships between thin descending limbs (*red tubules*), thin ascending limbs (*green tubules*), and collecting ducts (*dark blue tubules*). Thin ascending limbs were categorized into three groups related to their lateral proximity to collecting ducts. Members of each group are shown in a transverse section located at the base of the inner medulla: (A) group 1; (B) group 2; and (C) group 3. In (A), (B), and (C), *open red figures* represent aquaporin-1 (AQP1)-null thin descending limbs, *solid red figures* represent AQP1-expressing thin descending limbs, *white outlined figures* represent thin ascending limbs not associated with the collecting duct cluster, and *light blue figures* represent collecting ducts not associated with the collecting duct cluster. Two prebend segments from group 1 are included in (A). One thin ascending limb from each of groups 2 and 3 (B) and (C) extends below the region of reconstruction, and their thin descending limbs were therefore not reconstructed. (A'), (B'), and (C') show thin descending limbs and collecting ducts; (A''), (B''), and (C'') show thin ascending limbs and collecting ducts. Gray tubules in (A'), (B'), and (C') represent AQP1-null thin descending limbs. Scale bars, 100 μm . Reproduced with permission from Pannabecker TL, Dantzler WH. Three-dimensional lateral and vertical relationships of inner medullary loops of Henle and collecting ducts. *Am J Physiol Renal Physiol*. 2004;287:F767–F774.

the arcades are sites of vasopressin-regulated water reabsorption, similar to collecting ducts (see later). Tubular fluid exits the connecting tubules within the arcades and enters the initial collecting tubules, located in the superficial cortex, and then into the cortical collecting ducts. In most rodent species that have been studied, several nephrons merge to form a single cortical collecting duct.^{6,59}

COLLECTING DUCT SYSTEM

The collecting duct system spans all regions of the kidney, starting in the cortex and running to the tip of the inner medulla (see Fig. 10.2). The collecting ducts are the major site of vasopressin-regulated water and urea transport. The transport of water and urea is crucial to the urine-concentrating mechanism, and these are discussed in detail later in this chapter. The collecting ducts are arranged in parallel to the loops of Henle in the medullary rays, outer medulla, and inner medulla. Like the loops of Henle, several morphologically and functionally discrete segments are contained within the collecting duct system. In general, the collecting ducts descend straight through the medullary rays and outer medulla without joining with other collecting ducts. However, several collecting ducts merge as they descend within the inner medulla, resulting in a progressive reduction in the number of inner medullary collecting ducts from the inner-outer medullary border to the papillary tip.⁵⁹ The tapered structure of the renal papilla results from the reduction in collecting duct number, accompanied by a progressive reduction in the number of loops of Henle, reaching the deepest levels of the inner medulla.

The epithelial sodium channel (ENaC) is localized to the late distal convoluted tubule, connecting tubule, initial collecting tubule, and throughout the collecting duct.^{60,61} Vasopressin treatment increases the protein abundance of the beta- and gamma-subunits of ENaC.^{62–64} Acute vasopressin exposure also increases Na⁺ reabsorption in the cortical collecting duct by increasing apical Na⁺ entry via ENaC,^{65–67} due to adenylyl cyclase (AC) 6-dependent stimulation of ENaC open probability and apical membrane channel number.⁶⁸ Deletion of any of the ENaC subunits results in a severe phenotype with neonatal death.^{69–72} Alpha ENaC deletion from the collecting ducts alone, leaving intact ENaC expression in the connecting tubule and nonrenal tissues, results in viable mice that have little or no difficulty in maintaining salt and fluid homeostasis.⁷³ In contrast, alpha ENaC deletion from the connecting tubule and collecting duct together results in a mouse model with increased urine volume and decreased urine osmolality,⁷⁴ indicating that alpha ENaC expression within the connecting tubule and collecting duct is crucial for sodium and water homeostasis.

VASCULATURE

For detailed description of the renal vasculature, see Chapter 2 (Anatomy of the Kidney). The major blood vessels that carry blood into and out of the renal medulla are named the vasa recta. Blood enters the descending vasa recta from the efferent arterioles of juxtamedullary nephrons and supplies it to the capillary plexuses at each level of the medulla. The outer medullary capillary plexus is denser and better perfused than the plexus in the inner medulla.⁷⁵ Blood from the inner medullary capillary plexus feeds into the ascending

vasa recta (ascending vasa recta are never formed directly from descending vasa recta in a loop-like structure). Inner medullary ascending vasa recta traverse the inner stripe of the outer medulla in close physical association with the descending vasa recta in vascular bundles.²³ In many animal species, thin descending limbs of short-looped nephrons surround the vascular bundles, as shown in Fig. 10.5. Here the thin descending limb segments are labeled with an antibody to the UT-A2 urea transporter,⁸ suggesting a route for urea recycling from the vasa recta to the thin descending limbs of short-looped nephrons. The outer medullary capillary plexus is drained by vasa recta that ascend through the outer stripe of the outer medulla, separate from the descending vasa recta.²⁶ Recent computer-assisted digital tracing of the mouse kidney combined with AQP1 immunohistochemistry shows that the arrangement of tubules and vessels in the vascular bundles is important for providing a pathway for lateral osmolality heterogeneity for urine concentration.⁷⁶

The counterflow arrangement of the vasa recta in the medulla promotes countercurrent exchange of solutes and water, which is facilitated by the presence of AQP1^{77,78} and UT-B UTs^{79–81} in the endothelial cells of the descending portion of the vasa recta. In rats, UT-B is expressed in both the outer medullary and inner medullary descending vasa recta.^{81,82} In humans, UT-B is also expressed in the descending vasa recta, but its expression decreases with depth in the inner medulla.³⁰

Countercurrent exchange provides a means of reducing the effective blood flow to the medulla while maintaining a high absolute perfusion rate.⁸³ The low effective blood flow that results from countercurrent exchange is thought to be important for the preservation of solute concentration gradients in the medullary tissue (see later).

In contrast to the medulla, the cortical labyrinth has a high effective blood flow. The rapid vascular perfusion to this region promotes the rapid return of solutes and water reabsorbed from the nephron to the general circulation. The rapid perfusion is thought to maintain the interstitial concentrations of most solutes at levels close to those in the peripheral plasma. The medullary rays of the cortex have a capillary plexus that is considerably sparser than that of the cortical labyrinth. Consequently, the effective blood flow to the medullary rays has been postulated to be lower than that of the cortical labyrinth.³

MEDULLARY INTERSTITIUM

The renal medullary interstitium connects the tubules and vasculature.⁸⁴ It is a complex space that includes the medullary interstitial cells, microfibrils, extracellular matrix, and fluid.^{31,84–86} The interstitium is relatively small in volume in the outer medulla and the outer portion of the inner medulla, which may be important in limiting the diffusion of solutes upward along the medullary axis.^{3,27,84} In contrast, the interstitial space is much larger in the inner half of the inner medulla.^{3,27,84} Within this region, it consists of a gelatinous matrix containing large amounts of highly polymerized hyaluronic acid, consisting of alternating N-acetyl-D-glucosamine and D-glucuronate moieties.⁸⁷ Theories have been proposed in which the hyaluronic acid interstitial matrix plays a direct role in the generation of an inner medullary osmotic gradient through its ability to store and transduce energy

from the smooth muscle contractions of the renal pelvis (see later).⁸⁷

RENAL PELVIS

Urine exits the collecting duct system through the ducts of Bellini at the papillary tip and enters the renal pelvis (Fig. 10.8). The renal pelvis (or calyx in multipapillate kidneys) is a complex intrarenal urinary space that surrounds the papilla. The renal pelvis has portions that extend into the outer medulla, which are called fornices and secondary pouches. Although a transitional epithelium lines most of the pelvic space, the renal parenchyma is separated from the pelvic space by a simple cuboidal epithelium.⁸⁸ In humans, the UT-B urea transporter is expressed within this papillary surface epithelium.⁵⁰ It has been proposed that water and solute transport could occur across this epithelium, thereby modifying the composition of the renal medullary interstitial fluid.⁸⁹ There are two smooth muscle layers within the renal pelvic (calyceal) wall.⁹⁰ Contractions of these smooth muscle layers generate powerful peristaltic waves that appear to displace the renal papilla downward with a “milking” action.⁹¹ These peristaltic waves may intermittently propel urine along the collecting ducts. The contractions compress all structures within the renal inner medulla, including the interstitium, loops of Henle, vasa recta, and collecting ducts.⁹² Theories have been proposed whereby these contractions furnish part of the energy for concentrating solutes, and hence concentrating urine, within the inner medulla (see later).⁸⁷

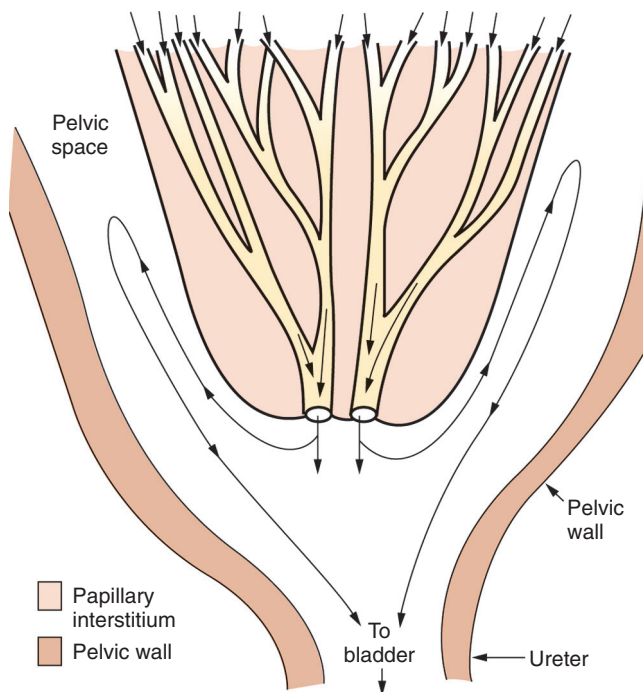


Fig. 10.8 Pattern of urine flow in papillary collecting ducts and renal pelvis. Urine exits the papillary collecting ducts (ducts of Bellini) at the tip of the renal papilla and is carried to the urinary bladder by the ureter. Under some circumstances, a fraction of the urine may reflux backward in the pelvic space and contact the outer surface of the renal papilla. Solute and water exchange across the papillary surface epithelium has been postulated (see text).

VASOPRESSIN AND THE TYPE 2 VASOPRESSIN RECEPTOR

The small peptide hormone vasopressin and the V_2R play a central role in the urinary concentrating mechanism. V_2R activation stimulates NaCl reabsorption by the thick ascending limbs of Henle, urea transport in terminal portions of the inner medullary collecting duct, and accumulation of a water channel, AQP2, on the plasma membrane of collecting duct principal cells. These events permit the collecting duct luminal fluid to equilibrate osmotically with the surrounding interstitium in the kidney, resulting in water reabsorption and urine concentration. Dysfunction of this reabsorption mechanism in the collecting duct results in the production of large amounts of dilute urine, up to 18 L/d, a disease known as diabetes insipidus. In the following we address how the V_2R and AQP2 interact via intracellular signaling pathways to regulate collecting duct water reabsorption and urine concentration.

Clinical Relevance

Nephrogenic Diabetes Insipidus

Nephrogenic diabetes insipidus (NDI) results from the inability of the kidney to respond to vasopressin and produce a concentrated urine. Congenital NDI results from mutations in the V_2R in 90% of families (in which the mutation is known) and in AQP2 in most of the other 10% (reviewed in Sands and Bichet⁴⁶⁹). Acquired forms of NDI occur much more frequently and arise as a consequence of drug treatments, electrolyte disturbances, and urinary tract obstruction. In most manifestations of acquired NDI, dysregulation of AQP2, either in terms of protein abundance or in AQP2 membrane targeting, plays a fundamental role in the development of polyuria.^{470,471} Downregulation of AQP2 observed in acquired NDI is most likely the primary cause of the NDI, rather than being a secondary event (e.g., as a consequence of the increased urine production or reduction in interstitial osmolality). For example, in models of hypokalemic and lithium-induced NDI, the changes in AQP2 expression in the kidney cortex are identical to those seen in the inner medulla,^{472–474} which indicates that interstitial tonicity is not a major factor. Moreover, washout of the medullary osmotic gradient for 1 or 5 days using the loop diuretic furosemide has no effect on AQP2 expression,^{474,475} which indicates that high urine flow in itself is not responsible for the reduced AQP2 expression in experimental NDI. Studies investigating the molecular physiology and signaling pathways regulating water and urea transport have identified several novel therapeutic possibilities for treating NDI (reviewed in Sands and Klein⁴⁰³).

VASOPRESSIN

The ADH of most mammals is a nine-amino acid peptide, vasopressin. Secretion of vasopressin from the posterior pituitary is stimulated by an increase in plasma osmolality,

but also by a reduction in plasma volume (reviewed in Sands et al.²). Vasopressin activates regulatory systems necessary to retain water and restore osmolality to normal.⁹³ The effects of vasopressin occur through the stimulation of receptors that are located on different cell types.^{94,95} Here we focus on the V_2R activation of a cyclic adenosine monophosphate (cAMP) pathway in renal epithelial cells for modulation of collecting duct water transport.

TYPE 2 VASOPRESSIN RECEPTOR

The V_2R is a seven transmembrane-spanning domain receptor that couples to heterotrimeric G proteins (GPCRs).^{96,97} In the kidney it is expressed from the thick ascending limb of

the loop of Henle through to the collecting duct principal cells.⁹⁸⁻¹⁰² When vasopressin binds to the V_2R , AC activity is stimulated and cytosolic cAMP levels increase.¹⁰³ This ultimately leads to an accumulation of AQP2 in the apical plasma membrane of collecting duct principal cells, thus increasing transepithelial water permeability and facilitating osmotically driven water reabsorption (Fig. 10.9). Intracellular calcium is also increased by vasopressin via a mechanism involving calmodulin¹⁰⁴; this is also involved in the regulated trafficking of AQP2.^{105,106} A critical role of the V_2R for urinary concentration has been demonstrated in two mouse models of X-linked nephrogenic diabetes insipidus (XNDI). Upon constitutive deletion,¹⁰⁷ male mutant mice ($V_2R^{-/-}$) die within 7 days after birth, with 3-day-old mice displaying severe hyponatremia,

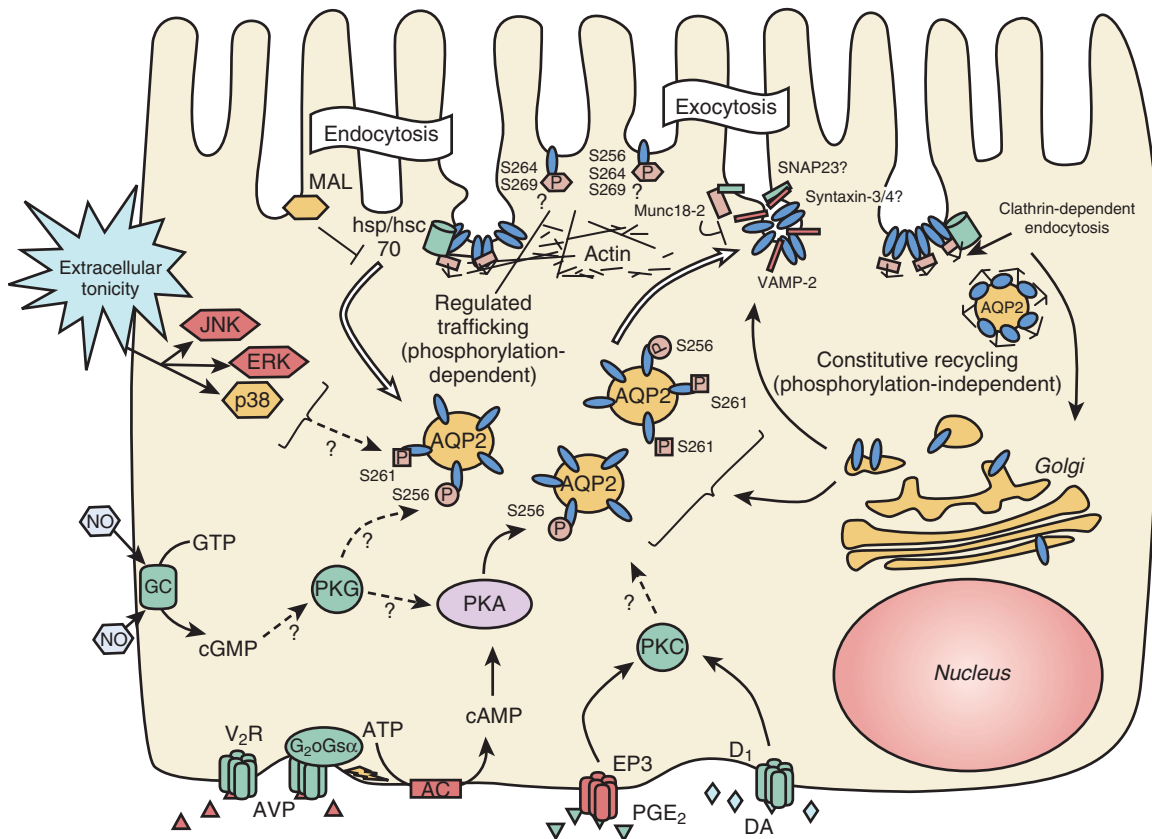


Fig. 10.9 Key events that contribute to the regulation of aquaporin-2 (AQP2) trafficking. The canonical pathway involves interaction of vasopressin with the type 2 receptor (V_2R) on the basolateral surface of the principal cell. This increases cyclic adenosine monophosphate (cAMP) formation after $G_{\alpha s}$ stimulation of adenylyl cyclase (AC). Phosphorylation of AQP2 occurs initially on residue S256, via protein kinase A (PKA) activation. After vasopressin stimulation, residue S261 on AQP2 is dephosphorylated, and residue S264 and S269 phosphorylation is increased. During exocytosis AQP2 interacts with soluble N-ethylmaleimide-sensitive factor attachment protein receptor (SNARE) proteins and their regulatory proteins such as Munc18-2, and these interactions may be regulated by phosphorylation. At the cell surface, phosphorylated AQP2 is present in endocytosis-resistant domains, and its interaction with heat shock protein/heat shock cognate 70 (hsp/hsc70), which is required for clathrin-mediated endocytosis, is inhibited. The myeloid and lymphocyte protein (MAL) also is involved in AQP2 endocytosis by an as-yet-unknown mechanism. Endocytosis of AQP2 is also facilitated by protein kinase C (PKC) activation (but possibly not by direct phosphorylation of AQP2), as well as by activation of dopamine (DA, D_1), prostaglandin E_2 (PGE_2), and PGE_2 receptor type 3 (EP3). However, constitutive exocytosis of AQP2 occurs without vasopressin stimulation and does not require AQP2 phosphorylation on residue S256. Accumulation of AQP2 at the plasma membrane is increased by inhibiting clathrin-mediated endocytosis. AQP2 phosphorylation can also be increased by stimulating the cyclic guanosine monophosphate/protein kinase G (cGMP/PKG) pathways using, for example, nitric oxide (NO). Extracellular hypertonicity activates the mitogen-activated protein (MAP) kinase pathway, and c-Jun N-terminal kinase (JNK), extracellular signal-regulated kinase (ERK), and p38 MAP kinase activities are all required for AQP2 surface accumulation after acute hypertonic shock. Finally, AQP2 trafficking involves the actin cytoskeleton, and actin depolymerization results in cell surface accumulation of AQP2 without the need for vasopressin stimulation. ATP, Adenosine triphosphate; GC, guanylyl cyclase; GTP, guanosine triphosphate; SNAP23, synaptosomal-associated protein 23; VAMP-2, vesicle-associated membrane protein 2.

drastically increased serum Na^+ and Cl^- levels, and significantly lower urine osmolality. In mice with conditional deletion of the V_2R ,^{108,109} adult mice display all of the characteristic symptoms of XNDI,^{110,111} including polyuria, polydipsia, and resistance to the antidiuretic actions of vasopressin.

The function of the V_2R depends on interaction with GPCRs and β -arrestin. Upon vasopressin binding, the V_2R assumes an active configuration and the bound heterotrimeric G protein, Gs, dissociates into $\text{Gs}\alpha$ and $\text{Gs}\beta\gamma$ subunits.¹⁰³ This G protein is localized on the basolateral plasma membrane of the thick ascending limb of Henle, distal convoluted tubule, and collecting duct principal cells.^{112,113} AC is stimulated by activated $\text{Gs}\alpha$, and cAMP levels are increased. The predominant AC isoform in the kidney is AC-6,¹¹⁴ and knockout mice lacking the AC-6 isoform have significant nephrogenic diabetes insipidus (NDI).^{115,116} After vasopressin binding,¹¹⁷ the V_2R is internalized, delivered to, and degraded in lysosomes, thus terminating the response. Many accessory proteins are involved in V_2R downregulation, including inhibitory G_i proteins,^{103,118,119} proteins involved in clathrin-mediated endocytosis,^{120,121} and proteins of the so-called retromer complex.^{122,123} Destruction of cAMP by cytosolic phosphodiesterases is also associated with limiting V_2R responses,¹²⁴ but cAMP levels in vasopressin target cells remain elevated for a considerable time after stimulation, and the V_2R continues to signal from endosomes after internalization.¹²²

A critical step in V_2R internalization is the binding of β -arrestin to the V_2R ,¹²⁵ which is triggered by phosphorylation of the V_2R by kinases, including G-protein-coupled receptor kinases (GRKs).¹²⁶ Following β -arrestin-dependent ubiquitination of the V_2R ,¹²⁷ arrestin-receptor complexes recruit the clathrin adaptor protein AP-2,¹¹⁹ and the complex is then internalized via clathrin-mediated endocytosis.^{120,128,129} Arrestins also uncouple GPCRs from GPCRs, producing a desensitized receptor.¹³⁰ Restoration of prestimulation levels of V_2R at the cell surface requires several hours.^{131–133} The majority of the V_2R that is internalized with vasopressin enters a lysosomal degradation compartment.^{127,134,135} Delivery of both the ligand and receptor to lysosomes may be required to terminate the physiologic response to vasopressin.¹³⁶ Restoration of prestimulation levels of the V_2R at the cell surface partly requires new protein synthesis.¹³⁴

VASOPRESSIN-REGULATED WATER TRANSPORT

COLLECTING DUCT WATER ABSORPTION AND OSMOTIC EQUILIBRATION

The urinary concentrating mechanism is dependent on two independent processes: (1) generation of a hypertonic medullary interstitium by concentration of NaCl and urea via countercurrent processes, and (2) osmotic equilibration of the tubule fluid within the medullary collecting ducts with the hypertonic medullary interstitium. As discussed, vasopressin is essential for determining the degree of water excretion because it increases NaCl reabsorption via the thick ascending limb and thus the hypertonicity of the medullary interstitium and it regulates collecting duct water permeability. When circulating vasopressin levels are low the water permeability of the collecting ducts is also extremely low; relatively little

water is reabsorbed from the tubule fluid and large volumes of hypotonic urine are produced. In contrast, high circulating levels of vasopressin increase the permeability of the apical membrane of the thick ascending limb to NaCl, leading to an increase in the osmolality of the peritubular interstitium (due to countercurrent multiplication) and increasing the water permeability of the collecting ducts to very high levels. Combined, this results in water being rapidly reabsorbed from the cortical and outer medullary portions of the collecting duct system via AQP water channels,^{137–139} resulting in the production of a small volume of hypertonic urine, with osmolality approaching that of the inner medullary interstitium.

The late distal tubule (the late distal convoluted tubule, the connecting tubule, and the initial collecting tubule) is the earliest site along the renal tubule where water absorption increases during antidiuresis (Fig. 10.10).¹⁴⁰ Although the

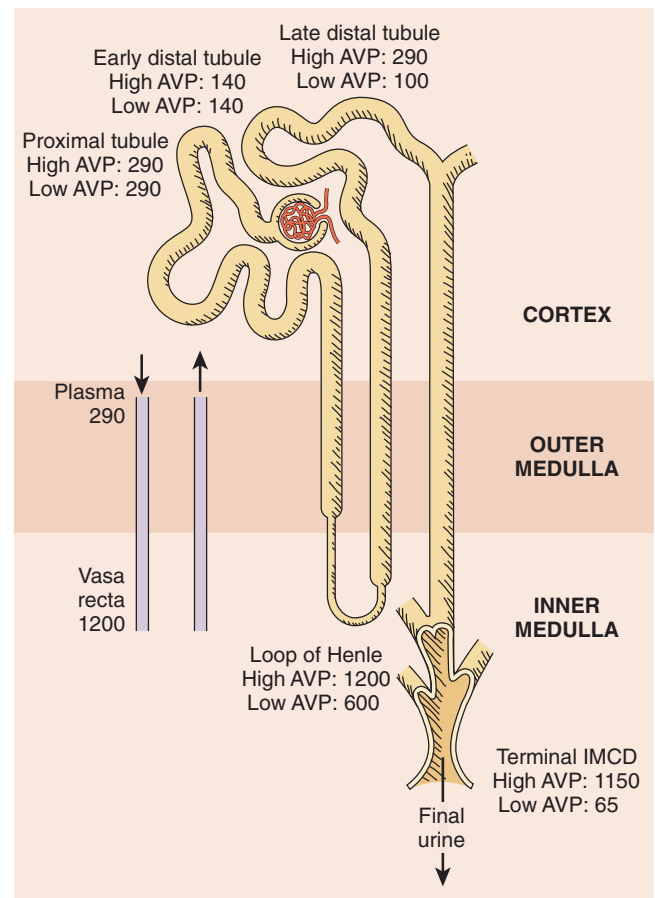


Fig. 10.10 Typical osmolalities (in mOsm/kg H₂O) found in various vascular (left) and renal tubule (right) sites in rat kidneys. Fluid in the proximal tubule is always isosmotic with plasma (290 mOsm/kg H₂O). Fluid emerging from the loop of Henle (entering the early distal tubule) is always hypotonic. Osmolality in the late distal tubule increases to plasma level only during antidiuresis. Final urine is hypertonic when the circulating vasopressin level is high, and hypotonic when the vasopressin level is low. A high osmolality is always maintained in the loop of Henle and vasa recta. During antidiuresis, osmolalities in all inner medullary structures are nearly equal. Osmolalities are somewhat attenuated in the loop and vasa recta during water diuresis (not shown). Based on micropuncture studies; see text. AVP, Vasopressin; IMCD, inner medullary collecting duct.

distal convoluted tubule does not express any water channels, it does express the V_2R and vasopressin regulates NaCl transport in this segment via increasing activity of the Na-Cl cotransport protein, NCC.^{141,142} In contrast, the connecting tubule and the cortical collecting duct express the V_2R and the vasopressin-regulated water channel AQP2.¹⁴³ Thus, it is likely that the connecting tubule and the cortical collecting duct segments are the earliest sites of distal tubular osmotic equilibration.

The volume of water absorption in the connecting segment and initial collecting tubule required to raise tubule fluid to isotonicity is considerably greater than the additional amount required to concentrate the urine above the osmolality of plasma in the medullary portion of the collecting duct system.³ Consequently, during antidiuresis, most of the water reabsorbed from the collecting duct system enters the cortical labyrinth, where the effective blood flow is high enough to return the reabsorbed water to the general circulation without diluting the interstitium. In contrast, if such a large volume of water was reabsorbed along the medullary collecting ducts, it would have a significant dilution effect on the medullary interstitium and thus impair concentrating ability).^{144,145}

During water diuresis, a modest corticomedullary osmolality gradient persists,^{146,147} and the water permeability of the

collecting ducts is low but not zero.^{148,149} Consequently, some water is reabsorbed by the collecting ducts during water diuresis, driven by the small transepithelial osmolality gradient. The majority of this water reabsorption occurs in the terminal inner medullary collecting ducts, where the transepithelial osmolality gradient is highest. In fact, more water is absorbed from the terminal inner medullary collecting ducts during water diuresis than during antidiuresis, owing to a much greater transepithelial osmolality gradient.^{144,145,150}

AQUAPORIN-2: THE VASOPRESSIN-SENSITIVE COLLECTING DUCT WATER CHANNEL

The first water channel, AQP1 was identified in 1991 by Peter Agre and his associates.^{151–154} AQP1 is expressed in proximal tubules and thin descending limbs of long-loop nephrons^{10,155,156} but not short-loop nephrons.¹⁷ AQP2, cloned in 1993, is the vasopressin-regulated water channel in kidney collecting duct principal cells.¹⁵⁷ Vasopressin stimulation of the collecting duct results in the accumulation of AQP2 on the plasma membrane of principal cells (Fig. 10.11). This involves the recycling of AQP2 between intracellular vesicles and the cell surface.^{157,158–164} However, aquaporin-3 (AQP3) and aquaporin-4 (AQP4), both of which are found in the

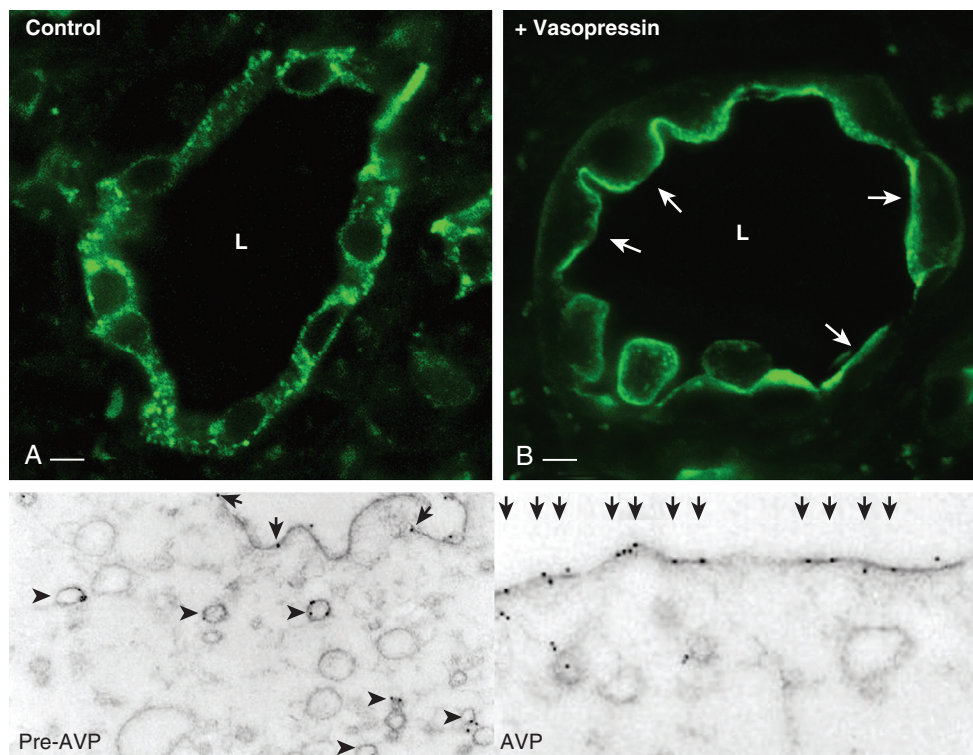


Fig. 10.11 Increased plasma membrane expression of AQP2 in principal cells of AVP-deficient Brattleboro rat kidney inner medullary collecting duct injected with vasopressin for 15 minutes. Kidneys were then fixed, sectioned and immunostained using anti-AQP2 antibodies. Under control conditions (A), AQP2 has a cytosolic distribution in principal cells. After perfusion with AVP (B), AQP2 shows an increased apical localization in principal cells (arrows). A weaker basolateral localization of AQP2 in principal cells is also visible in this section. The lower two panels show the effect of AVP on AQP2 distribution by immunogold electron microscopy. Tubules were perfused with 4 nM DDAVP for 60 minutes. The *left panel* (pre-AVP) shows the apical region of a principal cell, with gold particles (detecting AQP2) distributed on cytoplasmic vesicles, as well as a few on the apical plasma membrane (arrows). After AVP treatment, the number of gold particles on the apical plasma membrane is greatly increased (arrows), and the number of labeled cytoplasmic vesicles (arrowheads) is decreased. L, Tubule lumen. Scale bar, 5 μ m. (Lower panels adapted from Nielsen S, Chou CL, Marples D, et al. Vasopressin increases water permeability of kidney collecting duct by inducing translocation of aquaporin-CD water channels to plasma membrane. *Proc Natl Acad Sci U S A*. 1995;92:1013–1017.)

basolateral membrane of principal cells,^{165,166} are also regulated at the expression, and possibly functional level, by vasopressin and/or dehydration.¹⁶⁶⁻¹⁶⁹

OVERVIEW OF VASOPRESSIN-REGULATED AQP2 TRAFFICKING IN COLLECTING DUCT PRINCIPAL CELLS

The vasopressin-induced change from a low-to-high permeability state of collecting duct principal cells, and vice versa, involves the reversible redistribution of AQP2 from cytoplasmic vesicles to the apical plasma membrane. Early freeze-fracture electron microscopy studies using amphibian urinary bladder and skin suggested that clusters of water channels are located on intracellular vesicles that fuse with the apical plasma membrane upon vasopressin stimulation. The water channels are internalized back into the cell by endocytosis after vasopressin washout.¹⁷⁰⁻¹⁷⁴ Antibodies against AQP2 demonstrated that it is located in the apical plasma membrane of collecting duct principal cells, as well as in intracellular vesicles.^{157,175,176} In vitro and in vivo studies correlated the vasopressin-stimulated increase in collecting duct water permeability and urinary concentration with relocalization of AQP2 from intracellular vesicles to the plasma membrane of principal cells (see Fig. 10.11).¹⁷⁶⁻¹⁷⁹ This relocation was reversible upon vasopressin washout and in animals either infused with a V₂R antagonist or subjected to water loading to reduce circulating vasopressin levels.¹⁸⁰⁻¹⁸² One unexpected observation from initial studies was that significant amounts of AQP2 were present on principal cell basolateral membranes in some kidney regions, and that this staining tended to increase after vasopressin treatment. Recent studies have suggested that basolateral AQP2 is not only a potential pathway for water transport across the basolateral membrane, but may also have a role in cell migration and tubulogenesis due to interaction with β 1 integrin.^{183,184}

Some of the internalized AQP2 that accumulates in endosomes after vasopressin withdrawal follows a complex intracellular pathway before reinsertion into the plasma membrane.^{164,185-187} Unlike the V₂R,¹³⁴ de novo protein synthesis is not required for sequential responses to vasopressin stimulation.¹⁸⁸ A significant amount of AQP2 also accumulates in multivesicular bodies (MVBs).^{180,189} This pool of AQP2 can then be directed to lysosomes for degradation, be transferred to a recycling compartment, or be directly transported to the cell surface via transport vesicles that derive from the MVBs. The fate of internalized AQP2 seems to be at least in part regulated by ubiquitylation.^{190,193} Under certain conditions AQP2 can also be degraded in autophagosomes.^{194,195}

Some of the MVBs can fuse with the apical membrane of principal cells and release small nanovesicles known as exosomes into the tubule lumen. These exosomes contain a variety of different proteins,¹⁹⁶ including AQP2 on their limiting membranes,^{197,198} in addition to AQP2 mRNA and many other mRNAs and microRNAs within their lumen.^{199,200} AQP2 protein can be detected in urine, and the amount increases in conditions of antidiuresis, when more AQP2 is present in the apical membrane of principal cells. The physiologic relevance of this urinary excretion of AQP2 remains unknown, but the amount of exosomal AQP2 can be increased by vasopressin and urinary alkalization,²⁰¹ and a role in cell-cell communication has been proposed.²⁰⁰

BASOLATERAL AQUAPORINS IN PRINCIPAL CELLS

The presence of AQP3 and/or AQP4 renders the basolateral plasma membranes of collecting duct principal cells constitutively permeable to water.^{202,203} AQP3 expression is predominant in the cortex and decreases toward the inner medulla, with the reverse pattern for AQP4 (see Fig. 10.12), which is most abundant in the inner medulla.^{166,203} The abundances of AQP3 and AQP4 can be increased by the long-term action of vasopressin.²⁰²⁻²⁰⁴ AQP2 is also localized in the basolateral plasma membrane of these cells in some regions of the collecting duct.^{175,177,205-208} Basolateral expression of AQP2 is greatly increased by vasopressin^{209,210} or long-term (6 days) aldosterone.^{207,211,212} A proportion of basolateral AQP2 likely represents a transient step in an indirect apical targeting pathway for the AQP2 protein.^{213,214}

AQUAPORIN KNOCKOUT MICE

The physiological roles of various AQPs in the urinary concentrating mechanism have been uncovered by the use of various genetically modified mouse models.

AQUAPORIN-1 KNOCKOUT MICE

AQP1 knockout mice have increased urine volume and reduced urinary osmolality that does not increase in response to water deprivation.²¹⁵ Proximal tubule fluid absorption is markedly impaired in AQP1 knockout mice, but distal delivery of water and NaCl is not impaired due to a reduction in glomerular filtration rate via the tubular–glomerular feedback mechanism.²¹⁶ The osmotic water permeability of isolated perfused thin descending limbs from AQP1 knockout mice was markedly reduced compared with control animals.²¹⁷ As rapid water absorption from long-loop thin descending limbs is essential for countercurrent multiplication processes in the outer medulla, the reduced water reabsorption is one factor responsible for the concentrating defect in AQP1 knockout mice. Descending vasa recta, a second renal medullary site of AQP1 expression, also displayed a marked reduction in osmotic water permeability in AQP1 knockout mice,^{77,78} and thus countercurrent exchange processes are also likely to be impaired in AQP1 knockout mice. The results from studies in these mice show that AQP1 in the renal medulla is essential for the urine-concentrating mechanism.

AQUAPORIN-2 KNOCKOUT MICE

A number of different genetic models have been generated to assess the role of AQP2 in the urinary concentrating mechanism, including inducible and nephron-specific models of AQP2 deletion, models where essential phosphorylation sites in AQP2 are modified, and models of autosomal dominant NDI.^{192,218-226} The major phenotype in these models is severe polyuria; however, with free-access to water, plasma concentrations of electrolytes, urea, and creatinine are not different in knockout mice compared to controls. In contrast, a mouse model with connecting tubule-specific AQP2 deletion²²⁷ has indicated a role of the connecting tubule in regulating body water balance under basal conditions, but not for maximal concentration of the urine during antidiuresis. Taken together, these mouse models confirm that AQP2 is responsible for the

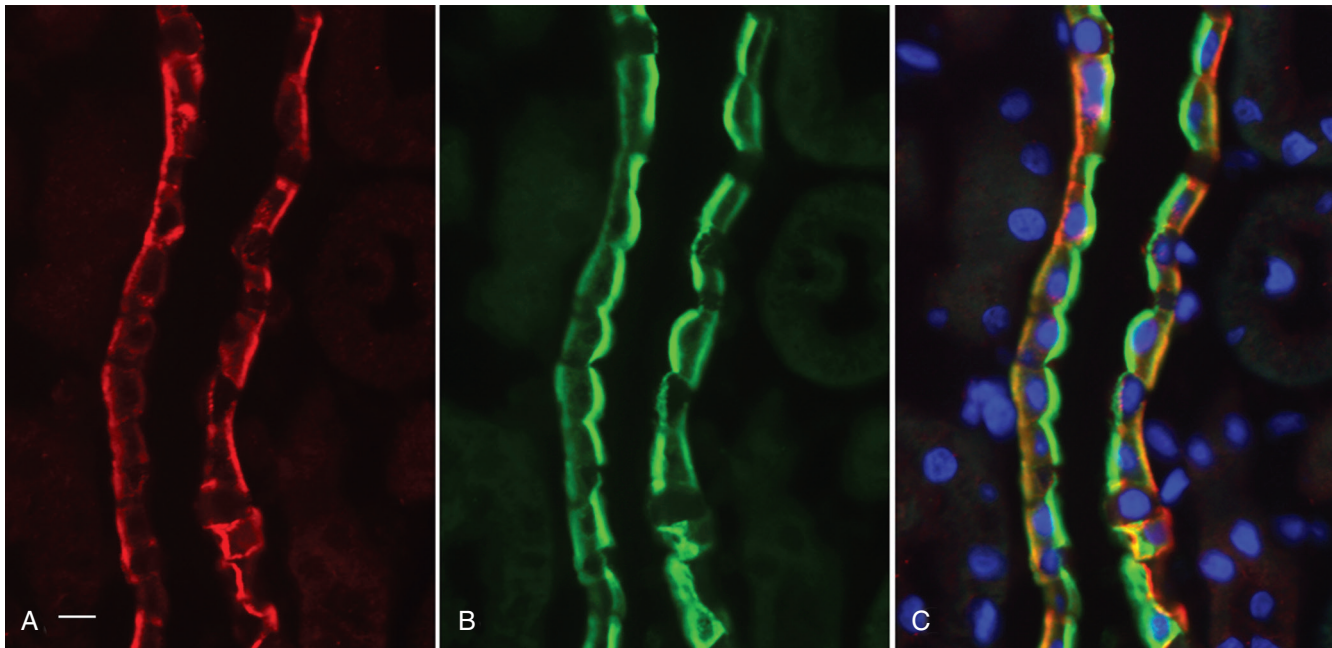


Fig. 10.12 Localization of aquaporins in the outer medullary collecting duct (outer stripe) of rat kidney. Images show sections immunostained in (A) for aquaporin-4 (AQP4) (red) and (B) for aquaporin-2 (AQP2) (green). The merged image in (C) shows that AQP2 is largely apical in this region, but both AQP2 and AQP4 are present on basolateral membranes. Intercalated cells are not stained with either antibody and appear as darker gaps among the other cells. In (C), nuclei are stained with 4',6-diamidino-2-phenylindole (DAPI). Scale bar, 10 μ m.

majority of transcellular water reabsorption in the connecting tubule and collecting duct system.

AQUAPORIN-3 AND AQUAPORIN-4 KNOCKOUT MICE

The osmotic water permeability of the basolateral membrane of cortical collecting duct cells from AQP3 knockout mice is reduced by greater than threefold compared with wild type control mice.²²⁸ Consequently, AQP3 knockout mice are markedly polyuric (10-fold greater daily urine volume than controls), but they can slightly increase their urine osmolality after either water deprivation or vasopressin treatment.³ AQP4 knockout mice have a fourfold decrease in inner medullary collecting duct osmotic water permeability, indicating that AQP4 is responsible for the majority of water movement across the basolateral membrane in this segment.^{229,230} Despite this reduced inner medullary collecting duct water permeability, AQP4 knockout mice have no difference in urine osmolality. However, after 36 hours of water deprivation, AQP4 knockout mice have a significantly reduced maximal urine osmolality that cannot be further increased by AVP administration. This modest decrease in urinary concentrating ability in AQP4 knockout mice, compared with the profound concentrating defect in AQP3 knockout mice, is likely due to the normal distribution of water transport along the collecting duct,³ with much greater osmotic reabsorption of water in the cortical portion of the collecting duct system (where AQP3 is predominant), than in the medullary collecting ducts (where AQP4 is the predominant basolateral water channel).

MECHANISMS OF AQUAPORIN-2 TRAFFICKING

A wealth of information regarding the regulated trafficking, function, structure, and water transport capacity of AQP2

has been generated by the use of various *in vitro* or *ex vivo* experimental systems.^{154,178,188,231–250} In the following sections, we discuss the various mechanisms of AQP2 trafficking that are continually evolving in parallel with new discoveries related to the targeting and trafficking of membrane proteins in general.

AQUAPORIN-2 RECYCLING

Clathrin-coated pits are critical for the internalization of both AQP2 and the V_2R ,^{119,120,128,251,252} with inhibition of clathrin-mediated endocytosis causing AQP2 plasma membrane accumulation (Fig. 10.13).^{159,185,186,251,253–256} Although caveolae have been proposed as an alternative endocytotic pathway for AQP2 in cultured cells,²⁵⁷ caveolae and caveolin are not present on the apical pole of principal cells *in vivo*.^{258,259} After internalization, AQP2 enters a subapical recycling compartment distinct from organelles such as the Golgi, the trans-Golgi network (TGN), and lysosomes,^{188,260,261} but it likely recycles via the classic endosomal recycling compartments^{186,262,263} with the vacuolar protein sorting-associated protein 35 (Vps35) playing an important role.²⁶⁴

ROLE OF THE CYTOSKELETON IN AQUAPORIN-2 TRAFFICKING

The cytoskeleton and soluble N-ethylmaleimide-sensitive factor attachment protein receptor (SNARE) complex play important roles in multiple aspects of vesicle trafficking, including exocytosis, endocytosis, and vesicle docking and fusion.^{265–273} Thus, it is no surprise that they are important for AQP2 trafficking.

Actin associates directly with AQP2^{274–276} or AQP2-containing vesicles²⁷⁷ and upon vasopressin-mediated depolymerization, AQP2 accumulates in the plasma membrane.^{278–281} Apical fluid shear stress also depolymerizes the apical actin cytoskeleton and causes AQP2 membrane accumulation.^{282,283} A

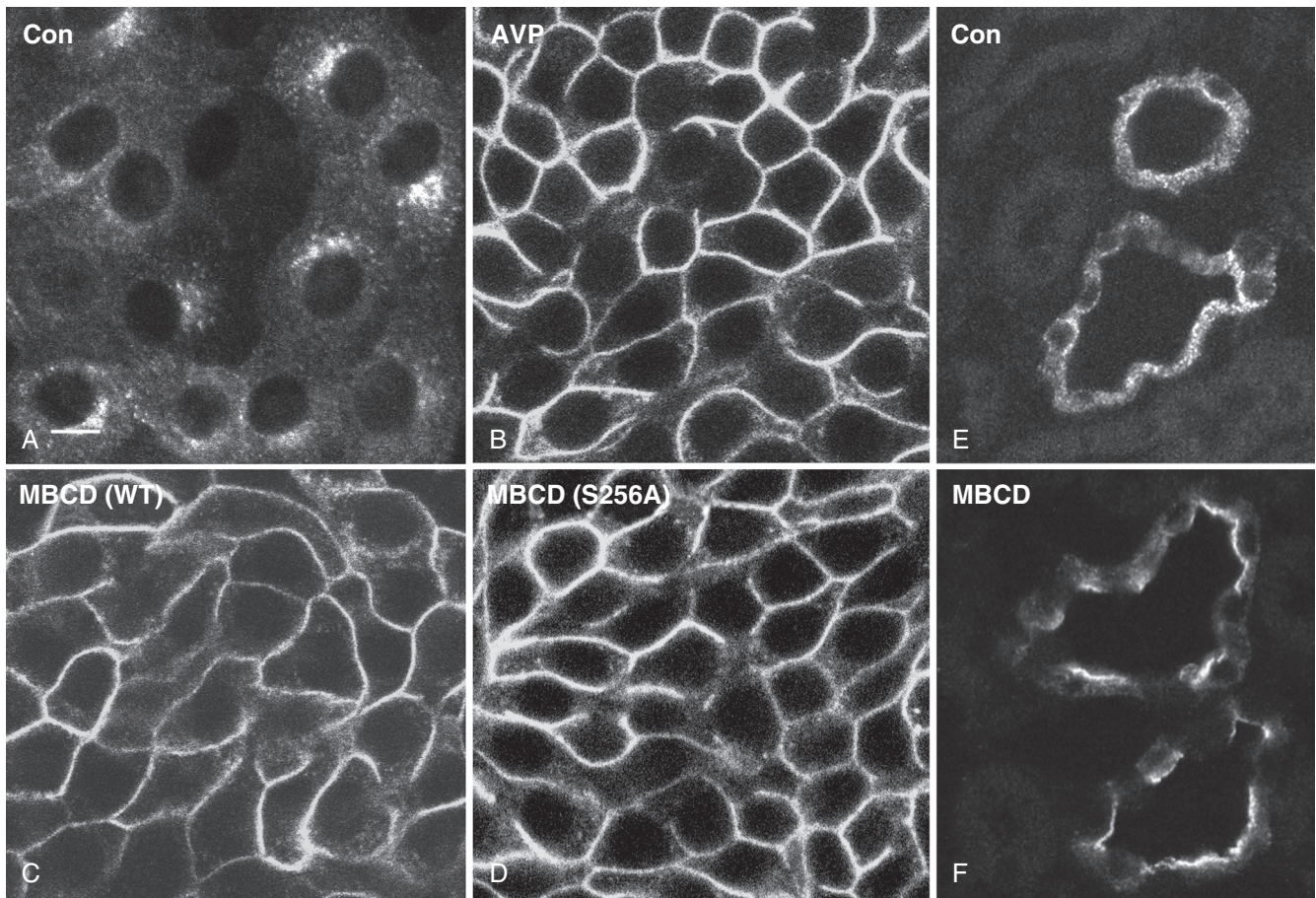


Fig. 10.13 Methyl- β -cyclodextrin (MBCD) stimulates aquaporin-2 (AQP2) membrane accumulation in LLC-PK₁ cells (A) to (D) and collecting duct principal cells in situ (E) and (F). Immunofluorescence staining for AQP2 in LLC-PK₁ cells expressing wild type AQP2 (A) to (C) or a mutant in which the S256 residue has been replaced by alanine (S256A) (D). Under baseline conditions, wild type AQP2 is located mainly on intracellular vesicles, often concentrated in the perinuclear region of the cell (A). After vasopressin (AVP) treatment, wild type AQP2 relocates to the plasma membrane (B). When endocytosis is inhibited by application of the cholesterol-depleting drug MBCD, both wild type and S256A AQP2 accumulate at the cell surface in the absence of AVP (C) and (D). This result shows that both wild type AQP2 and S256A AQP2 are constitutively recycling between intracellular vesicles and the plasma membrane, and that inhibiting endocytosis with MBCD is sufficient to cause membrane accumulation, even in the absence of S256 phosphorylation of AQP2. In collecting duct principal cells (inner stripe of outer medulla) in situ, AQP2 is located on vesicles scattered throughout the cytoplasm after perfusion of intact kidneys in vitro (E). However, after perfusion of kidneys for 60 minutes with 5 mmol/L MBCD, increased apical plasma membrane expression of AQP2 is seen (F). This finding indicates that AQP2 is constitutively recycling through the apical plasma membrane in principal cells in situ, and that membrane accumulation can be induced by blocking endocytosis (with MBCD) even in the absence of vasopressin. *Con*, Control; *WT*, wild type.

role for A-kinase anchoring protein 220 (AKAP220) and Rho GTPases in modulating the actin effects on AQP2 have been proposed.^{280,284–288} AQP2 also complexes with various other actin-associated proteins including myosins,^{277,281,289–291} Rab proteins,^{262,292} members of the ERM (ezrin-radixin-moesin) family,^{293,294} and the signal-induced proliferation-associated gene 1 (SPA-1).²⁸⁸ Although the mechanisms behind actin depolymerization and AQP2 trafficking are not clear (see Fig. 10.14), only vasopressin induces significant actin depolymerization in cells expressing AQP2,²⁸³ suggesting a novel mechanism of protein trafficking in which the channel protein itself critically regulates local actin reorganization to initiate its movement.²⁷⁵ The integrin-linked kinase (ILK) is also important in orchestrating cytoskeletal organization during AQP2 recycling and entry into the exocytotic pathway.^{295,296}

Dynein and dynactin, a protein complex linking microtubules and vesicles, are associated with AQP2-bearing vesicles²⁹⁷

and depolymerization of microtubules partially inhibits vasopressin-induced water permeability in target epithelia^{298–300} and apical localization of AQP2.^{176,249,301,302} A role of microtubules in the basolateral to apical transcytosis of AQP2 has also been suggested.²¹⁴ Together, the data on microtubules indicate that they are predominantly responsible for long-range trafficking of AQP2 vesicles toward the plasma membrane and localization of AQP2 inside the cell after internalization, but that the final steps of vesicle approach and fusion are microtubule independent.³⁰³

A variety of SNARE proteins are associated with AQP2-containing vesicles or colocalize with AQP2 in collecting duct cells, including VAMP-2 (vesicle-associated membrane protein 2, synaptobrevin-2), VAMP-3 (cellubrevin), VAMP-8, SNAP23 (synaptosomal-associated protein 23), the ATPase Hrs-2, syntaxin 3, syntaxin 4, syntaxin 7, syntaxin 12, and syntaxin 13.^{277,304–310} Of these, VAMP-2, VAMP-3, syntaxin 3,

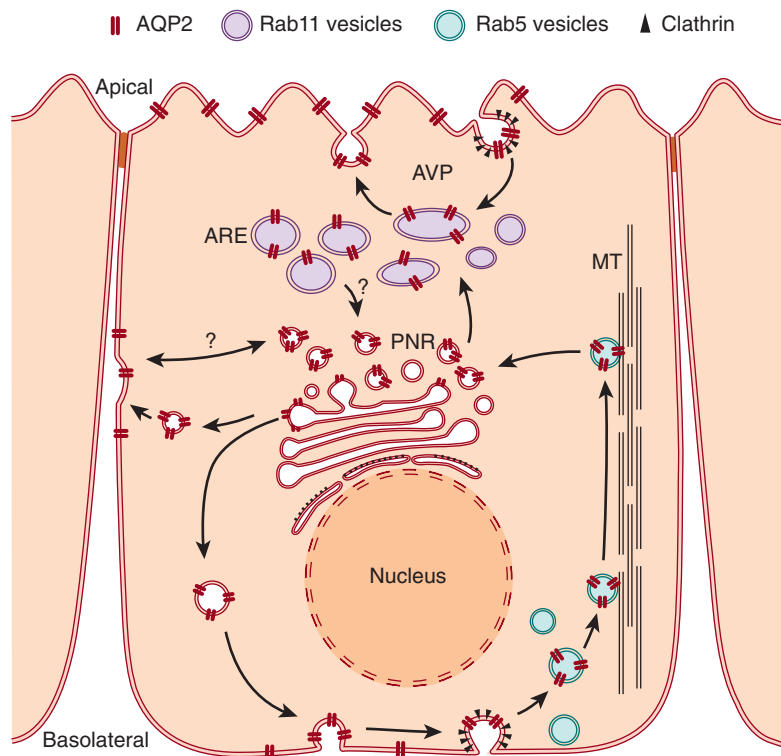


Fig. 10.14 Aquaporin-2 (AQP2) follows a transcytotic pathway before apical membrane delivery. From vesicles in the perinuclear region (*PNR*), probably originating from the trans-Golgi network, AQP2 can be delivered to the basolateral plasma membrane before reaching the apical surface of epithelial cells. From there, it is retrieved by clathrin-mediated endocytosis into Rab5-positive endosomes (*green*), which move in a microtubule (*MT*)-dependent manner to the *PNR* and ultimately to Rab11-positive apical recycling endosomes (*AREs*; *purple*). These Rab11-positive vesicles are involved in recycling AQP2 constitutively to and from the apical plasma membrane. The endocytotic branch of this recycling pathway is inhibited by the methyl- β -cyclodextrin treatment shown in Fig. 10.13, resulting in cell surface accumulation of AQP2. The physiologic stimulus, vasopressin (*AVP*), increases apical AQP2 expression in two ways. It increases exocytosis from the Rab11 compartment and also inhibits clathrin-mediated endocytosis of AQP2 from the apical plasma membrane. The delivery of AQP2 to the basolateral membrane of collecting duct principal cells may be important for collecting duct tubulogenesis,¹⁶³ whereas apical AQP2 is necessary for urine concentration. From Yui N, Lu HA, Chen Y, et al. Basolateral targeting and microtubule-dependent transcytosis of the aquaporin-2 water channel. *Am J Physiol Cell Physiol.* 2013;304:C38–C48.

and SNAP23 are the ones that have been functionally shown to be important for AQP2 trafficking.^{306,309,311} Interaction of AQP2 and the SNARE complex may be mediated by the protein snapin³¹² and/or by the angiotensin-converting enzyme 2 homolog collectrin, which has been implicated in salt-sensitive hypertension.³¹³

ESSENTIAL ROLE OF AQUAPORIN-2 PHOSPHORYLATION

The rise in intracellular cAMP following V_2R stimulation is important for modulating the abundance of AQP2 by modulation of AQP2 gene transcription.^{242,314} cAMP also plays a role in AQP2 trafficking by affecting the phosphorylation status of AQP2,^{262,315–317} with phosphatase inhibitors increasing cell surface accumulation of AQP2.^{318,319} However, V_2R -mediated increases in cAMP are not absolutely necessary for receptor-mediated AQP2 membrane targeting and alternative pathways to increase AQP2 membrane targeting exist.^{320–323}

AQP2 contains several phosphorylation sites for protein kinases,^{138,324–326} several of which are important for AQP2 trafficking alongside AQP2 ubiquitylation.^{190–193} Whether any of the phosphorylation sites are important for modulation of AQP2 unit water permeability is controversial.^{327–329} Early

work focused on the involvement of S256 phosphorylation in AQP2 trafficking, with the current consensus being that S256 phosphorylation is necessary for vasopressin-induced cell-surface accumulation of AQP2^{222,330–334} (Fig. 10.15). The importance of this site is highlighted by a mutation (S254L), which destroys the PKA phosphorylation site at S256 resulting in NDI in humans.^{334,335} The roles of S261, S264, and S269 (threonine in humans) are slowly being uncovered.³²⁸ All three phosphorylated forms are localized to some degree in the plasma membrane in vivo.^{169,189,336,337} Vasopressin decreases the abundance of pS261, whereas AMP-activated kinase (AMPK) activation increases the levels.³³⁸ However, this site alone is not required for AQP2 trafficking.^{339,340} Interestingly, activation of AMPK with metformin increases AQP2 phosphorylation in general,³⁴¹ whereas levels of phosphorylation are significantly attenuated under acidic conditions.³⁴² The pS269 form of AQP2 is exclusively detected in the apical plasma membrane, and a regulatory role of this phosphorylation site directly in the plasma membrane for inhibiting AQP2 endocytosis has been shown.*

*References 169, 189, 191, 336, 337, and 343.

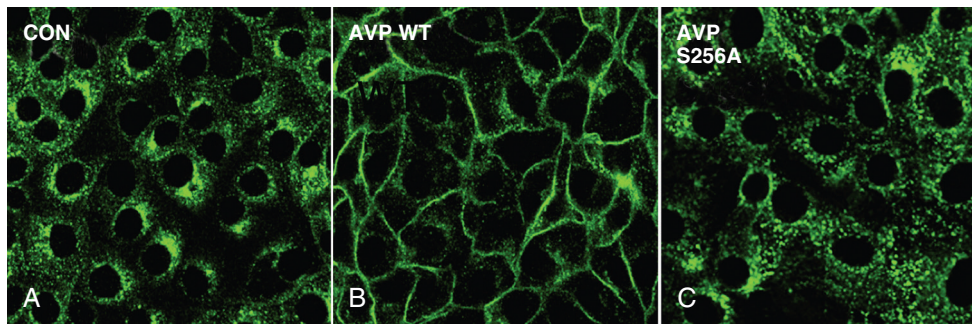


Fig. 10.15 Immunofluorescence staining showing aquaporin-2 (AQP2) expressed in LLC-PK₁ cells. Under control (CON) conditions (A), AQP2 is located on perinuclear and more diffusely distributed intracellular vesicles, with very little plasma membrane staining. After vasopressin (AVP) treatment for 10 minutes, AQP2 accumulates on the plasma membrane of cells expressing wild type (WT) AQP2 (B) but remains mainly on intracellular vesicles after vasopressin treatment of cells expressing AQP2-S256A, a mutation that prevents protein kinase A-mediated phosphorylation of this critical amino acid (C).

ROLE OF PHOSPHORYLATION IN EXOCYTOSIS AND ENDOCYTOSIS OF AQUAPORIN-2

Although S256 phosphorylation is necessary for vasopressin-induced cell-surface accumulation of AQP2, the role that phosphorylation plays in AQP2 exocytosis is complex. An AQP2 S256A mutant accumulates on the plasma membrane upon inhibition of endocytosis (see Fig. 10.13),²⁵³ suggesting that the exocytotic pathway is intact under these conditions. Vasopressin also increases exocytosis of vesicles in AQP2-expressing cells whether or not AQP2 is phosphorylated at S256.³⁴⁴ Thus, although vasopressin-induced accumulation of AQP2 at the cell surface requires S256 phosphorylation, and AQP2 is present in “endocytosis-resistant” membrane domains after vasopressin treatment,^{253,345,346} exocytotic insertion of AQP2 into the plasma membrane is probably independent of this phosphorylation event. Furthermore, the regulated endocytosis of AQP2 may not be dependent on its phosphorylation state.³⁴⁷ For example, prostaglandin E₂ (PGE₂)³⁴⁸ can induce AQP2 internalization independent of S256 phosphorylation, but other studies indicate that the effects of PGE₂ on AQP2 and urine concentration depend on which PGE₂ receptor it acts upon.^{109,250,344,349–351}

Accumulating evidence suggests that phosphorylation-mediated interaction of AQP2 with other regulatory proteins is important for modulating cell-surface accumulation of AQP2. For example, AQP2 phosphorylation modifies its interaction with key proteins of the vesicle docking/fusion apparatus or endocytotic machinery, including heat shock cognate/heat shock protein 70 (hsc/hsp70)^{345,352} dynamin and clathrin,^{340,352} annexin 2,¹⁶⁹ the myelin and lymphocyte protein (MAL),³⁵³ or 14-3-3 ζ .³⁵⁴

VASOPRESSIN-REGULATED UREA TRANSPORT IN THE INNER MEDULLA

UREA TRANSPORTER PROTEINS

Urea plays a central role in the urinary concentrating mechanism. Urea importance has been appreciated since 1934, when Gamble and colleagues initially described “an economy of water in renal function referable to urea,”³⁵⁵ findings which were recently confirmed and advanced in UT-A1/A3 knockout mice³⁵⁶ (discussed later). Many studies

show that maximal urine-concentrating ability is decreased in protein-deprived or malnourished humans (and other mammals), and that urea infusion restores urine-concentrating ability (reviewed in Sands and Layton³⁵⁷). Urine-concentrating defects have been demonstrated in UT-A1/A3,³⁵⁸ UT-A2,³⁵⁹ UT-B,^{360–362} and UT-A2/UT-B knockout mice.³⁶³ Thus, an effect due to urea or UTs must be part of the mechanism by which the inner medulla concentrates urine.

Two urea transporter genes have been cloned in mammals: the UT-A (*Slc14A2*) gene encodes 6 protein and 9 cDNA isoforms (reviewed in Sands and Layton³⁵⁷), and the UT-B (*Slc14A1*) gene encodes 2 protein isoforms.³⁶⁴ The UT-A gene, which has been cloned from rodents and humans, has two promoter elements: one upstream of exon 1 and a second that is located within intron 12 and drives the transcription of UT-A2 and UT-A2b (see references 365–368; also reviewed in Sands and Layton³⁵⁷). UT-B, which is also the Kidd blood group antigen in humans, has been cloned from humans and rodents³⁶⁹ (also reviewed by Sands and Layton³⁵⁷).

UT-A promoter I contains a tonicity enhancer (TonE) element and hyperosmolality increases its activity.^{366,370} UT-A1 is expressed in the terminal inner medullary collecting duct and is detected in the apical plasma membrane.^{367,371,372} UT-A3 is also expressed in the terminal inner medullary collecting duct; it is primarily detected in the basolateral plasma membrane but has been detected in the apical plasma membrane.^{373–375} UT-A2 is expressed in thin descending limbs.^{8,371,372,376} UT-B is expressed in descending vasa recta and red blood cells (reviewed by Sands and Layton³⁵⁷) (Fig. 10.16).

Vasopressin increases the phosphorylation and the apical plasma membrane accumulation of UT-A1 and of UT-A3 in rat inner medullary collecting ducts.^{375,377} UT-A1 is phosphorylated by vasopressin at serines 486 and 499.^{325,378} Both phospho-S486-UT-A1 and phospho-S499-UT-A1 are expressed predominantly in the apical plasma membrane in vasopressin-treated rat inner medullary collecting ducts.^{379,380} The site in UT-A3 that is phosphorylated by vasopressin has not been determined, except that neither of the two PKA consensus sites is involved.³⁸¹ Vasopressin stimulates urea transport, UT-A1 phosphorylation, and apical plasma membrane accumulation through two cAMP-dependent pathways: PKA and Epac (exchange protein activated by cAMP).³⁸² Epac increases UT-A1 phosphorylation but not at either serine 486 or 499.³⁸⁰

UT-A1 is dephosphorylated by multiple phosphatases, including calyculin and calcineurin.³⁸³ 14-3-3 proteins bind

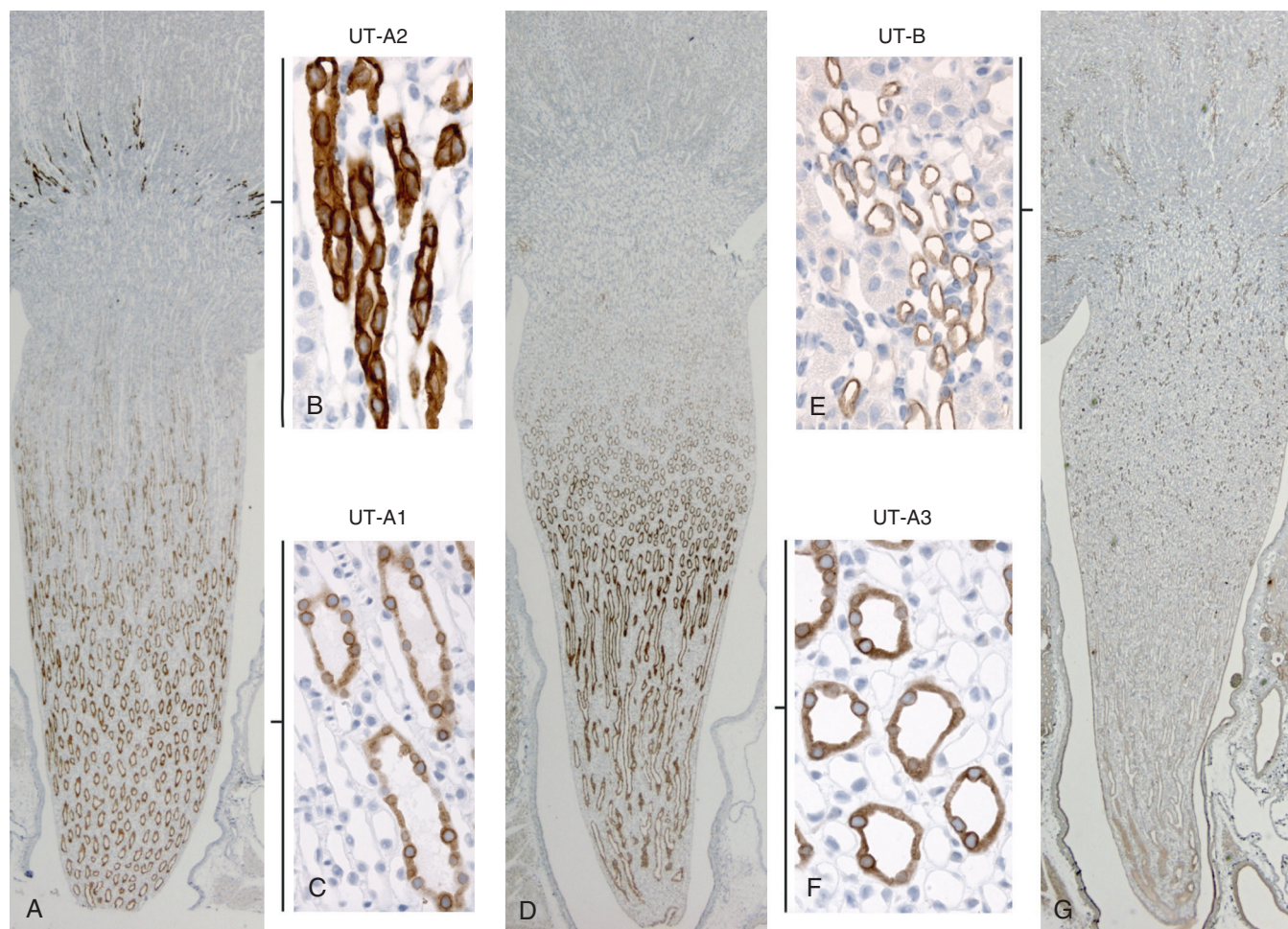


Fig. 10.16 Localization of urea transporters. UT-A1 is localized to the terminal portion of the inner medullary collecting duct, whereas UT-A2 is localized to the thin descending limbs of Henle loop in the inner stripe of outer medulla (A). Higher magnification shows that both UT-A2 (B) and UT-A1 (C) are predominantly intracellular. UT-A3 is localized to the terminal portion of the inner medullary collecting duct (D) and is both intracellular and in the basolateral membrane domains (F). UT-B is expressed in the descending vasa recta (G), where it is localized to the basolateral and apical regions (E). Adapted from Fenton RA, Knepper MA. Urea and renal function in the 21st century: insights from knockout mice. *J Am Soc Nephrol.* 2007;18: 679–688.

to phosphorylated serine or threonine residues and regulate protein function. UT-A1 and 14-3-3 γ bind, and PKA activation enhances this binding.³⁸⁴ 14-3-3 γ increases UT-A1 ubiquitination and degradation by interacting with the E3 ubiquitin ligase, MDM2, and decreases urea transport.³⁸⁴ Thus, UT-A1 phosphorylation is increased by PKA, and UT-A1 degradation is enhanced by subsequent binding to 14-3-3 γ , potentially providing a negative feedback mechanism to return UT-A1 function to its basal state following vasopressin stimulation.³⁸⁴ Although data showing these opposite effects of vasopressin/PKA are established, the physiologic significance remains to be determined.

Hyperosmolality increases urea permeability in rat terminal inner medullary collecting ducts, even in the absence of vasopressin,^{385–387} suggesting that it is an independent activator of urea transport. Hyperosmolality stimulates urea permeability via activation of PKC α and intracellular calcium,^{388–391} whereas vasopressin stimulates urea permeability via increases in cAMP.³⁹² Hyperosmolality increases the phosphorylation and the plasma membrane accumulation of both UT-A1 and UT-A3,^{375,377,393,394} similar to the effect of vasopressin. UT-A1 is phosphorylated by PKC α at serine 494.^{390,395–397}

Genetic knockout of PKC α in mice results in a urine-concentrating defect.^{395,398,399} PKC α knockout mice have reduced levels of UT-A1 protein abundance³⁹⁵ and UT-A1 sialylation.⁴⁰⁰ PKC α activation increases UT-A1 sialylation and UT-A1 accumulation in the apical plasma membrane, an effect mediated by Src kinase.⁴⁰⁰ PKC α also enhances UT-A3 sialylation, an effect mediated by ST6GalI.⁴⁰¹

Metformin, an AMPK activator, increases UT-A1 and AQP2 phosphorylation in inner medullary collecting duct suspensions, urea and water transport in perfused terminal inner medullary collecting ducts, and urine-concentrating ability in two rodent models of congenital NDI: tolvaptan-treated rats and V2R knockout mice.^{341,402} Thus, drugs that activate AMPK may be a future therapy for NDI.^{341,402,403}

UREA TRANSPORTER KNOCKOUT MICE

UT-A1/A3 KNOCKOUT MICE

A mouse model where the two inner medullary collecting duct UTs, UT-A1 and UT-A3, are deleted (*UT-A1/A3*^{-/-} mice) have a complete absence of phloretin-sensitive and vasopressin-regulated urea transport in the inner medullary collecting duct.^{358,404–406} These *UT-A1/A3*^{-/-} mice fed a normal or high protein diet have

a significantly greater fluid intake and urine flow, resulting in a decreased urine osmolality, compared with wild type mice.^{358,407} Under these dietary conditions, after an 18-hour water restriction, *UT-A1/A3^{-/-}* mice are unable to reduce their urine flow to levels below those observed under basal conditions, resulting in volume depletion and loss of body weight. In contrast, on a low-protein diet (4%), *UT-A1/A3^{-/-}* mice do not show a substantial degree of polyuria and can reduce their urine volume to a similar level as control mice after water restriction. On a low-protein diet, hepatic urea production is low and urea delivery to the inner medullary collecting duct is predicted to be low, thus rendering collecting duct urea transport largely immaterial to water balance. Thus, the concentrating defect in *UT-A1/A3^{-/-}* mice is due to a urea-dependent osmotic diuresis, results that are compatible with a model of urea handling proposed in the 1950s by Berliner and colleagues.⁸³

UT-A1/A3^{-/-} mice have also been exploited to study the “passive mechanism for urine concentration models” proposed in 1972 by Kokko and Rector and by Stephenson for concentration of Na⁺ and Cl⁻ in the inner medulla in the absence of active transport^{408,409} (see later). In these models, the passive electrochemical gradient that drives Na⁺ and Cl⁻ to exit from the thin ascending limb is indirectly dependent on rapid reabsorption of urea from the inner medullary collecting duct. However, despite a profound decrease in inner medulla urea accumulation in *UT-A1/A3^{-/-}* mice, three independent studies failed to demonstrate the predicted decline in Na⁺ and Cl⁻ concentrations in the inner medulla.^{355,358,405,406} Based on these results alone, the passive concentrating model in the form originally proposed does not appear to be the only mechanism by which NaCl is concentrated in the inner medulla. However, mathematical modeling analysis of these same data concluded that the results found in the *UT-A1/A3^{-/-}* mice are consistent with what one would predict for the passive mechanism.⁴¹⁰ Thus, the issue remains unresolved at present.

Another hypothesis regarding urea and the urinary concentrating mechanism was described over 80 years ago as “an economy of water in renal function referable to urea” and affectionately known as the Gamble phenomenon.³⁵⁵ Gamble described that (1) the water requirement for excretion of urea is less than for excretion of an osmotically equivalent amount of NaCl, and (2) less water is required for the excretion of urea and NaCl together than the water needed to excrete an osmotically equivalent amount of either urea or NaCl alone. In *UT-A1/A3^{-/-}* mice, both elements of the Gamble phenomenon were absent, indicating that inner medullary collecting duct UTs play an essential role.³⁵⁶ When wild type mice were given progressively increasing amounts of urea or NaCl in the diet, both substances induced osmotic diuresis, but at different excretion levels (6000 μmol/day for urea; 3500 μmol/day for NaCl). Mice were unable to increase urinary NaCl concentrations above 420 mM. Thus, the second component of the Gamble phenomenon derives from the fact that both urea and NaCl excretion are saturable, presumably resulting from an ability to exceed the respective reabsorptive capacity for urea and NaCl, rather than a specific interaction of urea transport and NaCl transport at an epithelial level.

A mouse lacking UT-A3 but expressing UT-A1 was created by transgenic restoration of UT-A1 into the *UT-A1/A3^{-/-}* knockout mouse in order to determine the effect of UT-A1 alone.⁴¹¹ Basal urea permeability in the inner medullary collecting duct of the UT-A1-only mouse was normal, but unlike wild type mice, vasopressin did not stimulate urea permeability

above basal levels.⁴¹¹ Surprisingly, urine-concentrating ability was restored to wild type levels in the UT-A1 only mice.⁴¹¹

UT-B AND UT-A2 KNOCKOUT MICE

UT-B knockout mice have a reduced urine-concentrating ability that is similar to humans lacking UT-B (reviewed by Fenton and Knepper⁴⁰⁶ and Klein et al.⁴¹²). In humans, UT-B is the Kidd blood group antigen, and people lacking the Kidd antigen are unable to concentrate their urine above 800 mOsm/kg H₂O, even following overnight water deprivation and exogenous vasopressin administration.⁴¹³

Mice lacking UT-A2 also have reduction in urine-concentrating ability (reviewed in Fenton and Knepper⁴⁰⁶ and Klein et al.⁴¹²). The urine-concentrating defect is thought to result from impairment of urea recycling (reviewed in Fenton and Knepper⁴⁰⁶ and Klein et al.⁴¹²). Because UT-B knockout may also interfere with urea recycling, a mouse lacking both UT-B and UT-A2 was generated.³⁶³ Unexpectedly, UT-A2 deletion appeared to partially correct the concentrating defect in mice lacking only UT-B.³⁶³ These results suggest that rather than playing a role in maintaining urea concentration during the normal steady state, UT-A2 may function to move urea during the acute transition from diuresis to antidiuresis.³⁶³

MICE LACKING ALL UREA TRANSPORTERS

Mice lacking all UTs have a 3.5-fold increase in urine output, produce dilute urine, and have reduced blood pressure.⁴¹⁴ The all-UT knockout mice do not increase urine osmolality or urea following water restriction, acute urea loading, or a high protein intake.⁴¹⁴ The all-UT knockout mice do not exhibit physiological abnormalities in extrarenal tissues.⁴¹⁴

Clinical Relevance

Urearetics

In recent years, urea transporter inhibitors have been developed as potential novel diuretics (reviewed in references 476 through 478). Dimethylthiourea (DMTU), a urea analog, inhibits UT-A1 and UT-B, results in a sustained and reversible reduction in urine osmolality, an increase in urine volume, and mild hypokalemia in rats.^{479,480} Other thiourea analogs are being investigated for selective inhibition of UT-A1 or UT-B.⁴⁷⁹ Another class of inhibitors, an indole thiazole or γ-sultambenzosulfonamide, is selective for UT-A and results in diuresis with more urea than salt excretion in rats, even when the rats were given dDAVP.⁴⁸¹ Another potential class of inhibitors are 2,7-distributed fluorenones, the most potent of which inhibited UT-A1 and UT-B with an IC₅₀ of 1 μM.⁴⁸² A fourth class are thienoquinolins that inhibit both UT-A and UT-B, PU-14, results in a diuresis in rats.^{483,484} The thienoquinolin PU-48 results in a diuresis in both wild type and UT-B knockout mice, indicating that its effect was to inhibit UT-A, and inhibits urea permeability in perfused rat inner medullary collecting ducts.⁴⁸⁵ Because the diuresis induced by PU-48 did not change serum sodium, chloride, or potassium levels, it supports the hypothesis that an agent that targets UT-A1, which is expressed in the last portion of the inner medullary collecting duct, may have less risk for side effects, such as hypokalemia, than conventional diuretics that act in more proximal portions of the nephron.⁴⁸⁵

ACCUMULATION OF UREA IN RENAL INNER MEDULLA

Urea accumulation within the inner medulla is partly dependent on variable urea permeabilities along the collecting duct system (Fig. 10.17). Within the collecting duct system, only the terminal inner medullary collecting duct possesses high urea permeability,⁴¹⁵ which can be further increased by vasopressin.^{148,416,417} UT-A1 and UT-A3 UTs are localized to the apical and basolateral plasma membranes of the inner medullary collecting duct cells and are responsible for the high urea permeability of the terminal portion of the inner medullary collecting duct. The mechanisms of urea accumulation in the renal medulla are depicted in Fig. 10.18. Accumulation of urea is predominantly a result of passive urea reabsorption from the inner medullary collecting duct. Tubular fluid entering the collecting duct system in the renal cortex has a relatively low urea concentration. However, during antidiuresis, water is osmotically reabsorbed from the urea-impermeable parts of the collecting duct system in the cortex and outer medulla, causing a progressive increase in the luminal urea concentration along the connecting tubules, cortical collecting ducts, and outer medullary collecting ducts. Thus, when the tubule fluid reaches the highly urea permeable terminal inner medullary collecting duct (due to the presence of UTs), urea rapidly exits from the lumen to the inner medullary interstitium, where it is “trapped” by countercurrent urea exchange between descending and ascending flows in both the vasa recta and loops of Henle. Under steady-state conditions, and in the continued presence of vasopressin, urea nearly equilibrates across the inner medullary collecting duct epithelium and thus osmotically balances the urea in the collecting duct lumen, preventing possible instances of osmotic diuresis (Fig. 10.19).

The descending and ascending vasa recta are in close association with each other in the inner medulla, facilitating

countercurrent exchange of urea between the two structures.⁸³ In the ascending vasa recta, aided by the extremely high ($>40 \times 10^{-5}$ cm/sec) permeability to urea, the concentration of urea exiting the inner medulla is similar to the concentration of urea in the descending vasa recta.^{79,416} This minimizes the washout of urea from the inner medulla. However, countercurrent exchange cannot completely eliminate loss of urea from the inner medullary interstitium, because the volume flow rate of blood in the ascending vasa recta exceeds that in the descending vasa recta.⁴¹⁸ During antidiuresis, water is added to the vasa recta from both inner medullary collecting ducts and descending limbs, resulting in a higher volume flow rate and an increased mass flow rate of urea. This ensures that the inner medullary vasculature continually removes urea from the inner medulla. Quantitatively, the most important loss of urea from the inner medullary interstitium is thought to occur via the vasa recta,⁴¹⁹ but urea recycling pathways play a major role in limiting the loss of urea from the inner medulla. Three major urea recycling pathways are described later in this section, and an overview of these is shown in Fig. 10.20).

1. Recycling of Urea Through the Ascending Limbs, Distal Tubules, and Collecting Ducts

Urea that escapes the inner medulla in the ascending limbs of the long loops of Henle is carried back through the thick ascending limbs, distal convoluted tubules, and early portions of the collecting duct system by the flow of tubule fluid.⁴²⁰ When it reaches the urea-permeable part of the inner medullary collecting ducts, it passively exits into the inner medullary interstitium and starts the cycle again.

2. Recycling of Urea Through the Vasa Recta, Short Loops of Henle, and Collecting Ducts

The delivery of urea to the superficial distal tubule exceeds the delivery out of the superficial proximal tubule.^{420–422} This

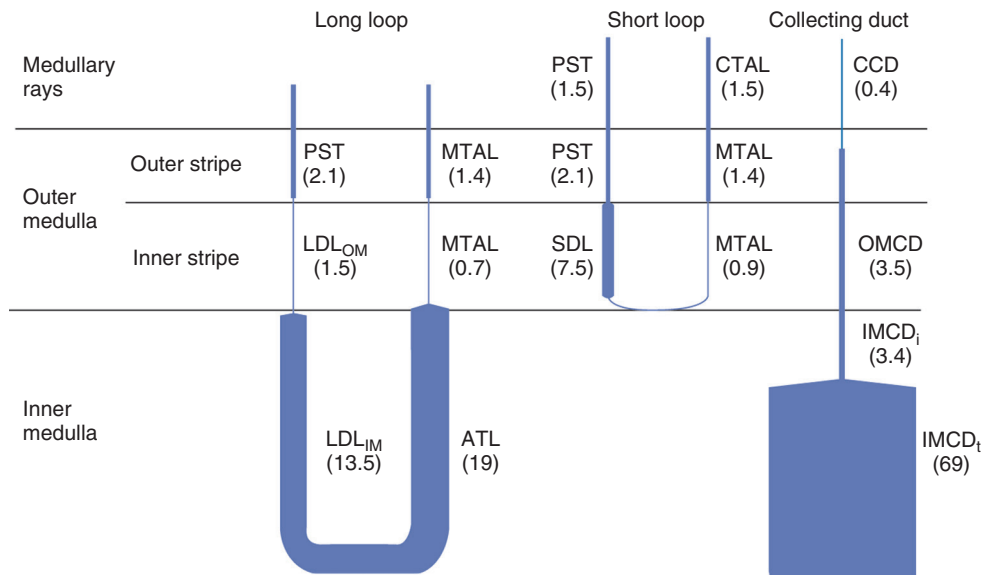


Fig. 10.17 Urea permeabilities of mammalian renal tubule segments. The width of each segment in the diagram is distorted to be proportional to the urea permeability of that segment. Numbers in parentheses are measured values for the permeability coefficient ($\times 10^{-5}$ cm/sec). Values are from isolated perfused tubule studies. *ATL*, Ascending thin limb; *CTAL*, cortical thick ascending limb; *IMCD_i*, initial inner medullary collecting duct; *IMCD_t*, terminal inner medullary collecting duct; *LDL*, thin descending limb of long-looped nephron; *MTAL*, medullary thick ascending limb; *OMCD*, outer medullary collecting duct; *PST*, proximal straight tubule; *SDL*, thin descending limb of short-looped nephron.

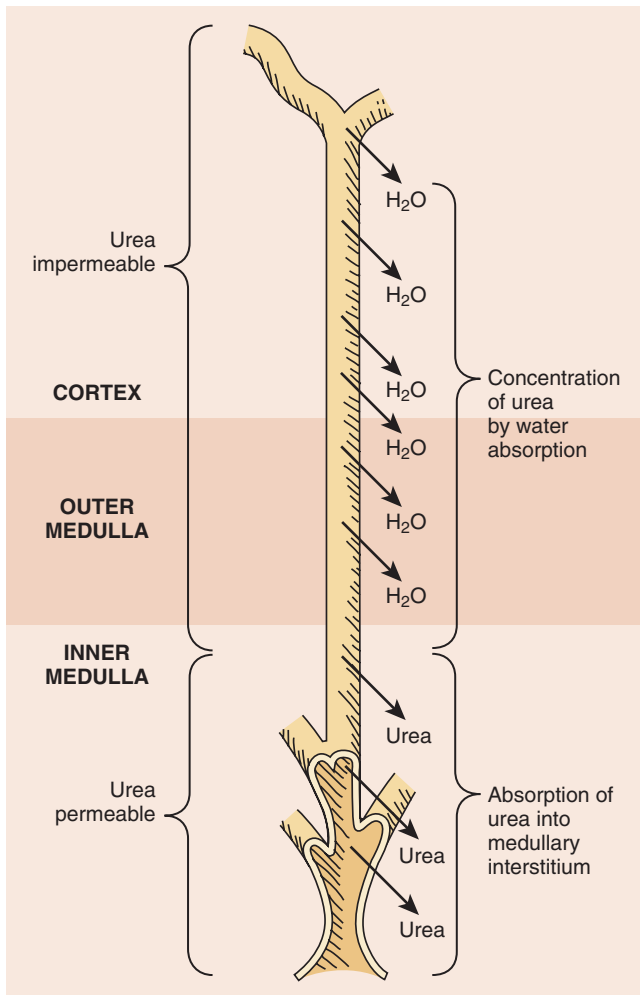


Fig. 10.18 Schematic representation of the mammalian collecting duct system showing principal sites of water absorption and urea absorption. Water is absorbed in the early part of the collecting duct system, driven by an osmotic gradient. Because urea permeabilities of cortical collecting duct, outer medullary collecting duct, and initial inner medullary collecting duct are very low, the water absorption concentrates urea in the lumen of these segments. When the tubule fluid reaches the terminal inner medullary collecting duct, which is highly permeable to urea, urea rapidly exits from the lumen. This urea is trapped in the inner medulla as a result of countercurrent exchange.

implies that net urea addition occurs somewhere along the short loops of Henle. One possible mechanism is that the urea leaving the inner medulla in the vasa recta is transferred to the descending limbs of the short loops of Henle⁴²¹ and is subsequently carried through the superficial distal tubules back to the urea-permeable part of the inner medullary collecting ducts, where it passively exits, completing the recycling pathway. The close physical association between the vasa recta and the descending limbs of the short loops in the vascular bundles of the inner stripe of the outer medulla would facilitate this transfer of urea from the vasa recta to the short loops of Henle.^{26,423} Furthermore, the existence of a facilitative UT, UT-A2, in the thin descending limb of short loops of Henle^{8,371} provides further support for this mechanism. However, as discussed earlier, recent studies on UT-A2

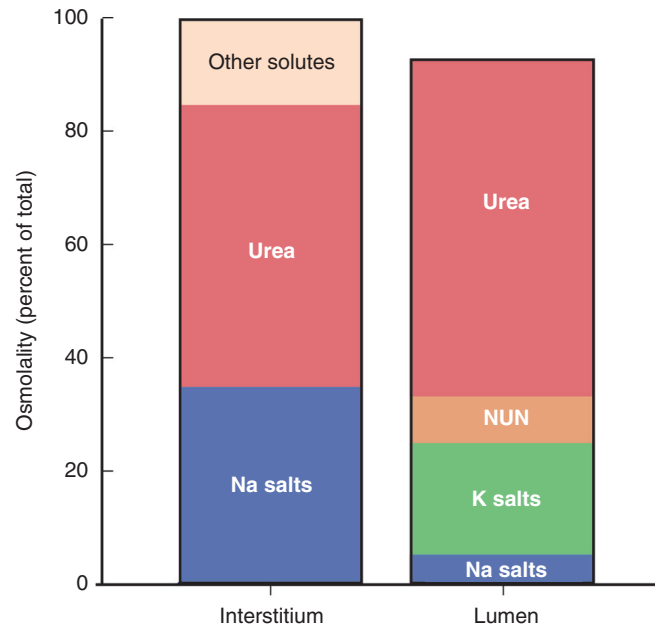


Fig. 10.19 Solutes that account for osmolality of medullary interstitium and tubule fluid in the inner medullary collecting duct during antidiuresis in rats. Urea nearly equilibrates across the inner medullary collecting duct epithelium as a result of rapid facilitated urea transport. Although the osmolalities of the fluid in the two spaces are nearly equal, the nonurea solutes can differ considerably between the two compartments. Typical values in untreated rats are presented. Values can differ considerably in other species and in the same species with different diets. *NUN*, Nonurea nitrogen.

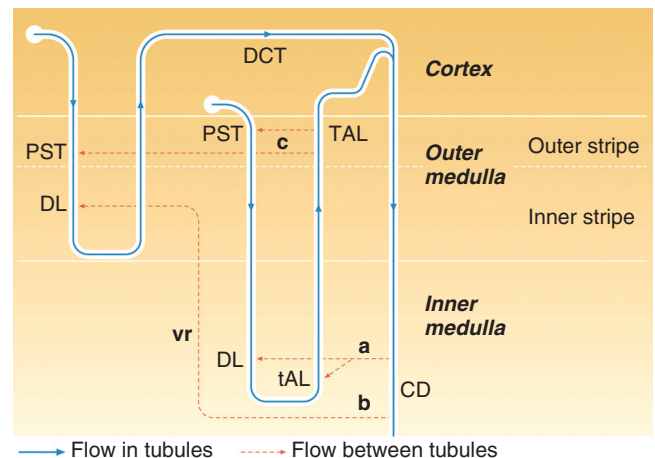


Fig. 10.20 Pathways of urea recycling in renal medulla. *Solid blue lines* represent a short-looped nephron (*left*) and a long-looped nephron (*right*). Transfer of urea between nephron segments is indicated by *dashed red arrows* labeled a, b, and c corresponding to recycling pathways described in the text. *CD*, Collecting duct; *DCT*, distal convoluted tubule; *DL*, descending limb; *PST*, proximal straight tubule; *tAL*, thin ascending limb; *TAL*, thick ascending limb; *vr*, vasa recta. Reproduced with permission from Knepper MA, Roch-Ramel F. Pathways of urea transport in the mammalian kidney. *Kidney Int.* 1987;31: 629–633.

knockout mice and UT-A2/UT-B knockout mice have raised doubts about the importance of this pathway.^{5,359}

3. Urea Recycling Between Ascending and Descending Limbs of the Loops of Henle

The urea permeability of thick ascending limbs from the inner stripe of the outer medulla is low.^{424,425} However, the urea permeability of thick ascending limbs from the outer stripe of the outer medulla and the medullary rays is relatively high.^{424,426} Based on this, a urea recycling pathway has been proposed in which urea is reabsorbed from thick ascending limbs and is secreted into neighboring proximal straight tubules, forming a recycling pathway between the ascending limb and descending limbs of the loop of Henle.^{3,419} Urea recycling from the thick ascending limbs and the proximal straight tubules is facilitated by the parallel relationship of these two structures in the outer stripe of the outer medulla and in the medullary rays. This transfer of urea is also likely to depend on a relatively attenuated effective blood flow in these regions. Urea secretion into the proximal straight tubules can occur by passive diffusion,⁴²⁶ active transport,⁴²⁷ or a combination of both. Urea presumably enters the proximal straight tubules of both short- and long-looped nephrons. The urea that enters the short-looped nephrons will be carried back to the inner medulla by the flow of tubule fluid through the superficial distal tubules and cortical collecting ducts, reentering the inner medullary interstitium by reabsorption from the terminal inner medullary collecting duct. The urea that enters proximal straight tubules of long-looped nephrons returns to the inner medulla directly through the descending limbs of the loops of Henle.⁴¹⁹

URINE CONCENTRATION AND DILUTION PROCESSES ALONG THE MAMMALIAN NEPHRON

SITES OF URINE CONCENTRATION AND DILUTION

Micropuncture studies of the mammalian nephron have determined the major sites of tubule fluid concentration and dilution (see Fig. 10.10). Regardless of whether the kidney is diluting or concentrating the urine, proximal tubule fluid is always isosmotic with plasma.⁴²⁸ Whereas early distal convoluted tubule fluid is always hypotonic, the earliest nephron segment where significant differences in tubule fluid osmolality can be detected is the late distal tubule. During water diuresis, the fluid in the distal tubule remains hypotonic. During antidiuresis, the fluid in the distal tubule becomes isosmotic with plasma, and the osmolality between the end of the late distal tubule and the inner medullary collecting ducts rises to a level greater than that of plasma. Thus, the conclusion from micropuncture studies is that the loop of Henle is the major site of dilution of tubule fluid, and that dilution processes in the loop occur regardless of whether the final urine is dilute or concentrated. Further dilution of the tubule fluid can occur in the collecting ducts during water diuresis.⁴²⁹ In contrast, the chief site of urine concentration is beyond the distal tubule (i.e., in the collecting duct system). The mechanisms of urinary dilution and of urinary concentration are discussed in the subsequent sections.

MECHANISMS OF TUBULE FLUID DILUTION

Micropuncture studies in rats show that the fluid in the early distal tubule is hypotonic, due mainly to a reduction in luminal NaCl concentration relative to that in the proximal tubule.⁴³⁰ The low luminal NaCl concentration could result either from active NaCl reabsorption from the loop of Henle or from water secretion into the loop of Henle. Micropuncture measurements in rats, performed using inulin as a volume marker, demonstrate net water reabsorption from the superficial loops of Henle during antidiuresis, thereby ruling out water secretion as a potential mechanism of tubule fluid dilution.⁴²⁰ Thus, one can conclude that luminal dilution occurs because of NaCl reabsorption from the loops of Henle, in excess of water reabsorption. Classic studies of isolated perfused rabbit thick ascending limbs established the mechanism of tubule fluid dilution.^{431,432} NaCl is rapidly reabsorbed by active transport, which lowers the luminal osmolality and NaCl concentration to levels below those in the peritubular fluid. The osmotic water permeability of the thick ascending limb is very low, which prevents dissipation of the trans-epithelial osmolality gradient by water flux.

The tubule fluid remains hypotonic throughout the distal tubule and collecting duct system during water diuresis, aided by the low osmotic water permeability of the collecting ducts when circulating levels of vasopressin are low. Even though the tubule fluid remains hypotonic in the collecting duct system, the solute composition of the tubule fluid is modified within the collecting duct, mainly by Na⁺ absorption and K⁺ secretion. Active NaCl reabsorption from the collecting duct results in a further dilution of the collecting duct fluid, beyond that achieved in the thick ascending limbs.⁴²⁹

MECHANISM OF TUBULE FLUID CONCENTRATION

When circulating vasopressin levels are high, net water absorption occurs between the late distal tubule and the collecting ducts.⁴²⁰ Because water is absorbed in excess of solutes, with a resulting rise in osmolality along the collecting ducts toward the papillary tip,⁴³³ it can be concluded that collecting duct fluid is concentrated chiefly by water absorption, rather than by solute addition.

An axial osmolality gradient in the renal medullary tissue, with the highest degree of hypertonicity at the papillary tip, provides the osmotic driving force for water absorption along the collecting ducts. This osmolality gradient was initially reported by Wirz and colleagues.⁴³⁴ In a classic study, they demonstrated, in antidiuretic rats, the existence of a continuously increasing osmolality gradient along the outer and inner medulla, with the highest osmolality in the deepest part of the inner medulla, the papillary tip. In addition, within the medulla the osmolality of the collecting ducts was as high as in the loops of Henle and the osmolality of vasa recta blood, sampled from near the papillary tip, was virtually equal to that of the final urine.⁴³⁴ Taken together these results demonstrate that the high tissue osmolality was not simply a manifestation of a high osmolality in a single structure, namely, the collecting duct. Micropuncture studies by Gottschalk and Mylle⁴²⁸ based on the superficial and thus accessible tubules and vessels confirmed that the osmolality of the fluid in the loops of Henle, the vasa recta, and the collecting ducts is approximately the same (see Fig. 10.10); thus, these studies

support the hypothesis that the collecting duct fluid is concentrated by osmotic equilibration with a hypertonic medullary interstitium. Furthermore, *in vitro* studies demonstrated that collecting ducts have a high water permeability in the presence of vasopressin,^{99,416} as is required for osmotic equilibration. The mechanism by which the corticomedullary osmolality gradient is generated is considered later.

Although the final axial osmolality gradient within the renal medulla is due to the combined gradients of several individual solutes, as initially demonstrated using tissue slice analysis by Ullrich and Jarausch,⁴³⁵ the principal solutes responsible for the osmolality gradient are NaCl and urea (Fig. 10.21). The increase in the NaCl concentration gradient along the corticomedullary axis occurs predominantly in the outer medulla, with only a small increase in the inner medulla. In contrast, the increase in urea concentration occurs predominantly in the inner medulla, with little or no increase in the initial outer medulla. The mechanisms for generating the NaCl gradient in the outer medulla and urea accumulation in the inner medulla are discussed later.

GENERATION OF THE AXIAL NaCl GRADIENT IN THE RENAL OUTER MEDULLA

In both diuresis and antidiuresis, an osmolality gradient is maintained along the corticomedullary axis of the outer medulla (see Fig. 10.21).⁴³⁶ That gradient arises mostly from an accumulation of NaCl and is generated by the concentrating mechanism of the outer medulla. Because the axial osmolality gradient is present in both diuresis and antidiuresis (in which the outer medullary collecting duct is water-permeable to varying degrees), the accumulation of NaCl in the outer medulla cannot depend on a sustained osmolality difference across the collecting duct epithelium. Thus, the concentrating mechanism must depend on the loops of Henle, on the vasculature, and on their interactions within the outer medulla. Moreover, a mass balance of water and NaCl must be maintained. Thus, for example, concentrated fluid that flows into the inner medulla must be balanced by dilute fluid that, in the presence of vasopressin, is absorbed from the cortical collecting duct, dilutes the cortical interstitial fluid, enters the cortical vasculature, and thus participates in maintaining an appropriate systemic level of blood plasma osmolality.

It has long been believed that the osmolality gradient of the outer medulla is generated by means of countercurrent multiplication of a single effect (“Vervielfachung des Einzeleffektes”). In this paradigm, proposed by Kuhn and Ryffle in 1942,⁴³⁷ osmotic pressure is raised along parallel but opposing flows in nearby tubes that are made contiguous by a hairpin turn (Fig. 10.22); a transfer of solute from one tubule to another (i.e., a single effect) would augment (multiply), or reinforce, the osmotic pressure in the parallel flows. Thus, by means of the countercurrent configuration, a small transverse osmotic difference would be multiplied into a relatively large difference along the axes of flow. In support of this paradigm, Kuhn and Ryffle provided both a mathematical model and an apparatus that exemplified countercurrent multiplication.

As anatomic and physiologic understanding of the renal medulla increased, the countercurrent multiplication paradigm was reinterpreted and modified. In 1951, Hargitay and Kuhn⁴³⁸ put the paradigm in the context of specific renal tubules. The loop of Henle was identified with the parallel

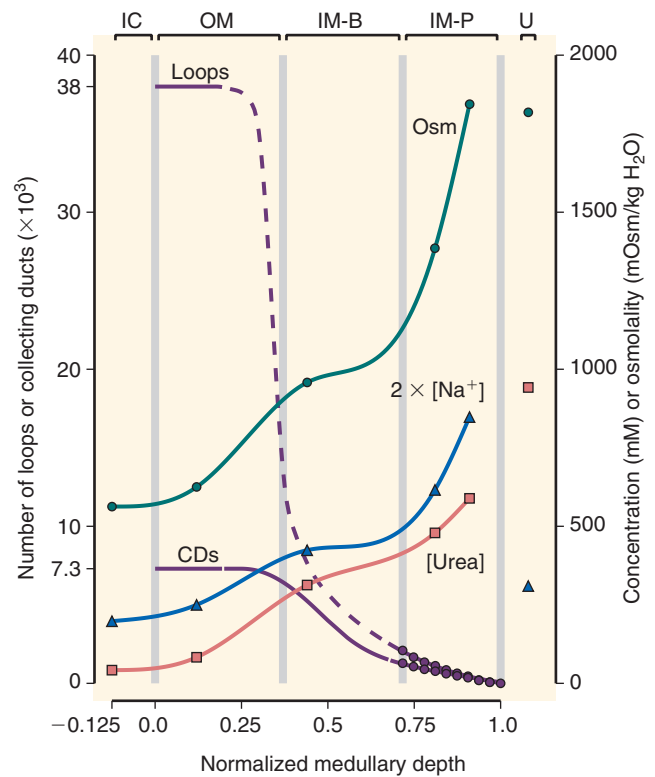


Fig. 10.21 Data from rat kidney in an antidiuretic state. Osmolality, urea concentration, and sodium concentration plus its anion are shown (scale at right), in addition to the loop of Henle and collecting duct populations (scale at left). Loop of Henle and collecting duct populations decrease in inner medulla because collecting ducts merge and loops turn back. The osmolality gradient is larger in the outer medulla and papilla than in the outer part of the inner medulla. The gradient is largest in the papilla, where the osmolality and concentration profiles appear to increase exponentially. The shape of the sodium profile has been corroborated by electron microprobe measurements.⁴⁸⁶ IC, Inner cortex; OM, outer part (base) of inner medulla; IM-B, papilla or inner part (tip) of inner medulla; IM-P, papilla; U, urine. Figure based on published data. Curves connecting data points are natural cubic splines, computed by standard algorithms.⁴⁸⁷ Dashed curve segments are interpolations without supporting measurements. Tubule populations in papilla are from Hans et al.⁴⁸⁸ tubule populations in outer medulla are based on estimates in Knepper et al.⁵⁹ Concentrations and osmolalities are from tissue slices and urine samples collected 4.5 hours after onset of vasopressin infusion at 15 μ U/min per 100 g body weight. Data are from Fig. 5 in Atherton et al.⁴⁸⁹ and Figs. 1, 3, 9 in Hai and Thomas⁴³⁶; slice locations were given in Wade et al.⁸ The osmolality reported in the inner cortex seems high relative to the reported plasma concentration of 314 mOsm/kg H₂O. The osmolality and concentration profiles, as drawn in the study by Hai and Thomas,⁴³⁶ apparently do not take into account relative distances between tissue sample sites. (From Sands JM, Layton HE. The urine-concentrating mechanism and urea transporters. In: Alpern RJ, Caplan MJ, Moe OW, eds. *The Kidney: Physiology and Pathophysiology*, ed 5. San Diego: Academic Press; 2013:1463–1510.)

tubes joined by a hairpin turn as proposed by Kuhn and Ryffle. Thus, the loops of Henle were proposed as the source of the outer medullary gradient, and that gradient was hypothesized to draw water out of water-permeable collecting ducts. In 1959, Kuhn and Ramel⁴³⁹ used a mathematical model to show that active transport of NaCl from thick ascending

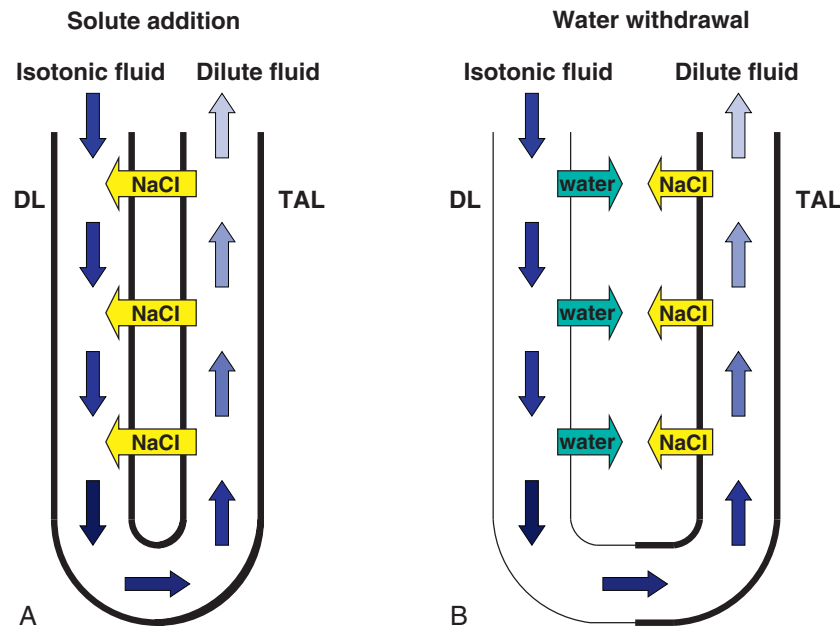


Fig. 10.22 (A) Countercurrent multiplication by means of NaCl transfer from an ascending flow to a descending flow. (B) Countercurrent multiplication by means of water withdrawal from a descending flow. NaCl transport from the ascending flow into the interstitium raises interstitial osmolality; this results in passive water transport from the descending flow, which has lower osmolality than the interstitium. In both panels, tubular fluid flow direction is indicated by *blue arrows*; increasing osmolality is indicated by *darkening shades of blue*. Ascending flow may be considered to be in the thick ascending limb of Henle (TAL); descending flow in the descending limb of Henle (DL). *Thick black lines* indicate that a tubule is impermeable to water; *thin lines* indicate high permeability to water. (From Layton AT, Layton HE. Countercurrent multiplication may not explain the axial osmolality gradient in the outer medulla of the rat kidney. *Am J Physiol Renal Physiol.* 2011; 301:F1047-F1056.)

limbs could serve as the single effect. Subsequent physiologic experiments confirmed the active NaCl transport and the osmotic absorption of water from collecting ducts.^{420,431–433} Experiments indicating high water permeability in hamster descending limbs of short loops⁴⁴⁰ and in descending limbs of long loops^{9,10,12} suggested that the accumulation of NaCl from thick limbs concentrated descending limb tubular fluid by osmotic water withdrawal, rather than by NaCl addition (see Fig. 10.22).

In more recent years, as anatomic details of the medulla emerged, it has become necessary to refine the paradigm of countercurrent multiplication to provide an accurate representation of the means by which the gradient is generated in the mammalian outer medulla. In particular, the descending limbs of short loops have been shown to be anatomically separated from ascending limbs, with inner stripe portions of short loops near (or within) the vascular bundles and thick limbs near the collecting ducts.^{23,441} This configuration is not consistent with direct interactions between counterflowing limbs. Furthermore, in short-looped rat nephrons, Wade et al.⁸ found that AQP1 is not expressed in portions of descending limb segments in the distal inner stripe. Zhai et al.¹⁷ found that AQP1 is not expressed in descending limbs of short loops in the inner stripes of mice, rats, and humans. The absence of AQP1 suggests that the assumption of high water permeability in descending limbs of short loops merits further experimental study.

From these considerations, it seems reasonable to hypothesize that the outer medullary osmolality gradient arises principally from vigorous active transport of NaCl,

without accompanying water, from the thick ascending limbs of short- and long-looped nephrons. The tubular fluid of the thick limbs that enters the cortex is diluted well below plasma osmolality, and thus the requirement of mass balance is met. In rats and mice, the thick limbs are localized near the collecting ducts⁴⁴²; mathematical models suggest that at a given level of the outer medulla, the interstitial osmolality will be higher near the collecting ducts than near the vascular bundles.^{443,444} This higher osmolality will facilitate water withdrawal from the descending limbs of long loops and from collecting ducts. Descending vasa recta are thought to be found only in the vascular bundles. Thus, the ascending vasa recta will act as the collectors of any NaCl that is absorbed from the loops of Henle and water that is absorbed from the descending limbs of long loops and from collecting ducts.

The countercurrent configuration of the ascending vasa recta, relative to the descending limbs and collecting ducts, is likely to participate in sustaining the axial gradient: as ascending vasa recta fluid ascends toward the cortex, its osmolality will exceed that in the descending limbs of long loops and in the collecting ducts. Thus, ascending vasa recta fluid will be progressively diluted as that fluid contributes to the concentrating of fluid in descending limbs of long loops and in collecting ducts, by giving up NaCl to, and absorbing water from, the interstitium (Fig. 10.23).

The previous summary appears to account for the elevation of osmolality in the outer medulla without invoking a role for countercurrent multiplication. However, a question remains: why does the osmolality gradient increase along the outer

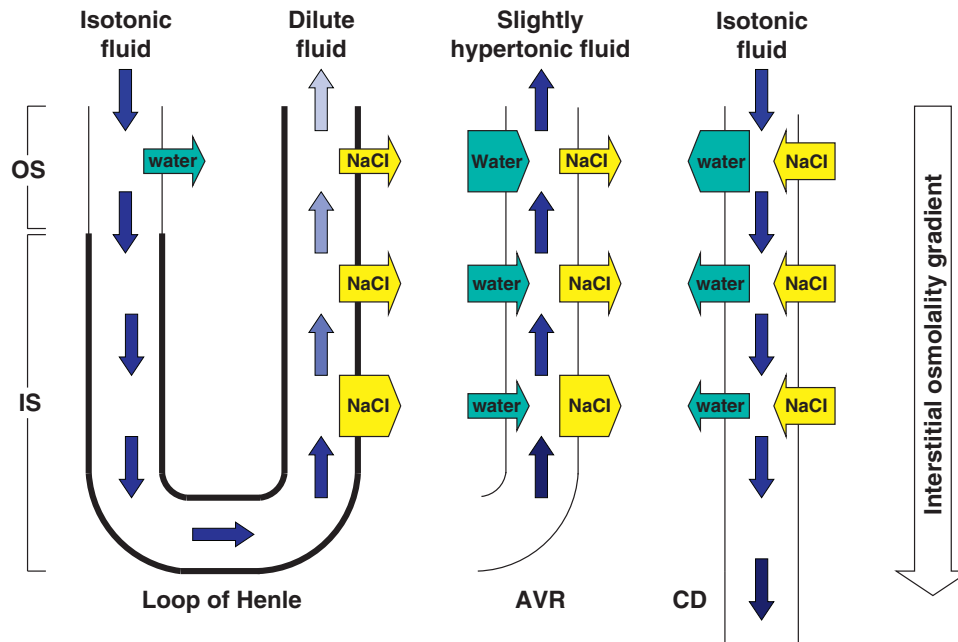


Fig. 10.23 Outer medullary concentrating mechanism based on NaCl addition to the interstitium but without water absorption from descending limbs of short loops. Arrows indicate water (cyan) and NaCl (yellow) transepithelial transport; arrow widths suggest relative transport magnitudes. Isotonic fluid is considered to have the same osmolality as blood plasma. Flow entering the AVR is assumed to arise from a descending vas rectum that is in, or near, a vascular bundle. Outflow from the collecting duct enters the inner medullary collecting duct. Tubular fluid flow direction is indicated by blue arrows; increasing osmolality is indicated by darkening shades of blue. Thick black lines indicate that a tubule is impermeable to water; thin lines indicate high permeability to water. AVR, Ascending vas rectum; CD, collecting duct; IS, inner stripe; OS, outer stripe. (From Layton AT, Layton HE. Countercurrent multiplication may not explain the axial osmolality gradient in the outer medulla of the rat kidney. *Am J Physiol Renal Physiol.* 2011; 301:F1047-F1056.)

medulla as a function of increasing medullary depth? The answer likely lies in the local balance of NaCl absorption from thick limbs and water absorption from descending limbs of long loops and from collecting ducts. At deeper medullary levels, the rate of NaCl absorption from thick limbs may be higher than at shallow levels, owing to a higher Na-K-ATPase activity at deeper levels⁴⁴⁵ and to a saturation of transport proteins by the higher NaCl concentration in thick limb tubular fluid before dilution. Moreover, because of the water already absorbed in the upper outer medulla, the load of water presented to the thick limbs deep in the outer medulla by descending limbs of long loops and by the collecting ducts is much reduced.

A caveat is in order: our understanding of the outer medulla is mostly based on information obtained from heavily studied laboratory animals, especially rats and mice. Outer medullary function and structure are likely to vary substantially in other species. For example, the human kidney has limited concentrating capability (relative to many other mammals) and only about one seventh of the loops of Henle are long⁴⁴⁶; the mountain beaver (*Aplodontia rufa*) has mostly cortical loops of Henle and essentially no inner medulla.⁴⁴⁷ It seems likely that the outer medullary structure in these species differ substantially from that in rats and mice. Finally, it should be acknowledged that the paradigm formulated above is similar to that proposed by Berliner et al. in 1958.⁸³

DETERMINANTS OF CONCENTRATING ABILITY

The overall concentrating ability of the kidney arises from interactions among several differing components. In addition

to the active transport of NaCl from the thick ascending limbs and the water permeability of the collecting ducts, two other factors play a significant role in determining the osmolality of the final urine. One important determinant is the delivery rate of NaCl and water to the loop of Henle, which sets an upper limit on the amount of NaCl actively reabsorbed by the thick ascending limb to drive the outer medullary concentrating mechanism. Another important determinant is the volume of tubular fluid delivered to the medullary collecting duct, which has an underappreciated effect on the concentrating process. Too much fluid delivery saturates water reabsorption processes along the medullary collecting ducts, leading to interstitial dilution due to rapid osmotic water transport. In contrast, too little fluid delivery to the medullary collecting ducts, even in the absence of vasopressin, results in sustained osmotic equilibration across the collecting duct epithelium owing to the nonzero osmotic water permeability of the inner medullary collecting duct.^{144,148,149}

AN UNRESOLVED QUESTION: CONCENTRATION OF NaCl IN THE RENAL INNER MEDULLA

Tissue slice studies demonstrate that the corticomedullary osmolality gradient is made up largely of a NaCl gradient in the outer medulla and a urea gradient in the inner medulla (see Fig. 10.21). Accordingly, in the previous sections we have emphasized the processes that concentrate NaCl in the outer medulla and the processes responsible for urea accumulation in the inner medulla (passive urea absorption from the inner medullary collecting duct plus countercurrent exchange of urea via diffusion). The concentrating

mechanism described previously functions only in the renal outer medulla and medullary rays of the cortex. The ascending limbs of loops of Henle that reach into the inner medulla are thin-walled and do not actively transport NaCl^{416,448,449}; nonetheless, in antidiuresis a substantial axial osmolality gradient is generated in the inner medulla of many mammals. For nearly 50 years, controversy has persisted regarding the nature of the mechanism that generates the inner medullary osmolality gradient. Moreover, the energy source for the concentrating of nonurea solutes in the inner medullary interstitium is not known. General analysis of inner medullary concentrating processes indicates that, to satisfy mass balance requirements, either an ascending stream (thin ascending limbs or ascending vasa recta) must be diluted relative to the inner medullary interstitium, or a descending stream (descending thin limbs, descending vasa recta, or collecting ducts) must be concentrated locally relative to the inner medulla.^{87,450}

Three major hypotheses have been proposed for the concentrating mechanism of the inner medulla.

1. The “Passive Mechanism”

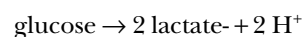
Kokko and Rector⁴⁰⁸ and Stephenson⁴⁰⁹ independently proposed a model by which the osmolality in the thin ascending limb could be lowered below that of the interstitium entirely by passive transport processes in the inner medulla. This mechanism is generally referred to as the “passive model” or the “passive countercurrent multiplier mechanism.” The passive mechanism depends on the separation of urea and NaCl that is accomplished by NaCl absorption from the thick ascending limbs; indeed, this absorption is the hypothesized energy source for the passive mechanism. In this model, rapid urea reabsorption from the inner medullary collecting duct generates and maintains a high urea concentration in the inner medullary interstitium, causing the osmotic withdrawal of water from the thin descending limb. This concentrates NaCl in the descending limb lumen and results in a transepithelial gradient favoring the passive reabsorption of NaCl from the thin ascending limb of Henle loop. Additionally, if the ascending limbs have extremely low urea permeability, then any NaCl that has been reabsorbed from the thin ascending limb will not be replaced by urea. Thus, the ascending limb fluid will be dilute relative to the fluid in other nephron segments, generating a “single effect” analogous to active NaCl absorption from thick ascending limbs. This single effect can then be multiplied by the counterflow between the ascending and descending limbs of Henle loops. This model requires that the thin descending limbs are highly permeable to water but not NaCl or urea, whereas the thin ascending limb would have to be permeable to NaCl but not water or urea. However, several objections to the passive mechanism have since been made. Contrary to the permeability requirements of the passive model, high urea permeabilities have been measured in the thin descending limb and thin ascending limb (summarized in Gamba and Knepper⁴⁵¹), whereas little or no osmotic water permeability has been measured in the lower portions of thin descending limbs in the inner medulla.²⁰ In addition, studies in UT-A1/A3 urea transporter knockout mice found that urea accumulation in the inner medulla was largely eliminated, but inner medullary NaCl accumulation was not affected^{143,358,407} (see “UT-A1/A3 knockout mice” in earlier section).

Layton and colleagues reevaluated the passive mechanism by incorporating measured loop NaCl, urea, and water permeabilities into a mathematical model.^{19,452,453} These studies suggest that water absorption from descending limbs is not a requirement for the passive mechanism to generate an osmolality gradient, and that the urea-permeable loops of Henle can serve as a highly effective countercurrent urea exchanger. However, the model was able to fully account for the high urine osmolalities attained by some animals.

2. Concentrating Mechanism Driven by External Solute

Jen and Stevenson⁴⁵⁴ proposed that the concentrating mechanism of the inner medulla depends on a solute other than NaCl and urea. By means of a mathematical model, they demonstrated, in principle, that the continuous addition of small amounts of an unspecified, but osmotically active, solute to the inner medullary interstitium could produce a substantial axial osmolality gradient. Such a solute would have to be generated in the inner medulla by a chemical reaction that produces more osmotically active particles than it consumes. The mechanism of concentration is similar to that driven by urea in the “passive” models proposed by Kokko and Rector and by Stephenson^{408,409}: the thin descending limbs in the inner medulla are assumed impermeable to the solute (thus it is an “external” solute), and as a result, water is withdrawn from the descending limbs and the concentration of NaCl is raised in descending limb tubular fluid. Beginning at the loop bend, elevated NaCl concentration within the loop will result in a substantial NaCl efflux that will dilute the ascending flow and that is sufficient to generate the axial gradient.

The feasibility of this mechanism was subsequently confirmed by Thomas and Wexler⁴⁵⁵ in the context of a more detailed mathematical model. In further modeling studies, Thomas,⁴⁵⁶ and Hervy and Thomas⁴⁵⁷ proposed that lactate, generated by anaerobic glycolysis (the predominant means of ATP generation in the inner medulla), could serve as the solute. Two lactate ions are generated per glucose consumed:



However, as pointed out by Knepper et al.,⁸⁷ the net generation of osmotically active particles depends on which buffering anions are titrated by the protons. If the protons titrate bicarbonate, there may be a net removal of osmotically active particles; if instead the protons titrate other buffers (e.g., phosphate or NH₃), there will be a net generation of osmotically active particles. Mathematical models developed by Zhang and Edwards⁴⁵⁸ and by Chen et al.⁴⁵⁹ predicted that vascular countercurrent exchange would tend to restrict significant glucose availability into the outer medulla and the upper inner medulla, thus limiting the rate of lactate generation in the deep inner medulla where the highest osmolalities are found.

3. Hyaluronan as a Mechano-osmotic Transducer

In the mechano-osmotic induction hypothesis,^{87,460} in which energy from the peristaltic contractions of the renal pelvic wall is used to concentrate solutes in the descending limbs and collecting ducts by water withdrawal, or, alternatively, the peristaltic contractions reduce sodium activity in the hyaluronan matrix of the interstitium, resulting in the

reabsorption of hypotonic fluid from that matrix into ascending vasa recta. Hyaluronan (or “hyaluronic acid”) is a glycosaminoglycan^{461,462} that is abundant in the interstitium of the renal inner medulla.^{463,464} The hyaluronan in the inner medulla is produced by a specialized interstitial cell (the type 1 interstitial cell), which forms characteristic “bridges” between the thin limbs of Henle and the vasa recta.⁴⁶⁵ These bridges may delimit, above and below, the nodal compartments identified by Pannabecker and Dantzer,²⁸ which were discussed previously. Thus, the inner medullary interstitium may be considered to be composed of a compressible, viscoelastic, hyaluronan matrix.

Several hypotheses have been advanced that depend on the peristalsis of the papilla as an integral component of the concentrating mechanism of the inner medulla.^{87,357,466} In one hypothesis, which was suggested in part by Schmidt-Nielsen,⁴⁶⁷ compression of the hyaluronan matrix stores some of the mechanical energy from the smooth muscle contraction that gives rise to the peristaltic wave. In the postwave decompression, the matrix exerts an elastic force that promotes water absorption from thin descending limbs and collecting ducts, and thereby increases tubular fluid osmolality. Water absorption from the descending limbs would raise tubular fluid NaCl concentration and thus promote a vigorous NaCl absorption from the loop bends and early ascending limbs. However, if, as is apparently the case in rat, the lower 60% of inner medullary descending limbs are water impermeable,²⁰ water is unlikely to be absorbed from descending limbs in the deep portion of the inner medulla where the highest osmolalities are achieved.

Another hypothesis involves special properties of hyaluronan.⁴⁶⁸ Hyaluronan is a large polyanion (1000 to 10,000 kDa). Its charge is due to the carboxylate (COO) groups of the glucuronic subunits. Hyaluronan is hydrophilic and assumes a highly expanded, random coil conformation that occupies a large volume of space relative to its mass. This extended state arises partly from electrostatic repulsion between carboxylate groups (which maximize the distances between neighboring negative charges), and partly from the extended conformations of the glycosidic bonds.

Knepper et al. proposed that the periodic compression of the papilla, and the effects of that compression on the hyaluronan matrix, could explain the osmolality gradient along the inner medulla.⁸⁷ When hyaluronan is compressed, the repulsive forces of neighboring carboxylate groups are overcome, in part, by a condensation of cations (mainly Na⁺), and a localized crystalloid structure is formed. Thus, compression of the hyaluronan gel results in a decrease of the local sodium ion activity in the gel.⁸⁷ In aqueous solutions that are in equilibrium with the gel, the NaCl concentration will decrease as a consequence of the compression-induced reduction in Na⁺ activity within the gel. Therefore, the free fluid that is expressed from the hyaluronan matrix during the contraction phase will have a lower total solute concentration than that of the gel as a whole. The slightly hypotonic fluid expressed from the matrix is likely to escape the inner medulla via the ascending vasa recta, the only structure that remains open during the compressive phase of the contraction cycle.⁴⁶⁷ As a consequence, the ascending fluid within the ascending vasa recta would have a lower osmolality than the local interstitium, and as a result, fluid in collecting ducts and descending vasa recta would be concentrated.

This mechanism is consistent with the nodal compartments found by Pannabecker and Dantzer²⁸; these compartments, which are likely rich in hyaluronan, are in contact with collecting ducts, thin ascending limbs, and ascending vasa recta. Thus, they are well-configured to be sites of transduction (i.e., sites where the mechanical energy of peristalsis is harnessed to generate an ascending flow that is dilute relative to average local osmolality). However, no quantitative analyses or mathematical models have examined the mass balance consistency or the thermodynamic adequacy of hypotheses that depend on the peristaltic contractions.

ACKNOWLEDGMENTS

This work was supported by National Institutes of Health grant R01-DK41707 to JMS. RAF is supported by the Danish Medical Research Council, the Novo Nordisk Foundation, the Carlsberg Foundation (Carlsbergfondet) and the Lundbeck Foundation.

Drs. Dennis Brown and Robert A. Fenton were coauthors of a chapter on the cell biology of vasopressin action in the 10th edition and some of the material in that chapter is incorporated into this chapter in the present edition.

 Complete reference list available at ExpertConsult.com.

KEY REFERENCES

5. Fenton RA, Knepper MA. Mouse models and the urinary concentrating mechanism in the new millennium. *Physiol Rev.* 2007;87:1083–1112.
15. Pannabecker TL. Comparative physiology and architecture associated with the mammalian urine concentrating mechanism: role of inner medullary water and urea transport pathways in the rodent medulla. *Am J Physiol Regul Integr Comp Physiol.* 2013;304(7):R488–R503.
18. Westrick KY, Serack B, Dantzer WH, et al. Axial compartmentation of descending and ascending thin limbs of Henle’s loops. *Am J Physiol Renal Physiol.* 2013;304(3):F308–F316.
87. Knepper MA, Saidel GM, Hascall VC, et al. Concentration of solutes in the renal inner medulla: interstitial hyaluronan as a mechano-osmotic transducer. *Am J Physiol Renal Physiol.* 2003;284(3):F433–F446.
97. Lolait SJ, O’Carroll A-M, McBride OW, et al. Cloning and characterization of a vasopressin V2 receptor and possible link to nephrogenic diabetes insipidus. *Nature.* 1992;357:336–339.
116. Roos KP, Strait KA, Raphael KL, et al. Collecting duct-specific knockout of adenylyl cyclase type VI causes a urinary concentration defect in mice. *Am J Physiol Renal Physiol.* 2012;302(1):F78–F84.
126. Ren XR, Reiter E, Ahn S, et al. Different G protein-coupled receptor kinases govern G protein and beta-arrestin-mediated signaling of V2 vasopressin receptor. *Proc Natl Acad Sci U S A.* 2005;102(5):1448–1453.
138. Fenton RA, Pedersen CN, Moeller HB. New insights into regulated aquaporin-2 function. *Curr Opin Nephrol Hypertens.* 2013;22(5):551–558.
148. Sands JM, Nonoguchi H, Knepper MA. Vasopressin effects on urea and H₂O transport in inner medullary collecting duct subsegments. *Am J Physiol.* 1987;253:F823–F832.
154. Preston GM, Carroll TP, Guggino WB, et al. Appearance of water channels in *Xenopus* oocytes expressing red cell CHIP28 protein. *Science.* 1992;256:385–387.
167. Poulsen SB, Kim YH, Frokiaer J, et al. Long-term vasopressin-v2-receptor stimulation induces regulation of aquaporin 4 protein in renal inner medulla and cortex of Brattleboro rats. *Nephrol Dial Transplant.* 2013;28(8):2058–2065.
169. Zwang NA, Hoffert JD, Pisitkun T, et al. Identification of phosphorylation-dependent binding partners of aquaporin-2 using protein mass spectrometry. *J Proteome Res.* 2009;8(3):1540–1554.
178. Nielsen S, Chou C-L, Marples D, et al. Vasopressin increases water permeability of kidney collecting duct by inducing translocation of aquaporin-CD water channels to plasma membrane. *Proc Natl Acad Sci U S A.* 1995;92:1013–1017.

185. Bouley R, Hasler U, Lu HA, et al. Bypassing vasopressin receptor signaling pathways in nephrogenic diabetes insipidus. *Semin Nephrol*. 2008;28(3):266–278.
191. Moeller HB, Aroankins TS, Slengerik-Hansen J, et al. Phosphorylation and ubiquitylation are opposing processes that regulate endocytosis of the water channel aquaporin-2. *J Cell Sci*. 2014;127(Pt 14):3174–3183.
195. Khositseth S, Charnkaew K, Boonkrai C, et al. Hypercalcemia induces targeted autophagic degradation of aquaporin-2 at the onset of nephrogenic diabetes insipidus. *Kidney Int*. 2017;91(5):1070–1087.
227. Kortenoeven ML, Pedersen NB, Miller RL, et al. Genetic ablation of aquaporin-2 in the mouse connecting tubules results in defective renal water handling. *J Physiol*. 2013;591(Pt 8):2205–2219.
243. Boone M, Kortenoeven ML, Robben JH, et al. Counteracting vasopressin-mediated water reabsorption by ATP, dopamine, and phorbol esters: mechanisms of action. *Am J Physiol Renal Physiol*. 2011;300(3):F761–F771.
248. Bouley R, Soler NP, Cohen O, et al. Stimulation of AQP2 membrane insertion in renal epithelial cells in vitro and in vivo by the cGMP phosphodiesterase inhibitor sildenafil citrate (Viagra). *Am J Physiol Renal Physiol*. 2005;288(6):F1103–F1112.
264. Lee MS, Choi HJ, Park EJ, et al. Depletion of vacuolar protein sorting-associated protein 35 is associated with increased lysosomal degradation of aquaporin-2. *Am J Physiol Renal Physiol*. 2016;311(6):F1294–F1307.
285. Li W, Zhang Y, Bouley R, et al. Simvastatin enhances aquaporin-2 surface expression and urinary concentration in vasopressin-deficient Brattleboro rats through modulation of Rho GTPase. *Am J Physiol Renal Physiol*. 2011;301(2):F309–F318.
320. Olesen ET, Moeller HB, Assentoft M, et al. The vasopressin type 2 receptor and prostaglandin receptors EP2 and EP4 can increase aquaporin-2 plasma membrane targeting through a cAMP-independent pathway. *Am J Physiol Renal Physiol*. 2016;311(5):F935–F944.
322. Cheung PW, Nomura N, Nair AV, et al. EGF receptor inhibition by erlotinib increases aquaporin 2-mediated renal water reabsorption. *J Am Soc Nephrol*. 2016;27(10):3105–3116.
326. Hoffert JD, Pisitkun T, Saeed F, et al. Dynamics of the G protein-coupled vasopressin V2 receptor signaling network revealed by quantitative phosphoproteomics. *Mol Cell Proteomics*. 2012;11(2):doi:10.1074/mcp.M111.014613.
328. Moeller HB, MacAulay N, Knepper MA, et al. Role of multiple phosphorylation sites in the COOH-terminal tail of aquaporin-2 for water transport: evidence against channel gating. *Am J Physiol Renal Physiol*. 2009;296(3):F649–F657.
340. Moeller HB, Praetorius J, Rutzler MR, et al. Phosphorylation of aquaporin-2 regulates its endocytosis and protein-protein interactions. *Proc Natl Acad Sci U S A*. 2010;107(1):424–429.
341. Klein JD, Wang Y, Blount MA, et al. Metformin, an AMPK activator, stimulates the phosphorylation of aquaporin 2 and urea transporter A1 in inner medullary collecting ducts. *Am J Physiol Renal Physiol*. 2016;310(10):F1008–F1012.
349. Olesen ET, Fenton RA. Is there a role for PGE2 in urinary concentration? *J Am Soc Nephrol*. 2013;24(2):169–178.
355. Gamble JL, McKhann CF, Butler AM, et al. An economy of water in renal function referable to urea. *Am J Physiol*. 1934;109:139–154.
358. Fenton RA, Chou C-L, Stewart GS, et al. Urinary concentrating defect in mice with selective deletion of phloretin-sensitive urea transporters in the renal collecting duct. *Proc Natl Acad Sci U S A*. 2004;101(19):7469–7474.
367. Bagnasco SM, Peng T, Janech MG, et al. Cloning and characterization of the human urea transporter UT-a1 and mapping of the human *Slc14a2* gene. *Am J Physiol Renal Physiol*. 2001;281:F400–F406.
371. Nielsen S, Terris J, Smith CP, et al. Cellular and subcellular localization of the vasopressin-regulated urea transporter in rat kidney. *Proc Natl Acad Sci U S A*. 1996;93:5495–5500.
376. You G, Smith CP, Kanai Y, et al. Cloning and characterization of the vasopressin-regulated urea transporter. *Nature*. 1993;365:844–847.
378. Blount MA, Mistry AC, Fröhlich O, et al. Phosphorylation of UT-a1 urea transporter at serines 486 and 499 is important for vasopressin-regulated activity and membrane accumulation. *Am J Physiol Renal Physiol*. 2008;295(1):F295–F299.
391. Wang Y, Klein JD, Fröhlich O, et al. Role of protein kinase C- α in hypertonicity-stimulated urea permeability in mouse inner medullary collecting ducts. *Am J Physiol Renal Physiol*. 2013;304:F233–F238.
402. Efe O, Klein JD, LaRocque LM, et al. Metformin improves urine concentration in rodents with nephrogenic diabetes insipidus. *JCI Insight*. 2016;1(11).
403. Sands JM, Klein JD. Physiological insights into novel therapies for nephrogenic diabetes insipidus. *Am J Physiol Renal Physiol*. 2016;doi:10.1152/ajprenal.00418.2016.
408. Kokko JP, Rector FC. Countercurrent multiplication system without active transport in inner medulla. *Kidney Int*. 1972;2:214–223.
409. Stephenson JL. Concentration of urine in a central core model of the renal counterflow system. *Kidney Int*. 1972;2:85–94.
410. Pannabecker TL, Dantzer WH, Layton HE, et al. Role of three-dimensional architecture in the urine concentrating mechanism of the rat renal inner medulla. *Am J Physiol Renal Physiol*. 2008;295(5):F1271–F1285.
428. Gottschalk CW, Mylle M. Micropuncture study of the mammalian urinary concentrating mechanism: evidence for the countercurrent hypothesis. *Am J Physiol*. 1959;196:927–936.
431. Burg MB, Green N. Function of the thick ascending limb of Henle's loop. *Am J Physiol*. 1973;224:659–668.
432. Rocha AS, Kokko JP. Sodium chloride and water transport in the medullary thick ascending limb of Henle. Evidence for active chloride transport. *J Clin Invest*. 1973;52:612–623.
434. Wirz H, Hargitay B, Kuhn W. Lokalisation des konzentrierungsprozesses in der niere durch direkte kryoskopie. *Helv Physiol Pharmacol Acta*. 1951;9:196–207.
437. Kuhn W, Ryffel K. Herstellung konzentrierter lösungen aus verdünnten durch blosse membranwirkung: ein modellversuch zur funktion der niere. *Hoppe Seylers Z Physiol Chem*. 1942;276:145–178.
453. Layton AT. A mathematical model of the urine concentrating mechanism in the rat renal medulla. I. Formulation and base-case results. *Am J Physiol Renal Physiol*. 2011;300(2):F356–F371.
454. Jen JF, Stephenson JL. Externally driven countercurrent multiplication in a mathematical model of the urinary concentrating mechanism of the renal inner medulla. *Bull Math Biol*. 1994;56(3):491–514.
457. Hervy S, Thomas SR. Inner medullary lactate production and urine-concentrating mechanism: a flat medullary model. *Am J Physiol Renal Physiol*. 2003;284(1):F65–F81.
467. Schmidt-Nielsen B. The renal concentrating mechanism in insects and mammals: a new hypothesis involving hydrostatic pressures. *Am J Physiol*. 1995;268:R1087–R1100.
478. Klein JD, Sands JM. Urea transport and clinical potential of urea-etics. *Curr Opin Nephrol Hypertens*. 2016;25(5):444–451.

REFERENCES

- Weiner ID, Mitch WE, Sands JM. Urea and ammonia metabolism and the control of renal nitrogen excretion. *Clin J Am Soc Nephrol*. 2015;10(8):1444–1458.
- Sands JM, Mount DB, Layton HE. The physiology of water homeostasis. In: Mount DB, Sayegh MH, Singh AK, eds. *Core Concepts in Disorders of Fluid, Electrolytes and Acid-Base Balance*. New York: Springer; 2013:1–28.
- Knepper MA, Burg MB. Organization of nephron function. *Am J Physiol Renal Physiol*. 1983;244:F579–F589.
- Knepper MA, Stephenson JL. Urinary concentrating and diluting processes. In: Andreoli TE, Hoffman JF, Fanestil DD, et al, eds. *Physiology of Membrane Disorders*. 1. 2nd ed. New York: Plenum; 1986:713–726.
- Fenton RA, Knepper MA. Mouse models and the urinary concentrating mechanism in the new millennium. *Physiol Rev*. 2007;87:1083–1112.
- Zhai XY, Thomsen JS, Birn H, et al. Three-dimensional reconstruction of the mouse kidney. *J Am Soc Nephrol*. 2006;17:77–88.
- Imai M, Taniguchi J, Tabei K. Function of thin loops of Henle. *Kidney Int*. 1987;31:565–579.
- Wade JB, Lee AJ, Liu J, et al. UT-a2: a 55 kDa urea transporter protein in thin descending limb of Henle's loop whose abundance is regulated by vasopressin. *Am J Physiol*. 2000;278(1):F52–F62.
- Imai M, Taniguchi J, Yoshitomi K. Transition of permeability properties along the descending limb of long-loop nephron. *Am J Physiol*. 1988;254:F323–F328.
- Chou C-L, Knepper MA. In vitro perfusion of chinchilla thin limb segments: segmentation and osmotic water permeability. *Am J Physiol Renal Physiol*. 1992;263:F417–F426.
- Chou C-L, Knepper MA. In vitro perfusion of chinchilla thin limb segments: urea and NaCl permeabilities. *Am J Physiol Renal Physiol*. 1993;264:F337–F343.
- Chou C-L, Nielsen S, Knepper MA. Structural-functional correlation in chinchilla long loop of Henle thin limbs: a novel papillary subsegment. *Am J Physiol*. 1993;265:F863–F874.
- Pannabecker TL. Structure and function of the thin limbs of the loop of Henle. *Compr Physiol*. 2012;2:2063–2086.
- Dantzler WH, Layton AT, Layton HE, et al. Urine-concentrating mechanism in the inner medulla: function of the thin limbs of the loops of Henle. *Clin J Am Soc Nephrol*. 2014;9(10):1781–1789.
- Pannabecker TL. Comparative physiology and architecture associated with the mammalian urine concentrating mechanism: role of inner medullary water and urea transport pathways in the rodent medulla. *Am J Physiol Regul Integr Comp Physiol*. 2013;304(7):R488–R503.
- Pannabecker TL, Abbott DE, Dantzler WH. Three-dimensional functional reconstruction of inner medullary thin limbs of Henle's loop. *Am J Physiol Renal Physiol*. 2004;286(1):F38–F45.
- Zhai XY, Fenton RA, Andreassen A, et al. Aquaporin-1 is not expressed in descending thin limbs of short-loop nephrons. *J Am Soc Nephrol*. 2007;18:2937–2944.
- Westrick KY, Serack B, Dantzler WH, et al. Axial compartmentation of descending and ascending thin limbs of Henle's loops. *Am J Physiol Renal Physiol*. 2013;304(3):F308–F316.
- Layton AT, Dantzler WH, Pannabecker TL. Urine concentrating mechanism: impact of vascular and tubular architecture and a proposed descending limb urea-Na⁺ cotransporter. *Am J Physiol Renal Physiol*. 2012;302(5):F591–F605.
- Nawata CM, Evans KK, Dantzler WH, et al. Transepithelial water and urea permeabilities of isolated perfused Munich-Wistar rat inner medullary thin limbs of Henle's loop. *Am J Physiol Renal Physiol*. 2014;306(1):F123–F129.
- Nawata CM, Dantzler WH, Pannabecker TL. Alternative channels for urea in the inner medulla of the rat kidney. *Am J Physiol Renal Physiol*. 2015;309(11):F916–F924.
- Pannabecker TL, Dantzler WH. Three-dimensional lateral and vertical relationships of inner medullary loops of Henle and collecting ducts. *Am J Physiol Renal Physiol*. 2004;287(4):F767–F774.
- Kriz W. Der architektonische und funktionelle aufbau der ratteniere. *Z Zellforsch*. 1967;82:495–535.
- Kriz W, Bankir L. Structural organization of the renal medullary counterflow system. *Fed Proc*. 1983;42:2379–2385.
- Kriz W, Schnermann J, Koepsell H. The position of short and long loops of Henle in the rat kidney. *Z Anat Entwicklungsgesch*. 1972;138:301–319.
- Lemley KV, Kriz W. Cycles and separations: the histotopography of the urinary concentrating process. *Kidney Int*. 1987;31:538–548.
- Pannabecker TL, Henderson CS, Dantzler WH. Quantitative analysis of functional reconstructions reveals lateral and axial zonation in the renal inner medulla. *Am J Physiol Renal Physiol*. 2008;294(6):F1306–F1314.
- Pannabecker TL, Dantzler WH. Three-dimensional architecture of collecting ducts, loops of Henle, and blood vessels in the renal papilla. *Am J Physiol Renal Physiol*. 2007;293(3):F696–F704.
- Issaian T, Urity VB, Dantzler WH, et al. Architecture of vasa recta in the renal inner medulla of the desert rodent *dipodomys merriami*: potential impact on the urine concentrating mechanism. *Am J Physiol Renal Physiol*. 2012;303(7):R748–F756.
- Wei G, Rosen S, Dantzler WH, et al. Architecture of the human renal inner medulla and functional implications. *Am J Physiol Renal Physiol*. 2015;309(7):F627–F637.
- Yuan J, Pannabecker TL. Architecture of inner medullary descending and ascending vasa recta: pathways for countercurrent exchange. *Am J Physiol Renal Physiol*. 2010;299(1):F265–F272.
- Gilbert RL, Pannabecker TL. Architecture of interstitial nodal spaces in the rodent renal inner medulla. *Am J Physiol Renal Physiol*. 2013;305(5):F745–F752.
- Layton AT, Gilbert RL, Pannabecker TL. Isolated interstitial nodal spaces may facilitate preferential solute and fluid mixing in the rat renal inner medulla. *Am J Physiol Renal Physiol*. 2012;302(7):F830–F839.
- Uchida S, Sasaki S, Nitta K, et al. Localization and functional characterization of rat kidney-specific chloride channel, ClC-k1. *J Clin Invest*. 1995;95(1):104–113.
- Vandewalle A, Cluzeaud F, Bens M, et al. Localization and induction by dehydration of ClC-K chloride channels in the rat kidney. *Am J Physiol Renal Physiol*. 1997;272:F678–F688.
- Takahashi N, Kondo Y, Ito O, et al. Vasopressin stimulates Cl⁻ transport in ascending thin limb of Henle's loop in hamster. *J Clin Invest*. 1995;95:1623–1627.
- Matsumura Y, Uchida S, Kondo Y, et al. Overt nephrogenic diabetes insipidus in mice lacking the ClC-K1 chloride channel. *Nat Genet*. 1999;21:95–98.
- Biemesderfer D, Rutherford PA, Nagy T, et al. Monoclonal antibodies for high-resolution localization of NHE3 in adult and neonatal rat kidney. *Am J Physiol Renal Physiol*. 1997;273:F289–F299.
- Ecelbarger CA, Terris J, Hoyer JR, et al. Localization and regulation of the rat renal Na⁺-K⁺-2Cl⁻ cotransporter, BSC-1. *Am J Physiol Renal Physiol*. 1996;271(3):F619–F628.
- Kaplan MR, Plotkin MD, Lee WS, et al. Apical localization of the Na-K-Cl cotransporter, *rBSC1*, on rat thick ascending limbs. *Kidney Int*. 1996;49(1):40–47.
- Nielsen S, Maunsbach AB, Ecelbarger CA, et al. Ultrastructural localization of Na-K-2Cl cotransporter in thick ascending limb and macula densa of rat kidney. *Am J Physiol Renal Physiol*. 1998;275(6):F885–F893.
- Schultheis PJ, Clarke LL, Meneton P, et al. Renal and intestinal absorptive defects in mice lacking the NHE3 Na⁺/H⁺ exchanger. *Nat Genet*. 1998;19:282–285.
- Cho CS, Elkahwaji J, Chang Z, et al. Modulation of the electrophoretic mobility of the linker for activation of T cells (LAT) by calcineurin inhibitors CsA and FK506: LAT is a potential substrate for PK and calcineurin signaling pathways. *Cell Signal*. 2003;15(1):85–93.
- Lorenz JN, Schultheis PJ, Traynor T, et al. Micropuncture analysis of single-nephron function in NHE3-deficient mice. *Am J Physiol Renal Physiol*. 1999;277:F447–F453.
- Amlal H, Ledoussal C, Sheriff S, et al. Downregulation of renal AQP2 water channel and NKCC2 in mice lacking the apical Na⁺-H⁺ exchanger NHE3. *J Physiol*. 2003;553(2):511–522.
- Fenton RA, Poulsen SB, de la Mora Chavez S, et al. Renal tubular NHE3 is required in the maintenance of water and sodium chloride homeostasis. *Kidney Int*. 2017.
- Oppermann M, Mizel D, Kim SM, et al. Renal function in mice with targeted disruption of the a isoform of the Na-K-2Cl co-transporter. *J Am Soc Nephrol*. 2007;18:440–448.
- Oppermann M, Mizel D, Huang G, et al. Macula densa control of renin secretion and preglomerular resistance in mice with selective deletion of the B isoform of the Na,K,2Cl co-transporter. *J Am Soc Nephrol*. 2006;17:2143–2153.
- Boim MA, Ho K, Shuck ME, et al. ROMK inwardly rectifying ATP-sensitive K⁺ channel. II. Cloning and distribution of alternative forms. *Am J Physiol Renal Physiol*. 1995;268:F1132–F1140.

50. Lee W-S, Hebert SC. ROMK inwardly rectifying ATP-sensitive K⁺ channel. I. Expression in rat distal nephron segments. *Am J Physiol*. 1995;268:F1124–F1131.
51. Kohda Y, Ding W, Phan E, et al. Localization of the ROMK potassium channel to the apical membrane of distal nephron in rat kidney. *Kidney Int*. 1998;54(4):1214–1223.
52. Mennitt PA, Wade JB, Ecelbarger CA, et al. Localization of ROMK channels in the rat kidney. *J Am Soc Nephrol*. 1997;8(12):1823–1830.
53. Xu JZ, Hall AE, Peterson LN, et al. Localization of the ROMK protein on apical membranes of rat kidney nephron segments. *Am J Physiol Renal Physiol*. 1997;273(5):F739–F748.
54. Besseghir K, Trimble ME, Stoner L. Action of ADH on isolated medullary thick ascending limb of the Brattleboro rat. *Am J Physiol*. 1986;251:F271–F277.
55. Ecelbarger CA, Kim GH, Knepper MA, et al. Regulation of potassium channel kir 1.1 (ROMK) abundance in the thick ascending limb of Henle's loop. *J Am Soc Nephrol*. 2001;12(1):10–18.
56. Lorenz JN, Baird NR, Judd LM, et al. Impaired renal NaCl absorption in mice lacking the ROMK potassium channel, a model for type II Bartter's syndrome. *J Biol Chem*. 2002;277:37871–37880.
57. Kaissling B, Kriz W. Structural analysis of the rabbit kidney. In: Brodal A, Hild W, VanLimborgh J, et al, eds. *Advances in Anatomy: Embryology and Cell Biology*. Vol. 56. Berlin: Springer Verlag; 1979:1–123.
58. Kishore BK, Mandon B, Oza NB, et al. Rat renal arcade segment expresses vasopressin-regulated water channel and vasopressin V₂ receptor. *J Clin Invest*. 1996;97(12):2763–2771.
59. Knepper MA, Danielson RA, Saidel GM, et al. Quantitative analysis of renal medullary anatomy in rats and rabbits. *Kidney Int*. 1977;12:313–323.
60. Hager H, Kwon TH, Vinnikova AK, et al. Immunocytochemical and immunoelectron microscopic localization of alpha-, beta-, and gamma-ENaC in rat kidney. *Am J Physiol Renal Physiol*. 2001;280(6):F1093–F1106.
61. Loffing J, Loffing-Cueni D, Macher A, et al. Localization of epithelial sodium channel and aquaporin-2 in rabbit kidney cortex. *Am J Physiol Renal Physiol*. 2000;278(F530):F539.
62. Ecelbarger CA, Kim GH, Terris J, et al. Vasopressin-mediated regulation of epithelial sodium channel abundance in rat kidney. *Am J Physiol Renal Physiol*. 2000;279(1):F46–F53.
63. Nicco C, Wittner M, DiStefano A, et al. Chronic exposure to vasopressin upregulates ENaC and sodium transport in the rat renal collecting duct and lung. *Hypertension*. 2001;38(5):1143–1149.
64. Sauter D, Fernandes S, Goncalves-Mendes N, et al. Long-term effects of vasopressin on the subcellular localization of ENaC in the renal collecting system. *Kidney Int*. 2006;69(6):1024–1032.
65. Schlatter E, Schafer JA. Electrophysiological studies in principal cells of rat cortical collecting tubules. ADH increases the apical membrane Na⁺ conductance. *Pfluegers Arch*. 1987;409:81–92.
66. Reif MC, Troutman SL, Schafer JA. Sodium transport by rat cortical collecting tubule. Effects of vasopressin and desoxycorticosterone. *J Clin Invest*. 1986;77:1291–1298.
67. Tomita K, Pisano JJ, Knepper MA. Control of sodium and potassium transport in the cortical collecting duct of the rat. Effects of bradykinin, vasopressin, and deoxycorticosterone. *J Clin Invest*. 1985;76:132–136.
68. Snyder PM. Minireview: regulation of epithelial Na⁺ channel trafficking. *Endocrinology*. 2005;146:5079–5085.
69. McDonald FJ, Yang B, Hrstka RF, et al. Disruption of the beta subunit of the epithelial Na⁺ channel in mice: hyperkalemia and neonatal death associated with a pseudohypoaldosteronism phenotype. *Proc Natl Acad Sci U S A*. 1999;96:1727–1731.
70. Hummler E, Barker P, Gatzky J, et al. Early death due to defective neonatal lung liquid clearance in alpha-ENaC-deficient mice. *Nat Genet*. 1996;12:325–328.
71. Hummler E, Barker P, Talbot C, et al. A mouse model for the renal salt-wasting syndrome pseudohypoaldosteronism. *Proc Natl Acad Sci U S A*. 1997;94:11710–11715.
72. Barker PM, Nguyen MS, Gatzky JT, et al. Role of gammaENaC subunit in lung liquid clearance and electrolyte balance in newborn mice. Insights into perinatal adaptation and pseudohypoaldosteronism. *J Clin Invest*. 1998;102:1634–1640.
73. Rubera I, Loffing J, Palmer LG, et al. Collecting duct-specific gene inactivation of alphaENaC in the mouse kidney does not impair sodium and potassium balance. *J Clin Invest*. 2003;112(4):554–565.
74. Christensen BM, Perrier R, Wang Q, et al. Sodium and potassium balance depends on alphaENaC expression in connecting tubule. *J Am Soc Nephrol*. 2010;21(11):1942–1951.
75. Rohuser H, Kriz W, Heinke W. Das gefässsystem der ratteniere. *Z Zellforsch Mikrosk Anat*. 1964;64:381–403.
76. Ren H, Gu L, Andreasen A, et al. Spatial organization of the vascular bundle and the interbundle region: three-dimensional reconstruction at the inner stripe of outer medulla in the mouse kidney. *Am J Physiol Renal Physiol*. 2014;306:F321–F326.
77. Nielsen S, Pallone T, Smith BL, et al. Aquaporin-1 water channels in short and long loop descending thin limbs and in descending vasa recta in rat kidney. *Am J Physiol*. 1995;268:F1023–F1037.
78. Pallone TL, Kishore BK, Nielsen S, et al. Evidence that aquaporin-1 mediates NaCl-induced water flux across descending vasa recta. *Am J Physiol Renal Physiol*. 1997;272:F587–F596.
79. Pallone TL. Characterization of the urea transporter in outer medullary descending vasa recta. *Am J Physiol*. 1994;267:R260–R267.
80. Xu Y, Olives B, Bailly P, et al. Endothelial cells of the kidney vasa recta express the urea transporter HUT11. *Kidney Int*. 1997;51(1):138–146.
81. Evans KK, Nawata CM, Pannabecker TL. Isolation and perfusion of rat inner medullary vasa recta. *Am J Physiol Renal Physiol*. 2015;309(4):F300–F304.
82. Pallone TL, Work J, Myers RL, et al. Transport of sodium and urea in outer medullary descending vasa recta. *J Clin Invest*. 1994;93:212–222.
83. Berliner RW, Levinsky NG, Davidson DG, et al. Dilution and concentration of the urine and the action of antidiuretic hormone. *Am J Med*. 1958;24:730–744.
84. Pannabecker TL. Loop of Henle interaction with interstitial nodal spaces in the renal inner medulla. *Am J Physiol Renal Physiol*. 2008;295(6):F1744–F1751.
85. Bulger RE, Nagle RB. Ultrastructure of the interstitium in the rabbit kidney. *Am J Anat*. 1973;136:183–204.
86. Pannabecker TL, Layton AT. Targeted delivery of solutes and oxygen in the renal medulla: role of microvessel architecture. *Am J Physiol Renal Physiol*. 2014;307(6):F649–F655.
87. Knepper MA, Saidel GM, Hascall VC, et al. Concentration of solutes in the renal inner medulla: interstitial hyaluronan as a mechano-osmotic transducer. *Am J Physiol Renal Physiol*. 2003;284(3):F433–F446.
88. Lacy ER, Schmidt-Nielsen B. Ultrastructural organization of the hamster renal pelvis. *Am J Anat*. 1979;155:403–424.
89. Schmidt-Nielsen B. Excretion in mammals: role of the renal pelvis in the modification of the urinary concentration and composition. *Fed Proc*. 1977;36:2493–2503.
90. Sheehan HL, Davis JC. Anatomy of the pelvis in the rabbit kidney. *J Anat*. 1959;93:499–502.
91. Reinking LN, Schmidt-Nielsen B. Peristaltic flow of urine in the renal papillary collecting ducts of hamsters. *Kidney Int*. 1981;20:55–60.
92. Schmidt-Nielsen B, Graves B. Changes in fluid compartments in hamster renal papilla due to peristalsis in the pelvic wall. *Kidney Int*. 1982;22:613–625.
93. Landry DW, Oliver JA. The pathogenesis of vasodilatory shock. *N Engl J Med*. 2001;345(8):588–595.
94. Morel A, O'Carroll A-M, Brownstein MJ, et al. Molecular cloning and expression of a rat V1a arginine vasopressin receptor. *Nature*. 1992;356:523–526.
95. Sugimoto T, Saito M, Mochizuki S, et al. Molecular cloning and functional expression of a cDNA encoding the human V1b vasopressin receptor. *J Biol Chem*. 1994;269:27088–27092.
96. Birnbaumer M, Seibold A, Gilbert S. Molecular cloning of the receptor for human antidiuretic hormone. *Nature*. 1992;357:333–335.
97. Lolait SJ, O'Carroll A-M, McBride OW, et al. Cloning and characterization of a vasopressin V2 receptor and possible link to nephrogenic diabetes insipidus. *Nature*. 1992;357:336–339.
98. Fejes-Toth G, Naray-Fejes-Toth A. Isolated principal and intercalated cells: hormone responsiveness and Na⁺K⁺-ATPase activity. *Am J Physiol*. 1989;256(4 Pt 2):F742–F750.
99. Grantham JJ, Burg MB. Effect of vasopressin and cyclic AMP on permeability of isolated collecting tubules. *Am J Physiol*. 1966;211:255–259.
100. Kirk K. Binding and internalization of a fluorescent vasopressin analogue by collecting duct cells. *Am J Physiol*. 1988;255:C622–C632.
101. Morel F, Imbert-Teboul M, Chabardes D. Distribution of hormone-dependent adenylate cyclase in the nephron and its physiologic significance. *Annual Rev Physiol*. 1981;43:569–581.

102. Woodhall PB, Tisher CC. Response of the distal tubule and cortical collecting duct to vasopressin in the rat. *J Clin Invest.* 1973;52(12):3095–3108.
103. Skorecki K, Brown D, Ercolani L, et al. Molecular mechanisms of vasopressin action in the kidney. In: Windhager EE, ed. *Handbook of Physiology*. New York: Oxford University Press; 1992:1185–1218.
104. Nickols HH, Shah VN, Chazin WJ, et al. Calmodulin interacts with the V2 vasopressin receptor: elimination of binding to the C terminus also eliminates arginine vasopressin-stimulated elevation of intracellular calcium. *J Biol Chem.* 2004;279(45):46969–46980.
105. Chou CL, Yip KP, Michea L, et al. Regulation of aquaporin-2 trafficking by vasopressin in the renal collecting duct. Roles of ryanodine-sensitive Ca^{2+} stores and calmodulin. *J Biol Chem.* 2000;275(47):36839–36846.
106. Hoffert JD, Chou C-L, Fenton RA, et al. Calmodulin is required for vasopressin-stimulated increase in cyclic AMP production in inner medullary collecting duct. *J Biol Chem.* 2005;280(14):13624–13630.
107. Yun J, Schöneberg T, Liu J, et al. Generation and phenotype of mice harboring a nonsense mutation in the V2 vasopressin receptor gene. *J Clin Invest.* 2000;106(11):1361–1371.
108. Schliebe N, Strotmann R, Busse K, et al. V2 vasopressin receptor deficiency causes changes in expression and function of renal and hypothalamic components involved in electrolyte and water homeostasis. *Am J Physiol Renal Physiol.* 2008;295:F1177–F1190.
109. Li JH, Chou CL, Li B, et al. A selective EP4 PGE2 receptor agonist alleviates disease in a new mouse model of X-linked nephrogenic diabetes insipidus. *J Clin Invest.* 2009;119(10):3115–3126.
110. Moeller HB, Fuglsang CH, Fenton RA. Renal aquaporins and water balance disorders. *Best Pract Res Clin Endocrinol Metab.* 2016;30(2):277–288.
111. Kortenoeven ML, Fenton RA. Renal aquaporins and water balance disorders. *Biochim Biophys Acta.* 2014;1840(5):1533–1549.
112. Brunskill N, Bastani B, Hayes C, et al. Localization and polar distribution of several G-protein subunits along nephron segments. *Kidney Int.* 1991;40(6):997–1006.
113. Stow J, Sabolic I, Brown D. Heterogeneous localization of G protein alpha-subunits in rat kidney. *Am J Physiol.* 1991;261:F831–F840.
114. Shen TS, Suzuki Y, Poyard M, et al. Expression of adenylate cyclase mRNAs in the adult, in developing, and in the Brattleboro rat kidney. *Am J Physiol Cell Physiol.* 1997;273(1):C323–C330.
115. Rieg T, Tang T, Murray F, et al. Adenylate cyclase 6 determines cAMP formation and aquaporin-2 phosphorylation and trafficking in inner medulla. *J Am Soc Nephrol.* 2010;21(12):2059–2068.
116. Roos KP, Strait KA, Raphael KL, et al. Collecting duct-specific knockout of adenylate cyclase type VI causes a urinary concentration defect in mice. *Am J Physiol Renal Physiol.* 2012;302(1):F78–F84.
117. Granier S, Terrillon S, Pascal R, et al. A cyclic peptide mimicking the third intracellular loop of the V2 vasopressin receptor inhibits signaling through its interaction with receptor dimer and G protein. *J Biol Chem.* 2004;279(49):50904–50914.
118. von Zastrow M. Mechanisms regulating membrane trafficking of G protein-coupled receptors in the endocytic pathway. *Life Sci.* 2003;74(2–3):217–224.
119. Wolfe BL, Trejo J. Clathrin-dependent mechanisms of G protein-coupled receptor endocytosis. *Traffic.* 2007;8(5):462–470.
120. Bouley R, Sun TX, Chenard M, et al. Functional role of the NPxxY motif in internalization of the type 2 vasopressin receptor in LLC-PK1 cells. *Am J Physiol Cell Physiol.* 2003;285(4):C750–C762.
121. Oakley RH, Laporte SA, Holt JA, et al. Differential affinities of visual arrestin, beta arrestin1, and beta arrestin2 for G protein-coupled receptors delineate two major classes of receptors. *J Biol Chem.* 2000;275(22):17201–17210.
122. Feinstein TN, Yui N, Webber MJ, et al. Noncanonical control of vasopressin receptor type 2 signaling by retromer and arrestin. *J Biol Chem.* 2013;288(39):27849–27860.
123. Terashima Y, Kondo K, Mizuno Y, et al. Influence of acute elevation of plasma AVP level on rat vasopressin V2 receptor and aquaporin-2 mRNA expression. *J Mol Endocrinol.* 1998;20(2):281–285.
124. Dousa TP. Cyclic-3',5'-nucleotide phosphodiesterases in the cyclic adenosine monophosphate (cAMP)-mediated actions of vasopressin. *Semin Nephrol.* 1994;14(4):333–340.
125. DeWire SM, Ahn S, Lefkowitz RJ, et al. Beta-arrestins and cell signaling. *Annu Rev Physiol.* 2007;69:483–510.
126. Ren XR, Reiter E, Ahn S, et al. Different G protein-coupled receptor kinases govern G protein and beta-arrestin-mediated signaling of V2 vasopressin receptor. *Proc Natl Acad Sci U S A.* 2005;102(5):1448–1453.
127. Martin NP, Lefkowitz RJ, Shenoy SK. Regulation of V2 vasopressin receptor degradation by agonist-promoted ubiquitination. *J Biol Chem.* 2003;278(46):45954–45959.
128. Oakley RH, Laporte SA, Holt JA, et al. Association of beta-arrestin with G protein-coupled receptors during clathrin-mediated endocytosis dictates the profile of receptor resensitization. *J Biol Chem.* 1999;274(45):32248–32257.
129. Pfeiffer R, Kirsch J, Fahrenholz F. Agonist and antagonist-dependent internalization of the human vasopressin V2 receptor. *Exp Cell Res.* 1998;244(1):327–339.
130. Perry SJ, Lefkowitz RJ. Arresting developments in heptahelical receptor signaling and regulation. *Trends Cell Biol.* 2002;12(3):130–138.
131. Bowen-Pidgeon D, Innamorati G, Sadeghi HM, et al. Arrestin effects on internalization of vasopressin receptors. *Mol Pharmacol.* 2001;59(6):1395–1401.
132. Innamorati G, Le Gouill C, Balamotis M, et al. The long and the short cycle. Alternative intracellular routes for trafficking of G-protein-coupled receptors. *J Biol Chem.* 2001;276(16):13096–13103.
133. Innamorati G, Sadeghi H, Birnbaumer M. Phosphorylation and recycling kinetics of G protein-coupled receptors. *J Recept Signal Transduct Res.* 1999;19(1–4):315–326.
134. Bouley R, Lin HY, Raychowdhury MK, et al. Downregulation of the vasopressin type 2 receptor after vasopressin-induced internalization: involvement of a lysosomal degradation pathway. *Am J Physiol Cell Physiol.* 2005;288(6):C1390–C1401.
135. Lutz W, Sanders M, Salisbury J, et al. Internalization of vasopressin analogs in kidney and smooth muscle cells: evidence for receptor-mediated endocytosis in cells with V2 or V1 receptors. *Proc Natl Acad Sci U S A.* 1990;87(17):6507–6511.
136. Zalyapin EA, Bouley R, Hasler U, et al. Effects of the renal medullary pH and ionic environment on vasopressin binding and signaling. *Kidney Int.* 2008;74(12):1557–1567.
137. Nielsen S, Frokiaer J, Marples D, et al. Aquaporins in the kidney: from molecules to medicine. *Physiol Rev.* 2002;82:205–244.
138. Fenton RA, Pedersen CN, Moeller HB. New insights into regulated aquaporin-2 function. *Curr Opin Nephrol Hypertens.* 2013;22(5):551–558.
139. Moeller HB, Fenton RA. Cell biology of vasopressin-regulated aquaporin-2 trafficking. *Pflugers Arch.* 2012;464(2):133–144.
140. Wirz H. Der osmotische druck in den corticocolin tubuli der rattenniere *Helv Physiol Pharmacol Acta.* 1956;14:353–362.
141. Elalouf JM, Roinel N, de Rouffignac C. Effects of antidiuretic hormone on electrolyte reabsorption and secretion in distal tubules of rat kidney. *Pflugers Arch.* 1984;401(2):167–173.
142. Pedersen NB, Hofmeister MV, Rosenbaek LL, et al. Vasopressin induces phosphorylation of the thiazide-sensitive sodium chloride cotransporter in the distal convoluted tubule. *Kidney Int.* 2010;78(2):160–169.
143. Fenton RA, Brond L, Nielsen S, et al. Cellular and subcellular distribution of the type II vasopressin receptor in kidney. *Am J Physiol Renal Physiol.* 2007;293:F748–F760.
144. Jamison RL, Buerkert J, Lacy FB. A micropuncture study of collecting tubule function in rats with hereditary diabetes insipidus. *J Clin Invest.* 1971;50:2444–2452.
145. Schmidt-Nielsen B, Graves B, Roth J. Water removal and solute additions determining increases in renal medullary osmolality. *Am J Physiol.* 1983;244:F472–F482.
146. Hai MA, Thomas S. Acute effects of lysine-vasopressin infusion on rat renal tissue osmolality. *J Physiol.* 1969;202(2):117P.
147. Saikia TC. Composition of the renal cortex and medulla of rats during water diuresis and antidiuresis. *Q J Exp Physiol Cogn Med Sci.* 1965;50:146–157.
148. Sands JM, Nonoguchi H, Knepper MA. Vasopressin effects on urea and H₂O transport in inner medullary collecting duct subsegments. *Am J Physiol.* 1987;253:F823–F832.
149. Lankford SP, Chou C-L, Terada Y, et al. Regulation of collecting duct water permeability independent of cAMP-mediated AVP response. *Am J Physiol.* 1991;261:F554–F566.
150. Atherton JC, Hai MA, Thomas S. The time course of changes in renal tissue composition during water diuresis in the rat. *J Physiol.* 1968;197:429–443.
151. Denker BM, Smith BL, Kuhajda FP, et al. Identification, purification, and partial characterization of a novel Mr 28,000 integral membrane protein from erythrocytes and renal tubules. *J Biol Chem.* 1988;263(30):15634–15642.

152. Knepper MA, Nielsen S, Peter Agre. 2003 Nobel Prize winner in chemistry. *J Am Soc Nephrol*. 2004;15(4):1093–1095.
153. Preston GM, Agre P. Isolation of the cDNA for erythrocyte integral membrane protein of 28 kilodaltons: member of an ancient channel family. *Proc Natl Acad Sci U S A*. 1991;88(24):11110–11114.
154. Preston GM, Carroll TP, Guggino WB, et al. Appearance of water channels in *Xenopus* oocytes expressing red cell CHIP28 protein. *Science*. 1992;256:385–387.
155. Nielsen S, Smith BL, Christensen EI, et al. CHIP28 water channels are localized in constitutively water-permeable segments of the nephron. *J Cell Biol*. 1993;120:371–383.
156. Sabolic I, Valenti G, Verbavatz J-M, et al. Localization of the CHIP28 water channel in rat kidney. *Am J Physiol Cell Physiol*. 1992;263:C1225–C1233.
157. Fushimi K, Uchida S, Hara Y, et al. Cloning and expression of apical membrane water channel of rat kidney collecting tubule. *Nature*. 1993;361:549–552.
158. Agre P, Kozono D. Aquaporin water channels: molecular mechanisms for human diseases. *FEBS Lett*. 2003;555(1):72–78.
159. Brown D. The ins and outs of aquaporin-2 trafficking. *Am J Physiol Renal Physiol*. 2003;284:F893–F901.
160. Frokiaer J, Nielsen S, Knepper MA. Molecular physiology of renal aquaporins and sodium transporters: exciting approaches to understand regulation of renal water handling. *J Am Soc Nephrol*. 2005;16(10):2827–2829.
161. Valenti G, Procinio G, Tamma G, et al. Minireview: aquaporin 2 trafficking. *Endocrinology*. 2005;146(12):5063–5070.
162. Deen PMT, Brown D. Trafficking of native and mutant mammalian MIP proteins. In: Hohmann S, Nielsen S, Agre P, eds. *Aquaporins: Current Topics in Membranes*. 51. New York: Academic Press; 2001:235–276.
163. Ishibashi K, Kuwahara M, Sasaki S. Molecular biology of aquaporins. *Rev Physiol Biochem Pharmacol*. 2000;141:1–32.
164. Nedvetzky PI, Tamma G, Beulshausen S, et al. Regulation of aquaporin-2 trafficking. *Handb Exp Pharmacol*. 2009;190:133–157.
165. Frigeri A, Gropper MA, Umenishi F, et al. Localization of M1WC and GLIP water channel homologs in neuromuscular, epithelial and glandular tissues. *J Cell Sci*. 1995;108(Pt 9):2993–3002.
166. Ishibashi K, Sasaki S, Fushimi K, et al. Immunolocalization and effect of dehydration on AQP3, a basolateral water channel of kidney collecting ducts. *Am J Physiol Renal Physiol*. 1997;272(2):F235–F241.
167. Poulsen SB, Kim YH, Frokiaer J, et al. Long-term vasopressin-V2-receptor stimulation induces regulation of aquaporin 4 protein in renal inner medulla and cortex of brattleboro rats. *Nephrol Dial Transplant*. 2013;28(8):2058–2065.
168. Van Hoek AN, Bouley R, Lu Y, et al. Vasopressin-induced differential stimulation of AQP4 splice variants regulates the in-membrane assembly of orthogonal arrays. *Am J Physiol Renal Physiol*. 2009;296(6):F1396–F1404.
169. Zwang NA, Hoffert JD, Pisitkun T, et al. Identification of phosphorylation-dependent binding partners of aquaporin-2 using protein mass spectrometry. *J Proteome Res*. 2009;8(3):1540–1554.
170. Brown D, Grosso A, DeSousa RC. Membrane architecture and water transport in epithelial cell membranes. In: Aloia R, ed. *Membrane Transport and Information Storage, Advances in Membrane Fluidity*. 4. New York: Wiley-Liss; 1990:103–132.
171. Brown D, Orci L. Vasopressin stimulates formation of coated pits in rat kidney collecting ducts. *Nature*. 1983;302(5905):253–255.
172. Chevalier J, Bourguet J, Hugon JS. Membrane associated particles: distribution in frog urinary bladder epithelium at rest and after oxytocin treatment. *Cell Tissue Res*. 1974;152(2):129–140.
173. Kachadorian WA, Wade JB, Uiterwyk CC, et al. Membrane structural and functional responses to vasopressin in toad bladder. *J Membr Biol*. 1977;30(4):381–401.
174. Wade JB. Membrane structural specialization of the toad urinary bladder revealed by the freeze-fracture technique. III. Location, structure and vasopressin dependence of intramembrane particle arrays. *J Membr Biol*. 1978;40 Spec No:281–296.
175. Nielsen S, DiGiovanni SR, Christensen EI, et al. Cellular and subcellular immunolocalization of vasopressin-regulated water channel in rat kidney. *Proc Natl Acad Sci U S A*. 1993;90:11663–11667.
176. Sabolic I, Katsura T, Verbavatz J-M, et al. The AQP2 water channel: effect of vasopressin treatment, microtubule disruption, and distribution in neonatal rats. *J Membr Biol*. 1995;143:165–175.
177. Marples D, Knepper MA, Christensen EI, et al. Redistribution of aquaporin-2 water channels induced by vasopressin in rat kidney inner medullary collecting duct. *Am J Physiol*. 1995;269(3):C655–C664.
178. Nielsen S, Chou C-L, Marples D, et al. Vasopressin increases water permeability of kidney collecting duct by inducing translocation of aquaporin-CD water channels to plasma membrane. *Proc Natl Acad Sci U S A*. 1995;92:1013–1017.
179. Yamamoto T, Sasaki S, Fushimi K, et al. Localization and expression of a collecting duct water channel, aquaporin, in hydrated and dehydrated rats. *Exp Nephrol*. 1995;3(3):193–201.
180. Christensen BM, Marples D, Jensen UB, et al. Acute effects of vasopressin V₂-receptor antagonist on kidney AQP2 expression and subcellular distribution. *Am J Physiol Renal Physiol*. 1998;275(2):F285–F297.
181. Hayashi M, Sasaki S, Tsuganezawa H, et al. Expression and distribution of aquaporin of collecting duct are regulated by vasopressin V₂ receptor in rat kidney. *J Clin Invest*. 1994;94(5):1778–1783.
182. Saito T, Ishikawa SE, Sasaki S, et al. Alteration in water channel AQP-2 by removal of AVP stimulation in collecting duct cells of dehydrated rats. *Am J Physiol Renal Physiol*. 1997;272(2):F183–F191.
183. Chen Y, Rice W, Gu Z, et al. Aquaporin 2 promotes cell migration and epithelial morphogenesis. *J Am Soc Nephrol*. 2012;24:in press.
184. Tamma G, Lasorsa D, Ranieri M, et al. Integrin signaling modulates AQP2 trafficking via Arg-Gly-Asp (RGD) motif. *Cell Physiol Biochem*. 2011;27:739–748.
185. Bouley R, Hasler U, Lu HA, et al. Bypassing vasopressin receptor signaling pathways in nephrogenic diabetes insipidus. *Semin Nephrol*. 2008;28(3):266–278.
186. Gustafson CE, Katsura T, McKee M, et al. Recycling of AQP2 occurs through a temperature- and bafilomycin-sensitive trans-golgi-associated compartment. *Am J Physiol Renal Physiol*. 2000;278(2):F317–F326.
187. Takata K. Aquaporin-2 (AQP2): its intracellular compartment and trafficking. *Cell Mol Biol (Noisy-le-Grand)*. 2006;52(7):34–39.
188. Katsura T, Ausiello DA, Brown D. Direct demonstration of aquaporin-2 water channel recycling in stably transfected LLC-PK₁ epithelial cells. *Am J Physiol*. 1996;270(3):F548–F553.
189. Moeller HB, Knepper MA, Fenton RA. Serine 269 phosphorylated aquaporin-2 is targeted to the apical membrane of collecting duct principal cells. *Kidney Int*. 2009;75(3):295–303.
190. Tamma G, Robben JH, Trimpert C, et al. Regulation of AQP2 localization by S256 and S261 phosphorylation and ubiquitination. *Am J Physiol Cell Physiol*. 2011;300(3):C636–C646.
191. Moeller HB, Aroankins TS, Slengerik-Hansen J, et al. Phosphorylation and ubiquitylation are opposing processes that regulate endocytosis of the water channel aquaporin-2. *J Cell Sci*. 2014;127(Pt 14):3174–3183.
192. Moeller HB, Olesen ET, Fenton RA. Regulation of the water channel aquaporin-2 by posttranslational modification. *Am J Physiol Renal Physiol*. 2011;300(5):F1062–F1073.
193. Kamsteeg EJ, Hendriks G, Boone M, et al. Short-chain ubiquitination mediates the regulated endocytosis of the aquaporin-2 water channel. *Proc Natl Acad Sci U S A*. 2006;103(48):18344–18349.
194. Khositseth S, Uawithya P, Somporn P, et al. Autophagic degradation of aquaporin-2 is an early event in hypokalemia-induced nephrogenic diabetes insipidus. *Sci Rep*. 2015;5:18311.
195. Khositseth S, Charnkaew K, Boonkrai C, et al. Hypercalcemia induces targeted autophagic degradation of aquaporin-2 at the onset of nephrogenic diabetes insipidus. *Kidney Int*. 2017;91(5):1070–1087.
196. Huebner AR, Cheng L, Somporn P, et al. Deubiquitylation of protein cargo is not an essential step in exosome formation. *Mol Cell Proteomics*. 2016;15(5):1556–1571.
197. Pisitkun T, Shen RF, Knepper MA. Identification and proteomic profiling of exosomes in human urine. *Proc Natl Acad Sci U S A*. 2004;101(36):13368–13373.
198. Wen HJ, Frokiaer J, Kwon TH, et al. Urinary excretion of aquaporin-2 in rat is mediated by a vasopressin-dependent apical pathway. *J Am Soc Nephrol*. 1999;10(7):1416–1429.
199. Miranda KC, Bond DT, McKee M, et al. Nucleic acids within urinary exosomes/microvesicles are potential biomarkers for renal disease. *Kidney Int*. 2010;78(2):191–199.
200. Street JM, Birkhoff W, Menzies RI, et al. Exosomal transmission of functional aquaporin 2 in kidney cortical collecting duct cells. *J Physiol*. 2011;589(Pt 24):6119–6127.
201. Higashijima Y, Sonoda H, Takahashi S, et al. Excretion of urinary exosomal AQP2 in rats is regulated by vasopressin and urinary pH. *Am J Physiol Renal Physiol*. 2013;305(10):F1412–F1421.

202. Ecelbarger CA, Terris J, Frindt G, et al. Aquaporin-3 water channel localization and regulation in rat kidney. *Am J Physiol*. 1995;269(5):F663–F672.
203. Terris J, Ecelbarger CA, Marples D, et al. Distribution of aquaporin-4 water channel expression within rat kidney. *Am J Physiol*. 1995;269(6):F775–F785.
204. Terris J, Ecelbarger CA, Nielsen S, et al. Long-term regulation of four renal aquaporins in rats. *Am J Physiol*. 1996;271(2):F414–F422.
205. Christensen BM, Marples D, Kim YH, et al. Changes in cellular composition of kidney collecting duct cells in rats with lithium-induced NDI. *Am J Physiol Cell Physiol*. 2004;286(4):C952–C964.
206. Christensen BM, Kim YH, Kwon TH, et al. Lithium treatment induces a marked proliferation of primarily principal cells in rat kidney inner medullary collecting duct. *Am J Physiol Renal Physiol*. 2006;291(1):F39–F48.
207. Christensen BM, Wang WD, Frokier J, et al. Axial heterogeneity in basolateral AQP2 localization in rat kidney: effect of vasopressin. *Am J Physiol Renal Physiol*. 2003;284(4):F701–F717.
208. Coleman RA, Wu DC, Liu J, et al. Expression of aquaporins in the renal connecting tubule. *Am J Physiol Renal Physiol*. 2000;279(5):F874–F883.
209. Jeon US, Joo KW, Na KY, et al. Oxytocin induces apical and basolateral redistribution of aquaporin-2 in rat kidney. *Exp Nephrol*. 2003;93(1):E36–E45.
210. Van Balkom BWM, Van Raak M, Breton S, et al. Hypertonicity is involved in redirecting the aquaporin-2 water channel into the basolateral, instead of the apical, plasma membrane of renal epithelial cells. *J Biol Chem*. 2003;278(2):1101–1107.
211. de Seigneux S, Nielsen J, Olesen ET, et al. Long-term aldosterone treatment induces decreased apical but increased basolateral expression of AQP2 in CCD of rat kidney. *Am J Physiol Renal Physiol*. 2007;293(1):F87–F99.
212. Nielsen J, Kwon TH, Praetorius J, et al. Aldosterone increases urine production and decreases apical AQP2 expression in rats with diabetes insipidus. *Am J Physiol Renal Physiol*. 2006;290(2):F438–F449.
213. Kamsteeg EJ, Bichet DG, Konings IBM, et al. Reversed polarized delivery of an aquaporin-2 mutant causes dominant nephrogenic diabetes insipidus. *J Cell Biol*. 2003;163(5):1099–1109.
214. Yui N, Lu HA, Chen Y, et al. Basolateral targeting and microtubule-dependent transcytosis of the aquaporin-2 water channel. *Am J Physiol Cell Physiol*. 2013;304(1):C38–C48.
215. Ma TH, Yang BX, Gillespie A, et al. Severely impaired urinary concentrating ability in transgenic mice lacking aquaporin-1 water channels. *J Biol Chem*. 1998;273(8):4296–4299.
216. Schnermann J, Chou CL, Ma TH, et al. Defective proximal tubular fluid reabsorption in transgenic aquaporin-1 null mice. *Proc Natl Acad Sci U S A*. 1998;95(16):9660–9664.
217. Chou CL, Knepper MA, Van Hoek AN, et al. Reduced water permeability and altered ultrastructure in thin descending limb of Henle in aquaporin-1 null mice. *J Clin Invest*. 1999;103(4):491–496.
218. Yang B, Gillespie A, Carlson EJ, et al. Neonatal mortality in an aquaporin-2 knock-in mouse model of recessive nephrogenic diabetes insipidus. *J Biol Chem*. 2001;276:2775–2779.
219. Lloyd DJ, Hall FW, Tarantino LM, et al. Diabetes insipidus in mice with a mutation in aquaporin-2. *PLoS Genet*. 2005;1:e20.
220. Rojek A, Fuechtbauer EM, Kwon TH, et al. Severe urinary concentrating defect in renal collecting duct-selective AQP2 conditional-knockout mice. *Proc Natl Acad Sci U S A*. 2006;103(15):6037–6042.
221. Yang BX, Zhao D, Qian LM, et al. Mouse model of inducible nephrogenic diabetes insipidus produced by floxed aquaporin-2 gene deletion. *Am J Physiol Renal Physiol*. 2006;291(2):F465–F472.
222. McDill BW, Li SZ, Kovach PA, et al. Congenital progressive hydro-nephrosis (CPH) is caused by an s256l mutation in aquaporin-2 that affects its phosphorylation and apical membrane accumulation. *Proc Natl Acad Sci U S A*. 2006;103:6952–6957.
223. Shi PP, Cao XR, Qu J, et al. Nephrogenic diabetes insipidus in mice caused by deleting COOH-terminal tail of aquaporin-2. *Am J Physiol Renal Physiol*. 2007;292(F1334):F1344.
224. Kuwahara M, Iwai K, Ooeda T, et al. Three families with autosomal dominant nephrogenic diabetes insipidus caused by aquaporin-2 mutations in the C-terminus. *Am J Hum Genet*. 2001;69(4):738–748.
225. Sohara E, Rai T, Yang SS, et al. Pathogenesis and treatment of autosomal-dominant nephrogenic diabetes insipidus caused by an aquaporin 2 mutation. *Proc Natl Acad Sci U S A*. 2006;103:14217–14222.
226. Yang B, Zhao D, Verkman AS. Hsp90 inhibitor partially corrects nephrogenic diabetes insipidus in a conditional knock-in mouse model of aquaporin-2 mutation. *FASEB J*. 2009;23(2):503–512.
227. Kortenoeven ML, Pedersen NB, Miller RL, et al. Genetic ablation of aquaporin-2 in the mouse connecting tubules results in defective renal water handling. *J Physiol*. 2013;591(Pt 8):2205–2219.
228. Ma TH, Song YL, Yang BX, et al. Nephrogenic diabetes insipidus in mice lacking aquaporin-3 water channels. *Proc Natl Acad Sci U S A*. 2000;97(8):4386–4391.
229. Ma TH, Yang BX, Gillespie A, et al. Generation and phenotype of a transgenic knockout mouse lacking the mercurial-insensitive water channel aquaporin-4. *J Clin Invest*. 1997;100(5):957–962.
230. Chou C-L, Ma TH, Yang BX, et al. Fourfold reduction of water permeability in inner medullary collecting duct of aquaporin-4 knockout mice. *Am J Physiol Cell Physiol*. 1998;274(2):C549–C554.
231. Zhang R, Logee KA, Verkman AS. Expression of mRNA coding for kidney and red cell water channels in *Xenopus* oocytes. *J Biol Chem*. 1990;265:15375–15378.
232. Kamsteeg EJ, Wormhoudt TA, Rijss JP, et al. An impaired routing of wild-type aquaporin-2 after tetramerization with an aquaporin-2 mutant explains dominant nephrogenic diabetes insipidus. *EMBO J*. 1999;18(9):2394–2400.
233. Mulders SM, Bichet DG, Rijss JP, et al. An aquaporin-2 water channel mutant which causes autosomal dominant nephrogenic diabetes insipidus is retained in the Golgi complex. *J Clin Invest*. 1998;102(1):57–66.
234. Canfield MC, Tamarappoo BK, Moses AM, et al. Identification and characterization of aquaporin-2 water channel mutations causing nephrogenic diabetes insipidus with partial vasopressin response. *Hum Mol Genet*. 1997;6(11):1865–1871.
235. Verbavatz J-M, Brown D, Sabolic I, et al. Tetrameric assembly of CHIP28 water channels in liposomes and cell membranes: a freeze-fracture study. *J Cell Biol*. 1993;123:605–618.
236. Zeidel ML, Nielsen S, Smith BL, et al. Ultrastructure, pharmacologic inhibition, and transport selectivity of aquaporin channel-forming integral protein in proteoliposomes. *Biochemistry*. 1994;33(6):1606–1615.
237. Tamarappoo BK, Yang BX, Verkman AS. Misfolding of mutant aquaporin-2 water channels in nephrogenic diabetes insipidus. *J Biol Chem*. 1999;274(49):34825–34831.
238. Maric K, Oksche A, Rosenthal W. Aquaporin-2 expression in primary cultured rat inner medullary collecting duct cells. *Am J Physiol Renal Physiol*. 1998;275(5):F796–F801.
239. Robert-Nicoud M, Flahaut M, Elalouf JM, et al. Transcriptome of a mouse kidney cortical collecting duct cell line: effects of aldosterone and vasopressin. *Proc Natl Acad Sci U S A*. 2001;98(5):2712–2716.
240. Hasler U, Leroy V, Martin PY, et al. Aquaporin-2 abundance in the renal collecting duct: new insights from cultured cell models. *Am J Physiol Renal Physiol*. 2009;297:F10–F18.
241. Li Y, Shaw S, Kamsteeg EJ, et al. Development of lithium-induced nephrogenic diabetes insipidus is dissociated from adenylyl cyclase activity. *J Am Soc Nephrol*. 2006;17(4):1063–1072.
242. Kortenoeven ML, Trimpert C, van den Brand M, et al. In mpkCCD cells, long-term regulation of aquaporin-2 by vasopressin occurs independent of protein kinase A and CREB but may involve Epac. *Am J Physiol Renal Physiol*. 2012;302(11):F1395–F1401.
243. Boone M, Kortenoeven ML, Robben JH, et al. Counteracting vasopressin-mediated water reabsorption by ATP, dopamine, and phorbol esters: mechanisms of action. *Am J Physiol Renal Physiol*. 2011;300(3):F761–F771.
244. Bustamante M, Hasler U, Kotova O, et al. Insulin potentiates AVP-induced AQP2 expression in cultured renal collecting duct principal cells. *Am J Physiol Renal Physiol*. 2005;288(2):F334–F344.
245. Hasler U, Nunes P, Bouley R, et al. Acute hypertonicity alters aquaporin-2 trafficking and induces a MAPK-dependent accumulation at the plasma membrane of renal epithelial cells. *J Biol Chem*. 2008;283(39):26643–26661.
246. Deen PMT, Rijss JPL, Mulders SM, et al. Aquaporin-2 transfection of Madin-Darby canine kidney cells reconstitutes vasopressin-regulated transcellular osmotic water transport. *J Am Soc Nephrol*. 1997;8(10):1493–1501.
247. Bouley R, Breton S, Sun TX, et al. Nitric oxide and atrial natriuretic factor stimulate cGMP-dependent membrane insertion of aquaporin 2 in renal epithelial cells. *J Clin Invest*. 2000;106(9):1115–1126.
248. Bouley R, Soler NP, Cohen O, et al. Stimulation of AQP2 membrane insertion in renal epithelial cells in vitro and in vivo by the cGMP

- phosphodiesterase inhibitor sildenafil citrate (Viagra). *Am J Physiol Renal Physiol*. 2005;288(6):F1103–F1112.
249. Breton S, Brown D. Cold-induced microtubule disruption and relocalization of membrane proteins in kidney epithelial cells. *J Am Soc Nephrol*. 1998;9(2):155–166.
 250. Olesen ET, Rutzler MR, Moeller HB, et al. Vasopressin-independent targeting of aquaporin-2 by selective E-prostanoid receptor agonists alleviates nephrogenic diabetes insipidus. *Proc Natl Acad Sci U S A*. 2011;108(31):12949–12954.
 251. Sun TX, Van Hoek A, Huang Y, et al. Aquaporin-2 localization in clathrin-coated pits: inhibition of endocytosis by dominant-negative dynamin. *Am J Physiol Renal Physiol*. 2002;282(6):F998–F1011.
 252. Brown D, Breton S, Ausiello DA, et al. Sensing, signaling and sorting events in kidney epithelial cell physiology. *Traffic*. 2009;10(3):275–284.
 253. Lu H, Sun TX, Bouley R, et al. Inhibition of endocytosis causes phosphorylation (S256)-independent plasma membrane accumulation of AQP2. *Am J Physiol Renal Physiol*. 2004;286(2):F233–F243.
 254. Rodal SK, Skretting G, Garred O, et al. Extraction of cholesterol with methyl-beta-cyclodextrin perturbs formation of clathrin-coated endocytic vesicles. *Mol Biol Cell*. 1999;10(4):961–974.
 255. Subtil A, Gaidarov I, Kobylarz K, et al. Acute cholesterol depletion inhibits clathrin-coated pit budding. *Proc Natl Acad Sci U S A*. 1999;96(12):6775–6780.
 256. Russo LM, McKee M, Brown D. Methyl-beta-cyclodextrin induces vasopressin-independent apical accumulation of aquaporin-2 in the isolated, perfused rat kidney. *Am J Physiol Renal Physiol*. 2006;291(1):F246–F253.
 257. Aoki T, Suzuki T, Hagiwara H, et al. Close association of aquaporin-2 internalization with caveolin-1. *Acta Histochem Cytochem*. 2012;45(2):139–146.
 258. Paunescu TG, Lu HA, Russo LM, et al. Vasopressin induces apical expression of caveolin in rat kidney collecting duct principal cells. *Am J Physiol Renal Physiol*. 2013;305(12):F1783–F1795.
 259. Zhuang Z, Marshansky V, Breton S, et al. Is caveolin involved in normal proximal tubule function? Presence in model PT systems but absence in situ. *Am J Physiol Renal Physiol*. 2011;300(1):F199–F206.
 260. Tajika Y, Matsuzaki T, Suzuki T, et al. Aquaporin-2 is retrieved to the apical storage compartment via early endosomes and phosphatidylinositol 3-kinase-dependent pathway. *Endocrinology*. 2004;145:4375–4383.
 261. Procino G, Caces DB, Valenti G, et al. Adipocytes support cAMP-dependent translocation of aquaporin-2 from intracellular sites distinct from the insulin-responsive GLUT4 storage compartment. *Am J Physiol Renal Physiol*. 2006;290(5):F985–F994.
 262. Nedvetsky PI, Stefan E, Frische S, et al. A role of myosin Vb and Rab11-FIP2 in the aquaporin-2 shuttle. *Traffic*. 2007;8(2):110–123.
 263. Tajika Y, Matsuzaki T, Suzuki T, et al. Differential regulation of AQP2 trafficking in endosomes by microtubules and actin filaments. *Histochem Cell Biol*. 2005;124(1):1–12.
 264. Lee MS, Choi HJ, Park EJ, et al. Depletion of vacuolar protein sorting-associated protein 35 is associated with increased lysosomal degradation of aquaporin-2. *Am J Physiol Renal Physiol*. 2016;311(6):F1294–F1307.
 265. Rothman JE, Sollner TH. Throttles and dampers: controlling the engine of membrane fusion. *Science*. 1997;276(5316):1212–1213.
 266. Rothman JE, Warren G. Implications of the SNARE hypothesis for intracellular membrane topology and dynamics. *Curr Biol*. 1994;4(3):220–233.
 267. Scheller RH. Membrane trafficking in the presynaptic nerve terminal. *Neuron*. 1995;14(5):893–897.
 268. Weber T, Zemelman BV, McNew JA, et al. SNAREpins: minimal machinery for membrane fusion. *Cell*. 1998;92(6):759–772.
 269. Allan VJ, Schroer TA. Membrane motors. *Curr Opin Cell Biol*. 1999;11(4):476–482.
 270. Schroer TA. Microtubules don and doff their caps: dynamic attachments at plus and minus ends. *Curr Opin Cell Biol*. 2001;13(1):92–96.
 271. Vale RD, Milligan RA. The way things move: looking under the hood of molecular motor proteins. *Science*. 2000;288(5463):88–95.
 272. Mooren OL, Galletta BJ, Cooper JA. Roles for actin assembly in endocytosis. *Annu Rev Biochem*. 2012;81:661–686.
 273. Zech T, Calaminus SD, Machesky LM. Actin on trafficking: could actin guide directed receptor transport? *Cell Adh Migr*. 2012;6(6):476–481.
 274. Brown D, Cunningham C, Hartwig J. Association of AQP2 with actin in transfected LLC-PK1 cells and rat papilla. *J Am Soc Nephrol*. 1996;7:1265.
 275. Noda Y, Horikawa S, Kanda E, et al. Reciprocal interaction with G-actin and tropomyosin is essential for aquaporin-2 trafficking. *J Cell Biol*. 2008;182(3):587–601.
 276. Noda Y, Horikawa S, Katayama Y, et al. Water channel aquaporin-2 directly binds to actin. *Biochem Biophys Res Commun*. 2004;322(3):740–745.
 277. Barile M, Pisitkun T, Yu MJ, et al. Large scale protein identification in intracellular aquaporin-2 vesicles from renal inner medullary collecting duct. *Mol Cell Proteomics*. 2005;4(8):1095–1106.
 278. Ding GH, Franki N, Condeelis J, et al. Vasopressin depolymerizes F-actin in toad bladder epithelial cells. *Am J Physiol*. 1991;260(1 Pt 1):C9–C16.
 279. Hays RM, Condeelis J, Gao Y, et al. The effect of vasopressin on the cytoskeleton of the epithelial cell. *Pediatr Nephrol*. 1993;7(5):672–679.
 280. Tamma G, Klussmann E, Maric K, et al. Rho inhibits cAMP-induced translocation of aquaporin-2 into the apical membrane of renal cells. *Am J Physiol Renal Physiol*. 2001;281(6):F1092–F1101.
 281. Loo CS, Chen CW, Wang PJ, et al. Quantitative apical membrane proteomics reveals vasopressin-induced actin dynamics in collecting duct cells. *Proc Natl Acad Sci U S A*. 2013;110(42):17119–17124.
 282. Jang KJ, Cho HS, Kang DH, et al. Fluid-shear-stress-induced translocation of aquaporin-2 and reorganization of actin cytoskeleton in renal tubular epithelial cells. *Integr Biol (Camb)*. 2011;3(2):134–141.
 283. Yui N, Lu HJ, Bouley R, et al. AQP2 is necessary for vasopressin- and forskolin-mediated filamentous actin depolymerization in renal epithelial cells. *Biology Open*. 2012;1(2):101–108.
 284. Ridley AJ. Rho proteins: linking signaling with membrane trafficking. *Traffic*. 2001;2(5):303–310.
 285. Li W, Zhang Y, Bouley R, et al. Simvastatin enhances aquaporin-2 surface expression and urinary concentration in vasopressin-deficient brattleboro rats through modulation of rho GTPase. *Am J Physiol Renal Physiol*. 2011;301(2):F309–F318.
 286. Procino G, Barbieri C, Carmosino M, et al. Lovastatin-induced cholesterol depletion affects both apical sorting and endocytosis of aquaporin-2 in renal cells. *Am J Physiol Renal Physiol*. 2010;298(2):F266–F278.
 287. Whiting JL, Ogier L, Forbush KA, et al. AKAP220 manages apical actin networks that coordinate aquaporin-2 location and renal water reabsorption. *Proc Natl Acad Sci U S A*. 2016;113(30):E4328–E4337.
 288. Noda Y, Horikawa S, Furukawa T, et al. Aquaporin-2 trafficking is regulated by PDZ-domain containing protein SPA-1. *FEBS Lett*. 2004;568:139–145.
 289. Marples D, Smith J, Nielsen S. Myosin-I is associated with AQP-2 water channel bearing vesicles in rat kidney and may be involved in the antidiuretic response to vasopressin. *J Am Soc Nephrol*. 1997;8:62.
 290. Chou CL, Christensen BM, Frische S, et al. Non-muscle myosin II and myosin light chain kinase are downstream targets for vasopressin signaling in the renal collecting duct. *J Biol Chem*. 2004;279(47):49026–49035.
 291. Noda Y, Saburo HC, Katayama Y, et al. Identification of a multiprotein “motor” complex binding to water channel aquaporin-2. *Biochem Biophys Res Commun*. 2005;330(4):1041–1047.
 292. Liebenhoff U, Rosenthal W. Identification of Rab3-, Rab5a- and synaptobrevin II-like proteins in a preparation of rat kidney vesicles containing the vasopressin-regulated water channel. *FEBS Lett*. 1995;365:209–213.
 293. Tamma G, Klussmann E, Oehlke J, et al. Actin remodeling requires ERM function to facilitate AQP2 apical targeting. *J Cell Sci*. 2005;118(16):3623–3630.
 294. Li W, Jin WW, Tsuji K, et al. Ezrin directly interacts with AQP2 and promotes its endocytosis. *J Cell Sci*. 2017;130(17):2914–2925.
 295. Mamuya FA, Cano-Penalver JL, Li W, et al. ILK and cytoskeletal architecture: an important determinant of AQP2 recycling and subsequent entry into the exocytotic pathway. *Am J Physiol Renal Physiol*. 2016;311(6):F1346–F1357.
 296. Cano-Penalver JL, Griera M, Serrano I, et al. Integrin-linked kinase regulates tubular aquaporin-2 content and intracellular location: a link between the extracellular matrix and water reabsorption. *FASEB J*. 2014;28(8):3645–3659.
 297. Marples D, Schroer TA, Ahrens N, et al. Dynein and dynactin colocalize with AQP2 water channels in intracellular vesicles from kidney collecting duct. *Am J Physiol Renal Physiol*. 1998;274(2):F384–F394.
 298. Dousa TP, Barnes LD. Effects of colchicine and vinblastine on the cellular action of vasopressin in mammalian kidney. A possible role of microtubules. *J Clin Invest*. 1974;54(2):252–262.

299. Phillips ME, Taylor A. Effect of nocodazole on the water permeability response to vasopressin in rabbit collecting tubules perfused in vitro. *J Physiol*. 1989;411:529–544.
300. Taylor A, Mamelak M, Golbetz H, et al. Evidence for involvement of microtubules in the action of vasopressin in toad urinary bladder. I. Functional studies on the effects of antimicrotubule agents on the response to vasopressin. *J Membr Biol*. 1978;40(3):213–235.
301. Bohn AB, Norregaard R, Stodkilde L, et al. Treatment with the vascular disrupting agent combretastatin is associated with impaired AQP2 trafficking and increased urine output. *Am J Physiol Renal Physiol*. 2012;303(2):R186–R198.
302. Vossenkamper A, Nedvetsky PI, Wiesner B, et al. Microtubules are needed for the perinuclear positioning of aquaporin-2 after its endocytic retrieval in renal principal cells. *Am J Physiol Cell Physiol*. 2007;293(3):C1129–C1138.
303. Chen S, Webber MJ, Vilardaga JP, et al. Visualizing microtubule-dependent vasopressin type 2 receptor trafficking using a new high-affinity fluorescent vasopressin ligand. *Endocrinology*. 2011;152(10):3893–3904.
304. Jo I, Harris HW, Amendt-Raduege AM, et al. Rat kidney papilla contains abundant synaptobrevin protein that participates in the fusion of antidiuretic hormone-regulated water channel-containing endosomes in vitro. *Proc Natl Acad Sci U S A*. 1995;92:1876–1880.
305. Nielsen S, Marples D, Birn H, et al. Expression of VAMP2-like protein in kidney collecting duct intracellular vesicles. Colocalization with aquaporin-2 water channels. *J Clin Invest*. 1995;96(4):1834–1844.
306. Gouraud S, Laera A, Calamita G, et al. Functional involvement of VAMP/synaptobrevin-2 in cAMP-stimulated aquaporin 2 translocation in renal collecting duct cells. *J Cell Sci*. 2002;115(18):3667–3674.
307. Inoue T, Nielsen S, Mandon B, et al. SNAP-23 in rat kidney: colocalization with aquaporin-2 in collecting duct vesicles. *Am J Physiol Renal Physiol*. 1998;275(5):F752–F760.
308. Shukla A, Hager H, Corydon TJ, et al. SNAP-25-associated Hrs-2 protein colocalizes with AQP2 in rat kidney collecting duct principal cells. *Am J Physiol Renal Physiol*. 2001;281(3):F546–F556.
309. Procino G, Barbieri C, Tamma G, et al. AQP2 exocytosis in the renal collecting duct—involvevement of SNARE isoforms and the regulatory role of munc18b. *J Cell Sci*. 2008;121(Pt 12):2097–2106.
310. Mandon B, Chou CL, Nielsen S, et al. Syntaxin-4 is localized to the apical plasma membrane of rat renal collecting duct cells: possible role in aquaporin-2 trafficking. *J Clin Invest*. 1996;98(4):906–913.
311. Wang CC, Ng CP, Shi H, et al. A role for VAMP8/endobrevin in surface deployment of the water channel aquaporin 2. *Mol Cell Biol*. 2010;30(1):333–343.
312. Mistry AC, Mallick R, Klein JD, et al. Syntaxin specificity of aquaporins in the inner medullary collecting duct. *Am J Physiol Renal Physiol*. 2009;297:F292–F300.
313. Yasuhara A, Wada J, Malakauskas SM, et al. Collectrin is involved in the development of salt-sensitive hypertension by facilitating the membrane trafficking of apical membrane proteins via interaction with soluble N-ethylmaleimide-sensitive factor attachment protein receptor complex. *Circulation*. 2008;118(21):2146–2155.
314. Kortenoeven ML, Sinke AP, Hadrup N, et al. Demeclocycline attenuates hyponatremia by reducing aquaporin-2 expression in the renal inner medulla. *Am J Physiol Renal Physiol*. 2013;305(12):F1705–F1718.
315. Klussmann E, Maric K, Wiesner B, et al. Protein kinase A anchoring proteins are required for vasopressin-mediated translocation of aquaporin-2 into cell membranes of renal principal cells. *J Biol Chem*. 1999;274(8):4934–4938.
316. Henn V, Edemir B, Stefan E, et al. Identification of a novel A-kinase anchoring protein 18 isoform and evidence for its role in the vasopressin-induced aquaporin-2 shuttle in renal principal cells. *J Biol Chem*. 2004;279(25):26654–26665.
317. Horner A, Goetz F, Tampe R, et al. Mechanism for targeting the A-kinase anchoring protein AKAP18δ to the membrane. *J Biol Chem*. 2012;287(51):42495–42501.
318. Valentí G, Procino G, Carosino M, et al. The phosphatase inhibitor okadaic acid induces AQP2 translocation independently from AQP2 phosphorylation in renal collecting duct cells. *J Cell Sci*. 2000;113(11):1985–1992.
319. Ren H, Yang B, Ruiz JA, et al. Phosphatase inhibition increases AQP2 accumulation in the rat IMCD apical plasma membrane. *Am J Physiol Renal Physiol*. 2016;311(6):F1189–F1197.
320. Olesen ET, Moeller HB, Assentoft M, et al. The vasopressin type 2 receptor and prostaglandin receptors EP2 and EP4 can increase aquaporin-2 plasma membrane targeting through a cAMP-independent pathway. *Am J Physiol Renal Physiol*. 2016;311(5):F935–F944.
321. Ando F, Sahara E, Morimoto T, et al. Wnt5a induces renal AQP2 expression by activating calcineurin signalling pathway. *Nat Commun*. 2016;7:13636.
322. Cheung PW, Nomura N, Nair AV, et al. EGF receptor inhibition by erlotinib increases aquaporin 2-mediated renal water reabsorption. *J Am Soc Nephrol*. 2016;27(10):3105–3116.
323. Bou Matar RN, Klein JD, Sands JM. Erlotinib preserves renal function and prevents salt retention in doxorubicin treated nephrotic rats. *PLoS ONE*. 2013;8(1):e54738.
324. Hoffert JD, Fenton RA, Moeller HB, et al. Vasopressin-stimulated increase in phosphorylation at ser269 potentiates plasma membrane retention of aquaporin-2. *J Biol Chem*. 2008;283(36):24617–24627.
325. Hoffert JD, Pisitkun T, Wang G, et al. Quantitative phosphoproteomics of vasopressin-sensitive renal cells: regulation of aquaporin-2 phosphorylation at two sites. *Proc Natl Acad Sci U S A*. 2006;103(18):7159–7164.
326. Hoffert JD, Pisitkun T, Saeed F, et al. Dynamics of the G protein-coupled vasopressin V2 receptor signaling network revealed by quantitative phosphoproteomics. *Mol Cell Proteomics*. 2012;11(2). doi:10.1074/mcp.M111.014613.
327. Kuwahara M, Fushimi K, Terada Y, et al. cAMP-dependent phosphorylation stimulates water permeability of aquaporin-collecting duct water channel protein expressed in *Xenopus* oocytes. *J Biol Chem*. 1995;270:10384–10387.
328. Moeller HB, MacAulay N, Knepper MA, et al. Role of multiple phosphorylation sites in the COOH-terminal tail of aquaporin-2 for water transport: evidence against channel gating. *Am J Physiol Renal Physiol*. 2009;296(3):F649–F657.
329. Lande MB, Jo I, Zeidel ML, et al. Phosphorylation of aquaporin-2 does not alter the membrane water permeability of rat papillary water channel-containing vesicles. *J Biol Chem*. 1996;271(10):5552–5557.
330. Arthur J, Huang J, Nomura N, et al. Characterization of the putative phosphorylation sites of the AQP2 C terminus and their role in AQP2 trafficking in LLC-PK1 cells. *Am J Physiol Renal Physiol*. 2015;309(8):F673–F679.
331. Fushimi K, Sasaki S, Marumo F. Phosphorylation of serine 256 is required for cAMP-dependent regulatory exocytosis of the aquaporin-2 water channel. *J Biol Chem*. 1997;272(23):14800–14804.
332. Katsura T, Gustafson CE, Ausiello DA, et al. Protein kinase A phosphorylation is involved in regulated exocytosis of aquaporin-2 in transfected LLC-PK₁ cells. *Am J Physiol Renal Physiol*. 1997;272(6):F816–F822.
333. Kamsteeg EJ, Heijnen I, Van Os CH, et al. The subcellular localization of an aquaporin-2 tetramer depends on the stoichiometry of phosphorylated and nonphosphorylated monomers. *J Cell Biol*. 2000;151(4):919–929.
334. Arnsperg EC, Login FH, Koffman JS, et al. AQP2 plasma membrane diffusion is altered by the degree of AQP2-S256 phosphorylation. *Int J Mol Sci*. 2016;17(11).
335. de Mattia F, Savelkoul PJM, Kamsteeg EJ, et al. Lack of arginine vasopressin-induced phosphorylation of aquaporin-2 mutant AQP2-R254L explains dominant nephrogenic diabetes insipidus. *J Am Soc Nephrol*. 2005;16(10):2872–2880.
336. Fenton RA, Moeller HB. Recent discoveries in vasopressin-regulated aquaporin-2 trafficking. *Prog Brain Res*. 2008;170:571–579.
337. Hoffert JD, Nielsen J, Yu MJ, et al. Dynamics of aquaporin-2 serine-261 phosphorylation in response to short-term vasopressin treatment in collecting duct. *Am J Physiol Renal Physiol*. 2007;292(2):F691–F700.
338. Al-Bataineh MM, Li H, Ohmi K, et al. Activation of the metabolic sensor AMP-activated protein kinase inhibits aquaporin-2 function in kidney principal cells. *Am J Physiol Renal Physiol*. 2016;311(5):F890–F900.
339. Lu HJ, Matsuzaki T, Bouley R, et al. The phosphorylation state of serine 256 is dominant over that of serine 261 in the regulation of AQP2 trafficking in renal epithelial cells. *Am J Physiol Renal Physiol*. 2008;295(1):F290–F294.
340. Moeller HB, Praetorius J, Rutzler MR, et al. Phosphorylation of aquaporin-2 regulates its endocytosis and protein-protein interactions. *Proc Natl Acad Sci U S A*. 2010;107(1):424–429.
341. Klein JD, Wang Y, Blount MA, et al. Metformin, an AMPK activator, stimulates the phosphorylation of aquaporin 2 and urea transporter AI in inner medullary collecting ducts. *Am J Physiol Renal Physiol*. 2016;310(10):F1008–F1012.

342. Choi HJ, Jung HJ, Kwon TH. Extracellular pH affects phosphorylation and intracellular trafficking of AQP2 in inner medullary collecting duct cells. *Am J Physiol Renal Physiol*. 2015;308(7):F737–F748.
343. Rice WL, Zhang Y, Chen Y, et al. Differential, phosphorylation dependent trafficking of AQP2 in LLC-PK1 cells. *PLoS ONE*. 2012;7(2):e32843.
344. Nunes P, Hasler U, McKee M, et al. A fluorimetry-based ssYFP secretion assay to monitor vasopressin-induced exocytosis in LLC-PK1 cells expressing aquaporin-2. *Am J Physiol Cell Physiol*. 2008;295(6):C1476–C1487.
345. Bouley R, Hawthorn G, Russot LM, et al. Aquaporin 2 (AQP2) and vasopressin type 2 receptor (V2R) endocytosis in kidney epithelial cells: AQP2 is located in 'endocytosis-resistant' membrane domains after vasopressin treatment. *Biol Cell*. 2006;98(4):215–232.
346. Procino G, Carosino M, Marin O, et al. Ser-256 phosphorylation dynamics of aquaporin 2 during maturation from the endoplasmic reticulum to the vesicular compartment in renal cells. *FASEB J*. 2003;17(13):1886–1888.
347. Zelenina M, Christensen BM, Palmer J, et al. Prostaglandin E(2) interaction with AVP: effects on AQP2 phosphorylation and distribution. *Am J Physiol Renal Physiol*. 2000;278(3):F388–F394.
348. Nejsum LN, Zelenina M, Aperia A, et al. Bidirectional regulation of AQP2 trafficking and recycling: involvement of AQP2-S256 phosphorylation. *Am J Physiol Renal Physiol*. 2005;288(5):F930–F938.
349. Olesen ET, Fenton RA. Is there a role for PGE2 in urinary concentration? *J Am Soc Nephrol*. 2013;24(2):169–178.
350. Gao M, Cao R, Du S, et al. Disruption of prostaglandin E2 receptor EP4 impairs urinary concentration via decreasing aquaporin 2 in renal collecting ducts. *Proc Natl Acad Sci U S A*. 2015;112(27):8397–8402.
351. Ren H, Yang B, Molina PA, et al. NSAIDs alter phosphorylated forms of AQP2 in the inner medullary tip. *PLoS ONE*. 2015;10(10):e0141714.
352. Lu HA, Sun TX, Matsuzaki T, et al. Heat shock protein 70 interacts with aquaporin-2 and regulates its trafficking. *J Biol Chem*. 2007;282(39):28721–28732.
353. Kamsteeg EJ, Duffield AS, Konings IB, et al. MAL decreases the internalization of the aquaporin-2 water channel. *Proc Natl Acad Sci U S A*. 2007;104(42):16696–16701.
354. Moeller HB, Slengerik-Hansen J, Aroankins T, et al. Regulation of the water channel Aquaporin-2 via 14-3-3 σ and - ζ . *J Biol Chem*. 2016;291(5):2469–2484.
355. Gamble JL, McKhann CF, Butler AM, et al. An economy of water in renal function referable to urea. *Am J Physiol*. 1934;109:139–154.
356. Fenton RA, Chou CL, Sowersby H, et al. Gamble's "economy of water" revisited: studies in urea transporter knockout mice. *Am J Physiol Renal Physiol*. 2006;291(1):F148–F154.
357. Sands JM, Layton HE. The urine concentrating mechanism and urea transporters. In: Alpern RJ, Caplan MJ, Moe OW, eds. *Seldin and Giebisch's the Kidney: Physiology and Pathophysiology*. 1. 5th ed. San Diego: Academic Press; 2013:1463–1510.
358. Fenton RA, Chou C-L, Stewart GS, et al. Urinary concentrating defect in mice with selective deletion of phloretin-sensitive urea transporters in the renal collecting duct. *Proc Natl Acad Sci U S A*. 2004;101(19):7469–7474.
359. Uchida S, Sohara E, Rai T, et al. Impaired urea accumulation in the inner medulla of mice lacking the urea transporter UT-a2. *Mol Cell Biol*. 2005;25(16):7357–7363.
360. Yang B, Bankir L, Gillespie A, et al. Urea-selective concentrating defect in transgenic mice lacking urea transporter UT-B. *J Biol Chem*. 2002;277:10633–10637.
361. Yang B, Verkman AS. Analysis of double knockout mice lacking aquaporin-1 and urea transporter UT-B. *J Biol Chem*. 2002;277(39):36782–36786.
362. Klein JD, Sands JM, Qian L, et al. Upregulation of urea transporter UT-a2 and water channels AQP2 and AQP3 in mice lacking urea transporter UT-B. *J Am Soc Nephrol*. 2004;15(5):1161–1167.
363. Lei T, Zhou L, Layton AT, et al. Role of thin descending limb urea transport in renal urea handling and the urine concentrating mechanism. *Am J Physiol Renal Physiol*. 2011;301(6):F1251–F1259.
364. Stewart GS, Graham C, Cattell S, et al. UT-B is expressed in bovine rumen: potential role in ruminal urea transport. *Am J Physiol Regul Integr Comp Physiol*. 2005;289(2):R605–R612.
365. Bagnasco SM, Peng T, Nakayama Y, et al. Differential expression of individual UT-a urea transporter isoforms in rat kidney. *J Am Soc Nephrol*. 2000;11(11):1980–1986.
366. Nakayama Y, Naruse M, Karakashian A, et al. Cloning of the rat *slc14a2* gene and genomic organization of the UT-a urea transporter. *Biochim Biophys Acta*. 2001;1518:19–26.
367. Bagnasco SM, Peng T, Janech MG, et al. Cloning and characterization of the human urea transporter UT-a1 and mapping of the human *Slc14a2* gene. *Am J Physiol Renal Physiol*. 2001;281:F400–F406.
368. Fenton RA, Cottingham CA, Stewart GS, et al. Structure and characterization of the mouse UT-a gene (*Slc14a2*). *Am J Physiol Renal Physiol*. 2002;282(4):F630–F638.
369. Olives B, Neau P, Bailly P, et al. Cloning and functional expression of a urea transporter from human bone marrow cells. *J Biol Chem*. 1994;269(50):31649–31652.
370. Nakayama Y, Peng T, Sands JM, et al. The TonE/tonEBP pathway mediates tonicity-responsive regulation of UT-A urea transporter expression. *J Biol Chem*. 2000;275(49):38275–38280.
371. Nielsen S, Terris J, Smith CP, et al. Cellular and subcellular localization of the vasopressin-regulated urea transporter in rat kidney. *Proc Natl Acad Sci U S A*. 1996;93:5495–5500.
372. Kim Y-H, Kim D-U, Han K-H, et al. Expression of urea transporters in the developing rat kidney. *Am J Physiol Renal Physiol*. 2002;282(3):F530–F540.
373. Terris JM, Knepper MA, Wade JB. UT-a3: localization and characterization of an additional urea transporter isoform in the IMCD. *Am J Physiol Renal Physiol*. 2001;280(2):F325–F332.
374. Stewart GS, Fenton RA, Wang W, et al. The basolateral expression of mUT-a3 in the mouse kidney. *Am J Physiol Renal Physiol*. 2004;286(5):F979–F987.
375. Blount MA, Klein JD, Martin CF, et al. Forskolin stimulates phosphorylation and membrane accumulation of UT-a3. *Am J Physiol Renal Physiol*. 2007;293(4):F1308–F1313.
376. You G, Smith CP, Kanai Y, et al. Cloning and characterization of the vasopressin-regulated urea transporter. *Nature*. 1993;365:844–847.
377. Zhang C, Sands JM, Klein JD. Vasopressin rapidly increases phosphorylation of UT-a1 urea transporter in rat IMCDs through PKA. *Am J Physiol Renal Physiol*. 2002;282(1):F85–F90.
378. Blount MA, Mistry AC, Fröhlich O, et al. Phosphorylation of UT-a1 urea transporter at serines 486 and 499 is important for vasopressin-regulated activity and membrane accumulation. *Am J Physiol Renal Physiol*. 2008;295(1):F295–F299.
379. Klein JD, Blount MA, Fröhlich O, et al. Phosphorylation of UT-a1 on serine 486 correlates with membrane accumulation and urea transport activity in both rat IMCDs and cultured cells. *Am J Physiol Renal Physiol*. 2010;298(4):F935–F940.
380. Hoban CA, Black LN, Ordas RJ, et al. Vasopressin regulation of multisite phosphorylation of UT-a1 in the inner medullary collecting duct. *Am J Physiol Renal Physiol*. 2015;308:F49–F55.
381. Smith CP, Potter EA, Fenton RA, et al. Characterization of a human colonic cDNA encoding a structurally novel urea transporter, UT-a6. *Am J Physiol Cell Physiol*. 2004;287(4):C1087–C1093.
382. Wang Y, Klein JD, Blount MA, et al. Epac regulation of the UT-A1 urea transporter in rat IMCDs. *J Am Soc Nephrol*. 2009;20(3):2018–2024.
383. Ilori TO, Wang Y, Blount MA, et al. Acute calcineurin inhibition with tacrolimus increases phosphorylated UT-A1. *Am J Physiol Renal Physiol*. 2012;302(8):F998–F1004.
384. Feng X, Li Z, Du Y, et al. Downregulation of urea transporter UT-A1 activity by 14-3-3 protein. *Am J Physiol Renal Physiol*. 2015;309(1):F71–F78.
385. Sands JM, Schrader DC. An independent effect of osmolality on urea transport in rat terminal IMCDs. *J Clin Invest*. 1991;88:137–142.
386. Gillin AG, Sands JM. Characteristics of osmolarity-stimulated urea transport in rat IMCD. *Am J Physiol*. 1992;262:F1061–F1067.
387. Kudo LH, César KR, Ping WC, et al. Effect of peritubular hypertonicity on water and urea transport of inner medullary collecting duct. *Am J Physiol*. 1992;262:F338–F347.
388. Gillin AG, Star RA, Sands JM. Osmolarity-stimulated urea transport in rat terminal IMCD: role of intracellular calcium. *Am J Physiol*. 1993;265:F272–F277.
389. Kato A, Klein JD, Zhang C, et al. Angiotensin II increases vasopressin-stimulated facilitated urea permeability in rat terminal IMCDs. *Am J Physiol Renal Physiol*. 2000;279(5):F835–F840.
390. Wang Y, Liedtke CM, Klein JD, et al. Protein kinase C regulates urea permeability in the rat inner medullary collecting duct. *Am J Physiol Renal Physiol*. 2010;299(6):F1401–F1406.
391. Wang Y, Klein JD, Fröhlich O, et al. Role of protein kinase C- α in hypertonicity-stimulated urea permeability in mouse inner medullary collecting ducts. *Am J Physiol Renal Physiol*. 2013;304:F233–F238.

392. Star RA, Nonoguchi H, Balaban R, et al. Calcium and cyclic adenosine monophosphate as second messengers for vasopressin in the rat inner medullary collecting duct. *J Clin Invest*. 1988;81:1879–1888.
393. Blessing NW, Blount MA, Sands JM, et al. Urea transporters UT-A1 and UT-A3 accumulate in the plasma membrane in response to increased hypertonicity. *Am J Physiol Renal Physiol*. 2008;295(5):F1336–F1341.
394. Klein JD, Fröhlich O, Blount MA, et al. Vasopressin increases plasma membrane accumulation of urea transporter UT-A1 in rat inner medullary collecting ducts. *J Am Soc Nephrol*. 2006;17:2680–2686.
395. Klein JD, Martin CF, Kent KJ, et al. Protein kinase C alpha mediates hypertonicity-stimulated increase in urea transporter phosphorylation in the inner medullary collecting duct. *Am J Physiol Renal Physiol*. 2012;302:F1098–F1103.
396. Wang Y, Klein JD, Fröhlich O, et al. Role of protein kinase C-alpha in hypertonicity-stimulated urea permeability in mouse inner medullary collecting ducts. *Am J Physiol Renal Physiol*. 2013;304(2):F233–F238.
397. Blount MA, Cipriani P, Redd SK, et al. Activation of protein kinase alpha increases phosphorylation of the UT-A1 urea transporter at serine 494 in the inner medullary collecting duct. *Am J Physiol Cell Physiol*. 2015;doi:10.1152/ajpcell.00171.2014.
398. Yao LJ, Huang DY, Pfaff IL, et al. Evidence for a role of protein kinase C-alpha in urine concentration. *Am J Physiol Renal Physiol*. 2004;287(2):F299–F304.
399. Sim JH, Himmel NJ, Redd SK, et al. Absence of PKC-alpha attenuates lithium-induced nephrogenic diabetes insipidus. *PLoS ONE*. 2014;9(7):e101753.
400. Li X, Yang B, Chen M, et al. Activation of protein kinase c-alpha and src kinase increases urea transporter A1 alpha-2, 6 sialylation. *J Am Soc Nephrol*. 2015;26(4):926–934.
401. Qian X, Sands JM, Song X, et al. Modulation of kidney urea transporter UT-a3 activity by alpha2,6-sialylation. *Pfluegers Arch*. 2016;468:1161–1170.
402. Efe O, Klein JD, LaRocque LM, et al. Metformin improves urine concentration in rodents with nephrogenic diabetes insipidus. *JCI Insight*. 2016;1(11):e88409.
403. Sands JM, Klein JD. Physiological insights into novel therapies for nephrogenic diabetes insipidus. *Am J Physiol Renal Physiol*. 2016;doi:10.1152/ajprenal.00418.2016.
404. Fenton RA. Urea transporters and renal function: lessons from knockout mice. *Curr Opin Nephrol Hypertens*. 2008;17:513–518.
405. Fenton RA. Essential role of vasopressin-regulated urea transport processes in the mammalian kidney. *Pfluegers Arch*. 2009;458:169–177.
406. Fenton RA, Knepper MA. Urea and renal function in the 21st century: insights from knockout mice. *J Am Soc Nephrol*. 2007;18(3):679–688.
407. Fenton RA, Flynn A, Shodeinde A, et al. Renal phenotype of UT-A urea transporter knockout mice. *J Am Soc Nephrol*. 2005;16(6):1583–1592.
408. Kokko JP, Rector FC. Countercurrent multiplication system without active transport in inner medulla. *Kidney Int*. 1972;2:214–223.
409. Stephenson JL. Concentration of urine in a central core model of the renal counterflow system. *Kidney Int*. 1972;2:85–94.
410. Pannabecker TL, Dantzer WH, Layton HE, et al. Role of three-dimensional architecture in the urine concentrating mechanism of the rat renal inner medulla. *Am J Physiol Renal Physiol*. 2008;295(5):F1271–F1285.
411. Klein JD, Wang Y, Mistry A, et al. Transgenic restoration of urea transporter A1 confers maximal urinary concentration in the absence of urea transporter A3. *J Am Soc Nephrol*. 2016;27(5):1448–1455.
412. Klein JD, Blount MA, Sands JM. Urea transport in the kidney. *Compr Physiol*. 2011;1(2):699–729.
413. Sands JM, Gargus JJ, Fröhlich O, et al. Urinary concentrating ability in patients with Jk(a-b-) blood type who lack carrier-mediated urea transport. *J Am Soc Nephrol*. 1992;2:1689–1696.
414. Jiang T, Li Y, Layton AT, et al. Generation and phenotypic analysis of mice lacking all urea transporters. *Kidney Int*. 2017;91(2):338–351.
415. Sands JM, Knepper MA. Urea permeability of mammalian inner medullary collecting duct system and papillary surface epithelium. *J Clin Invest*. 1987;79:138–147.
416. Morgan T, Berliner RW. Permeability of the loop of Henle, vasa recta, and collecting duct to water, urea, and sodium. *Am J Physiol*. 1968;215:108–115.
417. Rocha AS, Kudo LH. Water, urea, sodium, chloride, and potassium transport in the in vitro perfused papillary collecting duct. *Kidney Int*. 1982;22:485–491.
418. Zimmerhackl BL, Robertson CR, Jamison RL. The medullary microcirculation. *Kidney Int*. 1987;31(2):641–647.
419. Knepper MA, Roch-Ramel F. Pathways of urea transport in the mammalian kidney. *Kidney Int*. 1987;31:629–633.
420. Lassiter WE, Gottschalk CW, Mylle M. Micropuncture study of net transtubular movement of water and urea in nondiuretic mammalian kidney. *Am J Physiol*. 1961;200:1139–1146.
421. de Rouffignac C, Morel F. Micropuncture study of water, electrolytes and urea movements along the loop of Henle in *Psammomys*. *J Clin Invest*. 1969;48:474–486.
422. de Rouffignac C, Bankir L, Roinel N. Renal function and concentrating ability in a desert rodent: the gundi (*Ctenodactylus vali*). *Pfluegers Arch*. 1981;390:138–144.
423. Kriz W. Structural organization of the renal medulla: comparative and functional aspects. *Am J Physiol Regul Integr Comp Physiol*. 1981;241:R3–R16.
424. Knepper MA. Urea transport in isolated thick ascending limbs and collecting ducts from rats. *Am J Physiol*. 1983;245:F634–F639.
425. Rocha AS, Kokko JP. Permeability of medullary nephron segments to urea and water: effect of vasopressin. *Kidney Int*. 1974;6:379–387.
426. Knepper MA. Urea transport in nephron segments from medullary rays of rabbits. *Am J Physiol*. 1983;244:F622–F627.
427. Kawamura S, Kokko JP. Urea secretion by the straight segment of the proximal tubule. *J Clin Invest*. 1976;58:604–612.
428. Gottschalk CW, Mylle M. Micropuncture study of the mammalian urinary concentrating mechanism: evidence for the countercurrent hypothesis. *Am J Physiol*. 1959;196:927–936.
429. Jamison RL, Lacy ER. Evidence for urinary dilution by the collecting tubule. *Am J Physiol*. 1972;223:898–902.
430. Giebisch G, Windhager EE. Renal tubular transfer of sodium chloride and potassium. *Am J Med*. 1964;36:643–669.
431. Burg MB, Green N. Function of the thick ascending limb of Henle's loop. *Am J Physiol*. 1973;224:659–668.
432. Rocha AS, Kokko JP. Sodium chloride and water transport in the medullary thick ascending limb of Henle. Evidence for active chloride transport. *J Clin Invest*. 1973;52:612–623.
433. Ullrich KJ. Function of the collecting ducts. *Circulation*. 1960;21:869–874.
434. Wirz H, Hargitay B, Kuhn W. Lokalisation des konzentrierungsprozesses in der niere durch direkte kryoskopie. *Helv Physiol Pharmacol*. 1951;Acta 9:196–207.
435. Jarausch KH, Ullrich KJ. Untersuchungen zum problem der harnkonzentrierung und harnverdünnung: Über die verteilung von elektrolyten (na, K, Ca, Mg, Cl, anorganischem phosphat), Harnstoff, Aminosäuren und exogenem kreatinin in rinde und mark der hundeniere bei verschiedenen diuresezuständen. *Pfluegers Arch*. 1956;262:537–550.
436. Hai MA, Thomas S. The time-course of changes in renal tissue composition during lysine vasopressin infusion in the rat. *Pfluegers Arch*. 1969;310:297–319.
437. Kuhn W, Ryffel K. Herstellung konzentrierter lösungen aus verdünnten durch blasse membranwirkung: ein modellversuch zur funktion der niere. *Hoppe Seylers Z Physiol Chem*. 1942;276:145–178.
438. Hargitay B, Kuhn W. Das multiplikationsprinzip als grundlage der harnkonzentrierung in der niere. *Z Elektrochem*. 1951;55:539–558.
439. Kuhn W, Ramel A. Aktiver salztransport als möglicher (und wahrscheinlicher) einzeleffekt bei der harnkonzentrierung in der niere. *Helv Chim Acta*. 1959;42:628–660.
440. Imai M, Hayashi M, Araki M. Functional heterogeneity of the descending limbs of Henle's loop. I. internephron heterogeneity in the hamster kidney. *Pfluegers Arch*. 1984;402:385–392.
441. Rasch R, Grann BL, Andreassen A. 3D reconstruction of the bend of short loops from the loop of Henle [abstract]. *J Am Soc Nephrol*. 2002;13:SA VP0017.
442. Kriz W, Koepsell H. The structural organization of the mouse kidney. *Z Anat Entwicklungsgesch*. 1974;144:137–163.
443. Layton AT, Layton HE. A region-based mathematical model of the urine concentrating mechanism in the rat outer medulla. I. formulation and base-case results. *Am J Physiol Renal Physiol*. 2005;289(6):F1346–F1366.
444. Layton AT, Layton HE. A region-based mathematical model of the urine concentrating mechanism in the rat outer medulla. II. Parameter sensitivity and tubular inhomogeneity. *Am J Physiol Renal Physiol*. 2005;289(6):F1367–F1381.
445. Garg LC, Mackie S, Tisher CC. Effect of low potassium-diet on Na-K-ATPase in rat nephron segments. *Pfluegers Arch*. 1982;394:113–117.

446. Oliver J. *Nephrons and Kidneys: A Quantitative Study of Developmental and Evolutionary Mammalian Renal Architectonics*. New York: Harper and Row; 1968:1968.
447. Pfeiffer EW, Nungesser WC, Iverson DA, et al. The renal anatomy of the primitive rodent, *Aplodontia rufa*, and a consideration of its functional significance. *Anat Rec*. 1960;137:227–235.
448. Imai M, Kokko JP. Sodium, chloride, urea, and water transport in the thin ascending limb of Henle. *J Clin Invest*. 1974;53:393–402.
449. Kondo Y, Abe K, Igarashi Y, et al. Direct evidence for the absence of active Na⁺ reabsorption in hamster ascending thin limb of Henle's loop. *J Clin Invest*. 1993;91:5–11.
450. Knepper MA, Chou C-L, Layton HE. How is urine concentrated by the renal inner medulla? *Contrib Nephrol*. 1993;102:144–160.
451. Gamba G, Knepper MA. Urinary concentration and dilution. In: Brenner BM, ed. *Brenner and Rector's: The Kidney*. 7th ed. Philadelphia: Saunders; 2004:599–636.
452. Layton AT, Pannabecker TL, Dantzer WH, et al. Two modes for concentrating urine in rat inner medulla. *Am J Physiol Renal Physiol*. 2004;287(4):F816–F839.
453. Layton AT. A mathematical model of the urine concentrating mechanism in the rat renal medulla. I. Formulation and base-case results. *Am J Physiol Renal Physiol*. 2011;300(2):F356–F371.
454. Jen JF, Stephenson JL. Externally driven countercurrent multiplication in a mathematical model of the urinary concentrating mechanism of the renal inner medulla. *Bull Math Biol*. 1994;56(3):491–514.
455. Yang T, Huang YA, Singh I, et al. Localization of bumetanide- and thiazide-sensitive Na-K-Cl cotransporters along the rat nephron. *Am J Physiol*. 1996;271(4):F931–F939.
456. Thomas SR. Inner medullary lactate production and accumulation: a vasa recta model. *Am J Physiol Renal Physiol*. 2000;279:F468–F481.
457. Hery S, Thomas SR. Inner medullary lactate production and urine-concentrating mechanism: a flat medullary model. *Am J Physiol Renal Physiol*. 2003;284(1):F65–F81.
458. Zhang W, Edwards A. A model of glucose transport and conversion to lactate in the renal medullary microcirculation. *Am J Physiol Renal Physiol*. 2006;290:F87–F102.
459. Chen Y, Fry BC, Layton AT. Modeling glucose metabolism in the kidney. *Bull Math Biol*. 2016;78(6):1318–1336.
460. Pruitt ME, Knepper MA, Graves B, et al. Effect of peristaltic contractions of the renal pelvic wall on solute concentrations of the renal inner medulla in the hamster. *Am J Physiol Renal Physiol*. 2006;290:F892–F896.
461. Weigel PH, Hascall VC, Tammi M. Hyaluronan synthases. *J Biol Chem*. 1997;272:13997–14000.
462. Toole BP. Hyaluronan is not just goo! *J Clin Invest*. 2000;106:335–336.
463. Castor CW, Greene JA. Regional distribution of acid mucopolysaccharides in the kidney. *J Clin Invest*. 1968;47:2125–2132.
464. Dwyer TM, Banks SA, Alonso-Calicia M, et al. Distribution of renal medullary hyaluronan in lean and obese rabbits. *Kidney Int*. 2000;58:721–729.
465. Pitcock JA, Lyons H, Brown PS, et al. Glycosaminoglycans of the rat renomedullary interstitium: ultrastructural and biochemical observations. *Exp Mol Pathol*. 1988;49:373–387.
466. Sands JM, Layton HE. The physiology of urinary concentration: an update. *Semin Nephrol*. 2009;29(3):178–195.
467. Schmidt-Nielsen B. The renal concentrating mechanism in insects and mammals: a new hypothesis involving hydrostatic pressures. *Am J Physiol*. 1995;268:R1087–R1100.
468. Laurent TC. *The Chemistry, Biology and Medical Applications of Hyaluronan and Its Derivatives*. London: Portland Press; 1988:1988.
469. Sands JM, Bichet DG. Nephrogenic diabetes insipidus. *Ann Intern Med*. 2006;144(3):186–194.
470. Boone M, Deen PM. Congenital nephrogenic diabetes insipidus: what can we learn from mouse models? *Exp Physiol*. 2009;94(2):186–190.
471. Kwon TH, Nielsen J, Moller HB, et al. Aquaporins in the kidney. *Handb Exp Pharmacol*. 2009;190:95–132.
472. Kwon TH, Laursen UH, Marples D, et al. Altered expression of renal AQP2 and Na⁺ transporters in rats with lithium-induced NDI. *Am J Physiol Renal Physiol*. 2000;279(3):F552–F564.
473. Marples D, Christensen S, Christensen EI, et al. Lithium-induced downregulation of aquaporin-2 water channel expression in rat kidney medulla. *J Clin Invest*. 1995;95:1838–1845.
474. Marples D, Frokiaer J, Dorup J, et al. Hypokalemia-induced downregulation of aquaporin-2 water channel expression in rat kidney medulla and cortex. *J Clin Invest*. 1996;97(8):1960–1968.
475. Marples D, Christensen BM, Frokiaer J, et al. Dehydration reverses vasopressin antagonist-induced diuresis and aquaporin-2 downregulation in rats. *Am J Physiol Renal Physiol*. 1998;275(3):F400–F409.
476. Esteva-Font C, Anderson MO, Verkman AS. Urea transporter proteins as targets for small-molecule diuretics. *Nat Rev Nephrol*. 2015;11(2):113–123.
477. Sands JM. Urea transporter inhibitors: en route to new diuretics. *Chem Biol*. 2013;20(10):1201–1202.
478. Klein JD, Sands JM. Urea transport and clinical potential of urearetics. *Curr Opin Nephrol Hypertens*. 2016;25(5):444–451.
479. Esteva-Font C, Phuan PW, Lee S, et al. Structure-activity analysis of thiourea analogs as inhibitors of UT-A and UT-B urea transporters. *Biochim Biophys Acta*. 2015;1848(5):1075–1080.
480. Cil O, Esteva-Font C, Tas ST, et al. Salt-sparing diuretic action of a water-soluble urea analog inhibitor of urea transporters UT-A and UT-B in rats. *Kidney Int*. 2015;88(2):311–320.
481. Esteva-Font C, Cil O, Phuan PW, et al. Diuresis and reduced urinary osmolality in rats produced by small-molecule UT-A-selective urea transport inhibitors. *FASEB J*. 2014;28(9):3878–3890.
482. Lee S, Esteva-Font C, Phuan PW, et al. Discovery, synthesis and structure-activity analysis of symmetrical 2,7-disubstituted fluorenones as urea transporter inhibitors. *Med Chem Comm*. 2015;6:1278–1284.
483. Li F, Lei T, Zhu J, et al. A novel small-molecule thienoquinolin urea transporter inhibitor acts as a potential diuretic. *Kidney Int*. 2013;83(6):1076–1086.
484. Sun Y, Lau CW, Jia Y, et al. Functional inhibition of urea transporter UT-B enhances endothelial-dependent vasodilatation and lowers blood pressure via L-arginine-endothelial nitric oxide synthase-nitric oxide pathway. *Sci Rep*. 2016;6:18697.
485. Ren H, Wang Y, Xing Y, et al. Thienoquinolins exert diuresis by strongly inhibiting UT-A urea transporters. *Am J Physiol Renal Physiol*. 2014;307(12):F1363–F1372.
486. Koepsell H, Nicholson WAP, Kriz W, et al. Measurements of exponential gradients of sodium and chloride in the rat kidney medulla using the electron microprobe. *Pfluegers Arch*. 1974;350:167–184.
487. Press WH, Teukolsky SA, Vetterling WT, et al. *Numerical Recipes in FORTRAN: The Art of Scientific Computing*. 2nd ed. New York: Cambridge University Press; 1992:1992.
488. Han JS, Thompson KA, Chou C-L, et al. Experimental tests of three-dimensional model of urinary concentrating mechanism. *J Am Soc Nephrol*. 1992;2(12):1677–1688.
489. Atherton JC, Hai MA, Thomas S. Acute effects of lysine vasopressin injection (single and continuous) on urinary composition in the conscious water diuretic rat. *Pfluegers Arch*. 1969;310:281–296.

BOARD REVIEW QUESTIONS

1. Which diuretic will interfere with the ability to both concentrate and dilute the urine?
- Thiazide
 - Furosemide
 - Amiloride
 - Acetazolamide
 - Spirolonactone

Answer: b

Rationale: Furosemide inhibits NKCC2 in the thick ascending limb, thereby inhibiting NaCl reabsorption. The inability to remove NaCl from the luminal fluid interferes with the ability to generate dilute urine. The inability to add NaCl to the medullary interstitium prevents the generation of a hypertonic medulla and interferes with the ability to concentrate the urine. The other diuretic choices do not act on the thick ascending limb.

2. All of the following are required to reabsorb water across the collecting duct EXCEPT
- Hypertonic medulla
 - Vasopressin (ADH)
 - Aquaporin 1 water channels
 - Aquaporin 2 water channels
 - Aquaporin 3 water channels

Answer: c

Rationale: Vasopressin acts on the collecting duct to stimulate transcellular water reabsorption via aquaporin 2 in the apical membrane and aquaporin 3 in the basolateral membrane, provided that a hypertonic medulla exists to provide the osmotic driving force for water reabsorption. Aquaporin 1 is not expressed in the collecting duct.

3. Which urea recycling pathway is most likely to play a major role in urine concentration?
- Recycling of urea through the ascending limbs, distal tubules, and collecting ducts
 - Recycling of urea through the vasa recta, short loops of Henle, and collecting ducts
 - Urea recycling between ascending and descending limbs of the loops of Henle
 - Urea recycling across the renal pelvic (calyceal) epithelium
 - Urea recycling from the proximal tubule to peritubular capillaries

Answer: a

Rationale: Vasopressin stimulates urea reabsorption across the inner medullary collecting duct. The reabsorbed urea can be recycled into the thin ascending limb in the inner medulla. This recycled urea remains in the tubular fluid as it moves into the urea impermeable thick ascending limb, distal tubule, and cortical collecting duct. The other choices represent urea recycling pathways but are less important than the inner medullary urea recycling pathway in choice a.

4. Urine concentrating ability is improved by
- Hypokalemia
 - Protein malnutrition
 - Hypercalcemia
 - Decrease in medullary blood flow
 - Mutations in the V_2 receptor

Answer: d

Rationale: A decrease in medullary blood flow improves urine-concentrating ability but improving the efficiency of countercurrent exchange while an increase reduces urine concentrating ability by decreasing the efficiency of countercurrent exchange. The other choices all cause reduced urine-concentrating ability.